agriculture

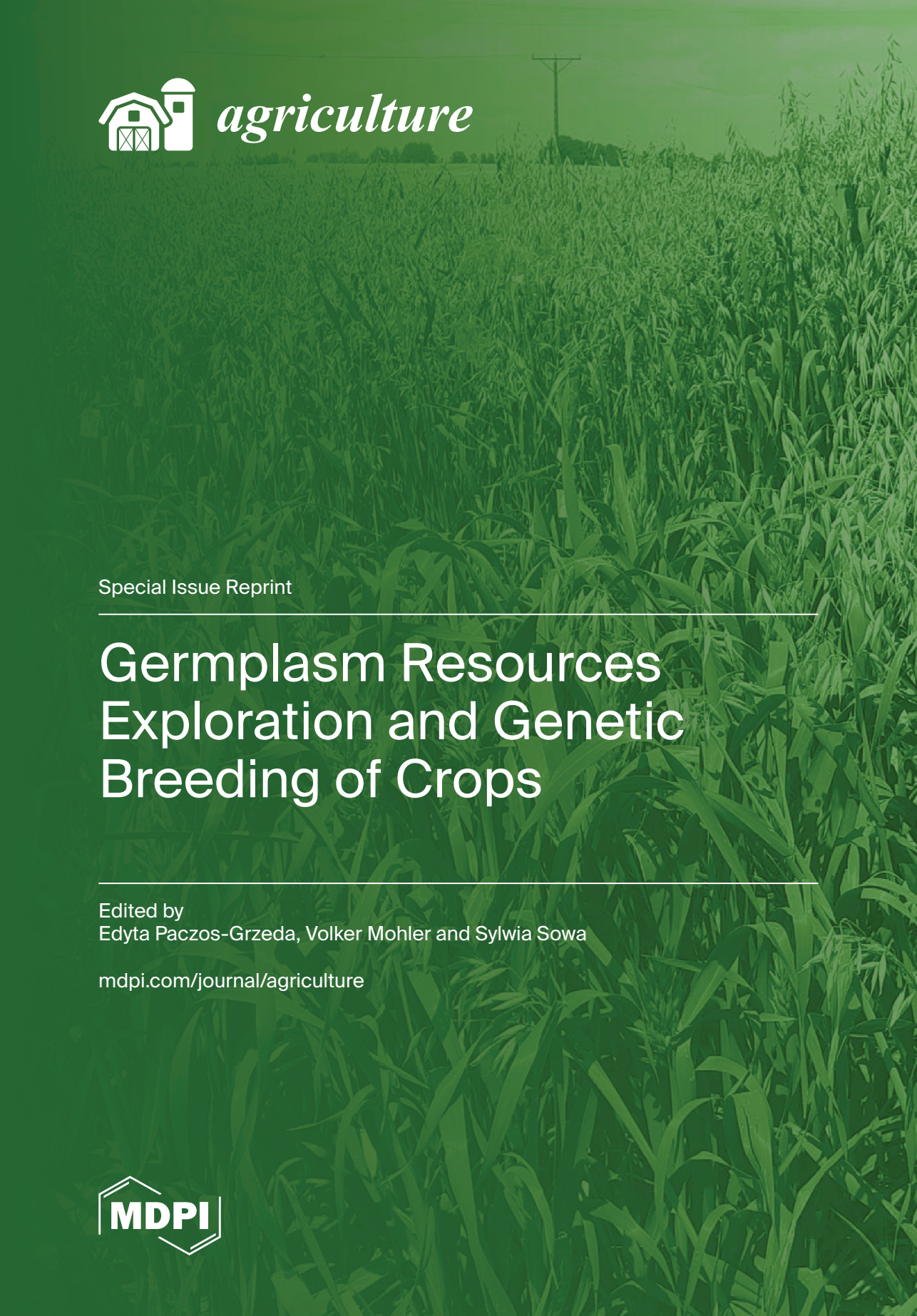

Special Issue Reprint

Germplasm Resources Exploration and Genetic Breeding of Crops

Edited by
Edyta Paczos-Grzeda, Volker Mohler and Sylwia Sowa

mdpi.com/journal/agriculture

MDPI

Germplasm Resources Exploration and Genetic Breeding of Crops

Germplasm Resources Exploration and Genetic Breeding of Crops

Editors

Edyta Paczos-Grzeda
Volker Mohler
Sylwia Sowa

MDPI

Basel • Beijing • Wuhan • Barcelona • Belgrade • Novi Sad • Cluj • Manchester

Editors

Edyta Paczos-Grzeda
Institute of Plant Genetics, Breeding and Biotechnology
University of Life Sciences in Lublin
Lublin, Poland

Volker Mohler
Institut für Pflanzenbau und Pflanzenzüchtung
Bayerische Landesanstalt für Landwirtschaft (LfL)
Freising, Germany

Sylwia Sowa
Institute of Plant Genetics, Breeding and Biotechnology
University of Life Sciences in Lublin
Lublin, Poland

Editorial Office
MDPI
St. Alban-Anlage 66
4052 Basel, Switzerland

This is a reprint of articles from the Special Issue published online in the open access journal *Agriculture* (ISSN 2077-0472) (available at: https://www.mdpi.com/journal/agriculture/special_issues/crops_germplasm_breeding).

For citation purposes, cite each article independently as indicated on the article page online and as indicated below:

Lastname, A.A.; Lastname, B.B. Article Title. *Journal Name* **Year**, *Volume Number*, Page Range.

ISBN 978-3-0365-9841-3 (Hbk)
ISBN 978-3-0365-9842-0 (PDF)
doi.org/10.3390/books978-3-0365-9842-0

Cover image courtesy of Edyta Paczos-Grzeda

Contents

Preface

To adapt to an increasingly demanding and changing environment, the genetic diversity of crops needs to be conserved and maintained in genebanks worldwide. Extensive genebank collections need to be genotypically and phenotypically characterized to effectively improve their management and generate knowledge that is useful to plant breeders. The availability of useful and properly characterized genetic variations is one of the key parameters for ensuring genetic gains in plant breeding programs. The Special Issue "Germplasm Resources Exploration and Genetic Breeding of Crops" covers many aspects of the characterization of crop genetic resources and their applications in conventional breeding, genetic research, and molecular breeding, including gene/QTL detection or gene functional analysis in crops.

Edyta Paczos-Grzeda, Volker Mohler, and Sylwia Sowa
Editors

agriculture

Editorial

Germplasm Resources Exploration and Genetic Breeding of Crops

Edyta Paczos-Grzęda [1,*], Volker Mohler [2,*] and Sylwia Sowa [1,*]

[1] Institute of Plant Genetics, Breeding and Biotechnology, University of Life Sciences in Lublin, 20-950 Lublin, Poland
[2] Institute for Crop Science and Plant Breeding, Bavarian State Research Center for Agriculture (LfL), 85354 Freising, Germany
* Correspondence: edyta.paczos@up.lublin.pl (E.P.-G.); volker.mohler@lfl.bayern.de (V.M.); sylwia.sowa@up.lublin.pl (S.S.)

1. Introduction

A continuously changing climate has negatively impacted agriculture and threatened food security worldwide. Climate change and the fast-growing human population have caused the shrinking of arable land, soil erosion, water shortages, and the loss of genetic resources in their natural locations. Environmental changes force plant breeders to develop new and improved cultivars with better adaptability to biotic and abiotic stresses. The genetic diversity of crops, gathered and protected from extinction in genebanks worldwide, is essential for dealing with changing and more demanding environments.

Plant genetic resources are not only items to collect but are vital for securing breeding gains in agricultural crops. An estimated number of 7.5 million samples are stored in approximately 1800 genebanks worldwide [1], of which most are at least recorded in information systems. There is a compelling need for the genotypic and phenotypic characterization of whole genebank collections to efficiently increase their management and generate information that is useful for plant breeders. Precise and comprehensive characterization can be achieved through the intensive phenotyping and genotyping of genebank collections, current and historic cultivars, landraces, and breeding materials using advanced molecular, biochemical, and physiological tools and methods.

Citation: Paczos-Grzęda, E.; Mohler, V.; Sowa, S. Germplasm Resources Exploration and Genetic Breeding of Crops. *Agriculture* **2023**, *13*, 2258. https://doi.org/10.3390/agriculture13122258

Received: 6 December 2023
Accepted: 7 December 2023
Published: 11 December 2023

2. Overview of the Special Issue

The Special Issue "Germplasm Resources Exploration and Genetic Breeding of Crops" was planned to cover all aspects of the characterization of crop genetic resources and their applications in breeding, as well as genetics research and molecular breeding, including gene/QTL detection or gene functional analysis in crops. In our Special Issue, we have united 16 papers addressing various aspects around the topic of plant genetic resources, including quantitative trait loci (QTL) mapping/gene discovery [2,3], genetic diversity/variation [4–9], breeding products [9–13], and genetic resource profiles for crops [14–16].

2.1. QTL Mapping

The first contribution [2] employed QTL analysis to investigate the genetic architecture of panicle length in a biparental rice population that involved an accession of Dongxiang wild rice (*Oryza rufipogon* L.). Three out of the four QTL found were derived from wild species. After the development of a near-isogenic line for a major wild rice QTL on chromosome 7 and the establishment of a high-resolution genetic mapping population, the locus was pinpointed to a genomic region that contains the well-known *grain length on chromosome 7* (*GL7*) gene. Further studies suggested the locus in Dongxiang wild rice to represent a new variant of *GL7* that appears to control, besides grain size, inflorescence length.

A second QTL study [3] addressed blast resistance in the Thai rice landrace variety Phaladum through a QTL-seq approach. Inheritance studies indicated the presence of a single, all-stage *Magnaporthe oryzae* resistance gene. QTL-seq analysis located the gene in a 3.6 Mb region on chromosome 4 that harbours, among four other genes with putative functions in disease resistance, the dominant resistance gene *Pi63*. Kompetitive Allele-Specific PCR (KASP) marker-trait association analysis showed that all five genes were highly associated with variation in disease reaction, with the highest phenotypic variance explained by *Pi63*.

2.2. Genetic Diversity/Variation

The characterization of germplasm genetic diversity is critical for gaining information on desirable traits and maximizing genetic resource exploitation for cultivar development.

Lee et al. [4] characterized the genetic diversity of Korean black soybean (*Glycine max* (L.) Merr.) with green cotyledons. The evaluation of twenty seed composition traits in 469 accessions indicated that black soybean germplasm was divided into four clusters by the differences observed in crude fat, lutein, chlorophyll, cyanidin-3-glucoside, palmitic, α-linolenic, and oleic acid contents. This study highlights the genetic diversity of black soybean germplasm, which may be useful for soybean breeding programs.

Mehmood et al. [5] assessed the genetic divergence and population structure of potato genotypes collected from Punjab, Pakistan, using polymorphic retrotransposon-based DNA markers. Analysis of molecular variance (AMOVA) and STRUCTURE arranged the eighty genotypes into five distinct groups and indicated genotypes especially valuable for potato cultivar improvement.

Kadluczka and Grzebelus [6] comparatively investigated the fruit morphology and anatomy of 13 wild *Daucus* species and four closely related non-*Daucus* species as potential sources of genetic diversity for carrot (*Daucus carota* subsp. *sativus* Hoffm.) improvement. Evaluation of fruit morphology and anatomy and observation by light and scanning electron microscopy revealed a wide range of variation in fruit morpho-anatomical characteristics, including fruit size, shape, and weight, as well as fruit surface sculpturing and some other anatomical characteristics.

In the study conducted by Madhavan Samyuktha et al. [7], 52 mungbean (*Vigna radiata* L.) genotypes were evaluated for resistance to bruchids (*Callosobruchus* ssp., *Coleoptera*, *Bruchidae*), insects that cause severe damage to seeds during storage, and 2 highly resistant genotypes (V2802BG and V2709) were identified. In a population developed by crossing V2802BG with a high-yielding bruchid-susceptible cultivar, seven highly resistant families were identified and evaluated in the F_4 and F_5 generations. As a result, five highly resistant lines were developed, which can be used as a potential source of genetic material for improving bruchid resistance in mungbean breeding programs.

Noweiska et al. [8] used a fluorescence in situ hybridization toolbox and molecular markers linked to the leaf rust resistance gene *Lr63* (located on the short arm of the $3A^m$ chromosome—$3A^mS$) to track polymorphisms between *Triticum monococcum* subsp. *monococcum*, *T. boeoticum,* and *T. urartu* (A-genome donor for hexaploid wheat) accessions collected in different regions of Europe, Asia, and Africa. The authors distinguished three groups of accessions and concluded that the polymorphisms observed in cultivated forms of *T. monococcum* were induced by adaptation to local environmental conditions.

2.3. Breeding Resources and Breeding Products

Progress in plant breeding is achieved through the search for and introduction of new valuable trait-conditioning genes into breeding materials. In this section, the authors scanned plants of the *Avena* L., *Setaria italica* L., *Zea mays* L., and *Brassica napus* L. species, utilizing phenotyping or molecular genotyping to detect useful breeding materials and assess the diversity of the available breeding resources.

Ma et al. [9] investigated the genetic basis of the foxtail millet (*Setaria italica* L.) discoloration rate caused by carotenoid degradation during storage and identified *SiLOX4*

as a potential key gene in regulating millet discoloration. This study provided critical information on the mechanism of carotenoid degradation during millet storage and laid the foundation for further understanding of carotenoid metabolism in millet.

Thiam et al. [10] evaluated the diversity, productivity, and stability of eleven advanced breeding lines and the control cultivar 'Avery' of *A. magna* ssp. *domestica* in five locations across three cropping seasons in Morocco. Consequently, they verified that the tested lines were beneficial to be incorporated into breeding programs in Morocco and chose line AT5 as one with the highest grain yield and AT7 as the most stable in all environments, making them the most promising breeding material.

Sowa et al. [11] tested the crown rust resistance of Polish National Genebank resources for *Avena strigosa Schreb*. In addition to identifying *Avena* accessions that might be ideal crown rust resistance gene donors (PI 51887) and sources of putatively new *Puccinia coronata* resistance, they also proved the complexity and heterogeneity of the accessions gathered in the genebanks. This confirms that once many potential sources of oat resistance have been overcome, it is advisable to conduct a thorough search for desired breeding features among the population plants of a given accession.

Sobiech et al. [12] scanned maize breeding lines with different field resistance to *Fusarium* fungi using molecular markers linked to *Fusarium verticillioides* quantitative resistance loci. They confirmed the utility of the markers used in evaluating fusarium-resistant materials, presented optimal parental selection for crossbreeding, and developed multiplex PCR reactions to facilitate the maize breeding process.

In the study of Wasuwatthanakool et al. [13], the genetic effect and combining ability for both total carotenoids and their fractions of S_2 super sweet corn lines developed from a cross between tropical and temperate germplasm were examined. The authors identified lines potentially useful in hybrid breeding of high-carotenoid content and improved nutritional values and determined that the inheritance of carotenoid content was controlled by non-additive gene activity, enabling further breeding strategies.

Finally, Łopatyńska et al. [14] assessed double haploid oilseed rape lines with varied seed coat color and selected valuable breeding material connecting a light color of seeds with high yielding. Based on the obtained results, the authors concluded that the most crucial factors in breeding rapeseed with improved seed properties are seed weight and color. They also proved the usefulness of statistical multivariate methods in the selection of breeding material for rapeseed.

2.4. Genetic Resource Profiles

Three review articles in this Special Issue offer insights into the wealth of genetic resources for wheat/oats [15], chestnuts [16], and tobacco [17]. All three articles point out the significance of these plant materials to breeding for disease resistance and that the potential of the wild relatives can only be fully used when coupled with genomics-assisted breeding. Further, the utilization of gene signatures from distantly related species will be accelerated by genome-editing techniques, as cross-compatibility is no longer a prerequisite for information transfer.

3. Conclusions

This editorial summarizes the main scientific input from 16 research papers and reviews comprising the Special Issue "Germplasm Resources Exploration and Genetic Breeding of Crops". The papers cover studies on QTL mapping, genetic diversity/variation, breeding resources and breeding products, as well as the genetic resource profiles of a variety of important crops. The Special Issue presents a variety of ideas, concepts, and tactics for readers and researchers aiming to accelerate plant breeding through the exploration of germplasm resources.

Author Contributions: The authors, E.P.-G., V.M. and S.S., contributed equally to writing and revising the manuscript. All authors have read and agreed to the published version of the manuscript.

Funding: This research received no external funding.

Data Availability Statement: All papers cited in this editorial are available at the following link: https://www.mdpi.com/journal/agriculture/special_issues/crops_germplasm_breeding (accessed on 20 November 2023).

Acknowledgments: The guest editors are thankful to all the eminent authors who accepted the invitation to submit their research to this Special Issue. In addition, they appreciate the support from the distinguished reviewers.

Conflicts of Interest: The authors declare no conflict of interest.

References

1. Keilwagen, J.; Lehnert, H.; Badaeva, E.D.; Özkan, H.; Sharma, S.; Civáň, P.; Kilian, B. Finding Needles in a Haystack: Identification of Inter-Specific Introgressions in Wheat Genebank Collections using Low-Coverage Sequencing Data. *Front. Plant Sci.* **2023**, *14*, 1166854. [CrossRef] [PubMed]
2. Li, S.; Rao, Y.; Duan, P.; Wang, Z.; Hu, P.; Yu, R.; Luo, C.; Tang, M.; Lu, C.; Wang, Y. Mapping and Candidate Gene Prediction of *qPL7-25*: A Panicle Length QTL in Dongxiang Wild Rice. *Agriculture* **2023**, *13*, 1623. [CrossRef]
3. Netpakdee, C.; Mathasiripakorn, S.; Sribunrueang, A.; Chankaew, S.; Monkham, T.; Arikit, S.; Sanitchon, J. QTL-Seq Approach Identified *Pi63* Conferring Blast Resistance at the Seedling and Tillering Stages of Thai Indigenous Rice Variety "Phaladum". *Agriculture* **2022**, *12*, 1166. [CrossRef]
4. Lee, J.Y.; Jo, H.; Son, C.K.; Bae, J.S.; Lee, J.D. Genetic Diversity of Korean Black Soybean (*Glycine max* L.) Germplasms with Green Cotyledons Based on Seed Composition Traits. *Agriculture* **2023**, *13*, 406. [CrossRef]
5. Mehmood, A.; Dracatos, P.M.; Maqsood, L.; Yousafi, Q.; Hussain, A.; Jaskani, M.J.; Sajid, M.W.; Haider, M.S.; Hussain, M.M. Genetic Variability and Population Structure of Pakistani Potato Genotypes Using Retrotransposon-Based Markers. *Agriculture* **2023**, *13*, 185. [CrossRef]
6. Kadluczka, D.; Grzebelus, E. Comparative Fruit Morphology and Anatomy of Wild Relatives of Carrot (*Daucus*, Apiaceae). *Agriculture* **2022**, *12*, 2104. [CrossRef]
7. Samyuktha, S.M.; Malarvizhi, D.; Mariyammal, I.; Karthikeyan, A.; Seram, D.; Dhasarathan, M.; Juliet Hepziba, S.; Sheela, V.; Thanga Hemavathy, A.; Kavithamani, D. The Hunt for Mungbean (*Vigna radiata* (L.) Wilczek) Genotypes and Breeding Lines Resistance to South Indian Bruchid Strain. *Agriculture* **2022**, *12*, 1050. [CrossRef]
8. Noweiska, A.; Bobrowska, R.; Kwiatek, M.T. Structural Polymorphisms of Chromosome 3Am Containing *Lr63* Leaf Rust Resistance Loci Reflect the Geographical Distribution of *Triticum monococcum* L. and Related Diploid Wheats. *Agriculture* **2022**, *12*, 966. [CrossRef]
9. Ma, Q.; Wang, J.; Cheng, L.; Li, Y.; Zhang, Q.; Li, H.; Han, Y.; Zhen, X.; Zhang, B. The Potential Function of *SiLOX4* on Millet Discoloration during Storage in Foxtail Millet. *Agriculture* **2022**, *12*, 1283. [CrossRef]
10. Thiam, E.H.; Jellen, E.N.; Jackson, E.W.; Nelson, M.; Rogers, W.; El Mouttaqi, A.; Benlhabib, O. Productivity and Stability Evaluation of 12 Selected *Avena magna* ssp. domestica Lines Based on Multi-Location Experiments during Three Cropping Seasons in Morocco. *Agriculture* **2023**, *13*, 1486. [CrossRef]
11. Sowa, S.; Mohler, V.; Paczos-Grzęda, E. Searching for Novel Oat Crown Rust Resistance in Diploid Oat *Avena strigosa* Schreb. Reveals the Complexity and Heterogeneity of the Analyzed Genebank Accessions. *Agriculture* **2023**, *13*, 296. [CrossRef]
12. Sobiech, A.; Tomkowiak, A.; Bocianowski, J.; Nowak, B.; Weigt, D.; Kurasiak-Popowska, D.; Kwiatek, M.; Mikołajczyk, S.; Niemann, J.; Szewczyk, K. Application Marker-Assisted Selection (MAS) and Multiplex PCR Reactions in Resistance Breeding of Maize (*Zea mays* L.). *Agriculture* **2022**, *12*, 1412. [CrossRef]
13. Wasuwatthanakool, W.; Harakotr, B.; Jirakiattikul, Y.; Lomthaisong, K.; Suriharn, K. Combining Ability and Testcross Performance for Carotenoid Content of S2 Super Sweet Corn Lines Derived from Temperate Germplasm. *Agriculture* **2022**, *12*, 1561. [CrossRef]
14. Łopatyńska, A.; Wolko, J.; Bocianowski, J.; Cyplik, A.; Gacek, K. Statistical Multivariate Methods for the Selection of High-Yielding Rapeseed Lines with Varied Seed Coat Color. *Agriculture* **2023**, *13*, 992. [CrossRef]
15. Mohler, V.; Paczos-Grzędarz, E.; Sowa, S. Loving the Alien: The Contribution of the Wild in Securing the Breeding of Cultivated Hexaploid Wheat and Oats. *Agriculture* **2023**, *13*, 2060. [CrossRef]
16. Braga, M.; Araújo, S.D.S.; Sales, H.; Pontes, R.; Nunes, J. Portuguese *Castanea sativa* Genetic Resources: Characterization, Productive Challenges and Breeding Efforts. *Agriculture* **2023**, *13*, 1629. [CrossRef]
17. Czubacka, A. The Use of the Polish Germplasm Collection of *Nicotiana tabacum* in Research and Tobacco Breeding for Disease Resistance. *Agriculture* **2022**, *12*, 1994. [CrossRef]

agriculture

MDPI

Article

Mapping and Candidate Gene Prediction of *qPL7-25*: A Panicle Length QTL in Dongxiang Wild Rice

Sanfeng Li [1,†], Yuchun Rao [2,†], Penggen Duan [1], Zhonghao Wang [1], Ping Hu [1], Ruoqian Yu [1], Chenxi Luo [1], Mengna Tang [1], Caolin Lu [1], Yuexing Wang [1] and Yijian Mao [1,*]

[1] State Key Laboratory of Rice Biology and Breeding, China National Rice Research Institute, Hangzhou 311400, China
[2] College of Life Sciences, Zhejiang Normal University, Jinhua 321004, China
* Correspondence: maoyijian@caas.cn
† These authors contributed equally to this work.

Abstract: Panicle length (PL) is an important trait closely related to rice yield. More than 200 quantitative trait loci (QTL) for PL have been identified, but only a few can be used for breeding. Dongxiang wild rice contains many excellent genes, and mining favorable PL-related QTL from DXWR is helpful for rice variety improvement. Here, we report a QTL analysis for PL using a recombinant inbred line population consisting of 143 individuals derived from a cross between Dongxiang wild rice and indica cultivar Guangluai 4. A total of four QTL (*qPL1-37*, *qPL4-26*, *qPL7-25*, and *qPL8-4*) for PL were identified and located on chromosomes 1, 4, 7, and 8. Among them, *qPL7-25* showed the largest F-value of 32.32 and 16.80, and the QTL explained 18.66% and 13.06% of the phenotypic variation of Dongxiang wild rice in Hangzhou and Hainan, respectively. QTL mapping was performed using a population of 1800 individuals derived from the crossing of NIL-*qPL7-25* and GLA4. *qPL7-25* was located between two InDel markers, InDel-24591 and InDel-24710, in a 119 kb region containing 14 predicted genes. Using Sanger sequencing and qRT-PCR analysis, we propose that *LOC_Os07g41200* is probably a new allele of the well-known *GL7* gene, which affects grain length and appearance quality in rice. These results provide new insights into the use of molecular marker-assisted selection for breeding high-yielding and high-quality rice varieties.

Keywords: Dongxiang wild rice; quantitative trait locus; near-isogenic lines; *qPL7-25*; fine mapping

Citation: Li, S.; Rao, Y.; Duan, P.; Wang, Z.; Hu, P.; Yu, R.; Luo, C.; Tang, M.; Lu, C.; Wang, Y.; et al. Mapping and Candidate Gene Prediction of *qPL7-25*: A Panicle Length QTL in Dongxiang Wild Rice. *Agriculture* **2023**, *13*, 1623. https://doi.org/10.3390/agriculture13081623

Academic Editors: Jaime Prohens, Volker Mohler, Edyta Paczos-Grzeda and Sylwia Sowa

Received: 12 July 2023
Revised: 11 August 2023
Accepted: 14 August 2023
Published: 18 August 2023

1. Introduction

Food security is a top priority for most countries. Rice is the staple food for more than 60% of the population in China, so improving rice production is crucial to ensuring national food security and is the goal of rice breeding. Rice yield is composed of the effective number of panicles per plant, the number of filled grains per panicle, the seed setting rate, and the kilogram grain weight. As a yield-related trait, panicle length (PL) directly determines the number and length of panicle branches in rice, which in turn affects the number of grains in the panicle [1,2]. Traditional rice breeding has made great strides, but there are also drawbacks of inefficiency, and molecular design breeding technology is beginning to show great potential for application, with mining for favorable alleles being the prerequisite for molecular design breeding.

Common wild rice (*Oryza rufipogon* Grff.) can provide favorable gene variants for many important agronomic traits in improved cultivated rice varieties [3–10]. Mining and exploiting favorable genes in *O. rufipogon* could be an effective way to overcome yield stagnation in cultivated rice. Dongxiang wild rice (DXWR) is the most northerly distributed *O. rufipogon* resource in the world, with many excellent characteristics and rich genetic diversity. Compared with other wild rice, DXWR is a close ancestor of cultivated rice, which is suitable for use as an excellent germplasm resource for cultivating rice genetic improvement. Previous studies have shown that DXWR could provide many favorable

genes controlling desirable traits such as high yield [11], cold tolerance [12], drought tolerance [13], and cytoplasmic male sterility [14]. Panicle traits are essential for yield and quality formation; the cloning of favorable panicle architecture genes from DXWR can provide new genetic resources for the high yield and quality breeding of rice, and introducing these favorable genes into the cultivated rice varieties by molecular breeding techniques can accelerate the breeding and use of DXWR.

Panicle traits in rice include the PL, primary branch number (PBN), secondary branch number (SBN), spikelets per panicle (SPP), and grain size. PL is a crucial determinant of panicle architecture, affecting rice yield and quality [15]. Therefore, PL can be used as a criterion for yield improvement breeding. More than 250 quantitative trait loci (QTL) for PL have been mapped and are located across all of the 12 rice chromosomes, but only a few of them have been cloned and used in breeding practice. In addition, some important QTLs for high-yielding traits have also been cloned and applied in rice genetic improvement, such as *Grain number 1a* (*Gn1a*), *DENSE AND ERECT PANICLE1* (*DEP1*), *Ideal Plant Architecture 1* (*IPA1*), *Grain number, plant height and heading date 7* (*Ghd7*), *Ghd8*, *grain size 3* (*GS3*), *grain weight 2* (*GW2*), and *ABERRANT PANICLE ORGANIZATION 1* (*APO1*). The characterization of these genes that supports molecular design breeding and pyramiding beneficial alleles by functional marker-assisted selection is of great help in increasing rice yield [16–18].

Rice PL is a quantitative trait controlled by multiple genes with low heritability, and some genes regulating other panicle traits may also affect PL. Based on the functions of the cloned genes, these genes regulating PL can be classified into the following categories: (1) Several genes/QTL regulate PL by modulating the hormone metabolism, such as *ELONGATED UPPERMOST INTERNODE1* (*EUI1*), *LONELY GUY* (*LOG*), *DEP1*, *Large Panicle* (*LP*)/*Erect Panicle 3* (*EP3*), *Oryza sativa PIN-FORMED 5b* (*OsPIN5b*), *HOMEOBOX12* (*HOX12*), *Oryza sativa GROWTH-REGULATING FACTOR4* (*OsGRF4*)/*PT2*, *Short Panicle* (*SP3*), and *semidwarf-1* (*sd1*) [19–27]. (2) Some genes control PL by affecting the heading date, such as *Ghd7*, *Ghd8*, and Heading date quantitative trait locus7.2 (*qHD7.2*) [28–30]. (3) Other genes are responsible for PL by regulating the cell wall components and nutrients required for growth, including *APO1*, *LARGE2*, *DEP3*, *Oryza sativa Curled leaf and Dwarf mutant1* (*OsCD1*), and *Oryza sativa Arginine* (*OsARG*) [31–37]. In addition, other genes such as *SP1*, *IPA1*, *DEP2, Aberrant spikelet and panicle1* (*ASP1*), *SHORT GRAIN1* (*SG1*), and *TAWAWA1* are involved in the regulation of PL development [38–44]. *Grain length on chromosome 7* (*GL7*) is a major QTL controlling grain length and grain width in rice, and Wang et al. (2015) found that tandem duplication of a 17.1-kb segment at the *GL7* locus led to the upregulation of *GL7* and downregulation of its nearby negative regulator, resulting in increased grain length and improved grain appearance quality [45]. *Slender grain on chromosome 7* (*SLG7*) was allelic to *GL7* and *GW7* [45,46], highly expressed alleles of *SLG7/GL7/GW7* produced slender grains with low chalkiness, and the PL of near-isogenic line (NIL)-*SLG7* was 14.2% longer than that of its background parent, 9311 [47]. *APO1* is an important panicle architecture gene that can directly interact with APO2 and positively regulate the PBN and SPP [48]. The weak allele *STRONG CULM2* (*SCM2*) carrying *APO1* can increase culm strength, which is useful for breeding applications [32,49]. The above results suggest that several factors, such as plant hormones, cell wall components, and heading date, are involved in the genetic regulation of PL.

In this study, a high-density single-nucleotide polymorphism (SNP) linkage map using specific locus-amplified fragment (SLAF) markers was constructed in the recombinant inbred line (RIL) population consisting of 143 individuals derived from a cross between DXWR and indica cultivar Guangluai 4 (GLA4) to detect the QTL associated with PL. The major QTL *qPL7-25* was stably detected on chromosome 7 in Hangzhou (HZ) and Hainan (HN) and was restricted to a 119 kb region between InDel-24591 and InDel-24710. Our results revealed that *qPL7-25* was probably a new allele of *GL7*, which can be used to improve the breeding of elite rice varieties.

2. Materials and Methods

2.1. Plant Materials

An RIL population was developed from a single seed offspring of a backcross (BC_1F_1) of DXWR as the donor and GLA4 as the recurrent parent. This population consisted of 143 lines backcrossed with GLA4 as the parent for one generation and then self-crossed for 12 generations. The parental lines DXWR and GLA4, together with the RIL population, were planted as a plot in the experimental field of the China National Rice Research Institute in Hangzhou (119.54′ E, 30.04′ N, May to October 2014) and Hainan (110.01′ E, 18.30′ N, December 2014 to May 2015). Each plot consisted of four rows separated by 20 cm, with each row consisting of ten plants, each separated from its neighbor by 20 cm. All experimental plots had uniform fertility and medium fertilizer application, and field management was carried out according to general field cultivation techniques.

2.2. Measurement of Traits

To find the relationships between PL and other agronomic traits, ten and five plants from two parents and 143 lines, respectively, were harvested at the maturity stage to measure the plant height (PH), PL, PBN, SBN, and SPP. PH was measured as the distance from the ground to the tip of the main panicle. PL was measured as the distance from the neck node to the tip of the main panicle using a ruler. More than 100 fully filled grains were used to measure seed length, width and length/width ratio using a seed phenotyping system (Wan Sheng, Hangzhou, China). The 1000-grain weight was measured by weighing 1000 full-filled grains with an electronic balance with three replicates. The mean values of all the characters measured were used for the analysis.

2.3. Linkage Map Construction and QTL Analysis

The SLAF sample preparation, sequencing, sequence comparison, polymorphic analysis, and associated marker identification were processed as previously reported [50]. Briefly, two restriction enzymes (*Hae* III and *Hpy* 166II) were selected for their uniform distribution and prevalence in the simulations of fragment alignments to the NPB reference genome. *Arabidopsis thaliana* was used as a control genome to verify the accuracy of the restriction digestion protocol. Fragments of 200–350 bp were isolated to be used as the SLAF tags. The fragments were sequenced on the Illumina HiSeq 2500 system. The SLAFs were grouped into 12 linkage groups with their positions in the reference genome. The modified logarithm of odds scores (MLOD) value between two adjacent markers was determined [51], and SLAFs with MLOD values less than 5 were filtered out. QTL analysis was performed using the QTL Network 2.0 software based on a mixed linear model with all the genotype data from the RIL mapping population. The contribution rates and additive effects of each QTL to the PL were calculated, and the detected QTL were named according to the method proposed by McCouch et al. [52]. If the additive effect value was positive, then the allele was from the DXWR parent, and if the additive effect value was negative, then the allele was from the GLA4 parent.

2.4. Construction of NIL

A VB431 line of RILs with the DXWR genotype was selected for backcrossing with the recurrent parent GLA4. The F_1 generation was then backcrossed with GLA4, combined with the PL phenotype of the progeny, and two InDel markers (InDel-24091 and InDel-25971) on either side of *qPL7-25* were used for marker-assisted selection (MAS) of each generation. After three consecutive backcrosses and one self-cross, a BC_3F_2 population containing 100 individuals with a GLA4 genetic background was isolated and used for primary mapping of *qPL7-25* (Figure S2A). The NIL-*qPL7-25* contains 1.88 Mb of the *qPL7-25* locus from a fragment of DXWR located on chromosome 7 between the InDel markers InDel-24091 and InDel-25971 (Figure S2B). Rice variety P13 with the *GL7* gene was used as the male, the restoring line Huazhan as the female, and the F_1 generation was then backcrossed with recurrent parent Huazhan. A pair of dominant functional markers

(NGL7-F: TGACACGCCACAGTCCAAGACGAGCAGT, NGL7-R: AAGGGAGTTGAGAG-TAGAAAAAA) was used for MAS of each generation. After four consecutive backcrosses and one self-cross, a BC_4F_2 population was obtained. An NIL carrying a homozygous allele of P13 in the target QTL region between markers NGL7-F and NGL7-R, designated NIL-Huazhan-*GL7*^{p13}, was also developed on a Huazhan background.

2.5. QTL Mapping and Statistical Analysis

QTL analysis was performed with the QTLNetwork2.0 software using the mixed linear models [53]. The VB431 line was crossed with the GLA4 variety to develop a mapping population. The F2 population was constructed by self-crossing of the F1 hybrid. A primary linkage of the QTLs for PL was obtained using 100 recessive plants from the F2 population. According to the resequencing and alignment results of GLA4 and DXWR, the InDel loci were identified on chromosome 7. Primers were designed using Vector NTI 11.5 biological software with the following design parameters: GC % 40–55%, base length 19–30 bp, and Tm value 55–60 °C. Seven new InDel markers were developed for fine mapping of the *qPL7-25* locus (Table S1), and the *qPL7-25* locus was mapped to the interval between InDel-24591 and InDel-24710 using a population of 1800 individuals derived from the crossing of NIL-*qPL7-25* and GLA4. All statistical analyses were performed using Student's *t*-test (*, $p < 0.05$; **, $p < 0.01$).

2.6. RNA Extraction and QRT-PCR Analysis

Total RNA was isolated from 3 cm young panicles of DXWR and GLA4 plants according to the manufacturer's instructions of the AxyPerp Multisource Total RNA miniprep kit (Corning Life Sciences (WuJiang) Co., Ltd, Suzhou, China). DNAase-treated RNA (1 µg) was reverse transcribed using a ReverTra Ace qPCR RT master mix (FSQ-301, Toyobo, Osaka, Japan). qRT-PCR was performed using *GL7* gene-specific primers, as described by Wang et al. [45], using the SYBR Green Real-Time-PCR master mix (QPK-201, Toyobo) and the Bio-Rad (Hercules, CA, USA) CFX96 Real Time-PCR system. Ubiquitin was used as an internal standard, and the results were calculated using the $2^{-\Delta\Delta CT}$ method [54].

3. Results

3.1. Phenotypic Data of Panicle Traits of Two Parents and RIL Population

The phenotypes of the DXWR and GLA4 parents were relatively different. The PH of GLA4 in HZ and HN was 54.09% and 64.66% of that of DXWR, respectively. The PL of DXWR was 23.7 cm and 22.1 cm, while that of GLA4 was 21.2 cm and 20.0 cm in HZ and HN, respectively, and was significantly shorter than that of DXWR (Table 1). The grain length and grain length/width ratio of DXWR were significantly greater than those of GLA4, but the grain width and 1000-grain weight were significantly lower than those of GLA4 (Figure S1). In addition, the PBN and SBN of DXWR were significantly higher than those of GLA4, but there was no significant difference in the SPP between the parents (Figure 1, Table 1). The skewness and kurtosis values of the PL in HZ and HN were both less than 1, indicating that the PL was normally distributed and was a polygene-controlled quantitative trait. The data obtained for the PL in the RIL population conformed to a continuous normal distribution with a wide range (Figure 2). In addition, we identified significant positive correlations between PL pairs, the PBN, SBN, and SPP in both HZ and HN (Table 2).

Table 1. Data collection of panicle traits of DXWR, GLA4, and their RIL population.

Traits	Loc	Parents			RIL Population			
		DXWR	GLA4	Average	SD	Variation	Skewness	Kurtosis
PH (cm)	HZ	154.3 ± 3.5 **	83.3 ± 0.8	127.3	29.2	79.0–190.3	0.315	−1.062
	HN	133.7 ± 2.6 **	86.2 ± 1.2	107.5	25.3	64.8–159.6	0.106	−1.237
PL (cm)	HZ	23.7 ± 0.5 **	21.2 ± 0.7	22.1	3.1	14.8–29.8	−0.120	−0.281
	HN	22.1 ± 0.3 **	20.0 ± 0.3	19.5	3.0	13.7–27.0	0.278	−0.516
PBN	HZ	15.7 ± 0.3 *	12.3 ± 0.9	14.5	1.9	10.0–19.0	0.062	−0.646
	HN	11.7 ± 0.7 *	9.3 ± 0.3	9.7	1.5	5.7–13.3	−0.145	−0.238
SBN	HZ	18.3 ± 0.9 *	26.0 ± 2.7	27.3	10.1	8.6–52.0	0.424	−0.262
	HN	13.7 ± 1.5 **	24.3 ± 1.5	21.4	8.7	6.7–44.0	0.335	−0.679
SPP	HZ	133.5 ± 6.5	125.3 ± 3.8	125.4	33.2	58.8–233.9	0.702	0.795
	HN	142.5 ± 3.3	136.9 ± 3.6	99.8	30.3	45.5–170.1	0.349	−0.735

Means ± SD (n = 10 for parents, and n = 5 for RIL lines). * and ** indicate a significant difference between DXWR and GLA4 at the 0.05 and 0.01 levels according to the t-test, respectively. Abbreviations: RIL, recombinant inbred line; DXWR, Dongxiang wild rice; GLA4, Guangluai 4; SD, standard deviation; PH, plant height; PL, panicle length; PBN, primary branch number; SBN, secondary branch number; SPP, spikelet number per panicle; HZ, Hangzhou; HN, Hainan; Loc, location.

Figure 1. Plant and panicle of GLA4 and DXWR at the mature stage. (**A**) Outward appearance comparison of the plants, scale bar = 20 cm. (**B**) Outward appearance comparison of the panicles, scale bar = 3 cm.

Table 2. Correlation analysis of the panicle traits in Hangzhou and Hainan recombinant inbred lines.

Traits	Loc	PBN	SBN	SPP	PL (cm)
PBN	HZ	1			
	HN	1			
SBN	HZ	0.6173 **	1		
	HN	0.6347 **	1		
SPP	HZ	0.5484 **	0.7837 **	1	
	HN	0.7484 **	0.8470 **	1	
PL (cm)	HZ	0.2934 **	0.3321 **	0.4884 **	1
	HN	0.4575 **	0.5049 **	0.6124 **	1

The data in the table were the correlation coefficients between the traits in Hangzhou and Hainan, respectively; ** indicates a 0.01 significant level. Abbreviations: PL, panicle length; PBN, primary branch number; SBN, secondary branch number; SPP, spikelet number per panicle; HZ, Hangzhou; HN, Hainan; Loc, location.

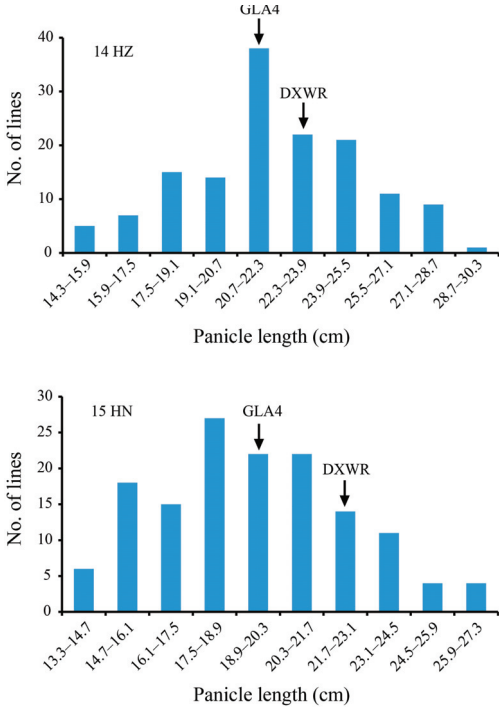

Figure 2. Frequency distribution of panicle length in recombinant inbred line populations in Hangzhou and Hainan. DXWR, Dongxiang wild rice; GLA4, Guangluai 4; HZ, Hangzhou; HN, Hainan.

3.2. QTL Analysis of PL

The 368 polymorphic SNP markers were evenly distributed among the 12 chromosomes and were used to construct a molecular linkage map with the SLAF markers. QTL analysis was performed using QTLNetwork2.0 software based on a mixed linear model, and $p = 0.005$ was used as the statistical detection threshold. A total of four QTL were detected for the PL and were distributed on chromosomes 1, 4, 7, and 8. Among them, *qPL1-37*, *qPL4-26*, and *qPL7-25* were detected repeatedly in both HZ and HN, but *qPL8-4* was detected only in HN (Figure 3, Table 3). *qPL1-37* was located in the marker M37-M38 on chromosome 1, with a physical distance of 1.0 Mb and an F-value of 17.13 and 9.42, and the QTL explained 8.99% and 7.31% of the phenotypic variation in HZ and HN, respectively. *qPL4-26* was located in the marker M142-M143 on chromosome 4 with a physical distance of 1.0 Mb and an F-value of 18.77 and 10.28, and the QTL explained 12.92% and 7.48% of the phenotypic variation in HZ and HN, respectively. *qPL7-25* was located in the marker M234-M235 on chromosome 7 with a physical distance of 1.0 Mb and an F-value of 32.32 and 16.80, and the QTL explained 18.66% and 13.06% of the phenotypic variation in HZ and HN, respectively. *qPL8-4* was located in the marker M242-M243 on chromosome 8 with a physical distance of 1.2 Mb and an F-value of 10.25, and the QTL explained 6.17% of the phenotypic variation in HN. The enhanced alleles *qPL1-37*, *qPL7-25*, and *qPL8-4* were from the DXWR parent (Table 3). As the PBN and SBN of DXWR were significantly different from GLA4, we also identified other QTL related to the panicle traits, and three QTL (*qPBN1-8*, *qPBN2-4*, and *qPBN7-25*) for the PBN and five QTL (*qSBN1-2*, *qSBN1-5*, *qSBN1-6*, *qSBN5-22*, and *qSBN7-20*) for the SBN were also detected. *qPBN1-8* and *qPBN2-4* were repeatedly detected in both HZ and HN, but other QTL were only detected in HZ or HN. Notably, *qPBN7-25* was mapped to the same interval as *qPL7-25* on chromosome 7 (Figure 3, Table 3).

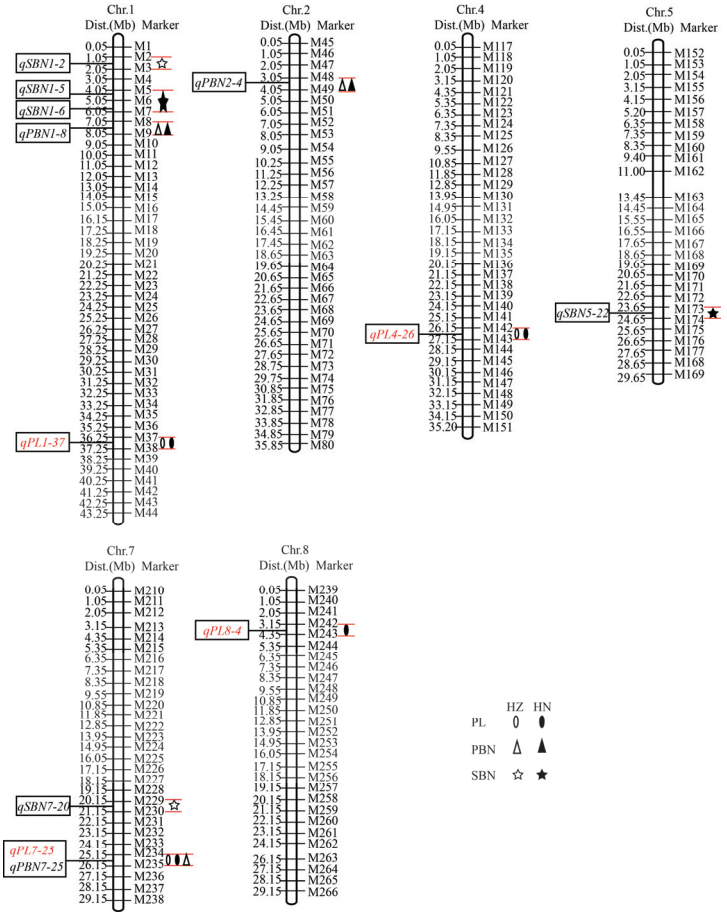

Figure 3. Location of the quantitative trait loci for panicle traits on the single-nucleotide polymorphism map. The number indicates the physical distance (Mb) along each chromosome. Abbreviations: PL, panicle length; PBN, primary branch number; SBN, secondary branch number; HZ, Hangzhou; HN, Hainan.

Table 3. Quantitative trait loci for panicle length were detected in recombinant inbred line populations in Hangzhou and Hainan.

Trait	Loc	Chr.	QTL	Marker Interval	F-Value	*p*-Value	Additive	PVE (%)
PL	HZ	1	*qPL1-37*	M37–M38	17.13	0.000025	0.9532	8.99
		4	*qPL4-26*	M142–M143	18.77	0.000000	0.000000	12.92
		7	*qPL7-25*	M234–M235	32.32	0.000000	1.3373	18.66
	HN	1	*qPL1-37*	M37–M38	9.42	0.000646	0.8259	7.31
		4	*qPL4-26*	M142–M143	10.28	0.000412	−0.8356	7.48
		7	*qPL7-25*	M234–M235	16.80	0.000007	1.1858	13.06
		8	*qPL8-4*	M242–M243	10.25	0.003005	0.7589	6.17
PBN	HZ	1	*qPBN1-8*	M8–M9	17.22	0.000005	−0.6958	12.62
	HN	1	*qPBN1-8*	M8–M9	18.89	0.000001	−0.6390	16.12
	HZ	2	*qPBN2-4*	M48–M49	8.44	0.005070	−0.4330	4.89
	HN	2	*qPBN2-4*	M48–M49	9.30	0.000710	−0.4365	7.53
	HZ	7	*qPBN7-25*	M234–M235	14.84	0.000145	0.5493	7.87

Table 3. *Cont.*

Trait	Loc	Chr.	QTL	Marker Interval	F-Value	*p*-Value	Additive	PVE (%)
SBN	HZ	1	*qSBN1-2*	M2–M3	11.76	0.000330	−2.6833	9.26
	HN	1	*qSBN1-5*	M5–M6	19.28	0.000004	−3.8478	13.91
	HN	1	*qSBN1-6*	M6–M7	24.31	0.000004	−3.1235	12.55
	HN	5	*qSBN5-22*	M173–M174	8.87	0.000447	2.3278	6.97
	HZ	7	*qSBN7-20*	M229–M230	10.99	0.001025	2.8319	7.54

Additives indicate the additive effects. PVE (%) represents the percentage of total phenotypic variance explained by the QTL. Abbreviations: HZ, Hangzhou; HN, Hainan. QTL, quantitative trait locus; Chr, chromosome; Loc, location.

3.3. Fine Mapping of *qPL7-25*

As *qPL7-25* showed the greatest potential to increase the PL, we focused on determining its underlying gene using a map-based cloning strategy. The VB431 line from the RILs with the DXWR genotype in the *qPL7-25* region was selected to backcross with the recurrent GLA4 parent to construct the near-isogenic line (NIL-*qPL7-25*). The phenotypic characteristics were measured in the F_2 population, which included 100 individuals derived from a BC_3F_1 line with a GLA4 genetic background (Figure S2A). By combining the genotype and phenotype of individuals, the QTL was mapped primarily between the two insertion-deletion (InDel) markers, InDel-24091 and InDel-25971, at 1.88 Mb intervals (Figure S2B). To delineate the genomic region of the *qPL7-25*, InDel markers were designed from the re-sequenced genome sequences and tested to predict the probability of polymorphism between the NIL-*qPL7-25* line and the GLA4 cultivar. In the end, seven InDel markers were successfully developed (Table S1). Genotyping of all recombinant genes was performed using seven polymorphic markers, and the *qPL7-25* was located between the two InDel markers, InDel-24591 and InDel-24710 on chromosome 7, with an interval of 119 kb, using a population of 1800 recessive plants derived from the crossing of NIL-*qPL7-25* and GLA4 (Figure 4A). The target region contains 14 predicted genes based on the Rice Genome Annotation Project website (http://rice.plantbiology.msu.edu/), accessed on 10 August 2020 (Figure 4B, Table S2).

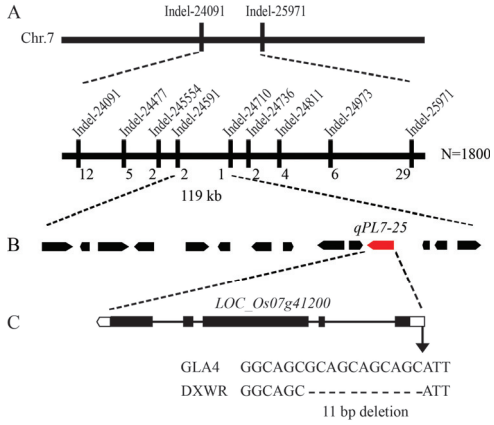

Figure 4. Fine mapping of *qPL7-25*. (**A**) *qPL7-25* was narrowed down to a 119 kb interval on chromosome 7, defined by the InDel markers InDel-24591 and InDel-24710. The numbers below the bars in the panel indicate the number of recombinant lines between each adjacent marker. (**B**) The positions of the 14 predicted genes in the target region. (**C**) The structure and allelic variation of the candidate gene *LOC_Os07g41200*/*GL7*. Introns are shown as lines, exons as black boxes, and the white boxes indicate non-coding regions. Black lines indicate deleted nucleotides. DXWR, Dongxiang wild rice; GLA4, Guangluai 4.

3.4. Candidate Gene Analysis of qPL7-25

Among these 14 predicted genes (Table S2), *LOC_Os07g41100* encodes a conserved hypothetical protein, *LOC_Os07g41110* encodes a retrotransposon protein, and *LOC_Os07g41170* encodes an expressed protein. We used Genevestigator (https://genevestigator.com accessed on 10 August 2020) software to analyze the temporal and spatial expression of the remaining 11 genes. *LOC_Os07g41220* has no expression data in this software, *LOC_Os07g41150* showed pollen-specific expression, *LOC_Os07g41180*, and *LOC_Os07g41190* were highly expressed in root tips, and *LOC_Os07g41230* was a cloned gene related to disease resistance in rice. It is unlikely that the above genes were candidate genes. *LOC_Os07g41090*, *LOC_Os07g41120*, *LOC_Os07g41140*, and *LOC_Os07g41200* were highly expressed in the panicle, *LOC_Os07g41200* (*GL7/GW7*) was a previously cloned major QTL, controlling the grain length and width [45,46], and its expression showed a positive correlation with the critical period of spike development, both in terms of timing and tissue specificity (Figure S3A). In addition, NIL-Huazhan-$GL7^{P13}$ and NIL-*qPL7-25* also showed increased grain length compared to Huazhan and GLA4, respectively (Figure S3B). Therefore, we propose that *LOC_Os07g41200/GL7* could be a candidate gene for *qPL7-25*.

To further confirm that *LOC_Os07g41200/GL7* could be a candidate gene for *qPL7-25*, we sequenced and analyzed the coding sequence and promoter region of *GL7* in the low *GL7*-expressing variety, Nipponbare (NPB) and the high *GL7* expressing variety, landrace Ping13 (P13), DXWR, and GLA4. There were no SNP differences resulting in amino acid changes in the coding region of DXWR and GLA4, but there were SNP and InDel differences in the 5′ untranslated region (UTR) and promoter, especially in the region from -111 to -101 (transcription start site, +1), with an 11 bp deletion in the *GL7* promoter of DXWR compared to GLA4, and P13 had an 8 bp deletion. In contrast, the sequence of GLA4 was similar to that of NPB (Figure 4C, Figure S4). This 11 bp deletion of *GL7* was expressed 2.4-fold higher than GLA4 in young panicles of DXWR, as determined by qRT-PCR assays (Figure 5). These results suggest that this deletion could enhance the function of *GL7* and thus affect the PL in rice. The *GL7* gene from P13 was introduced into the indica rice variety "Huazhan" to construct NIL-Huazhan-$GL7^{P13}$. The PH, PL, PBN, grain length, and grain length/width ratio of NIL-Huazhan-$GL7^{P13}$ were significantly increased compared to Huazhan (Table S3), which was consistent with the comparative trend between NIL-*qPL7-25* and GLA4 phenotypes (Table S4).

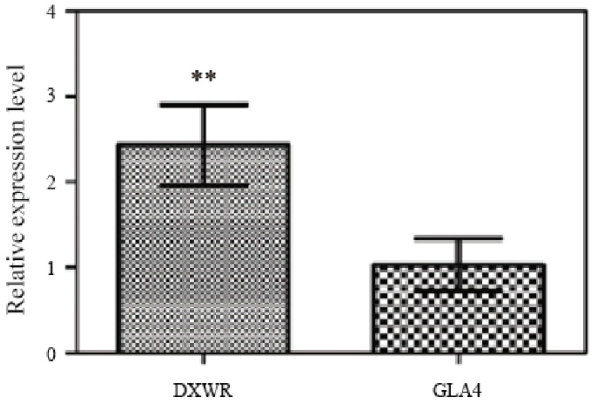

Figure 5. Expression analysis of *GL7* in young panicles of Dongxiang wild rice (DXWR) and Guangluai 4 (GLA4) by qRT-PCR; the rice's *Ubiquitin* gene was used as an internal control. Data indicate means ± SD. (n = 3 biological replicates). ** indicates a significant difference between DXWR and GLA4 at the 0.01 levels, according to the t-test. DXWR, Dongxiang wild rice; GLA4, Guangluai 4.

We performed a haplotype network analysis of the *GL7* gene promoter region and the 5′ UTR region according to the RiceVarMap V2.0 website (http://ricevarmap.ncpgr.cn/v2/), accessed on 15 October 2020 [55,56]. The results showed that NPB is type I, P13 is type II, DXWR is closest to type III, and GLA4 is closer to type IV (Figure 6). There are 1047 rice varieties in type I, and these include mainly temperate Japonica rice (547 haplotypes), some IndI (164 haplotypes), and AUS rice (106 haplotypes), as well as several other rice subspecies. Type II rice had 1010 haplotypes, including P13, tropical Japonica rice (471 haplotypes), and mixed Japonica (214 haplotypes). Type III had 1964 haplotypes and contained 882 IndIII Indica haplotypes, 353 IndII Indica haplotypes, and 443 mixed Indica haplotypes. Type IV rice contained 673 haplotypes and was dominated by IndI rice with 393 haplotypes and mixed indica with 216 haplotypes. As seen above, the promoter region and the 5′ UTR region of the *GL7* gene are evolutionarily distinct, and different SNP haplotypes were derived from each of the Japonica and Indica rice species and are closely related to each rice subtype. The NPB and P13 belong to different haplotypes, and the *GL7* genes of both have significantly different regulatory roles in grain length. DXWR and GLA4 also belong to different haplotypes, and their *GL7* genes may also have similar differences leading to changes in the PL, and this type of difference may be widespread in indica rice with different typing. In conclusion, the *LOC_Os07g41200* gene in DXWR can be tentatively identified as the candidate gene for *qPL7-25* and is a new *GL7* allele.

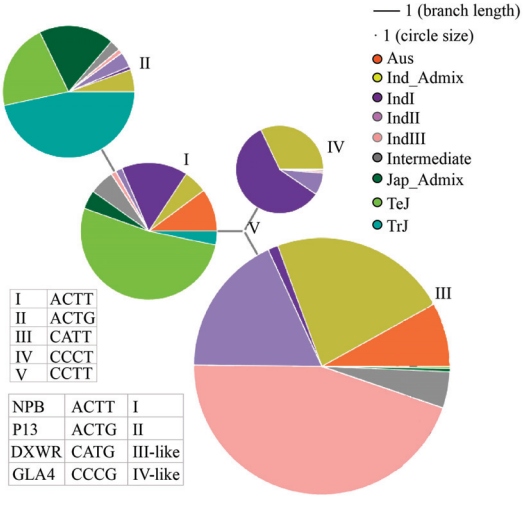

Figure 6. Haplotype network analysis results using the single-nucleotide polymorphisms from the promoter and 5′ untranslated region of the *GL7* gene.

4. Discussion

PL is an important trait related to rice yield, and breeding long and large panicle rice varieties is an effective method to achieve higher yields. Therefore, the study of the PL QTL has important and far-reaching implications for improving rice yield and quality. The QTL of PL are controlled by multiple genes and influenced by environmental factors, which are difficult to map in individual plants [57]. Although a number of QTL affecting the rice PL have been localized by previous studies, few of them have been cloned, especially those located on chromosome 7. *qPL6*, *LP1*, *qPL7*, and *qpl9* are some finely mapped QTL directly related to PL [30,58,59]. In this study, *qPL7-25* was localized on chromosome 7 between InDel-24591 and InDel-24710 in a 119 kb interval (Figure 4A), which did not overlap with the previously reported QTL/gene position of PL. Therefore, *qPL7-25* should be considered as a new PL QTL and as an enhanced allele from the DXWR parents. Previous studies have shown that the change in PL can be accompanied by a change in other panicle traits. Loss

of function of *SP1*, *SP3*, and *DEP3* not only shortened the PL but also reduced the number of branches and SPP [26,35,38]. *DEP1*, *OsAPC6*, and *PT2* mutations result in reduced PL and grain size [21,25,60]. In our study, *qPBN7-25*, a QTL for PBN, was mapped to the same interval as *qPL7-25* on chromosome 7, and both were potential alleles of the QTL from DXWR (Figure 3). Phenotypic analysis showed that both NIL-*qPL7-25* and NIL-Huazhan-$GL7^{P13}$ had more PBN than their parents (Tables S3 and S4). Our results were consistent with previous reports, and we propose that these two QTL were single-causal multiple effects of the same QTL/gene. Compared with other common wild and cultivated rice, DXWR has more abundant rare allelic variants (including SNPs and InDels), but many QTLs coexist with unfavorable genes and are masked. Gene editing technology can be used to quickly and efficiently break the tight linkage between favorable and unfavorable genes [61], thus enabling better and faster use of the favorable genes from DXWR.

There were 14 candidate genes in the fine mapping interval of *qPL7-25* (Figure 4B, Table S2); *LOC_Os07g41200* is a well-known cloned gene of *GL7*, which controls the grain length. Previous studies have shown that overexpression of *GL7* in NPB and ZF802 (Zhefu802) backgrounds, and *SLG7* in the NPB background, can increase the grain length and length/width ratio, and upregulation of *GL7/GW7/SLG7* expression increases the cell length and decreases the cell width for epidermal cells of the outer and inner glumes [45–47]. We hypothesized that this cell division pattern is consistent with panicle elongation in the direction that leads to increased PL, and thus increased *GL7* expression promotes increased PL. NIL-*SLG7* showed a higher level of expression in the panicle and produced longer panicles (+14.2%) compared to NIL-*slg7* [47], confirming our hypothesis. In addition, there were 14 bp and 36 bp deletions in the promoter of *slg7* mutants constructed using CRISPR/Cas9, which resulted in an increased expression level of *SLG7* and produced more slender grains compared with WYJ30 [62]. Sequence alignment analysis showed that there was also an 11 bp deletion in the *GL7* promoter of DXWR compared with GLA4, and the expression level of *GL7* was 2.4-fold higher in DXWR than in GLA4 performed by qRT-PCR analysis (Figure S4 and Figure 5). Unfortunately, we subsequently lost the seeds of NIL-*qPL7-25* due to improper storage, so we could not provide data on the expression level of the *GL7* gene in the young panicles of NIL-*qPL7-25*. However, another experiment provided strong support for our analysis: when we transferred *GL7* from P13 (a long grain, long panicle, *GL7* high expressing variety) to the relatively short panicle, short-grained Huazhan variety by backcrossing using MAS, the NIL-Huazhan-$GL7^{P13}$ showed a significant increase in the PL, grain length, and grain length/width ratio, as well as a significant increase in the PBN compared to the Huazhan parent (Table S3). This showed a consistent trend with the comparison between the phenotypes of NIL-*qPL7-25* and GLA4 (Table S4). Our results were consistent with the previous studies. In addition, DXWR and GLA4 belong to different haplotypes in the promoter and 5′ UTR regions of the *GL7* gene (Figure 6). In view of the above, we propose that *qPL7-25* is a new allele of *GL7* with a greater breeding utilization value in improving rice quality rather than increasing rice yield. We are currently introducing *GL7* into the promoted varieties to simultaneously improve the yield and quality of existing varieties through gene polymerization breeding.

In addition, the parents and RIL populations in this study were re-sequenced when the QTL was first located. Although the cost was high, a large amount of SNP and InDel information was obtained. Combined with the biological information analysis, it provides convenience for our subsequent future research and provides a good experimental basis for the further fine mapping or cloning of QTL genes on other chromosomes.

5. Conclusions

In this study, four PL QTL (*qPL1-37*, *qPL4-26*, *qPL7-25*, and *qPL8-4*) were detected using an RIL population consisting of 143 individuals derived from a cross between DXWR and GLA4. Among these, *qPL7-25* showed great potential to increase the PL, which was further localized to a 119 kb region on chromosome 7 by a map-based cloning strategy using 1800 individuals derived from a cross between NIL-*qPL7-25* and GLA4. Sequence

alignment and qRT-PCR analysis suggested that *qPL7-25* was probably a new allele of *GL7*, a major QTL regulating grain length. The introduction of *qPL7-25* into the population varieties will help to improve the yield and quality of the existing varieties.

Supplementary Materials: The following supporting information can be downloaded at: https://www.mdpi.com/article/10.3390/agriculture13081623/s1, Figure S1: The morphology and grain size comparisons of mature grains from GLA4 and DXWR; Figure S2: Construction of NIL and linkage map of *qPL7-25* on chromosome 7 in the NIL; Figure S3: Expression patterns of candidate genes; Figure S4: Sequence alignment of promoter region and 5′ UTR region of *GL7* gene; Table S1: InDel primers used in fine mapping of *qPL7-25*; Table S2: Predicted ORF on RGAP; Table S3: Data collection of main agronomic traits of Huazhan and NIL-Huazhan-$GL7^{P13}$ in Hangzhou.; Table S4: Data collection of main agronomic traits of GLA4 and NIL-*qPL7-25* in Hangzhou.

Author Contributions: Conceptualization, Y.M. and Y.W.; methodology, S.L., Z.W., P.H. and R.Y.; software, P.D. and Z.W.; validation, S.L. and Z.W.; formal analysis, C.L. (Chenxi Luo) and S.L.; investigation, M.T. and C.L. (Caolin Lu); resources, Y.M.; data curation, Y.M., S.L. and Y.R.; writing—original draft preparation, S.L., Y.R. and P.D.; writing—review and editing, S.L., Y.R., P.D. and Y.W.; supervision, Y.M. and Y.W. All authors have read and agreed to the published version of the manuscript.

Funding: This research was funded by the Natural Science Foundation of Zhejiang Province (Grant No. LQ21C130004), the Zhejiang Provincial Natural Science Outstanding Youth Fund (Grant No. LR20C130001), Hainan Yazhou Bay Seed Lab (Grant No. B21HJ0219), and the Central Public-interest Scientific Institution Basal Research Fund (Grant No. CPSIBRF-CNRRI-202109).

Institutional Review Board Statement: Not applicable.

Data Availability Statement: The datasets presented in this study can be found in the article and Supplementary Materials.

Conflicts of Interest: The authors declare no conflict of interest.

References

1. Cho, Y.G.; Kang, H.J.; Lee, J.S.; Lee, Y.T.; Mccouch, S.R. Identification of quantitative trait loci in rice for yield, yield components, and agronomic traits across years and locations. *Crop Sci.* **2007**, *47*, 2403–2417. [CrossRef]
2. Marathi, B.; Guleria, S.; Mohapatra, T.; Parsad, R.; Mariappan, N.; Kurungara, V.; Atwal, S.; Prabhu, K.; Singh, N.; Singh, A. QTL analysis of novel genomic regions associated with yield and yield related traits in new plant type based recombinant inbred lines of rice (*Oryza sativa* L.). *BMC Plant Biol.* **2012**, *12*, 137. [CrossRef] [PubMed]
3. Moncada, P.; Martinez, C.P.; Borrero, J.; Chatel, M.; Gauch, H.; Guimaraes, E.; Tohme, J.; McCouch, S.R. Quantitative trait loci for yield and yield components in an *Oryza sativa* × *Oryza rufipogon* BC2F2 population evaluated in an upland environment. *Theor. Appl. Genet.* **2001**, *102*, 41–52. [CrossRef]
4. Septiningsih, E.M.; Prasetiyono, J.; Lubis, E.; Tai, T.H.; Tjubaryat, T.; Moeljopawiro, S.; McCouch, S.R. Identification of quantitative trait loci for yield and yield components in an advanced backcross population derived from the *Oryza sativa* variety IR64 and the wild relative *O. rufipogon*. *Theor. Appl. Genet.* **2003**, *107*, 1419–1432. [CrossRef]
5. Septiningsih, E.M.; Trijatmiko, K.R.; Moeljopawiro, S.; McCouch, S.R. Identification of quantitative trait loci for grain quality in an advanced backcross population derived from the *Oryza sativa* variety IR64 and the wild relative *O. rufipogon*. *Theor. Appl. Genet.* **2003**, *107*, 1433–1441. [CrossRef]
6. Thomson, M.J.; Tai, T.H.; McClung, A.M.; Lai, X.H.; Hinga, M.E.; Lobos, K.B.; Xu, Y.; Martinez, C.P.; McCouch, S.R. Mapping quantitative trait loci for yield, yield components and morphological traits in an advanced backcross population between *Oryza rufipogon* and the *Oryza sativa* cultivar Jefferson. *Theor. Appl. Genet.* **2003**, *107*, 479–493. [CrossRef]
7. Nguyen, B.D.; Brar, D.S.; Bui, B.C.; Nguyen, T.V.; Pham, L.N.; Nguyen, H.T. Identification and mapping of the QTL for aluminum tolerance introgressed from the new source, *Oryza rufipogon* Griff., into indica rice (*Oryza sativa* L.). *Theor. Appl. Genet.* **2003**, *106*, 583–593. [CrossRef]
8. Marri, P.R.; Sarla, N.; Reddy, L.V.; Siddiq, E.A. Identification and mapping of yield and yield related QTHN from an Indian accession of *Oryza rufipogon*. *BMC Genet.* **2005**, *6*, 33–46. [CrossRef]
9. Sweeney, M.; McCouch, S. The complex history of the domestication of rice. *Ann. Bot.* **2007**, *100*, 951–957. [CrossRef]
10. Koseki, M.; Kitazawa, N.; Yonebayashi, S.; Maehara, Y.; Wang, Z.X.; Minobe, Y. Identification and fine mapping of a major quantitative trait locus originating from wild rice, controlling cold tolerance at the seedling stage. *Mol. Genet. Genom.* **2010**, *284*, 45–54. [CrossRef]
11. Dong, X.X.; Wang, X.Y.; Zhang, L.S.; Yang, Z.T.; Xin, X.Y.; Wu, S.; Sun, C.Q.; Liu, J.X.; Yang, J.S.; Luo, X.J. Identification and characterization of *OsEBS*, a gene involved in enhanced plant biomass and spikelet number in rice. *Plant Biotechnol. J.* **2013**, *11*, 1044–1057. [CrossRef] [PubMed]

12. Mao, D.; Yu, L.; Chen, D.; Li, L.; Zhu, Y.; Xiao, Y.; Zhang, D.; Chen, C. Multiple cold resistance loci confer the high cold tolerance adaptation of Dongxiang wild rice (*Oryza rufipogon*) to its high-latitude habitat. *Theor. Appl. Genet.* **2015**, *128*, 1359–1371. [CrossRef]
13. Zhang, X.; Zhou, S.; Fu, Y.; Su, Z.; Wang, X.; Sun, C. Identification of a drought tolerant introgression line derived from Dongxiang common wild rice (*O. rufipogon* Griff.). *Plant Mol. Biol.* **2006**, *62*, 247–259. [CrossRef] [PubMed]
14. Xie, H.W.; Peng, X.J.; Qian, M.J.; Cai, Y.C.; Ding, X.; Chen, Q.S.; Cai, Q.Y.; Zhu, Y.L.; Yan, L.G.; Cai, Y.H. The chimeric mitochondrial gene *orf182* causes non-pollen-type abortion in Dongxiang cytoplasmic male-sterile rice. *Plant J.* **2018**, *95*, 715–726. [CrossRef] [PubMed]
15. Yadav, S.K.; Pandey, P.; Kumar, B.; Suresh, B.G. Genetic architecture, inter-relationship and selection criteria for yield improvement in rice (*Oryza sativa* L.). *Pak. J. Biol. Sci.* **2011**, *14*, 540–545. [CrossRef]
16. Miura, K.; Ashikari, M.; Matsuoka, M. The role of QTLs in the breeding of high-yielding rice. *Trends Plant Sci.* **2011**, *16*, 319–326. [CrossRef]
17. Bai, X.F.; Wu, B.; Xing, Y.Z. Yield-related QTLs and their applications in rice genetic improvement. *J. Integr. Plant Biol.* **2012**, *54*, 300–311. [CrossRef]
18. Khahani, B.; Tavakol, E.; Shariati, V.; Rossini, L. Meta-QTL and ortho-MQTL analyses identifed genomic regions controlling rice yield, yield-related traits and root architecture under water defcit conditions. *Sci. Rep.* **2021**, *11*, 6942. [CrossRef]
19. Zhu, Y.Y.; Nomura, T.; Xu, Y.H.; Zhang, Y.Y.; Peng, Y.; Mao, B.Z.; Hanada, A.; Zhou, H.C.; Wang, R.X.; Li, P.J.; et al. *ELONGATED UPPERMOST INTERNODE* encodes a cytochrome P450 monooxygenase that epoxidizes gibberellins in a novel deactivation reaction in rice. *Plant Cell* **2006**, *18*, 442–456. [CrossRef]
20. Kurakawa, T.; Ueda, N.; Maekawa, M.; Kobayashi, K.; Kojima, M.; Nagato, Y.; Sakakibara, H.; Kyozuka, J. Direct control of shoot meristem activity by a cytokinin-activating enzyme. *Nature* **2007**, *445*, 652–655. [CrossRef]
21. Huang, X.Z.; Qian, Q.; Liu, Z.B.; Sun, H.Y.; He, S.Y.; Luo, D.; Xia, G.M.; Chu, C.C.; Li, J.Y.; Fu, X.D. Natural variation at the *DEP1* locus enhances grain yield in rice. *Nat. Genet.* **2009**, *41*, 494–497. [CrossRef] [PubMed]
22. Li, M.; Tang, D.; Wang, K.J.; Wu, X.R.; Lu, L.L.; Yu, H.X.; Gu, M.H.; Yan, C.J.; Cheng, Z.K. Mutations in the F-box gene *LARGER PANICLE* improve the panicle architecture and enhance the grain yield in rice. *Plant Biotechnol. J.* **2011**, *9*, 1002–1013. [CrossRef] [PubMed]
23. Lu, G.W.; Coneva, V.; Casaretto, J.A.; Ying, S.; Mahmood, K.; Liu, F.; Nambara, E.; Bi, Y.M.; Rothstein, S.J. *OsPIN5b* modulates rice (*Oryza sativa*) plant architecture and yield by changing auxin homeostasis, transport and distribution. *Plant J.* **2015**, *83*, 913–925. [CrossRef] [PubMed]
24. Gao, S.P.; Fang, J.; Xu, F.; Wang, W.; Chu, C.C. Rice HOX12 regulates panicle exsertion by directly modulating the expression of *ELONGATED UPPERMOST INTERNODE1*. *Plant Cell* **2016**, *28*, 680–695. [CrossRef]
25. Sun, P.Y.; Zhang, W.H.; Wang, Y.H.; He, Q.; Shu, F.; Liu, H.; Wang, J.; Wang, J.M.; Yuan, L.P.; Deng, H.F. *OsGRF4* controls grain shape, panicle length and seed shattering in rice. *J. Integr. Plant Biol.* **2016**, *58*, 836–847. [CrossRef]
26. Huang, Y.; Bai, Y.F.; Luo, M.F.; Ying, Y.Z. *Short Panicle 3* controls panicle architecture by upregulating *APO2/RFL* and increasing cytokinin content in rice. *J. Integr. Plant Biol.* **2019**, *61*, 987–999. [CrossRef]
27. Su, S.; Hong, J.; Chen, X.; Zhang, C.; Chen, M.; Luo, Z.; Chang, S.; Bai, S.; Liang, W.; Liu, Q.; et al. Gibberellins orchestrate panicle architecture mediated by DELLA-KNOX signalling in rice. *Plant Biotechnol. J.* **2021**, *19*, 2304–2318. [CrossRef]
28. Xue, W.Y.; Xing, Y.Z.; Weng, X.Y.; Zhao, Y.; Tang, W.J.; Wang, L.; Zhou, H.J.; Yu, S.B.; Xu, C.G.; Li, X.H.; et al. Natural variation in *Ghd7* is an important regulator of heading date and yield potential in rice. *Nat. Genet.* **2008**, *40*, 761–767. [CrossRef]
29. Yan, W.H.; Wang, P.; Chen, H.X.; Zhou, H.J.; Li, Q.P.; Wang, C.R.; Ding, Z.H.; Zhang, Y.S.; Yu, S.B.; Xing, Y.Z.; et al. A Major QTL, *Ghd8*, plays pleiotropic roles in regulating grain productivity, plant height, and heading date in rice. *Mol. Plant* **2011**, *4*, 319–330. [CrossRef]
30. Li, J.; Xu, R.; Wang, C.C.; Qi, L.; Zheng, X.M.; Wang, W.S.; Ding, Y.B.; Zhang, L.Z.; Wang, Y.Y.; Cheng, Y.L.; et al. A heading date QTL, *qHD7.2*, from wild rice (*Oryza rufipogon*) delays flowering and shortens panicle length under long-day conditions. *Sci. Rep.* **2018**, *8*, 2928.
31. Ikeda, K.; Ito, M.; Nagasawa, N.; Kyozuka, J.; Nagato, Y. Rice *ABERRANT PANICLE ORGANIZATION 1*, encoding an F-box protein, regulates meristem fate. *Plant J.* **2007**, *51*, 1030–1040. [CrossRef] [PubMed]
32. Ookawa, T.; Hobo, T.; Yano, M.; Murata, K.; Ando, T.; Miura, H.; Asano, K.; Ochiai, Y.; Ikeda, M.; Nishitani, R.; et al. New approach for rice improvement using a pleiotropic QTL gene for lodging resistance and yield. *Nat. Commun.* **2010**, *1*, 132. [CrossRef] [PubMed]
33. Terao, T.; Nagata, K.; Morino, K.; Hirose, T. A gene controlling the number of primary rachis branches also controls the vascular bundle formation and hence is responsible to increase the harvest index and grain yield in rice. *Theor. Appl. Genet.* **2010**, *120*, 875–893. [CrossRef] [PubMed]
34. Luan, W.J.; Liu, Y.Q.; Zhang, F.X.; Song, Y.L.; Wang, Z.Y.; Peng, Y.K.; Sun, Z.X. *OsCD1* encodes a putative member of the cellulose synthase-like D sub-family and is essential for rice plant architecture and growth. *Plant Biotech. J.* **2011**, *9*, 513–524. [CrossRef] [PubMed]
35. Qiao, Y.L.; Piao, R.H.; Shi, J.X.; Lee, S.I.; Jiang, W.Z.; Kim, B.K.; Lee, J.; Han, L.Z.; Ma, W.B.; Koh, H.J. Fine mapping and candidate gene analysis of *dense and erect panicle 3*, *DEP3*, which confers high grain yield in rice (*Oryza sativa* L.). *Theor. Appl. Genet.* **2011**, *122*, 1439–1449. [CrossRef]

36. Ma, X.F.; Cheng, Z.J.; Qin, R.Z.; Qiu, Y.; Heng, Y.Q.; Yang, H.; Ren, Y.L.; Wang, X.L.; Bi, J.C.; Ma, X.D.; et al. *OsARG* encodes an arginase that plays critical roles in panicle development and grain production in rice. *Plant J.* **2013**, *73*, 190–200. [CrossRef]
37. Huang, L.J.; Hua, K.; Xu, R.; Zeng, D.L.; Wang, R.C.; Dong, G.J.; Zhang, G.Z.; Lu, X.L.; Fang, N.; Wang, D.K.; et al. The LARGE2-APO1/APO2 regulatory module controls panicle size and grain number in rice. *Plant Cell* **2021**, *33*, 1212–1228. [CrossRef]
38. Li, S.B.; Qian, Q.; Fu, Z.M.; Zeng, D.L.; Meng, X.B.; Kyozuka, J.; Maekawa, M.; Zhu, X.D.; Zhang, J.; Li, J.Y.; et al. *Short panicle1* encodes a putative PTR family transporter and determines rice panicle size. *Plant J.* **2009**, *58*, 592–605. [CrossRef]
39. Miura, K.; Ikeda, M.A.; Matsubara, A.; Song, X.J.; Ito, M.; Asano, K.; Matsuoka, M.; Kitano, H.; Ashikari, M. OsSPL14 promotes panicle branching and higher grain productivity in rice. *Nat. Genet.* **2010**, *42*, 545–549. [CrossRef]
40. Li, F.; Liu, W.B.; Tang, J.Y.; Chen, J.F.; Tong, H.N.; Hu, B.; Li, C.L.; Fang, J.; Chen, M.S.; Chu, C.C. Rice DENSE AND ERECT PANICLE 2 is essential for determining panicle outgrowth and elongation. *Cell Res.* **2010**, *20*, 838–849. [CrossRef]
41. Nakagawa, H.; Tanaka, A.; Tanabata, T.; Ohtake, M.; Fujioka, S.; Nakamura, H.; Ichikawa, H.; Mori, M. *SHORT GRAIN1* decreases organ elongation and brassinosteroid response in rice. *Plant Physiol.* **2012**, *158*, 1208–1219. [CrossRef] [PubMed]
42. Yoshida, A.; Ohmori, Y.; Kitano, H.; Taguchi-Shiobara, F.; Hirano, H.Y. *Aberrant spikelet and panicle1*, encoding a TOPLESS-related transcriptional co-repressor, is involved in the regulation of meristem fate in rice. *Plant J.* **2012**, *70*, 327–339. [CrossRef] [PubMed]
43. Yoshida, A.; Sasao, M.; Yasuno, N.; Takagi, K.; Daimon, Y.; Chen, R.H.; Yamazaki, R.; Tokunaga, H.; Kitaguchi, Y.; Sato, Y.; et al. *TAWAWA1*, a regulator of rice inflorescence architecture, functions through the suppression of meristem phase transition. *Proc. Natl. Acad. Sci. USA* **2013**, *110*, 767–772. [CrossRef] [PubMed]
44. Léran, S.; Varala, K.; Boyer, J.C.; Chiurazzi, M.; Crawford, N.; Daniel-Vedele, F.; David, L.; Dickstein, R.; Fernandez, E.; Forde, B.; et al. A unified nomenclature of NITRATE TRANSPORTER 1/PEPTIDE TRANSPORTER family members in plants. *Trends Plant Sci.* **2014**, *19*, 5–9. [CrossRef] [PubMed]
45. Wang, Y.X.; Xiong, G.S.; Hu, J.; Jiang, L.; Yu, H.; Xu, J.; Fang, Y.X.; Zeng, L.J.; Xu, E.B.; Xu, J.; et al. Copy number variation at the *GL7* locus contributes to grain size diversity in rice. *Nat. Genet.* **2015**, *47*, 944–948. [CrossRef]
46. Wang, S.K.; Li, S.; Liu, Q.; Wu, K.; Zhang, J.Q.; Wang, S.S.; Wang, Y.; Chen, X.B.; Zhang, Y.; Gao, C.X.; et al. The *OsSPL16-GW7* regulatory module determines grain shape and simultaneously improves rice yield and grain quality. *Nat. Genet.* **2015**, *47*, 949–954. [CrossRef]
47. Zhou, Y.; Miao, J.; Gu, H.Y.; Peng, X.R.; Leburu, M.; Yuan, F.H.; Gu, H.W.; Gao, Y.; Tao, Y.J.; Zhu, J.Y.; et al. Natural variations in *SLG7* regulate grain shape in rice. *Genetics* **2015**, *201*, 1591–1599. [CrossRef]
48. Ikeda-Kawakatsu, K.; Maekawa, M.; Izawa, T.; Itoh, J.I.; Nagato, Y. *ABERRANT PANICLE ORGANIZATION 2/RFL*, the rice ortholog of Arabidopsis LEAFY, suppresses the transition from inflorescence meristem to floral meristem through interaction with APO1. *Plant J.* **2015**, *69*, 168–180. [CrossRef]
49. Ikeda-Kawakatsu, K.; Yasuno, N.; Oikawa, T.; Iida, S.; Nagato, Y.; Maekawa, M.; Kyozuka, J. Expression level of *ABERRANT PANICLE ORGANIZATION1* determines rice inflorescence form through control of cell proliferation in the meristem. *Plant Physiol.* **2009**, *150*, 736–747. [CrossRef]
50. Sun, X.W.; Liu, D.Y.; Zhang, X.F.; Li, W.B.; Liu, H.; Hong, W.G.; Jiang, C.B.; Guan, N.; Ma, C.X.; Zeng, H.P.; et al. SLAF-seq: An efficient method of large-scale de novo SNP discovery and genotyping using high-throughput sequencing. *PLoS ONE* **2013**, *8*, e58700. [CrossRef]
51. Vision, T.J.; Brown, D.G.; Shmoys, D.B.; Durrett, R.T.; Tanksley, S.D. Selective mapping: A strategy for optimizing the construction of high-density linkage maps. *Genetics* **2000**, *155*, 407–420. [CrossRef]
52. McCouch, S.R.; Cho, Y.G.; Yano, M.; Paul, E.; Blinstrub, M.; Morishima, H.; Kinoshita, T. Suggestions for QTL nomenclature for rice, Rice Genet. *News* **1997**, *14*, 11–13.
53. Yang, J.; Zhu, J. Methods for predicting superior genotypes under multiple environments based on QTL effects. *Theor. Appl. Genet.* **2005**, *110*, 1268–1274. [CrossRef] [PubMed]
54. Livak, K.J.; Schmittgen, T.D. Analysis of relative gene expression data using real-time quantitative PCR and the $2^{-\Delta\Delta CT}$ method. *Methods* **2001**, *25*, 402–408. [CrossRef] [PubMed]
55. Zhao, H.; Yao, W.; Ouyang, Y.D.; Yang, W.N.; Wang, G.W.; Lian, X.M.; Xing, Y.Z.; Chen, L.L.; Xie, W.B. RiceVarMap: A comprehensive database of rice genomic variations. *Nucleic Acids Res.* **2015**, *43*, 1018–1022. [CrossRef] [PubMed]
56. Zhao, H.; Li, J.C.; Yang, L.; Qin, G.; Xia, C.J.; Xu, X.B.; Su, Y.M.; Liu, Y.M.; Ming, L.C.; Chen, L.L.; et al. An inferred functional impact map of genetic variants in rice. *Mol. Plant.* **2021**, *14*, 1584–1599. [CrossRef]
57. Adriani, D.E.; Dingkuhn, M.; Dardou, A.; Adam, H.; Luquet, D.; Lafarge, T. Rice panicle plasticity in near isogenic lines carrying a QTL for larger panicle is genotype and environment dependent. *Rice* **2016**, *9*, 28. [CrossRef]
58. Zhang, L.; Wang, J.J.; Wang, J.M.; Wang, L.Y.; He, Z.H. Quantitative trait locus analysis and fine mapping of the *qPL6* locus for panicle length in rice. *Theor. Appl. Genet.* **2015**, *128*, 1151–1161. [CrossRef]
59. Liu, E.B.; Liu, Y.; Wu, G.C.; Zeng, S.Y.; Thi, T.; Liang, L.J.; Liang, Y.F.; Dong, Z.Y.; She, D.; Wang, H.; et al. Identification of a candidate gene for panicle length in rice (*Oryza sativa* L.) via association and linkage analysis. *Front. Plant Sci.* **2016**, *7*, 596. [CrossRef]
60. Kumar, M.; Basha, P.O.; Puri, A.; Rajpurohit, D.; Randhawa, G.S.; Sharma, T.R.; Dhaliwal, H.S. A candidate gene *OsAPC6* of anaphase-promoting complex of rice identified through T-DNA insertion. *Funct. Integr. Genom.* **2010**, *10*, 349–358. [CrossRef]

61. Li, S.F.; Shen, L.; Hu, P.; Wu, X.M.; Yuan, Q.L.; Rao, Y.C.; Qian, Q.; Wang, K.J.; Zhu, X.D.; Shang, L.G.; et al. A method for effectively overcoming tight functional linkage between genes in rice by CRISPR/Cas9 system. *Rice Sci.* **2020**, *27*, 180–183.
62. Tan, W.C.; Miao, J.; Xu, B.; Zhou, C.T.; Wang, Y.R.; Gu, X.Q.; Liang, S.N.; Wang, B.X.; Chen, C.; Zhu, J.Y.; et al. Rapid production of novel beneficial alleles for improving rice appearance quality by targeting a regulatory element of *SLG7*. *Plant Biotechnol. J.* **2023**, *21*, 1305–1307. [CrossRef] [PubMed]

agriculture

MDPI

Article

QTL-Seq Approach Identified *Pi63* Conferring Blast Resistance at the Seedling and Tillering Stages of Thai Indigenous Rice Variety "Phaladum"

Chaiwat Netpakdee [1,2], Sittiwut Mathasiripakorn [1], Arthit Sribunrueang [1], Sompong Chankaew [1,2], Tidarat Monkham [1], Siwaret Arikit [3] and Jirawat Sanitchon [1,*]

[1] Department of Agronomy, Faculty of Agriculture, Khon Kaen University, Khon Kaen 40002, Thailand
[2] Center of Excellence on Agricultural Biotechnology: (AG-BIO/MHESI), Bangkok 10900, Thailand
[3] Department of Agronomy, Faculty of Agriculture at Kamphaeng Saen, Kasetsart University, Kamphaeng Saen, Nakhon Pathom 73140, Thailand
* Correspondence: jirawat@kku.ac.th; Tel.: +66-81567-4364

Abstract: Rice blast (BL) caused by *Magnaporthe oryzae* is a fungal disease causing significant yield losses in rice production worldwide. To overcome the breakdown of resistance by the rapid adaptation of pathogens, identifying resistance (*R*) genes or QTLs in indigenous rice, which harbors the *R* genes that co-evolved with the local pathogen race, is necessary. In this study, a recombinant inbred line (RIL) population derived from a cross between RD6 and Phaladum (PLD) was used to map quantitative trait loci (QTL) for BL resistance through a QTL-seq approach. A single QTL (*qBLchr4*) associated with BL resistance at the seedling and maximum tillering stages was mapped on the long arm of chromosome 4. Five genes, *LOC_Os04g0616600, LOC_Os04g0617900 (OsGLP4-1), LOC_Os04g0619600 (OsRLCK161), LOC_Os04g0620800 (Pi63),* and *LOC_Os04g0621500*, were considered the candidate genes representing *qBLchr4*. Subsequently, the Kompetitive Allele-Specific PCR (KASP) markers specific for the SNP variant and position of each gene were designed for validation in the mapping population. These markers showed the high phenotypic variance explained (PVE) values in all testing methods and/or environments, signifying the major effect of *qBLchr4*. Among these markers, the *Pi63*-KASP marker explained the highest and most stable phenotypic variation across all testing methods and/or environments, with 84.18%, 80.34%, and 23.43% in the upland short row (USR) method, Sila environment, and Mueang environment, respectively. Therefore, *Pi63* was suggested to be the strongest candidate gene. These results represent the potential utility of future BL resistance breeding and/or pyramiding using marker-assisted selection (MAS).

Keywords: multiple-stage resistance; rice germplasm; rapid generation advance; upland short row; SNP index

Citation: Netpakdee, C.; Mathasiripakorn, S.; Sribunrueang, A.; Chankaew, S.; Monkham, T.; Arikit, S.; Sanitchon, J. QTL-Seq Approach Identified *Pi63* Conferring Blast Resistance at the Seedling and Tillering Stages of Thai Indigenous Rice Variety "Phaladum". *Agriculture* **2022**, *12*, 1166. https://doi.org/10.3390/agriculture12081166

Academic Editors: Edyta Paczos-Grzeda, Volker Mohler and Sylwia Sowa

Received: 25 June 2022
Accepted: 3 August 2022
Published: 5 August 2022

1. Introduction

Rice blast (BL) caused by *Magnaporthe oryzae* (*M. oryzae*) is a major and devastating disease in rice production throughout the world [1], in which outbreaks can result in decreasing rice grain yields by up to 10–35% [2]. For the sake of controlling this disease, the application of resistant varieties is regarded as the most effective and economical strategy [3]. However, cultivation of a resistant variety carrying a single resistance (*R*) gene for short periods often leads to resistance breakdown, as a consequence of pathogen adaptation [4]. To mitigate the breakdown of resistance, integrating multiple *R* genes (each with a different function) through a marker-assisted method is deployed for long-lasting and broad-spectrum resistance [5–8]. Therefore, there is an imperative need to explore new *R* genes to broaden the availability of a resistance source in rice breeding.

To date, approximately 100 BL *R* genes conferring resistance to *M. oryzae* have been identified [9]. The BL *R* genes are distributed across almost all rice chromosomes, except

chromosome 3 [10]. Most of the BL *R* genes reported have been identified in exotic rice cultivars and wild species of rice [10], which may not prove effective when exploited in rice breeding programs in Thailand, as a result of the race specificity of the *R* genes. On the other hand, the utilization of the *R* genes from Thai indigenous rice that co-evolved with local pathogen races [11] could offer an effective tool for rice breeding in Thailand. It is worth noting that among the identified *R* genes, several BL *R* genes have been discovered in indigenous rice varieties, such as *Pi-67* [12], *Pi54* [13], *Pigm* [14], *Pi-jnw1* [15], *Pi-d(t)1* [16], and *Pid(t)2* [16]. These *R* genes identified in indigenous rice have provided potential genetic resources in rice improvement for BL resistance. A good example of the utilization of such resistance resources is the Chinese indigenous rice Gumei 4 carrying the *Pigm* gene, which exhibited broad-spectrum resistance to *M. oryzae* and has been used as a BL resistance donor in rice improvement for the past five decades [14]. Although numerous *R* genes have been identified, many unexplored genes remain. Recently, a large number of indigenous rice varieties have been identified for disease resistance. Khannetah et al. [17] identified 4 and 34 Indian indigenous rice accessions as 'resistant' and 'moderately resistant' to bacterial blight (BB) disease, respectively. In Thailand, ten Thai indigenous lowland rice germplasms were also reported to confer resistance to BB, in which five of ten were identified as BB-resistant and showed some favorable agronomic traits [18]. Similarly, Chumpol et al. [19] identified ten Thai indigenous upland rice varieties as resistant to leaf blast, six of which were found to be resistant to both leaf blast and neck blast. Notably, in a previous study, we found that the Thai indica indigenous lowland rice variety Phaladum (PLD), collected from the Yasothon province in Northeastern Thailand, exhibited a high level of BL (both leaf blast and neck blast) and BB resistance, and possessed several superior agronomic traits. These results indicated that some resistant indigenous rice may contain the unidentified *R* gene. Thus, the identification of unexplored genes or QTLs conferring BL resistance in indigenous rice is necessary for their meaningful utilization in future resistant rice breeding programs.

For the rapid identification of genes or QTLs, a QTL-seq approach was developed by combining bulked-segregant analysis (BSA) and whole-genome resequencing of two DNA bulks of progeny showing contrasting phenotypes to identify genomic regions associated with focal traits, without marker developing and genotyping [20]. With these advantages, QTL-seq analysis successfully identified the genes or QTLs associated with several traits in rice [21–28], including blast disease [20]. In the present study, we employed the QTL-seq approach to identify the QTL for BL resistance in the recombinant inbred line (F_6 RIL) population derived from a cross between a BL-susceptible variety, RD6, and the BL-resistance indigenous variety PLD. The QTLs, as well as candidate genes for BL resistance, obtained in this study could provide a valuable tool for the molecular breeding of disease resistance in rice.

2. Materials and Methods

2.1. Development of Mapping Population

Two parental varieties/accessions, RD6 and Phaladum (PLD), were used to generate the F_6 RIL population. RD6, the most favorable glutinous variety in Thailand, is both blast- and bacterial-blight-susceptible. PLD is a blast- and bacterial-blight-resistant variety that was obtained from the Rice Project, Khon Kaen University, Khon Kaen, Thailand. A single F_1 seed from an RD6/PLD cross was selfed to generate F_2 seeds; then, the mapping populations of 450 F_6 RILs were developed through the rapid generation advance (RGA) technique [29] (Figure 1).

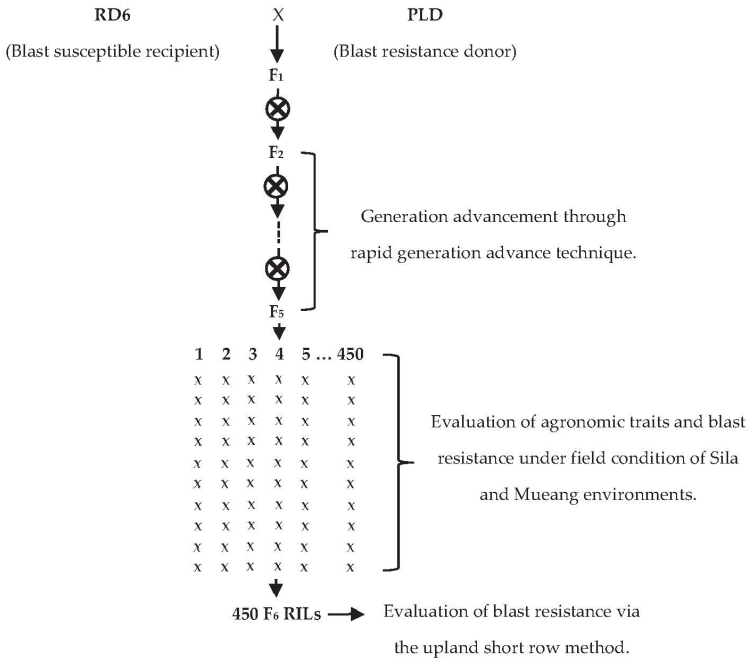

Figure 1. Scheme of the mapping population development from a cross between RD6 and PLD.

2.2. Evaluation of Blast Resistance

To understand the genetic basis of BL in PLD, a total of 450 F_6 RILs derived from a cross between RD6 and PLD were investigated for the segregation of disease reaction against *M. oryzae*. Evaluations of BL resistance were conducted in both field conditions and via the upland short row (USR) method in 2020. For the field evaluations, thirty-day seedlings of each line were transplanted in single rows (2 m long), with a spacing of 25 cm between and within each row, in two environments, the Mueang and Sila sub-districts in Khon Kean, Thailand. Natural infection was utilized by transplanting the susceptible KDML105 variety in the experiment border rows. BL resistance was scored for ten plants at their maximum tillering stage (approximately 45 days after transplanting) using the 0–9 rating scale of the Standard Evaluation System for rice (SES) [30]. The testing lines with 0–5 scores were considered resistant (R) while 6–9 were deemed susceptible (S).

In addition to the field evaluation, BL resistance was also evaluated at the seedling stage of rice through the USR method, at the Agronomy Field Crop Station, Faculty of Agriculture, Khon Kaen University, Khon Kaen, Thailand. The USR method evaluation was laid out in a randomized complete block design (RCB) with two replications. The local 'susceptible' KDML105 variety was planted in border strips 14 days before planting, to serve as a source of inoculum and as a spreader. Then, seeds of the parent, each RIL, and the 'resistant' check varieties (IR62266, P0489, and Jao Hom Nin) were sown in rows, 10 cm long and 7 cm apart. To ensure the uniform spread of the disease, the KDML105 variety was also planted after every ten test lines. Diseased plants of the BL-susceptible varieties (KDML105 and RD6), containing a mixture of natural *M. oryzae* strains, were collected from the Khon Kean rice fields. They were additionally used as an inoculum source, sprayed on all testing lines at the fourteen-day growth stage. Disease reactions were recorded ten days post-inoculation on a scale of 0–9 following the SES method [30], as described above.

2.3. Construction of Bulks, DNA Extraction, and Whole-Genome Resequencing

Contrasting phenotype bulks were generated for BL resistance based on disease reaction data of the RIL population. In constructing the contrasting phenotype bulks for BL resistance, 19 and 20 RILs showing the high and stable resistance and susceptible phenotypes were selected to generate resistant (BLR) and susceptible (BLS) bulks, respectively. The genomic DNA of each RIL in each bulk, as well as parental lines (PLD and RD6), were individually extracted using the GeneJET Plant Genomic DNA Purification Mini Kit (Thermo Scientific™, Waltham, MA, USA). The quantity of DNA was measured and adjusted to equal concentrations. Each DNA bulk (BLR and BLS) was formed by pooling equal quantities of genomic DNA for each RIL. Later, the genomic DNA of two parents and two bulks was used to prepare DNA-seq libraries and was sequenced the whole genome via the Illumina HiSeq. 2500 platform (Illumina, Inc., Hayward, CA, USA).

2.4. QTL-Seq Analysis

The QTL-seq pipeline, developed by Takagi et al. [20], was used for QTL-seq analysis. First, to obtain high-quality reads, raw reads were trimmed by removing low-quality and adapter-contained reads. According to the requirement of reference genome generation for read mapping of two bulk samples, the high-quality reads of RD6 were aligned to the public reference genome of Nipponbare (IRGSP1.0) using a BWA aligner [31]. Subsequently, the RD6 reference genome was generated by substituting the base in the Nipponbare reference genome with the variants representing the RD6 parent. The high-quality reads of the two bulks were then aligned onto the RD6 reference genome to call DNA variants (SNP, single nucleotide polymorphism and Indel, small insertion/deletion) in BLR and BLS bulks. The SNP index calculation of both bulks was performed for each SNP position, as previously described [20,32]. SNPs with an SNP index <0.3 in both bulks were excluded, and the remaining SNPs (SNP index $\geq$0.3 in either bulk) were considered as the real SNPs, and were used for Δ(SNP index) calculation. The Δ(SNP index) was calculated by subtracting the SNP index of the BLR bulk from the SNP index of the BLS bulk. An average SNP index and Δ(SNP index) in a given genomic region were obtained from a sliding window analysis (with 2 Mb window size and 10 kb increment) to generate the plots of the distribution of average SNP index and Δ(SNP index) compared between the two bulks. Circos was applied for visualization of the plots of average SNP index and Δ(SNP index) compared between the two bulks [33]. The QTL for BL resistance was determined as a peak or valley of the SNP index plots that exhibited an average Δ(SNP index) higher than the statistical confidence intervals under the null hypothesis of no QTL (p-value < 0.05) [20].

2.5. Candidate Gene Annotation

Candidate genes presented in the detected QTL region were identified from the whole-genome resequencing data of the two parents (RD6 and PLD) that were aligned to the reference genome of Nipponbare using a BWA aligner. The alignment files obtained in the alignment step were converted to BAM files to identify the SNPs using Samtools [34]. The variance effect predictor (VEP: https://plants.ensembl.org/oryza_sativa/Tools/VEP) (accessed on 22 September 2021) was applied to determine the effect of the SNPs in each gene. Only the genes containing nonsynonymous SNPs were selected as candidate genes [25].

2.6. Development of KASP Markers and Marker-Trait Association Analysis

To validate the association of markers with the BL resistance phenotype, we designed five Kompetitive Allele Specific PCR (KASP) markers for *LOC_Os04g0616600*, *LOC_Os04g0617900* (*OsGLP4-1*), *LOC_Os04g0619600* (*OsRLCK161*), *LOC_Os04g0620800* (*Pi63*), and *LOC_Os04g0621500* to genotype 200 RILs (randomly selected from the 450 F_6 RIL mapping population). Each KASP marker was developed based on the specific SNP variant and position of each gene, i.e., a nonsynonymous SNP (C/G) at position 31,309,180 for *LOC_Os04g0616600*, a nonsynonymous SNP (G/A) at position 31,395,022 for *OsGLP4-1*, a nonsynonymous SNP (A/G) at position 31,478,782 for *OsRLCK161*, a nonsynonymous

SNP (C/A) at position 31,552,051 for *Pi63*, and a nonsynonymous SNP (T/C) at position 31,581,570 for *LOC_Os04g0621500*. The genotypic data from the KASP markers and the phenotypic data of 200 RILs were used for single-marker analysis [25].

3. Results

3.1. Evaluation of Blast Resistance and Plant Selection for Bulk Preparation

For the rapid identification of QTLs capable of controlling blast (BL) resistance through the QTL-seq approach, we constructed a 450 F_6 RIL mapping population derived from a cross between the susceptible rice variety RD6 and resistance rice Phaladum (PLD). An F_6 RIL mapping population and parents were evaluated via the upland short row (USR) method (seedling stage) and in two environments (Sila and Mueang) during the maximum tillering stage for disease reaction against *M. oryzae*. Variations in resistance were observed, in which those in the Mueang population were less severe (Figure 2). Thus, we exclusively considered the disease reaction data obtained from USR and the Sila environment in this study. The results determined that the donor parent PLD was found to be resistant, with an average score of 3 and 2.57 for USR and Sila, respectively, while RD6 was found to be susceptible with an average score of 9 and 7.38 for USR and Sila, respectively. In the RIL population, the score ranged from 0.75 to 9 for USR and 1 to 8.78 for Sila. Across the two environments and/or methods, 203 RILs exhibited stable resistance against *M. oryzae*. The frequency distribution of F_6 RILs in USR and Sila appeared to follow a bimodal distribution (Figure 2). The segregation ratio of the F_6 RIL population tested under USR and Sila fitted to 1:1 ($X^2 = 1.91$, $p > 0.01$ and $X^2 = 2.72$, $p > 0.01$), with 244 resistant and 201 susceptible, and 250 resistant and 201 susceptible, respectively. These results suggested a single resistance gene conferring *M. oryzae* resistance in PLD. Additionally, correlations of the scores between USR and Sila were significant and strong ($r = 0.76$, $p < 0.01$) (Table S1), indicating that the single blast resistance gene of PLD contributes to both seedling and tillering stage resistance.

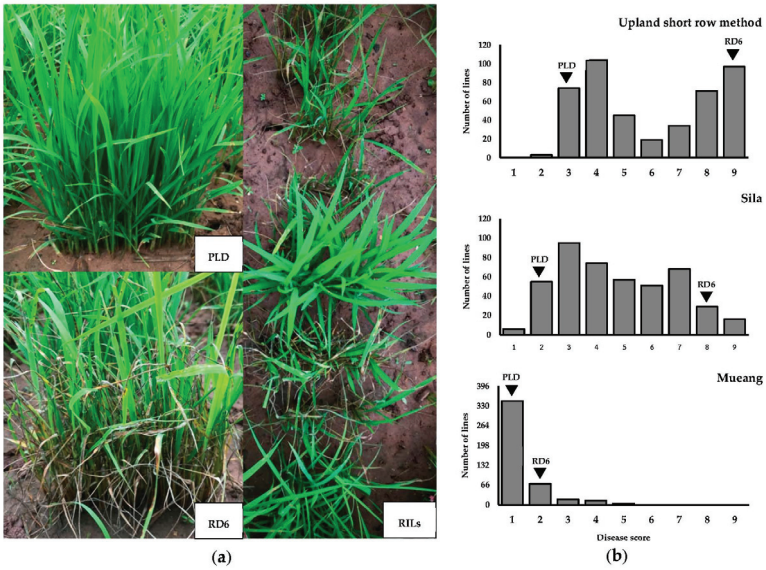

Figure 2. Blast (BL) phenotype in two parents and RILs: (**a**) the BL symptoms of the resistance parent PLD and susceptible parent RD6 and in RILs; (**b**) frequency distribution of disease reaction to a mixture of natural *M. oryzae* strains in 450 RD6/PLD F_6 RIL populations evaluated via USR method (top) and in two environments, Sila (middle) and Mueang (bottom). Disease scores of the parental lines (PLD and RD6) are indicated by a black triangle.

For QTL-seq analysis, we selected RILs that exhibited a consistent reaction (resistance or susceptible) to BL according to disease reaction data obtained from USR and Sila, but not Mueang, as disease infection was not severe. Disease scores from 19 resistance RILs and 20 susceptible RILs ranged from 1 to 3 and 7.13 to 9 for resistant (BLR) bulk and susceptible (BLS) bulk, respectively (Table S2).

3.2. QTL-Seq Analysis Identified QTL for Blast Resistance in PLD

Four DNA libraries, consisting of two contrasting bulks (i.e., BLR-bulk (blast resistance) and BLS-bulk (blast susceptible)) and two parents (i.e., resistance donor PLD and susceptible recipient RD6) were sequenced with the whole genome using Illumina HiSeq. 2500. In total, approximately 109 million reads for BLR-bulk, 113 million reads for BLS-bulk, 106 million reads for PLD, and 110 million reads for RD6 (with 150 bp in length) were generated, which were equivalent to 16.30, 17.00, 15.90, and 16.40 Gb for BLR-bulk, BLS-bulk, PLD, and RD6, respectively. The average sequencing depths of BLR-bulk, BLS-bulk, PLD, and RD6 were 33.20, 33.00, 35.10, and 34.80, respectively. The alignment of the reads from two bulks and parents to the reference genome of Nipponbare revealed 76.12%, 73.02%, 86.65%, and 85.52% of read alignments in BLR-bulk, BLS-bulk, PLD, and RD6, respectively, corresponding to 94.53%, 94.43%, 92.49%, and 92.83% of rice genome coverage (Table 1). The high-quality reads of RD6 were used to generate the reference sequence of RD6. Then, read mapping against the reference sequence of RD6 was performed to identify the common SNPs between BLR-bulk and BLS-bulk for QTL-seq analysis. As a result, a total of 1,457,210 SNPs with read support of at least three reads were obtained in both bulks (Table 2). According to a read support criterion of at least 29 reads, 719,720 SNPs existing in both bulks were selected for further SNP index and Δ(SNP index) calculation (Table 2). The SNP index in each bulk and the Δ(SNP index) were physically plotted across all rice chromosomes to identify the QTL responsible for BL resistance in PLD (Figure 3).

Table 1. Summary of Illumina sequencing data of parental lines and resistant and susceptible bulks.

Sample	Clean Reads	Clean Data (Gb)	Read Alignment (%)	Genome Coverage (%)	Average Depth
BLR-Bulk	108,940,496	16.30	76.12	94.53	33.20
BLS-Bulk	113,062,190	17.00	73.02	94.43	33.00
PLD	106,155,076	15.90	86.65	92.49	35.10
RD6	109,607,418	16.40	85.52	92.83	34.80

Table 2. Chromosome-wise distribution of single-nucleotide polymorphisms (SNPs) between two bulks.

Chromosome	Length	Number of SNPs [1]	Selected SNPs [2]
1	43,270,923	174,528	88,590
2	35,937,250	154,536	78,724
3	36,413,819	144,210	75,668
4	35,502,694	116,622	59,979
5	29,958,434	108,057	56,814
6	31,248,787	121,894	59,695
7	29,697,621	110,016	50,525
8	28,443,022	119,664	61,922
9	23,012,720	90,455	42,175
10	23,207,287	95,062	43,039
11	29,021,106	118,196	52,202
12	27,531,856	103,970	50,387
Total	373,245,519	1,457,210	719,720

[1] Number of SNPs with read support of at least three reads. [2] Selected SNPs with read support of at least 29 reads.

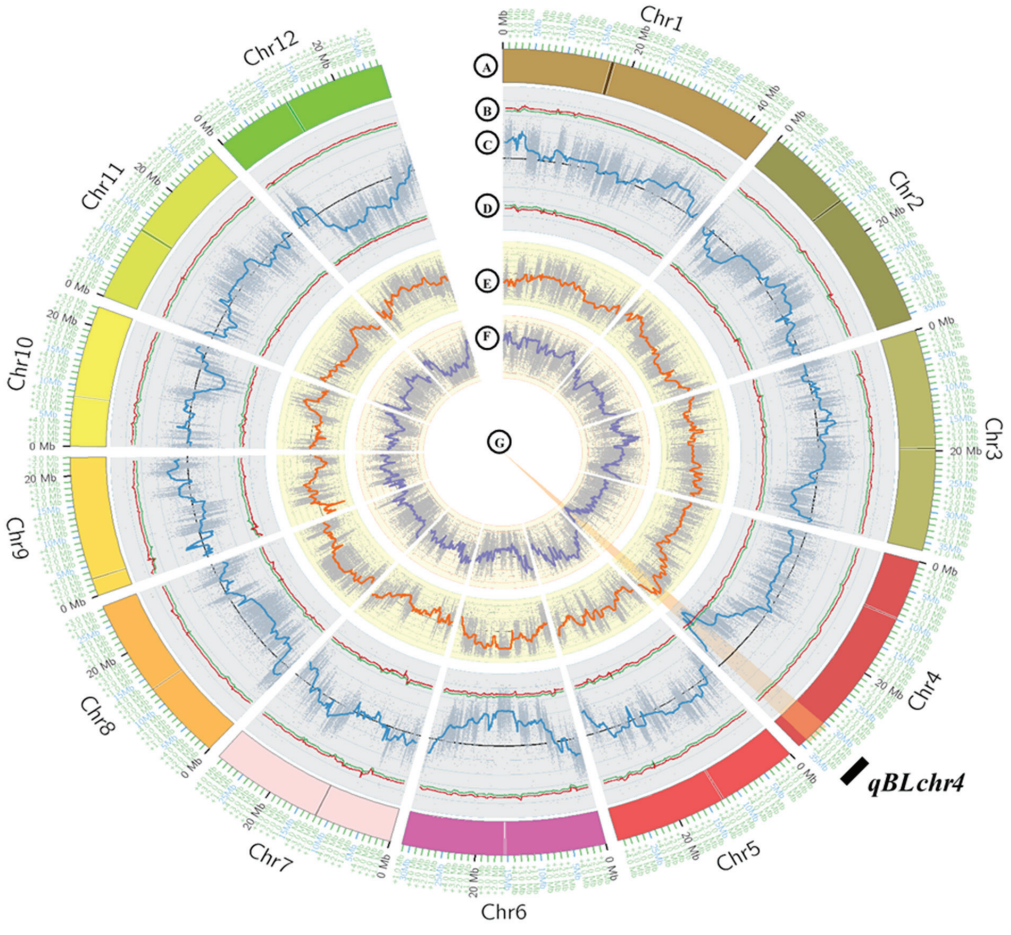

Figure 3. SNP index plots of BLR-bulk and BLS-bulk and plots of Δ(SNP index) obtained by subtracting between them: (A) pseudomolecules of Nipponbare reference genome (IRGSP 1.0); (B) upper probability values at 95% ($p < 0.05$; green line) and 99% confidence ($p < 0.01$; red lines); (C) plots of Δ(SNP index) with a window size of 2 Mb and 10 kb increment; (D) lower probability values at 99% ($p < 0.01$; red lines) and 95% confidence ($p < 0.05$; green line); (E) SNP index plots of BLR-bulk with a window size of 2 Mb and 10 kb increment; (F) SNP index plots of BLS bulk with a window size of 2 Mb and 10 kb increment; and (G) candidate genomic regions encompassing *qBLchr4* for blast resistance.

For the identification of putative QTLs, one QTL on the long arm of chromosome 4, namely *qBLchr4*, was detected based on the Δ(SNP index) plot that was greater than the threshold (confidence intervals > 95%) (Figure 3, Table 3). In the *qBLchr4* region, the average SNP index of BLR-bulk and BLS-bulk was 0.88 and 0.08, respectively, and the Δ(SNP index) was −0.80 (Figure 4, Table 3), indicating that plants in the BLR-bulk primarily contained the PLD-type genome in this QTL, whereas those in the BLS-bulk mostly contained the RD6-type genome.

Table 3. QTL detected for blast resistance in PLD.

QTL	Chromosome	Location		Interval (Mb)	Delta (SNP Index)		Confidence Interval	
		Start	End		Min	Max	95%	99%
qBLchr4	4	30,300,000	33,900,000	3.6	−0.60	−0.96	−0.73	−0.76

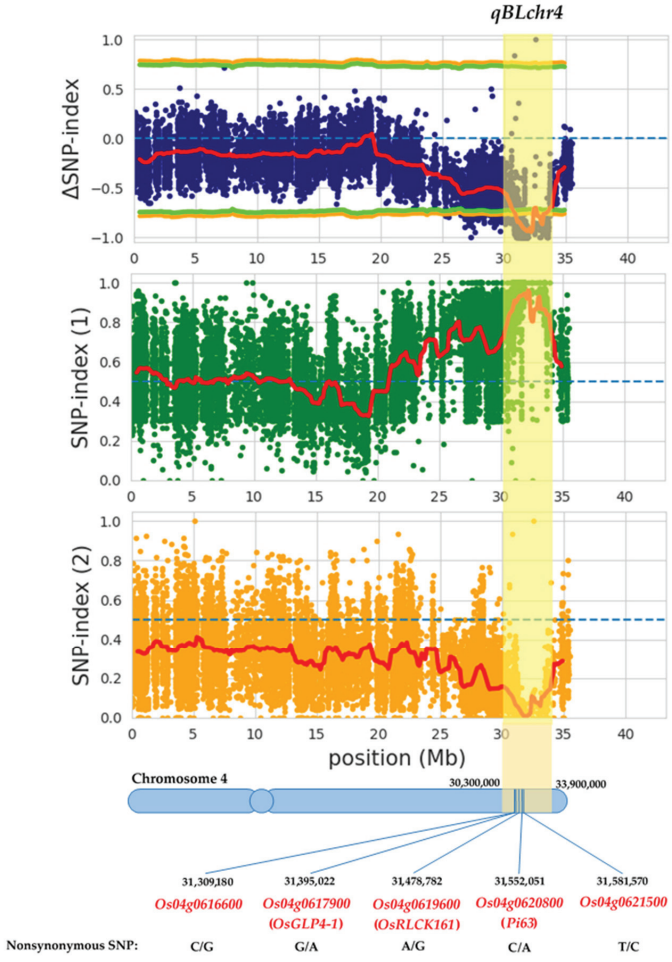

Figure 4. SNP index plots between resistance bulks (middle, BLR) and susceptible bulks (bottom, BLS) and Δ(SNP index) plots (top) on chromosome 4. The cream shade highlights the detected QTL regions with contrasting SNP indexes in two bulks.

qBLchr4 was mapped to the 3.6 Mb region (between 30.3 and 33.9 Mb) with 339 annotated genes. Of these, 117 genes were in the 1 Mb region covering the valley of *qBLchr4* and only 41 genes contained nonsynonymous SNPs. Among them, five genes—LOC_Os04g0616600, encoding a serine/threonine protein kinase-related domain-containing protein; LOC_Os04g0617900 (*OsGLP4-1*), encoding a similar to germin-like protein subfamily 1 member 11; LOC_Os04g0619600 (*OsRLCK161*), encoding a similar to resistance protein candidate (Fragment); LOC_Os04g0620800 (*Pi63*), encoding a similar to H0714H04.10 protein; and LOC_Os04g0621500, encoding a disease resistance protein domain-containing protein—were known to be involved in disease resistance and were selected as the putative

candidate genes representing *qBLchr4* in this study (Figure 4). Notably, in this region, *Pi63* was previously reported as the BL *R* gene.

3.3. Validation and Confirmation of Identified QTL on Chromosome 4

Based on the *qBLchr4* region identified by QTL-seq analysis, five genes, *LOC_Os04g0616600*, *LOC_Os04g0617900* (*OsGLP4-1*), *LOC_Os04g0619600* (*OsRLCK161*), *LOC_Os04g0620800* (*Pi63*), and *LOC_Os04g0621500*, were selected as the putative candidate genes for BL (Figure 4). The KASP marker specific for each gene was then developed and used for genotyping in 200 RILs that were randomly selected from the 450 mapping population. The association between the KASP marker and BL resistance phenotypes was validated through single-marker analysis. As a result, the high phenotypic variance explained (PVE) value for all five markers was found in all testing methods and/or environments. These markers explained 58.58–84.18%, 55.81–80.34%, and 18.63–23.73% of phenotypic variation in USR, Sila, and Mueang, respectively (Table 4). It is noted that the PVE value was still high in Mueang, where the disease infection was not severe. Among the five markers, the marker specific to *LOC_Os04g0620800* (*Pi63*) explained the highest and most stable phenotypic variation across all testing methods and/or environments (Table 4).

Table 4. Single marker analysis of the five markers, *LOC_Os04g0616600*, *LOC_Os04g0617900* (*OsGLP4-1*), *LOC_Os04g0619600* (*OsRLCK161*), *LOC_Os04g0620800* (*Pi63*), and *LOC_ Os04g0621500*, and BL resistance of the F_6 RIL population.

Markers	Chr	Upland Short Row Method				Sila				Mueang			
		LOD	PVE (%)	Add	Dom	LOD	PVE (%)	Add	Dom	LOD	PVE (%)	Add	Dom
LOC_Os04g0616600	4	36.86	58.58	−1.93	−0.69	34.14	55.81	−1.74	−0.46	9.64	20.63	−0.44	−0.35
LOC_Os04g0617900	4	51.78	70.94	−2.12	−0.61	45.81	66.52	−1.90	−0.56	8.59	18.63	−0.43	0.00
LOC_Os04g0619600	4	73.28	82.48	−2.22	−1.65	65.76	79.10	−2.01	−1.36	11.30	23.73	−0.46	−0.49
LOC_Os04g0620800	4	77.65	84.18	−2.23	−1.72	68.35	80.34	−2.03	−1.37	11.14	23.43	−0.46	−0.34
LOC_Os04g0621500	4	75.06	83.20	−2.25	−1.21	66.23	79.33	−2.03	−0.94	9.66	20.68	−0.44	−0.11

Chr = chromosome, LOD = logarithm of odds, PVE = phenotypic variation explained, Add = additive effect, and Dom = dominant effect.

4. Discussion

Rice blast (BL) epidemics are a major challenge for rice production worldwide. According to the rapid adaptation of the pathogen to overcome the *R* genes of the host plant, the use of a resistance variety carrying a single *R* gene with broad-spectrum resistance or multiple *R* genes is considered to be the most effective and economical way to control this disease. To meet the demand, identification of the genes or QTLs responsible for BL resistance is crucial for rice breeding. Indigenous rice is considered to be a valuable source for BL resistance as it has harbored the *R* genes that co-evolved along with local pathogen races for a very long time [11]. Therefore, the main focus of the current study was to utilize the QTL-seq approach to locate QTLs for BL resistance in Thai indica indigenous rice Phaladum (PLD).

To identify the QTL for BL resistance, an F_6 RIL population derived from the two parents (RD6 and PLD), differing in BL resistance, was used for phenotyping in the QTL analysis. According to our correlation analysis of seedling stage resistance and tillering stage resistance for BL, a strong positive correlation of BL resistance between the seedling stage and tillering stage was found, implying that the BL *R* gene in PLD likely functions at both stages of growth. These many stages of resistance correspond with the previous result of Gerema et al. [35], which reported that two rice cultivars, Chewaga and Edget, conferred leaf blast resistance at both seedling and adult (maximum tillering) stages. Moreover, in addition to leaf and neck blast, panicle blast is also a common symptom caused by *M. oryzae* at the adult stage of rice. Three landraces, Yangmaogu, Jingnanwan, and Gumei 4, carrying the *R* genes *Pi64*, *Pi-jnw1,* and *Pigm*, respectively, were reported to confer both leaf blast (seedling) and neck blast resistance [15,36,37]. Similarly, Chumpol et al. [19] also reported that ten Thai indigenous upland rice varieties (including PLD) exhibited resistance to both

leaf blast and neck blast. In addition to the seedling and neck blast resistance of PLD, we additionally demonstrated the resistance of PLD at the tillering stage. The resistance expressed at many stages in growth is more desirable agronomically than that expressed at one particular stage (developmental stage-specific manner) [38]. Nevertheless, there are exceptions where plants are resistant at particular stages of growth. For example, a panicle blast resistance gene *Pb1* from indica rice variety Modan is susceptible to leaf blast during its young vegetative stage, but the resistance level then increases steadily and persists after heading [39,40].

In genetic analysis using 450 RILs, the mapping population showed a 1:1 segregation ratio. Generally, this 1:1 segregation ratio in the RIL population suggested the monogenic inheritance controlling the trait [41]. This follows previous reports that stated that the inheritance of BL resistance is controlled by a single gene [41–44]. The monogenic inheritance of BL resistance in PLD was confirmed by QTL-seq analysis. The results of this RIL population identified only one significant QTL (*qBLchr4*) on the long arm of chromosome 4. Furthermore, as high phenotypic variation explained (PVE) was achieved through single-marker analysis, *qBLchr4* was considered a major QTL in this study. This provides additional support for Miyamoto et al. [45], who identified major QTLs *qBFR4-1* (designated as *Pikahei-1(t)* and *Pi63* after fine mapping and cloning, respectively) for BL resistance, which explained 61.6% of phenotypic variance. Although numerous genes and QTLs for BL resistance have been identified [9,46], these sources have not been utilized effectively in rice breeding. This is because the genetic control of quantitative resistance is complex and the causal genes within resistance QTLs are still unknown [47]. Additionally, QTLs are frequently identified in the regions covering large DNA fragments, which might exhibit linkage drag, causing undesired traits when QTLs with different genetic backgrounds were pyramided into an improved commercial cultivar [47]. Identification of candidate genes underlying resistance QTLs will facilitate the effective utilization of these QTLs in rice breeding through marker-assisted selection (MAS) [47]. Among the molecular markers used in MAS, single-nucleotide polymorphisms (SNPs) have been considered to be the most promising, due to their high abundance in genomes and their potential for high-throughput automated genotyping [48].

In the present study, we identified five genes, *LOC_Os04g0616600*, *LOC_Os04g0617900* (*OsGLP4-1*), *LOC_Os04g0619600* (*OsRLCK161*), *LOC_Os04g0620800* (*Pi63*) and *LOC_Os04g0621500*, as the candidate genes representing *qBLchr4*. The KASP markers specific to the SNP variant and position of each gene were developed and used for validating the associations of markers with BL resistance phenotypes. According to the results of our single-marker analyses, the high phenotypic variance explained (PVE) value was found across each testing method and/or environment using all five markers, suggesting that these five markers can be potentially used in MAS for BL-resistant rice breeding. Previously, Yang et al. [48] also developed three KASP markers, each specific to SNP on the BL *R* gene: *Pita*; *Pik*; and *Pi2*. They were effectively used for BL resistance. It should be noted that the QTL identified in this study was stable across all testing methods and/or environments, even in the Mueang environment, where disease infection was minimal. Across the testing methods and/or environments, the *Pi63*-KASP marker explained the highest and most stable PVE value compared to other KASP markers used in this study. Therefore, *Pi63* is suggested to be the best candidate gene associated with BL resistance in PLD.

Pi63 was previously reported as a BL-resistant gene capable of encoding a typical coiled-coil (CC) nucleotide-binding site and leucine-rich repeat (CC-NBS-LRR) protein [49], one of two NBS–LRR protein sub-classes [40]. The CC domain was found to have a function in pathogen recognition and defense signaling through intramolecular interactions [50]. The central NBS domain participates in nucleotide binding and plays an important role in transducing pathogen perception by LRR to resistance protein activation [40,51–53]. Additionally, Xu et al. [49] reported that *Pi63* exhibited partial resistance and isolate specificity to *M. oryzae* (resistance to two of four isolates used). This is in agreement with previous reports that many rice cultivars conferred partial resistance and isolate specificity

to *M. oryzae* [36,41,54,55]. According to the isolate specificity of *Pi63*, resistance can be overcome by the emergence of a new virulent isolate of *M. oryzae*. Thus, pyramiding *Pi63* from PLD with other *R* genes into a high-yielding rice variety, locally, through marker-assisted selection (MAS), is needed for broad-spectrum and durable resistance rice breeding in Thailand.

PLD is an indica indigenous lowland rice variety that confers resistance to local *M. oryzae* isolates and possesses some favorable agronomic traits, which provides beneficial breeding material for enhancing BL resistance and yield, as it might reduce genetic linkage dragging. To utilize this elite resistance source in future BL resistance rice improvement programs, selecting the RILs (obtained from a cross between RD6 and PLD that exhibited different BL resistance) showing different BL resistance with satisfactory agronomic traits may be attained. In the study herein, seven RILs conferred resistance to BL and possessed some desirable agronomic traits, i.e., early maturity (DTF, days to flowering), high tillering ability (TN, tiller number), short plant height (PH), and long and slender grains (SL, seed length and SW, seed width) (Table 5). These RILs may potentially be used as breeding materials for further BL resistance rice improvement programs in Thailand. Nevertheless, some agronomic traits of these RILs, such as the number of filled grains per panicle (NFGP), which will directly affect the grain yield per plant (GYP), indicated the need for improvement. To achieve this, marker-assisted backcrossing (MABC) is considered a promising approach to achieve both the desired agronomic traits with BL resistance.

Table 5. Blast scores and agronomic traits of selected RILs.

Lines	Blast Score		DTF	TN	PH	SL	SW	PL	NFGP	1000 GW	GYP (g)
	USR	Sila			(cm)	(mm)	(mm)			(g)	
100	3.50	1.67	107	11	136	10.30	3.12	26.33	119	28.73	36.12
124	3.00	1.11	71	14	118	9.99	2.68	27.00	131	21.23	29.35
126-1	4.00	2.67	91	14	159	10.10	2.66	29.43	144	23.16	22.85
132	2.50	1.00	71	12	166	10.32	2.66	30.50	185	25.12	29.62
238	4.00	1.00	70	17	143	9.73	2.64	26.75	183	23.47	30.44
335	4.00	1.56	89	13	126	9.97	2.74	26.50	141	24.51	32.00
361	3.00	2.00	90	10	150	10.39	2.80	26.67	143	26.80	29.49
PLD	3.00	2.57	69	13	126	9.54	2.91	26.35	145	26.35	28.16
RD6	9.00	5.72	102	11	175	10.17	2.78	27.38	196	25.14	32.00

USR = upland short row method, DTF = days to flowering, TN = tiller number, SL = seed length, SW = seed width, PL = panicle length, NFGP = number of filled grain per panicle, GW = 1000-grain weight, GYP = grain yield per plant.

5. Conclusions

By applying QTL-seq analysis in the F_6 RIL population (RD6 × PLD), we successfully identified one major QTL (*qBLchr4*) on the long arm of chromosome 4, associated with BL resistance in both the seedling and tillering stages. Five genes—*LOC_Os04g0616600*; *LOC_Os04g0617900* (*OsGLP4-1*); *LOC_Os04g0619600* (*OsRLCK161*); *LOC_Os04g0620800* (*Pi63*); and *LOC_Os04g0621500*—were considered as candidate genes. The KASP marker designed for these genes was found to be effective in selecting plants with BL resistance. With the highest and most stable PVE value, *Pi63* was suggested as the best candidate gene for BL resistance. Moreover, the RILs selected from this population exhibited BL resistance and possessed desired agronomic traits; thus, they could provide good breeding materials for further BL-resistant rice breeding.

Supplementary Materials: The following supporting information can be downloaded at: https://www.mdpi.com/article/10.3390/agriculture12081166/s1, Table S1: Correlation coefficient of blast score of the mapping population evaluated at seedling (USR method) and maximum tillering (Sila and Mueang environments) stages; Table S2: Blast score of RILs in the resistance bulk (BLR) and susceptible bulk (BLS) investigated via upland short row (USR) method and in the Sila environment.

Author Contributions: Conceptualization, C.N., S.C. and J.S.; methodology, C.N., S.M. and A.S.; software, C.N. and S.A.; validation, S.A., T.M., S.C. and J.S.; formal analysis, C.N.; investigation, S.C. and J.S.; resources, S.C., T.M. and J.S.; data curation, C.N.; writing (original draft preparation), C.N.; writing (review and editing), S.C. and J.S.; visualization, T.M., S.C., S.A. and J.S; supervision, J.S.; project administration, S.C.; funding acquisition, S.C. All authors have read and agreed to the published version of the manuscript.

Funding: This research was funded by the Center of Excellence on Agricultural Biotechnology, Office of the Permanent Secretary, Ministry of Higher Education, Science, Research and Innovation. (AG-BIO/MHESI).

Institutional Review Board Statement: Not applicable.

Informed Consent Statement: Not applicable.

Data Availability Statement: The data presented in this study are available upon request from the corresponding author.

Acknowledgments: This research was supported by the Plant Breeding Research Center for Sustainable Agriculture, Khon Kaen University, Khon Kaen, Thailand, and the Center of Excellence on Agricultural Biotechnology, Office of the Permanent Secretary, Ministry of Higher Education, Science, Research and Innovation. (AG-BIO/MHESI).

Conflicts of Interest: The authors declare no conflict of interest.

References

1. Srivastava, D.; Shamim, M.; Kumar, M.; Mishra, A.; Pandey, P.; Kumar, D.; Yadav, P.; Siddiqui, M.H.; Singh, K.N. Current status of conventional and molecular interventions for blast resistance in rice. *Rice Sci.* **2017**, *24*, 299–321. [CrossRef]
2. Lee, K.S.; Rasabandith, S.; Angeles, E.R.; Khush, G.S. Inheritance of resistance to bacterial blight in 21 cultivars of rice. *Phytopathology* **2003**, *93*, 147–152. [CrossRef]
3. Wu, Y.Y.; Xiao, N.; Yu, L.; Pan, C.H.; Li, Y.H.; Zhang, X.X.; Liu, G.Q.; Dai, Z.Y.; Pan, X.B.; Li, A.H. Combination patterns of major *R* genes determine the level of resistance to the *M. oryzae* in rice (*Oryza sativa* L.). *PLoS ONE* **2015**, *10*, e0126130. [CrossRef] [PubMed]
4. Xiao, N.; Wu, Y.; Li, A. Strategy for use of rice blast resistance genes in rice molecular breeding. *Rice Sci.* **2020**, *27*, 263–277. [CrossRef]
5. Datta, K.; Baisakh, N.; Maung Thet, K.; Tu, J.; Datta, S.K. Pyramiding transgenes for multiple resistance in rice against bacterial blight, yellow stem borer, and sheath blight. *Theor. Appl. Genet.* **2002**, *106*, 1–8. [CrossRef]
6. Maruthasalam, S.; Kalpana, K.; Kumar, K.K.; Loganathan, M.; Poovannan, K.; Raja, J.A.J.; Kokiladevi, E.; Samiyappan, R.; Sudhakar, D.; Balasubramanian, P. Pyramiding transgenic resistance in elite indica rice cultivars against the sheath blight and bacterial blight. *Plant. Cell Rep.* **2007**, *26*, 791–804. [CrossRef]
7. Vasudevan, K.; Vera Cruz, M.C.; Gruissem, W.; Bhullar, N.K. Large-scale germplasm screening for identification of novel rice blast resistance sources. *Front. Plant. Sci.* **2014**, *5*, 505. [CrossRef]
8. Jiang, N.; Yan, J.; Liang, Y.; Shi, Y.; He, Z.; Wu, Y.; Zeng, Q.; Liu, X.; Peng, J. Resistance genes and their interactions with bacterial blight/leaf streak pathogens (*Xanthomonas oryzae*) in rice (*Oryza sativa* L.). *Rice* **2020**, *13*, 3. [CrossRef]
9. Ashkani, S.; Yusop, M.R.; Shabanimofrad, M.; Azadi, A.; Ghasemzadeh, A.; Azizi, P.; Latif, M.A. Allele mining strategies: Principles and utilisation for blast resistance genes in rice (*Oryza sativa* L.). *Curr. Issues Mol. Biol.* **2015**, *17*, 57–74.
10. Ashkani, S.; Rafii, M.Y.; Shabanimofrad, M.; Ghasemzadeh, A.; Ravanfar, S.A.; Latif, M.A. Molecular progress on the mapping and cloning of functional genes for blast disease in rice (*Oryza sativa* L.): Current status and future considerations. *Crit. Rev. Biotechnol.* **2014**, *36*, 353–367. [CrossRef]
11. Yaday, M.K.; Aravindan, S.; Ngangkham, U.; Raghu, S.; Praphukarthikeyan, S.R.; Keerthana, U.; Marndi, B.C.; Adak, T.; Munda, S.; Deshmukh, R.; et al. Blast resistance in Indian rice landraces: Genetic dissection by gene-specific markers. *PLoS ONE* **2019**, *14*, e0211061. [CrossRef]
12. Joshi, S.; Dhatwalia, S.; Kaachra, A.; Sharma, K.D.; Rathour, R. Genetic and physical mapping of a new rice blast resistance specificity Pi-67 from a broad spectrum resistant genotype Tetep. *Euphytica* **2019**, *215*, 9. [CrossRef]
13. Sharma, T.R.; Rai, A.K.; Gupta, S.K.; Singh, N.K. Broad-spectrum blast resistance gene Pi-k^{h} cloned from rice line Tetep designated as Pi54. *J. Plant. Biochem. Biotechnol.* **2010**, *19*, 87–89. [CrossRef]
14. Deng, Y.W.; Zhai, K.R.; Xie, Z.; Yang, D.Y.; Zhu, X.D.; Liu, J.Z.; Wang, X.; Qin, P.; Yang, Y.Z.; Zhang, G.M.; et al. Epigenetic regulation of antagonistic receptors confers rice blast resistance with yield balance. *Science* **2017**, *355*, 962–965. [CrossRef]
15. Wang, R.; Fang, N.; Guan, C.; He, W.; Bao, Y.; Zhang, H. Characterization and fine mapping of a blast-resistant gene *Pi-jnw1* from the *japonica* rice landrace Jiangnanwan. *PLoS ONE* **2016**, *11*, e0169417. [CrossRef]

16. Chen, X.W.; Li, S.G.; Xu, J.C.; Zhai, W.X.; Ling, Z.Z.; Ma, B.T.; Wang, Y.P.; Wang, W.M.; Cao, G.; Ma, Y.Q.; et al. Identification of two blast resistance genes in a rice variety, Digsu. *J. Phytopathol.* **2004**, *152*, 77–85. [CrossRef]
17. Khannetah, K.R.; Ramchander, S.; Leon, M.T.A.P.; Shoba, D.; Saravanan, S.; Kannan, R.; Yasin, J.K.; Pillai, M.A. Genetic diversity analysis in indigenous rice (*Oryza sativa* L.) germplasm for bacterial leaf blight (Xanthomonas oryzae pv. eryzae) (BB) using resistance genes-linked markers. *Euphytica* **2021**, *217*, 145. [CrossRef]
18. Kwanwah, M.R.; Wongsa, T.; Monkham, T.; Chankaew, S.; Falab, S.; Sanitchon, J. Thai indigenous lowland rice germplasms: Sources of bacterial blight disease resistance and agronomic attributes. *AGRIVITA J. Agric. Sci.* **2020**, *42*, 367–380. [CrossRef]
19. Chumpol, A.; Chankaew, S.; Saepaisan, S.; Monkham, T.; Sanitchon, J. New sources of rice blast resistance obtained from Thai indigenous upland rice germplasm. *Euphytica* **2018**, *214*, 183. [CrossRef]
20. Takagi, H.; Abe, A.; Yoshida, K.; Kosugi, S.; Natsume, S.; Mitsuoka, C.; Uemura, A.; Utsushi, H.; Tamiru, M.; Takuno, S.; et al. QTL-seq: Rapid mapping of quantitative trait loci in rice by whole-genome resequencing of DNA from two bulked populations. *Plant. J.* **2013**, *74*, 174–183. [CrossRef]
21. Ogiso-Tanaka, E.; Tanaka, T.; Tanaka, K.; Nonoue, Y.; Sasaki, T.; Fushimi, E.; Koide, Y.; Okumoto, Y.; Yano, M.; Saito, H. Detection of novel QTLs QDTH4.5 and QDTH6.3, which confer late heading under short-day conditions, by SSR marker-based and QTL-seq analysis. *Breed. Sci.* **2017**, *67*, 101–109. [CrossRef] [PubMed]
22. Yang, X.; Xia, X.; Zhang, Z.; Nong, B.; Zeng, Y.; Xiong, F.; Wu, Y.; Gao, J.; Deng, G.; Li, D. QTL mapping by whole genome re-sequencing and analysis of candidate genes for nitrogen use efficiency in rice. *Front. Plant. Sci.* **2017**, *8*, 1634. [CrossRef]
23. Kadambari, G.; Vemireddy, L.R.; Srividhya, A.; Nagireddy, R.; Jena, S.S.; Gandikota, M.; Patil, S.; Veeraghattapu, R.; Deborah, D.A.K.; Reddy, G.E.; et al. QTL-seq-based genetic analysis identifies a major genomic region governing dwarfness in rice (*Oryza sativa* L.). *Plant. Cell Rep.* **2018**, *37*, 677–687. [CrossRef] [PubMed]
24. Qin, Y.; Cheng, P.; Cheng, Y.; Feng, Y.; Huang, D.; Huang, T.; Song, X.; Ying, J. QTL-seq identified a major QTL for grain length and weight in rice using near-isogenic F_2 population. *Rice Sci.* **2018**, *25*, 121–131. [CrossRef]
25. Arikit, S.; Wanchana, S.; Khanthong, S.; Saensuk, C.; Thianthavon, T.; Vanavichit, A.; Toojinda, T. QTL-seq identifies cooked grain elongation QTLs near soluble starch synthase and starch branching enzymes in rice (*Oryza Sativa* L.). *Sci. Rep.* **2019**, *9*, 8328. [CrossRef] [PubMed]
26. Bommisetty, R.; Chakravartty, N.; Bodanapu, R.; Naik, J.B.; Panda, S.K.; Lekkala, S.P.; Lalam, K.; Thomas, G.; Mallikarjuna, S.J.; Eswar, G.R.; et al. Discovery of genomic regions and candidate genes for grain weight employing next-generation sequencing-based QTL-seq approach in rice (*Oryza Sativa* L.). *Mol. Biol. Rep.* **2020**, *47*, 8615–8627. [CrossRef]
27. Nubankoh, P.; Wanchana, S.; Saensuk, C.; Ruanjaichon, V.; Cheabu, S.; Vanavichit, A.; Toojinda, T.; Malumpong, C.; Arikit, S. QTL-seq reveals genomic regions associated with spikelet fertility in response to a high temperature in rice (*Oryza Sativa* L.). *Plant. Cell Rep.* **2020**, *39*, 149–162. [CrossRef]
28. Thianthavon, T.; Aesomnuk, W.; Pitaloka, M.K.; Sattayachiti, W.; Sonsom, Y.; Nubankoh, P.; Malichan, S.; Riangwong, K.; Ruanjaichon, V.; Toojinda, T.; et al. Identification, and validation of a QTL for bacterial leaf streak resistance in rice (*Oryza sativa* L.) against Thai Xoc strains. *Genes* **2021**, *12*, 1587. [CrossRef]
29. Beredo, J.; Mendoza, R.; Reyes, E.; Hermosada, H.; Javier, M.A.; Islam, M.R.; Collard, B. Use of a rapid generation advance (RGA) system for IRRI's irrigated breeding pipeline. In In Proceedings of the IRRI-BMGF's Transforming Rice Breeding (TRB) Project Objective 3.0, Metro Manila, Philippines, 6 June 2016.
30. International Rice Research Institute. *Standard Evaluation System (SES) for Rice*, 5th ed.; International Rice Research Institute: Manila, Philippines, 2013; p. 18.
31. Li, H.; Durbin, R. Fast and accurate short read alignment with burrows-wheeler transform. *Bioinformatics* **2009**, *25*, 1754–1760. [CrossRef]
32. Abe, A.; Kosugi, S.; Yoshida, K.; Natsume, S.; Takagi, H.; Kanzaki, H.; Matsumura, H.; Yoshida, K.; Mitsuoka, C.; Tamiru, M.; et al. Genome sequencing reveals agronomically important loci in rice using MutMap. *Nat. Biotechnol.* **2012**, *30*, 174–178. [CrossRef]
33. Krzywinski, M.; Schein, J.; Birol, I.; Connors, J.; Gascoyne, R.; Horsman, D.; Jones, S.J.; Marra, M.A. Circos: An information aesthetic for comparative genomics. *Genome Res.* **2009**, *19*, 1639–1645. [CrossRef] [PubMed]
34. Li, H.; Handsaker, B.; Wysoker, A.; Fennell, T.; Ruan, J.; Homer, N.; Marth, G.; Abecasis, G.; Durbin, R. The sequence alignment/Map format and SAMtools. *Bioinformatics* **2009**, *25*, 2078–2079. [CrossRef]
35. Gerema, G.; Mengistu, G.; Kebede, M.; Lule, D.; Desalegn, K.; Birahanu, C.; Debela, M. Seedling, and adult plant resistance to Pyricularia oryzae in Ethiopian rice cultivars. *Acta Univ. Sapientiae Agric. Environ.* **2020**, *12*, 45–57. [CrossRef]
36. Ma, J.; Lei, C.L.; Xu, X.T.; Hao, K.; Wang, J.L.; Cheng, Z.J.; Ma, X.D.; Ma, J.; Zhou, K.N.; Zhang, X.; et al. Pi64, encoding a novel CC-NBS-LRR protein, confers resistance to leaf and neck blast in rice. *Mol. Plant. Microbe Interact.* **2015**, *28*, 558–568. [CrossRef] [PubMed]
37. Wu, Y.Y.; Yu, L.; Pan, C.H.; Dai, Z.Y.; Li, Y.H.; Xiao, N.; Zhang, X.X.; Ji, H.J.; Huang, N.S.; Zhao, B.H.; et al. Development of near-isogenic lines with different alleles of *Piz* locus and analysis of their breeding effect under Yangdao 6 background. *Mol. Breed.* **2016**, *36*, 1–12. [CrossRef]
38. Century, K.S.; Lagman, R.A.; Adkisson, M.; Morlan, J.; Tobias, R.; Schwartz, K.; Smith, A.; Love, J.; Ronald, P.C.; Whalen, M.C. Developmental control of *Xa21*-mediated disease resistance in rice. *Plant. J.* **1999**, *20*, 231–236. [CrossRef]
39. Fuji, K.; Hayano-Saito, Y. Genetics of durable resistance to rice panicle blast derived from an indica rice variety Modan. *Jpn. J. Plant. Sci.* **2017**, *1*, 69–76.

40. Hayashi, N.; Inoue, H.; Kato, T.; Funao, T.; Shirota, M.; Shimizu, T.; Kanamori, H.; Yamane, H.; Hayano-Saito, Y.; Matsumoto, T.; et al. Durable panicle blast-resistance gene Pb1 encodes an atypical CC-NBS-LRR protein and was generated by acquiring a promoter through local genome duplication. *Plant. J.* **2010**, *64*, 498–510. [CrossRef]
41. Sun, P.; Liu, J.; Wang, Y.; Jiang, N.; Wang, S.; Dai, Y.; Gao, J.; Li, Z.; Pan, S.; Wang, D.; et al. Molecular mapping of the blast resistance gene Pi49 in the durably resistant rice cultivar Mowanggu. *Euphytica* **2013**, *192*, 45–54. [CrossRef]
42. Zenbayashi-Sawata, K.; Ashizawa, T.; Koizumi, S. Pi34-AVRPi34: A new gene-for-gene interaction for partial resistance in rice to blast caused by Magnaporthe grisea. *J. Gen. Plant. Pathol.* **2005**, *71*, 395–401. [CrossRef]
43. Khumbar, S.D.; Kulwal, P.L.; Patil, J.V.; Gaikwad, A.P.; Jadhav, A.S. Inheritance of blast resistance and identification of SSR marker associated with it in rice cultivar RDN 98-2. *J. Genet.* **2013**, *92*, 317–321. [CrossRef] [PubMed]
44. Lei, C.; Hao, K.; Yang, Y.; Ma, J.; Wang, S.; Wang, J.; Cheng, Z.; Zhao, S.; Zhang, X.; Guo, X.; et al. Identification and fine mapping of two blast resistance genes in rice cultivar 93-11. *Crop. J.* **2013**, *1*, 2–14. [CrossRef]
45. Miyamoto, M.; Yano, M.; Hirasawa, H. Mapping of quantitative trait loci conferring blast field resistance in the Japanese upland rice variety Kahei. *Breed. Sci.* **2001**, *51*, 257–261. [CrossRef]
46. Li, W.T.; Chern, M.S.; Yin, J.J.; Wang, J.; Chen, X.W. Recent advances in broad-spectrum resistance to the rice blast disease. *Curr. Opin. Plant. Biol.* **2019**, *50*, 114–120. [CrossRef]
47. Hu, M.; Qiu, D.; Shen, X.; Li, X.; Wang, S. Isolation and manipulation of quantitative trait loci for disease resistance in rice using a candidate gene approach. *Mol. Plant.* **2008**, *1*, 786–793. [CrossRef]
48. Yang, G.L.; Chen, S.P.; Chen, L.K.; Sun, K.; Huang, C.H.; Zhou, D.H.; Huang, Y.T.; Wang, J.F.; Liu, Y.Z.; Wang, H.; et al. Development of core SNP arrays based on the KASP method for molecular breeding of rice. *Rice* **2019**, *12*, 21. [CrossRef]
49. Xu, X.; Hayashi, N.; Wang, C.; Fukuoka, S.; Kawasaki, S.; Takatsuji, H.; Jiang, C. Rice blast resistance gene Pikahei-1(t), a member of a resistance gene cluster on chromosome 4, encodes a nucleotide-binding site and leucine-rich repeat protein. *Mol. Breed.* **2014**, *34*, 691–700. [CrossRef]
50. Raidan, G.J.; Collier, S.M.; Sacco, M.A.; Baldwin, T.T.; Boettrich, T.; Moffett, P. The coiled-coil and nucleotide-binding domains of the potato Rx disease resistance protein function in pathogen recognition and signaling. *Plant. Cell* **2008**, *20*, 739–751. [CrossRef]
51. Tameling, W.I.; Elzinga, S.D.; Darmin, P.S.; Vossen, J.H.; Takken, F.L.; Haring, M.A.; Cornelissen, B.J. The tomato *R* gene products I-2 and MI-1 are functional ATP binding proteins with ATPase activity. *Plant. Cell.* **2002**, *14*, 2929–2939. [CrossRef]
52. Takken, F.L.; Albrecht, M.; Tameling, W.I. Resistance proteins: Molecular switches of plant defence. *Curr. Opin. Plant. Biol.* **2006**, *9*, 383–390. [CrossRef]
53. Van Ooijen, G.; Mayr, G.; Kasiem, M.M.A.; Albrecht, M.; Cornelissen, B.J.C.; Takken, F.L.W. Structure-function analysis of the NB-ARC domain of plant disease resistance proteins. *J. Exp. Bot.* **2008**, *59*, 1383–1397. [CrossRef] [PubMed]
54. Talukder, Z.I.; Tharreau, D.; Price, A.H. Quantitative trait loci analysis suggests that partial resistance to rice blast is mostly determined by race-specific interactions. *N. Phytol.* **2004**, *162*, 197–209. [CrossRef]
55. Miah, G.; Rafii, Y.R.; Ismail, M.R.; Puteh, A.B.; Rahim, H.A.; Asfaliza, R.; Latif, M.A. Blast resistance in rice: A review of conventional breeding to molecular approaches. *Mol. Biol. Rep.* **2013**, *40*, 2369–2388. [CrossRef] [PubMed]

agriculture

MDPI

Article

Genetic Diversity of Korean Black Soybean (*Glycine max* L.) Germplasms with Green Cotyledons Based on Seed Composition Traits

Ji Yun Lee [1,†], Hyun Jo [2,3,†], Chang Ki Son [1], Jeong Suk Bae [1] and Jeong-Dong Lee [2,4,*]

[1] Gyeongsangbuk-do Provincial Agricultural Research & Extension Service, Daegu 41404, Republic of Korea
[2] Department of Applied Biosciences, Kyungpook National University, Daegu 41566, Republic of Korea
[3] Upland-Field Machinery Research Center, Kyungpook National University, Daegu 41566, Republic of Korea
[4] Department of Integrative Biology, Kyungpook National University, Daegu 41566, Republic of Korea
* Correspondence: jdlee@knu.ac.kr; Tel.: +82-53-950-5709; Fax: +82-53-958-6880
† These authors contributed equally to this work.

Abstract: The demand for black soybeans (*Glycine max* (L.) Merr.) with green cotyledons is increasing because of their health benefits. Therefore, it is important to understand the genetic diversity of black soybean germplasms and to develop a new soybean cultivar. This study aimed to evaluate genetic diversity among 469 black soybean germplasms with green cotyledons based on seed composition traits. Twenty seed composition traits were analyzed to conduct correlation analysis, principal component analysis (PCA), and cluster analysis, which indicated that black soybean germplasms were divided into four clusters. Black soybean germplasms in cluster 1 had higher crude fat, lutein, chlorophyll *a*, chlorophyll *b*, and total chlorophyll contents, but lower cyanidin-3-glucoside content than those in clusters 2 and 3. However, germplasms in clusters 2 and 3 had the highest cyanidin-3-glucoside content. Moreover, germplasms in cluster 1 had significantly higher palmitic acid content than those in clusters 2 and 3. Germplasms in clusters 2 and 3 had relatively high α-linolenic acid content. Germplasms in cluster 4 had the highest oleic acid content. This study highlights the genetic diversity of black soybean germplasms with different seed composition traits, and the results of this study can be beneficial for soybean breeding programs, enabling them to develop new black soybean cultivars with green cotyledons and improved seed composition traits.

Keywords: genetic diversity; black soybean; green cotyledon; seed composition; breeding

Citation: Lee, J.Y.; Jo, H.; Son, C.K.; Bae, J.S.; Lee, J.-D. Genetic Diversity of Korean Black Soybean (*Glycine max* L.) Germplasms with Green Cotyledons Based on Seed Composition Traits. *Agriculture* **2023**, *13*, 406. https://doi.org/10.3390/agriculture13020406

Academic Editors: Edyta Paczos-Grzeda, Volker Mohler and Sylwia Sowa

Received: 10 January 2023
Revised: 6 February 2023
Accepted: 7 February 2023
Published: 9 February 2023

1. Introduction

Black soybeans (*Glycine max* (L.) Merr.) are one of the most significant food crops in Asian countries, including Korea, due to the high amount of protein, oil, and chemicals with health benefits in the soybean seeds [1]. Soybean paste and soy sauce are fermented foods that have been proven to have antiaging, anticancer, antibacterial, and antidiabetic properties [2]. In addition, soybeans are a valuable source of nutrition and one of the most important raw materials for vegetable oil as they contain 20% vegetable fat [3]. Soybean oil consists of five major fatty acids: 12% palmitic acid (16:0, PA), 4% stearic acid (18:0, SA), 23% oleic acid (18:1, OA), 53% linoleic acid (18:2, LA), and 8% α-linolenic acid (18:3, LNA) [4]. Furthermore, the alternation of fatty acid profiles affects the physicochemical properties of soybean oil, indicating that fatty acids are a major factor in determining the commercial use of soybean oil [5,6]. In addition to serving as a source of essential fatty acids, soybean oil exhibits pharmacological effects, such as lowering cholesterol levels and preventing cardiovascular diseases. Moreover, soybeans can be used as cosmetic raw materials, biodiesel, and industrial oil [5,7–17]. Soybeans also contain phytochemicals, such as isoflavones, tocopherols, and saponins, as well as antioxidants, including minerals

and vitamins. Consequently, it is widely known that soybeans provide excellent health benefits [18,19].

In Korea, black soybeans with green cotyledons have received attention as a functional food. Black soybeans contain a greater number of biologically functional compounds than yellow commodity soybeans, but they contain very similar nutrients. The seed coats of black soybeans contain pigments known as anthocyanins, which affect the color of the seed coat [20–30]. The seed coats of black soybeans consist of 11 anthocyanins: cyanidin-3-O-glucoside (C3G), delphinidin-3-O-glucoside (D3G), petunidin-3-O-glucoside (Pt3G), peonidin-3-O-glucoside (Pn3G), malvidin-3-O-glucoside (M3G), pelargonidin-3-O-lucoside (Pl3G), cyanidin-3-O-galactoside, cyanidin, catechin-cyanidin-3-O-glucoside, delphinidin-3-O-galactoside, and cyanidin-3-O-galactoside. Among them, the three main anthocyanins in the seed coats of black soybeans are C3G, D3G, and Pt3G [21,22,25,31].

Cotyledons in soybean seeds are green or yellow. Pigments, such as chlorophyll and lutein, play a major role in determining the color of the cotyledons in soybean seeds [32–34]. In general, the cotyledons, leaves, and pods of soybeans are green during the development stages. The plants turn yellow as they reach maturity because the chlorophyll and chloroplast components are decomposed. This is a natural aging process that occurs in various plants, including soybeans, at the maturity stage [35–38]. However, green senescent leaves and green cotyledons of matured seeds have been reported in various crops, and this phenomenon is known as "stay-green" [39–42]. Furthermore, nuclear inheritance and cytoplasmic inheritance have been identified as impairing chlorophyll degradations in soybeans, resulting in the green cotyledons seed trait. *D1* (*Glyma.01g214600* in W82.a2.v1 assembly) and *D2* (*Glyma.11g027400*) are involved in chlorophyll degradation and are nuclear genes inherited by green cotyledons in soybean seeds. Soybeans having double recessive mutations of *D1* and *D2* produce green colored cotyledons [43]. In addition, *cytG* in the chloroplast genome is associated with the decomposition of chlorophyll during senescence [40,43–47]. Lutein, a carotenoid pigment component that protects the photosynthetic system and absorbs light energy, was more abundant in green soybeans than in yellow ones [48,49]. Carotenoids and chlorophyll are biosynthesized in the chloroplast and the metabolisms of the two components are closely linked [50].

Black soybeans with green cotyledons contain anthocyanin, chlorophyll, and lutein, which reduce the risks of cardiovascular diseases and increase anticancer and antioxidant effects [21,51–55]. The seed compositions in soybean seeds are the major factors that determine the availability and use of soybeans. Therefore, it is essential to secure black soybean germplasms by evaluating morphological traits, such as seed size, color, maturity, and length, as well as various nutritional and bioactive substances (protein, fat, anthocyanin, and pigment components). This approach will aid in the development of new cultivars with a high content of functional substances. In the present study, the objective was to analyze the genetic diversity of 469 black soybean germplasms with green cotyledons and with 20 seed composition traits, and this information will be helpful in developing a new black soybean cultivar with green cotyledons.

2. Materials and Methods

2.1. Growth Conditions of Black Soybean Germplasms with Green Cotyledons

To understand the genetic diversity based on the seed composition traits, a collection of 470 soybean accessions, including three check cultivars, was used in this study. The collection consisted of a yellow soybean check cultivar, 'Uram' [56], and 469 black soybean germplasms with green cotyledons, including check cultivars 'Cheongja 3' [57] and 'Cheongja' [58]. Among the 469 black soybean germplasms with green cotyledons, 405 accessions were obtained from the National Agrobiodiversity Center in Jeonju, Republic of Korea, and 47 accessions were derived from the pure line selection of germplasms with different seed characteristics, plant appearance, flowering, and maturity. Fifteen black soybean accessions with green cotyledons were collected from Gyeongsanbuk-do, Republic of Korea. A total of 470 soybean accessions were grown at Gyeongsanbuk-do Agricultural

Research and Extension Service, Daegu, Republic of Korea, over 3 years from 2013 to 2015, and the planting dates were 14 June 2013, 29 May 2014, and 15 June 2015. The planting density was 80 × 15 cm, and each plot was 1.5 m in length (a single row). Each plot was planted with two replications, and two seedlings per hill were grown during the growing season. Finally, each plot was harvested in bulk and combined into one [33,59].

2.2. Seed Composition Analysis

The anthocyanin, chlorophyll, and lutein contents in the black soybean accessions with green cotyledons were determined using the methods described by Jo et al. [59]. The values for chlorophyll *a*, chlorophyll *b*, lutein, and six anthocyanins (D3G, C3G, Pt3G, Pl3G, Pn3G, and M3G) were obtained from our previous studies [33,59].

The fatty acid composition analysis was conducted using the method described by Bilyeu et al. [60], with some modifications. Briefly, 1.5 mL of chloroform:hexane:methanol (8:5:2, $v/v/v$) solution was added to 0.5 g of pulverized sample, followed by extraction at room temperature for 12 h for the fatty acid analysis. Later, 75 µL of a methylating reagent (0.25 M sodium methoxide:petroleum ether:ethyl ether (1:5:2, $v/v/v$)) was added to 100 µL of the extracted solvent, and hexane was added to adjust the total volume to 1 mL. The methylating agent was used to obtain methyl derivatives of fatty acids (fatty acid methyl esters, FAME), decrease polarity, increase volatility, and separate fatty acids more efficiently. A gas chromatography system (7890A, Agilent Technologies Inc., Santa Clara, CA, USA) attached to a flame ionization detector and an Agilent DB-FFAP capillary GC column (30 m × 0.25 mm, 0.25 µm) was used for the qualitative analysis of the fatty acids. The temperature of the sample injector was set to 230 °C and the temperature of the detector was set to 250 °C. The peak areas for the fatty acids were calculated based on standard curves of standard fatty acids (Fame #16, Restek) and the retention time of standard fatty acids.

The crude protein content (% crude protein = % N × 6.25) was calculated with an elemental analyzer (Vario Max CNS, Elementar Analysensysteme GmbH, Langenselbold, Main-Kinzig, Germany) using the Dumas method based on the AOAC method [61]. The pulverized sample (200 mg) was heated to 1200 °C to measure the nitrogen gas and obtain the nitrogen content. The crude fat content was extracted by utilizing a Soxtherm Automated Soxhlet Extraction System (Gerhardt, Königswinter, North Rhine-Westphalia, Germany) according to the AOAC method [61], and petroleum ether was used as the extraction solvent.

The crude fat was extracted with boiling, rinsing, solvent recovery, and drying steps after placing 2 g of the pulverized sample in a cylindrical filter paper, adding 140 mL petroleum ether, and connecting it to the machine. The crude fat content value was calculated as crude fat (%) = (weight of the glass and extracted fat—weight of the empty glass) × (100/sample weight).

2.3. Statistical Analysis

The results from the experiments were statistically analyzed using the SAS package (version 9.4 and Enterprise Guide 7.1, SAS Institute, Inc., Cary, NC, USA) and R analysis (version 3.5.3 and R studio). The principal component analysis (PCA) and the cluster analysis were conducted using the sample correlation matrix for the 468 germplasms, in which the 20 seed composition traits, including crude protein, crude fat, fatty acids, lutein, chlorophyll, and anthocyanin, were studied. Lutein, chlorophyll, and anthocyanin data from our previous studies were used [33,59]. However, one accession (IT186154) was excluded from the PCA and cluster analysis due to missing data for several measured seed compositions. In the principal component analyses, the optimal number of principal components was determined by referring to Kaiser's rule [62] and the Scree test [63]. The PCA was conducted using the SAS PRINCOMP procedure in SAS, and the results of the PCA were analyzed using the ggplot2 package in R software.

K-means cluster analysis was utilized for the cluster analysis in this study. R-square (RSQ) and RSQ/(1-RSQ) values were used as indicators to determine the influence of variables on cluster formation [64], and whether the number of clusters was optimal was determined by using the Cubic Clustering Criterion (CCC) and Pseudo F (PSF) values. The CCC is a statistic indicating the bias degree of clusters under the assumption that observation values follow a uniform distribution. The optimal number of clusters can be confirmed through the CCC distribution based on the change in the number of clusters, and the study shows that the larger CCC value ($\geq$3) provides a better clustering result. PSF is a statistic that measures the degree of clusters, and the higher the PSF value indicates the degree of separation between clusters [65–67]. The SAS' FASTCLUS procedure was utilized for the cluster analysis, and the results were shown on the scatterplots through the SAS' CANDISC and GPLOT procedures.

3. Results and Discussion

3.1. Seed Composition Traits of Black Soybean Germplasms with Green Cotyledons

The results of a statistical analysis of the measured seed composition traits in 470 soybean germplasms, including Cheongja 3, Cheongja, and a yellow soybean cultivar, Uram, are shown in Table 1. The range of crude protein content in the 470 accessions was 35.6–45.8%, with an average of 39.7%. A total of 55 germplasms had <38.0% protein content, whereas 387 germplasms had 38.1–42.0% protein content. A total of 27 germplasms had >42.1% protein content. The mean protein content values of the Cheongja 3, Cheongja, and Uram cultivars were 42.5%, 42.7%, and 40.2%, respectively. Furthermore, the crude fat content in the 470 accessions ranged from 15.9% to 22.4%, with an average of 18.6%. Only 2 black soybean germplasms had <16.0% fat content, whereas 124 germplasms had 16.1–18.0% fat content. A total of 315 germplasms had 18.1–20.0% fat content. A total of 28 germplasms had >20.1% fat content. The fat content values of the Cheongja3, Cheongja, and Uram cultivars were 19.5%, 21.8%, and 18.8%, respectively.

Yellow soybeans have been used as a main ingredient in foods such as tofu, soy sauce, and oil due to their seed color. Although the seed compositions of black soybeans are similar to those of yellow soybeans, the availability of black soybeans is limited. The protein content of 179 black soybeans with green cotyledon accessions was higher than that of Uram. In addition, 191 black soybean accessions had higher fat content than Uram. These black soybeans with green cotyledons containing high amounts of protein or fat can serve as useful genetic materials for expanding the availability of black soybeans.

Regarding the fatty acid compositions, the following results were obtained: PA ranged from 9.4% to 15.3%, with an average of 11.3%; SA ranged from 2.4% to 4.9%, with an average of 3.7%; OA ranged from 13.7% to 40.6%, with an average of 23.1%; LA ranged from 40.2% to 60.2%, with an average of 53.7%; and LNA ranged from 5.2% to 12.3%, with an average of 8.2%. In Cheongja 3, Cheongja, and Uram, the respective PA contents were 13.1%, 12.1%, and 11.1%; the respective SA contents were 4.4%, 3.7%, and 4.8%; the respective OA contents were 21.2%, 22.9%, and 24.4%; the respective LA contents were 54.0%, 53.7%, and 52.0%; and the respective LNA contents were 7.4%, 7.6%, and 7.8%. These results were similar to those of previous studies [5,6,16]. Of the 469 black soybean germplasms with green cotyledons, 10 germplasms contained <10.0% PA, 6 contained >30.0% OA, 16 contained <50.0% LA, 60 contained <7.0% LNA, and 9 contained >10.0% LNA. Altered fatty acid profiles in soybean seeds affect the quality of soybean oil and play a significant role in determining its use. In saturated fatty acids (SFAs), PA acts as a health-threatening compound as it increases the cholesterol content, whereas SA has the least effect on increased cholesterol levels [6,16]. However, PA and SA have the advantage of reducing the generation of trans fats because there is no need for hydrogenation during food processing [4,68]. Since elevated OA content increases the oxidative stability of soybean oil, soybean oils with high OA content can be used in various industries. In addition, OA exhibits excellent health benefits, such as lowering cholesterol levels and preventing cardiovascular diseases and cancer; hence, it is highly useful as a functional food [6,7,9,10,16]. Moreover, higher

amounts of LA (ω-6) and LNA (ω-3) lower the oxidative stability of soybean oil, thereby decreasing its quality. Since ω-6 and ω-3 are essential fatty acids, they have high utility as health foods and can reduce cardiovascular diseases and increase anti-inflammatory and antioxidant functions [6,7,10,13,15–17]. Thus, soybean seeds with altered fatty acid profiles can be used in various food-based industries [6,69].

Table 1. Statistical data for seed composition traits of 469 black soybean germplasms with green cotyledons (including check cultivars 'Cheongja 3' and 'Cheongja'), and a yellow soybean check cultivar, 'Uram', over three years (2013–2015).

Trait	Mean	SD	CV	Maximum	Minimum	Median	PCS	Kurtosis	Uram
Crude protein (%)	39.7	1.5	3.8	45.8	35.6	39.5	0.7	1.3	40.2
Crude fat (%)	18.6	1.0	5.3	22.4	15.9	18.5	0.4	0.8	18.8
Lutein (μg/g)	47.6	2.7	5.7	59.7	42.7	47.3	0.9	1.2	41.6
Chlorophyll a (μg/g)	33.9	15.6	46.0	88.4	11.5	28.6	1.2	0.3	0.0
Chlorophyll b (μg/g)	21.9	5.9	27.0	40.8	7.7	23.5	−0.3	−0.6	0.0
Total chlorophyll (μg/g)	55.8	15.4	27.6	120.0	22.6	54.1	0.7	1.3	0.0
C3G (mg/g)	9.7	4.1	41.8	19.8	1.7	11.2	−0.7	−0.9	0.0
D3G (mg/g)	2.5	0.9	36.8	4.8	0.0	2.7	−1.0	0.5	0.0
Pt3G (mg/g)	0.6	0.3	56.3	1.6	0.0	0.6	0.6	1.1	0.0
Pl3G (mg/g)	0.2	0.1	86.5	0.7	0.0	0.2	0.7	0.1	0.0
Pn3G (mg/g)	0.1	0.0	45.6	0.2	0.0	0.1	−0.6	0.3	0.0
M3G (mg/g)	0.0	0.1	116.6	0.3	0.0	0.0	2.4	5.4	0.0
Total anthocyanin (mg/g)	13.0	5.0	38.6	24.3	2.3	15.0	−0.9	−0.6	0.0
PA (%)	11.3	0.8	6.9	15.3	9.4	11.2	1.5	4.4	11.1
SA (%)	3.7	0.4	9.7	4.9	2.4	3.7	0.2	0.8	4.8
OA (%)	23.1	2.7	11.6	40.6	13.7	22.7	1.4	7.3	24.4
LA (%)	53.7	2.0	3.7	60.2	40.2	54.0	−1.3	7.6	52.0
LNA (%)	8.2	1.0	11.8	12.3	5.2	8.3	−0.1	0.4	7.8
SFA (%)	15.0	0.9	6.1	19.5	12.9	14.8	1.5	4.0	15.8
UFA (%)	85.0	0.9	1.1	87.1	80.5	85.2	−1.5	4.0	84.2

SD: standard deviation; CV: coefficient of variation; PCS: Pearson's coefficient of skewness (PCS > 0, skewed to the right = positively skewed distribution; PCS < 0, skewed to the left = negatively skewed distribution; PCS = 0, normal distribution); K: kurtosis (K > 3, narrow curved; K < 3, broad curved; K = 3, normal distribution); Uram: check cultivar with yellow seed coat and cotyledon; crude protein~crude fat: in the whole seed; lutein~total chlorophyll: in cotyledons removed seed coats; the number of black soybean resources is 469 for lutein and chlorophyll, including check cultivars Cheongja and Cheongja 3; C3G~total anthocyanin: in seed coats (C3G: cyanidin-3-glucoside; D3G: delphinidin-3-glucoside; Pt3G: petunidin-3-glucoside; Pl3G: pelargonidin-3-glucoside; Pn3G: peonidin-3-glucoside; M3G: malvidin-3-galactoside); palmitic acid~unsaturated fatty acid: in the whole seed (PA: palmitic acid; SA: stearic acid; OA: oleic acid; LA: linoleic acid; LNA: α-linolenic acid; SFA: saturated fatty acid; UFA: unsaturated fatty acid).

3.2. Correlation Analysis of Germplasms

The results of a correlation analysis of the seed component traits of black soybean germplasms with green cotyledons is presented in Table 2 and is intended to explain the linear associations between two traits. The anthocyanin, chlorophyll, and lutein contents of the black soybean accessions with green cotyledons were obtained from our previous studies [33,59]. The crude protein content showed significantly negative correlations with chlorophyll *b* ($r = -0.56$, $p < 0.001$), C3G ($r = -0.42$, $p < 0.001$), D3G ($r = -0.43$, $p < 0.001$), and total anthocyanin contents ($r = -0.44$, $p < 0.001$). Kim et al. [12] reported a significant negative correlation between the protein and fat contents of black soybeans ($r = -0.22$ $p < 0.05$). Similarly, Tajuddin et al. [70] reported a negative correlation between protein and fat contents. In the present study, there was a weak negative correlation between crude protein and crude fat contents ($r = -0.22$, $p < 0.001$). Crude fat content showed a significant positive correlation with lutein ($r = 0.37$, $p < 0.001$), chlorophyll *a* ($r = 0.35$, $p < 0.001$), total chlorophyll ($r = 0.34$, $p < 0.001$), and OA ($r = 0.32$, $p < 0.001$) contents. However, crude fat content showed a significant negative correlation with LNA content ($r = -0.38$, $p < 0.001$).

Table 2. Simple linear correlation coefficients for 20 seed composition traits of 469 black soybean germplasms with green cotyledons, including check cultivars 'Cheongja 3' and 'Cheongja', over three years (2013–2015).

Trait	CP	CF	Lut	Chl *a*	Chl *b*	Total Chl	C3G	D3G	Pt3G	Pl3G	Pn3G	M3G	Total Ant	PA	SA	OA	LA	LNA	SFA	UFA
CP	1																			
CF	−0.21 ***	1																		
Lut	−0.11 *	0.37 ***	1																	
Chl *a*	0.14 **	0.35 ***	0.82 ***	1																
Chl *b*	−0.56 ***	−0.04 ns	0.10 *	−0.22 ***	1															
Total Chl	−0.07 ns	0.34 ***	0.86 ***	0.93 ***	0.16 ***															
C3G	−0.42 ***	−0.21 ***	−0.54 ***	−0.74 ***	0.51 ***	−0.56 ***	1													
D3G	−0.43 ***	−0.13 **	−0.31 ***	−0.47 ***	0.61 ***	−0.24 ***	0.63 ***	1												
Pt3G	−0.11 *	−0.17 ***	−0.52 ***	−0.69 ***	0.25 ***	−0.60 ***	0.61 ***	0.65 ***	1											
Pl3G	−0.42 ***	−0.17 ***	−0.34 ***	−0.48 ***	0.46 ***	−0.31 ***	0.65 ***	0.43 ***	0.27 ***	1										
Pn3G	−0.22 ***	−0.08 ns	−0.46 ***	−0.62 ***	0.43 ***	−0.46 ***	0.71 ***	0.56 ***	0.71 ***	0.38 ***	1									
M3G	0.11 *	−0.10 *	−0.44 ***	−0.55 ***	−0.03 ns	−0.56 ***	0.37 ***	0.28 ***	0.89 ***	0.03 ns	0.58 ***	1								
Total Ant	−0.44 ***	−0.29 ***	−0.54 ***	−0.75 ***	0.56 ***	−0.55 ***	0.99 ***	0.75 ***	0.69 ***	0.65 ***	0.74 ***	0.42 ***	1							
PA	0.12 *	0.07 ns	0.07 ns	0.13 **	−0.08 ns	0.10 *	−0.17 ***	−0.10 *	−0.10 *	−0.07 ns	−0.12 *	−0.08 ns	−0.16 ***	1						
SA	0.22 ***	−0.08 ns	−0.06 ns	0.01 ns	−0.05 ns	−0.01 ns	−0.10 *	0.02 ns	0.07 ns	−0.20 ***	−0.06 ns	0.11 *	−0.08 ns	0.16 ***	1					
OA	0.15 **	0.32 ***	0.38 ***	0.47 ***	−0.43 ***	0.31 ***	−0.42 ***	−0.43 ***	−0.26 ***	−0.42 ***	−0.31 ***	−0.05 ns	−0.45 ***	−0.21 ***	−0.09 ns	1				
LA	−0.14 **	−0.26 ***	−0.33 ***	−0.41 ***	0.39 ***	−0.27 ***	0.36 ***	0.41 ***	0.25 ***	0.37 ***	0.29 ***	0.07 ns	0.39 ***	−0.06 ns	−0.02 ns	−0.92 ***	1			
LNA	−0.29 ***	−0.38 ***	−0.40 ***	−0.56 ***	0.48 ***	−0.38 ***	0.58 ***	0.43 ***	0.26 ***	0.55 ***	0.39 ***	0.02 ns	0.58 ***	−0.15 **	−0.22 ***	−0.69 ***	0.54 ***	1		
SFA	0.18 ***	0.03 ns	0.04 ns	0.12 *	−0.09 ns	0.09 ns	−0.18 ***	−0.08 ns	−0.06 ns	−0.14 **	−0.13 **	−0.02 ns	−0.17 ***	0.92 ***	0.53 ***	−0.21 ***	−0.07 ns	−0.21 ***	1	
UFA	−0.18 ***	−0.03 ns	−0.04 ns	−0.12 *	0.09 ns	−0.09 ns	0.18 ***	0.08 ns	0.06 ns	0.15 **	0.13 **	0.02 ns	0.17 ***	−0.92 ***	−0.53 ***	0.21 ***	0.07 ns	0.21 ***	−1.00 ***	1

CP: crude protein; CF: crude fat; Lut: lutein; Chl a: chlorophyll a; Chl b: chlorophyll b; Total Chl: total chlorophyll; C3G: cyanidin-3-glucoside; D3G: delphinidin-3-glucoside; Pt3G: petunidin-3-glucoside; Pl3G: pelargonidin-3-glucoside; Pn3G: peonidin-3-glucoside; M3G: malvidin-3-galactoside; Total Ant: total anthocyanin; PA: palmitic acid; SA: stearic acid; OA: oleic acid; LA: linoleic acid; LNA: α-linolenic acid; SFA: saturated fatty acid; UFA: unsaturated fatty acid. *** Significant at the 0.001 probability level. ** Significant at the 0.01 probability level. * Significant at the 0.05 probability level. NS: non-significance.

The correlation between lutein and chlorophyll demonstrates that lutein showed a highly significant positive correlation with chlorophyll *a* ($r = 0.82$, $p < 0.001$) and total chlorophyll content ($r = 0.86$, $p < 0.001$). Monma et al. [49] also reported that there was a correlation between lutein content and total chlorophyll content. The significant correlation between lutein and chlorophyll is a result of their biosyntheses and metabolisms being closely linked [50]. However, despite this close correlation, chlorophyll *b* seems to have a weak positive correlation with lutein and a negative correlation with chlorophyll *a*. However, the scatterplots below show that there were three divided groups (arrows) showing positive correlations (Figure 1). These results could be due to the involvement of genetic traits in green cotyledons, which are divided into germplasms with nuclear inheritance (*d1d2*) and cytoplasmic inheritance (*cytG*) [59]. Studies have reported that black soybeans with nuclear inheritance (*d1d2*) show higher total chlorophyll content than soybeans with cytoplasmic inheritance (*cytG*), and that the values of chlorophyll *a*/*b* are higher in the composition ratio [32,45,59].

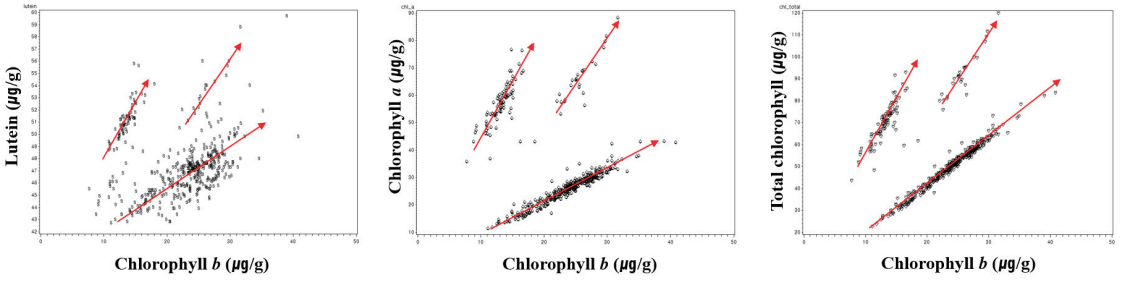

Figure 1. Scatterplots showing positive correlations between chlorophyll *b* and lutein, chlorophyll *b* and chlorophyll *a*, and chlorophyll *b* and total chlorophyll in 469 black soybean germplasms with green cotyledons, including check cultivars 'Cheongja 3' and 'Cheongja', over three years (2013–2015).

The total anthocyanin content, including C3G, showed significantly negative correlations with lutein (r = –0.54, $p < 0.001$), chlorophyll *a* ($r = -0.75$, $p < 0.001$), and total chlorophyll ($r = -0.55$, $p < 0.001$) contents and significantly positive correlations with chlorophyll *b* content ($r = 0.56$, $p < 0.001$). Furthermore, according to previous studies, anthocyanin and chlorophyll are closely linked in the biosynthesis stage in poinsettia leaves and apple peels [71–73].

In addition, lutein and chlorophyll had no significant correlation with PA and SA, which are SFAs. However, OA, which is a monounsaturated fatty acid, showed a significant positive correlation with lutein ($r = 0.38$, $p < 0.001$), chlorophyll *a* ($r = 0.47$, $p < 0.001$), and total chlorophyll content ($r = 0.31$, $p < 0.001$), but it showed a significant negative correlation with chlorophyll *b* ($r = -0.43$, $p < 0.001$). Conversely, LA and LNA showed a significant negative correlation with lutein ($r = -0.33$, $r = -0.40$, $p < 0.001$), chlorophyll *a* ($r = -0.41$, $r = -0.56$, $p < 0.001$), and total chlorophyll content ($r = -0.27$, $r = -0.38$, $p < 0.001$). However, LA and LNA showed a significant positive correlation with chlorophyll *b* ($r = 0.39$, $r = 0.48$, $p < 0.001$). These results are supported by other studies on the correlations between lutein and fatty acid compositions [74]. During the embryogenesis of "green seeds" such as soybeans, Arabidopsis, and rapeseed seeds, the genes involved in photosynthesis and fatty acid synthesis pathways are very tightly linked, resulting in controlled chlorophyll and fatty acid synthesis [75,76].

In the correlation analysis of anthocyanin components, C3G showed a highly significant positive correlation with D3G ($r = 0.63$, $p < 0.001$), Pt3G ($r = 0.61$, $p < 0.001$), and Pn3G ($r = 0.71$, $p < 0.001$). Furthermore, D3G showed a highly significant positive correlation with C3G ($r = 0.63$, $p < 0.001$), Pt3G ($r = 0.65$, $p < 0.001$), and Pn3G ($r = 0.56$, $p < 0.001$). In addition, Pt3G showed a highly significant positive correlation with Pn3G ($r = 0.71$, $p < 0.001$) and M3G ($r = 0.89$, $p < 0.001$). These results support the hypothesis that the anthocyanin pigments should show a highly significant positive correlation with each other [77]. However, Pl3G, Pn3G, and M3G showed statistically weak correlations with the components due to the small amounts of anthocyanin components they contain. In addition, since C3G has the highest content, the correlation analysis between total anthocyanin content and other component traits showed a trend similar to that of C3G.

The correlations between fatty acid compositions indicated that SFA and unsaturated fatty acid (UFA) showed a highly significant negative correlation ($r = -1.00$, $p < 0.001$). However, SFA (PA and SA) showed a weak negative correlation with OA and LA. OA showed a highly significant negative correlation with LA ($r = -0.92$, $p < 0.001$) and LNA ($r = -0.69$, $p < 0.001$). In addition, a highly significant positive correlation was shown between LA and LNA ($r = 0.54$, $p < 0.001$). These results are consistent with those of previous studies [5,78,79].

3.3. Principal Component Analysis

A PCA was conducted on 469 germplasms with 20 seed composition traits using a sample correlation matrix (Table 3). The anthocyanin, chlorophyll, and lutein contents in black soybean accessions with green cotyledons were obtained from our previous PCA study (Jo et al. 2021; Lee et al. 2021). Furthermore, the four principal components were the most important components in determining variations in the 469 soybean germplasms based on the criterion of Kaiser [62] and the Scree plot. The four components accounted for 76.2% of the total variations. The first principal component had an eigenvalue of 7.5477 and a 37.7% rate of contribution to the total variation. The second principal component had an eigenvalue of 3.2648 and a contribution rate of 16.3%. The third principal component had an eigenvalue of 2.6188 and a contribution rate of 13.0%. The fourth principal component had an eigenvalue of 1.8189 and a contribution rate of 9.0% (Table 3).

Table 3. Eigenvalues and proportions of principal components to 20 quantitative traits of 468 black soybean germplasms with green cotyledons, including check cultivars 'Cheongja 3' and 'Cheongja'.

Principal Component	Eigenvalue	Difference	Proportion	Cumulative
1	7.5477	4.2829	0.3774	0.3774
2	3.2648	0.6460	0.1632	0.5406
3	2.6188	0.7999	0.1309	0.6716
4	1.8189	0.7363	0.0909	0.7625
5	1.0826	0.2485	0.0541	0.8166
6	0.8341	0.1371	0.0417	0.8583
7	0.6970	0.2301	0.0349	0.8932
8	0.4669	0.0507	0.0233	0.9165
9	0.4163	0.0381	0.0208	0.9374
10	0.3782	0.0856	0.0189	0.9563
11	0.2925	0.0670	0.0146	0.9709
12	0.2255	0.0152	0.0113	0.9822
13	0.2103	0.0815	0.0105	0.9927
14	0.1288	0.1136	0.0064	0.9991
15	0.0152	0.0130	0.0008	0.9999
16	0.0021	0.0019	0.0001	1.0000
17	0.0002	0.0002	0.0000	1.0000
18	0.0001	0.0000	0.0000	1.0000
19	0.0000	0.0000	0.0000	1.0000
20	0.0000	0.0000	0.0000	1.0000

Table 4 shows the correlations between these 4 principal components and the 20 component traits. The first principal component showed a positive correlation with chlorophyll *b*, total anthocyanin, C3G, LNA, LA, and UFAs, whereas it showed a negative correlation with crude protein, crude fat, lutein, chlorophyll *a*, total chlorophyll, PA, SA, OA, and SFA. In particular, total anthocyanin (0.337) and C3G (0.325) were the phenotypic measurements with the biggest positive contributions to the first principal component, whereas chlorophyll *a* (−0.319) contributed negatively to the first principal component. The second principal component showed a highly positive correlation with the total SFAs (0.516), PA (0.452), and SA (0.325) (Table 4). The second principal component showed a highly negative correlation with the total unsaturated fatty acids (−0.516). Chlorophyll *b*, total chlorophyll content, and crude protein were correlated with the third principal component. The fourth principal component showed a highly positive correlation with crude fat and OA, and a negative correlation with LA and LNA.

In this study, the first and second principal components explained 54.0% of the black soybean germplasms with green cotyledons. Figure 2 presents a scatter plot showing the first principal component against the second principal component. On the upper side of the horizontal axis, black soybean germplasms with high total UFA are present, whereas on the lower side, black soybean germplasms with high total SFA are present. The results indicate that C3G and total anthocyanin positively contributed to the PCA plot consisting

of principal components 1 and 2, whereas lutein, chlorophyll *a*, total chlorophyll, and OA contributed negatively.

Table 4. The 4 principal components among 20 seed composition traits of 468 black soybean germplasms with green cotyledons, including check cultivars 'Cheongja 3' and 'Cheongja'.

Trait	Principal Component (Eigenvectors)			
	1	2	3	4
Crude protein	−0.127	0.176	−0.335	−0.267
Crude fat	−0.122	−0.081	0.086	0.413
Lutein	−0.248	−0.141	0.273	0.202
Chlorophyll *a*	−0.319	−0.085	0.181	0.083
Chlorophyll *b*	0.185	−0.086	0.413	0.179
Total chlorophyll	−0.252	−0.119	0.341	0.152
C3G	0.325	−0.028	0.047	0.119
D3G	0.263	0.003	0.166	0.219
Pt3G	0.274	0.096	−0.211	0.287
Pl3G	0.238	−0.062	0.206	−0.052
Pn3G	0.279	0.024	−0.057	0.257
M3G	0.183	0.122	−0.362	0.285
Total anthocyanin	0.337	−0.016	0.057	0.156
PA (16:0)	−0.077	0.452	0.185	0.067
SA (18:0)	−0.034	0.325	−0.032	0.075
OA (18:1)	−0.220	−0.192	−0.275	0.330
LA (18:2)	0.208	0.052	0.212	−0.338
LNA (18:3)	0.255	−0.059	0.189	−0.298
SFA	−0.080	0.516	0.145	0.089
UFA	0.080	−0.516	−0.146	−0.089

C3G: cyanidin-3-glucoside; D3G: delphinidin-3-glucoside; Pt3G: petunidin-3-glucoside; Pl3G: pelargonidin-3-glucoside; Pn3G: peonidin-3-glucoside; M3G: malvidin-3-galactoside; PA: palmitic acid; SA: stearic acid; OA: oleic acid; LA: linoleic acid; LNA: α-linolenic acid; SFA: saturated fatty acid; UFA: unsaturated fatty acid. The underlined values are the traits that showed a higher correlation with the principal component.

3.4. Cluster Analysis with Seed Composition Traits

The anthocyanin, chlorophyll, and lutein contents in the black soybean accessions with green cotyledons were obtained from our previous cluster analysis study [33,59]. A K-means cluster analysis was performed on 469 black soybean germplasms with green cotyledons to classify them into 4 clusters. In addition, this study used CCC and PSF values to determine the appropriate number of clusters. Furthermore, based on the CCC and PSF values for the population (*K*) numbers from 2 to 6, the highest CCC value was 26 and the highest PSF value was 655 when *K* was 4, indicating that the 469 black soybean germplasms in this study were divided into 4 clusters (Table 5). In addition, a canonical discriminant analysis with *K* = 4 revealed that cluster 1 is the smallest group, consisting of 10 germplasms, which is 2.1% of the total number of germplasms. Cluster 2 consisted of 108 germplasms, which is 23.1% of the total number of germplasms. Cluster 3 is the largest group, containing 254 germplasms, which is 54.3% of the total number of germplasms. Cluster 4 consisted of 96 germplasms, which is 20.5% of the total number of germplasms (Figure 3, Table S1). Our previous study revealed that there were four clusters of black soybean accessions with green cotyledons based on their agronomic traits [33]. However, genotypic data from 470 soybean accessions with 6 K single nucleotide polymorphic loci determined 3 clusters based on PCA and phylogenetic tree analyses [59].

Chlorophyll *a*, total chlorophyll, and total anthocyanin had relatively higher R-square (RSQ) and RSQ/(1-RSQ) values than other traits (Table 5). The results of the present study revealed that chlorophyll *a*, total chlorophyll, and total anthocyanin greatly contributed to the classification of the clusters. Furthermore, chlorophyll *a* showed the highest RSQ/(1-RSQ) value (9.7482), suggesting that it had the greatest influence on cluster classification in these black soybean germplasms. The black soybean germplasms in cluster 1 had higher

crude fat, lutein, chlorophyll *a*, chlorophyll *b*, and total chlorophyll contents than the other clusters, whereas the C3G content in cluster 1 was significantly lower than that in clusters 2 and 3 (Figure 4). Clusters 2 and 3 were located closest to each other (Figure 4), indicating that the black soybean germplasms included in these two clusters showed a similar pattern of measured seed compositions in this study. The black soybean germplasms in clusters 2 and 3 had the highest anthocyanin (e.g., C3G) content, whereas they had lower lutein, chlorophyll *b*, and total chlorophyll contents than the other clusters (Figure 4). Figure 5 shows fatty acid profiles in four clusters of distribution. Cluster 1 had significantly higher PA content than clusters 2 and 3. However, there was no significant difference in SA content among the clusters. Clusters 2 and 3 had relatively high LNA content. Cluster 4 had the highest OA content and the lowest LA and LNA contents.

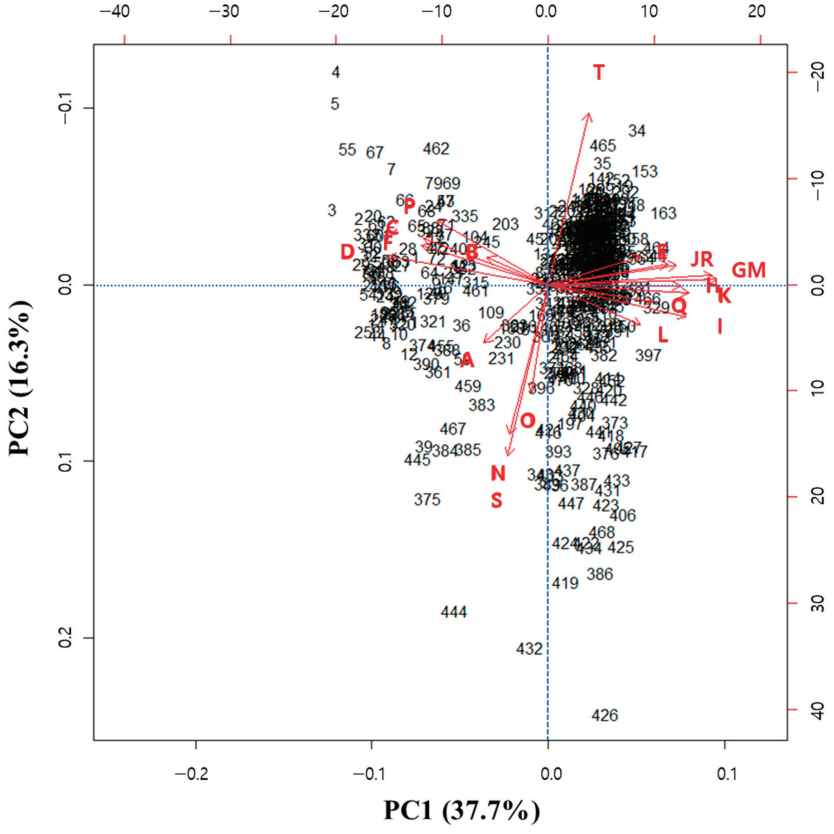

Figure 2. Scatterplot of principal component 1 (PC1: 37.7%) and principal component 2 (PC2: 16.3%) based on 20 seed composition traits of 468 black soybean germplasms with green cotyledons, including check cultivars 'Cheongja 3' and 'Cheongja'. A: crude protein; B: crude fat; C: lutein; D: chlorophyll a; E: chlorophyll b; F: total chlorophyll; G: C3G (cyanidin-3-glucoside); H: D3G (delphinidin-3-glucoside); I: Pt3G (petunidin-3-glucoside); J: Pl3G (pelargonidin-3-glucoside); K: Pn3G (peonidin-3-glucoside); L: M3G (malvidin-3-galactoside); M: total anthocyanin; N: palmitic acid; O: stearic acid; P: oleic acid; Q: linoleic acid; R: α-linolenic acid; S: saturated acid; T: unsaturated acid.

Table 5. Statistical variables for clusters of 20 seed composition traits of 468 black soybean germplasms with green cotyledons, including check cultivars 'Cheongja 3' and 'Cheongja'.

Variable	Total SD	within SD	R-Square	RSQ/(1-RSQ)
Crude protein	1.5157	1.3176	0.2492	0.3319
Crude fat	0.9748	0.9065	0.1408	0.1638
Lutein	2.7305	1.6903	0.6193	1.6265
Chlorophyll *a*	15.6020	4.7743	0.9070n	9.7482
Chlorophyll *b*	5.9057	4.1003	0.5210	1.0879
Total chlorophyll	15.4317	6.4765	0.8250	4.7141
C3G	4.0595	2.4189	0.6472	1.8348
D3G	0.9037	0.6641	0.4635	0.8638
Pt3G	0.3145	0.2241	0.4957	0.9831
Pl3G	0.1413	0.1112	0.3847	0.6251
Pn3G	0.0292	0.0213	0.4718	0.8933
M3G	0.0459	0.0363	0.3780	0.6077
Total anthocyanin	5.0218	2.8425	0.6817	2.1413
PA (16:0)	0.7834	0.7757	0.0259	0.0266
SA (18:0)	0.3627	0.3632	0.0037	0.0037
OA (18:1)	2.6856	2.2171	0.3228	0.4767
LA (18:2)	1.9999	1.7277	0.2585	0.3486
LNA (18:3)	0.9684	0.7336	0.4299	0.7540
SFA	0.9111	0.9037	0.0224	0.0229
UFA	0.9116	0.9043	0.0222	0.0227
Overall	5.4053	2.3687	0.8092	4.2412
Pseudo F Statistic = 655.97				
Cubic Clustering Criterion (CCC) = 26.025				

Total SD: standard deviation for the total sample; Within SD: pooled within cluster standard deviation; R-Square: for predicting the variable from the cluster; RSQ/(1-RSQ): the ratio of between-cluster variance to within-cluster variance ($R^2/(1-R^2)$); Pseudo F Statistic: estimating the number of clusters; Cubic Clustering Criterion (CCC): computed under the assumption that the variables are uncorrelated; C3G: cyanidin-3-glucoside; D3G: delphinidin-3-glucoside; Pt3G: petunidin-3-glucoside; Pl3G: pelargonidin-3-glucoside; Pn3G: peonidin-3-glucoside; M3G: malvidin-3-galactoside; PA: palmitic acid; SA: stearic acid; OA: oleic acid; LA: linoleic acid; LNA: α-linolenic acid; SFA: saturated fatty acid; UFA: unsaturated fatty acid.

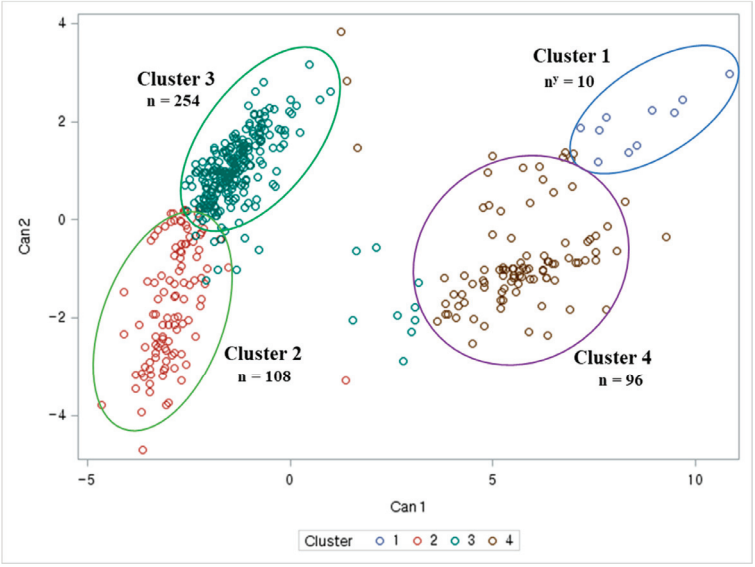

Figure 3. The 4 clusters based on 5 principal components of 468 black soybean germplasms with green cotyledons, including check cultivars 'Cheongja 3' and 'Cheongja'. Can: canonical variables; n: number of resources in each cluster.

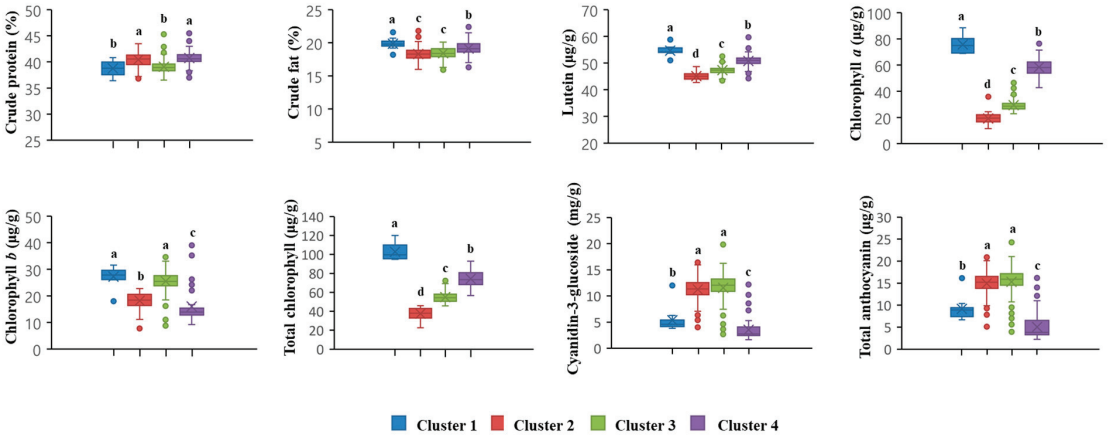

Figure 4. Box plots of crude protein, crude fat, lutein, chlorophylls, and anthocyanins in 4 clusters of 468 black soybean germplasms with green cotyledons, including check cultivars 'Cheongja' and 'Cheongja 3'. The letters above the bars are statistically different based on the least square difference.

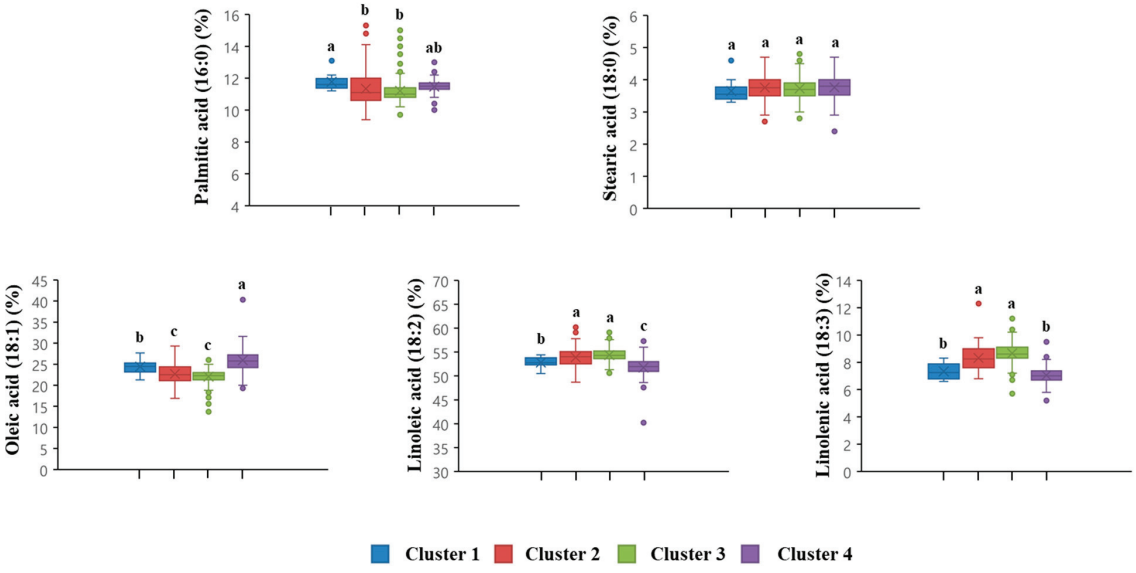

Figure 5. Box plots of fatty acids in 4 clusters of 468 black soybean germplasms with green cotyledons, including check cultivars 'Cheongja 3' and 'Cheongja'. The letters above the bars are statistically different based on the least square difference.

Anthocyanin, lutein, and chlorophyll are major antioxidants in black soybean germplasms with green cotyledons [20–30]. Furthermore, OA prevents cardiovascular diseases, and LNA is an ω-3 fatty acid directly related to brain health [5,6]. Black soybeans with high levels of anthocyanin, lutein, chlorophyll, OA, and LNA are highly utilized as raw materials for preparing healthy foods [6,7,9,10,13,15,21,30,51–55,80]. Protein in soybean seeds is one of the most important sources of vegetable protein. From a nutritional perspective, a combination of higher protein and anthocyanins can provide novel functional foods with desirable health benefits. However, we did not discover a black soybean germplasm with high protein and anthocyanin content in this study, so this could be a breeding goal. There has been a change in the consumer perception of black soybeans with green cotyledons.

Therefore, the development of new black soybean cultivars with green cotyledons and with altered seed compositions is warranted. This study provides useful information for improving seed composition in soybean breeding programs.

4. Conclusions

Black soybeans with green cotyledons contain anthocyanin, chlorophyll, and lutein, which reduce the risks of cardiovascular diseases and increase anticancer and antioxidant effects [21,51–55]. Therefore, it is essential to secure black soybean germplasms with green cotyledons by evaluating various nutritional and bioactive substances. This study analyzed the genetic diversity of 469 black soybean germplasms with green cotyledons and with 20 seed composition traits. Twenty seed composition traits were analyzed to conduct correlation analysis, principal component analysis (PCA), and cluster analysis, which indicated that black soybean germplasms were divided into four clusters. Black soybean germplasms in cluster 1 had higher crude fat, lutein, chlorophyll *a*, chlorophyll *b*, and total chlorophyll contents, but lower C3G content than those in clusters 2 and 3. However, germplasms in clusters 2 and 3 had the highest C3G content. Moreover, germplasms in cluster 1 had significantly higher PA content than those in clusters 2 and 3. Germplasms in clusters 2 and 3 had relatively high LNA content. Germplasms in cluster 4 had the highest OA content. This study highlights the genetic diversity of black soybean germplasms with different seed composition traits, and the results of this study can be beneficial for soybean breeding programs, enabling them to develop new black soybean cultivars with green cotyledons and improved seed composition traits.

Supplementary Materials: The following supporting information can be downloaded at: https://www.mdpi.com/article/10.3390/agriculture13020406/s1, Figure S1: Calibration curves of anthocyain (D3G, C3G, Pt3G, Pl3G, Pn3G, M3G) for the anaylsis of black soybean germplasms with green cotyledon. D3G: delphinidin-3-glucoside, C3G: cyanidin-3-glucoside, Pt3G: petunidin-3-glucoside, Pl3G: pelargonidin-3-glucoside, Pn3G: peonidin-3-glucoside, M3G: malvidin-3-galactoside. Table S1: Four clusters based on 20 seed composition traits of 468 black soybean accessions including two checks (Cheongja 3, and Cheongja) by K-means cluster analysis.

Author Contributions: Conceptualization, J.-D.L.; methodology, J.Y.L., C.K.S. and J.S.B.; formal analysis, J.Y.L. and H.J.; writing—original draft preparation, J.Y.L. and H.J.; writing—review and editing, H.J., C.K.S., J.S.B. and J.-D.L.; supervision, J.-D.L. All authors have read and agreed to the published version of the manuscript.

Funding: This work was carried out with the support of the "Cooperative Research Program for Agriculture Science and Technology Development (Project No. PJ01416803)", Rural Development Administration, Republic of Korea.

Institutional Review Board Statement: Not applicable.

Data Availability Statement: The datasets generated during this study are available from the corresponding author on reasonable request.

Acknowledgments: The authors would like to acknowledge the personnel from the Plant Genetics and Breeding Lab at the Kyungpook National University and the Gyeongsangbuk-do Provincial Agricultural Research and Extension Service for their time and work on the field experiments.

Conflicts of Interest: The authors declare no conflict of interest.

References

1. Lee, C.Y.; Choi, M.S.; Kim, H.T.; Yun, H.T.; Lee, B.; Chung, Y.S.; Kim, R.W.; Choi, H.K. Soybean [*Glycine max* (L.) Merrill]: Importance as a crop and pedigree reconstruction of Korean varieties. *Plant Breed. Biotech.* **2015**, *3*, 179–196. [CrossRef]
2. Sanjukta, S.; Rai, A.K. Production of bioactive peptides during soybean fermentation and their potential health benefits. *Trends Food Sci. Tech.* **2016**, *50*, 1–10. [CrossRef]
3. Goldsmith, P.D. Economics of soybean production, marketing, and utilization. In *Soybeans: Chemistry, Production, and Utilization*; AOCS Press: Urbana, IL, USA, 2015; pp. 117–150. [CrossRef]
4. Fehr, W.R. Breeding for modified fatty acid composition in soybean. *Crop Sci.* **2007**, *47*, 72–87. [CrossRef]

5. Choung, M.G. Variation of oil contents and fatty acid compositions in Korean soybean germplasms. *Korean J. Crop Sci.* **2006**, *51*, 139–145.
6. Lee, J.D.; Bilyeu, K.D.; Shannon, J.G. Genetics and breeding for modified fatty acid profile in soybean seed oil. *J. Crop Sci. Biotech.* **2007**, *10*, 201–210.
7. Asif, M. Health effects of omega-3,6,9 fatty acids: *Perilla frutescens* is a good example of plant oils. *Orient Pharm. Exp. Med.* **2011**, *11*, 51–59. [CrossRef]
8. Cahoon, E.B. Genetic enhancement of soybean oil for industrial uses: Prospects and challenges. *AgBioForum* **2003**, *6*, 11–13.
9. Chang, N.W.; Huang, P.C. Effects of the ratio of polyunsaturated and monounsaturated fatty acid to saturated fatty acid on rat plasma and liver lipid concentrations. *Lipids* **1998**, *33*, 481–487. [CrossRef]
10. De Jong, A.J.; Kloppenburg, M.; Toes, R.E.; Ioan-Facsinay, A. Fatty acids, lipid mediators, and T-cell function. *Front. Immunol.* **2014**, *5*, 483. [CrossRef]
11. Gerde, J.A.; White, P.J. Lipid. In *Soybeans: Chemistry, Production, and Utilization*; Johnson, L.A., White, P.J., Galloway, R., Eds.; AOCS Press: Urbana, IL, USA, 2015; pp. 193–227. [CrossRef]
12. Kim, S.L.; Lee, Y.H.; Chi, H.Y.; Lee, S.J.; Kim, S.J. Diversity in lipid contents and fatty acid composition of soybean seeds cultivated in Korea. *Korean J. Crop Sci.* **2007**, *52*, 348–357.
13. Kris-Etherton, P.M.; Harris, W.S.; Appel, L.J. Fish consumption, fish oil, omega-3 fatty acids, and cardiovascular disease. *Arterioscler. Thromb. Vas.* **2003**, *23*, 20–30. [CrossRef]
14. Neff, W.E. Oxidative stability of natural and randomized high palmitic-and high-stearic-acid oils from genetically modified soybean varieties. *J. Am. Oil Chem. Soc.* **1999**, *76*, 825–831. [CrossRef]
15. Wall, R.; Ross, R.P.; Fitzgerald, G.F.; Stanton, C. Fatty acids from fish: The anti-inflammatory potential of long-chain omega-3 fatty acids. *Nutr. Rev.* **2010**, *68*, 280–289. [CrossRef]
16. Wilson, R.F. Seed composition. In *Soybeans: Improvement, Production and Uses*, 3rd ed.; Boerma, H.R., Specht, J.E., Eds.; ASA, CSSA, SSSA: Madison, WI, USA, 2004; pp. 621–629. [CrossRef]
17. Zhu, X.; Wang, B.; Zhang, X.; Chen, X.; Zhu, J.; Zou, Y.; Li, J. Alpha-linolenic acid protects against lipopolysaccharide-induced acute lung injury through anti-inflammatory and anti-oxidative pathways. *Microb. Pathogenesis* **2020**, *142*, 104077. [CrossRef]
18. Barnes, S. Evolution of the health benefits of soy isoflavone. *Proc. Soc. Exp. Biol. Med.* **1998**, *217*, 386–392. [CrossRef]
19. Tomomatsu, H. Health effects of oligosaccharides. *Food Technol.* **1994**, *48*, 61–65.
20. Astadi, I.R.; Astuti, M.; Santoso, U.; Nugraheni, P.S. In vitro antioxidant activity of anthocyanins of black soybean seed coat in human low density lipoprotein (LDL). *Food Chem.* **2009**, *112*, 659–663. [CrossRef]
21. Cho, K.M.; Ha, T.J.; Lee, Y.B.; Seo, W.D.; Kim, J.Y.; Ryu, H.W.; Jeong, S.H.; Kang, Y.M.; Lee, J.H. Soluble phenolics and antioxidant properties of soybean (*Glycine max* L.) cultivars with varying seed coat colors. *J. Funct. Foods* **2013**, *5*, 1065–1076. [CrossRef]
22. Choung, M.G.; Baek, I.Y.; Kang, S.T.; Han, W.Y.; Shin, D.C.; Moon, H.P.; Kang, K.H. Isolation and determination of anthocyanins in seed coats of black soybean (*Glycine max* (L.) Merr.). *J. Agric. Food Chem.* **2001**, *49*, 5848–5851. [CrossRef]
23. Correa, C.R.; Li, L.; Aldini, G.; Carini, M.; Chen, C.Y.O.; Chun, H.K.; Cho, S.M.; Park, K.M.; Russell, R.M.; Blumberg, J.B.; et al. Composition and stability of phytochemicals in five varieties of black soybeans (*Glycine max*). *Food Chem.* **2010**, *123*, 1176–1184. [CrossRef]
24. Dajanta, K.; Janpum, P.; Leksing, W. Antioxidant capacities, total phenolics and flavonoids in black and yellow soybeans fermented by *Bacillus subtilis*. A comparative study of Thai fermented soybeans (*thuanao*). *Int. Food Res. J.* **2013**, *20*, 3125–3132.
25. Lee, J.H.; Kang, N.S.; Shin, S.O.; Shin, S.H.; Lim, S.G.; Suh, D.Y.; Baek, I.Y.; Park, K.Y.; Ha, T.J. Characterisation of anthocyanins in the black soybean (*Glycine max* L.) by HPLC-DAD-ESI/MS analysis. *Food Chem.* **2009**, *112*, 226–231. [CrossRef]
26. Lee, K.J.; Lee, J.R.; Ma, K.H.; Cho, Y.H.; Lee, G.A.; Chung, J.W. Anthocyanin and isoflavone contents in Korean black soybean landraces and their antioxidant activities. *Plant Breed. Biotech.* **2016**, *4*, 441–452. [CrossRef]
27. Lee, K.J.; Baek, D.Y.; Lee, G.A.; Cho, G.T.; So, Y.S.; Lee, J.R.; Ma, K.H.; Chung, J.W.; Hyun, D.Y. Phytochemicals and antioxidant activity of Korean black soybean (*Glycine max* L.) landraces. *Antioxidants* **2020**, *9*, 213. [CrossRef]
28. Todd, J.J.; Vodkin, L.O. Pigmented soybean (*Glycine max*) seed coats accumulate proanthocyanins during development. *Plant Physiol.* **1993**, *102*, 663–670. [CrossRef]
29. Xu, B.; Chang, S.K.C. Antioxidant capacity of seed coat, dehulled bean, and whole black soybeans in relation to their distributions of total phenolics, phenolic acids, anthocyanins, and isoflavones. *J. Agric. Food Chem.* **2008**, *56*, 8365–8373. [CrossRef]
30. Yamashita, Y.; Wang, L.; Nakamura, A.; Nanba, F.; Saito, S.; Toda, T.; Nakagawa, J.; Ashida, H. Black soybean improves the vascular function through an increase in nitric oxide and a decrease in oxidative stress in healthy women. *Arch. Biochem. Biophys.* **2020**, *688*, 108408. [CrossRef]
31. Choi, Y.M.; Yoon, H.; Lee, S.; Ko, H.C.; Shin, M.J.; Lee, M.C.; Hur, O.S.; Ro, N.Y.; Desta, K.T. Isoflavones, anthocyanins, phenolic content, and antioxidant activities of black soybeans (*Glycine max* (L.) Merrill) as affected by seed weight. *Sci. Rep.* **2020**, *10*, 1–13. [CrossRef]
32. Kang, S.T.; Seo, M.J.; Moon, J.K.; Yun, H.T.; Lee, Y.H.; Kim, S.J.; Hwang, Y.S.; Lee, S.K.; Choung, M.G. Introduction of stay green mutant for the development of black seed coat and green cotyledon soybean variety. *Korean J. Crop Sci.* **2010**, *55*, 187–194.
33. Lee, J.Y.; Choi, H.J.; Son, C.K.; Bae, J.S.; Jo, H.; Lee, J.D. Genetic diversity of black soybean germplasms with green cotyledons based on agronomic traits and cotyledon pigments. *Korean J. Breed. Sci.* **2021**, *53*, 127–139. [CrossRef]

34. Sinnecker, P.; Gomes, M.S.O.; Arêas, J.A.; Lanfer-Marquez, U.M. Relationship between color (Instrumental and visual) and chlorophyll contents in soybean seeds during ripening. *J. Agric. Food Chem.* **2002**, *50*, 3961–3966. [CrossRef]
35. Crookston, R.K.; Hill, D.S. A visual indicator of the physiological maturity of soybean seed. *Crop Sci.* **1978**, *18*, 867–870. [CrossRef]
36. Nooden, L.D. The phenomena of senescence and aging. In *Senescence and Aging in Plants*; Noodén, L.D., Leopold, A.C., Eds.; Academic Press: San Diego, CA, USA, 1988; pp. 2–50. [CrossRef]
37. Noodén, L.D.; Guiamét, J.J.; John, I. Senescence mechanisms. *Physiol. Plant.* **1997**, *101*, 746–753. [CrossRef]
38. Okatan, Y.; Kahanak, G.M.; Noodén, L.D. Characterization and kinetics of soybean maturation and monocarpic senescence. *Physiol. Plant.* **1981**, *52*, 330–338. [CrossRef]
39. Cha, K.W.; Lee, Y.J.; Koh, H.J.; Lee, B.M.; Nam, Y.W.; Paek, N.C. Isolation, characterization, and mapping of the stay green mutant in rice. *Theor. Appl. Genet.* **2002**, *104*, 526–532. [CrossRef]
40. Park, S.Y.; Yu, J.W.; Park, J.S.; Li, J.; Yoo, S.C.; Lee, N.Y.; Lee, S.K.; Jeong, S.W.; Seo, H.S.; Koh, H.J. The senescence-induced staygreen protein regulates chlorophyll degradation. *Plant Cell* **2007**, *19*, 1649–1664. [CrossRef]
41. Thomas, H.; Smart, C.M. Crops that stay green 1. *Ann. Appl. Biol.* **1993**, *123*, 193–219. [CrossRef]
42. Thomas, H.; Howarth, C.J. Five ways to stay green. *J. Exp. Bot.* **2000**, *51*, 329–337. [CrossRef]
43. Fang, C.; Li, C.; Li, W.; Wang, Z.; Zhou, Z.; Shen, Y.; Wu, M.; Wu, Y.; Li, G.; Kong, L.A. Concerted evolution of D1 and D2 to regulate chlorophyll degradation in soybean. *Plant J.* **2014**, *77*, 700–712. [CrossRef]
44. Guiamet, J.J.; Teeri, J.A.; Nooden, L.D. Effects of nuclear and cytoplasmic genes altering chlorophyll loss on gas exchange during monocarpic senescence in soybean. *Plant Cell Physiol.* **1990**, *31*, 1123–1130.
45. Guiamet, J.J.; Schwartz, E.; Pichersky, E.; Noodén, L.D. Characterization of cytoplasmic and nuclear mutations affecting chlorophyll and chlorophyll-binding proteins during senescence in soybean. *Plant Physiol.* **1991**, *96*, 227–231. [CrossRef]
46. Ott, A.; Yang, Y.; Bhattacharyya, M.; Horner, H.T.; Palmer, R.G.; Sandhu, D. Molecular mapping of D1, D2 and ms5 revealed linkage between the cotyledon color locus D2 and the male-sterile locus ms5 in soybean. *Plants* **2013**, *2*, 441–454. [CrossRef]
47. Palmer, R.; Pfeiffer, T.W.; Buss, G.R.; Kilen, T.C. Qualitative genetics. In *Soybeans: Improvement, Production, and Uses*, 3rd ed.; Boerma, H.R., Specht, J.E., Eds.; ASA, CSSA, SSSA: Madison, WI, USA, 2004; pp. 137–233. [CrossRef]
48. Gitelson, A.A.; Keydan, G.P.; Merzlyak, M.N. Three-band model for noninvasive estimation of chlorophyll, carotenoids, and anthocyanin contents in higher plant leaves. *Geophys. Res. Lett.* **2006**, *33*, L11402. [CrossRef]
49. Monma, M.; Terao, J.; Ito, M.; Saito, M.; Chikuni, K. Carotenoid components in soybean seeds varying with seed color and maturation stage. *Biosci. Biotech. Bioch.* **1994**, *58*, 926–930. [CrossRef]
50. Brotosudarmo, T.H.P.; Limantara, L.; Chandra, R.D.; Heriyanto. Chloroplast pigments: Structure, function, assembly and characterization. In *Plant Growth and Regulation-Alterations to Sustain Unfavorable Conditions*; IntechOpen: London, UK, 2018; pp. 43–80.
51. Granado, F.; Olmedilla, B.; Blanco, I. Nutritional and clinical relevance of lutein in human health. *Brit. J. Nutr.* **2003**, *90*, 487–502. [CrossRef]
52. İnanç, A.L. Chlorophyll: Structural properties, health benefits and its occurrence in virgin olive oils. *Acad. Food J. Akad. GIDA* **2011**, *9*, 26–32.
53. Kizhedath, A.; Suneetha, V. Estimation of chlorophyll content in common household medicinal leaves and their utilization to avail health benefits of chlorophyll. *J. Pharm. Res.* **2011**, *4*, 1412–1413.
54. Landrum, J.T.; Bone, R.A. Lutein, zeaxanthin, and the macular pigment. *Arch. Biochem. Biophys.* **2001**, *385*, 28–40. [CrossRef]
55. Zhang, R.F.; Zhang, F.X.; Zhang, M.W.; Wei, Z.C.; Yang, C.Y.; Zhang, Y.; Tang, X.J.; Deng, Y.Y.; Chi, J.W. Phenolic composition and antioxidant activity in seed coats of 60 Chinese black soybean (*Glycine max* L. Merr.) varieties. *J. Agric. Food Chem.* **2011**, *59*, 5935–5944. [CrossRef]
56. Ko, J.M.; Han, W.Y.; Kim, H.T.; Lee, Y.H.; Choi, M.S.; Lee, B.W.; Shin, S.U.; Seo, J.H.; Oh, K.W.; Yun, H.T.; et al. Soybean cultivar for soy-paste, 'Uram' with mechanization harvesting, large seed, disease resistance and high yield. *Korean J. Breed. Sci.* **2016**, *48*, 301–306. [CrossRef]
57. Yun, H.T.; Park, K.Y.; Moon, J.K.; Kim, Y.H.; Kim, S.L.; Ku, J.H.; Lee, Y.H.; Ryu, Y.H.; Baek, I.Y.; Han, W.Y.; et al. A new black soybean cultivar, Cheongja 3, with green cotyledon, medium-late maturity and high anthocyanin. *Korean J. Breed. Sci.* **2005**, *37*, 261–262.
58. Baek, I.Y.; Kang, S.T.; Shin, D.C.; Choung, M.G.; Han, W.Y.; Kwack, Y.H.; Moon, H.P. A new black soybean variety with green cotyledon, early maturity and large seed size "Cheongjakong". *Korean J. Breed. Sci.* **2001**, *33*, 240–241.
59. Jo, H.; Lee, J.Y.; Cho, H.T.; Choi, H.J.; Son, C.K.; Bae, J.S.; Bilyeu, K.; Song, J.T.; Lee, J.D. Genetic diversity of soybeans (*Glycine max* (L.) merr.) with black seed coats and green cotyledons in Korean germplasm. *Agronomy* **2021**, *11*, 581. [CrossRef]
60. Bilyeu, K.; Palavalli, L.; Sleper, D.; Beuselinck, P. Mutations in soybean microsomal omega-3 fatty acid desaturase genes reduce linolenic acid concentration in soybean seeds. *Crop Sci.* **2005**, *45*, 1830–1836. [CrossRef]
61. Association of Official and Analytical Chemists (AOAC). *Official Methods of Analysis*, 18th revision ed.; AOAC: Rockville, MD, USA, 2011.
62. Kaiser, H.F. The application of electronic computers to factor analysis. *Educ. Psychol. Meas.* **1960**, *20*, 141–151. [CrossRef]
63. Cattell, R.B. The screen test for the number of factors. *Multivar. Behav. Res.* **1966**, *1*, 245–276. [CrossRef]
64. Ryo, H.C. A study on the categorization of the strategy group of program provider (PP). *J. Korean Data Inf. Sci. Soc.* **2008**, *19*, 913–924.

65. Caliński, T.; Harabasz, J. A dendrite method for cluster analysis. *Commun. Stat.-Theor. M.* **1974**, *3*, 1–27. [CrossRef]
66. Cooper, M.C.; Milligan, G.W. The effect of measurement error on determining the number of clusters in cluster analysis. In *Data, Expert Knowledge and Decisions*; Gaul, W., Schader, M., Eds.; Springer: Berlin/Heidelberg, Germany, 1988; pp. 319–328. [CrossRef]
67. Milligan, G.W.; Cooper, M.C. An examination of procedures for determining the number of clusters in a data set. *Psychometrika* **1985**, *50*, 159–179. [CrossRef]
68. Hunter, J.E.; Zhang, J.; Kris-Etherton, P.M. Cardiovascular disease risk of dietary stearic acid compared with trans, other saturated, and unsaturated fatty acids: A systematic review. *Am. J. Clin. Nutr.* **2010**, *91*, 46–63. [CrossRef]
69. Cardinal, A.J.; Burton, J.W.; Camacho-Roger, A.M.; Yang, J.H.; Wilson, R.F.; Dewey, R.E. Molecular analysis of soybean lines with low palmitic acid content in the seed oil. *Crop Sci.* **2007**, *47*, 304–310. [CrossRef]
70. Tajuddin, T.; Watanabe, S.; Yamanaka, N.; Harada, K. Analysis of quantitative trait loci for protein and lipid contents in soybean seeds using recombinant inbred lines. *Breed. Sci.* **2003**, *53*, 133–140. [CrossRef]
71. Downs, R.J.; Siegelman, H.W.; Butler, W.L.; Hendricks, S.B. Photoreceptive pigments for anthocyanin synthesis in apple skin. *Nature* **1965**, *205*, 909–910. [CrossRef]
72. Kannangara, C.G.; Hansson, M. Arrest of chlorophyll accumulation prior to anthocyanin formation in *Euphorbia pulcherrima*. *Plant Physiol. Bioch.* **1998**, *36*, 843–848. [CrossRef]
73. Slatnar, A.; Mikulic-Petkovsek, M.; Veberic, R.; Stampar, F.; Schmitzer, V. Anthocyanin and chlorophyll content during poinsettia bract development. *Sci. Hortic.* **2013**, *150*, 142–145. [CrossRef]
74. Lee, J.D.; Shannon, J.G.; So, Y.S.; Sleper, D.A.; Nelson, R.L.; Lee, J.H.; Choung, M.G. Environmental effects on lutein content and relationship of lutein and other seed components in soybean. *Plant Breed.* **2009**, *128*, 97–100. [CrossRef]
75. Wu, X.L.; Liu, Z.H.; Hu, Z.H.; Huang, R.Z. BnWRI1 coordinates fatty acid biosynthesis and photosynthesis pathways during oil accumulation in rapeseed. *J. Integr. Plant Biol.* **2014**, *56*, 582–593. [CrossRef]
76. Ruuska, S.A.; Schwender, J.; Ohlrogge, J.B. The capacity of green oilseeds to utilize photosynthesis to drive biosynthetic processes. *Plant Physiol.* **2004**, *136*, 2700–2709. [CrossRef]
77. Joo, Y.H.; Park, J.H.; Choung, M.G.; Yun, S.G.; Chung, K.W. Variation of contents and color difference of anthocyanin by different cultivation year in black soybean seed. *Korean J. Crop Sci.* **2004**, *49*, 507–511.
78. Liu, K.; Orthoefer, F.; Brown, E.A. Association of seed size with genotypic variation in the chemical constituents of soybeans. *J. Am. Oil Chem. Soc.* **1995**, *72*, 189–192. [CrossRef]
79. Yoon, T.H.; Im, K.J.; Kim, D.H. Fatty acid composition of lipids obtained from Korean soybean varieties. *Korean J. Food Sci. Technol.* **1984**, *16*, 375–382.
80. Adhvaryu, A.; Erhan, S.Z.; Perez, J.M. Preparation of soybean oil-based greases: Effect of composition and structure on physical properties. *J. Agric. Food Chem.* **2004**, *52*, 6456–6459. [CrossRef]

agriculture

MDPI

Article

Genetic Variability and Population Structure of Pakistani Potato Genotypes Using Retrotransposon-Based Markers

Asim Mehmood [1,*], Peter M. Dracatos [2,*], Linta Maqsood [1], Qudsia Yousafi [1], Abrar Hussain [1], Muhammad J. Jaskani [3], Muhammad W. Sajid [1], Muhammad S. Haider [4] and Muhammad M. Hussain [5]

[1] Department of Biosciences, COMSATS University Islamabad, Sahiwal Campus, COMSATS Road off GT Road, Sahiwal 57000, Pakistan
[2] Department of Animal, Plant and Soil Sciences, La Trobe University, Bundoora 3086, Australia
[3] Institute of Horticultural Sciences, University of Agriculture, Faisalabad 38040, Pakistan
[4] Department of Horticulture, Ghazi University, Dera Ghazi Khan 32200, Pakistan
[5] Potato Research Institute, Sahiwal 57000, Pakistan
* Correspondence: assim_324@cuisahiwal.edu.pk (A.M.); p.dracatos@latrobe.edu.au (P.M.D.)

Abstract: Molecular germplasm characterization is essential for gathering information on favorable attributes and varietal improvement. The current study evaluated the genetic divergence and population structure of 80 potato genotypes collected from Punjab, Pakistan, using polymorphic retrotransposon-DNA-based markers (iPBS). A total of 11 iPBS primers generated 787 alleles with a mean value of 8.9 alleles per primer, of which ~95% were polymorphic across the 80 genotypes. Different variation attributes, such as mean expected heterozygosity (H = 0.21), mean unbiased expected heterozygosity (μHe = 0.22), and mean Shannon's information index (I = 0.32), showed the existence of sufficient genetic diversity in the studied potato genotypes. Analysis of molecular variance (AMOVA) showed that genetic variation within the population was higher (84%) than between populations (16%). A neighbor-joining tree was constructed based on the distance matrices that arranged the 80 genotypes into five distinct groups, and the genotypes FD61-3 and potato 2 had the highest genetic distance. A STRUCTURE analysis corroborated the dendrogram results and distributed the 80 genotypes also into five clusters. Our results determined that retrotransposon-based markers are highly polymorphic and could be used to evaluate genetic diversity between local and exotic potato genotypes. The genotypic data and population structure dissection analysis reported in this study will enhance potato varietal improvement and development.

Keywords: molecular characterization; varietal improvement; heterozygosity; neighbor-joining tree

Citation: Mehmood, A.; Dracatos, P.M.; Maqsood, L.; Yousafi, Q.; Hussain, A.; Jaskani, M.J.; Sajid, M.W.; Haider, M.S.; Hussain, M.M. Genetic Variability and Population Structure of Pakistani Potato Genotypes Using Retrotransposon-Based Markers. *Agriculture* **2023**, *13*, 185. https://doi.org/10.3390/agriculture13010185

Academic Editors: Edyta Paczos-Grzeda, Volker Mohler and Sylwia Sowa

Received: 27 November 2022
Revised: 31 December 2022
Accepted: 4 January 2023
Published: 11 January 2023

1. Introduction

Among food crops, potato (*Solanum tuberosum* L.) is considered a vital staple food cultivated commercially across temperate and sub-tropical regions [1]. Global potato production was recently estimated at over 370 million metric tons annually and is cultivated over more than 17 million hectares [2]. Potatoes were first grown in modern-day southern Peru and northwestern Bolivia from 5000 to 8000 BC [1]. China is the leading producer of potatoes and produces approximately 22% of global potato production, followed by India, Russia, Ukraine, and the United States [3]. It is estimated that potato is cultivated in Pakistan on approximately 185,360 hectares, with an average production of 4.5 million tons annually, and it is extensively grown in the Punjab region [4].

The potato genome has 12 chromosomes and is an autopolyploid, having different ploidy states, including diploid (2 × n = 24), triploid (3 × n = 36), tetraploid (24 × n = 48), pentaploid (5 × n = 60), and hexaploid (6 × n = 72). The population structure and genetic characterization of potatoes has been well characterized relative to other solanaceous plants [5,6]. Determining the extent and distribution of genetic divergence in distinct gene pools, evaluating germplasm collections, and improving the efficient preservation and

management approaches are all critical factors for successful potato breeding programs. Conventionally, varietal characterization is conducted by assessing morphological traits; however, physical characteristics are often influenced by environmental variability, epistatic interactions, and pleiotropic effects, which restrict only a few traits, leading to low levels of polymorphism [7]. Inherent molecular variation in plant genomes makes it possible to establish and utilize genetic differences between various taxonomic groups, which assists researchers in assessing genetic diversity in gene pools of interest.

Commonly, DNA-based molecular markers are utilized to explore genetic diversity both within and between different crop plant species [8]. The inter-priming binding sites (iPBS) are a retrotransposon-based marker system based in the amplification of a target region incorporated through reverse transcriptase primer binding sites of two adjacent retrotransposons that are in opposite and anti-parallel directions [9]. The iPBS method uses a universal tRNA for primer binding and, therefore, does not rely on pre-defined sequence information, making it an attractive cost-effective proposition for efficient genotyping [10]. The iPBS method has been used for genetic diversity analysis in several crop species, such as date palm, guava, okra, beans, peas, and tobacco [11–16]. The iPBS markers have also been used extensively in genetic diversity studies of Turkish potatoes [17]. Earlier research has confirmed the universality of iPBS markers for molecular and phylogenetic studies and reported that iPBS markers are powerful tools for assessing genetic diversity [11,14,17]. Moreover, iPBS markers have been shown to be consistently more polymorphic than SSR markers [17].

The Pakistani potato is the only germplasm characterized on a morphological basis [18]. Previously, five cultivars were also evaluated for genetic diversity using RAPD markers [19]. These studies suggest that most Pakistani potato accessions need further genetic characterization, to provide vital information for potential use in local breeding programs. The current study has been designed to determine the relationship between the population structure and genetic diversity of 80 potato accessions sourced from the Punjab region in Pakistan using iPBS retrotransposon-based markers. This study will improve the efficacy of incorporating desired traits, such as disease/stress resistance, yield, and environmental adaptability.

2. Materials and Methods

2.1. Plant Material and Genomic DNA Extraction

We collected 80 potato accessions from the Potato Research Institute, Sahiwal; all genotypes and passport data are listed in Table 1. DNA The was extracted from 16-day-old potato leaves using a modified CTAB method [20]. The DNA quality was checked using gel electrophoresis (1% agarose), and quantity was measured with a known λ-DNA concentration.

Table 1. Details of 80 potato (*Solanum tuberosum* L.) genotypes collected from the Potato Research Institute Sahiwal used for genetic diversity analysis in this study.

Accession	Variety Name	Source	Cross	Morphological Characters (Color, Shape, Eyes)
LS 1	FD44-26	Local Strains	385270-163 × Dura	Dark red, oblong, shallow
LS 2	FD48-4	Local Strains	384640-3 × 385270-163	Red, round
LS 3	FD48-54	Local Strains	384640-3 × 385270-163	White, round, shallow
LS 4	FD61-3	Local Strains	Diamant × FD12-24	White, round, shallow
LS 5	FD63-4	Local Strains	384636-1 × FD1-8	White, round, deep
LS 6	FD69-2	Local Strains	FD4-2 × SH-5	Dark red, round, deep
LS 7	FD71-1	Local Strains	FD8-3 × ultimas	Red, round/oval, medium
LS 8	FD73-75	Local Strains	FD35-36 × SH-5	Red, round, shallow
LS 9	FD73-77	Local Strains	FD35-36 × SH-5	Red, round, deep

Table 1. *Cont.*

Accession	Variety Name	Source	Cross	Morphological Characters (Color, Shape, Eyes)
LS 10	FD74-19	Local Strains	9619 × FD49-28	White, round, shallow
LS 11	FD74-33	Local Strains	9619 × FD49-28	White, oblong, shallow
LS 12	FD74-40	Local Strains	9619 × FD49-28	White, round, medium
LS 13	FD74-47	Local Strains	9619 × FD49-28	White, round, deep
LS 14	FD74-50	Local Strains	9619 × FD49-28	White, oval, shallow
LS 15	FD74-51	Local Strains	9619 × FD49-28	White, oblong, shallow
LS 16	FD75-3	Local Strains	FD49-28 × SH-5	White, round, shallow
LS 17	FD75-55	Local Strains	FD49-28 × SH-5	Red, round, deep
LS 18	FD76-13	Local Strains	FD3-15 × SH- 5	Red, oblong, medium
LS 19	FD76-27	Local Strains	FD3-15 × SH- 5	Red, oblong, shallow
LS 20	FD76-35	Local Strains	FD3-15 × SH- 5	Dark red, oblong, shallow
LS 21	FD76-48	Local Strains	FD3-15 × SH- 5	White, round, shallow
LS 22	FD77-62	Local Strains	FD3-9 × SH-5	Dark red, oblong, deep
LS 23	FD80-6	Local Strains	FD3-15 × FD35-36	Light red, round, deep
LS 24	FD51-5	Local Strains	Dura × SH-5	White, round, shallow
LS 25	SL 1-4	Local strains	SH-5 × Red fantasy	Red, oblong, medium
LS 26	SL 1-47	Local strains	SH-5 × Red fantasy	Red, oblong, shallow
LS 27	SL 4-26	Local strains	FD48-4 × SH-5	Dark red, oblong, deep
LS 28	SL13-64	Local strains	SH -5 × FD 48- 54	Red, oblong, shallow
LS 29	SL 13-78	Local strains	FD51-5 × FD69-1	White, oblong, shallow
LS 30	SL14-15	Local strains	Saghitta × SH-5	Red, round, deep
LC 31	FSD white	Local Cultivar	————————	White, round, shallow
LC 32	FSD red	Local Cultivar	————————	Red, round, deep
LC 33	Sadaf	Local Cultivar	FD3-15 × FD35-36	White, round, shallow
LC 34	Ruby	Local Cultivar	384636-1 × FD1-8	Dark red, round, shallow
LC 35	PRI Red	Local Cultivar	FD44-24 × FD12-24	Red, oblong, shallow
NARC 36	Potato 3	NARC Cultivar	————————	————————
NARC 37	Potato2	NARC Cultivar	————————	————————
NARC 38	NARC	NARC Cultivar		
NARC 39	N-13	NARC Cultivar	————————	Light yellow, oval, medium
NARC 40	N-15	NARC Cultivar	————————	Light red, oval, medium
NARC 41	N-18	NARC Cultivar	————————	Light red, oval, medium
NARC 42	N-34	NARC Cultivar	————————	White, oval, medium
NARC 43	N-2005-1	NARC Cultivar	————————	Red, oval, medium
NARC 44	N-2005-4	NARC Cultivar		
NARC 45	N-393619-44	NARC Cultivar	————————	Light red, round, deep
NARC 46	N-4	NARC Cultivar	————————	White, round, medium
EC 47	Aurea	Exotic Cultivar	Lady Rosetta × (Satruna × Pentland dell)	White, round, medium
EC 48	Dolly	Exotic Cultivar	Lady Rosetta × Britta	Light red, round, deep
EC 49	Elbieda	Exotic Cultivar	————————	White, oval, shallow
EC 50	Elodie	Exotic Cultivar	80F66.25 × 81F145.14	White, oval, shallow

Table 1. *Cont.*

Accession	Variety Name	Source	Cross	Morphological Characters (Color, Shape, Eyes)
EC 51	Eldorodo	Exotic Cultivar	————————	Red, oval, medium
EC 52	Estima	Exotic Cultivar	Nopol × G3014	Light yellow, oval, medium
EC 53	El-mundo	Exotic Cultivar	————————	White, oval, medium
EC 54	Erora	Exotic Cultivar	————————	White, oval, medium
EC 55	Paramount	Exotic Cultivar	Janat × Dutch seeding	Red, oval, medium
EC 56	Hybrid 202-05-01	Exotic Cultivar	———————-	Light red, oval, medium
EC 57	Simply red	Exotic Cultivar	Asterix × HZ86 AM75	Light red, oblong, medium
EC 58	Santana	Exotic Cultivar	Spunta × VK69-491	White, oblong, shallow
EC 59	Romera	Exotic Cultivar	Belladonna × Laura	Light red, oval, medium
EC 60	Monika	Exotic Cultivar	Krasa × Velox	White, oval, medium
EC 61	Verdi	Exotic Cultivar	Tomnsa × Diana	White, oval, medium
EC 62	Safrane	Exotic Cultivar	————————	White, oval, medium
EC 63	Terka	Exotic Cultivar	Fabula × Pamir	Light yellow, round, shallow
EC 64	Red Valentine	Exotic Cultivar	Mondial × Amadeus	Red, oval, medium
EC 65	Red Sonia	Exotic Cultivar	————————	Red, oval, medium
EC 66	Red Sun	Exotic Cultivar	Inova × Amadeus	Red, oblong, medium
EC 67	Rositta	Exotic Cultivar	———————-	Light red, oval, medium
EC 68	Sagitta	Exotic Cultivar	Gallia × RZ-86-2918	Light yellow, oblong, medium
EC 69	Suzen	Exotic Cultivar	————————	White, oval, medium
EC 70	Sassy	Exotic Cultivar	G82TTT37 × Propmesse	White, round, medium
EC 71	Focus	Exotic Cultivar	Agria × Bru 82-78	Light yellow, round, shallow
EC 72	Florice	Exotic Cultivar	Fanette × Inra72.68.5	Light yellow, oblong, medium
EC 73	HZD-04-684	Exotic Cultivar	————————	Red, oval, shallow
EC 74	Shepody	Exotic Cultivar	Bake king × F58050	White, oval, medium
EC 75	Orchestra	Exotic Cultivar	Maradonna × Cupido	Light yellow, oval, medium
EC 76	Jitka	Exotic Cultivar	M22/12 × Bonita	Light yellow, round, medium
EC 77	Red river	Exotic Cultivar	————————	Red, oval, medium
EC 78	Kuroda	Exotic Cultivar	AR76-199-3 × Konst80-1407	Red, oval, medium
EC 79	KWS-06-125	Exotic Cultivar	————-	Dark red, oval, medium
EC 80	Pirol	Exotic Cultivar	Agriax × 1.214.226-84	

Abbreviations are as follows: LS, local strains; LC, local cultivars; NARC, National Agriculture Research Centre; EC, exotic cultivars.

2.2. Amplification Profile of Retrotransposon-Based iPBS Primers

Initially, 16 iPBS primers (detailed in Table 2) previously developed and characterized by Kalender et al. [9] were assessed for their polymorphism and utility. A total of 11 primers that gave clear polymorphic bands were selected for molecular profiling of the 80 potato accessions detailed in Table 1. Here, PCR reactions were performed in 20 µL reactions consisting of 11.5 µL double-distilled H_2O, 2 µL 10× Taq buffer with (NH_2) SO_4, (Thermo Scientific, Waltham, MA, USA), 2 µL (20 mM) $MgCl_2$ (Thermo Scientific), 1 µL (2 mM) dNTPs (Deoxyribonucleotide triphosphate), 1 µL iPBS primer (Macrogen, Seoul, Republic of Korea), 0.5 µL Taq polymerase (Thermo Scientific), and 2 µL (10 ng) template DNA. The PCR conditions involved an initial denaturation cycle of 5 min at 94 °C, 35 cycles for 1 min at 94 °C, 1 min at an annealing temperature range between 30–50 °C, 2 min at the temperature of 72 °C, then a final extension of 10 min at a temperature of 72 °C, and storage temperature of 4 °C for 1 hour.

Table 2. List of 16 inter-primer binding site (iPBS) retrotransposon primers with their sequence and annealing temperature used in this study.

Serial No	iPBS Primers	Base Pair Sequence (5′-3′)	Annealing Temp (°C)	GC Content (%)
1	2257	CTCTCAATGAAAGCACCA	46	44
2	2229	CGACCTGTTCTGATACCA	46	50
3	2252	TCATGGCTCATGATACCA	43	44
4	2277	GGCGATGATACCA	46	54
5	2375	TCGCATCAACCA	30	50
6	2376	TAGATGGCACCA	46	50
7	2387	GCGCAATACCCA	46	58
8	2391	ATCTGTCAGCCA	46	50
9	2374	CCCAGCAAACCA	30	58
10	2377	ACGAAGGGACCA	46	67
11	2383	GCATGGCCTCCA	46	66
12	2232	AGAGAGGCTCGGATACCA	48	56
13	2239	ACCTAGGCTCGGATGCCA	50	61
14	2272	GGCTCAGATGCCA	46	62
15	2373	GCTCATCATGCCA	46	54
16	2390	GCAACAACCCCA	46	58

The iPBS primers by Kalender et al. [9] were used in the initial screening.

2.3. Band Counting and Statistical Measurement

To confirm band pattern uniformity, three experimental replicates were performed for each PCR for all iPBS markers on the potato accessions. The PCR bands were examined using a 2% agarose gel using a transilluminator and were scored manually; only clear visible bands were scored with the assumption that bands of the same size represented the same single locus. A binary matrix was constructed for the presence of an allele on a specific locus denoted as '1', and for the absence of an allele marked as '0' for a particular locus. To estimate the polymorphism of each dominant marker, polymorphic information content (PIC) was calculated as PIC = $1 - [f^2 + (1 - f)^2]$, where 'f' indicates the frequency of the marker in the data set. Statistical parameters, such as Shannon's information index (I), heterozygosity (He), unbiased heterozygosity (μHe), number of different alleles, number of effective alleles, and principal coordinate analysis (PCoA), were calculated using GeneAlex 6.5 [21]. The binary matrix was imported to construct a neighbor-joining (NJ) tree using MEGA 7.0.14 [22]. The model-based software STRUCTURE v. 2.3.4 created the population structure and allocated individual genotypes to sub-populations [23]. A Bayesian approach was applied to determine the population structure of the potato genotypes used in this study. Data from 11 distinct iPBS markers were analyzed using STRUCTURE software; using the value of K (10 runs at each K), the highest number of clusters was estimated by running combination data among the population and allelic frequency of 10,000 steps followed by 50,000 simulations of a Monte Carlo Markov chain (MCMC). The most probable K value was determined by measuring the assessed data of log probability of LnP(D), and the value of ΔK was calculated for the rate of change in LnP(D) between consecutive K-values [24]. We used the STRUCTURE HARVESTER for computational analysis of 80 potato accessions based on iPBS markers, and the maximum number of Ln Pr (X | K) was selected for bar plots among all 10 independent runs [25].

3. Results

3.1. Molecular Assessment of iPBS Markers

The 11 primers detailed in Table 3 gave stable, precise, and polymorphic PCR amplicons, and were subsequently selected for further genetic analysis of the 80 potato accessions. The banding pattern of the PCR products of 80 potato genotypes using iPBS primer 2252 is shown in Figure 1. The highest polymorphic band size of 1800 bp was obtained in Ruby and N-34 genotypes for primer 2229. Across 11 primers, 787 alleles were identified, out of which 752 were polymorphic, showing 96% polymorphism. Primer 2229 amplified the

highest number of bands (60), and primers 2390 and 2391 amplified the lowest number of bands (25). The highest PIC value amongst the 11 polymorphic iPBS markers was marker 2277 (0.39), whereas marker 2391 had the lowest PIC value of 0.14 (Table 3). The highest values of Shannon's information index (I = 0.48), heterozygosity (He = 0.33), and unbiased expected heterozygosity (μHe = 0.34) was observed for marker 2229.

Table 3. Detection of polymorphism and summary statistics for mean values of 11 iPBS primers used to assess genetic diversity among 80 potato genotypes.

iPBS Primers	AN	Size Range (bp)	PM	% PM	MM	PIC	Na	Ne	I	He	μHe	f
2229	86	500–2000	85	99	1	0.37	1.83	1.58	0.48	0.33	0.34	0.45
2232	86	550–1350	86	100	0	0.33	1.61	1.40	0.36	0.24	0.25	0.46
2239	86	600–1500	80	93	6	0.24	1.45	1.37	0.33	0.22	0.23	0.35
2252	86	650–2000	85	99	1	0.25	1.63	1.38	0.35	0.23	0.24	0.39
2272	84	500–1750	79	94	5	0.19	0.67	1.11	0.12	0.07	0.08	0.13
2277	80	450–1000	80	100	0	0.39	1.71	1.54	0.45	0.31	0.32	0.47
2374	82	400–1250	60	73	22	0.22	1.25	1.15	0.19	0.11	0.11	0.14
2375	80	350–3500	65	81	15	0.25	1.23	1.2	0.23	0.14	0.14	0.17
2377	83	300–3500	75	90	8	0.36	1.75	1.52	0.44	0.3	0.31	0.45
2390	85	280–1000	80	94	5	0.36	1.66	1.57	0,47	0.32	0.34	0.54
2391	75	250–1000	60	80	15	0.14	1.07	1.08	0.13	0.07	0.07	0.81

Abbreviations are as follows: AN, allelic number; PM, number of polymorphic bands; MM, number of monomorphic bands; PIC, polymorphic information content; Na, number of different alleles; Ne, number of effective alleles; I, Shannon's information index: He, heterozygosity; μHe, unbiased expected heterozygosity; f, frequency.

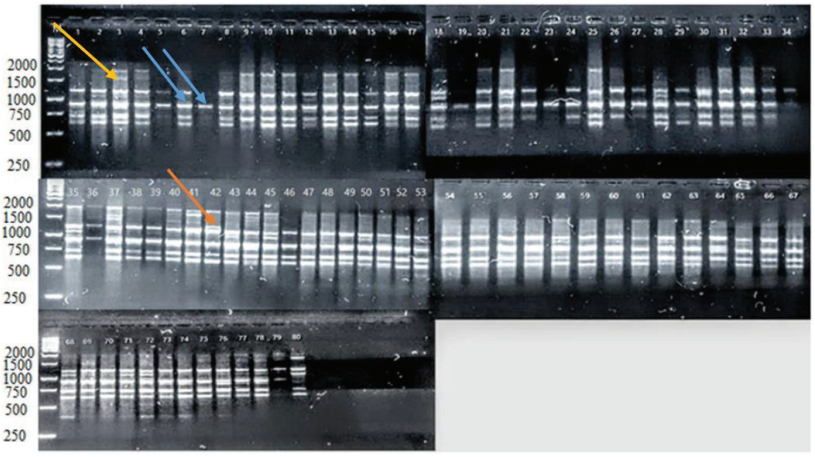

Figure 1. The banding pattern of PCR products of 80 potato genotypes using 2252 iPBS primers. Well 1 includes a 1 kb size ladder, wells 2–30 include local strains, wells 31–35 are local cultivars, wells 36–46 represent NARC accessions, and wells 47–80 contain exotic cultivars. Yellow-colored arrows point to polymorphic alleles of sizes 1700 bp, and blue-colored arrows point to monomorphic alleles of size 900 bp, while the orange color represents a unique allele of size 1300 bp.

3.2. Heterozygosity and Molecular Variance (AMOVA) of 80 Potato Genotypes

Shannon's information index (I) ranged from 0.29 (NARC) to 0.37 (EC), with an average of 0.32. Expected heterozygosity (He) ranged from 0.18 (NARC) to 0.24 (EC) with an average value of 0.21, and the unbiased heterozygosity (μHe) ranged between 0.19 (NARC) and 0.24 (EC) with an average value of 0.22 (Table 4). Among all populations, the population of ECs (exotic cultivars) showed the highest Shannon's information index (0.37), expected heterozygosity (0.24), and unbiased expected heterozygosity (0.24), while genotypes from

the NARC population showed the lowest Shannon's information index (0.29), expected heterozygosity (0.19), and unbiased expected heterozygosity (0.19). The genotypes included in the EC population had the highest genetic distance from the genotypes of the local strain population, local cultivar population, and NARC population.

Table 4. The summary of statistical analysis of genetic diversity across 80 potato genotypes based on 11 iPBS primers.

Groups	N	Na	Ne	I	He	μHe
LS	30	1.56	1.36	0.34	0.22	0.22
LC	5	1.11	1.35	0.29	0.2	0.22
NARC	11	1.36	1.30	0.29	0.19	0.19
EC	34	1.75	1.39	0.37	0.24	0.24
Mean	20	1.45	1.35	0.32	0.21	0.22

Abbreviations are as follows: N, number of sample size; Na, number of different alleles; Ne, number of effective alleles; I, Shannon's information index: He, heterozygosity; μHe, unbiased expected heterozygosity; LS, local strain population; LC, local cultivar population; NARC, NARC population; EC, exotic cultivar population.

Analysis of molecular variance (AMOVA) was performed to determine the diversity both among and between the 80 potato genotypes according to their four geographic regions of origin (Table 5). Results from AMOVA revealed greater molecular variation within populations (85%) relative to between populations (15%).

Table 5. Analysis of molecular variance (AMOVA) of 80 potato genotypes based on 11 iPBS markers presenting the percentage of molecular variance among and within the population.

SV	df	SS	MS	Est. Var.	%	PhiPT
Among Pops	3	166.47	55.49	2.30	15%	0.021 ***
Within Pops	82	1056.16	12.88	12.88	85%	
Total	85	1222.63		15.18	100%	

Abbreviations are as follows: SV, source of variation; df, degrees of freedom; SS, sum of squares; MS, mean square; Est. Var., estimated variance; %, percentage of variation; *** $p < 0.001$.

3.3. Principal Coordinate analysis (PCoA) and Hierarchical Clustering of 80 Potato Genotypes

Principal coordinate analysis (PCoA) depicted the 80 potato genotypes based on their genetic distance (Figure 2). The 2 axis of the principal coordinate accounted for 20.6% of the total molecular variation, which distributed 80 genotypes in thee main groups, while six genotypes, including NARC37, NARC46, LC34, LS7, LS9, EC78, and EC47, were distinct from other genotypes.

Genetic distance was calculated using the dissimilarity index for constructing a NJ tree using 11 iPBS markers. Among the local strain (LS) population, LS9 (22.74) and LS3 (19.72) revealed the highest genetic distance. Among the local cultivar (LC) population, LC36 showed the highest genetic distance (17.35). Cultivars NARC37 (23.97) and NARC46 (19.88) indicated the maximum genetic length among the NARC cultivars population, and EC78 (23.65), EC69 (21.80), EC80 (21.65), and EC77 (21.34) had the maximum genetic distance among the EC (exotic cultivar) population. The NJ dendrogram separated 80 potato accessions into three major clusters with five sub-clusters (Figure 3). Cluster 1 consists of 16 genotypes, including 14 local strains, 1 NARC cultivar, and 1 local cultivar, of which LS14 (FD74-50) and LS10 (FD74-19) showed the closest genetic similarity, while LS7 (FD71-1), LS9 (FD73-77), LC34 (Ruby), and NARC46 (N-4) were more genetically diversified than other genotypes. Cluster 2 consists of 22 potato genotypes, including 17 exotic cultivars (ECs), 3 local strains, and 2 NARC cultivars, of which EC53 (El-mundo) and EC51 (Eldorodo) showed the closest genetic similarity while EC47 (Aurea), EC50 (Elodie), and EC54 (Erora) were genetically distinct. Cluster 3 consists of 17 exotic cultivars, of which EC73 (HZD-04-684) and EC70 (Sassy) had the closest genetic similarity, while EC71 (Focus), EC78 (Kuroda), EC65 (Red Sonia), and EC80 (Pirol) were genetically distinct. Cluster

4 consists of 13 genotypes, including 9 local strains and 4 local cultivars, of which LC32 (FSD red), LS18 (FD76-13), and LS25 (SL1-4) were genetically dissimilar. Similarly, cluster 5 consists of 12 genotypes, including 8 NARC cultivars and 4 local strains, of which LS29 (SL13-78) and LS24 (FD51-5) were closely related, while LS22 (FD77-62) and NARC39 (N-13) were more genetically dissimilar than other genotypes (Figure 3).

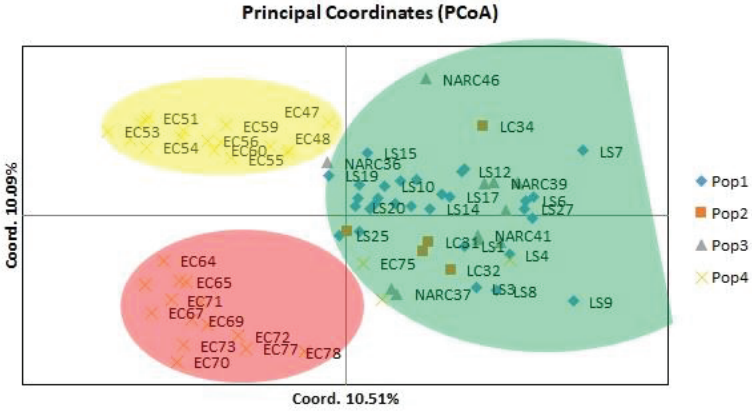

Figure 2. Principle coordinate analysis of 80 potato genotypes indicated the 20.6% variation based on retrotransposon markers; population 1 represents local strains, population 2 represents local cultivars, population 3 represent NARC cultivars, and population 4 represents exotic cultivars.

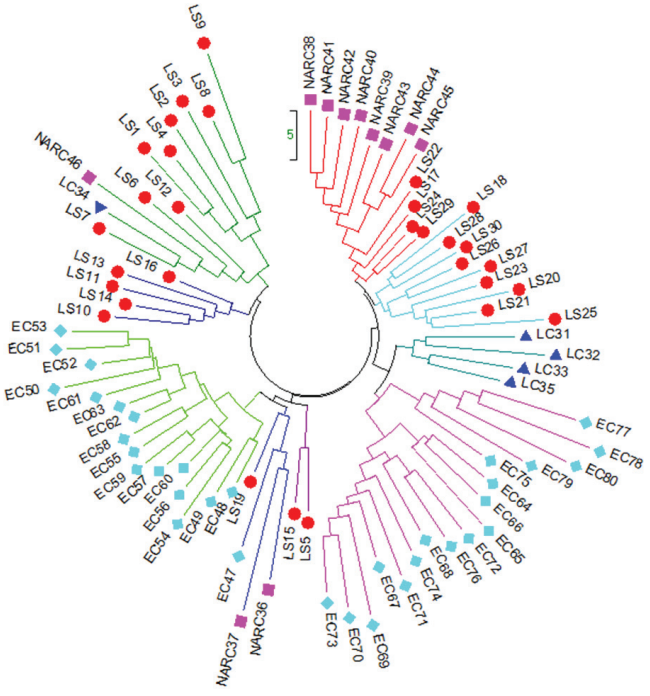

Figure 3. Neighbor-joining tree of 80 genotypes of potato generated with data from 11 iPBS primers showing 5 main clusters with some clusters containing sub-groups. Abbreviations are as follows: LS (●), local strains; LC (▲), local cultivars; NARC (■), and EC (◆), exotic cultivars.

3.4. Genetic Structure of 80 Potato Genotypes

The Bayesian methodology [23] used in STRUCTURE was applied to calculate the genetic structure of binary data extracted from 11 iPBS primers, and the data suggested that an optimum number of K = 5 represents the presence of five main clusters among 80 potato genotypes (Figure 4). A total of 11 iPBS primers distributed 80 potato genotypes into five major groups identified in yellow, red, blue, purple, and green (Figure 5). If a genotype has a member coefficient of 80% in K = 5, it belongs to that population. The result of iPBS data showed that population 1 had 7 genotypes (yellow), population 2 had 14 genotypes (red), population 3 had 7 genotypes (blue), population 4 had 13 genotypes (green), and population 5 had 14 potato genotypes (purple). In terms of the population structure of some the potato genotypes collected, namely LS18, LS28, NARC41, NARC45, EC51, EC52, EC54, EC56, EC59, EC60, EC61, EC62, EC67, EC68, EC70, EC73, and EC74, it was proposed that they do not share a common ancestor and represent pure genetic material. At the same time, genotypes with multiple colors are a mixture from numerous clusters, i.e., LC31, LC32, LC33, LC34, LC35, and LC36.

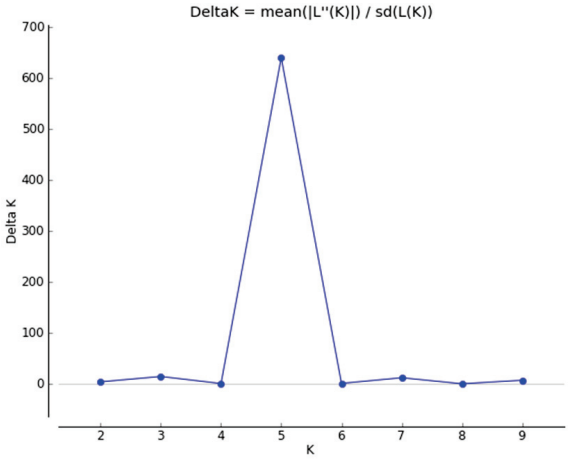

Figure 4. Plot of delta K calculated as the mean of the second-order rate of change in the likelihood of K divided by the standard deviation of the likelihood of K, m(|L″(K)|)/sd[L(K)]. Delta K = 5 is the potential number of genetic clusters that may exist in the overall sample of individuals.

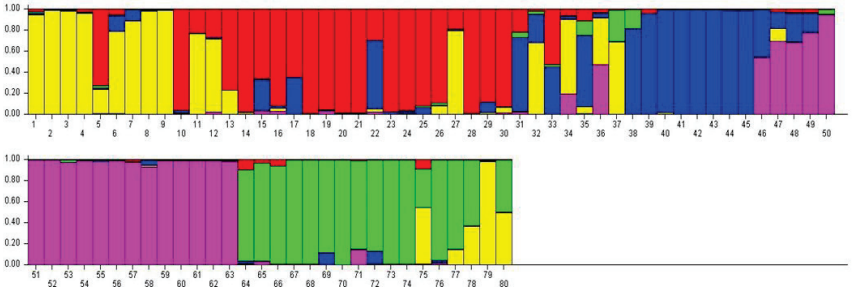

Figure 5. The population structure of 80 genotypes assessed using Bayesian analysis with allelic variation from the 11 iPBS markers. Five populations (yellow, red, blue, purple, and green) were defined using the method described in Evanno et al. (2005). Each vertical line symbolizes an individual multi-locus genotype.

4. Discussion

Despite low labor requirements, potato production in Pakistan is poor relative to neighboring countries, such as India and Bangladesh. This is thought to be due to several biotic and abiotic stresses, as well as the limited allocation of arable land. To overcome biotic and abiotic stresses using a breeding approach understanding the genetic diversity within breeding lines, landraces, and germplasm is critical. According to previous studies, retrotransposons comprise half of the plant genome's repetitive DNA. Potato has been reported to contain 214 Mb of LTR-transposons comprising 30% of total genome size. The iPBS markers are derived from retrotransposons and are not reliant on prior sequence information. Furthermore, iPBS markers have been applied in several different genetic evaluation studies of plant species, such as *Cicer* ssp. [26], *Saussurea esthonica* [27], *Diospyros* ssp. [28], *Myrica rubra* [29], and grape [30]. The iPBS markers typically generate multiple polymorphic bands per locus, are highly reproducible, and are inexpensive compared to other marker systems [30].

A total of 11 polymorphic iPBS markers were effective in characterizing the genetic variation between and within 80 potato genotypes. Unique alleles were found in Red River, Sagitta, FD 61-3, and PRI-RED genotypes with primers 2229, 2232, 2375, and 2239, respectively; these alleles could be sequenced in the future for primer design. The PIC values estimate the marker power of discrimination for a locus and provide the size of alleles. The PIC value recorded for each primer ranged from 0.13 to 0.38, with a mean value of 0.28, which is higher than the PIC value (0.12–0.31) reported in Turkish potato accessions by Demirel et al. [17]. This is likely due to the selection of more specific transposable base iPBS markers in this study into the genetic diversity of the Pakistani potato germplasm. The molecular analysis of 80 genotypes revealed the average recorded heterozygosity (He) for 11 iPBS primers was 0.2. The low He and Shannon's information index (I) values observed in this study are due to using a limited number of iPBS markers, leading to selection bias.

A dendrogram was constructed based on data gathered from 11 iPBS primers by using the NJ method, and this distributed the 80 potato genotypes into five main clusters. Further cluster analysis showed that genetic diversity was higher among and between the potato genotypes due to genetic drift. The dendrogram was built based on dissimilarity coefficient values that showed a wide range of variable values of the similarity index and indicates that iPBS markers can be used effectively in genetic diversity studies. To further enhance the Pakistani potato industry, phylogenetic characterization based on genetic distance could be helpful for crop breeding, facilitating the development new breeding programs. Wild relatives and primitive cultivars of potatoes contribute to diversity in genetic resources for production programs for the potato crop [31–33]. The current study's genetic dissimilarity results showed the highest genetic distance among the genotypes, including LS9 (FD73-77), LS3 (FD48-54), LC36 (Potato 3), NARC37 (Potato2), NARC46 (N-4), EC78 (Kuroda), EC69 (Suzen), EC80 (Pirol), and EC77 (Red River). These results provide a basis for enhanced diversification for parental selection for potato breeding in Pakistan.

Potato has been reported to show higher heterozygosity, as it is a tetraploid outcrossing crop [34]. The present study has shown a high level of genetic diversity in the potato genotypes selected. The heterozygosity results are in agreement with the previously reported studies [34]. Furthermore, heterosis and mutation-positive selection could also be the important factor contributing to the high heterozygosity in potato. Shannon's information index (I) is important in order to understand genetic variation among cultivars, as it is related to genetic differences in uniformity and population combining abundance. The variation in I observed among genetic groups might be due to geographic factors, habitat destruction, restriction in gene flow, and type of breeding system. Further variation could be the result of the inclusion of wild accessions in the present study. These results are in contrast with a Chinese study [35] that showed that I varied from 0.73 to 1.76 among the 149 main potato cultivars of China. Analysis of molecular variance (AMOVA) showed the presence of high variation within potato genotypes, with the percentage of total variance being 85%. It has been previously stated that higher variations in varieties may be due to

reasons, such as selection, adaptation, gene flow, genetic drift, and variation in ecotypes and pollination method [36].

The PCoA approach is a widely used method for assessing genetic diversity based on quantitative and qualitative traits that scale distance data to multidimensional planes for the characterization of genetic diversity. The data acquired from this study of population structure and heterozygosity of potato germplasm indicate that NARC cultivars clustered together in the dendrogram due to their low heterozygosity. Despite their extensive distribution and cultivation, these findings indicate that only a few NARC cultivars have been used in potato breeding programs. Our results showed that the local cultivar population and NARC cultivars tended to be closely related based on their clustering showing minimal genetic diversity that can be exploited for breeding purposes. Individuals with multiple colors, such as LC31, LC32, LC33, LC34, LC35, and LC36, are admixtures indicating the maximum genetic drift and, thus, inform future studies into enhancing potato genetic diversity for germplasm collection and conservation [8]. The genotypes were clustered based on geographical distribution and morphological features to execute a similarity index analysis. The PCoA method has been used previously to study the genetic relatedness among different potato genotypes [37]. The genetic diversity for 26 potato genotypes grown in Turkey was previously analyzed using six AFLP primers, resulting in the production of 191 polymorphic bands which distributed potato genotypes into six distinct subgroups [38]. Another study in Turkey used SSR markers for fingerprinting major potato landraces and varieties grown in Central Anatolia [39]. Among 16 SSR primers, five markers (STM19, STM31, STM3012, STI32, and STI42) distinguished the 15 potato genotypes into five groups [39]. In our study, 11 transposon-based markers distributed the potato accessions into 5 groups according to their genetic structures.

5. Conclusions

The study of the genetic variation of 80 Pakistani potato genotypes using iPBS-based markers provided data about their relatedness and diversity. This data can be submitted to the relevant molecular databases to incorporate new information in the national gene pool. Other techniques, such as genotype-by-sequencing (GBS) and DArT-Seq, can also be used to enhance genetic diversity studies using an increased number of accessions to better assess genetic distances among divergent genotypes. A comprehensive genome-wide association mapping study is required to better understand and further explore genetic diversity studies in a highly diverse collection of potato accessions. Establishing germplasm consisting of a core collection used in breeding programs is necessary. The findings of this study confirm the extent of diversity within the Pakistani potato germplasm. Further molecular diversity, trait dissection, and characterization studies are required for germplasm preservation and crop improvement.

Author Contributions: L.M. and A.M. performed data collection and original draft preparation; P.M.D. performed substantial reviewing, editing and formatting M.S.H. and M.J.J. were also responsible for reviewing and editing; A.M. and A.H. were responsible for software; supervision and lab work data analysis was by M.W.S.; Q.Y. and M.M.H. were responsible for the fieldwork and methodology. All authors have read and agreed to the published version of the manuscript.

Funding: This research received no external funding.

Institutional Review Board Statement: Not applicable.

Conflicts of Interest: The authors declare no conflict of interest.

References

1. De Haan, S.; Rodriguez, F. Potato origin and production. In *Advances in Potato Chemistry and Technology*, 2nd ed.; Singh, J., Kaur, L., Eds.; Academic Press: Cambridge, MA, USA, 2016; pp. 1–32.
2. FAO. Available online: https://www.fao.org/faostat/en/#data/QCL (accessed on 18 June 2022).
3. Dongyu, Q. *Role and Potential of Potato in Global Food Security*; FAO: Rome, Italy, 2022; pp. 23–30. Available online: https://www.fao.org/3/cc0330en/cc0330en.pdf (accessed on 2 July 2022).

4. FAOSTAT. Food and Agricultural Organization Statistical Database, Crop Production. 2020. Available online: http://faostat3.fao.org/download/Q/QC/E (accessed on 22 March 2022).
5. Watanabe, K. Potato genetics, genomics, and applications. *Breed. Sci.* **2015**, *65*, 53–68. [CrossRef] [PubMed]
6. Lee, K.J.; Sebastin, R.; Cho, G.T.; Yoon, M.; Lee, G.A.; Hyun, D.Y. Genetic Diversity and Population Structure of Potato Germplasm in RDA-Genebank: Utilization for Breeding and Conservation. *Plants* **2021**, *10*, 752. [CrossRef] [PubMed]
7. Schulman, A.H. Molecular markers to assess genetic diversity. *Euphytica* **2007**, *158*, 313–321. [CrossRef]
8. Nadeem, M.A.; Muhammad, A.N.; Muhammad, Q.S.; Yıldız, D.; Gonul, C.; Mehtap, Y.; Rüştü, H.; Fiaz, A.; Ahmad, A.; Nitin, L.; et al. DNA molecular markers in plant breeding: Status and recent advancements in genomic selection and genome editing. *Biotechnol. Equip.* **2018**, *32*, 261–285. [CrossRef]
9. Kalendar, R.; Antonius, K.; Smýkal, P.; Schulman, A.H. iPBS: A universal method for DNA fingerprinting and retrotransposon isolation. Theor. *Appl. Genet.* **2010**, *121*, 1419–1430. [CrossRef]
10. Yildiz, M.; Kocak, M.; Nadeem, M.A.; Cavagnaro, P.; Barboza, K.; Baloch, F.S.; Argün, D.; Keleş, D. Genetic diversity analysis in the Turkish pepper germplasm using iPBS retrotransposon-based markers. *Turk. J. Agric. For.* **2020**, *44*, 1–14. [CrossRef]
11. Mehmood, A.; Jaskani, M.J.; Ahmad, S.; Ahmad, R. Evaluation of genetic diversity in open pollinated guava by iPBS primers. *Pak. J. Agric. Sci.* **2013**, *50*, 591–597.
12. Baloch, F.S.; Ahmad, A.; Luis, E.; Sáenzde, M.; Rüştü, H.; Vahdettin, Ç.; Tolga, K.; Mehtap, Y.; Hakan, Ö. DNA based iPBS-retrotransposon markers for investigating the population structure of pea (*Pisum sativum*) germplasm from Turkey. *Biochem. Syst. Ecol.* **2015**, *61*, 244–252. [CrossRef]
13. Yıldız, M.; Koçak, M.; Baloch, F.S. Genetic bottlenecks in Turkish okra germplasm and utility of iPBS retrotransposon markers for genetic diversity assessment. *Genet. Mol. Res.* **2015**, *14*, 10588–10602. [CrossRef]
14. Al-Najm, A.; Luo, S.; Ahmad, N.M.; Trethowan, R. Molecular variability and genetic relationships of date palm (*Phoenix dactylifera* L.) cultivars based on inter-primer binding site (iPBS) markers. *Aust. J. Crop Sci.* **2016**, *10*, 732–740. [CrossRef]
15. Yaldiz, G.; Camlica, M.; Nadeem, M.A.; Nawaz, M.A.; Baloch, F.S. Genetic diversity assessment in *Nicotiana tabacum* L. with iPBS-retrotransposons. *Turk. J. Agric. For.* **2018**, *42*, 154–164. [CrossRef]
16. Nemli, S.; Kianoosh, T.; Tanyolac, M.B. Genetic diversity and population structure of common bean (*Phaseolus vulgaris* L.) accessions through retrotransposon-based interprimer binding sites (iPBSs) markers. *Turk. J. Agric. For.* **2015**, *39*, 940–948. [CrossRef]
17. Demirel, U.; Tındaş, İ.; Yavuz, C.; Baloch, F.S.; Çalışkan, M.E. Assessing genetic diversity of potato genotypes using inter-PBS retrotransposon marker system. *Plant Genet. Resour.* **2018**, *16*, 137–145. [CrossRef]
18. Khan, M.F.; Tabassum, N.; Latif, A.; Khaliq, A.; Malik, M. Morphological characterization of potato (*Solanum tuberosum* L.) germplasm under rainfed environment. *Afr. J. Biotechnol.* **2013**, *21*, 3214–3223.
19. Abbas, S.J.; Rasool, G.; Shah, S.R.U.; Iqbal, A. Analysis of genetic diversity in Pakistani potato cultivars by using randomly amplified polymorphic DNA (RAPD) primers. *Am.-Eurasian J. Sustain. Agric.* **2008**, *2*, 50–54.
20. Murray, M.; Thompson, W.F. Rapid isolation of high molecular weight plant DNA. *Nucleic Acids Res.* **1980**, *8*, 4321–4325. [CrossRef]
21. Peakall, R.; Smouse, P.E. GenAlEx tutorials-part 2: Genetic distance and analysis of molecular variance (AMOVA). *Bioinformatics* **2012**, *28*, 2537–2539. [CrossRef]
22. Kumar, S.; Stecher, G.; Tamura, K. MEGA7: Molecular evolutionary genetics analysis version 7.0 for bigger datasets. *Mol. Biol. Evol.* **2016**, *33*, 1870–1874. [CrossRef]
23. Pritchard, J.K.; Stephens, M.; Donnelly, P. Inference of population structure using multilocus genotype data. *Genetics* **2000**, *155*, 945–959. [CrossRef]
24. Evanno, G.; Regnaut, S.; Goudet, J. Detecting the number of clusters of individuals using the software STRUCTURE: A simulation study. *Mol. Ecol.* **2005**, *14*, 2611–2620. [CrossRef]
25. Earl, D.A. STRUCTURE HARVESTER: A website and program for visualizing STRUCTURE output and implementing the Evanno method. *Conserv. Genet. Resour.* **2012**, *4*, 359–361. [CrossRef]
26. Andeden, E.E.; Baloch, F.S.; Derya, M.; Kilian, B.; Özkan, H. iPBS-Retrotransposons-based genetic diversity and relationship among wild annual Cicer species. *J. Plant Biochem. Biotechnol.* **2013**, *22*, 453–466. [CrossRef]
27. Gailīte, A.; Ievinsh, G.; Runģis, D. Genetic diversity analysis of Latvian and Estonian Saussurea esthonica populations. *Environ. Exp. Bot.* **2011**, *9*, 115–119.
28. Raddová, J.; Ptáčková, H.; Čechová, J.; Ondrášek, I. Genetic analysis of the genus *Diospyros* ssp. using RAPD and i-PBS methods. *Acta Univ. Agric. Silvic. Mendelianae Brun.* **2012**, *60*, 205–216. [CrossRef]
29. Fang-Yong, C.; Ji-Hong, L. Germplasm genetic diversity of Myrica rubra in Zhejiang Province studied using inter-primer binding site and start codon-targeted polymorphism markers. *Sci. Hortic.* **2014**, *170*, 169–175. [CrossRef]
30. Guo, D.L.; Guo, M.X.; Hou, X.G.; Zhang, G.H. Molecular diversity analysis of grape varieties based on iPBS markers. *Biochem. Syst. Ecol.* **2014**, *52*, 27–32. [CrossRef]
31. Bamberg, J.B.; del Rio, A. Conservation of Potato Genetic Resources. In *Genetic Improvement of Solanaceous Crops, Volume I: Potato*; Razdan, M.K., Mattoo, A.K., Eds.; Science Publishers, Inc.: Plymouth, UK, 2005; p. 476.
32. D'hoop, B.B.; Paulo, M.J.; Mank, R.A.; van Eck, H.J.; van Eeuwijk, F.A. Association mapping of quality traits in potato (*Solanum tuberosum* L.). *Euphytica* **2008**, *161*, 47–60. [CrossRef]

33. Jansky, S. Breeding for Disease Resistance in Potato. In *Plant Breeding Reviews*; Janick, J., Ed.; John Wiley & Sons, Inc.: Oxford, UK, 2010; Volume 19, pp. 69–155. [CrossRef]
34. Meirmans, P.G.; Liu, S.; van Tienderen, P.H. The analysis of polyploid genetic data. *J. Hered.* **2018**, *109*, 283–296. [CrossRef]
35. Hu, J.; Mei, M.; Jin, F.; Xu, J.; Duan, S.; Bian, C.; Li, G.; Wang, X.; Jin, L. Phenotypic variability and genetic diversity analysis of cultivated potatoes in China. *Front. Plant Sci.* **2022**, *13*, 954162. [CrossRef]
36. Bohn, M.; Utz, H.F.; Melchinger, A.E. Genetic similarities among winter wheat cultivars determined on the basis of RFLPs, AFLPs, and SSRs and their use for predicting progeny variance. *Crop Sci.* **1999**, *39*, 228–237. [CrossRef]
37. Khodadadi, M.; Fotokian, M.H.; Miransari, M. Genetic diversity of wheat (*Triticum aestivum* L.) genotypes based on cluster and principal component analyses for breeding strategies. *Aust. J. Crop Sci.* **2011**, *5*, 17–24.
38. Akkale, C.; Yildirim, Z.; Yildirim, M.B.; Kaya, C.; Öztürk, G.; Tanyolaç, B. Assessing genetic diversity of some potato (*Solanum tuberosum* L.) genotypes grown in Turkey using the AFLP marker technique. *Turk. J. Field Crop.* **2010**, *15*, 73–78.
39. Kandemir, N.; Yılmaz, G.; Karan, Y.B.; Borazan, D. Development of a simple sequence repeat (SSR) marker set to fingerprint local and modern potato varieties grown in central Anatolian Plateau in Turkey. *Afr. J. Biotechnol.* **2010**, *9*, 5516–5522.

agriculture

MDPI

Article

Comparative Fruit Morphology and Anatomy of Wild Relatives of Carrot (*Daucus*, Apiaceae)

Dariusz Kadluczka and Ewa Grzebelus *

Department of Plant Biology and Biotechnology, Faculty of Biotechnology and Horticulture, University of Agriculture in Krakow, Al. Mickiewicza 21, 31-120 Krakow, Poland
* Correspondence: ewa.grzebelus@urk.edu.pl

Abstract: Fruit morphological and anatomical characteristics are essential in the taxonomy of Apiaceae. *Daucus* L. is one of the most important genera of the family Apiaceae, as it contains the cultivated carrot, a crop of great economic importance, and about 40 wild species that could serve as potential sources of genetic diversity for crop improvement. However, the taxonomic and phylogenetic relationships among these species have not yet been fully clarified. In this study, we comparatively investigated the fruit morphology and anatomy of 13 *Daucus* taxa and four closely related non-*Daucus* species using light and scanning electron microscopy to evaluate the taxonomic value of these characteristics. A wide range of variations was observed in the fruit morpho-anatomical characteristics across the taxa and revealed several diagnostically valuable features, thus proving to be taxonomically useful. For *Daucus*, the observed differences included the fruit size (2.1–8.4 mm), shape (from ellipsoid to oblong), and weight (0.079–1.349 g/100 fruits), as well as the fruit surface sculpturing and some anatomical characteristics, i.e., the presence/absence and size of vittae, the shape and size of vascular bundles, and the shape of exocarp cells. This study contributes to a better understanding of the relationships among the genus *Daucus*.

Keywords: Apioideae; carpology; crop wild relatives; Daucinae; mericarp; plant systematics; schizocarp; Torilidinae

Citation: Kadluczka, D.; Grzebelus, E. Comparative Fruit Morphology and Anatomy of Wild Relatives of Carrot (*Daucus*, Apiaceae). *Agriculture* **2022**, *12*, 2104. https://doi.org/10.3390/agriculture12122104

Academic Editors: Edyta Paczos-Grzeda, Volker Mohler and Sylwia Sowa

Received: 25 October 2022
Accepted: 6 December 2022
Published: 8 December 2022

1. Introduction

The genus *Daucus* L. belongs to the large and complex family Apiaceae, which comprises approximately 3820 species in 466 genera that are widely distributed all around the world, especially in the temperate regions of Eurasia and North America [1]. This cosmopolitan family is considered one of the most economically important families, and it includes a number of food crops, herbs, and spices [2]. *Daucus* contains carrot (*D. carota* subsp. *sativus* Hoffm.), the only cultivated member of the genus, which is a crop of great importance for human nutrition as it serves as a major source of α- and β-carotene (vitamin A precursors) in the diet [3,4]. The taxonomic and phylogenetic relationships among *Daucus* species have not yet been fully clarified. Traditionally, the genus comprised 20–25 species, as inferred from morphological and anatomical data [2,5]. However, recent studies based on different molecular data have led to a better understanding of the species boundaries and phylogenetic relationships among *Daucus* and its close relatives in the Apioideae subfamily [6–13]. Following these revisions, the genus has been extended to include nine other genera, and it now contains about 40 species positioned in two main clades [11].

The wild species of *Daucus* are widespread in the temperate parts of the Northern Hemisphere, most commonly in the Mediterranean region, which is considered the center of this genus's diversity; however, few species occur in South America, Australia, and tropical Africa [14,15]. They are mostly herbaceous biennials, rarely annuals [14], but a few rosette treelets (endemic to Macaronesia) also exist [16]. Most *Daucus* species are diploids with chromosome numbers of $2n = 16$, 18, 20, or 22; however, some tetra- and hexaploids

have also been reported [15,17,18]. Regarding the genome size within the genus, nuclear DNA content estimates based on flow cytometry are available for several wild species and subspecies, as well as for many cultivated carrots, ranging from 0.920 to 3.228 pg/2C DNA [19–21].

The fruit of Apiaceae is typically a schizocarp that splits at maturity into two—usually equal—ribbed, one-seeded mericarps. Each mericarp has five primary ribs: three dorsal (one median and two lateral) and two marginal (closest to the commissure), which are separated by furrows (valleculae). The primary ribs enclose one or more vascular bundles that are often associated with schizogenous secretory canals (rib oil ducts). Another set of secretory canals (vittae) are located in the valleculae and the commissural area but are not associated with the vasculature. In some groups, secondary ribs develop from the valleculae, and they have no vascular bundles (see Figure 1) [1,22,23]. The fruit's structural characteristics, especially the number and distribution of vittae and vascular bundles, as well as rib/wing morphology, have proven to be exceptionally useful for the taxonomy of Apiaceae (e.g., [24–32]). Regarding *Daucus*, several decades ago, Sáenz Laín [5] published a taxonomic monograph of the genus based on morpho-anatomical analyses, providing some observations of the fruit morphology and anatomy of *Daucus* taxa; however, this was a largely intuitive classification that did not contain specimen citations, detailed descriptions, or distribution maps [33]. More recently, Mezghani et al. [34] studied the patterns of phenotypic diversity of fruits among Tunisian *Daucus* germplasm collection, whereas Wojewódzka et al. [35] investigated fruit evolution in many members of the Apiaceae tribe Scandiceae, including some *Daucus* taxa, and outgroups to assess adaptive shifts associated with the evolutionary switches between anemochory and epizoochory, as well as to identify possible dispersal syndromes.

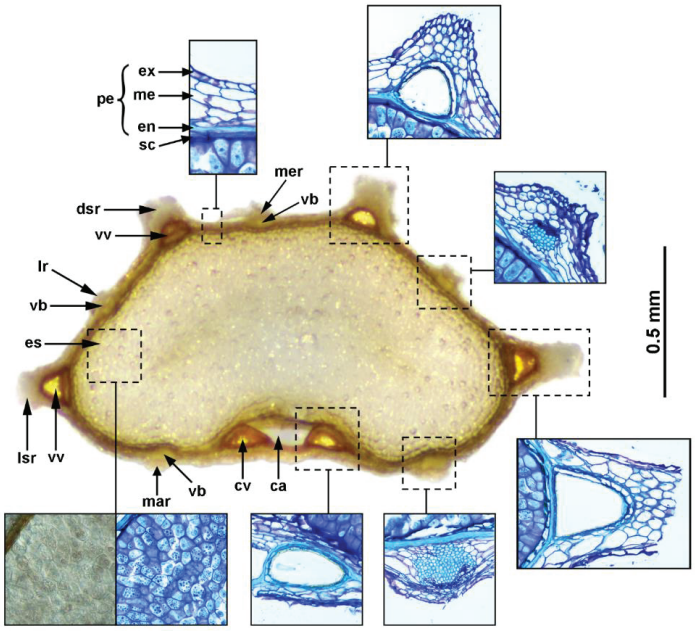

Figure 1. Transverse section of a mericarp of *Daucus* sp., indicating the anatomical structures considered in this study and their terminology. The insets show the corresponding structures, as seen by light microscopy. Abbreviations: ca, cavity; cv, commissural vitta; dsr, dorsal secondary rib; en, endocarp; es, endosperm; ex, exocarp; lr, lateral primary rib; lsr, lateral secondary rib; mar, marginal primary rib; me, mesocarp; mer, median primary rib; pe, pericarp; sc, seed coat; vb, vascular bundle; vv, vallecular vitta.

To address the rising need for food and to ensure food security for a constantly growing population, plant breeders require access to new genetic resources that could be used in crop breeding programs to expand the genetic variation of crops that has been lost during domestication. Such a large pool of genetic diversity can be found in crop wild relatives, which—due to their high adaptability to a wide range of habitats and environmental conditions—represent an important reservoir of agronomically important genes [36–38]. In this context, wild *Daucus* species may play a crucial role in the process of improving modern agriculture, being a valuable source of genes potentially useful for breeding purposes, e.g., for producing new crop varieties that could be disease-resistant, tolerant to abiotic stress, higher-yielding, male-sterile, or more nutritious [9,14]. In light of this, a better understanding of species relationships within the genus *Daucus* may greatly contribute to the development of future carrot breeding programs.

Given the significance of wild *Daucus* species and the great economic importance of the cultivated carrot, as well as the taxonomical usefulness of fruit structural characteristics in Apiaceae, this study aimed to compare the fruit morphology and anatomy of *Daucus* taxa using light and scanning electron microscopy (SEM) and to evaluate the diagnostic value of these characteristics. In this study, which is a continuation of our previous work [21], we selected a representative sample that covered the two main *Daucus* subclades (13 taxa) and four closely related non-*Daucus* species. We used the same accessions that have commonly been used in previous phylogenetic and (cyto)taxonomic research on the genus [9,12,13,21,39].

2. Materials and Methods

2.1. Plant Material

The study materials were ripe fruits (mericarps) of 13 *Daucus* taxa (14 accessions) and four closely related non-*Daucus* species (outgroup). The *Daucus* accessions comprised 12 wild taxa belonging to *Daucus* subclades I and II, as well as two cultivated carrots. The fruit samples of wild *Daucus* and non-*Daucus* accessions were provided by the USDA-ARS North Central Regional Plant Introduction Station (Ames, IA, USA), whereas the fruits of the carrot accessions were either purchased from commercial sources or obtained from the collections of the Department of Plant Biology and Biotechnology, University of Agriculture in Krakow (Krakow, Poland). The following taxa were used (chromosome numbers [17,18] and accession numbers [PI = USDA Plant Introduction numbers] are given in brackets): *Daucus aureus* Desf. (2*n* = 22; PI 319403), *D. conchitae* Greuter (2*n* = 22; Ames 25835), *D. carota* subsp. *capillifolius* (Gilli) C. Arbizu (2*n* = 18; PI 279764), *D. carota* subsp. *sativus* Hoffm. (2*n* = 18; DH1, a doubled haploid orange Nantes-type carrot), *D. carota* subsp. *sativus* (2*n* = 18; 'Dolanka'), *D. glochidiatus* (Labill.) Fisch & C.A. Mey (2*n* = 44; PI 285038), *D. guttatus* Sm. (2*n* = 20; PI 652233), *D. involucratus* Sm. (2*n* = 22; PI 652332), *D. littoralis* Sm. (2*n* = 20; PI 295857), *D. muricatus* (L.) L. (2*n* = 22; PI 295863), *D. pusillus* Michx. (2*n* = 22; PI 349267), *D. rouyi* Spalik & Reduron (2*n* = 20; PI 674284), *D. sahariensis* Murb. (2*n* = 18; Ames 29096), *D. syrticus* Murb. (2*n* = 18; Ames 29108), *Caucalis platycarpos* L. (2*n* = 20; PI 649446), *Orlaya daucoides* (L.) Greuter (2*n* = 16; PI 649477), *O. daucorlaya* Murb. (2*n* = 14; PI 649478), and *Torilis arvensis* (Huds.) Link (2*n* = 12; PI 649391).

2.2. Fruit Morphology

To characterize fruit morphology, 50 dry mericarps of each accession were placed on graph paper and photographed with a Flexacam C1 digital camera (Leica Microsystems, Heerbrugg, Switzerland) under a Leica S6D stereomicroscope (Leica Microsystems). The images were processed using Leica Application Suite X (Leica Microsystems) software, and the mericarp length (L) and width (W) were measured using AxioVision 4.8.2 software (Carl Zeiss MicroImaging, Jena, Germany). The fruit shape was described on the basis of the mean ratio of the mericarp length to width (L/W), and the following shape classes were used: ovoid (L/W $\leq$ 1.5), ellipsoid (L/W = 1.6–2.0), and narrowly ellipsoid or oblong (L/W $\geq$ 2.0), according to Lee et al. [40] and Mustafina et al. [41].

For scanning electron microscopy (SEM) analysis, dry fruit samples were mounted on stubs and sputter-coated with gold using a JFC-1100E ion sputter coater (JEOL, Tokyo, Japan); then, the dorsal side of the mericarps was examined under a JSM-5410 scanning electron microscope with a wolfram cathode (JEOL). The terminology used to describe the fruit surface sculpturing pattern was adopted from Stearn [42] and Ostroumova [43].

The fruit weight of each accession was expressed as grams per 100 mericarps and estimated by weighing four subsamples (each containing 50 randomly selected mericarps) using a WPS 510/C analytical balance (Radwag, Radom, Poland). The mean value was then calculated to obtain the weight of 100 mericarps.

2.3. Fruit Anatomy

For anatomical examination, 5–10 fruit samples (schizocarps or individual mericarps) of each accession were rehydrated in distilled water for 24–48 h, fixed in freshly prepared FAA (formalin, glacial acetic acid, and 70% ethanol, 6:4:90, *v*/*v*/*v*) for 48–72 h at room temperature, and stored in 70% ethanol at 4 °C until further use. The samples were then dehydrated in a graded ethanol series (80% and 90% for 2 h each) and left overnight in absolute ethanol. The dehydrated material was embedded in Technovit® 7100 resin (Kulzer, Hanau, Germany), following the manufacturer's protocol, with minor modifications involving prolonged infiltration with embedding solutions, i.e., the material was treated with increasing concentrations of Technovit relative to ethanol (1:3, 1:1, 3:1, *v*/*v*) for 24 h each and then left in pure Technovit for 5 days. The fixation, dehydration, and infiltration steps were performed on an orbital shaker (150 rpm) at room temperature, with 15 min vacuum pumping during each solution change. When polymerized, cross-sections of 4–8 µm thickness were made using a Leica RM2145 rotary microtome (Leica Microsystems, Wetzlar, Germany) with a Leica TC-65 carbide blade (Leica Microsystems). The sections were then stained with 0.2% (*w*/*v*) toluidine blue O (Sigma-Aldrich, Steinheim, Germany) for 30–60 s, mounted in Entellan® (Merck, Darmstadt, Germany), and analyzed under an Axio Imager.M2 microscope (Carl Zeiss, Göttingen, Germany). Three quantitative anatomical characteristics were measured (from five mericarps per accession): width of commissural vittae, width of vallecular vittae, and pericarp thickness. The terminology used to describe fruit anatomy follows that of Kljuykov et al. [22,23] and Wojewódzka et al. [35].

Another fruit sample was rehydrated in distilled water for 24 h and hand-sectioned using a disposable razor blade. The sections were then photographed under a stereomicroscope with the same camera as described in Section 2.2.

The transverse section of an exemplary mericarp showing the anatomical structures considered in this study, along with their terminology, is given in Figure 1.

2.4. Statistical Analysis

For each accession, the means and standard errors (SE) of the means were calculated for the measured quantitative parameters and then subjected to a one-way analysis of variance (ANOVA), followed by Tukey's honestly significant difference (HSD) test using Statistica 13.3 software (TIBCO Software Inc., Palo Alto, CA, USA). The differences were considered significant at $p \leq 0.05$.

3. Results

3.1. Fruit Morphology

The fruits of the studied taxa were schizocarps consisting of two homomorphic mericarps. The mericarps were pale yellow to brown in color and ovoid to oblong in shape in dorsal view (Figure 2 and Table 1). All taxa had spiny fruits, except for *D. rouyi* (Figure 2l), whose fruits were winged; however, since the material was mostly obtained from gene bank collections, the fruits often had broken spikes/wings or were devoid of these structures. In almost all taxa, the primary ribs were more or less inconspicuous or rarely prominent, covered with hairs or pointed thorns, whereas the secondary ribs (two dorsal and two

lateral) were remarkably prominent (Figure 2). *Torilis arvensis*, however, had numerous additional secondary ribs covering almost the entire surface of the fruit (Figure 2r).

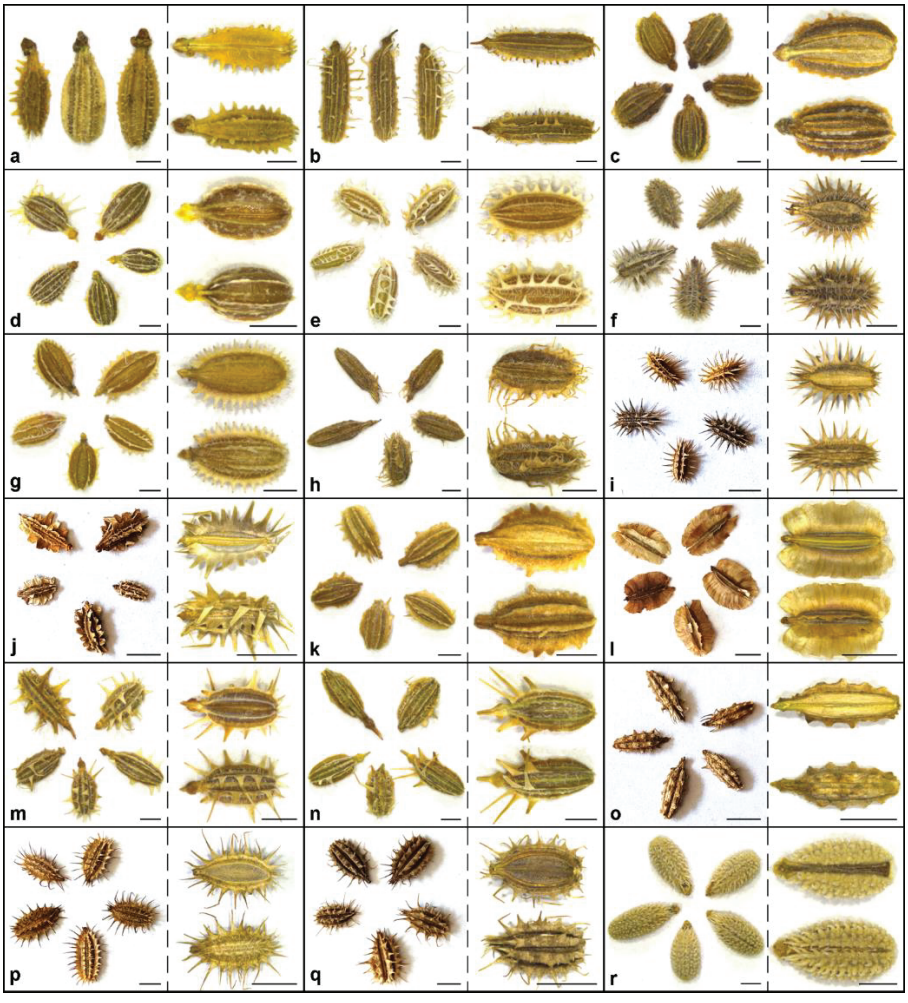

Figure 2. Variation in fruit morphology of the investigated *Daucus* and closely related non-*Daucus* taxa. The insets show magnified views of the dorsal (lower) and ventral (upper) sides of the mericarps. (**a**) *D. aureus*; (**b**) *D. carota* subsp. *capillifolius*; (**c**) subsp. *sativus* (DH); (**d**) subsp. *sativus* ('Dolanka'); (**e**) *D. conchitae*; (**f**) *D. glochidiatus*; (**g**) *D. guttatus*; (**h**) *D. involucratus*; (**i**) *D. littoralis*; (**j**) *D. muricatus*; (**k**) *D. pusillus*; (**l**) *D. rouyi*; (**m**) *D. sahariensis*; (**n**) *D. syrticus*; (**o**) *Caucalis platycarpos*; (**p**) *Orlaya daucoides*; (**q**) *O. daucorlaya*; (**r**) *Torilis arvensis*. Scale bars: 1 mm (**a**–**h**,**k**,**m**,**n**,**r**); 5 mm (**i**,**j**,**l**,**o**–**q**).

The mean mericarp length (L) varied from 2.1 (*D. carota* subsp. *sativus* 'Dolanka') to 11.4 mm (*O. daucoides*), whereas the average mericarp width (W) ranged from 1.1 (*D. conchitae* and *D. involucratus*) to 7.7 mm (*D. rouyi*) (Table 1). The ratio of these two parameters (L/W) was recorded in the range between 1.1 (*D. rouyi*) and 3.6 (*D. carota* subsp. *capillifolius*).

A closer look at the dorsal side of the mericarps, as examined under SEM (Figure 3), showed that the vast majority of *Daucus* taxa exhibited more or less rugose fruit surface sculpturing (Figure 3b–f,h,k,l). The most distinct pattern was found in *D. aureus* (Figure 3a), whose whole fruit surface was densely covered with tubercles (tuberculate type of sculpturing). Moreover, a few other or mixed types were detected. In *D. guttatus*, a rugose–tuberculate pattern was observed, i.e., rugose in the furrows between ribs, tuberculate on the surface of the secondary ribs (Figure 3g). *Daucus littoralis* showed a lineolate–tuberculate (lineolate furrows and tuberculate secondary ribs) surface (Figure 3i), whereas *D. rouyi* displayed ribbed–striate sculpturing (Figure 3j). In *D. muricatus*, the furrows were not clearly seen, but the surface of the secondary ribs was tuberculate (Figure 3m).

Among the outgroup species, variations in the types of sculpturing were also observed. In *T. arvensis*, the secondary ribs were densely covered with pointed tubercles (Figure 3n); *Caucalis platycarpos* exhibited a smooth surface (Figure 3o), while both *O. daucoides* and *O. daucorlaya* showed an undulate sculpturing pattern (Figure 3p,q, respectively).

In all cases, the outlines of the exocarp cells were not visible.

The lowest mean weight of 100 fruits (mericarps) was recorded for *D. glochidiatus* (0.079 g/100 fruits) and *D. syrticus* (0.080 g/100 fruits) (Table 1). *Orlaya daucorlaya* and *O. daucoides* had the heaviest fruits (3.451 and 3.407 g/100 fruits, respectively).

Table 1. Fruit (mericarp) morphological characteristics of the investigated *Daucus* and closely related non-*Daucus* (outgroup) taxa.

Taxon	Length (L; mm)		Width (W; mm)		L/W	Shape	100 Fruit Weight (g)
	Min–Max	Mean ± SE	Min–Max	Mean ± SE			Mean ± SE
***Daucus*I subclade**							
D. aureus	2.5–4.4	3.3 ± 0.06 h	1.2–2.1	1.5 ± 0.03 de	2.2	NE	0.136 ± 0.002 f–h
D. carota subsp. *capillifolius*	4.0–6.5	4.9 ± 0.07 g	1.1–1.7	1.4 ± 0.02 d–f	3.6	OB	0.206 ± 0.002 f
D. carota subsp. *sativus* (DH)	2.3–3.4	2.8 ± 0.04 i	1.5–1.7	1.6 ± 0.01 d	1.7	E	0.117 ± 0.003 f–h
D. carota subsp. *sativus* ('Dolanka')	1.6–2.8	2.1 ± 0.04 k	0.9–1.7	1.3 ± 0.02 fg	1.7	E	0.139 ± 0.005 f–h
D. muricatus	4.5–8.4	6.5 ± 0.12 e	2.1–4.0	2.6 ± 0.05 c	2.5	NE	1.076 ± 0.020 d
D. rouyi	6.8–12.1	8.4 ± 0.13 c	5.6–10.9	7.7 ± 0.15 a	1.1	OV	1.349 ± 0.012 c
D. sahariensis	2.0–3.8	2.7 ± 0.05 i	0.9–1.6	1.3 ± 0.03 e–g	2.1	NE	0.098 ± 0.002 gh
D. syrticus	1.9–3.7	2.7 ± 0.06 i	0.9–1.7	1.2 ± 0.03 fg	2.2	NE	0.080 ± 0.002 h
***Daucus*II subclade**							
D. conchitae	1.9–3.7	2.5 ± 0.05 i–k	0.8–1.5	1.1 ± 0.03 fg	2.2	NE	0.106 ± 0.003 gh
D. glochidiatus	1.8–3.0	2.2 ± 0.04 jk	0.9–1.5	1.2 ± 0.02 fg	1.9	E	0.079 ± 0.004 h
D. guttatus	2.2–3.8	2.8 ± 0.05 i	1.1–1.8	1.4 ± 0.03 d–f	2.1	NE	0.109 ± 0.001 f–h
D. involucratus	2.5–3.4	2.9 ± 0.03 i	0.9–1.6	1.1 ± 0.02 g	2.6	OB	0.098 ± 0.002 gh
D. littoralis	4.8–6.7	5.7 ± 0.07 f	2.1–3.3	2.6 ± 0.04 c	2.3	NE	0.596 ± 0.011 e
D. pusillus	2.0–2.9	2.5 ± 0.03 ij	1.1–1.6	1.3 ± 0.02 e–g	2.0	NE	0.091 ± 0.002 gh
Outgroup							
Caucalis platycarpos	5.8–8.2	7.1 ± 0.07 d	2.3–3.5	2.8 ± 0.03 c	2.6	OB	1.664 ± 0.023 b
Orlaya daucoides	8.7–14.0	11.4 ± 0.18 a	4.2–8.1	5.8 ± 0.11 b	2.0	NE	3.407 ± 0.061 a
O. daucorlaya	6.8–12.5	10.1 ± 0.18 b	3.8–7.3	5.8 ± 0.09 b	1.8	E	3.451 ± 0.035 a
Torilis arvensis	2.2–3.6	2.7 ± 0.03 i	1.2–1.8	1.4 ± 0.02 d–g	2.0	NE	0.178 ± 0.005 fg

Means followed by the same letter in a column were not significantly different at $p \leq 0.05$. E, ellipsoid; NE, narrowly ellipsoid; OB, oblong; OV, ovoid; SE, standard error.

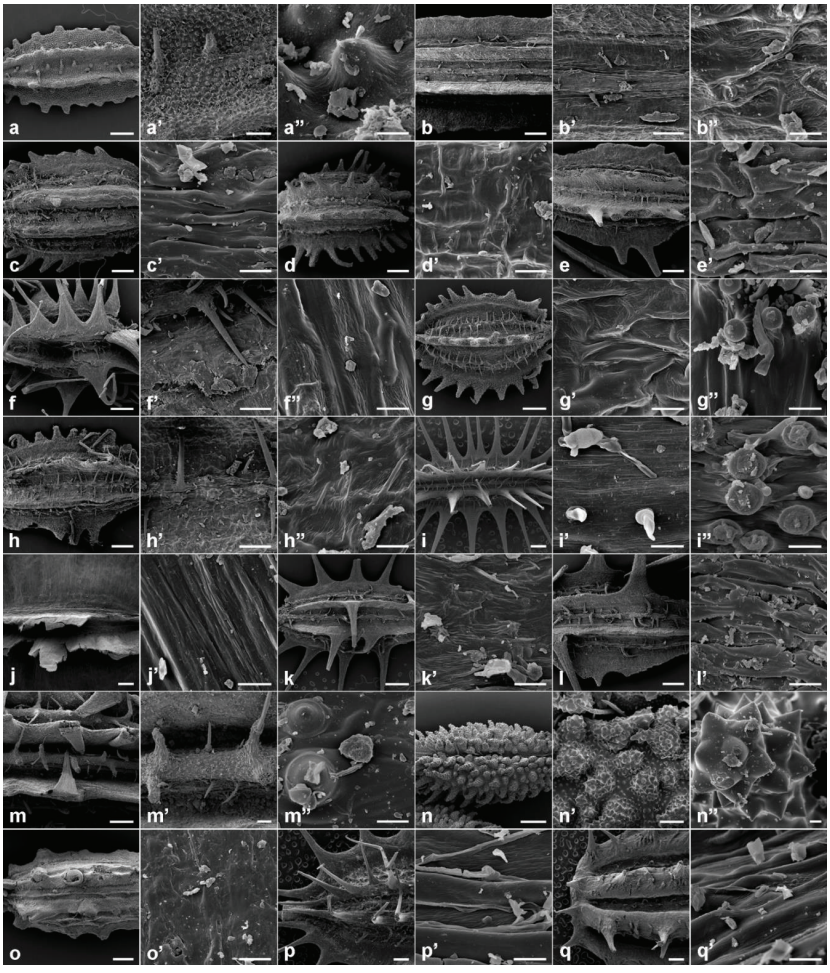

Figure 3. Fruit morphology and its surface micromorphology of the investigated *Daucus* and closely related non-*Daucus* taxa by scanning electron microscopy. (**a**–**a″**) *D. aureus*: (**a**) dorsal view and close-ups on (**a′**) the median primary rib and (**a″**) tubercle; (**b**–**b″**) *D. carota* subsp. *capillifolius*: (**b**) dorsal view and close-ups on (**b′**) the median primary rib and (**b″**) surface between ribs; (**c**,**c′**) subsp. *sativus* (DH): (**c**) dorsal view, (**c′**) close-up on the surface between ribs; (**d**–**d′**) subsp. *sativus* ('Dolanka'): (**d**) dorsal view, (**d′**) close-up on the surface between ribs; (**e**,**e′**) *D. pusillus*: (**e**) dorsal view, (**e′**) close-up on the surface between ribs; (**f**–**f″**) *D. conchitae*: (**f**) dorsal view and close-ups on (**f′**) the primary rib and (**f″**) surface between ribs; (**g**–**g″**) *D. guttatus*: (g) dorsal view and close-ups on (**g′**) the surface between ribs and (**g″**) tubercles; (**h**–**h″**) *D. involucratus*: (**h**) dorsal view and close-ups on (**h′**) the median primary rib and (**h″**) surface between ribs; (**i**–**i″**) *D. littoralis*: (**i**) dorsal view and close-ups on (**i′**) the surface between ribs and (**i″**) tubercles; (**j**,**j′**) *D. rouyi*: (**j**) dorsal view, (**j′**) close-up on the surface of the wing; (**k**,**k′**) *D. sahariensis*: (**k**) dorsal view, (**k′**) close-up on the surface between ribs; (**l**,**l′**) *D. syrticus*: (**l**) dorsal view, (**l′**) close-up on the surface between ribs; (**m**–**m″**) *D. muricatus*: (**m**) dorsal view and close-ups on (**m′**) the primary rib and (**m″**) tubercles; (**n**–**n″**) *Torilis arvensis*: (**n**) dorsal view and close-ups on (**n′**) the additional secondary ribs and (**n″**) tubercle; (**o**–**o′**) *Caucalis platycarpos*: (**o**) dorsal view, (**o′**) close-up on the surface between ribs; (**p**,**p′**) *Orlaya daucoides*: (**p**) dorsal view, (**p′**) close-up on the surface between ribs; (**q**,**q′**) *O. daucorlaya*: (**q**) dorsal view, (**q′**) close-up on the surface between ribs. Scale bars: 600 μm (**i**,**j**,**o**–**q**); 400 μm (**a**,**f**,**g**,**k**,**m**,**n**); 300 μm (**b**–**e**,**h**,**l**); 100 μm (**a′**,**b′**,**f′**,**h′**,**m′**,**n′**); 10 μm (**c′**–**e′**,**g′**,**i′**–**l′**,**o′**–**q′**,**a″**,**b″**,**f″**–**i″**,**m″**,**n″**).

3.2. Fruit Anatomy

The mericarp outline in the transverse section of almost all examined taxa was slightly compressed dorsally (Figures 4–6 and Table 2), except for *C. platycarpos*, which was slightly compressed laterally (Figure 6d).

Although the primary ribs of *Daucus* fruits were not prominent compared to the secondary ones (Figures 3–6), they were distinctly large in *D. muricatus* but still not larger than the secondary ribs (Figures 3m and 6c). The primary ribs were more or less similar in size and shape, whereas the secondary ribs often differed, with lateral secondary ribs usually longer than dorsal ones. The number of ribs in the mericarps was typically constant among taxa, i.e., five primary and four secondary, except for *D. littoralis*, in which mericarps with one additional primary and one additional secondary rib were rarely found (Figure 7a). Among the outgroup, the rib architectural pattern was similar to *Daucus*, i.e., more or less inconspicuous primary ribs and prominent secondary ribs; however, some distinct features of the latter were observed. The secondary ribs of *C. platycarpos* were wide and thick, often with a sunken apex (Figure 6d). *Orlaya daucoides* sometimes had bifurcated secondary ribs (Figure 6f), whereas those of *O. daucorlaya* were massive and thick, often clavate-shaped, with a thin base (Figure 6g). The fruits of *T. arvensis* were characterized by the presence of numerous additional secondary ribs (Figures 3n and 6e).

Table 2. Fruit (mericarp) anatomical characteristics of the investigated *Daucus* and closely related non-*Daucus* (outgroup) taxa.

Taxon	Width (μm)		Pericarp Thickness (μm)	Mericarp Outline [a]	Exocarp [b]	Hypendocarp	Endosperm [c]	Surface Micromorphology
	VV	CV						
***Daucus*I subclade**								
D. aureus	absent	absent	51 ± 5 c–e	SCD	T	–	F/C	Tuberculate
D. carota subsp. *capillifolius*	139 ± 6 bc	181 ± 16 cd	28 ± 1 e	SCD	–	–	F/C	Rugose
D. carota subsp. *sativus* (DH)	91 ± 4 ef	115 ± 6 e–g	38 ± 1 e	SCD	–	–	F/C	Rugose
D. carota subsp. *sativus* ('Dolanka')	82 ± 8 fg	78 ± 3 f–h	32 ± 3 e	SCD	–	–	F/C	Rugose
D. muricatus	33 ± 2 i	83 ± 6 f–h	108 ± 7 ab	SCD	–	–	F/C	Tuberculate
D. rouyi	168 ± 7 a	200 ± 7 c	132 ± 9 a	SCD	–	–	F/C	Ribbed–striate
D. sahariensis	75 ± 4 f–h	122 ± 5 e–g	42 ± 5 e	SCD	A	–	F/C	Rugose
D. syrticus	70 ± 3 f–h	144 ± 14 de	48 ± 4 de	SCD	–	–	F/C	Rugose
***Daucus*II subclade**								
D. conchitae	64 ± 3 gh	71 ± 5 gh	35 ± 2 e	SCD	–	–	F/C	Rugose
D. glochidiatus	53 ± 3 hi	53 ± 3 h	34 ± 6 e	SCD	A	–	F/C	N/A
D. guttatus	87 ± 4 e–g	108 ± 8 e–g	51 ± 4 c–e	SCD	–	–	F/C	Rugose–tuberculate
D. involucratus	75 ± 2 f–h	81 ± 2 f–h	31 ± 2 e	SCD	–	–	F/C	Rugose
D. littoralis	110 ± 5 de	127 ± 8 ef	80 ± 5 bc	SCD	–	–	F/C	Lineolate–tuberculate
D. pusillus	85 ± 2 e–g	125 ± 5 ef	38 ± 5 e	SCD	–	–	F/C	Rugose
Outgroup								
Caucalis platycarpos	93 ± 2 ef	87 ± 3 f–h	117 ± 7 a	SCL	–	–	MG	Smooth
Orlaya daucoides	125 ± 5 cd	273 ± 17 b	129 ± 6 a	SCD	–	+	F/C	Undulate
O. daucorlaya	150 ± 12 ab	329 ± 26 a	118 ± 13 a	SCD	–	+	F/C	Undulate
Torilis arvensis	81 ± 3 fg	106 ± 7 e–g	77 ± 6 cd	SCD	T	–	MG	Tuberculate

[a] Mericarp outline in transverse section. [b] The presence or absence of exocarp protuberances or appendages. [c] Endosperm shape at commissure. Means followed by the same letter in a column were not significantly different at $p \leq 0.05$. A, cells with triangular appendages; CV, width of commissural vittae; F/C, flat or more or less concave; MG, mushroom-like grooved; N/A, not analyzed; SCD, slightly compressed dorsally; SCL, slightly compressed laterally; SE, standard error; T, covered with tubercles; VV, width of vallecular vittae.

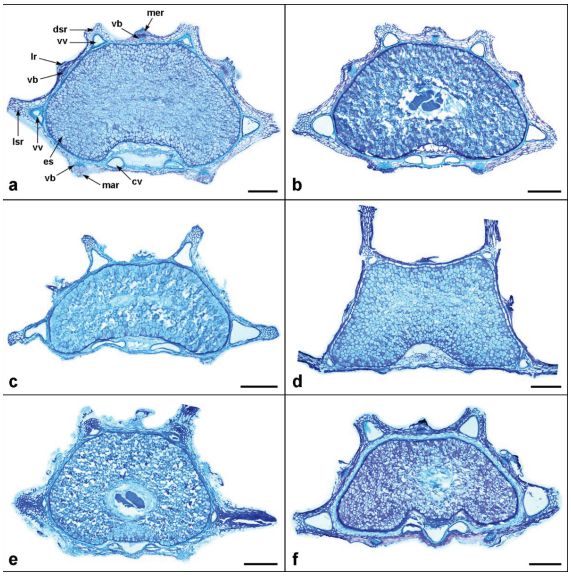

Figure 4. Mericarp structure of the investigated *Daucus* taxa, as seen in a transverse section. (**a**) *D. carota* subsp. *sativus* (DH); (**b**) subsp. *sativus* ('Dolanka'); (**c**) subsp. *capillifolius*; (**d**) *D. conchitae*; (**e**) *D. glochidiatus*; (**f**) *D. guttatus*. Abbreviations: cv, commissural vitta; dsr, dorsal secondary rib; es, endosperm; lr, lateral primary rib; lsr, lateral secondary rib; mar, marginal primary rib; mer, median primary rib; vb, vascular bundle; vv, vallecular vitta. Scale bar = 200 μm.

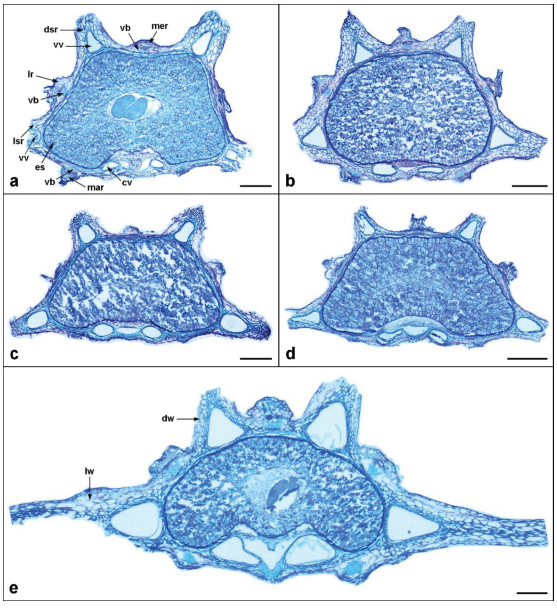

Figure 5. Mericarp structure of the investigated *Daucus* taxa, as seen in a transverse section. (**a**) *D. involucratus*; (**b**) *D. pusillus*; (**c**) *D. sahariensis*; (**d**) *D. syrticus*; (**e**) *D. rouyi*. Abbreviations: cv, commissural vitta; dsr, dorsal secondary rib; dw, dorsal wing; es, endosperm; lr, lateral primary rib; lsr, lateral secondary rib; lw, lateral wing; mar, marginal primary rib; mer, median primary rib; vb, vascular bundle; vv, vallecular vitta. Scale bar = 200 μm.

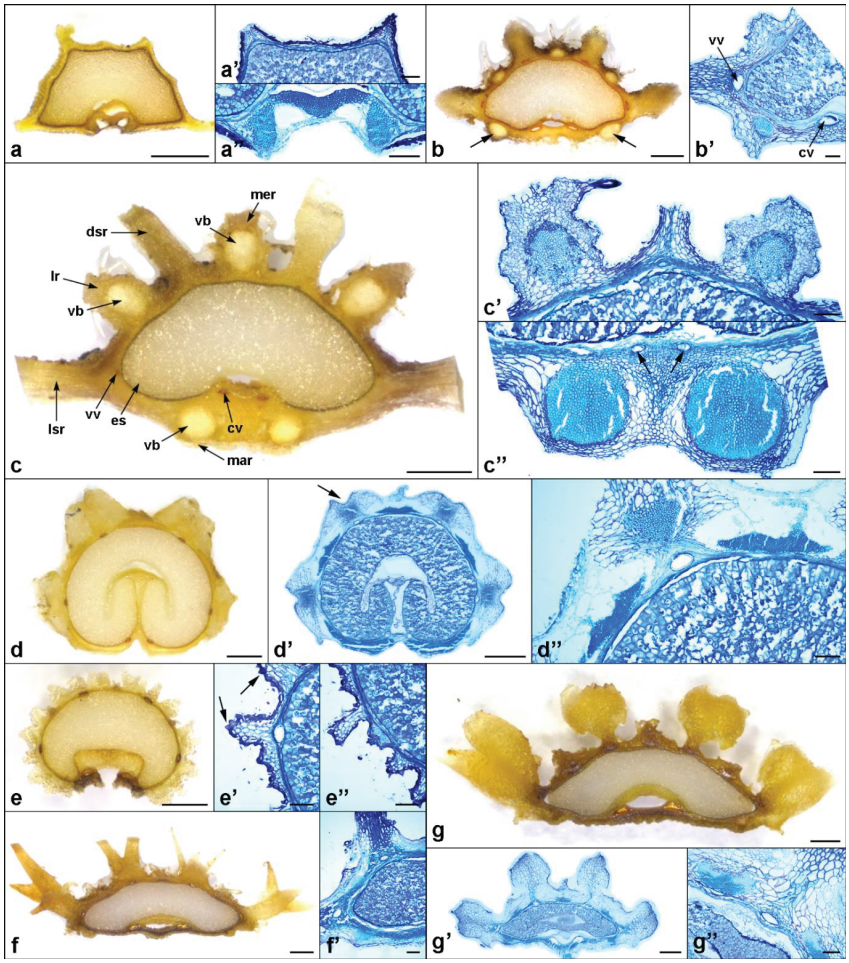

Figure 6. Mericarp structure of the investigated *Daucus* and closely related non-*Daucus* taxa, as seen in a transverse section. (**a**–**a″**) *D. aureus*; (**a′**) the upper part of the mericarp showing the absence of the vallecular vittae; (**a″**) M-shaped vascular bundle at the commissural side; (**b**,**b′**) *D. littoralis*, arrows indicate the larger vascular bundles in the marginal primary ribs; (**c**–**c″**) *D. muricatus*; (**c′**) the upper part of the mericarp showing two primary ribs with vascular bundles and the secondary rib in the middle enclosing the vallecular vitta; (**c″**) vascular bundles in the marginal primary ribs, arrows indicate commissural vittae; (**d**–**d″**) *Caucalis platycarpos*, arrow in (**d′**) indicates the sunken apex of the secondary rib; (**d″**) close-up on the upper part of the mericarp showing the flattened and elongated vascular bundles and a patch of collenchyma above the vallecular vitta; (**e**–**e″**) *Torilis arvensis*; (**e′**) close-up on the secondary rib enclosing the vallecular vitta, arrows indicate tubercles covering the exocarp; (**e″**) close-up on the part of the mericarp with secondary ribs and the primary rib in the middle; (**f**,**f′**) *Orlaya daucoides*; (**g**–**g″**) *O. daucorlaya*; (**g″**) close-up on the upper part of the mericarp showing the vasculature and the vallecular vitta. Abbreviations: cv, commissural vitta; dsr, dorsal secondary rib; es, endosperm; lr, lateral primary rib; lsr, lateral secondary rib; mar, marginal primary rib; mer, median primary rib; vb, vascular bundle; vv, vallecular vitta. Scale bars: 0.5 mm (**a**–**g**,**d′**,**g′**); 100 μm (**a′**–**c′**,**e′**,**f′**,**a″**,**c″**–**e″**,**g″**).

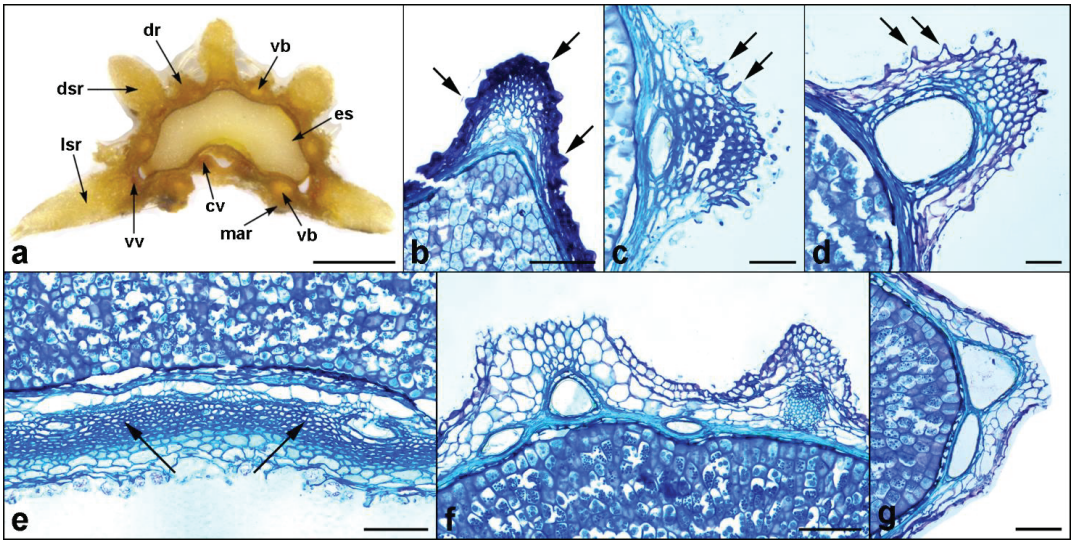

Figure 7. Selected distinct features or abnormalities found in the mericarps of *Daucus* and related taxa. (**a**) Abnormal mericarp of *D. littoralis* with additional dorsal primary and secondary ribs; (**b**) tubercles (arrows) on the exocarp of *D. aureus*; (**c**) characteristic exocarp cells with triangular appendages (arrows) covering the primary ribs of *D. glochidiatus* and (**d**) *D. sahariensis*; (**e**) close-up on the commissural side of *Orlaya daucoides* mericarps showing a hypendocarp (arrows); (**f**,**g**) additional smaller vallecular vittae in the cultivated carrot mericarps. Abbreviations: cv, commissural vitta; dr, dorsal primary rib; dsr, dorsal secondary rib; es, endosperm; lsr, lateral secondary rib; mar, marginal primary rib; vb, vascular bundle; vv, vallecular vitta. Scale bars: 1 mm (**a**); 50 μm (**c**,**d**); 100 μm (**b**,**e**–**g**).

The fruit wall (pericarp) of the investigated taxa had a typical structure of three layers: exocarp, mesocarp, and endocarp (see Figure 1), varying in thickness from 28 to 132 μm (Table 2). The single-layered exocarp consisted of small, thick-walled cells, usually flattened rectangular or more or less isodiametric in shape (Figure 1), but some exceptions were also found. In *D. aureus*, the exocarp was covered with numerous tubercles (Figures 3a and 7b), whereas, in *D. glochidiatus* and *D. sahariensis*, the part of the exocarp that covered the secondary ribs was composed of cells with triangular appendages (Figure 7c,d). The mesocarp consisted of a few to several layers of irregular thin-walled parenchymatic cells, typically larger than the exocarpic cells (Figure 1). The endocarp was a single compressed layer of somewhat lignified cells that usually adhered tightly to the seed coat (Figure 1). Regarding deviations in the pericarp structure among the outgroup taxa, we observed that the exocarp of *T. arvensis* was covered with numerous tubercles (Figures 3n and 6e), whereas the fruits of both *Orlaya* species were characterized by the presence of a hypendocarp, i.e., the inner fibrous mesocarp consisting of several layers of lignified fibers (Figure 7e).

Vallecular vittae were typically well developed in most members of *Daucus* and were triangular or ovate in shape (Figures 4–6); only *D. aureus* was devoid of these structures (Figure 6a). Among all taxa, *D. rouyi* exhibited the largest vallecular vittae (168 μm), whereas *D. muricatus* had the smallest (33 μm) (Table 2). The largest commissural vittae were found in *O. daucorlaya* (329 μm), and the smallest were found in *D. glochidiatus* (53 μm). Generally, each secondary rib enclosed one vitta; however, some variations were observed in carrots in which one or two additional smaller vittae—alongside the larger ones—were sometimes noticed (Figure 7f,g). All taxa, except for *D. aureus*, always had two commissural vittae that were ovate or compressed ovate in shape. Among the outgroups, the number and arrangement of both vallecular and commissural vittae were the same as in *Daucus*.

All *Daucus* taxa had a single compact vascular bundle embedded in the mesocarp below each primary rib. In *D. aureus*, however, the vasculature in the marginal primary ribs was connected in the commissure, forming a distinct M-shaped vascular bundle (Figure 6a). The size of the vascular bundles was more or less similar between the ribs of a given accession, except for *D. littoralis*, whose vascular bundles in the marginal primary ribs were distinctly larger than those in the dorsal primary ribs (Figure 6b). Among the outgroups, the most distinct differences in vasculature were flattened and elongated vascular bundles in the primary ribs of *C. platycarpos* (Figure 6d); the fruits of this taxon were also characterized by the presence of collenchyma in the secondary ribs.

In almost all taxa, the endosperm (commissural side) was flat or more or less concave, except for *C. platycarpos* (Figure 6d) and *T. arvensis* (Figure 6e), whose endosperm was mushroom-like grooved; *C. platycarpos* had strongly revolute margins.

4. Discussion

Traditionally, the taxonomic classification of the family Apiaceae has relied on the morpho-anatomical features of the fruits. However, many of the relationships inferred from this approach appear to be incongruent when confronted with molecular evidence. This is due to the high level of homoplasy among the fruit characteristics, which can be partially explained by selection [44]. Generally morphological characteristics are greatly affected by environmental factors [45–47]. Nevertheless, fruit characteristics can still provide useful information to support or supplement conclusions drawn from molecular data [27,32,44,48–50].

Here, we explored the morphology and anatomy of fruits in 13 *Daucus* and four closely related non-*Daucus* taxa. The results revealed a wide range of variation across the investigated taxa in terms of fruit size, shape, and weight, as well as fruit surface sculpturing and some anatomical characteristics. Thus, we pointed out several diagnostically valuable features of some of the *Daucus* taxa that we discuss below.

The morphometric characteristics and weights of the fruits differed significantly among the taxa (Table 1), which can be helpful—to some extent—in distinguishing between them. However, intra(sub)specific variations may occur in this regard, as observed here for cultivated carrot accessions. Moreover, in many cases, the quantitative values overlapped, which makes these data of limited taxonomic value. Therefore, the micromorphological features of the fruit surface, as well as fruit anatomy, appear to be more advantageous for distinguishing species.

Exocarp cell shape, exomesocarp protuberances, and cuticles are those components that contribute to fruit surface sculpturing, often providing taxonomically useful data [51]. In our study, as revealed by SEM, most of the investigated *Daucus* taxa had a rugose type of ornamentation, which can also be found, for instance, in *Ferula dshizakensis* [41] or some species of *Pimpinella* [52]. In *D. rouyi*, ribbed–striate fruit surface ornamentation was observed. This sculpturing pattern has also been reported, for example, in a few members of *Grammosciadium* [53] and *Pimpinella ibradiensis* [52]. Four *Daucus* taxa were characterized by the presence of tubercles, of which only *D. aureus* was covered on the entire surface of the mericarp, whereas *D. guttatus*, *D. littoralis*, and *D. muricatus* had only tuberculate secondary ribs. As for the exocarp cell shape (not visible by SEM), only *D. glochidiatus* and *D. sahariensis* were marked by the presence of distinct exocarp cells with triangular appendages that covered the surface of the secondary ribs; cells of this shape are characteristic of, for example, *Alepidea serrata* var. *serrata* [51]. Nonetheless, although the micromorphological characteristics of fruit surfaces have proven to be of taxonomic value, the application of these traits is difficult due to the lack of generally accepted terminology [54].

Species of *Daucus* and *Orlaya* (subtribe Daucinae), as well as *Caucalis* and *Torilis* (Torilidinae), are characterized by the presence of prominent secondary ribs, which is an almost unique trait among the members of these two subtribes and the genus *Artedia* [35,50]. In *Daucus*, the secondary ribs form spines or wings, the presence of which is a distinct adaptation to seed dispersal by epizoochory (animal-mediated dispersal) or anemochory

(wind-mediated dispersal). The genus *Daucus* has traditionally comprised only spiny-fruited species [5]; however, following a recent taxonomic revision by Banasiak et al. [11], numerous species with winged or obsolete fruits have been included in the genus. However, fruit appendages are characterized as highly homoplastic and are, thus, of limited utility in delimiting monophyletic groups [11,15].

The number and arrangement of both vallecular and commissural vittae within the pericarp are often of great taxonomic importance in Apiaceae. These secretory canals, located also in roots, stems, and leaves, are responsible for the specific odors of Apiaceae species as they contain essential oils, mucilage, gums, or resins [1], some of which are toxic to insects [55]. In our study, all taxa but one (*D. aureus*) had six vittae per mericarp: one below each secondary rib and two in the commissure, which is a common feature in most genera of Daucinae and Torilidinae [25]. Although we observed some variations in this regard in the cultivated carrot accessions that rarely had additional smaller vittae, these were presumably dwarf vittae, which could also be found, for instance, in *Apium graveolens* [56] or in many members of the Heteromorpheae tribe [57]. However, the size of the vittae seems to be more useful since this feature varied between many taxa.

In *Daucus* and related taxa, each mericarp had five vascular bundles—three in the dorsal primary ribs and two in the marginal primary ribs—as in almost all other members of Apiaceae. However, some exceptions to this pattern were found, for instance, in *Choritaenia capensis* [58] or *Cryptotaenia canadensis* [59], characterized by having seven vascular bundles, of which five were located on the dorsal side and two on the commissural side of the mericarp.

A lignified endocarp, composed of one layer of compressed and elongated cells, was present in all of the investigated *Daucus* taxa. De Miranda et al. [60] evidenced the process of lignin deposition in the endocarp cells of carrot fruit, along with their development, and reported that this process begins 21 days after anthesis.

Although the results showed considerable variations in the fruit morpho-anatomical characteristics, these variations were not sufficient enough to distinguish all of the investigated taxa. Exclusively on the basis of fruit characteristics, the most easily distinguishable taxon among *Daucus* was *D. aureus*, as it was characterized by several unique traits, i.e., entirely tuberculate fruit surface, lack of vittae, and distinct M-shaped vascular bundle on the commissural side. The partially tuberculate taxa (*D. guttatus*, *D. littoralis*, and *D. muricatus*) were distinguished by the length and weight of the mericarps, as well as by the features of their vascular bundles. The two taxa with characteristic exocarp cells with triangular appendages (*D. glochidiatus* and *D. sahariensis*) were differentiated according to the size of their vittae. In the case of *D. carota* subspecies, *D. carota* subsp. *capillifolius* differed from carrot accessions (subsp. *sativus*) by means of its mericarp length and oblong shape. *Daucus rouyi* was the only wing-fruited taxon in our sample. The remaining *Daucus* taxa (*D. syrticus*, *D. conchitae*, *D. involucratus*, *D. pusillus*, and the cultivated carrot) were morphologically and anatomically very similar to each other; thus, we were unable to unambiguously separate them.

5. Conclusions

This study provides detailed information on the morphology and anatomy of fruits from 13 *Daucus* and four closely related non-*Daucus* taxa. The results showed a wide range of variation in the fruit morpho-anatomical characteristics across the investigated taxa, as well as revealed several diagnostically valuable features of the fruits. For *Daucus*, the observed differences included the fruit size, shape (from ellipsoid to oblong), and weight, as well as the fruit surface sculpturing and some anatomical characteristics, i.e., the presence/absence and size of vittae, pericarp thickness, and the shape of exocarp cells. This study broadens the knowledge of the fruits of *Daucus* and may be useful for future taxonomical research on the genus and its close relatives.

However, to gain better insight into the relationships among the genus *Daucus*, further studies with a broader sample, including the remaining members of the genus, are needed.

Author Contributions: Conceptualization, D.K.; methodology, D.K.; formal analysis, D.K.; investigation, D.K.; resources, D.K. and E.G.; data curation, D.K.; writing—original draft preparation, D.K.; writing—review and editing, D.K. and E.G.; visualization, D.K.; supervision, E.G.; project administration, D.K. and E.G.; funding acquisition, D.K. All authors have read and agreed to the published version of the manuscript.

Funding: This research was funded by the National Science Center, Poland (grant number UMO-2019/35/N/NZ9/00959).

Institutional Review Board Statement: Not applicable.

Data Availability Statement: The data presented in this study are available in this article.

Conflicts of Interest: The authors declare no conflict of interest.

References

1. Plunkett, G.M.; Pimenov, M.G.; Reduron, J.-P.; Kljuykov, E.V.; van Wyk, B.-E.; Ostroumova, T.A.; Henwood, M.J.; Tilney, P.M.; Spalik, K.; Watson, M.F.; et al. *Flowering Plants. Eudicots. The Families and Genera of Vascular Plants*; Kadereit, J., Bittrich, V., Eds.; Springer: Cham, Switzerland, 2019; Volume 15, pp. 9–206. [CrossRef]
2. Rubatzky, V.E.; Quiros, C.F.; Simon, P.W. *Carrots and Related Vegetable Umbelliferae*; CABI: New York, NY, USA, 1999; pp. 1–294.
3. Heinonen, M.I. Carotenoids and provitamin A activity of carrot (*Daucus carota* L.) cultivars. *J. Agric. Food. Chem.* **1990**, *38*, 609–612. [CrossRef]
4. Khoo, H.-E.; Prasad, K.N.; Kong, K.-W.; Jiang, Y.; Ismail, A. Carotenoids and their isomers: Color pigments in fruits and vegetables. *Molecules* **2011**, *16*, 1710–1738. [CrossRef] [PubMed]
5. Sáenz Lain, C. Research on *Daucus* L. (Umbelliferae). *An. Jard. Bot. Madrid* **1981**, *37*, 481–533.
6. Spalik, K.; Downie, S.R. Intercontinental disjunctions in *Cryptotaenia* (Apiaceae, Oenantheae): An appraisal using molecular data. *J. Biogeogr.* **2007**, *34*, 2039–2054. [CrossRef]
7. Zhou, J.; Gong, X.; Downie, S.R.; Peng, H. Towards a more robust molecular phylogeny of Chinese Apiaceae subfamily Apioideae: Additional evidence from nrDNA ITS and cpDNA intron (*rpl16* and *rps16*) sequences. *Mol. Phylogenet. Evol.* **2009**, *53*, 56–68. [CrossRef]
8. Spooner, D.; Rojas, P.; Bonierbale, M.; Mueller, L.A.; Srivastav, M.; Senalik, D.; Simon, P. Molecular phylogeny of *Daucus* (Apiaceae). *Syst. Bot.* **2013**, *38*, 850–857. [CrossRef]
9. Arbizu, C.; Ruess, H.; Senalik, D.; Simon, P.W.; Spooner, D.M. Phylogenomics of the carrot genus (*Daucus*, Apiaceae). *Am. J. Bot.* **2014**, *101*, 1666–1685. [CrossRef]
10. Arbizu, C.I.; Ellison, S.L.; Senalik, D.; Simon, P.W.; Spooner, D.M. Genotyping-by-sequencing provides the discriminating power to investigate the subspecies of *Daucus carota* (Apiaceae). *BMC Evol. Biol.* **2016**, *16*, 234. [CrossRef]
11. Banasiak, Ł.; Wojewódzka, A.; Baczyński, J.; Reduron, J.P.; Piwczyński, M.; Kurzyna-Młynik, R.; Gutaker, R.; Czarnocka-Cieciura, A.; Kosmala-Grzechnik, S.; Spalik, K. Phylogeny of Apiaceae subtribe Daucinae and the taxonomic delineation of its genera. *Taxon* **2016**, *65*, 563–585. [CrossRef]
12. Spooner, D.M.; Ruess, H.; Iorizzo, M.; Senalik, D.; Simon, P. Entire plastid phylogeny of the carrot genus (*Daucus*, Apiaceae): Concordance with nuclear data and mitochondrial and nuclear DNA insertion to the plastid. *Am. J. Bot.* **2017**, *104*, 296–312. [CrossRef]
13. Spooner, D.M.; Ruess, H.; Ellison, S.; Senalik, D.; Simon, P. What is truth: Consensus and discordance in next-generation phylogenetic analyses of *Daucus*. *J. Syst. Evol.* **2020**, *58*, 1059–1070. [CrossRef]
14. Grzebelus, D.; Baranski, R.; Spalik, K.; Allender, C.; Simon, P.W. *Daucus*. In *Wild Crop Relatives: Genomic and Breeding Resources. Vegetables*; Kole, C., Ed.; Springer: Berlin/Heidelberg, Germany, 2011; pp. 91–113. [CrossRef]
15. Spooner, D.M. *Daucus*: Taxonomy, phylogeny, distribution. In *The Carrot Genome. Compendium of Plant Genomes*; Simon, P., Iorizzo, M., Grzebelus, D., Baranski, R., Eds.; Springer: Cham, Switzerland, 2019; pp. 9–26. [CrossRef]
16. Frankiewicz, K.E.; Oskolski, A.; Banasiak, Ł.; Fernandes, F.; Reduron, J.-P.; Reyes-Betancort, J.-A.; Szczeparska, L.; Alsarraf, M.; Baczyński, J.; Spalik, K. Parallel evolution of arborescent carrots (*Daucus*) in Macaronesia. *Am. J. Bot.* **2020**, *107*, 394–412. [CrossRef] [PubMed]
17. Iovene, M.; Grzebelus, E.; Carputo, D.; Jiang, J.; Simon, P.W. Major cytogenetic landmarks and karyotype analysis in *Daucus carota* and other Apiaceae. *Am. J. Bot.* **2008**, *95*, 793–804. [CrossRef] [PubMed]
18. Rice, A.; Glick, L.; Abadi, S.; Einhorn, M.; Kopelman, N.M.; Salman-Minkov, A.; Mayzel, J.; Chay, O.; Mayrose, I. The chromosome counts database (CCDB)—A community resource of plant chromosome numbers. *New Phytol.* **2015**, *206*, 19–26. [CrossRef]
19. Nowicka, A.; Sliwinska, E.; Grzebelus, D.; Baranski, R.; Simon, P.W.; Nothnagel, T.; Grzebelus, E. Nuclear DNA content variation within the genus *Daucus* (Apiaceae) determined by flow cytometry. *Sci. Hortic.* **2016**, *209*, 132–138. [CrossRef]
20. Roxo, G.; Moura, M.; Talhinhas, P.; Costa, J.C.; Silva, L.; Vasconcelos, R.; Menezes de Sequeira, M.; Romeiras, M.M. Diversity and cytogenomic characterization of wild carrots in the Macaronesian islands. *Plants* **2021**, *10*, 1954. [CrossRef]
21. Kadluczka, D.; Sliwinska, E.; Grzebelus, E. Combining genome size and pollen morphology data to study species relationships in the genus *Daucus* (Apiaceae). *BMC Plant Biol.* **2022**, *22*, 382. [CrossRef]

22. Kljuykov, E.V.; Liu, M.; Ostroumova, T.A.; Pimenov, M.G.; Tilney, P.M.; van Wyk, B.-E.; van Staden, J. Towards a standardised terminology for taxonomically important morphological characters in the Umbelliferae. *S. Afr. J. Bot.* **2004**, *70*, 488–496. [CrossRef]
23. Kljuykov, E.V.; Zakharova, E.A.; Ostroumova, T.A.; Tilney, P.M. Most important carpological anatomical characters in the taxonomy of Apiaceae. *Bot. J. Linn. Soc.* **2021**, *195*, 532–544. [CrossRef]
24. Pimenov, M.G.; Leonov, M.V. *The Genera of the Umbelliferae: A Nomenclator*; Royal Botanic Gardens, Kew: Richmond, UK, 1993; pp. 1–156.
25. Spalik, K.; Wojewódzka, A.; Downie, S.R. The evolution of fruit in Scandiceae subtribe Scandicinae (Apiaceae). *Can. J. Bot.* **2001**, *79*, 1358–1374. [CrossRef]
26. Liu, M.; van Wyk, B.-E.; Tilney, P.M. The taxonomic value of fruit structure in the subfamily Saniculoideae and related African genera (Apiaceae). *Taxon* **2003**, *52*, 261–270. [CrossRef]
27. Liu, M.; Plunkett, G.M.; Lowry, P.P.; van Wyk, B.-E.; Tilney, P.M. The taxonomic value of fruit wing types in the order Apiales. *Am. J. Bot.* **2006**, *93*, 1357–1368. [CrossRef] [PubMed]
28. Liu, M.; van Wyk, B.-E.; Tilney, P.M.; Plunkett, G.M.; Lowry, P.P. Evidence from fruit structure supports in general the circumscription of Apiaceae subfamily Azorelloideae. *Plant Syst. Evol.* **2009**, *280*, 1–13. [CrossRef]
29. Khajepiri, M.; Ghahremaninejad, F.; Mozaffarian, V. Fruit anatomy of the genus *Pimpinella* L. (Apiaceae) in Iran. *Flora* **2010**, *205*, 344–356. [CrossRef]
30. Akalın Uruşak, E. Fruit anatomy of some *Ferulago* (Apiaceae) species in Turkey. *Turk. J. Bot.* **2013**, *37*, 434–445. [CrossRef]
31. Akalın, E.; Yeşil, Y.; Akpulat, A. Fruit anatomy of the Turkish *Pimpinella* species. *Flora* **2016**, *223*, 62–73. [CrossRef]
32. Liu, M.; Downie, S.R. The phylogenetic significance of fruit anatomical and micromorphological structures in Chinese *Heracleum* species and related taxa (Apiaceae). *Syst. Bot.* **2017**, *42*, 313–325. [CrossRef]
33. Arbizu, C.I.; Simon, P.W.; Martínez-Flores, F.; Ruess, H.; Crespo, M.B.; Spooner, D.M. Integrated molecular and morphological studies of the *Daucus guttatus* complex (Apiaceae). *Syst. Bot.* **2016**, *41*, 479–492. [CrossRef]
34. Mezghani, N.; Zaouali, I.; Bel Amri, W.; Rouz, S.; Simon, P.W.; Hannachi, C.; Ghrabi, Z.; Neffati, M.; Bouzbida, B.; Spooner, D.M. Fruit morphological descriptors as a tool for discrimination of *Daucus* L. germplasm. *Genet. Resour. Crop Evol.* **2014**, *61*, 499–510. [CrossRef]
35. Wojewódzka, A.; Baczyński, J.; Banasiak, Ł.; Downie, S.R.; Czarnocka-Cieciura, A.; Gierek, M.; Frankiewicz, K.; Spalik, K. Evolutionary shifts in fruit dispersal syndromes in Apiaceae tribe Scandiceae. *Plant Syst. Evol.* **2019**, *305*, 401–414. [CrossRef]
36. Brozynska, M.; Furtado, A.; Henry, R.J. Genomics of crop wild relatives: Expanding the gene pool for crop improvement. *Plant Biotechnol. J.* **2016**, *14*, 1070–1085. [CrossRef]
37. Dempewolf, H.; Baute, G.; Anderson, J.; Kilian, B.; Smith, C.; Guarino, L. Past and future use of wild relatives in crop breeding. *Crop Sci.* **2017**, *57*, 1070–1082. [CrossRef]
38. Prohens, J.; Gramazio, P.; Plazas, M.; Dempewolf, H.; Kilian, B.; Díez, M.J.; Fita, A.; Herraiz, F.J.; Rodríguez-Burruezo, A.; Soler, S.; et al. Introgressiomics: A new approach for using crop wild relatives in breeding for adaptation to climate change. *Euphytica* **2017**, *213*, 158. [CrossRef]
39. Kadluczka, D.; Grzebelus, E. Using carrot centromeric repeats to study karyotype relationships in the genus *Daucus* (Apiaceae). *BMC Genomics* **2021**, *22*, 508. [CrossRef] [PubMed]
40. Lee, C.; Kim, J.; Darshetkar, A.M.; Choudhary, R.K.; Park, S.-H.; Lee, J.; Choi, S. Mericarp morphology of the tribe Selineae (Apiaceae, Apioideae) and its taxonomic implications in Korea. *Bangladesh J. Plant Taxon.* **2018**, *25*, 175–186. [CrossRef]
41. Mustafina, F.U.; Lee, H.; Sharipova, V.K.; Lee, A.; Kim, D.W.; Choi, M.N.; Jang, J.W.; Kim, Y.-S. Comparative fruit morphology and its systematic significance in *Ferula* (Apiaceae) species from different growth habitats. *Flora* **2021**, *283*, 151899. [CrossRef]
42. Stearn, W.T. *Botanical Latin. History, Grammar, Syntax, Terminology and Vocabulary*, 3rd ed.; David & Charles: New Abbot, UK, 1983; pp. 506–507.
43. Ostroumova, T.A. Fruit micromorphology in the Umbelliferae of the Russian Far East. *Bot. Pac.* **2018**, *7*, 41–49. [CrossRef]
44. Piwczyński, M.; Puchałka, R.; Spalik, K. The infrageneric taxonomy of *Chaerophyllum* (Apiaceae) revisited: New evidence from nuclear ribosomal DNA ITS sequences and fruit anatomy. *Bot. J. Linn. Soc.* **2015**, *178*, 298–313. [CrossRef]
45. Sharma, G.P.; Esler, K.J. Phenotypic plasticity among *Echium plantagineum* populations in different habitats of Western Cape, South Africa. *S. Afr. J. Bot.* **2008**, *74*, 746–749. [CrossRef]
46. Nicotra, A.B.; Atkin, O.K.; Bonser, S.P.; Davidson, A.M.; Finnegan, E.J.; Mathesius, U.; Poot, P.; Purugganan, M.D.; Richards, C.L.; Valladares, F.; et al. Plant phenotypic plasticity in a changing climate. *Trends Plant Sci.* **2010**, *15*, 684–692. [CrossRef]
47. Abdurahman, M.; Sabirhazi, G.; Liu, B.; Yin, L.; Pan, B. Comparison of five *Calligonum* species in Tarim Basin based on morphological and molecular data. *EXCLI J.* **2012**, *11*, 776–782. [PubMed]
48. Feist, M.A.E.; Downie, S.R.; Magee, A.R.; Liu, M.R. Revised generic delimitations for *Oxypolis* and *Ptilimnium* (Apiaceae) based on leaf morphology, comparative fruit anatomy, and phylogenetic analysis of nuclear rDNA ITS and cpDNA trnQ–trnK intergenic spacer sequence data. *Taxon* **2012**, *61*, 402–418. [CrossRef]
49. Liao, C.; Downie, S.R.; Li, Q.; Yu, Y.; He, X.; Zhou, B. New insights into the phylogeny of *Angelica* and its allies (Apiaceae) with emphasis on East Asian species, inferred from nrDNA, cpDNA, and morphological evidence. *Syst. Bot.* **2013**, *38*, 266–281. [CrossRef]
50. Lyskov, D.; Degtjareva, G.; Samigullin, T.; Pimenov, M. Systematic placement of the Turkish endemic genus *Ekimia* (Apiaceae) based on morphological and molecular data. *Turk. J. Bot.* **2015**, *39*, 673–680. [CrossRef]

51. Yembaturova, E.Y.; van Wyk, B.-E.; Tilney, P.M.; Winter, P.J.D. The taxonomic significance of fruit morphology and anatomy in the genus *Alepidea* Delaroche (Apiaceae, subfamily Saniculoideae). *Plant Divers. Evol.* **2010**, *128*, 369–385. [CrossRef]
52. Yeşil, Y.; Akalın, E.; Akpulat, A.; Vural, C. Fruit morphology of the genus *Pimpinella* (Apiaceae) in Turkey. *An. Jard. Bot. Madr.* **2018**, *75*, e072. [CrossRef]
53. Bani, B.; Karakaya, M.A.; Çeter, T. Fruit micromorphological characters of the genus *Grammosciadium* DC. (Apiaceae) in Turkey. *Phytotaxa* **2016**, *246*, 184–191. [CrossRef]
54. Ostroumova, T.A.; Kljuykov, E.V. Fruit structure and microsculpture in the annual species of the genus *Bupleurum*, section Perfoliata (Umbelliferae). *Phytol. Balc.* **2015**, *21*, 117–127.
55. Berenbaum, M.R. Evolution of specialization in insect-umbellifer associations. *Annu. Rev. Entomol.* **1990**, *35*, 319–343. [CrossRef]
56. Ronse, A.C.; Popper, Z.A.; Preston, J.C.; Watson, M.F. Taxonomic revision of European *Apium* L. s.l.: *Helosciadium* W.D.J.Koch restored. *Plant Syst. Evol.* **2010**, *287*, 1–17. [CrossRef]
57. Liu, M.; van Wyk, B.-E.; Tilney, P.; Plunkett, G.M.; Lowry, P.P.; Magee, A.R. The phylogenetic significance of fruit structural variation in the tribe Heteromorpheae (Apiaceae). *Pak. J. Bot.* **2016**, *48*, 201–210.
58. Liu, M.; van Wyk, B.-E.; Tilney, P.M. A revision of the genus *Choritaenia* (Apiaceae). *S. Afr. J. Bot.* **2007**, *73*, 184–189. [CrossRef]
59. Magee, A.R.; van Wyk, B.-E.; Tilney, P.M.; Downie, S.R. Phylogenetic position of African and Malagasy *Pimpinella* species and related genera (Apiaceae, Pimpinelleae). *Plant Syst. Evol.* **2010**, *288*, 201–211. [CrossRef]
60. de Miranda, R.M.; Dias, D.C.F.D.; Picoli, E.A.D.; da Silva, P.P.; Nascimento, W.M. Physiological quality, anatomy and histochemistry during the development of carrot seeds (*Daucus carota* L.). *Ciênc. Agrotec.* **2017**, *41*, 169–180. [CrossRef]

agriculture

MDPI

Article

The Hunt for Mungbean (*Vigna radiata* (L.) Wilczek) Genotypes and Breeding Lines Resistance to South Indian Bruchid Strain

Santhi Madhavan Samyuktha [1], Devarajan Malarvizhi [2], Irulappan Mariyammal [1], Adhimoolam Karthikeyan [3], Devina Seram [4], Manickam Dhasarathan [5], Sundarrajan Juliet Hepziba [1], Venugopal Sheela [6], Arumugam Thanga Hemavathy [7], Duraisamy Kavithamani [8], Shanmugam Kavitha [9] and Natesan Senthil [10,*]

[1] Department of Plant Breeding and Genetics, Agricultural College and Research Institute, Tamil Nadu Agricultural University, Madurai 625104, India; samyukthaliea@gmail.com (S.M.S.); mari.tnau@gmail.com (I.M.); juliethepziba.s@tnau.ac.in (S.J.H.)
[2] Agricultural Research Station, Tamil Nadu Agricultural University, Bhavanisagar 638451, India; dmalarvizhi@tnau.ac.in
[3] Department of Biotechnology, Centre of Innovation, Agricultural College and Research Institute, Tamil Nadu Agricultural University, Madurai 625104, India; karthik2373@gmail.com
[4] Department of Entomology, School of Agriculture, Lovely Professional University, Phagwara 144001, India; devnah@gmail.com
[5] Agro Climate Research Centre, Directorate of Crop Management, Tamil Nadu Agricultural University, Coimbatore 641003, India; plantdr.dhasarathan@gmail.com
[6] Department of Rice, Centre for Plant Breeding and Genetics, Tamil Nadu Agricultural University, Coimbatore 641003, India; sheelavenugopal@tnau.ac.in
[7] Department of Pulses, Centre for Plant Breeding and Genetics, Tamil Nadu Agricultural University, Coimbatore 641003, India; thangahemavathy@tnau.ac.in
[8] Department of Millets, Centre for Plant Breeding and Genetics, Tamil Nadu Agricultural University, Coimbatore 641003, India; dkavithamani@tnau.ac.in
[9] Department of Plant Genetic Resources, Centre for Plant Breeding and Genetics, Tamil Nadu Agricultural University, Coimbatore 641003, India; skavitha@tnau.ac.in
[10] Department of Plant Molecular Biology and Bioinformatics, Centre for Plant Molecular Biology and Biotechnology, Tamil Nadu Agricultural University, Coimbatore 641003, India
* Correspondence: senthil_natesan@tnau.ac.in

Citation: Samyuktha, S.M.; Malarvizhi, D.; Mariyammal, I.; Karthikeyan, A.; Seram, D.; Dhasarathan, M.; Juliet Hepziba, S.; Sheela, V.; Thanga Hemavathy, A.; Kavithamani, D.; et al. The Hunt for Mungbean (*Vigna radiata* (L.) Wilczek) Genotypes and Breeding Lines Resistance to South Indian Bruchid Strain. *Agriculture* **2022**, *12*, 1050. https://doi.org/10.3390/agriculture12071050

Academic Editors: Edyta Paczos-Grzeda, Volker Mohler and Sylwia Sowa

Received: 15 June 2022
Accepted: 15 July 2022
Published: 18 July 2022

Abstract: Mungbean (*Vigna radiata*) is an important short-season legume widely cultivated in Asia, particularly India. It is highly susceptible to bruchids and developing bruchid resistance is an important goal in mungbean breeding programs. In the present study, 52 mungbean genotypes were evaluated for bruchid resistance based on the "no-choice test" and identified two highly resistant genotypes (V2802BG and V2709) with no adult emergence and seed damage. Further, these two resistant genotypes were crossed with six high-yielding bruchid susceptible cultivars (CO 5, CO 6, CO 7, CO 8, VBN 2, and VBN 3), and 12 independent F_1 populations were generated. Of these, one population derived from CO 6 × V2802BG was selected (based on the good combining ability of the parents) and forwarded to later generations to trace the bruchid-resistant lines. A total of 159 $F_{2:3}$ families were screened for bruchid resistance, and the results showed that seven families were highly resistant, whereas the remainder were resistant to highly susceptible. Further, those seven families were evaluated in F_4 and F_5 generations. As a result, five highly resistant lines (BSR-GG-1-49-3-1, BSR-GG-1-56-2-2, BSR-GG-1-160-5-3, BSR-GG-1-170-2-4, and BSR-GG-1-198-1-4) with good agronomic performances were identified. The newly developed lines could be tested in multi-location trials and then be utilized as a potential source of genetic material for improving the bruchid resistance in mungbean breeding programs.

Keywords: bruchid resistance; *Callosobruchus* spp.; introgression breeding; mungbean

1. Introduction

Mungbean (*Vigna radiata*) is a major grain legume and versatile crop cultivated throughout Asia. It is an excellent source of protein, carbohydrates, minerals, and vitamins for people [1,2]. Mungbean has the ability to fix nitrogen even in poor soils. Also, it is compatible with growing as an intercrop with many cereals and root crops, as well as with cotton, sugarcane, and several plantation crops [1,3–6]. With these characteristics, the mung bean is highly adaptable for sustainable agriculture in marginal lands and drier tropical regions. Asia alone accounts for 90% of mungbean production, and some mung bean is also produced in Africa, Australia, and the United States [2]. The important mungbean growing countries are India, Pakistan, Bangladesh, China, Myanmar, and Nepal. India is the largest producer in the world and produces a significant amount of mung bean. The total mungbean area in India was 4.07 million ha, with a total production of 1.9 million tonnes [7]. However, the standard yield of mungbean is low, and its production has not been significantly increased yet.

Insect pests are a formidable threat to flourishing mungbean production in Asia, including India. The outbreak of insect pests seriously reduces the yield and quality of mungbean. Among the insect pests, bruchids (*Callosobruchus* spp. Coleoptera, Bruchidae) are major insects causing severe damage to seeds in storage conditions [8–10]. The two most common species infecting mungbean seeds are *Callosobruchus chinensis* (L.) and *Callosobruchus maculatus* (F.) [11]. Bruchid infection in field conditions have no severe impacts because of oviposition on the surface of green pods. However, infection in storage conditions leads to severe damage to seeds [12,13]. A single insect-infested seed is a potential source for bruchid population development under storage conditions. Bruchid damage significantly reduces the grain's commercial and nutritional values [14–16]. Therefore, the seeds are not suitable for human consumption and agricultural use.

Breeding resistant cultivars is a cost-effective and environment-friendly method for managing bruchids in mungbean production [10,17–20]. However, over the past decade, limited progress has been made in mungbean breeding to identify resistance sources and develop resistant varieties. So far, several genotypes with resistance to bruchids have been identified by screening a set of mungbean germplasm [21–25]. However, the resistance breakdown occurs with the emergence of a new bruchid population. Moreover, resistant genotypes are not well adapted to different agro-climatic zones, and their agronomic performance is low. Therefore, it is essential to develop bruchid-resistant high-yielding genotypes adapted to different agro-climatic zones. With this backdrop, the objectives of the present study were to: (i) screen mungbean genotypes' resistance to South Indian bruchid strain based on "no-choice" testing; (ii) develop the breeding lines with bruchid resistance, (iii) assess the agronomic performance of the resistant lines.

2. Materials and Methods

2.1. Plant Genetic Materials

Fifty-two mungbean genotypes from different parts of Asian and African countries were used to evaluate resistance to bruchids (*C. maculatus*). The mungbean seeds were obtained from the Department of Plant Genetic Resources, Tamil Nadu Agricultural University (TNAU), Coimbatore, India; National Bureau of Plant Genetic Resources (NBPGR), New Delhi, India; and Asian Vegetable Research and Development Center (AVRDC), Taiwan.

2.2. Source and Identification of Callosobruchus maculatus

The culture of the test insect was maintained in the plastic containers (20 × 10 cm) on a BOD-incubator (Bio-Oxygen Demand) under the temperature of 27 ± 1 °C with 65 ± 5% of relative humidity (RH) at the storage laboratory, Agricultural Research Station (ARS), TNAU, Bhavanisagar, Tamil Nadu, India. To raise the culture in the laboratory, bruchid adults were collected from the local grain market, and *C. maculatus* was carefully separated based on the morphological characters with the support of a stereo zoom microscope (Olympus SZ61, Tokyo, Japan). Adult males and females of *C. maculatus* were differentiated

through readily observable morphological characters (i.e., the abdomen's size and shape) (Figure 1). Males had a shorter abdomen than females, with the dorsal side of terminal segments bent strongly downwards. Females have dark stripes on each side of their posterior dorsal belly, but males do not have dark stripes [26].

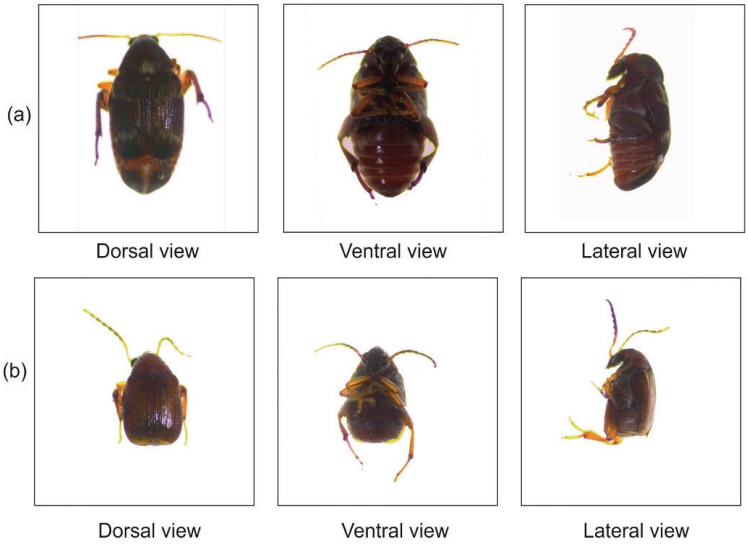

Figure 1. Female (**a**) and male (**b**) bruchid beetles (*Callosobruchus maculatus*).

2.3. Mass Culturing and Maintenance of Callosobruchus maculatus

The infested mungbean seeds collected from the local grain markets of Bhavanisagar, Tamil Nadu, India, were kept for one generation as a source of initial bruchid cultures (*Callosobruchus maculatus*). The pests obtained from initial cultures were reared on fresh CO 6 mungbean seeds susceptible to bruchids following the procedure adopted by Seram et al. [27] with some modifications. Around 50 pairs of *C. maculatus* adults were placed into 600 mL plastic containers containing 200 g of mungbean seeds (CO 6). The containers were covered using a muslin cloth, which allowed adequate ventilation but prevented insects from escaping and placed inside the incubator at 27 ± 1 °C with relative humidity (RH) of 65 ± 5% to facilitate maximum oviposition. The insects were allowed to oviposit for 10 days before being discarded. The dead adults were discarded from each container daily by visual screening using a microscope. Freshly emerging progenies were used to generate the subsequent generations of the laboratory population after 25–30 days. A specific number of females were collected from stock culture, transferred individually to different containers, and maintained as subcultures adopting the above-mentioned procedure. Infested seeds were regularly replaced with fresh ones at monthly intervals.

2.4. Assay Methodology for Screening Mungbean Genotypes and Resistance Evaluation

Bruchid resistance evaluation was made in 52 mungbean genotypes using a "no-choice" test according to the method described by Venkataramana et al. [28] with minor modifications. The stepwise procedures for conducting a "no-choice" test are detailed. Briefly, the sample containers were first labeled (i.e., Genotype name, replication number, and date of infestation), and then each sample was kept in respective containers in three replications containing 20 seeds each replication. Five pairs of freshly emerged adults were introduced per container, covered with muslin cloth on the top and tied with rubber bands. For oviposition, the containers were left undisturbed for three days. Containers were kept inside an incubator at 27 ± 1 °C with RH of 65 ± 5% to facilitate proper oviposition. After three days, containers with egg-laden seeds were carefully taken out, and the number of

eggs oviposited on each seed sample was counted. The presence of frass was checked, and the number of eggs hatched on the 4th and 5th day (After oviposition or release of insects) was recorded. Containers (with egg-laden seeds) were undisturbed until the first adult emergence of a new insect generation. Then, the observations were taken up to the cessation of adult emergence. The observations were recorded based on the following biological and damage assessment parameters:

I. The number of eggs laid: The total number of eggs laid was counted in each genotype for seven days after adult release;
II. The number of adults emerged: The total number of adults emerged was counted daily to determine the mean developmental period (days) and continued till the cessation of emergence;
III. Adult emergence percentage: (Number of adults emerged/number of eggs laid) × 100;
IV. Female to male ratio;
V. Mean developmental period (MDP) recorded in days.

The mean developmental period is the time required for the emergence of 50% of adults. It was calculated by the formula given by Howe [29]

$$MDP = D_1A_1 + D_2A_2 + D_3A_3 + \ldots + D_nA_n / \text{Total number of adults emerged}$$

where D_1 = day at which the first adult started emerging (1st day), A_1 = total number of adults emerged on the D_1th day

a. Susceptibility Index: log (per cent adult emergence)/mean developmental period.
b. Percentage of (%) seed damage: Number of seeds damaged/Number of seeds taken × 100. Based on seed damage percent, the genotypes were categorized as highly resistant (0–10%), resistant (10.1–20%), moderately resistant (20.1–40%), susceptible (40.1–80%), and highly susceptible (80.1–100%) [10].

2.5. Generation of Breeding Population Using Resistant and Susceptible Genotypes

The two resistant genotypes (V2802BG and V2709) and six high-yielding susceptible cultivars (CO 5, CO 6, CO 7, CO 8, VBN 2, and VBN 3) were raised in a crossing block during June to September 2018 at ARS, Bhavanisagar. The genotypes were raised on 4-m length ridges at 30 cm spacing between ridges and 10 cm between plants. Two-staggered sowing of parents was used to synchronize flowering and continuous supply of pollen for the crossing program. The crossed pods from the following cross combinations *viz.*, CO 5 × V2802BG, CO 5 × V2709, CO 6 × V2802BG, CO 6 × V2709, CO 7 × V2802BG, CO 7 × V2709, CO 8 × V2802BG, CO 8 × V2709, VBN 2 × V2802BG, VBN 2 × V2709, VBN 3 × V2802BG and VBN 3 × V2709 were collected separately, threshed, and used to raise the F_1 generation at ARS, Bhavanisagar during November 2018 to February 2019. Then, F_2 generation was raised during March to June 2019, and the seeds of each plant were collected individually, and the selected progenies were forwarded to F_3–F_5. The F_3, F_4, and F_5 generations were raised during July to October 2019, December 2019 to March 2020, and April to July 2020. All the generations were raised at ARS, Bhavanisagar.

2.6. Assessment of Grub and Morphological Traits

Grub development and morphological traits were examined in five resistant genotypes (BSR-GG-1-49-3-1, BSR-GG-1-56-2-2, BSR-GG-1-160-5-3, BSR-GG-1-170-2-4, and BSR-GG-1-198-1-4) in the F_5 generation and parents of the cross CO 6 × V2802BG. The morphometric measurement (length and breadth) of the grub of *Callosobruchus maculatus* was measured with the help of a stereo zoom microscope with ten replications. At about 20 days after insect infestation (DAI), seeds with developing grubs inside were carefully cut open, and the measurements were taken. The morphological traits were evaluated in five stable resistant lines from the F_5 generation raised in three replications to determine the agronomic performance. The morphological observations were recorded based on the standard descriptors of mungbean [30]. The traits recorded were plant height (cm), days to fifty

percent flowering, number of pods per plant, pod length (cm), number of seeds per pod, hundred seed weight (g), and single plant yield (g).

2.7. Statistical Analysis

The data on the biological and damage assessment parameters of *C. maculatus* in different genotypes and breeding populations were subjected to square root transformation in case of number values and angular transformation in case of percent values and analyzed using a Completely Randomized Design suggested by Panse and Sukhatme [31]. Analysis of variance (ANOVA) was carried out using SPSS 16.0 version. The general combining ability effects of the parents was worked out as suggested by Kempthorne [32]. Combining ability analysis was carried out using the TNAUSTAT software package [33].

3. Results

3.1. Bruchid Resistance Determination on 52 Mungbean Genotypes

Seed characteristics showed only slight variation among the 52 mungbean genotypes examined. The majority of the genotypes had light green color seeds with shiny lustre. Greenish-yellow or dark green seeds with a dull lustre were seen in a few genotypes. Both oval (24 accessions) and drum (28 accessions) types of seeds were common among the genotypes. The total number of eggs in each genotype ranged from 22 (V2802BG) to 69 (EC 396121), which was significantly higher and lower than the overall mean (Table 1; Figure 2).

Figure 2. Mungbean genotypes response to bruchid beetles (*Callosobruchus maculatus)* Note: V2802BG and V2709 (Highly resistant); EC 396113, EC 396106, BDYR2, Barimung 7, AVRDC 1785/5, and EC 396126 (Highly susceptible).

Table 1. Screening of 52 mungbean genotypes for bruchid resistance.

S.No.	Genotypes	No.of Eggs Laid	No. of Adults Emerged	Adult Emergence Percentage	Mean Developmental Period	No. of Males Emerged	No. of Females Emerged	Female to Male Ratio	Susceptibility Index	Damage Percentage	Category
1	NM94	52 ± 3.28^{h}	20	38.46^{pq}	25.75 ± 0.65^{qrstuv}	14 ± 0.88^{b}	6 ± 0.88^{j}	0.43^{j}	$0.062^{defghijklmnopq}$	100	HS
2	Binamung 2	30 ± 3.76^{x}	20	66.67^{a}	23.35 ± 0.63^{y}	12 ± 1.15^{d}	8 ± 1.15^{h}	0.67^{h}	0.078^{a}	100	HS
3	Barimung 7	50 ± 5.29^{i}	20	40.00^{op}	25.75 ± 0.88^{qrstuv}	11 ± 1.45^{e}	9 ± 1.45^{g}	0.82^{g}	$0.062^{cdefghijklmnop}$	100	HS
4	Barimung 4	63 ± 2.96^{c}	20	31.75^{t}	24.85 ± 0.49^{vwx}	11 ± 0.88^{e}	9 ± 0.88^{g}	0.82^{g}	$0.060^{ghijklmnopq}$	100	HS
5	Binamung 7	36 ± 4.33^{u}	20	55.56^{d}	25.80 ± 0.28^{pqrstu}	6 ± 0.33^{j}	14 ± 0.33^{b}	2.33^{b}	0.068^{bcdefg}	100	HS
6	Barimung 5	48 ± 2.73^{j}	20	41.67^{no}	28.95 ± 0.58^{cdefg}	10 ± 0.58^{f}	10 ± 0.58^{f}	1.00^{f}	$0.056^{mnopqrs}$	100	HS
7	Nigerian variety	40 ± 2.19^{qr}	20	50.00^{gh}	$26.80 \pm 0.65^{jklmnopq}$	13 ± 0.88^{c}	7 ± 0.88^{i}	0.54^{i}	$0.063^{bcdefjklm}$	100	HS
8	DM 2	58 ± 2.91^{d}	20	34.48^{s}	26.60 ± 0.62^{y}	7 ± 0.58^{i}	13 ± 0.58^{c}	1.86^{c}	$0.058^{bcdefghi}$	100	HS
9	Ilangai 2	36 ± 3.18^{u}	20	55.56^{d}	25.15 ± 0.82^{tuvw}	13 ± 0.88^{c}	7 ± 0.88^{i}	0.54^{i}	0.069^{bc}	100	HS
10	Ilangai 1	32 ± 3.18^{w}	20	62.50^{b}	25.45 ± 0.85^{rstuvw}	10 ± 1.33^{f}	10 ± 1.33^{f}	1.00^{f}	0.071^{b}	100	HS
11	EC 396097	42 ± 6.08^{op}	20	47.62^{ij}	27.95 ± 0.69^{fghij}	13 ± 1.53^{c}	7 ± 1.53^{i}	0.54^{i}	$0.060^{hijklmnopq}$	100	HS
12	HUM 2	41 ± 3.79^{pq}	20	48.78^{hi}	26.20 ± 0.70^{nopqrst}	7 ± 0.88^{i}	13 ± 0.88^{c}	1.86^{c}	$0.064^{bcdefghijk}$	100	HS
13	EC 396099	41 ± 2.91^{pq}	20	48.78^{hi}	29.05 ± 0.66^{cdef}	12 ± 1.86^{d}	8 ± 1.86^{h}	0.67^{h}	$0.058^{jklmnopqr}$	100	HS
14	EC 396103	38 ± 3.84^{st}	20	52.63^{ef}	28.15 ± 0.17^{efghi}	8 ± 0.88^{h}	12 ± 0.88^{d}	1.50^{d}	$0.061^{efghijklmnopq}$	100	HS
15	EC 396107	32 ± 5.04^{w}	20	62.50^{b}	27.75 ± 0.88^{ghijk}	12 ± 1.53^{d}	8 ± 1.53^{h}	0.67^{h}	$0.065^{bcdefghijk}$	100	HS
16	EC 396104	48 ± 4.33^{j}	20	41.67^{no}	29.25 ± 0.69^{bcde}	11 ± 0.58^{e}	9 ± 0.58^{g}	0.82^{g}	0.055^{opqrs}	100	HS
17	EC 396114	51 ± 3.18^{hi}	20	39.22^{p}	26.15 ± 0.89^{nopqrst}	8 ± 0.88^{h}	12 ± 0.88^{d}	1.50^{d}	$0.061^{fghijklmnopq}$	100	HS
18	EC 396115	48 ± 2.73^{j}	20	41.67^{no}	29.05 ± 0.81^{cdef}	12 ± 1.45^{d}	8 ± 1.45^{h}	0.67^{h}	0.056^{nopqrs}	100	HS
19	EC 396126	39 ± 2.85^{rs}	20	51.28^{fg}	27.65 ± 0.69^{hijkl}	7 ± 0.33^{i}	13 ± 0.33^{c}	1.86^{c}	$0.062^{defghijklmnopq}$	100	HS
20	EC 396100	41 ± 2.65^{pq}	20	48.78^{hi}	26.40 ± 0.32^{mnopqrs}	11 ± 1.45^{e}	9 ± 1.45^{g}	0.82^{g}	$0.064^{bcdefghijk}$	100	HS
21	EC 396121	69 ± 1.73^{a}	20	28.99^{u}	25.05 ± 0.92^{tuvw}	15 ± 0.58^{a}	5 ± 0.58^{k}	0.33^{k}	$0.058^{ijklmnopqr}$	100	HS
22	BDYR 3	34 ± 1.53^{v}	20	58.82^{c}	26.05 ± 0.45^{opqrstu}	9 ± 1.53^{g}	11 ± 1.53^{e}	1.22^{e}	0.068^{bcdef}	100	HS
23	EC 396106	62 ± 0.88^{c}	20	32.26^{t}	27.75 ± 0.37^{ghijk}	12 ± 1.20^{d}	8 ± 1.20^{h}	0.67^{h}	0.054^{qrs}	100	HS
24	EC 396110	46 ± 3.76^{kl}	20	43.48^{mn}	28.45 ± 0.91^{defgh}	13 ± 1.33^{c}	7 ± 1.33^{i}	0.54^{i}	$0.058^{klmnopqr}$	100	HS
25	EC 396108	41 ± 1.15^{pq}	20	48.78^{hi}	28.05 ± 0.50^{efghi}	8 ± 1.45^{h}	12 ± 1.45^{d}	1.50^{d}	$0.060^{ghijklmnopq}$	100	HS
26	EC 396105	56 ± 4.62^{ef}	20	35.71^{rs}	$27.00 \pm 0.18^{ijklmnop}$	11 ± 1.20^{e}	9 ± 1.20^{g}	0.82^{g}	$0.058^{klmnopqr}$	100	HS
27	EC 396118	41 ± 1.76^{p}	20	48.78^{hi}	30.30 ± 0.23^{ab}	10 ± 1.45^{f}	10 ± 1.45^{f}	1.00^{f}	0.056^{t}	100	HS
28	EC 396120	57 ± 2.96^{de}	20	35.09^{gs}	$26.45 \pm 0.42^{lmnopqrs}$	8 ± 0.88^{h}	12 ± 0.88^{d}	1.50^{d}	$0.058^{ikmnopqr}$	100	HS
29	EC 118889	39 ± 3.76^{rs}	20	51.28^{f}	26.10 ± 0.56^{opqrst}	14 ± 0.33^{b}	6 ± 0.33^{j}	0.43^{j}	$0.066^{bcdefghij}$	100	HS
30	AVRDC 1785/5	38 ± 1.15^{st}	20	52.63^{ef}	24.40 ± 0.49^{wxy}	5 ± 0.33^{k}	15 ± 0.33^{a}	3.00^{a}	0.071^{b}	100	HS
31	BDYR 2	45 ± 1.76^{lm}	20	44.44^{lm}	25.05 ± 0.42^{tuvw}	12 ± 0.88^{d}	8 ± 0.88^{h}	0.67^{h}	$0.066^{bcdefghi}$	100	HS
32	EC 396101	54 ± 3.18^{g}	20	37.04^{q}	26.30 ± 0.56^{vwx}	13 ± 0.88^{c}	7 ± 0.88^{i}	0.54^{i}	$0.060^{bcdefghijklmn}$	100	HS
33	EC 396102	44 ± 1.73^{mn}	20	45.45^{kl}	29.45 ± 0.75^{bcd}	6 ± 0.67^{j}	14 ± 0.67^{b}	2.33^{b}	$0.056^{lmnopqrs}$	100	HS
34	EC 396111	65 ± 2.03^{b}	20	30.77^{tu}	30.00 ± 0.22^{bc}	14 ± 0.33^{b}	6 ± 0.33^{j}	0.43^{j}	0.050^{s}	100	HS
35	EC 396116	38 ± 1.45^{st}	20	52.63^{ef}	27.45 ± 0.86^{gijklm}	13 ± 1.15^{c}	7 ± 1.15^{i}	0.54^{i}	$0.063^{cdefijklmno}$	100	HS
36	EC 396117	37 ± 1.45^{tu}	20	54.05^{de}	31.50 ± 0.71^{a}	12 ± 1.15^{d}	8 ± 1.15^{h}	0.67^{h}	0.055^{pqrs}	100	HS
37	EC 396125	33 ± 2.03^{vw}	20	60.61^{bc}	27.10 ± 0.26^{ijklmno}	11 ± 0.88^{e}	9 ± 0.88^{g}	0.82^{g}	$0.066^{bcdefghi}$	100	HS
38	EC 396113	63 ± 2.03^{c}	20	31.75^{t}	25.75 ± 0.71^{qrstuv}	7 ± 0.88^{i}	13 ± 0.88^{c}	1.86^{c}	$0.058^{ijklpqr}$	100	HS

Table 1. *Cont.*

S.No.	Genotypes	No.of Eggs Laid	No. of Adults Emerged	Adult Emergence Percentage	Mean Developmental Period	No. of Males Emerged	No. of Females Emerged	Female to Male Ratio	Susceptibility Index	Damage Percentage	Category
39	EC 396123	47 ± 1.45^{jk}	20	42.55^{mn}	23.75 ± 0.20^{xy}	10 ± 1.20^{f}	10 ± 1.20^{f}	1.00^{f}	0.069^{bcde}	100	HS
40	EC 396122	42 ± 3.48^{op}	20	47.62^{ij}	25.50 ± 0.45^{rstuvw}	13 ± 0.33^{c}	7 ± 0.33^{i}	0.54^{i}	$0.066^{bcdefghi}$	100	HS
41	BDYR 1	55 ± 2.96^{fg}	20	36.36^{rs}	30.15 ± 0.76^{bc}	14 ± 0.88^{b}	6 ± 0.88^{j}	0.43^{j}	0.052^{rs}	100	HS
42	V2709	25 ± 2.40^{y}	0	0.00^{v}	0.00 ± 0.00^{z}	0 ± 0.00^{l}	0 ± 0.00^{l}	0.00^{l}	0.000^{u}	0	HR
43	HG 22	32 ± 4.36^{w}	20	62.50^{b}	26.10 ± 0.45^{opqrst}	12 ± 0.58^{d}	8 ± 0.58^{h}	0.67^{h}	0.069^{bcd}	100	HS
44	ML 818	42 ± 6.06^{op}	20	47.62^{ij}	27.35 ± 0.75^{gijklmn}	13 ± 1.45^{c}	7 ± 1.45^{i}	0.54^{i}	$0.061^{defghijklmnopq}$	100	HS
45	VGGRU 1	58 ± 3.06^{d}	20	34.48^{s}	25.60 ± 0.19^{qrstuvw}	9 ± 1.45^{g}	11 ± 1.45^{e}	1.22^{e}	$0.060^{hijklmnopq}$	100	HS
46	ML 1108	62 ± 5.13^{c}	20	32.26^{t}	26.15 ± 0.51^{nopqrst}	12 ± 0.88^{d}	8 ± 0.88^{h}	0.67^{h}	$0.058^{klmnopqr}$	100	HS
47	Basanti	34 ± 3.21^{v}	20	58.82^{c}	$26.55 \pm 0.42^{klmnopqr}$	5 ± 0.58^{k}	15 ± 0.58^{a}	3.00^{a}	$0.067^{bcdefgh}$	100	HS
48	KMG 189	39 ± 6.06^{rs}	20	51.28^{fg}	25.30 ± 0.92^{stuvw}	12 ± 1.15^{d}	8 ± 1.15^{h}	0.67^{h}	0.068^{bcdef}	100	HS
49	EC 396098	40 ± 6.11^{qr}	20	50.00^{gh}	26.05 ± 1.08^{opqrstu}	6 ± 0.33^{j}	14 ± 0.33^{b}	2.33^{b}	$0.065^{bcdefghij}$	100	HS
50	LM 469	43 ± 5.49^{no}	20	46.51^{hjk}	26.20 ± 0.78^{nopqrst}	13 ± 1.20^{c}	7 ± 1.20^{i}	0.54^{i}	$0.064^{bcdefghijkl}$	100	HS
51	T 1	41 ± 6.17^{pq}	20	48.78^{i}	25.75 ± 1.22^{qrstuv}	9 ± 0.58^{g}	11 ± 0.58^{e}	1.22^{e}	$0.066^{bcdefghij}$	100	HS
52	V2802 BG	22 ± 3.46^{z}	0	0.00^{v}	0.00 ± 0.00^{z}	0 ± 0.00^{l}	0 ± 0.00^{l}	0.00^{l}	0.000^{u}	0	HR
Mean		44.42	19.23	44.44	25.73	10.17	9.06	1.01	0.059	96.15	-
SEd		0.91	-	0.96	0.61	0.24	0.19	0.02	0.004	-	-
CD ($p = 0.05$)		1.81	-	1.91	1.21	0.48	0.38	0.04	0.008	-	-

Values are mean ± SE of three replicates; Mean values followed by different letters in the same column are significantly different at the 5% level by LSD.

Two mungbean genotypes, V2709 and V2802BG, exhibited no adult emergence, whereas a maximum of 20 adults emerged from the remaining 50 genotypes. The adult emergence percentage was significantly higher in Binamung 2 (66.67%), followed by 62.50% in Ilangai 1, EC 396107, and HG 22. EC 396117 had a considerably higher mean developmental period (31.50 days), comparable to EC 396118 (30.30 days). The mean developmental period cannot be calculated since there was no adult emergence in V2709 and V2802BG. Other than these two genotypes (V2709 and V2802BG), Binamung 2 exhibited a significantly minimum mean developmental period of 23.35 days that was found to be on par with the following genotypes, EC 396123 (23.75 days), AVRDC 1785/5 (24.40 days), and Barimung 4 (24.85 days). Apart from V2709 and V2802BG, a significant minimum female to male ratio of 0.33 was observed from EC 396121. The significantly highest female to male ratio of 3.00 was shown by AVRDC 1785/5 and Basanti, followed by 2.33 in Binamung 7, EC 396102, and EC 396098. The susceptibility index was zero for V2709 and V2802BG, whereas a significantly higher susceptibility index of 0.078 was observed in Binamung 2, followed by 0.071 (Ilangai 1, AVRDC 1785/5) and 0.069 (Ilangai 2, HG 22, EC 396123). V2709 and V2802BG were categorized as highly resistant (HR) with 0% seed damage, and all other genotypes were classified as highly susceptible (HS) with 100% seed damage.

3.2. Development of Breeding Lines with Bruchid Resistance

Two resistant genotypes (V2709 and V2802BG) were crossed with six high-yielding cultivars (CO 5, CO 6, CO 7, CO 8, VBN 2, and VBN 3), and 12 independent populations of F_1 were generated. Of these, one population derived from CO 6 × V2802BG was selected based on good combining ability (Table 2; Figure 3) and forwarded to later generations.

Table 2. General combining ability effects for different morphological traits.

Parents	Plant Height	Days to 50% Flowering	No. of Pods/Plant	Pod Length	No. of Seeds/Pod	Hundred Seed Weight	Single Plant Yield
Lines							
CO 5	6.28 **	0.31	3.44	0.15	0.03	−0.14 **	0.82
CO 6	10.83 **	−0.03	7.11 **	0.95 **	0.86 **	0.09 **	5.63 **
CO 7	2.31 **	−0.53 *	−3.56	0.32 **	0.86 **	0.30 **	2.24
CO 8	−4.75 **	−0.19	−4.89 *	−0.85 **	0.19	−0.21 **	−3.50 **
VBN 2	−8.72 **	−1.53 **	6.11 *	−0.12	−0.47	0.09 **	1.70
VBN 3	−5.95 **	1.97 **	−8.22 **	−0.44 **	−1.47	−0.13 **	−6.89 **
Testers							
V2802BG	0.03	−0.36 **	0.83	0.12 *	−0.25	0.01	0.05
V2709	−0.03	0.36 **	−0.83	−0.12 *	0.25	−0.01	−0.05
SE (Lines)	1.06	0.21	2.24	0.08	0.28	0.02	1.17
SE (Testers)	0.61	0.11	1.29	0.05	0.16	0.02	0.67

* Significant at 5% level, ** Significant at 1% level.

CO 6 × V2802BG population comprising 159 $F_{2:3}$ families were screened for bruchid resistance, and results showed that seven $F_{2:3}$ families exhibited high resistance with 0% seed damage, whereas the remainder were resistant to highly susceptible. Further, these seven $F_{2:3}$ families were (BSR-GG-1-42, BSR-GG-1-49, BSR-GG-1-56, BSR-GG-1-97, BSR-GG-1-160, BSR-GG-1-170, and BSR-GG-1-198) evaluated for bruchid resistance in the F_4 generation. Of these, five families *viz.*, BSR-GG-1-49, BSR-GG-1-56, BSR-GG-1-160, BSR-GG-1-170, and BSR-GG-1-198 exhibited high resistance with 0% seed damage. Two families, namely BSR-GG-1-42 and BSR-GG-1-97, showed segregation with 0–35% seed damage (Table 3). Further, we have evaluated the five resistant lines in the F_5 generation and confirmed the resistance.

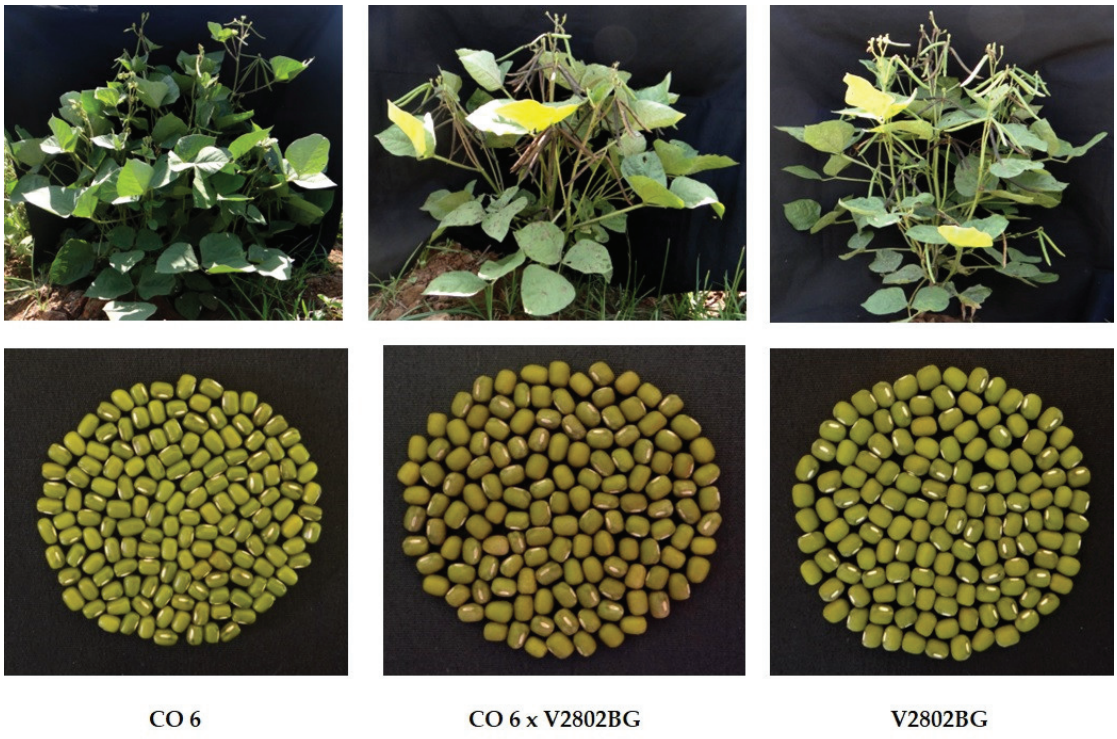

Figure 3. Parents, F_2 plants, and F_3 seeds of the cross CO 6 × V2802BG.

3.3. Grub Development in the Resistant Lines

The development of grub in five resistant lines in the F_5 generation was examined along with the parents (Table 4, Figure 4). Grub length was observed as follows in the resistant lines *viz.*, BSR-GG-1-49-3-1 (0.19 mm), BSR-GG-1-56-2-2 (0.20 mm), BSR-GG-1-160-5-3 (0.20 mm), BSR-GG-1-170-2-4 (0.22 mm) and BSR-GG-1-198-1-4 (0.21 mm), which was found to be on par with the resistant parent V2802BG (0.21 mm). However, grub length was significantly higher in CO 6 (4.05 mm) than in resistant lines. On the other hand, the grub breadth of resistant lines varied from 0.11 to 0.14 mm and was on par with the resistant parent V2802BG (0.13 mm), while in CO 6, grub breadth (2.65 mm) was significantly higher than the resistant lines.

Table 3. Screening of bruchid resistance in seven F_4 families derived from the cross of CO 6 × V2802BG.

S.No.	Genotypes	No. of Eggs Laid	Adult Emergence	Adult Emergence Percentage	Mean Developmental Period	No. of Males Emerged	No. of Females Emerged	Female to Male Ratio	Susceptibility Index	Damage Percentage	Score
1	BSR-GG-1-42-1	23 ^{q}	0 ^{f}	0.00 ^{h}	0.00 ^{e}	0 ^{f}	0 ^{e}	0.00 ^{e}	0.000 ^{e}	0.00 ^{f}	HR
2	BSR-GG-1-42-2	28 ^{m}	1 ^{f}	3.57 ^{d}	31.00 ^{a}	1 ^{e}	0 ^{e}	0.00 ^{e}	0.018 ^{d}	5.00 ^{e}	HR
3	BSR-GG-1-42-3	78 ^{a}	3 ^{d}	3.85 ^{g}	31.67 ^{a}	3 ^{c}	0 ^{c}	0.00 ^{e}	0.019 ^{d}	15.00 ^{d}	R
4	BSR-GG-1-42-4	50 ^{f}	7 ^{b}	14.00 ^{f}	31.71 ^{a}	4 ^{b}	3 ^{c}	0.75 ^{c}	0.036 ^{c}	35.00 ^{b}	MR
5	BSR-GG-1-42-5	48 ^{g}	0 ^{f}	0.00 ^{h}	0.00 ^{e}	0 ^{f}	0 ^{e}	0.00 ^{e}	0.000 ^{e}	0.00 ^{f}	HR
6	BSR-GG-1-49-1	21 ^{rs}	0 ^{f}	0.00 ^{h}	0.00 ^{e}	0 ^{f}	0 ^{e}	0.00 ^{e}	0.000 ^{e}	0.00 ^{f}	HR
7	BSR-GG-1-49-2	26 ^{op}	0 ^{f}	0.00 ^{h}	0.00 ^{e}	0 ^{f}	0 ^{e}	0.00 ^{e}	0.000 ^{e}	0.00 ^{f}	HR
8	BSR-GG-1-49-3	51 ^{f}	0 ^{f}	0.00 ^{h}	0.00 ^{e}	0 ^{f}	0 ^{e}	0.00 ^{e}	0.000 ^{e}	0.00 ^{f}	HR
9	BSR-GG-1-49-4	22 ^{qr}	0 ^{f}	0.00 ^{h}	0.00 ^{e}	0 ^{f}	0 ^{e}	0.00 ^{e}	0.000 ^{e}	0.00 ^{f}	HR
10	BSR-GG-1-49-5	23 ^{q}	0 ^{f}	0.00 ^{h}	0.00 ^{e}	0 ^{f}	0 ^{e}	0.00 ^{e}	0.000 ^{e}	0.00 ^{f}	HR
11	BSR-GG-1-56-1	32 ^{j}	0 ^{f}	0.00 ^{h}	0.00 ^{e}	0 ^{f}	0 ^{e}	0.00 ^{e}	0.000 ^{e}	0.00 ^{f}	HR
12	BSR-GG-1-56-2	28 ^{m}	0 ^{f}	0.00 ^{h}	0.00 ^{e}	0 ^{f}	0 ^{e}	0.00 ^{e}	0.000 ^{e}	0.00 ^{f}	HR
13	BSR-GG-1-56-3	36 ^{i}	0 ^{f}	0.00 ^{h}	0.00 ^{e}	0 ^{f}	0 ^{e}	0.00 ^{e}	0.000 ^{e}	0.00 ^{f}	HR
14	BSR-GG-1-56-4	67 ^{b}	0 ^{f}	0.00 ^{h}	0.00 ^{e}	0 ^{f}	0 ^{e}	0.00 ^{e}	0.000 ^{e}	0.00 ^{f}	HR
15	BSR-GG-1-56-5	60 ^{c}	0 ^{f}	0.00 ^{h}	0.00 ^{e}	0 ^{f}	0 ^{e}	0.00 ^{e}	0.000 ^{e}	0.00 ^{f}	HR
16	BSR-GG-1-97-1	27 ^{o}	0 ^{f}	0.00 ^{h}	0.00 ^{e}	0 ^{f}	0 ^{e}	0.00 ^{e}	0.000 ^{e}	0.00 ^{f}	HR
17	BSR-GG-1-97-2	27 ^{o}	5 ^{c}	18.52 ^{b}	26.20 ^{c}	3 ^{c}	1 ^{d}	0.33 ^{d}	0.048 ^{b}	25.00 ^{c}	MR
18	BSR-GG-1-97-3	38 ^{h}	1 ^{e}	2.63 ^{e}	25.00 ^{d}	1 ^{e}	0 ^{e}	0.00 ^{e}	0.017 ^{d}	5.00 ^{e}	HR
19	BSR-GG-1-97-4	58 ^{d}	7 ^{b}	12.07 ^{c}	29.28 ^{b}	2 ^{d}	5 ^{b}	2.50 ^{a}	0.037 ^{c}	35.00 ^{b}	MR
20	BSR-GG-1-97-5	30 ^{kl}	0 ^{f}	0.00 ^{h}	0.00 ^{e}	0 ^{f}	0 ^{e}	0.00 ^{e}	0.000 ^{e}	0.00 ^{f}	HR
21	BSR-GG-1-160-1	25 ^{p}	0 ^{f}	0.00 ^{h}	0.00 ^{e}	0 ^{f}	0 ^{e}	0.00 ^{e}	0.000 ^{e}	0.00 ^{f}	HR
22	BSR-GG-1-160-2	20 ^{s}	0 ^{f}	0.00 ^{h}	0.00 ^{e}	0 ^{f}	0 ^{e}	0.00 ^{e}	0.000 ^{e}	0.00 ^{f}	HR
23	BSR-GG-1-160-3	31 ^{jk}	0 ^{f}	0.00 ^{h}	0.00 ^{e}	0 ^{f}	0 ^{e}	0.00 ^{e}	0.000 ^{e}	0.00 ^{f}	HR
24	BSR-GG-1-160-4	55 ^{e}	0 ^{f}	0.00 ^{h}	0.00 ^{e}	0 ^{f}	0 ^{e}	0.00 ^{e}	0.000 ^{e}	0.00 ^{f}	HR
25	BSR-GG-1-160-5	48 ^{g}	0 ^{f}	0.00 ^{h}	0.00 ^{e}	0 ^{f}	0 ^{e}	0.00 ^{e}	0.000 ^{e}	0.00 ^{f}	HR
26	BSR-GG-1-170-1	23 ^{q}	0 ^{f}	0.00 ^{h}	0.00 ^{e}	0 ^{f}	0 ^{e}	0.00 ^{e}	0.000 ^{e}	0.00 ^{f}	HR
27	BSR-GG-1-170-2	25 ^{p}	0 ^{f}	0.00 ^{h}	0.00 ^{e}	0 ^{f}	0 ^{e}	0.00 ^{e}	0.000 ^{e}	0.00 ^{f}	HR
28	BSR-GG-1-170-3	26 ^{op}	0 ^{f}	0.00 ^{h}	0.00 ^{e}	0 ^{f}	0 ^{e}	0.00 ^{e}	0.000 ^{e}	0.00 ^{f}	HR
29	BSR-GG-1-170-4	32 ^{j}	0 ^{f}	0.00 ^{h}	0.00 ^{e}	0 ^{f}	0 ^{e}	0.00 ^{e}	0.000 ^{e}	0.00 ^{f}	HR
30	BSR-GG-1-170-5	30 ^{kl}	0 ^{f}	0.00 ^{h}	0.00 ^{e}	0 ^{f}	0 ^{e}	0.00 ^{e}	0.000 ^{e}	0.00 ^{f}	HR

Table 3. *Cont.*

S.No.	Genotypes	No. of Eggs Laid	Adult Emergence	Adult Emergence Percentage	Mean Developmental Period	No. of Males Emerged	No. of Females Emerged	Female to Male Ratio	Susceptibility Index	Damage Percentage	Score
31	BSR-GG-1-198-1	39 ^{h}	0 ^{f}	0.00 ^{h}	0.00 ^{e}	0 ^{f}	0 ^{e}	0.00 ^{e}	0.000 ^{e}	0.00 ^{f}	HR
32	BSR-GG-1-198-2	29 ^{lm}	0 ^{f}	0.00 ^{h}	0.00 ^{e}	0 ^{f}	0 ^{e}	0.00 ^{e}	0.000 ^{e}	0.00 ^{f}	HR
33	BSR-GG-1-198-3	27 ^{o}	0 ^{f}	0.00 ^{h}	0.00 ^{e}	0 ^{f}	0 ^{e}	0.00 ^{e}	0.000 ^{e}	0.00 ^{f}	HR
34	BSR-GG-1-198-4	60 ^{c}	0 ^{f}	0.00 ^{h}	0.00 ^{e}	0 ^{f}	0 ^{e}	0.00 ^{e}	0.000 ^{e}	0.00 ^{f}	HR
35	BSR-GG-1-198-5	32 ^{j}	0 ^{f}	0.00 ^{h}	0.00 ^{e}	0 ^{f}	0 ^{e}	0.00 ^{e}	0.000 ^{e}	0.00 ^{f}	HR
					Parents						
36	CO6	48 ^{g}	20 ^{a}	41.67 ^{a}	26.10 ^{c}	9 ^{a}	11 ^{a}	1.22 ^{b}	0.062 ^{a}	100.00 ^{a}	HS
37	V2802 BG	16 ^{t}	0 ^{f}	0.00 ^{h}	0.00 ^{e}	0 ^{f}	0 ^{e}	0.00 ^{e}	0.000 ^{e}	0.00 ^{f}	HR
	Mean	36.33	1.00	2.21	5.72	0.49	0.46	0.11	0.01	4.86	-
	SEd	0.91	0.11	0.07	0.22	0.02	0.03	0.01	0.00	0.57	-
	CD ($p = 0.05$)	1.82	0.22	0.13	0.44	0.05	0.05	0.02	0.00	1.13	-

Values are the mean of three replicates; Mean values followed by different letters in the same column are significantly different at 5% level by LSD. HR, Highly resistant; R, Resistant; MR, Moderately resistant; HS, Highly susceptible.

Table 4. Grub dimensions of *Callosobruchus maculatus* in five stable resistant lines from F_5 generation derived from the cross of CO 6 × V2802BG.

S.No.	Parents and Resistant Lines	Length (mm)	Breadth (mm)
1.	BSR-GG-1-49-3-1	0.19 [b]	0.12 [b]
2.	BSR-GG-1-56-2-2	0.20 [b]	0.14 [b]
3.	BSR-GG-1-160-5-3	0.20 [b]	0.11 [b]
4.	BSR-GG-1-170-2-4	0.22 [b]	0.13 [b]
5.	BSR-GG-1-198-1-4	0.21 [b]	0.13 [b]
6.	CO 6	4.05 [a]	2.65 [a]
7.	V2802 BG	0.21 [b]	0.13 [b]
	Mean	0.75	0.49
	SEd	0.04	0.01
	CV%	6.41	3.56

Values are the mean of three replicates; Mean values followed by different letters in the same column are significantly different at the 5% level by LSD.

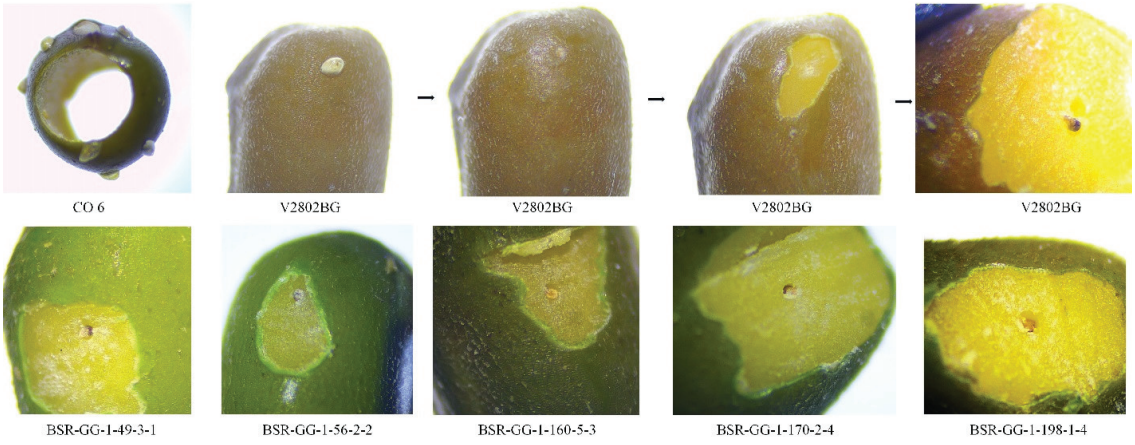

Figure 4. Grub development in five highly resistant lines from the cross of CO6 × V2802BG. CO 6 (Highly susceptible) and V2802BG (Highly resistant). BSR-GG-1-49-3-1, BSR-GG-1-56-2-2, BSR-GG-1-160-5-3, BSR-GG-1-170-2-4, and BSR-GG-1-198-1-4 (Highly resistant lines).

3.4. Agronomic Performance of the Resistant Lines

The agronomic performance of five resistant lines in the F_5 generation was evaluated along with CO 6 (Table 5). Apart from BSR-GG-1-56-2-2 (60.17 cm), all the four resistant lines had increased mean plant height compared to CO 6 (60.62 cm). Two resistant lines, BSR-GG-1-160-5-3, and BSR-GG-1-49-3-1 attained 50 percent flowering at 35 days after sowing was earlier than CO 6 (36 days). Excluding BSR-GG-1-49-3-1 (41.33), all the resistant lines produced more pods per plant than CO 6. The maximum number of pods per plant was exhibited by BSR-GG-1-198-1-4 (48.33). All the resistant lines expressed increased pod length. The mean value for the number of seeds per pod of BSR-GG-1-170-2-4 (12.33) was found to be on par with CO 6, whereas other resistant lines exhibited a higher number of seeds per pod. All the resistant lines expressed a higher hundred seed weight and single plant yield than CO 6.

Table 5. Agronomic performance of five stable resistant lines from F_5 generation derived from the cross of CO 6 × V2802BG.

S.No.	Genotypes	PH	DFPF	PPP	PL	SPP	HSW	SPY
1	BSR-GG-1-49-3-1	64.23 ± 6.31	35.33 ± 0.33	41.33 ± 1.76	8.27 ± 0.15	13.00 ± 0.58	3.95 ± 0.02	16.71 ± 0.66
2	BSR-GG-1-56-2-2	60.17 ± 4.13	35.67 ± 0.33	43.67 ± 3.38	7.83 ± 0.12	12.67 ± 0.33	4.04 ± 0.05	18.18 ± 0.83
3	BSR-GG-1-160-5-3	62.40 ± 2.15	34.67 ± 0.33	45.67 ± 2.73	8.53 ± 0.06 *	13.00 ± 0.58	4.02 ± 0.06	19.70 ± 1.41
4	BSR-GG-1-170-2-4	61.97 ± 2.44	35.67 ± 0.33	44.00 ± 2.52	7.73 ± 0.15	12.33 ± 0.33	3.98 ± 0.03	16.31 ± 0.50
5	BSR-GG-1-198-1-4	62.73 ± 3.46	36.33 ± 0.33	48.33 ± 2.60	8.23 ± 0.15	12.67 ± 0.33	3.90 ± 0.04	18.72 ± 1.00
6	CO 6	60.62 ± 2.66	35.67 ± 0.33	42.33 ±2.03	7.33 ± 0.06	12.33 ± 0.33	3.79 ± 0.04	15.99 ± 0.34
	Mean	62.02	35.56	44.22	7.99	12.67	3.95	17.60
	SEd	5.45	0.41	3.56	0.11	0.62	0.06	1.31
	CD (p = 0.05)	12.15	0.92	7.93	0.24	1.37	0.14	2.91

Values are mean ± SE of three replicates; * Significance at 5% level; PH, Plant height (cm); DFPF, Days to fifty percent flowering; PPP, Number of pods per plant; PL, Pod length (cm); SPP, Number of seeds per pod; HSW, Hundred seed weight (g); SPY, Single plant yield (g).

4. Discussion

4.1. Search for Mungbean Genotypes Resistance to South Indian Bruchid Strain

The initial screening for identifying bruchid-resistant genotypes was made in a set of 52 mungbean genotypes. The genotypes comprised the high frequency of light green seeds with shiny lustre, whereas few genotypes possessed greenish-yellow or dark green seeds with dull lustre. The proportion of oval and drum-shaped seeds was almost equal among the mungbean genotypes. First, we observed the egg deposition in all the mungbean genotypes used in the study. There was no significant difference in egg deposition among the mungbean genotypes of various sizes and shapes. The egg distribution also revealed no difference among seeds with dull and shiny lustres. It showed that the seed texture had no role in preventing the pest from laying eggs. AVRDC [34] reported that the texture layer could not prevent mungbean seeds from the damage caused by *C. maculatus* and *C. chinensis*. Singh and Singh [35] also reported that the seed coat texture of cowpea could not be considered a reliable trait in breeding against *C. maculatus*. Edde and Amatobi [36] reported that the type of seed coat (Wrinkled or smooth) had no effect on the ovipositional intensity of *C. maculatus* on cowpea. Hence, it is concluded that none of the seed traits, *viz.*, seed colour, seed shape, and seed lustre prevented the bruchid infestation in mungbean.

Further, the seed damage is measured by observing the following traits *viz.*, the number of eggs laid, adult emergence percentage, mean developmental period, female to male ratio, susceptibility index, and seed damage percentage (%). Results showed that no adult emergence and seed damage were reported in two genotypes (V2709 and V2802BG). In contrast, the maximum number of adult emergence, with 100% seed damage, was found in the remaining 50 mungbean genotypes. The adult emergence percentage, mean developmental period, female to male ratio, and susceptibility index of 50 highly susceptible genotypes ranged from 28.99 to 66.67%, 23.75 to 31.50 days, 0.33–3.00, and 0.050–0.078, respectively. Similar findings for adult emergence percentage, mean developmental period, and susceptibility index were reported by Soumia et al. [24] in mungbean infested with *C. maculatus*. A lower number of females than males of *C. maculatus* in mungbean was reported by Bashir et al. [37] and Sharma et al. [38]. The egg-laying and hatching were observed in the resistant (V2802BG and V2709) and all remaining susceptible genotypes. This indicates that the antixenosis mechanism exhibited by seed traits *viz.*, seed colour, seed lustre, and seed shape had no role in imparting resistance against bruchids and coupled with the results of Seram et al. [27].

4.2. Breeding Resistant Lines with Better Agronomic Performances

To develop the widely adopted resistant lines, two resistant genotypes (V2709 and V2802BG) were crossed with six high-yielding cultivars (CO 5, CO 6, CO 7, CO 8, VBN 2, and VBN 3), and 12 independent populations of F_1 were generated. Of these, one population derived from CO 6 × V2802BG was selected based on the good combining ability of the parents (CO 6 and V2802BG) for most of the promising traits and forwarded to later

generations. Good combiners will yield better recombinant progenies in later generations. Furthermore, CO 6 is the high-yielding and ruling variety in Tamil Nadu. A total of 159 $F_{2:3}$ families were examined for bruchid resistance. The results revealed that seven F2:3 families were highly resistant with 0% seed damage, and the rest were resistant to highly susceptible. The percentage of seed damage varied from 0 to 100%, with a mean of 44.4%. Similarly, the F_2 population derived from Kamphaeng Saen 2 (Susceptible) × ACC41 (Resistant) exhibited 0 to 100% seed damage (*C. maculatus*) with a mean of 46.30% [39]. The $BC_{11}F_2$ population derived two crosses, KPS1 × V2802 [40] and KPS 1 and V2709 [41], also recorded 0 to 100% seed damage (*C. maculatus*) with a mean of 48.58% and 44.60%, respectively. Chen et al. [42] also recorded 0 to 100% seed damage in F_{12} RILs derived from the cross NM92 × TC1966. The F_{10} population of the cross Berken × ACC41 also recorded 0 to 100% seed damage with a mean of 46.5% [43]. Further, we evaluated the seven $F_{2:3}$ families in the advanced generations (F_4 and F_5) and found five highly resistant lines (BSR-GG-1-49-3-1, BSR-GG-1-56-2-2, BSR-GG-1-160-5-3, BSR-GG-1-170-2-4, and BSR-GG-1-198-1-4) in the F_5 generation.

4.3. Development of Grub and Agronomic Performance of the Resistant Lines

When we compare the development of grub in resistant lines with the parental lines, it showed that the underdevelopment of grub in all the five stable resistant lines was the same as that of the resistant parent, V2802BG, at the early instar level and confirmed the transfer of resistance from V2802BG to the population of CO 6 × V2802BG. These results are consistent with the reports of Somta et al. [44], who described the death (62.9%) of bruchids (*C. chinensis* and *C. maculatus*) at the first instar larval stage in undamaged seeds. The present study recorded normal growth of grub from the susceptible genotypes. In contrast, in resistant genotypes, the underdevelopment of grub and death of grub was observed at a lower instar level in the undamaged seeds. It was already discussed that there was no role of antixenosis factors in imparting resistance against *C. maculatus.* Hence, the resistance was due to the compounds in the seed's cotyledon. Antibiosis resistance resulted in grub mortality, disturbance in the life cycle, reduction in fecundity, and insect fertility [45,46]. Plant morphological traits and some chemical factors are responsible for the antibiosis mechanism of host plants against insects [46,47]. Edwards and Singh [48] and Eduardo et al. [49] reported antibiosis as an effective defense strategy exhibited by the legumes against stored seed insect pests. The *C. maculatus* grub with morphometric measurements *viz.*, length (3.64 mm) and breadth (2.00 mm) reared on mungbean was reported by Devi and Devi [50]. The fate of *C. maculatus* during development is determined by the biochemical factors operating after hatching and commencement of feeding by the developing grub [51–53]. The antibiosis mechanism of resistance due to the presence of toxic secondary metabolites in mungbean was reported by AVRDC [54] and Talekar and Lin [55]. The antibiosis mechanism of resistance against bruchids in various legume crops was reported by several researchers Seram et al. [27], Souframanien and Gopalakrishna [56], Castro et al. [57], Kaur et al. [58], Miesho et al. [59], Grazziotin et al. [60], Jaba et al. [61] and Caroline et al. [62]. Furthermore, the stable resistant lines recorded a comparable yield to the CO6. The five resistant lines in the F_5 generation showed good agronomic performance like high-yielding parent CO 6. An agronomic performance similar to parents in the F_5 generation was reported by Krisnawati et al. [63].

5. Conclusions

In summary, we have successfully developed the bruchid resistance lines with good agronomic performance. Furthermore, in the present study, the mechanism of bruchid resistance is described as antibiosis. The resistant lines developed in this study could be evaluated in multi-location trials and then exploited as a budding source of genetic material for improving bruchid resistance in mungbean breeding programs.

Author Contributions: D.M., N.S., V.S. and S.M.S. conceived and designed the methods and experiments. S.M.S., D.M. and V.S. managed the fieldwork. S.M.S., I.M. and A.K. conducted the phenotype screening. S.M.S., I.M., D.S., M.D., A.K. and S.J.H. performed data analysis. S.J.H., D.M., N.S., A.T.H., D.K. and S.K. provided suggestions on experiments. S.M.S. and A.K. drafted the manuscript. All authors have read and agreed to the published version of the manuscript.

Funding: The work was financially supported through grants from the Department of Biotechnology, Government of India, under the BioCARe (No. BT/PR19568/BIC/101/321/2016 dt. 19.06.2017) scheme entitled Introgression of bruchid resistant gene (s) from *Vigna* genotypes into popular mungbean (*Vigna radiata* L.) variety through marker-assisted backcross breeding.

Institutional Review Board Statement: Not applicable.

Informed Consent Statement: Not applicable.

Data Availability Statement: Data are available upon request to the authors.

Conflicts of Interest: The authors declare that the research was conducted in the absence of any commercial or financial relationships that could be construed as a potential conflict of interest.

References

1. Nair, R.M.; Yang, R.Y.; Easdown, W.J.; Thavarajah, D.; Thavarajah, P.; Hughes, J.A.; Keatinge, J.D.H. Biofortification of mungbean (*Vigna radiata*) as a whole food to enhance human health. *J. Sci. Food Agric.* **2013**, *93*, 1805–1813. [CrossRef] [PubMed]
2. Karthikeyan, A.; Shobhana, V.G.; Sudha, M.; Raveendran, M.; Senthil, N.; Pandiyan, M.; Nagarajan, P. Mungbean yellow mosaic virus (MYMV): A threat to green gram (*Vigna radiata*) production in Asia. *Int. J. Pest Manag.* **2014**, *60*, 314–324. [CrossRef]
3. Karthikeyan, A.; Sudha, M.; Pandiyan, M.; Senthil, N.; Shobhana, V.G.; Nagarajan, P. Screening of MYMV resistant mungbean (*Vigna radiata* (L.) Wilczek) progenies through Agroinoculation. *Int. J. Plant Pathol.* **2011**, *2*, 115–125. [CrossRef]
4. Amin, M.R.; Islam, M.S.; Hasan, M.K.; Sabagh, A.E. Improvement of production and net economic return through intercropping of upland cotton with mungbean. *Azarian J. Agric.* **2018**, *5*, 67–75.
5. He, T.G.; Su, L.R.; Li, Y.R.; Su, T.M.; Qin, F.; Li, Q. Nutrient decomposition rate and sugarcane yield as influenced by mungbean intercropping and crop residue recycling. *Sugar Tech.* **2018**, *20*, 154–162. [CrossRef]
6. Diatta, A.A.; Thomason, W.E.; Abaye, O.; Thompson, T.L.; Battaglia, M.L.; Vaughan, L.J.; Lo, M. Assessment of Nitrogen Fixation by Mungbean Genotypes in Different Soil Textures Using 15 N Natural Abundance Method. *J. Soil Sci. Plant Nutr.* **2020**, *20*, 2230–2240. [CrossRef]
7. Ministry of Agriculture and Farmers Welfare, Department of Agriculture, Cooperation and Farmers Welfare, Government of India. Pulses Revolution from Food to Nutritional Security. 2018. Available online: http://dpd.gov.in (accessed on 20 February 2019).
8. Gahukar, R.T.; Reddy, G.V. Management of insect pests in the production and storage of minor pulses. *Ann. Entomol. Soc. Am.* **2018**, *111*, 172–183. [CrossRef]
9. Mishra, S.K.; Macedo, M.L.R.; Panda, S.K.; Panigrahi, J. Bruchid pest management in pulses: Past practices, present status and use of modern breeding tools for development of resistant varieties. *Ann. App. Biol.* **2018**, *172*, 4–19. [CrossRef]
10. Mariyammal, I.; Seram, D.; Samyuktha, S.M.; Karthikeyan, A.; Dhasarathan, M.; Murukarthick, J.; Kennedy, J.S.; Malarvizhi, D.; Yang, T.J.; Pandiyan, M.; et al. QTL mapping in *Vigna radiata*× *Vigna umbellata* population uncovers major genomic regions associated with bruchid resistance. *Mol. Breed.* **2019**, *39*, 1–13. [CrossRef]
11. Young, N.D.; Kumar, L.; Menancio-Hautea, D.; Danesh, D.; Talekar, N.S.; Shanmugasundarum, S.; Kim, D.H. RFLP mapping of a major bruchid resistance gene in mungbean (*Vigna radiata*, L. Wilczek). *Theor. Appl. Genet.* **1992**, *84*, 839–884. [CrossRef]
12. Tripathi, A.; Tripathi, D.K.; Chauhan, D.K.; Kumar, N.; Singh, G.S. Paradigms of climate change impacts on some major food sources of the world: A review on current knowledge and future prospects. *Agric. Ecosyst. Environ.* **2016**, *216*, 356–373. [CrossRef]
13. Chawe, K.G.; Venkataramana, P.B.; Ndakidemi, P.A. Assessment of farmers' indigenous knowledge and preferences: A tool for sustainable lablab bean (Lablab purpureus L. Sweet) improvement and utilization in Northern Tanzania. *J. Adv. Biol. Biotechnol.* **2019**, *21*, 1–14. [CrossRef]
14. Mofunanya, A.A.J.; Namgbe, E.E. Assessment of damage due to *Callosobruchus maculatus* (Coleoptera: Bruchidae) infestation on germination and nutrient quality of *Vigna unguiculata* L. (Walp). *IOSR-J. Agric. Vet. Sci.* **2016**, *9*, 96–101. [CrossRef]
15. Hamdi, S.H.; Abidi, S.; Sfayhi, D.; Dhraief, M.Z.; Amri, M.; Boushih, E.; Hedjal-Chebheb, M.; Larbi, K.M.; Jemaa, J.M.B. Nutritional alterations and damages to stored chickpea in relation with the pest status of *Callosobruchus maculatus* (Chrysomelidae). *J. Asia Pac. Entomol.* **2017**, *20*, 1067–1076. [CrossRef]
16. Sreedhar, M.; Singh, D.V.; Reddy, D.C.; Vasudha, A. Biochemical changes in groundnut pods due to infestation of bruchid *Caryedon serratus* (Olivier) under stored conditions. *J. Stored Prod. Res.* **2020**, *88*, 101678. [CrossRef]
17. Somta, P.; Ammaranan, C.; Ooi, P.A.C.; Srinives, P. Inheritance of seed resistance to bruchids in cultivated mungbean (*Vigna radiata*, L. Wilczek). *Euphytica* **2007**, *155*, 47–55. [CrossRef]
18. Soumia, P.S.; Srivastava, C.; Dikshit, H.K.; Pandi, G.G.P. Screening for resistance against pulse beetle, *Callosobruchus analis* (F.) in greengram (*Vigna radiata* (L.) Wilczek) accessions. *Proc. Natl. Acad. Sci. India Sect. B Biol. Sci.* **2015**, *87*, 551–558. [CrossRef]

19. Liu, M.S.; Kuo, T.C.Y.; Ko, C.Y.; Wu, D.C.; Li, K.Y.; Lin, W.J.; Lin, C.P.; Wang, Y.W.; Schafleitner, R.; Lo, H.F.; et al. Genomic and transcriptomic comparison of nucleotide variations for insights into bruchid resistance of mungbean (*Vigna radiata* [L.] R. Wilczek). *BMC Plant Biol.* **2016**, *16*, 1–16. [CrossRef]
20. Singh, C.M.; Singh, P.; Pratap, A.; Pandey, R.; Purwar, S.; Douglas, C.A.; Baek, K.H.; Mishra, A.K. Breeding for enhancing Legumovirus resistance in mungbean: Current understanding and future directions. *Agronomy* **2019**, *9*, 622. [CrossRef]
21. Somta, C.; Somta, P.; Tomooka, N.; Ooi, P.A.C.; Vaughan, D.A.; Srinives, P. Characterization of new sources of mungbean (*Vigna radiata* (L.) Wilczek) resistance to bruchids, *Callosobruchus* spp. (Coleoptera: Bruchidae). *J. Stored Prod. Res.* **2008**, *44*, 316–321. [CrossRef]
22. Ponnusamy, D.; Pratap, A.; Singh, S.K.; Gupta, S. Evaluation of screening methods for bruchid beetle (*Callosobruchus chinensis*) resistance in green gram (*Vigna radiata*) and blackgram (*Vigna mungo*) genotypes and influence of seed physical characteristics on its infestation. *Vegetos* **2014**, *27*, 60–67. [CrossRef]
23. Sarkar, S.; Bhattacharyya, S. Screening of green gram genotypes for Bruchid (*Callosobruchus chinensis* L.) resistance and selection of parental lines for hybridization programme. *Legume Res.* **2015**, *38*, 704–706. [CrossRef]
24. Soumia, P.S.; Srivastava, C.; Pandi, G.; Subramanian, S. Varietal preference of pulse beetle, *Callosobruchus maculatus* (F.) in greengram. *Indian J. Entomol.* **2017**, *79*, 86–91. [CrossRef]
25. Soumia, P.S.; Chitra, S.; Guru, P.P.G.; Subramanian, S. Screening of green gram accessions against pulse beetle *Callosobruchus chinensis* (L.). *Indian J. Entomol.* **2018**, *80*, 1635–1641. [CrossRef]
26. Beck, C.W.; Blumer, L.S.; Habib, J. Effects of evolutionary history on adaptation in bean beetles, a model system for inquiry-based laboratories. *Evol. Educ. Outreach* **2013**, *6*, 5. [CrossRef]
27. Seram, D.; Senthil, N.; Pandiyan, M.; Kennedy, J.S. Resistance determination of a South Indian bruchid strain against rice bean landraces of Manipur (India). *J. Stored Prod. Res.* **2016**, *69*, 199–206. [CrossRef]
28. Venkataramana, P.B.; Gowda, R.; Somta, P.; Ramesh, S.; Rao, A.M.; Bhanuprakash, K.; Srinives, P.; Gireesh, C.; Pramila, C.K. Mapping QTL for bruchid resistance in rice bean (*Vigna umbellata*). *Euphytica* **2016**, *207*, 135–147. [CrossRef]
29. Howe, R. A parameter for experssing the suitability of an environment for insect development. *J. Stored Prod. Res.* **1971**, *7*, 63–65. [CrossRef]
30. IBPGR. *Descriptors for Vigna Mungo and Vigna Radiata*; International Board for Plant Genetic Resources: Rome, Italy, 1980; pp. 11–15.
31. Panse, V.; Sukhatme, P. Statistical methods for agricultural research. *ICAR New Delhi India* **1985**, *8*, 308–318.
32. Kempthorne, O. *An Introduction to Genetic Statistics*; John Willey & Sons. Inc.: New York, NY, USA, 1957.
33. Manivannan N TNAUSTAT-Statistical Package. 2014. Available online: https://sites.google.com/site/tnaustat (accessed on 10 January 2019).
34. Asian Vegetable Research and Development Center [AVRDC]. *Progress Report, 1987*; AVRDC: Shanhua, Taiwan, 1990; 480p.
35. Singh, B.B.; Singh., S.R. Breeding for bruchid resistance in cowpea. In *Bruchids and Legumes: Economics, Ecology and Coevolution*; Springer: Dordrecht, The Netherlands, 1990; pp. 219–228. [CrossRef]
36. Edde, P.A.; Amatobi, C.I. Seed coat has no value in protecting cowpea seed against attack by *Callosobruchus maculatus* (F.). *J. Stored Prod. Res.* **2003**, *39*, 1–10. [CrossRef]
37. Bashir, M.A.; Alvi, A.M.; Naz, H. Screening of legume and cereal seeds against *Callosobruchus maculatus* on the basis of fecundity and longevity. *J. Environ. Agric. Sci.* **2014**, *1*, 11.
38. Sharma, R.; Devi, R.; Soni, A.; Sharma, U.; Yadav, S.; Sharma, R. Growth and developmental responses of *Callosobruchus maculatus* (F.) on various pulses. *Legume Res.* **2016**, *39*, 840–843. [CrossRef]
39. Kaewwongwal, A.; Liu, C.; Somta, P.; Chen, J.; Tian, J.; Yuan, X.; Chen, X. A second VrPGIP1 allele is associated with bruchid resistance (Callosobruchus spp.) in wild mungbean (*Vigna radiata* var. *sublobata*) accession ACC41. *Mol. Genet. Genom.* **2020**, *295*, 275–286. [CrossRef] [PubMed]
40. Chotechung, S.; Somta, P.; Chen, J.; Yimram, T.; Chen, X.; Srinives, P. A gene encoding a polygalacturonase-inhibiting protein (PGIP) is a candidate gene for bruchid (Coleoptera: Bruchidae) resistance in mungbean (*Vigna radiata*). *Theor. Appl. Genet.* **2016**, *129*, 1673–1683. [CrossRef] [PubMed]
41. Kaewwongwal, A.; Chen, J.; Somta, P.; Kongjaimun, A.; Yimram, T.; Chen, X.; Srinives, P. Novel Alleles of Two Tightly Linked Genes Encoding Polygalacturonase-Inhibiting Proteins (VrPGIP1 and VrPGIP2) Associated with the Br Locus That Confer Bruchid (*Callosobruchus* spp.) Resistance to Mungbean (*Vigna radiata*) Accession V2709. *Front. Plant Sci.* **2017**, *8*, 1692. [CrossRef] [PubMed]
42. Chen, H.M.; Ku, H.; Shafleitner, R.; Bains, T.S.; Kuo, C.G.; Liu, C.; Nair, R.M. The major quantitative trait locus for mungbean yellow mosaic Indian virus resistance is tightly linked in repulsion phase to the major bruchid resistance locus in a cross between mungbean [*Vigna radiata* (L.) Wilczek] and its wild relative *Vigna radiata* ssp. *sublobata*. *Euphytica* **2013**, *192*, 205–216. [CrossRef]
43. Wang, L.; Wu, C.; Zhong, M.; Zhao, D.; Mei, L.; Chen, H.; Wang, S.; Liu, C.; Cheng, X. Construction of an integrated map and location of a bruchid resistance gene in mungbean. *Crop J.* **2016**, *4*, 60–366. [CrossRef]
44. Somta, P.; Kaga, A.; Tomooka, N.; Kashiwaba, K.; Isemura, T.; Chaitieng, B.; Srinives, P.; Vaughan, D.A. Development of an interspecific Vigna linkage map between *Vigna umbellata* (Thunb.) Ohwi & Ohashi and *V. nakashimae* (Ohwi) Ohwi & Ohashi and its use in analysis of bruchid resistance and comparative genomics. *Plant Breed.* **2006**, *125*, 77–84.
45. Smith, C.M. *Plant Resistance to Arthropods: Molecular and Conventional Approaches*; Springer: Dordrecht, The Netherlands, 2005.
46. Smith, C.M.; Clement, S.L. Molecular bases of plant resistance to arthropods. *Annu. Rev. Entomol.* **2012**, *57*, 309–328. [CrossRef]
47. Sadasivam, S.; Thayumanayan, B. *Molecular Host Plant Resistance to Pests*; CRC Press: Boca Raton, FL, USA, 2003. [CrossRef]

48. Edwards, O.; Singh, K.B. Resistance to insect pests: What do legumes have to offer? *Euphytica* **2006**, *147*, 273–285. [CrossRef]
49. Eduardo, W.I.; Junior, A.L.B.; de Moraes, R.F.O.; Chiorato, A.F.; Perlatti, B.; Forim, M.R. Antibiosis levels of common bean genotypes toward Zabrotes subfasciatus (Boheman) (Coleoptera: Bruchidae) and its correlation with flavonoids. *J. Stored Prod. Res.* **2016**, *67*, 63–70. [CrossRef]
50. Devi, M.B.; Devi, N.V. Biology and morphometric measurement of cowpea weevil, *Callosobruchus maculatus* Fab. (Coleoptera: Chrysomelidae) in green gram. *J. Entomol. Zool. Stud.* **2014**, *2*, 74–76.
51. Dick, K.M. Bionomic Variation among Three Populations of the Southern Cowpea Weevil, *Callosobruchus maculatus*, and Their Responses to Resistant Varieties of the Primary Host. Ph.D. Thesis, University of London, Bedford College, Bedford, UK, 1984.
52. Dick, K.M.; Credland, P.F. Changes in the response of *Callosobruchus maculatus* (Coleoptera: Bruchidae) to a resistant variety of cowpea. *J. Stored Prod. Res.* **1986**, *22*, 227–233. [CrossRef]
53. Edde, P.A.; Amatobi, C.I. Relative resistance of some cowpea varieties to *Callosobruchus maculatus* (F.) (Coleoptera: Bruchidae). *J. Sustain. Agric.* **2001**, *17*, 67–77. [CrossRef]
54. Asian Vegetable Research and Development Center [AVRDC]. *Progress Report for 1991*; AVRDC: Shanhua, Taiwan, 1992; p. 410.
55. Talekar, N.S.; Lin, C.P. Characterization of *Callosobruchus chinensis* (Coleoptera: Bruchidae) resistance in mungbean. *J. Econ. Entomol.* **1992**, *85*, 1150–1153. [CrossRef]
56. Souframanien, J.; Gopalakrishna, T. Source for bruchid resistance and its inheritance in Trombay wild urdbean Vigna. *J. Food Legumes* **2007**, *20*, 19–21.
57. Castro, M.D.; Baldin, E.L.; Cruz, P.L.; Souza, C.M.; Silva, P.H. Characterization of cowpea genotype resistance to *Callosobruchus maculatus*. *Pesqui. Agropecu. Bras.* **2013**, *48*, 1201–1209. [CrossRef]
58. Kaur, H.; Gill, R.S.; Kaur, S. Antinutritional factors in rice bean, *Vigna umbellata* Thunb. (Ohwi and Ohashi) against *Callosobruchus maculatus* F. (Coleoptera: Bruchidae). *Phytoparasitica* **2016**, *44*, 609–614. [CrossRef]
59. Miesho, B.; Msiska, U.; Hailay, M.; Malinga, G.; Odong, T.; Edema, R.; Gibson, P.; Rubaihayo, P.; Kyamanywa, S. Biochemical basis of cowpea resistance to bruchid, *Callosobruchus maculatus* (F.). *IJACR* **2017**, *5*, 219–227.
60. Grazziotin, M.A.; Cabral, G.B.; Ibrahim, A.B.; Machado, R.B.; Aragao, F.J. Expression of the Arcelin 1 gene from *Phaseolus vulgaris* L. in cowpea seeds (*Vigna unguiculata* L.) confers bruchid resistance. *Ann. App. Biol.* **2020**, *176*, 268–274. [CrossRef]
61. Jaba, J.; Bhandi, S.; Deshmukh, S.; Pallipparambil, G.R.; Mishra, S.P.; Arora, N. Identification, evaluation and utilization of resistance to insect pests in grain legumes: Advancement and restrictions. In *Genetic Enhancement in Major Food Legumes*; Springer: Cham, Germany, 2021; pp. 197–230.
62. Caroline, N.M.; Deogracious, P.M.; George, M.T.; James, R.M.; Joel, W.D.; Paul, M.K. Identification of potential seed storage protein responsible for bruchid resistance in common bean landraces from Tanzania and Malawi. *Afr. J. Biotechnol.* **2022**, *21*, 35–45. [CrossRef]
63. Krisnawati, A.; Adie, M.M.; Soegianto, A.; Waluyo, B. Pod shattering resistance and agronomic traits in F_5 segregating populations of soybean. *SABRAO J. Breed. Genet.* **2019**, *51*, 266–280.

agriculture

MDPI

Article

Structural Polymorphisms of Chromosome 3A^m Containing *Lr63* Leaf Rust Resistance Loci Reflect the Geographical Distribution of *Triticum monococcum* L. and Related Diploid Wheats

Aleksandra Noweiska, Roksana Bobrowska and Michał Tomasz Kwiatek *

Department of Genetics and Plant Breeding, Faculty of Agronomy, Horticulture and Bioengineering, Poznań University of Life Sciences, 11 Dojazd Str., 60-632 Poznań, Poland; aleksandra.noweiska@up.poznan.pl (A.N.); roksana.bobrowska@up.poznan.pl (R.B.)
* Correspondence: michal.kwiatek@up.poznan.pl

Abstract: Wheat is one of the world's crucial staple food crops. In turn, einkorn wheat (*Triticum monococcum* L.) is considered a wild relative of wheat (*Triticum aestivum* L.) and can be used as a source of agronomically important genes for breeding purposes. Cultivated *T. monococcum* subsp. *monococcum* originated from *T. monococcum* subsp. *aegilopoides* (syn. *T. boeticum*). For the better utilization of valuable genes from these species, it is crucial to discern the genetic diversity at their cytological and molecular levels. Here, we used a fluorescence in situ hybridization toolbox and molecular markers linked to the leaf rust resistance gene *Lr63* (located on the short arm of the 3A^m chromosome—3A^{m}S) to track the polymorphisms between *T. monococcum* subsp. *monococcum*, *T. boeticum* and *T. urartu* (A-genome donor for hexaploid wheat) accessions, which were collected in different regions of Europe, Asia, and Africa. We distinguished three groups of accessions based on polymorphisms of cytomolecular and leaf rust resistance gene *Lr63* markers. We observed that the cultivated forms of *T. monococcum* revealed additional marker signals, which are characteristic for genomic alternations induced by the domestication process. Based on the structural analysis of the 3A^{m}S chromosome arm, we concluded that the polymorphisms were induced by geographical dispersion and could be related to adaptation to local environmental conditions.

Keywords: chromosome alternations; diploid wheat; species dispersion; domestication; einkorn; leaf rust resistance

Citation: Noweiska, A.; Bobrowska, R.; Kwiatek, M.T. Structural Polymorphisms of Chromosome 3A^m Containing *Lr63* Leaf Rust Resistance Loci Reflect the Geographical Distribution of *Triticum monococcum* L. and Related Diploid Wheats. *Agriculture* **2022**, *12*, 966. https://doi.org/10.3390/agriculture12070966

Academic Editors: Edyta Paczos-Grzeda, Volker Mohler and Sylwia Sowa

Received: 9 June 2022
Accepted: 2 July 2022
Published: 5 July 2022

1. Introduction

Crop wild relatives (CWRs) are considered wild species that have sufficient levels of interfertility with other crops [1]. CWRs carry many beneficial traits for breeding, especially those, which have been lost during domestication and breeding selection, as well as novel adaptive alleles that can enhance crop diversity and productivity [2]. Initially, the classification for CWRs was established through the empirical crossing that resulted in four major germplasm categories: primary (no crossing barriers), secondary (benign crossing barriers), tertiary (requires special methods to obtain hybrid organisms, such as embryo rescue), and quaternary (genetic engineering technics are necessary to be performed) [1]. *Triticum monococcum* L. (2n = 2x = 14 chromosomes; A^{m}A^m) is closely related to *Triticum urartu* Thumanjan ex Gandilyan (2n = 2x = 14; A^{u}A^u), which has been reported as one of the primary gene pool ancestors of hexaploid wheat (*Triticum aestivum* L.; 2n = 6x = 42; BBAADD) from which the A-genome originated [3]. *T. monococcum* presents a high genetic variability, making it a significant gene pool for other species. Due to its close affinity to common wheat, it has been reported as a source of valuable genes, i.e., disease resistance genes, including leaf rust resistance genes [4]. Leaf rust (*Lr*) is a fungal disease caused by *Puccinia triticina* Eriksson. It is the most widespread of the wheat rust diseases, which

occurs in almost all growing areas and limits wheat production worldwide. The disease can take the form of an epidemic, which can lead to severe economic losses [5]. Until now, over 80 *Lr* resistance genes have been identified within the Triticeae tribe [6]. Some of these genes have been used to develop resistance to leaf rust in wheat varieties [5], including the *Lr63* gene, which is located on a short arm of chromosome $3A^m$ ($3A^mS$) of *T. monococcum*. It is the only mapped leaf rust resistance gene on the distal part of chromosome $3A^mS$, and is linked with microsatellites locus *Xbarc321* and *Xbarc57* markers (2.9 cM) [7].

Crop domestication is a process inseparably linked to the transition from hunter–gatherer societies to settled agriculture (the 'Neolithic revolution'; [8]), which independently appeared over a dozen times in various regions around the world from 10,000 to 12,000 years ago (ya) ca., to as recently as 3000–4000 ya [9–11]. This process can be called a conscious artificial selection of plants used in order to enhance their relevance to human demands, such as flavor, harvest, preservation, and methods of breeding. However, this process has been reported to be unconscious as well [12]. It is claimed that the factors which are responsible for early domestication include (1) the relocation of plants to new environmental niches, (2) human migration, and (3) genetic and genomic alternations, which are specific to selection [12]. Demographic effects often associated with domestication resulted in conspicuous impacts on genomic architecture, such as reductions in ineffective population sizes, reductions in diversity, and changes in the mating system, as well as targeted selection of specific traits [13,14]. There are also a number of reports showing evidence of large-scale chromosomal structural changes [15], changes in repetitive sequence content [16], and changes in gene variations and their copy numbers [17]. Cultivated *T. monococcum* L. subsp. *monococcum* originated from *T. boeticum* (syn. *T. monococcum* subsp. *aegilopoides*), which was widespread in southern Europe and western Asia. Even before domestication, *T. boeticum* was divided by the strong genetic differentiation into three races: race α, race β, and race γ [18]. However, only one race (β) has been exploited by mankind [18]. Precisely, wild *T. boeticum* was domesticated in the Karacadag mountains in southeast Turkey [19] and spread to several locations of the Fertile Crescent as the first cultivated wheat, called einkorn (*T. monococcum* L. subsp. *monococcum*) (Kilian et al. 2007). The common name was derived from the German "Einkorn", which means 'single grain', and relates to the occurrence of only a single grain per spikelet [20]. However, the name einkorn is used sometimes for both the wild (subsp. *aegilopoides*) and the cultivated (subsp. *monococcum*) forms. This cereal was important in the early Neolithic agriculture, but now is extensively grown in western Turkey, the Balkans, Switzerland, Germany, Spain, and the Caucasus [21]. During the last 5000 years, einkorn was eradicated and replaced by tetra- and hexaploid wheat. What is interesting is that both *T. monococcum* and *T. boeticum* (*T. monococcum* subsp. *aegilopoides*) are reproductively isolated from wild *T. urartu* (a progenitor of the A-genome of hexaploid wheat) with interspecific hybrids being sterile, although the two wild forms have comparable morphologies [22]. Cultivated einkorn is represented by a broad genetic variation [20]. This taxon includes nearly twenty identified botanical varieties [23] and six ecogeographical groups. The geographical diversification of *T. monococcum* from the domestication area was well restored through grain remains discovered in archaeological excavations [18,20], and is an example of well-documented speciation in the background of time and location.

What is interesting is that *T. monococcum*, *T. boeticum,* and *T. urartu* are karyotypically similar and have similar Giemsa C-banding patterns [24]. However, it was reported that fluorescence in situ hybridization (FISH), which allows for the direct localization of DNA sequences on chromosomes, revealed a number of intra- and interspecific divergence within diploid species of wheat [4,25–28]. FISH in plants commonly involves the application of probes containing conservative high-copy sequences. One of them is the *Afa*-family DNA probe, which is one of the most useful ones for the chromosome identification of diploid A-genome wheats. The *Afa*-family probe allowed for the recognition of the majority of chromosomes of cultivated einkorn [28] and *T. urartu* [4]. Other repeat DNA families, which were isolated from the bread wheat genome, among others, include pTa-86, pTa-465, pTa-

535, and pTa-713 [29–31] which can also provide informative labelling patterns for wheat chromosome discrimination. Among them, the probe pTa-535 was reported to generate the largest number of signals on the A-genome chromosomes, which are chromosome-specific. This clone is a 342 bp tandemly repeated DNA sequence, showing ~80% homology with the clone pTa-173, a member of the *Afa*-family [29].

In this study, we used molecular cytogenetics to analyze the karyotypes of *T. monococcum* accessions originating from different regions of eastern Europe, western Asia, and North Africa. Precisely, we analyzed the structural changes of the short arm of chromosome $3A^m$, which were probably induced by geographical dispersion and adaptation to local environmental conditions using cytomolecular tools and molecular markers linked to the *Lr63* locus.

2. Materials and Methods

2.1. Plant Material

Sixteen diploid wheat genotypes (Table 1) collected from different geographical regions were used in this study. One hexaploid wheat (*Triticum aestivum* L. subsp. *aestivum*) 'was the reference for the presence of locus *Lr63* (GSTR 444). Chinese Spring (CS) wheat was used as a standard control and for molecular probe generation as well. All accessions were provided by the National Small Grain Collection located at the Agricultural Research Station in Aberdeen, WA, USA.

Table 1. Origin and presence of *Xbarc321* and *Xbarc57* markers linked to *Lr63* locus in tested diploid wheat. "+"—presence of marker; "-"—absence of marker.

No.	Plant ID	Cultivar	Species	Origin	*Xbarc321*	*Xbarc57*
1.	GSTR 444	Lr63	*Triticum aestivum* subsp. *aestivum*	Canada	+	+
2.	CLTR17667	-	*Triticum urartu*	Turkey	-	+
3.	PI428316	G3220	*Triticum urartu*	Iran	-	+
4.	PI225164	Kaploutras	*Triticum monococcum* subsp. *monococcum*	Greece	+	-
5.	PI428011	G3224	*Triticum monococcum* subsp. *aegilopoides*	Azerbaijan	+	+
6.	PI554513	84TK154-028.00	*Triticum monococcum* subsp. *aegilopoides*	Soviet Union	+	-
7.	PI668147	Kromeriz	*Triticum monococcum* subsp. *monococcum*	Former Czechoslovakia	+	+
8.	PI277130	A TRI 613/59	*Triticum monococcum* subsp. *monococcum*	Albania	+	+
9.	PI614649	UKR-99-075	*Triticum monococcum* subsp. *aegilopoides*	Ukraine	+	-
10.	PI290508	V.J. 388	*Triticum monococcum* subsp. *monococcum*	Hungary	+	+
11.	PI662221	GR05-052	*Triticum monococcum* subsp. *aegilopoides*	Greece	+	-
12.	PI307984	K930	*Triticum monococcum* subsp. *monococcum*	Morocco	-	+
13.	CLTR17664	-	*Triticum urartu*	Lebanon	-	-
14.	PI170196	2498	*Triticum monococcum* subsp. *monococcum*	Turkey	+	+
15.	PI326317	WIR 18140	*Triticum monococcum* subsp. *monococcum*	Azerbaijan	+	+
16.	PI591871	SN-264	*Triticum monococcum* subsp. *monococcum*	Georgia	+	+
17.	PI487265	SY 20033	*Triticum urartu*	Syria	-	+

2.2. Identification of Molecular Markers Linked to Lr63

GeneMATRIX Plant and Fungi DNA Purification Kit was used to perform DNA isolation from the leaves of 10-day-old seedlings (EURx Ltd., Gdansk, Poland). DNA quality and concentration were measured using a DeNovix spectrophotometer (DeNovix Inc., Wilmington, DE, USA) at the spectral length of 260 and 280 nm. The samples were diluted with Tris buffer (EURx Ltd., Gdansk, Poland) to attain a concentration of 50 ng/μL. To identify gene *Lr63*, the molecular markers *Xbarc57* and *Xbarc321* [7] were used. PCR reaction was carried out in 25 μL volumes, consisting of the following: 1μL of two primers (Sigma); 12.5 μL FastGene® Optima HotStart ReadyMix (NIPPON Genetics, Europe GmbH, Düren, Germany), which included FastGene® Optima DNA Polymerase blend (0.2 U per μL reaction), FastGene® Optima Buffer (1X), dNTPs (0.4 mM of each dNTP at 1X), $MgCl_2$ (4 mM at 1X), and stabilizers; 2 μL of DNA templates; and PCR-grade water. A PCR procedure was adjusted based on the standard protocol. The primer annealing temperatures of the marker primers were 52 °C for *Xbarc321* and 60 °C for *Xbarc57* [7]. The PCR final reaction included an initial denaturation at 94 °C for 5 min, followed by 35 cycles (denaturation, 94 °C for 45 s; primer annealing, 52 or 60 °C for 30s; elongation, 72 °C for 1 min), followed by the final extension for 7 min at 72 °C and storage at 4 °C. Polymerase chain reaction (PCR) was performed with the Labcycler thermocycler (SensoQuest GmbH, Göttingen, Germany). Amplification products were separated on 2% agarose gel (Bioshop, Canada Inc., Burlington, ON, Canada) in 1xTBE buffer (Bioshop, Canada Inc., Burlington, ON, Canada) for one and a half hours. Midori Green Advanced DNA Stain (Nippon Genetics Europe, Düren, Germany) was added to agarose gel. The UV Molecular Imager Gel Doc™ XR system with Biorad Bio Image™ software (Biorad, Berkeley, CA, USA) was used to visualize the amplification products.

2.3. Chromosome Preparation

Seeds were germinated in Petri dishes laid out with filter paper and flooded with water at room temperature (22 °C) for 4–6 days. After this time, root tips were cut off and stored in ice-cold water for 26 h. Fixation of the root tips was performed using ethanol and acetic acid (3:1, *v*/*v*). Mitotic preparations were created from root tips by digesting them with an enzyme mixture consisting of 20% (*v*/*v*) pectinase (Sigma), 1% (*w*/*v*) cellulose (Calbiochem), and 1% (*w*/*v*) cellulase 'Onozuka R-10' (Serva). By previously washing them with 0.01 M sodium citric buffer, slides were prepared according to the Kwiatek et al. [30] procedure.

2.4. DNA Molecular Probes

Genomic DNA from "CS" wheat was used to amplify the following repetitive sequences: pTa-86, pTa-535, and pTa-713, which were used as molecular probes (Table 2) [30]. According to Komuro et al. [30], two clones (pTa-535 and pTa-713) were determined to have especially valuable sequences for chromosome identification. In combination with pTa-86 (the pSc119 homologous sequence), these probes enabled the unambiguous discrimination of all wheat chromosomes, including orientation.

Table 2. Primer sequence and PCR terms for amplification of wheat repetitive sequences [29,30].

Clone	NCBI GenBank Sequence Number	Primer Sequences (5′ to 3′)	Annealing Temperature (°C)
pTa-86	KC290896	ACGATTGACCAATCTCGGGG ACCGACCCAAATTACGAGAGT	58.5
pTa-535	KC290894	GCATAGCATGTGCGAAAGAG TCGTCCGAAACCCTGATAC	59
pTa-535	KC290894	GGGGCGGACGTCGTTG CCGTAAGATAGACAGGGTGGG	59

The PCR mixture contained 12.5 µL of TaqNovaHS Master Mix, 1 µL of forward/reverse primers, 2 µL of DNA, and 8.5 µL of nuclease-free water. PCR reactions were performed under conditions of 95 °C for 3 min, 34 cycles of 95 °C for 30 s, annealing temperature at 59 °C for 30 s, 72 °C for 60 s, and 72 °C for 5 min. Labeling of molecular probes was performed using the nick translation method using the Nick Translation Kit (Roche/Merck). The pTa-535 sequence was labeled with tetramethyl-5-dUTP-rhodamine (Roche), whereas pTa-713 was labeled with digoxigenin-11-dUTP (Roche), and pTa-86 was labeled with Atto647 (Jena Bioscience, Jena, Germany).

2.5. DNA Molecular Probes

According to Kwiatek et al. [30], FISH was carried out with modifications. The repeat sequences of pTa-86, pTa-535, and pTa-713 were used as molecular probes. The hybridization mixture (10 µL/slide) contained: 50% formamide, 20% dextran sulphate, 10% 20×SSC, and 5% salmon sperm DNA and molecular probes. It was denatured at 70 °C for 10 min, 75 °C for 3 min, and then stored on ice for 10 min. Chromosomal DNA was denatured for 4 min at 70 °C with a hybridization mix and allowed to hybridize for 24 h at 37 °C. Digoxigenin-11-dUTP detection was conducted using antidigoxigenin-fluorescein antibody (Roche). Specific chromosomes were identified by comparing signal patterns and by comparing them to Komuro's et al. [29] work. Slides were analyzed at 1000× using a Delta Optical FMA050 microscope with a DLT-Cam PRO 12MP camera and DLT-Cam Viewer software. Image editing and karyotyping were performed using Adobe Photoshop C6 software.

3. Results

3.1. Intraspecific Polymorphism of Chromosome Markers

We performed a cytogenetic analysis based on the following probes: pTa-713, pTa-535, and pTa-86. All molecular probes provided signals on chromosomes of diploid wheat. FISH-painted chromosomes were categorized according to Komuro et al. [29]. The hybridization of the pTa-535 probe to chromosomes of einkorn species revealed clear and highly specific labeling patterns. All chromosomes carried 1–2 hybridization sites in chromosome-specific positions, although some intraspecific variation in signal localization and intensity has been observed. Hybridization patterns of pTa-86 in *T. urartu*, *T. monococcum* ssp. *Aegilopides*, and *T. monococcum* ssp. *Monococcum* were absent. In the *T. urartu* hybridization patterns of pTa-535, only two genotypes (CLTR17664 and PI487265) were observed on chromosome $3A^{u}$ in distal regions of long arms (Figure 1). The hybridization of the pTa-535 probe on the *T. monococcum* ssp. *Aegilopoides* chromosome revealed one very small signal in the subtelomeric region of the long arm in accession PI614649. A similar pattern was observed in the distal part of the short arm in genotype PI428011 of *T. boeticum*, and the additional hybridization sites of pTa-713 were found in the pericentromeric region (Figure 1).

Similar signal distributions of pTa-535 were observed in four accessions of *T. monococcum* ssp. *monococcum* (PI290508, PI591871, PI668147, and PI277130); one signal in the pericentromeric region of chromosome 3A in the hexaploid wheat overlap with sites of these accessions and the other pattern was noticed in the distal part of the short arms of chromosome $3A^{mm}$. Two accessions (PI170196 and PI326317) contained signals located in the subtelomeric region of the short arm. A weak signal was found in genotype PI225164 of einkorn in the subtelomeric region of chromosome $3A^{mm}L$ (Figure 1). In accessions CLTR17667, PI428316 (*T. urartu*); PI554513, PI662221 (*T. monococcum* ssp. *aegilopoides*), and PI307984 (*T. monococcum* ssp. *monococcum*), we observed a lack of hybridization patterns of pTa-535 and pTa-713 (Figure 1).

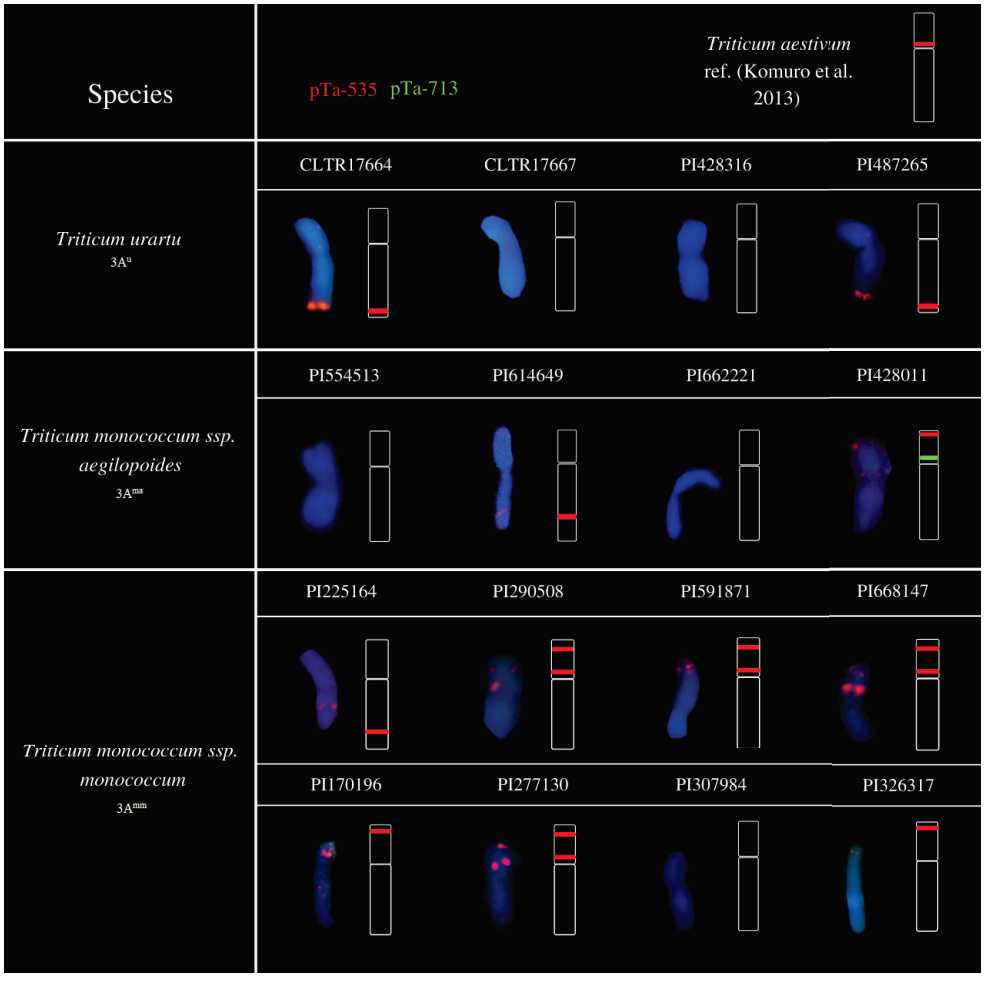

Figure 1. Chromosomes 3A after FISH with pTa-713 (**green**) and pTa-535 (**red**) probes of CLTR17664, CLTR17667, PI428316, PI487265, PI554513, PI614649, PI662221, PI428011, PI225164, PI290508, PI591871, PI668147, PI170196, PI277130, PI307984, and PI326317.

3.2. Polymorphism of Lr63 Loci

In parallel to the cytogenetic analysis, we analyzed the allelic variation in the *Lr63* leaf rust resistance loci at chromosome 3A (Figure 2). The expected specific product for marker *Xbarc321* was 191 bp according to Kolmer et al. [7]. In this experiment, 11 genotypes (PI 225164, PI 428011, PI 554513, PI 668147, PI 277130, PI 614649, PI 290508, PI 662221, PI 170196, PI 326317, and PI 591871) revealed PCR products, which were identical to one specific to GSTR 444 (reference genotype to locus *Lr63*) (Table 1 and Figure 2). Moreover, *Xbarc57* was used as the second marker in order to analyze the *Lr63* locus. Compared to the reference genotype (GSTR 444), the expected 240 bp products were identified in 11 genotypes (CLTR 17667, PI 428316, PI 428011, PI 668147, PI 277130, PI 290508, PI 307984, PI 170196, PI 326317, PI 591871, and PI 487265) (Table 1, Figure 2). The comparison of *Xbarc321* and *Xbarc57* marker analyses showed that both markers allowed to identify the *Lr63* gene locus in seven genotypes. Among them, six genotypes were considered as domesticated forms (*Triticum monococcoccum* subsp. *monococcum*) (PI 668147, PI 277130, PI 290508, PI 170196, PI 326317,

and PI 591871) and one was a nondomestication form (PI 428011) (*Triticum monococcoccum* subsp. *aegilopoides*).

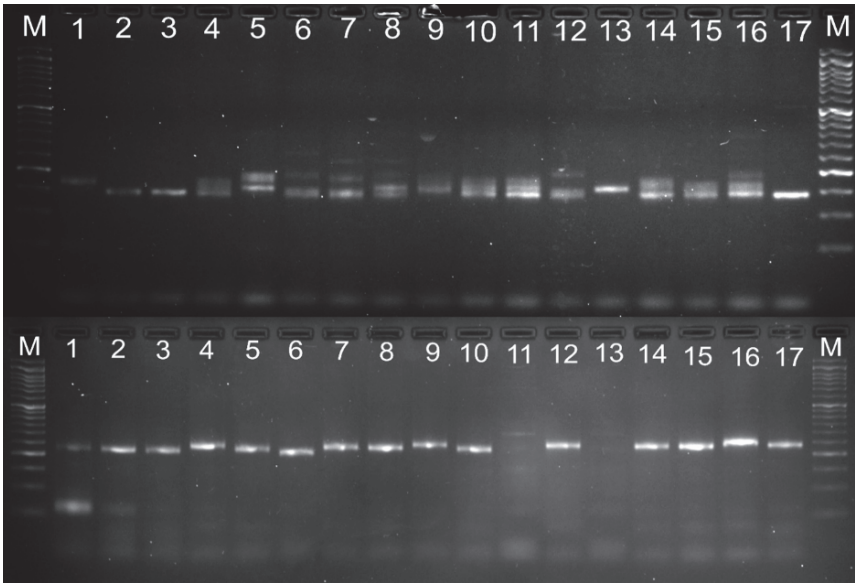

Figure 2. PCR amplification products of wheat genotypes with *xbarc321* and *xbarc57* markers linked to *Lr63* locus. M-50 bp DNA Ladder (NIPPON Genetics EUROPE GmbH); 1–17—wheat genotypes.

3.3. Rearrangements of Short Arm of 3A Chromosome

Taking into consideration the presence of molecular markers (*Xbarc321* and *Xbarc57*) and the signals of the pTa-535 probe on chromosome 3A of the short arm, it was possible to divide the accessions into three groups (Figure 3). The first group included seven genotypes carrying *Lr63* markers and possessed hybridization patterns on chromosome 3A. These accessions were as follows: PI 428011, PI 668147, PI 277130, PI 290508, PI 170196, PI 326317, and PI 591871, originating from Azerbaijan, Czechoslovakia, Albania, Hungary, Turkey, Azerbaijan, and Georgia (Figure 3). The genotypes in the second group were characterized by the presence of one marker (*Xbarc321* or *Xbarc57)* and the absence of the pTa-535 probe signal, including CLTR 17667, PI 428316, PI 225164, PI 554513, PI 614649, PI 662221, PI 307984, and PI 487265, originating from Turkey, Iran, Greece, the Soviet Union, Ukraine, Greece, Morocco, and Syria (Figure 3). One accession (CLTR 17664 from Lebanon), included in the last group, revealed the absence of *Lr63* markers and hybridization signals (Figure 3).

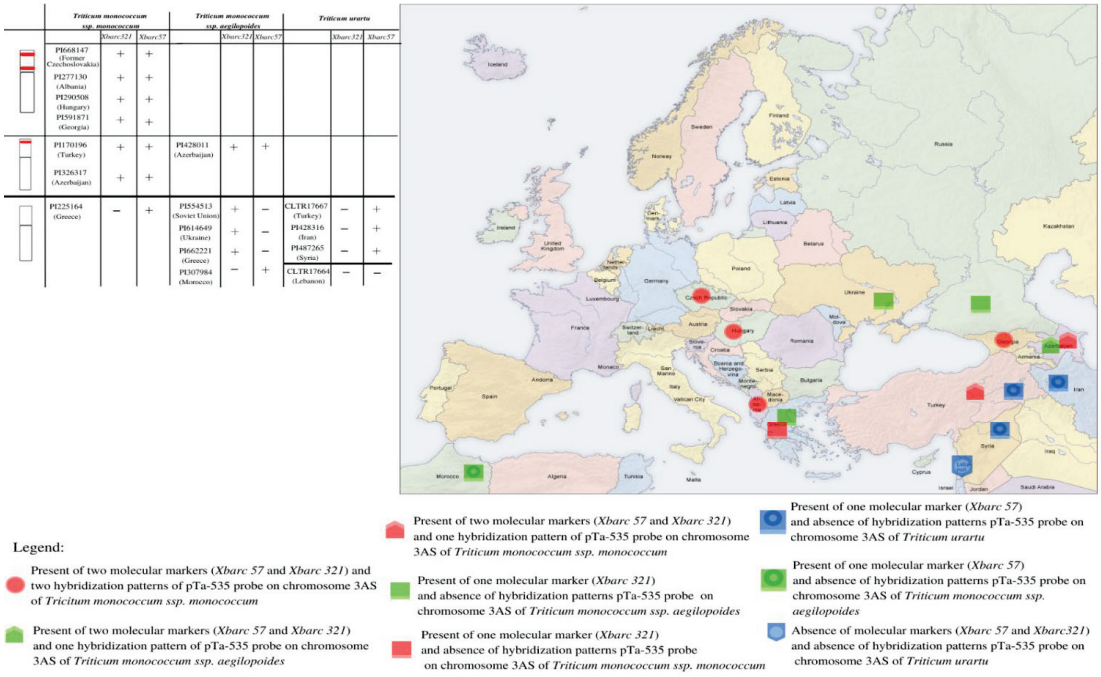

Figure 3. Geographical distribution of the studied accessions divided into three groups according pTa-535 signal location, as well as molecular markers, the presence of a particular amplification product.

4. Discussion

Revealing how domestication and selection impact disease-related genes is one of the crucial issues in plant genetics connected to resistance breeding. It has been reported that hexaploid wheat originated due to two hybridization events [32]. First, two wild species, *Triticum urartu* (A-genome donor) and an extinct species from the *Sitopsis* section (B-genome donor), hybridized and formed wild tetraploid wheat (*T. turgidum* ssp. *dicoccoides*). After the domestication of this wild form to cultivated tetraploid wheat (*T. turgidum* ssp. *dicoccum*), a second hybridization occurred with the wild grass *Ae. tauschii* (D-genome donor) resulting in the hexaploid wheat. The evolution of the resistance genes of wheat can be determined with comparative analyses and the allele mining of diverse germplasms. For example, the leaf rust resistance gene *Lr10* (located on chromosome arm 1AS) was cloned from bread cv. Thatcher *Lr10* [33]. It was reported that diploid (*T. urartu*; A-genome donor) and tetraploid (wild and domesticated) wheats carry a homologous sequence of *Lr10*, which has two haplotypes at the *Lr10* locus [34]. What is more, [35] suggested a balanced polymorphism and maintenance of both haplotypes of the *Lr10* gene sequence in the wheat gene pool, which is similar to the evolutionary pathway of genes in other species, such as *Rpm1* in Arabidopsis.

It is known that *T. monococcum* subsp. *aegilopoides*, *T. monococcum* subsp. *Monococcum*, and *T. urartu* carry the genome A, which is the axial subgenome for all wheats (*Triticum* sp.) [32]. Genes from these species can be introduced into wheat using direct crossing and chromosomal recombination. Diversified collections of these species are present in nature, widely distributed in different regions. The domestication of the diploid wheat *T. monococcum* ssp. *aegilopoides* was located in the geographical region of the Karaca Dağ (Karacadag) volcanic mountain, located in present-day south-eastern Turkey [18]. The wild form was first harvested and then transported to different geographical areas and cultivated there. Transport involved migrating farmers or exchanging seeds for other material goods,

because not all soils in the "Fertile Crescent" area were adjusted to cultivate crops. The directions of the early spread of diploid wheat included areas of present-day Turkey, Iraq, Syria, and Iran. In the later phase of agricultural expansion, crops were transported in an already nascent state of domestication [18,36]. According to Kolmer et al. [7], only one gene resistant to leaf rust (*Lr63*) has been mapped on the short arm of chromosome $3A^m$. The short arm of the $3A^m$ chromosome is also a region, where the main QTL for seed dormancy [37] *FLOWERING LOCUS T* (*FT*)-like, *TERMINAL FLOWER1* (*TFL1*)-like, and *MFT*-like [38] is located. Those loci are considered to be the most agronomically important traits considering crop domestication. It could, therefore, be stated that the selection pressure could alter this chromosome region with particular intensity. After all, it is known that in the transition from gathering to cultivation, early farmers selected CWRs with useful genetic modifications and developed improved populations with desirable traits [39]. The abovementioned traits, as well as the loss of seed dispersal mechanisms, increased grain size, the loss of vulnerability to environmental factors for germination and flowering, synchronous ripening, and a compact growth habit are included in the "domestication syndrome" characters, which are the most important adaptive traits selected by mankind [40]. In this research, we observed the presence of two markers (*Xbarc321* and *Xbarc57*) and hybridization patterns of probe pTa-535 on chromosome 3A accessions, which strongly indicated intra- and interspecific polymorphisms. The direction of the expansion of the first group of accessions proved the later phase of agricultural spread. The second group allowed to prove the early spread of einkorn, through directions of expansion and intra- and interspecific polymorphisms. The third group (*T. urartu*) was never domesticated and located near the Fertile Crescent. According to our cytogenetic observations, it could be stated that a similar organization of the $3A^m$ chromosome (lack of pTa-535 signals and lack of one or two SSR markers) of *T. monococcum* spp. *monococcum* and *T. monococcum* spp. *aegilopoides* compared to *T. urartu* was observed only in accessions collected from the regions which were located closely to the domestication centers of einkorn wheat (Turkey, Azerbaijan, Greece, and Ukraine). Additional pTa-535 signals which appeared on the short arm of the $3A^m$ chromosome were observed in the accessions, which revealed both markers linked to *Lr63* loci. Interestingly, those accessions were collected near the domestication center of *T. monococcum* (Turkey), as well as in central Europe (Hungary, former Czechoslovakia, and Albania), and Georgia. Hence, it could be stated that forms belonging to the first and second groups were more prone to be selected and perform desirable domestication traits. Both repetitive sequence redundancies and proximities to genes were reported to vary between cultivated and wild genotypes [41,42]. Such differences suggest the potential function of repetitive sequences in crop domestication. For example, differences in the proximity of retrotransposons to genes could contribute to the significant phenotypic differences between wild and cultivated sunflowers [43]. Recently, Ebrahizadegan et al. [44] reported that different classes of repetitive DNA sequences have differentially accumulated between *Aegilops tauschii* subsp. *strangulata* and the other two subspecies of *Ae. tauschii* that were in parallel with spike morphology, implying that factors affecting the so called "repeatome" evolution are variable even among highly closely related lineages. In our study, we observed that both markers linked with *Lr63* loci were present only in those accessions which revealed one or two additional pTa-535 sites. This chromosome organization pattern was characteristic to most of the *T. monococcum* subsp. *monococcum* accessions. Anker et al. [45] proposed that *Triticum monococcum* has a nonhost status to the pathogens responsible for leaf rust, and showed that *Triticum monococcum* subsp. *monococcum* is more rust-resistant compared to *Triticum monococcum* subp. *aegilopoides* and *Triticum urartu* [45].

5. Conclusions

Considering that new virulence pathotypes and races keep on appearing constantly, one of the key challenges for wheat breeders is the systematic development of new, elite varieties carrying effective resistance genes. In the description of the domestication model

of diploid wheat, Kilian et al. [36] reported that einkorn wheat retained a high level of genetic diversity in the domesticated lines, which can be used to improve common wheat. Alterations and reorganization of the repetitive DNA sequences are the strongest indications of evolution and speciation processes. Therefore, the identification of polymorphisms in chromosome structures of different accessions of einkorn wheat may be helpful in further basic and application research.

Author Contributions: M.T.K. initiated the project. A.N. conducted the experiments and analyses. A.N. and R.B. wrote the first draft of the manuscript. M.T.K. revised the draft and improved the manuscript. All authors have read and agreed to the published version of the manuscript.

Funding: This publication was co-financed by the framework of the Ministry of Science and Higher Education program as "Regional Initiative Excellence" in years 2019–2022, project No. 005/RID/2018/19.

Informed Consent Statement: Not applicable.

Acknowledgments: The authors would like to acknowledge Harrold Bockelman at the USDA/ARS Small Grains Laboratory, (Aberdeen, ID, USA), for providing the seed samples.

Conflicts of Interest: The authors declare no conflict of interest.

References

1. Harlan, J.R.; de Wet, J.M.J. Toward a Rational Classification of Cultivated Plants. *TAXON* **1971**, *20*, 509–517. [CrossRef]
2. Dempewolf, H.; Baute, G.; Anderson, J.; Kilian, B.; Smith, C.; Guarino, L. Past and Future Use of Wild Relatives in Crop Breeding. *Crop Sci.* **2017**, *57*, 1070–1082. [CrossRef]
3. Feldman, M.; Levy, A.A. Origin and Evolution of Wheat and Related Triticeae Species. In *Alien Introgression in Wheat*; Molnár-Láng, M., Ceoloni, C., Doležel, J., Eds.; Springer International Publishing: Cham, Switzerland, 2015; pp. 21–76. ISBN 978-3-319-23493-9.
4. Badaeva, E.D.; Amosova, A.V.; Goncharov, N.P.; Macas, J.; Ruban, A.S.; Grechishnikova, I.V.; Zoshchuk, S.A.; Houben, A. A Set of Cytogenetic Markers Allows the Precise Identification of All A-Genome Chromosomes in Diploid and Polyploid Wheat. *Cytogenet Genome Res.* **2015**, *146*, 71–79. [CrossRef]
5. Prasad, P.; Savadi, S.; Bhardwaj, S.C.; Gupta, P.K. The Progress of Leaf Rust Research in Wheat. *Fungal Biol.* **2020**, *124*, 537–550. [CrossRef] [PubMed]
6. McIntosh, R.A.; Dubcovsky, J.; Rogers, W.J.; Morris, C.; Xia, X.C. Catalogue of Gene Symbols For Wheat: 2017 Supplement. 20. Available online: https://shigen.nig.ac.jp/wheat/komugi/genes/macgene/supplement2017.pdf (accessed on 30 March 2022).
7. Kolmer, J.A.; Anderson, J.A.; Flor, J.M. Chromosome Location, Linkage with Simple Sequence Repeat Markers, and Leaf Rust Resistance Conditioned by Gene *Lr63* in Wheat. *Crop Sci.* **2010**, *50*, 2392–2395. [CrossRef]
8. Childe, V.G. The Origin of Neolithic Culture in Northern Europe. *Antiquity* **1949**, *23*, 129–135. [CrossRef]
9. Diamond, J. Evolution, Consequences and Future of Plant and Animal Domestication. *Nature* **2002**, *418*, 700–707. [CrossRef]
10. Diamond, J.; Bellwood, P. Farmers and Their Languages: The First Expansions. *Science* **2003**, *300*, 597–603. [CrossRef]
11. Skoglund, P.; Malmström, H.; Raghavan, M.; Storå, J.; Hall, P.; Willerslev, E.; Gilbert, M.T.P.; Götherström, A.; Jakobsson, M. Origins and Genetic Legacy of Neolithic Farmers and Hunter-Gatherers in Europe. *Science* **2012**, *336*, 466–469. [CrossRef]
12. Meyer, R.S.; DuVal, A.E.; Jensen, H.R. Patterns and Processes in Crop Domestication: An Historical Review and Quantitative Analysis of 203 Global Food Crops. *New Phytol.* **2012**, *196*, 29–48. [CrossRef]
13. Beissinger, T.M.; Wang, L.; Crosby, K.; Durvasula, A.; Hufford, M.B.; Ross-Ibarra, J. Recent Demography Drives Changes in Linked Selection across the Maize Genome. *Nat. Plants* **2016**, *2*, 16084. [CrossRef] [PubMed]
14. Kantar, M.B.; Nashoba, A.R.; Anderson, J.E.; Blackman, B.K.; Rieseberg, L.H. The Genetics and Genomics of Plant Domestication. *BioScience* **2017**, *67*, 971–982. [CrossRef]
15. Yang, L.; Koo, D.-H.; Li, Y.; Zhang, X.; Luan, F.; Havey, M.J.; Jiang, J.; Weng, Y. Chromosome Rearrangements during Domestication of Cucumber as Revealed by High-Density Genetic Mapping and Draft Genome Assembly. *Plant. J.* **2012**, *71*, 895–906. [CrossRef] [PubMed]
16. Chia, J.-M.; Song, C.; Bradbury, P.J.; Costich, D.; de Leon, N.; Doebley, J.; Elshire, R.J.; Gaut, B.; Geller, L.; Glaubitz, J.C.; et al. Maize HapMap2 Identifies Extant Variation from a Genome in Flux. *Nat. Genet.* **2012**, *44*, 803–807. [CrossRef]
17. Wang, Y.; Xiong, G.; Hu, J.; Jiang, L.; Yu, H.; Xu, J.; Fang, Y.; Zeng, L.; Xu, E.; Xu, J.; et al. Copy Number Variation at the GL7 Locus Contributes to Grain Size Diversity in Rice. *Nat. Genet.* **2015**, *47*, 944–948. [CrossRef]
18. Kilian, B.; Ozkan, H.; Walther, A.; Kohl, J.; Dagan, T.; Salamini, F.; Martin, W. Molecular Diversity at 18 Loci in 321 Wild and 92 Domesticate Lines Reveal No Reduction of Nucleotide Diversity during *Triticum Monococcum* (Einkorn) Domestication: Implications for the Origin of Agriculture. *Mol. Biol. Evol.* **2007**, *24*, 2657–2668. [CrossRef]
19. Heun, M.; Schäfer-Pregl, R.; Klawan, D.; Castagna, R.; Accerbi, M.; Borghi, B.; Salamini, F. Site of Einkorn Wheat Domestication Identified by DNA Fingerprinting. *Science* **1997**, *278*, 1312–1314. [CrossRef]

20. Zaharieva, M.; Monneveux, P. Cultivated Einkorn Wheat (*Triticum Monococcum* L. Subsp. *Monococcum*): The Long Life of a Founder Crop of Agriculture. *Genet. Resour. Crop Evol.* **2014**, *61*, 677–706. [CrossRef]
21. Nesbitt, M. From Staple Crop to Extinction? The Archaeology and History of Hulled Wheat. In *Hulled Wheats. Promoting the Conservation and Use of Underutilized and Neglected Crops*; IPRGI: Serdang, Malaysia, 1996; pp. 1–100.
22. Nevo, E. Triticum. In *Wild Crop Relatives: Genomic and Breeding Resources*; Kole, C., Ed.; Springer: Berlin/Heidelberg, Germany, 2011; pp. 407–456. ISBN 978-3-642-14227-7.
23. Filatenko, A.; Hammer, K. New Descriptions of Hulled Wheats on the Infraspecific Level. *Genet. Resour. Crop Evol.* **1997**, *44*, 285–288. [CrossRef]
24. Gill, B.S.; Friebe, B. Plant Cytogenetics at the Dawn of the 21st Century. *Curr. Opin. Plant. Biol.* **1998**, *1*, 109–115. [CrossRef]
25. Pedersen, C.; Langridge, P. Identification of the Entire Chromosome Complement of Bread Wheat by Two-Colour FISH. *Genome* **1997**, *40*, 589–593. [CrossRef] [PubMed]
26. Cuadrado, A.; Schwarzacher, T.; Jouve, N. Identification of Different Chromatin Classes in Wheat Using In Situ Hybridization with Simple Sequence Repeat Oligonucleotides. *Theor. Appl. Genet.* **2000**, *101*, 711–717. [CrossRef]
27. Cuadrado, A.; Cardoso, M.; Jouve, N. Physical Organisation of Simple Sequence Repeats (SSRs) in Triticeae: Structural, Functional and Evolutionary Implications. *Cytogenet Genome Res.* **2008**, *120*, 210–219. [CrossRef] [PubMed]
28. Megyeri, M.; Farkas, A.; Varga, M.; Kovács, G.; Molnár-Láng, M.; Molnár, I. Karyotypic Analysis of Triticum Monococcum Using Standard Repetitive DNA Probes and Simple Sequence Repeats. *Acta Agron. Hung.* **2012**, *60*, 87–95. [CrossRef]
29. Komuro, S.; Endo, R.; Shikata, K.; Kato, A. Genomic and Chromosomal Distribution Patterns of Various Repeated DNA Sequences in Wheat Revealed by a Fluorescence In Situ Hybridization Procedure. *Genome* **2013**, *56*, 131–137. [CrossRef] [PubMed]
30. Kwiatek, M.; Majka, M.; Majka, J.; Belter, J.; Suchowilska, E.; Wachowska, U.; Wiwart, M.; Wiśniewska, H. Intraspecific Polymorphisms of Cytogenetic Markers Mapped on Chromosomes of *Triticum Polonicum* L. *PLoS ONE* **2016**, *11*, e0158883. [CrossRef]
31. Goriewa-Duba, K.; Duba, A.; Kwiatek, M.; Wiśniewska, H.; Wachowska, U.; Wiwart, M. Correction: Chromosomal Distribution of PTa-535, PTa-86, PTa-713, 35S RDNA Repetitive Sequences in Interspecific Hexaploid Hybrids of Common Wheat (*Triticum Aestivum* L.) and Spelt (*Triticum Spelta* L.). *PLoS ONE* **2018**, *13*, e0203162. [CrossRef]
32. Venske, E.; Schreinert dos Santos, R.; Busanello, C.; Gustafson, P.; Costa de Oliveira, A. Bread Wheat: A Role Model for Plant Domestication and Breeding. *Hereditas* **2019**, *156*, 16. [CrossRef]
33. Feuillet, C.; Travella, S.; Stein, N.; Albar, L.; Nublat, A.; Keller, B. Map-Based Isolation of the Leaf Rust Disease Resistance Gene Lr10 from the Hexaploid Wheat (*Triticum Aestivum* L.) Genome. *Proc. Natl. Acad. Sci. USA* **2003**, *100*, 15253–15258. [CrossRef]
34. Loutre, C.; Wicker, T.; Travella, S.; Galli, P.; Scofield, S.; Fahima, T.; Feuillet, C.; Keller, B. Two different CC-NBS-LRR genes are required for *Lr10*-mediated leaf rust resistance in tetraploid and hexaploid wheat. *Plant J.* **2009**, *60*, 1043–1054. [CrossRef]
35. Tian, D.; Traw, M.B.; Chen, J.Q.; Kreitman, M.; Bergelson, J. Fitness costs of R-gene-mediated resistance in *Arabidopsis thaliana*. *Nature* **2003**, *423*, 74–77. [CrossRef] [PubMed]
36. Muehlbauer, G.J.; Feuillet, C. (Eds.) *Genetics and Genomics of the Triticeae*; Springer: New York, NY, USA, 2009; ISBN 978-0-387-77488-6.
37. Zhang, L.; Wang, S.; Li, H.; Deng, Q.; Zheng, A.; Li, S.; Li, P.; Li, Z.; Wang, J. Effects of Missing Marker and Segregation Distortion on QTL Mapping in F2 Populations. *Appl. Genet.* **2010**, *121*, 1071–1082. [CrossRef] [PubMed]
38. Nakamura, S.; Abe, F.; Kawahigashi, H.; Nakazono, K.; Tagiri, A.; Matsumoto, T.; Utsugi, S.; Ogawa, T.; Handa, H.; Ishida, H.; et al. A Wheat Homolog of Mother of FT and TFL1 Acts in the Regulation of Germination. *Plant. Cell.* **2011**, *23*, 3215–3229. [CrossRef]
39. Vaughan, D.A.; Balázs, E.; Heslop-Harrison, J.S. From Crop Domestication to Super-Domestication. *Ann. Bot.* **2007**, *100*, 893–901. [CrossRef]
40. Gao, L.; Zhao, G.; Huang, D.; Jia, J. Candidate Loci Involved in Domestication and Improvement Detected by a Published 90K Wheat SNP Array. *Sci. Rep.* **2017**, *7*, 44530. [CrossRef] [PubMed]
41. Ramírez-González, R.H.; Borrill, P.; Lang, D.; Harrington, S.A.; Brinton, J.; Venturini, L.; Davey, M.; Jacobs, J.; van Ex, F.; Pasha, A.; et al. The Transcriptional Landscape of Polyploid Wheat. *Science* **2018**, *361*, eaar6089. [CrossRef] [PubMed]
42. Bariah, I.; Keidar-Friedman, D.; Kashkush, K. Where the Wild Things Are: Transposable Elements as Drivers of Structural and Functional Variations in the Wheat Genome. *Front. Plant Sci.* **2020**, *11*, 585515. [CrossRef]
43. Mascagni, F.; Barghini, E.; Giordani, T.; Rieseberg, L.H.; Cavallini, A.; Natali, L. Repetitive DNA and Plant Domestication: Variation in Copy Number and Proximity to Genes of LTR-Retrotransposons among Wild and Cultivated Sunflower (*Helianthus Annuus*) Genotypes. *Genome Biol. Evol.* **2015**, *7*, 3368–3382. [CrossRef]
44. Ebrahimzadegan, R.; Orooji, F.; Ma, P.; Mirzaghaderi, G. Differentially Amplified Repetitive Sequences Among *Aegilops Tauschii* Subspecies and Genotypes. *Front. Plant Sci.* **2021**, *12*, 716750. [CrossRef]
45. Anker, C.C.; Niks, R.E. Prehaustorial Resistance to the Wheat Leaf Rust Fungus, Puccinia Triticina, in *Triticum Monococcum*. *Euphytica* **2001**, *117*, 209–215. [CrossRef]

agriculture

MDPI

Article

The Potential Function of *SiLOX4* on Millet Discoloration during Storage in Foxtail Millet

Qi Ma [1], Junjie Wang [1], Lu Cheng [1], Yaqiong Li [1,2], Qianxiang Zhang [1], Hongying Li [1,2,3], Yuanhuai Han [1,2,3], Xiaoxi Zhen [3,*] and Bin Zhang [1,2,*]

[1] College of Agriculture, Shanxi Agricultural University, Jinzhong 030801, China
[2] Institute of Agricultural Bioengineering, Shanxi Agricultural University, Jinzhong 030801, China
[3] Shanxi Key Laboratory of Minor Crop Germplasm Innovation and Molecular Breeding, Shanxi Agricultural University, Taiyuan 030031, China
* Correspondence: xiaoxizhen@sxau.edu.cn (X.Z.); binzhang@sxau.edu.cn (B.Z.)

Abstract: Millet color is an important index for consumers to assess foxtail millet quality. The yellow color of millet is mainly because of the accumulation of carotenoids, which are essential for human nutrition. However, the discoloration of millet during storage due to carotenoid degradation seriously reduces the nutritional and commercial value of millet products. The essential quality traits of millet discoloration during storage were analyzed using two foxtail millet varieties, namely 9806-1 and Baomihunzi. We observed that the millet discoloration was caused by carotenoid degradation during storage, and different genotypes exhibited different discoloration rates. The carotenoid reduction rate in 9806-1 (32.2%) was higher than that in Baomihunzi (10.5%). The positive correlation between carotenoid reduction and the expression of SiLOX protein indicated that SiLOX from foxtail millet played a major role in carotenoid reduction during storage. The expression profiles of the *SiLOX* gene family were analyzed at different grain maturing stages, from S1 to S3, in these two varieties to determine the key *SiLOX* genes responsive to millet discoloration in foxtail millet. The consecutively low expression of *SiLOX2*, *SiLOX3*, and *SiLOX4* contributed to the low level of SiLOX protein in Baomihunzi. Furthermore, the undetectable expression of *SiLOX4* in the later stage of maturation in Baomihunzi was associated with low discoloration, indicating that *SiLOX4* might be a key gene in regulating the discoloration of millet. This study provided critical information on the mechanism of carotenoid degradation during millet storage and laid the foundation for further understanding of carotenoid metabolism in foxtail millet.

Keywords: foxtail millet; lipoxygenase; carotenoid; discoloration

Citation: Ma, Q.; Wang, J.; Cheng, L.; Li, Y.; Zhang, Q.; Li, H.; Han, Y.; Zhen, X.; Zhang, B. The Potential Function of *SiLOX4* on Millet Discoloration during Storage in Foxtail Millet. *Agriculture* **2022**, *12*, 1283. https://doi.org/10.3390/agriculture12081283

Academic Editors: Edyta Paczos-Grzeda, Volker Mohler and Sylwia Sowa

Received: 14 July 2022
Accepted: 19 August 2022
Published: 22 August 2022

1. Introduction

Carotenoids are the principal pigments responsible for yellow, orange, and red colors in different plant organs, including flowers, fruits, vegetables, and seeds. They play multiple roles in plant survival, such as acting as light-harvesting antennae in photosynthesis, protecting plants from light damage by quenching triplet-excised states in chlorophyll II, and attracting pollinators and seed distributors in non-photosynthesis processes [1,2]. Carotenoids cannot be synthesized in the human body and must be obtained from the diet. They provide valuable nutrition and health benefits for humans. They produce biologically active molecules that are important antioxidants and free-radical scavengers, which can protect against age-related macular durations and reduce the risk of cancer and cardiovascular diseases [3,4]. The degradation rate is an important contributory factor to the final carotenoid content in plant tissues [5]. The advances in the understanding of carotenoid degradation would be critical for improving the nutritional quality of various plant-based food sources.

Foxtail millet [*Setaria italica* (L.) Beauv.], a minor crop, is essential for food security in semiarid regions of Asia and Africa [6]. Hulled foxtail millet is popular because of its rich

and balanced nutrients. Millet porridge is a favorite daily food for most people in northern China, especially for pregnant and postnatal women [7,8]. Carotenoids, which impart a bright yellow color to millet, are important nutrients in millet [9]. The millet color is the key index to determining foxtail millet quality [10]. However, the discoloration of millet during storage reduces the value and nutritional qualities of millet and millet products, which causes serious economic losses for the millet industry. However, the mechanism underlying the carotenoid degradation in foxtail millet during storage is unclear to date.

Previous studies on wheat, golden rice, and sweet corn have reported that lipoxygenase (LOX) activity was responsible for carotenoid degradation during storage or staleness [11–13]. LOXs are nonheme, iron-containing dioxygenases in plants, animals, and fungi. In plants, they are classified into two major groups 9-LOX and 13-LOX. They play a key role in plant development and defense by various oxidizing lipids, especially through their metabolites, such as jasmonates (JA), green leaf volatiles (GLVs), and death acid, which are involved in response to biotic and abiotic stresses [14]. The *13-LOX TomloxC* is reported to be essential for the synthesis of the flavor volatiles in both tomato fruits and leaves [15]. Similarly, the high expression of two *13-LOXs* (*SbLOX9* and *SbLOX5*) in sorghum-resistant lines induced by the sugarcane aphid infestation and exogenous MeJA treatment predicts the putative function of these genes in the biosynthesis of JA and GLVs [16]. The gene of *cssap92*, encoding a 9-LOX protein, is responsive to *Aspergillu* spp. infection in maize [17]. In addition, 9-LOXs are more involved in the seed qualities related to storage. In rice, 9-LOXs are the major factor influencing seed longevity and viability. Over-expression of *LOX3* in LOX3-normal rice cultivar can accelerate the decrease in seed longevity and germination ability, and the rice seeds with *LOX3* knockout exhibited an improved storability [18,19]. Furthermore, it was reported that *r9-LOX1* was directly responsible for the degradation of carotenoids in golden rice after artificial aging treatment [20]. The deletion of *Lpx-B1* in durum wheat resulted in a 4.5-fold reduction in LOX activity and significant improvement in yellow pigments in pasta [21].

Considering the important function of *LOX* genes on the carotenoid degradation in cereal grains, we investigated the relationship between the LOXs in foxtail millet and the discoloration of millet during storage. For the study, "9806-1" with a fast millet discoloration rate and "Baomihunzi" with a slow millet discoloration rate were selected as research materials. At different storage stages, the total carotenoid contents (TCC) of the two varieties were investigated. The expression patterns of SiLOX protein and *SiLOX* gene family members were compared between the two varieties during grain maturing stages to determine which *SiLOX* gene plays a major role in the discoloration of millet. This study improved the understanding of the molecular mechanism of millet discoloration during storage, which could lay a foundation for developing molecular markers and promoting the molecular breeding of high-quality foxtail millet.

2. Materials and Methods

2.1. Plant Materials

Two foxtail millet varieties, 9806-1 (Crop Research Institute of the Jilin Academy of Agricultural Sciences, Jilin City, Jilin Province, China) and Baomihunzi (Farming variety of Hulan County, Harbin City, Heilongjiang Province, China), were selected from the core germplasm of foxtail millet in China based on the significant difference in millet discoloration between the two varieties. Maturing grains (S1, initial maturation stage, 14 days of filling stage; S2, mid maturation stage, 21 DOFS; S3, last stage of maturation, 29 DOFS) were collected, hulled, and immediately frozen in liquid nitrogen for RNA and protein isolation [22]. In early October, the foxtail millet was harvested, and the hulled grains of the two varieties were separately kept in Kraft paper bags and stored at room temperature (approximately 23 °C) in the dark. Samples of matured grains from the two varieties were collected at 0, 1, 2, 3, 4, 5, 6, and 7 months during storage for carotenoid extraction analysis.

2.2. Experimental Site and Field Experiment

The sowing of the foxtail millets was performed on 1st May, 2020 (Average temperature of 24 °C) at the research station in Shanxi Agriculture University, Taigu, Shanxi province, China (112.31° E, 37.26° N). The study site is located 803.2 m above sea level, and the climate is continental monsoon, warm, and with much rain in the summer. The annual average rainfall is 500–650 mm, and 60% is distributed between June and August. The average temperature range is from a maximum of 25 °C during May and October to an average maximum of −2 °C during November and April of the following year. The crop was sown with row spacing of 0.3 m, plant spacing of 0.2 m, the sowing depth was 5 cm, and the planting plot with 13.5 m^2 (4.5 × 3.0 m) for each variety.

2.3. The Total Carotenoid Content (TCC) Analysis

The TCC of each variety was analyzed once a month during the storage from November 2020 to June 2021. A modified method based on the version developed by the American Association of Cereal Chemists (AACC) was used to extract carotenoids from grains [10,23]. The harvested grains were freeze-dried for 48 h in a lyophilization chamber guard (−30 °C, 37 pa, CHRIST, Osterode, Germany) and ground into powder (TissueLyser 2, Qiagen, Shanghai, China). Overall, 2 g of millet powder was homogenized in 20 mL water-saturated n-butanol by vortexing for 30 s, followed by being shaken for 3 h at room temperature. The extract was centrifuged at 10,000 g for 10 min at 4 °C (Allegra X-30R, Beckman Colulter, Brea, CA, USA). The supernatant was transferred to a new 50-mL centrifuge tube and diluted to the volume to 25 mL with water-saturated n-butanol. The whole process needed to be protected from light. The absorbance of the extract was measured at 448 nm using a biological spectrometer (BioSpectrometer basic, Eppendorf, Hamburg, Germany). All samples were analyzed in triplicates with three biological replicates.

2.4. Chemicals and Solvents

Lutein and zeaxanthin (98% pure, Sigma, St. Louis, MA, USA) were used as standards for quantitative HPLC analysis. Methanol and methyl tert-butyl ether (HPLC-grade, Thermo Fisher Scientific, Shanghai, China) were utilized for chromatographic separations.

2.5. HPLC Analysis of Lutein and Zeaxanthin

Carotenoid extracts from samples after storage for 0 and 3 months were separated using a Thermo Fisher HPLC system according to the protocol described previously [22]. Briefly, A C30 column (250 cm × 4.6 mm, 5 mm, YMC, Kyoto, Japan) was maintained at 35 °C. The samples were eluted using a linear mobile phase gradient containing (A) methanol/methyl tert-butyl ether/nanopure water (81:15:4, *v/v/v*) and (B) methyl tert-butyl ether/methanol (90:10, *v/v*) at a flow rate of 1 mL/min, over 30 min. The procedure was as follows: 0–20 min 0%–22.2% B, 20–25 min 22.2%–0% B, 25–30 min 0% B. Lutein and zeaxanthin in the sample extracts were identified through their characteristic absorption spectra and quantified by corresponding peak areas based on the established standard curves.

2.6. Western-Blot Analysis

Total proteins from grains at maturing stages (S1, 2, 3) and storage stages (m-0, 7) were extracted. Samples (0.1 g) were ground to form a powder in liquid nitrogen and suspended in 1 mL lysis buffer (2 × SDT lysis buffer, Coolaber, Beijing, China). The extract was homogenized in an ice water bath for 30 min followed by centrifugation (Allegra X-30R, Beckman Colulter, Brea, CA, USA) at 12,000 rpm for 20 min. The protein concentration was quantified using a micronucleus concentration meter (μLite spectrophotometer, BioDrop, Cambridge, UK). Proteins (300 μg) were separated in a 10% SDS-PAGE gel (10% SDS-PAGE Gel Preparation Kit, Coolaber, Beijing, China) and blotted onto nitrocellulose membranes (0.45 nitrocellulose membranes, Coolaber, Beijing, China). The membranes were treated with blocking solution (TBST (10× TBST Buffer, Coolaber, Beijing, China) containing 5% (*w/v*) dried skimmed milk powder) for 1 h and incubated overnight with anti-LOX antibody

in the same solution as the closed solution. Signals were detected using the ECL Western Blotting Analysis System (GE Healthcare, Marlborough, New Zealand). Affinity-purified anti-LOX polyclonal antibody was prepared by Sangon (Anti-LOX rabbit polyclonal antibody, Sangon, Shanghai, China). Peptide sequence from LOX (GVTGKGIPNSTSIC) was synthesized, conjugated with keyhole limpet hemocyanin, and used as an antigen. The antibody against LOX was raised in rabbit antibodyand further purified from immunoblots [24]. The dilution of the LOX antibody for immunoblotting was 1:1000. Quantification was performed using software Image Lab (Bio-Rad Laboratories, Inc., Hercules, CA, USA).

2.7. Isolation and Sequence Retrieval of LOX Gene Family from Foxtail Millet

Protein sequences of foxtail millet LOX were obtained from a genome-sequencing library (Phytozome V12.1). LOX sequences from wheat and rice were downloaded from NCBI (http://www.ncbi.nlm.nih.gov/ (accessed on 1 October 2021)). A phylogenetic tree was constructed using Molecular Evolutionary Genetics Analysis (MEGA7) Software (University of Kent, Canterbury, UK) with the Neighbor-Joining (NJ) method having 1000 bootstrap values.

2.8. RNA Extraction and Real-Time PCR Analysis

To identify the transcript abundance, total RNA samples were isolated from grains at different maturing stages (S1, 2, and 3) according to the manufacturer's instruction of RNAiso Plus (TaKaRa, Beijing, China). Total RNA was reverse-transcribed using a Takara PrimeScriptTM RT reagent Kit (TaKaRa, Beijing, China) with gDNA Eraser. The synthesized cDNAs were diluted 10 times in ddH2O. Quantitative real-time PCR (qRT-PCR) was performed using the SYBR Premix Ex Taq II (Tli RNaseH Plus, TaKaRa, Beijing, China) Kit in the CFX96™ Real-Time System (Bio-rad, Hercules, CA, USA). The reaction mixture contained 5 μL of SYBR Premix Ex Taq II, 1 μL each of the forward and reverse primers (10 μM), 1 μL of diluted cDNA, and ddH2O to a final volume of 10 μL. The cycling program consisted of 95 °C for 30 s, followed by 40 cycles of 95 °C for 5 s, and 58 °C for 30 s. To confirm the product specificity for each gene primer reaction, a melt curve analysis was performed with continual fluorescence data acquisition during the 60–95 °C melting [25]. Transcript abundance of the housekeeping gene *SiACTIN* was quantified as a reference. At least three biological replicates, each with three replicates, were analyzed for each sample. The primers used in this study are listed in Table 1

Table 1. Primer's information for RT-PCR of LOX gene in foxtail millet.

Gene	Forward Primer Sequence (5′ to 3′)	Reverse Primer Sequence (5′ to 3′)
SiACTIN	TGC TCA GTG GAG GCT CAA CA	CAA GAC ACT GTA CTT GCG CTC
SiLOX1	AAA TCA CTG GCT GAG GAC ACA T	CAG GAG CTT GAA GAT CGG GT
SiLOX2	GGT CCT CGG AAA TGT GTT GG	GCT GAA CTT TAC GCA GGC TTA
SiLOX3	AGG AGT TTG GAC GGG AGA TT	CGAGGTTCCTCTCGATGT
SiLOX4	CCC TGG AGA TGT CCT CAA AG	ATT GCC GTC CAG ATT TCG
SiLOX5	GGA CCT AAG GCA GTA TGG A	AGG ATG AAG AGC TTG TTG TT
SiLOX6	CTG CTG TCC TCG CAC TCC	CTC GCT GTC ATC GTT CCA T
SiLOX7	GAC CGT CTT CCC TCG CAA	GTC GTC GGG GTA GTA GAT GG
SiLOX8	CCC AAC AGC GTC ACC ATC TA	CCC CGC CCG AGT ATA ATG AG
SiLOX9	GCG GGT GAT GAT GAC ATA AGT A	TCT TTG TGG CTA TGA TGA ACG
SiLOX10	TAC CAC TAC GGC GGC TAC TT	TCT GCG TTG GGA GCA TGT C
SiLOX11	AAC CTC CTG TCG TCG CAC TC	GGG GTC CTT GTT CCT ACT ATC G
SiLOX12	TAGAAGCCTACACCGATGATAC	CTTCCAGGTTGTGCTGAATAT

3. Results

3.1. Changes in the Content and Composition of Carotenoid in the Two Varieties of Foxtail Millet during Storage

To assess the dynamic profiles of the TCC during the millet storage, two varieties of foxtail millet that exhibited an extreme difference in millet discoloration in our preliminary

experiments were analyzed over a storage period of 7 months. The results revealed that the genotype had a significant impact on the degradation of millet color. As shown in Figure 1a, similar curves were observed in both varieties. However, 9806-1, with a 32.2% discoloration rate, exhibited more discoloration than Baomihunzi (with a discoloration rate of 10.5%). After 1-month storage (M0–M1), the TCC in both varieties was decreased (from 19.23 to 16.60 mg kg^{-1} in 9806-1 and from 11.99 to 11.37 mg kg^{-1} in Baomihunzi). Interestingly, it was noted that the TCC increased at M2 for both varieties. In the following 1-month storage (M1–M2), the TCC in 9806-1 slightly increased to 16.84 mg kg^{-1} and then steadily decreased to 13.03 mg kg^{-1} after five months of storage. However, the TCC in Baomihunzi increased to 12.15 mg kg^{-1} at the M2 stage but decreased to 10.73 mg kg^{-1} after storage for a long duration. Clearly, the significant difference in millet discoloration between both varieties was in the first (M0–M3) period, especially in the first month of storage.

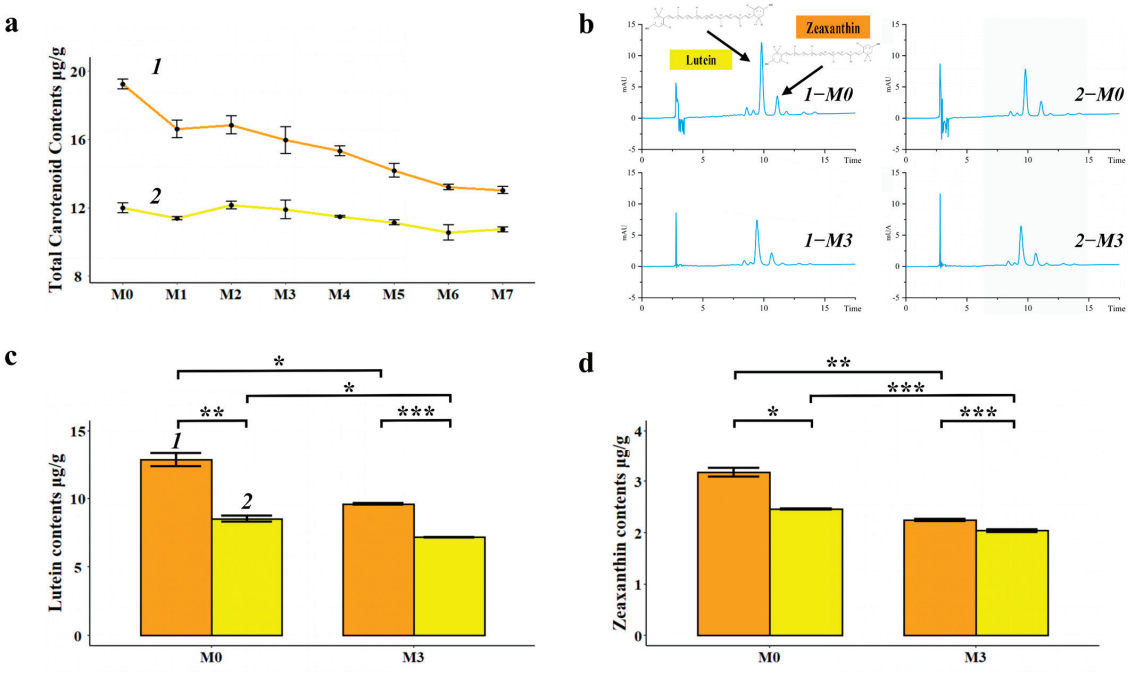

Figure 1. Changes in the total carotenoids, lutein, and zeaxanthin contents in the grains of 9806-1 (1, orange) and Baomihunzi (2, yellow) varieties at different storage stages. (**a**) The changes in total carotenoids in the grains of the two varieties during 7-month storage. (**b**) HPLC analysis of carotenoids in two varieties at M0 and M3 stages. Characteristic peaks of lutein and zeaxanthin. (**c**) Comparison of lutein content in the grains of two varieties at M0 and M3 stages. (**d**) Comparison of zeaxanthin content in the grains of two varieties at M0 and M3 stages. The bars represent the standard error (SE) from three biological replicates. Asterisks indicate significant differences; * $p < 0.05$, ** $p < 0.01$, and *** $p<0.001$.

The YMC C30 carotenoid column was used to isolate carotenoids from these millet samples of the initial (M0) and middle (M3) storage stages; HPLC analysis was performed to quantify changes in the composition of carotenoids during storage. The carotenoid compositions in grains of foxtail millet were comprised mainly of lutein and zeaxanthin (Figure 1b). After three consecutive months of storage, the lutein content decreased from 12.83 to 9.60 mg kg^{-1} in 9806-1 and from 8.52 to 7.17 mg kg^{-1} in Baomihunzi (Figure 1c); however, the zeaxanthin content decreased from 3.18 to 2.24 mg kg^{-1} in 9806-1 and from 2.46 to 2.04 mg kg^{-1} in Baomihunzi (Figure 1d). As expected, the decrease in lutein and

zeaxanthin contents reflected the decrease in the TCC, resulting in the millet discoloration of foxtail millet.

3.2. Expression Patterns of SiLOX Protein in the Two Millet Varieties

To investigate if the difference in millet discoloration between the two varieties was related to the expression of SiLOX protein, western blot analysis was performed with polyclonal antibody against LOX. SiLOX protein expression was species-specific (Figure 2), and its expression in Baomihunzi was constantly and significantly lower than that in 9806-1 at all stages of grain maturation and millet storage. It appeared that the higher level of SiLOX protein in 9806-1 was positively related to the higher discoloration rate of carotenoids, in contrast to that in Baomihunzi.

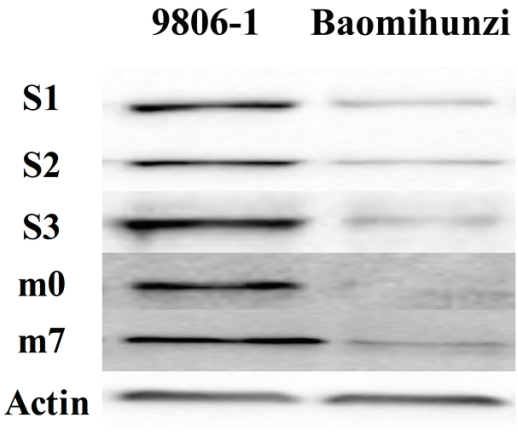

Figure 2. Comparison of the expression patterns of SiLOX protein between the grains of 9806-1 and Baomihunzi varieties at three grain development stages and two storage stages.

3.3. Phylogenetic Analysis of SiLOX Genes in Foxtail Millet

In total, 12 *SiLOX* genes were identified in foxtail millet by bioinformatic methods. To understand the classification and evolutionary relationship of foxtail millet SiLOXs, a phylogenetic tree was constructed using LOX proteins of foxtail millet and other plants. The SiLOX proteins of foxtail millet can be explicitly categorized into two subfamilies, with seven SiLOXs clustering into the 9-LOX group and five SiLOXs into the 13-LOX group (Figure 3). Phylogenetic analysis revealed that SiLOX2, SiLOX3, SiLOX4, and SiLOX7 were clustered with those of 9-LOXs that were involved in regulating seed longevity and degradation of carotenoids in wheat and rice, indicating that SiLOX2, SiLOX3, SiLOX4, and SiLOX7 may have the same functions.

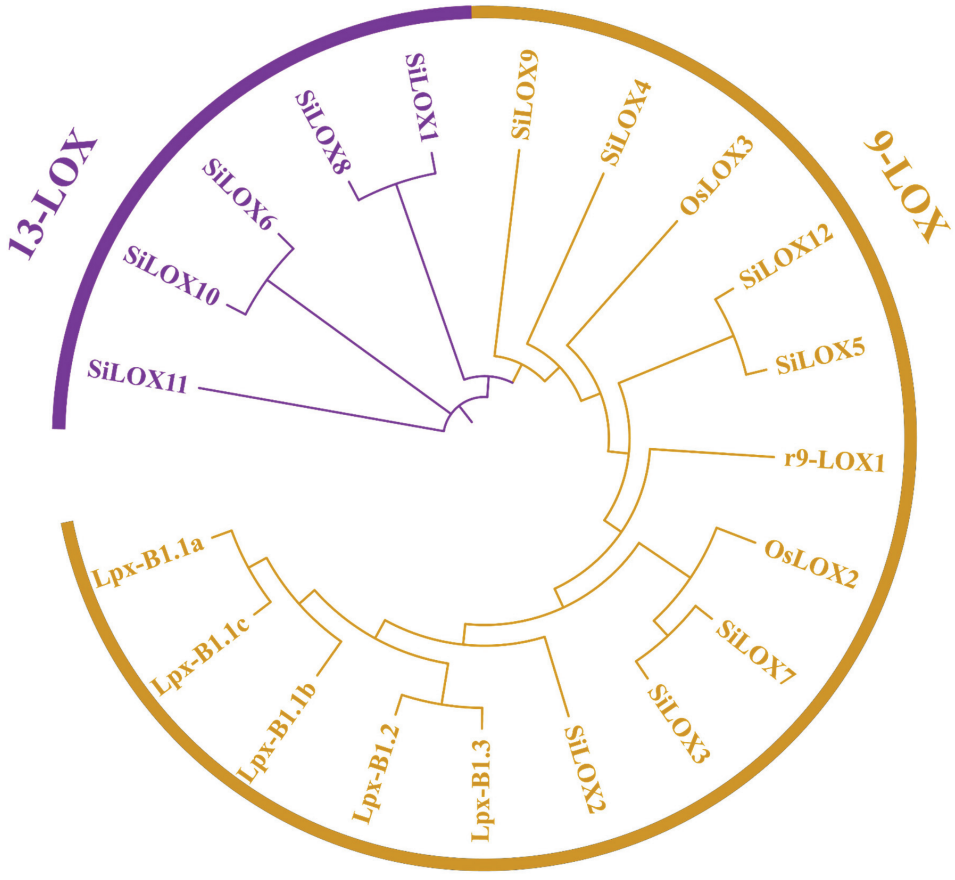

Figure 3. Phylogenetic analysis of LOX proteins from *Setaria italica*, *Oryza sativa*, and *Triticum turgidum*. The LOX proteins were divided into two phylogenetic subgroups (9-LOX and 13-LOX) and marked with different line colors.

3.4. Tissue-Specific Expression Patterns of SiLOX Genes

To identify the genes related to millet discoloration, the expression profiles of *SiLOXs* in different tissues were analyzed using RT-PCR (Figure 4). The transcripts of *SiLOX1*, *SiLOX5*, and *SiLOX8* could be detected in all the tested tissues. Seven *SiLOX* genes (*SiLOX5*, *SiLOX6*, *SiLOX7*, *SiLOX8*, *SiLOX9*, *SiLOX10* and *SiLOX11*) exhibited high expression levels in leaves, with much higher expression observed for *SiLOX6*, *SiLOX7*, and *SiLOX8*. In addition, *SiLOX10* and *SiLOX11* were highly expressed in seedlings. *SiLOX1*, *SiLOX5*, *SiLOX8*, and *SiLOX9* were strongly expressed in roots. It was noticeable that *SiLOX2*, *SiLOX3*, and *SiLOX4* exhibited stronger expression in grains than in other tissues, especially for *SiLOX3* and *SiLOX4*, which were almost only expressed in grains and their expression was significantly higher. However, *SiLOX9*, *SiLOX10*, and *SiLOX11* were not expressed much in grains. The transcripts of *SiLOX12* could not be detected in any tested tissues.

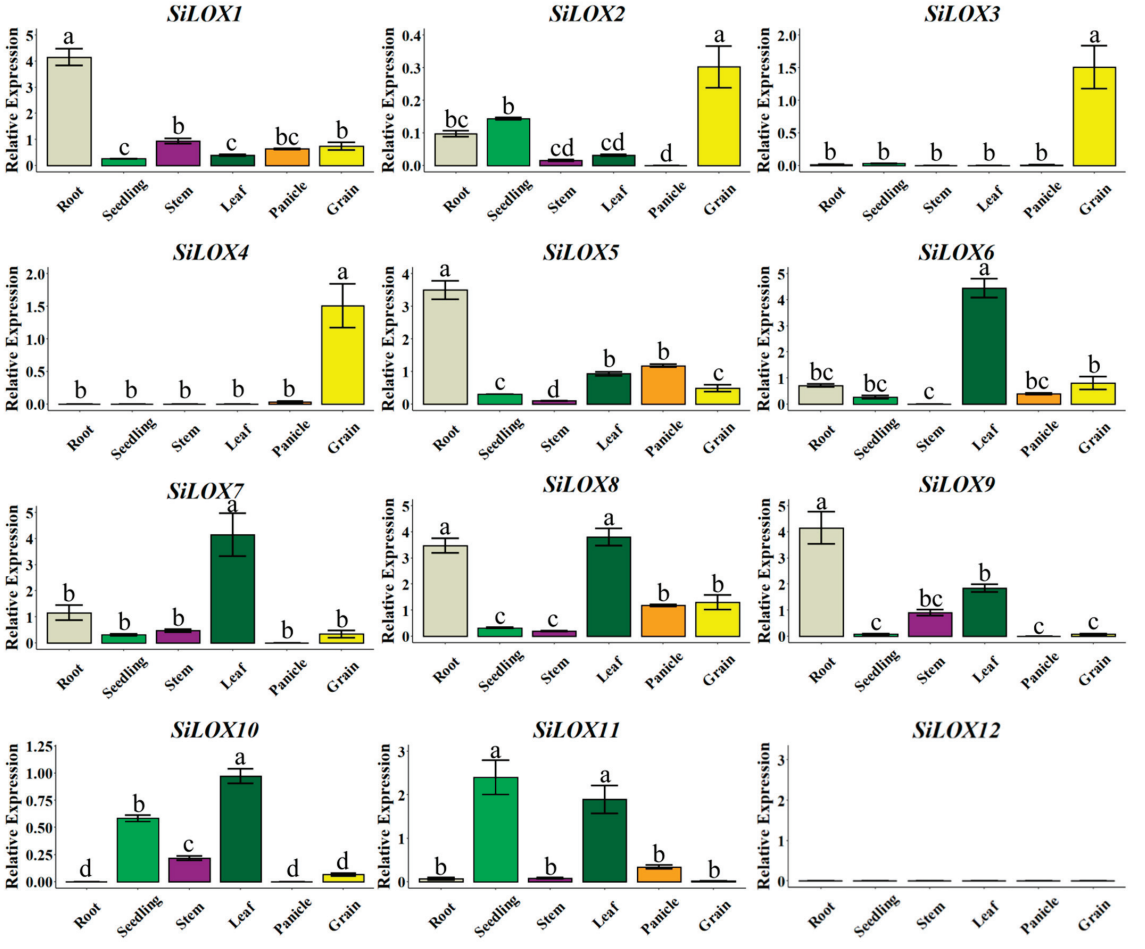

Figure 4. The expression profiles of *SiLOX* genes in various tissues of foxtail millet as analyzed by quantitative real-time RT-PCR. The data represent the mean from three replicates with three biological repeats. The bars represent the SE from three biological replicates. The lowercase letters indicated the statistical significance at the level of 0.05 ($p < 0.05$).

3.5. Expression Patterns of SiLOX Genes during Grain Maturation

To determine which *SiLOX* gene plays a major role in the discoloration of millet, the expression profiles of the *SiLOX* genes that can be detected in grains were analyzed in two millet varieties during three grain maturation stages (Figure 5). In general, most *SiLOX* genes exhibited higher expression in 9806-1 than in Baomihunzi at all stages, except *SiLOX6* and *SiLOX8*, which exhibited slightly lower expression consistently in 9806-1 than in Baomihunzi. The mRNA levels of *SiLOX1*, *SiLOX5*, and *SiLOX7* exhibited a major increase during grain maturation and were higher in 9806-1 than in Baomihunzi except for *SiLOX5*, which exhibited slightly lower expression in 9806-1 than in Baomihunzi at the S2 stage. The expression of *SiLOX3* kept decreasing during grain maturation in the two varieties and was higher in 9806-1 than in Baomihunzi. The expression levels of *SiLOX4* first increased with grain maturation, peaked at the S2 stage, and then decreased dramatically at the S3 stage in both varieties. *SiLOX2*, *SiLOX3*, and *SiLOX4* exhibited significantly higher expression in 9806-1 than in Baomihunzi at the last two stages, especially at the

S3 stage. The expression of *SiLOX2* and *SiLOX3* in 9806-1 was approximately 2.5 times higher than that in Baomihunzi, and the expression of *SiLOX4* could not be detected in Baomihunzi. This indicated that the extremely low expression of *SiLOX2*, *SiLOX3*, and *SiLOX4* contributed to the low level of SiLOX protein in Baomihunzi. Furthermore, it was noteworthy that the expression of *SiLOX4* was undetectable at the last maturing stage.

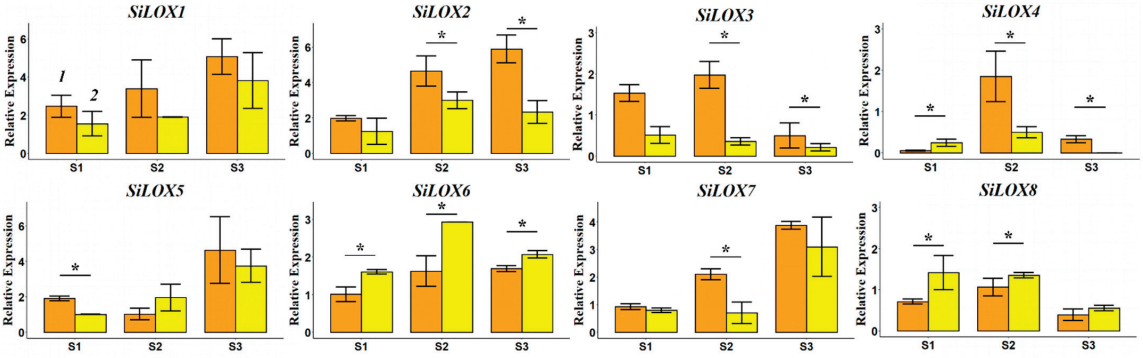

Figure 5. Quantitative real-time RT-PCR analysis of the mRNA levels of *SiLOX* genes that can be detected in grains at three grain development stages in 9806-1 (1, orange) and Baomihunzi (2, yellow) varieties. The data represent the mean from three replicates with three biological repeats. The bars represent the SE from three biological replicates. Asterisks indicate significant differences; * $p < 0.05$.

4. Discussion

Foxtail millet is an ancient cereal grain crop that is extensively cultured for food in the arid and semiarid regions of China [26]. The primary processing product of the crop is millets. Because of increasing awareness of the health benefits of millet, it is gaining increasing popularity among consumers [10,27]. Carotenoids, a class of important nutrients in foxtail millet, give the millet its yellow color. Unfortunately, the instability of carotenoids due to its high susceptibility to oxidation results in the loss of both color and nutritional qualities of millet products [28]. To date, no information is available on the carotenoid degradation in foxtail millet during storage. In this study, we have explored the potential link between millet discoloration and LOX in foxtail millet. Based on the changes in the TCC in the two millet varieties during storage, it appeared that the genotype had a significant influence on millet discoloration. After long-term storage, the TCC of 9806-1 decreased by 32.25%; however, that of Baomihunzi decreased by only 10.46%. In our prior study, lutein and zeaxanthin were proved to be the two major carotenoid components in millet [22]. Further analysis by HPLC revealed that millet discoloration was mainly caused by the decreasing of lutein and zeaxanthin contents. During the storage of grains in the first month, some water remained in the grains after harvesting. This indicated that the enzymes responsible for the discoloration could be more active; a relatively rapid reduction in the TCC was observed in both varieties. Furthermore, a significant difference in millet discoloration between the two varieties was also observed in M0–M1. The slight increase in the TCC during the following 1-month storage (M1–M2) could be interpreted as the result of regulation by postharvest maturation. The enhancement of carotenoid content in millet during postharvest maturation was commonly observed in other varieties of foxtail millet, and such carotenoid accumulation was accompanied by the starch breakdown in our previous studies. Besides cultivation, the development of carotenoids occurs during postharvest storage [29]. For example, during the storage for the first two months of winter squash, the TCC increased 3-4 times in comparison with that at the time of harvest [30]. Similarly, the analysis of changes in the carotenoid content in mango revealed that while β-carotene and lycopene contents first increased and then decreased, violaxanthin contents

steadily increased during postharvest storage [31]. In our study, during the consecutive last 5 months of storage, although the TCC of both varieties decreased, 9806-1 exhibited a faster degradation rate than Baomihunzi.

Carotenoids are prone to degradation during storage and food production by a lipoxygenase-assisted process. Some evidence has illustrated that LOX was related to the carotenoid degradation during storage or staleness in staple crops [20,21,32]. LOX is a class of nonheme iron-containing dioxygenases that co-oxidize carotenoids by the random attack of the carotenoid molecules [33]. Soybean LOX enzymes are reported to be used as the pigment bleacher to bleach carotenoids in the process of white bread making [34,35]. ZAF1, a maize variety lacking LOX-1and 2, exhibited superior storage stability to other normal varieties [36]. In addition, considerable genetic variability was observed in terms of TCC and LOX activity; genotypes with a high-carotenoid loss may also express low LOX activities [11]. A key constituent involved in carotenoid degradation is endogenous lipoxygenases, and a higher lipoxygenase concentration is associated with an increased loss in lutein content [37]. In this study, the significant difference in the expression of SiLOX protein between the two varieties at all stages supported our hypothesis that SiLOX was involved in the millet discoloration process.

The endogenous lipoxygenase in grain is significantly important in terms of food quality because they have negative implications for color, off-flavor, and nutritional quality. In our previous study, 12 *SiLOX* genes were identified in foxtail millet [38]. Among them, 8 *SiLOX* genes (*SiLOX1-8*) were expressed in the grains of foxtail millet, and the transcript levels of *SiLOX2*, *SiLOX3*, and *SiLOX4* were significantly higher in 9806-1 with a faster discoloration than that in Baomihunzi, especially at the last stage of maturation. *SiLOX2*, *SiLOX3*, and *SiLOX4* were clustered together with *OsLOX3*, *r9-LOX1*, and *Lpx-B1*, which were reported to regulate the storage stability and carotenoid degradation in seeds of rice and wheat [19,21,39]. LOXs in wheat are the best characterized, and their physiological functions are well studied. In durum wheat, the deletion in a lipoxygenase gene, *Lpx-B1.1*, is associated with a strong reduction in LOX activities, leading to improved pasta color [11]. A further study revealed that the expression levels of the *Lpx-B1* gene family contributed to the most total LOX activity, thereby positively correlating with the β-carotene bleaching activities in mature grains [40]. During golden rice storage, the *r9-LOX1* gene plays an important role in carotenoid degradation. After artificial aging treatment, the downregulation of *LOX1* activity by LOX-RNAi can prevent the loss of carotenoids in golden rice seeds [20]. Based on the grain-specific expression characteristic of *SiLOX3* and *SiLOX4* (that they were only expressed in grains of foxtail millet) and reported role of their orthologues in rice and wheat, it was concluded that they might be mainly related to the SiLOX protein expression corresponding to the discoloration of millet during storage. It was noteworthy that the lack of *SiLOX4* expression at the last maturing stage appeared to account for the extremely low expression of SiLOX protein in Baomihunzi, which exhibited slow discoloration. Collectively, our results indicated that *SiLOX4* might be the key factor that affected the millet discoloration rate in foxtail millet during storage.

5. Conclusions

In this present study, our objective was to investigate the molecular mechanism of millet discoloration during storage in foxtail millet. Our results suggested that SiLOX played a major role in carotenoid reduction during millet storage. In addition, we found that *SiLOX4* was a key gene in regulating millet discoloration. However, to further determine the function of *SiLOX4* on the carotenoid reduction during storage in foxtail millet, studies with a transgenic approach are necessary.

Author Contributions: Conceptualization, B.Z.; Methodology, B.Z.; Formal Analysis, Q.M. and J.W.; Resources, H.L.; Data Curation, Q.M. and L.C.; Writing—Original Draft Preparation, Q.M.; Writing—Review and Editing Y.H., X.Z., and Y.L., Visualization, Q.M. and Q.Z.; Supervision, B.Z. and Y.H.; Project Administration, B.Z.; Funding Acquisition, B.Z. All authors have read and agreed to the published version of the manuscript.

Funding: This work was supported by the National Natural Science Foundation of China (grant numbers 31971906, 31601369), Grand Science and Technology Special Project in Shanxi Province (grant numbers 202101140601027), Shanxi Key Laboratory of Minor Crops Germplasm Innovation and Molecular Breeding, Shanxi Agricultural University (grant number 202204010910001), and Shanxi Province Science Found for Excellent Young Scholar (grant number 201901D211382).

Institutional Review Board Statement: Not applicable.

Data Availability Statement: Not applicable.

Conflicts of Interest: The authors declare no conflict of interest.

References

1. Tanaka, Y.; Sasaki, N.; Ohmiya, A. Biosynthesis of plant pigments: Anthocyanins, betalains and carotenoids. *Plant J.* **2008**, *54*, 733–749. [CrossRef]
2. Howitt, C.A.; Pogson, B.J. Carotenoid accumulation and function in seeds and non-green tissues. *Plant Cell Environ.* **2006**, *29*, 435–445. [CrossRef] [PubMed]
3. Ficco, D.; Mastrangelo, A.M.; Trono, D.; Borrelli, G.M.; Vita, P.D.; Fares, C.; Beleggia, R.; Platani, C.; Papa, R. The colours of durum wheat: A review. *Crop Pasture Sci.* **2014**, *65*, 1–15. [CrossRef]
4. Botella-Pavía, P.; Rodríguez-Concepción, M. Carotenoid biotechnology in plants for nutritionally improved foods. *Physiol. Plant.* **2010**, *126*, 369–381. [CrossRef]
5. Sun, T.H.; Yuan, H.; Cao, H.B.; Yazdani, M.; Tadmor, Y.; Li, L. Carotenoid metabolism in plants: The role of plastids. *Mol. Plant* **2018**, *11*, 58–74. [CrossRef] [PubMed]
6. Ceasar, S.A.; Baker, A.; Ignacimuthu, S. Functional characterization of the PHT1 family transporters of foxtail millet with development of a novel *Agrobacterium*-mediated transformation procedure. *Sci. Rep.* **2017**, *7*, 14064. [CrossRef] [PubMed]
7. He, L.; Zhang, B.; Wang, X.; Li, H.Y.; Han, Y.H. Foxtail millet: Nutritional and eating quality, and prospects for genetic improvement. *Front. Agr. Sci. Eng.* **2015**, *2*, 124–133. [CrossRef]
8. Yang, X.S.; Wang, L.L.; Zhou, X.R.; Shuang, S.M.; Zhu, Z.H.; Li, N.; Li, Y.; Liu, F.; Liu, S.C.; Lu, P. Determination of protein, fat, starch, and amino acids in foxtail millet [*Setaria italica* (L.) Beauv.] by fourier transform near-infrared reflectance spectroscopy. *Food Sci. Biotechnol.* **2013**, *22*, 1495–1500. [CrossRef]
9. He, L.; Cheng, L.; Wang, J.J.; Liu, J.; Cheng, J.J.; Yang, Z.R.; Cao, R.; Han, Y.H.; Li, H.Y.; Zhang, B. Carotenoid Cleavage Dioxygenase 1 Catalyzes Lutein Degradation To Influence Carotenoid Accumulation and Color Development in Foxtail Millet Grains. *J. Agric. Food Chem.* **2022**, *70*, 9283–9294. [CrossRef]
10. Shen, R.; Yang, S.P.; Zhao, G.H.; Shen, Q.; Diao, X.M. Identification of carotenoids in foxtail millet (*Setaria italica*) and the effects of cooking methods on carotenoid content. *J. Cereal Sci.* **2015**, *61*, 86–93. [CrossRef]
11. Leenhardt, F.; Lyan, B.; Rock, E.; Boussard, A.; Potus, J.; Chanliaud, E.; Remesy, C. Genetic variability of carotenoid concentration, and lipoxygenase and peroxidase activities among cultivated wheat species and bread wheat varieties. *Eur. J. Agron.* **2006**, *25*, 170–176. [CrossRef]
12. Zhang, Y.; Yu, Z.L.; Lu, Y.X.; Wang, Y.; She, D.; Song, M.; Wu, Y.J. Effect of the absence of lipoxygenase isoenzymes on the storage characteristics of rice grains. *J. Stored Prod. Res.* **2007**, *43*, 87–91. [CrossRef]
13. Sun, Y.N.; Wang, K.; Dong, Y.H.; Li, K.K.; Liu, H.H.; Cui, B.Z.; Fu, H.F.; Chen, X.W.; Wang, Y.Q.; Wang, Y.Y. Effects of radiofrequency blanching on lipoxygenase inactivation, physicochemical properties of sweet corn (*Zea mays* L.), and its correlation with cell morphology. *Food Chem.* **2022**, *394*, 133498. [CrossRef] [PubMed]
14. Brash, A.R. Lipoxygenases: Occurrence, functions, catalysis, and acquisition of substrate. *J. Biol. Chem.* **1999**, *274*, 23679–23682. [CrossRef]
15. Shen, J.; Tieman, D.; Jones, J.B.; Taylor, M.G.; Schmelz, E.; Huffaker, A.; Bies, D.; Chen, K.; Klee, H.J. A 13-lipoxygenase, TomloxC, is essential for synthesis of C5 flavour volatiles in tomato. *J. Exp. Bot.* **2014**, *65*, 419–428. [CrossRef]
16. Shrestha, K.; Pant, S.; Huang, Y. Genome-wide identification and classification of Lipoxygenase gene family and their roles in sorghum-aphid interaction. *Plant Mol. Biol.* **2021**, *105*, 527–541. [CrossRef]
17. Wilson, R.A.; Gardner, H.W.; Keller, N.P. Cultivar-dependent expression of a maize lipoxygenase responsive to seed infesting fungi. *Mol. Plant Microbe Interact.* **2001**, *14*, 980–987. [CrossRef]
18. Long, Q.; Zhang, W.; Wang, P.; Shen, W.B.; Zhou, T.; Liu, N.N.; Wang, R.; Jiang, L.; Huang, J.X.; Wang, Y.H.; et al. Molecular genetic characterization of rice seed lipoxygenase 3 and assessment of its effects on seed longevity. *J. Plant Biol.* **2013**, *56*, 232–242. [CrossRef]
19. Ma, L.; Zhu, F.G.; Li, Z.W.; Zhang, J.F.; Li, X.; Dong, J.L.; Wang, T. TALEN-Based mutagenesis of lipoxygenase LOX3 enhances the storage tolerance of rice (*Oryza sativa*) seeds. *PLoS ONE.* **2015**, *10*, e0143877. [CrossRef]

20. Gayen, D.; Ali, N.; Sarkar, S.N.; Datta, S.K.; Datta, K. Down-regulation of *lipoxygenase* gene reduces degradation of carotenoids of golden rice during storage. *Planta* **2015**, *242*, 353–363. [CrossRef]
21. Carrera, A.; Echenique, V.; Zhang, W.; Helguera, M.; Manthey, F.; Schrager, A.; Picca, A.; Cervigni, G.; Dubcovsky, J. A deletion at the *Lpx-B1* locus is associated with low lipoxygenase activity and improved pasta color in durum wheat (*Triticum turgidum ssp. durum*). *J. Cereal Sci.* **2007**, *45*, 67–77. [CrossRef]
22. Zhang, B.; Liu, J.; Cheng, L.; Zhang, Y.Y.; Hou, S.Y.; Sun, Z.X.; Li, H.Y.; Han, Y.H. Carotenoid composition and expression of biosynthetic genes in yellow and white foxtail millet [*Setaria italica* (L.) Beauv]. *J. Cereal Sci.* **2019**, *85*, 84–90. [CrossRef]
23. Quinton, L.A.; Kennedy, J.F. American association of cereal chemists approved methods, 10th ed. CD-ROM. *Carbohydr. Polym.* **2002**, *49*, 515–517. [CrossRef]
24. Kurien, B.T.; Scofield, R.H. Western blotting. *Methods* **2006**, *38*, 283–293. [CrossRef]
25. Noguchi, A.; Nakamura, K.; Sakata, K.; Sato-Fukuda, N.; Ishigaki, T.; Mano, J.; Takabatake, R.; Kitta, K.; Teshima, R.; Kondo, K.; et al. Development and Interlaboratory Validation of a Simple Screening Method for Genetically Modified Maize Using a ΔΔC(q)-Based Multiplex Real-Time PCR Assay. *Anal. Chem.* **2016**, *88*, 4285–4293. [CrossRef] [PubMed]
26. Barton, L.; Newsome, S.D.; Chen, F.H.; Wang, H.; Guilderson, T.P.; Bettinger, R.L. Agricultural origins and the isotopic identity of domestication in northern China. *Proc. Natl. Acad. Sci. USA* **2009**, *106*, 5523–5528. [CrossRef]
27. Liu, J.K.; Tang, X.; Zhang, Y.Z.; Zhao, W. Determination of the volatile composition in brown millet, milled millet and millet bran by gas chromatography/mass spectrometry. *Molecules* **2012**, *17*, 2271–2282. [CrossRef] [PubMed]
28. Boon, C.S.; McClements, D.J.; Weiss, J.; Decker, E.A. Factors influencing the chemical stability of carotenoids in foods. *Crit. Rev. Food Sci. Nutr.* **2010**, *50*, 515–532. [CrossRef]
29. Ngamwonglumlert, L.; Devahastin, S.; Chiewchan, N.; Raghavan, V. Plant carotenoids evolution during cultivation, postharvest storage, and food processing: A review. *Compr. Rev. Food Sci. Food Saf.* **2020**, *19*, 1561–1604. [CrossRef]
30. Zhang, M.K.; Zhang, M.P.; Mazourek, M.; Tadmor, Y.; Li, L. Regulatory control of carotenoid accumulation in winter squash during storage. *Planta* **2014**, *240*, 1063–1074. [CrossRef]
31. Zhao, J.J.; Zhou, Z.X.; Zhu, M.; Zhao, L.; Gao, A.P.; Chen, Y.Y.; Wang, J.B.; University, H. Changes of carotenoids during dynamic development and ripening of mango fruits. *Xi Nan Nong Ye Xue Bao.* **2014**, *27*, 2124–2130.
32. Dua, P.N.; Day, E.J.; Grogan, C.O. Loss of carotenoids in stored commercial and high-carotenoid yellow corn, *Zea mays* L. *Agron. J.* **1965**, *57*, 501–502. [CrossRef]
33. Chedea, V.S.; Jisaka, M. Lipoxygenase and carotenoids: A co-oxidation story. *Afr. J. Biotechnol.* **2013**, *12*, 2786–2791.
34. Wu, Z.; Robinson, D.S.; Domoney, C.; Casey, R. High-performance liquid chromatographic analysis of the products of linoleic acid oxidation catalysed by pea (*Pisum sativum*) seed lipoxygenases. *J. Agric. Food Chem.* **1995**, *43*, 337–342. [CrossRef]
35. Pokorny, J.; Yanishlieva, N.; Gordon, M. *Antioxidants in Food Practical Applications*; CRC Woodhead Publishing Ltd.: Boca Raton, FL, USA, 2001; p. 288.
36. Li, J.K.; Zhang, Y.; Yu, Z.L.; Wang, Y.J.; Yang, Y.; Liu, Z.; Jiang, J.Y.; Song, M.; Wu, Y.J. Superior storage stability in low lipoxygenase maize varieties. *J. Stored Prod. Res.* **2007**, *43*, 530–534. [CrossRef]
37. Mares, D.J.; Cheong, J.; Goonetilleke, S.N.; Mather, D.E. Lipoxygenase in wheat: Genetic control and impact on stability of lutein and lutein esters. *Foods* **2021**, *10*, 1149. [CrossRef]
38. Zhang, Q.X.; Zhao, Y.F.; Zhang, J.L.; Li, X.K.; Ma, F.F.; Duan, M.; Zhang, B.; Li, H.Y. The responses of the lipoxygenase gene fmily to salt and frought stress in foxtail millet (*Setaria italica*). *Life* **2021**, *11*, 1169. [CrossRef] [PubMed]
39. RoyChowdhury, M.; Li, X.B.; Qi, H.Y.; Li, W.X.; Sun, J.; Huang, C.; Wu, D.X. Functional characterization of *9-/13-LOXs* in rice and silencing their expressions to improve grain qualities. *Biomed. Res. Int.* **2016**, *2016*, 4275904. [CrossRef]
40. Verlotta, A.; Simone, V.D.; Mastrangelo, A.M.; Cattivelli, L.; Papa, R.; Trono, D. Insight into durum wheat *Lpx-B1*: A small gene family coding for the lipoxygenase responsible for carotenoid bleaching in mature grains. *BMC Plant Biol.* **2010**, *10*, 263. [CrossRef]

agriculture

MDPI

Article

Productivity and Stability Evaluation of 12 Selected *Avena magna* ssp. *domestica* Lines Based on Multi-Location Experiments during Three Cropping Seasons in Morocco

El hadji Thiam [1], Eric N. Jellen [2], Eric W. Jackson [3], Mark Nelson [4], Will Rogers [4], Ayoub El Mouttaqi [1] and Ouafae Benlhabib [1,*]

[1] Institut Agronomique et Vétérinaire Hassan II, Rabat 10000, Morocco; elasthiam0@gmail.com (E.h.T.); elmouttaqi.ayoub@gmail.com (A.E.M.)
[2] Plant Genetic Resources Laboratory, Department of Plant & Wildlife Sciences, Brigham Young University, Provo, UT 84602, USA; jellen@byu.edu
[3] 25:2 Solutions, 815 S First Ave Suite A, Pocatello, ID 83201, USA; eric.jackson@25-2.com
[4] Context Global Development, 9666 Olive Blvd Suite 750, St. Louis, MO 63132, USA; mark.nelson@contextglobal.org (M.N.); will.rogers@contextglobal.org (W.R.)
* Correspondence: o.benlhabib@gmail.com; Tel.: +212-668-194085

Abstract: *Avena magna* (2n = 4x = 28) is a tetraploid oat with a very high protein content compared to the hexaploid common oat, *A. sativa* (2n = 6x = 42). The wild type of *A. magna* originates from Morocco; its domestication has been achieved only within the past 25 years. The present study aimed to evaluate the productivity potential of an *A. magna* ssp. *domestica* collection of 11 advanced lines and a control variety, 'Avery'. Twelve trials were conducted during three cropping seasons at four, three, and five locations and revealed significant differences among the accessions. Data on twelve agro-morphological characters and two disease traits were collected, and they confirmed the presence of variability in this oat germplasm set. Mean grain yield was 30.76 q/ha and varied from site to site, ranging from 6.89 q/ha at Bouchane_19 to 85.5 q/ha at Alnif_21. Across experimental sites, plant height ranged from 48.93 to 120.47 cm; thousand kernel weight from 32.83 to 49.73 g; and harvest index from 20.43 to 31.33%. Line AT6 was relatively tolerant of BYDV and crown rust infections, based on disease severity scoring at the heading stage. According to AMMI analysis, 78% of the grain yield variability was due to the environment factor and 4% was explained by the genetic factor. Among the highest-yielding lines, AT5 and ATC were relatively unstable. Line AT5 was more productive at the elevated site of El Kbab_19, and ATC performed better at the oasis location of Alnif_21 under irrigation. Line AT7 showed the most stable behavior; it was high yielding across the five environments and exceeded the general mean of the experiments. The *A. magna* ssp. *domestica* lines proved their suitability for cultivation under local farming conditions. Their nutritional quality, especially their high protein content, makes them good candidates for further testing in the Moroccan breeding program and for integration into local cropping systems.

Keywords: *Avena magna* ssp. *domestica*; oat; advanced lines; agro-morphological traits; yield; productivity; stability

Citation: Thiam, E.h.; Jellen, E.N.; Jackson, E.W.; Nelson, M.; Rogers, W.; El Mouttaqi, A.; Benlhabib, O. Productivity and Stability Evaluation of 12 Selected *Avena magna* ssp. *domestica* Lines Based on Multi-Location Experiments during Three Cropping Seasons in Morocco. *Agriculture* **2023**, *13*, 1486. https://doi.org/10.3390/agriculture13081486

Academic Editors: Edyta Paczos-Grzeda, Volker Mohler and Sylwia Sowa

Received: 19 June 2023
Revised: 18 July 2023
Accepted: 19 July 2023
Published: 26 July 2023

1. Introduction

An ever-increasing world population and climate change are among the major contributors to famine. Crop yields must continue to increase to attain the Sustainable Development Goals and ensure safe, nutritious, and adequate food for everyone. Cereals and derivatives should play a key role in this challenge since they are the staple food of most countries of the world and the primary food for livestock. Cereal grains constitute more than half of the food energy and half of the protein consumed on Earth [1]. With the pressure on resources and the climate change scenario, future food supplies not only need to be

increased but also enriched especially in nutrients and protein to address food and nutrient security. Nutrition deficiencies have a significant impact on a country's productivity and can reduce its gross domestic product (GDP) by as much as 7% globally and up to 9–10% in African and South Asian countries [2]. In this context, there is a need to develop new sustainable sources of protein and nutrients to avoid the 150 more people expected to be at risk of protein deficiencies by 2050 [3]. It is evident that protein plays an essential role within the human body, including building muscle and bone and brain development. Its components, amino acids, are the building blocks of this development and are critically important in the first 1000 days of life and throughout the lifecycle [4]. Animal-based foods are excellent sources of protein but contribute 14.5% of all greenhouse gas emissions [5]. In this view, development of new nutrient-rich crops such as high-protein oat, *Avena magna* ssp. *domestica*, becomes one of the pathways to diversify the sources of protein and help attack the dual challenge of increasing supply in a sustainable manner.

Oat ranks sixth in world cereal production after wheat, maize, rice, barley, and sorghum [6]. The most widespread cultivated species of oat is common oat (*Avena sativa*), with Abyssinian oat (*A. abyssinica*), diploid naked or hulless oats (*A. nuda*), and lopsided oat (*A. strigosa*) being of relatively minor importance [7]. Morocco is the center of origin and a major center of diversity of the *Avena* genus [8]; consequently, it represents an essential country for expanding genetic resource conservation efforts and an interesting location for expanding oat production.

Oat is a cereal that has long been prized for its nutritional attributes, particularly in terms of mixed-linkage soluble beta-glucan, protein, oil, and antioxidants. Oat grain is also free-gluten and has the highest protein content among cereals; as a consequence, it is tolerated by most celiac disease patients [9]. Several previous studies have shown oat's health-promoting effects in preventing obesity, type II diabetes, gastrointestinal diseases, coronary heart disease, and certain types of cancer [10]. For human consumption, an increasing supply of oat-based products has been exhibited in the market, including a diverse array of breads, oatcakes, biscuits, granola bars, and ever more novel foods such as yogurt-type products and oat-based drinks [11–13].

The newly domesticated Moroccan tetraploid species *A. magna* (2n = 4x = 28, CCDD genome) was developed via sexual transfer of the domestication syndrome from the hexaploid common oat *A. sativa* (2n = 6x = 42, AACCDD; [14]). Subsequently, Jackson [7] produced a set of *A. magna* ssp. *domestica* lines via mutagenesis within a population of $F_{2:8}$ recombinant inbred lines (RILs) from a cross between a stable domesticated backcross line, Ba13-13, and a wild *A. magna* parent [15]. Oliver et al. [15] also mapped three of the domestication syndrome genes, for shattering (*Ba*), geniculate awn (*Awn*), and lemma pubescence (*Lp*), and measured the linkage of *Awn* and *Ba* with a terminal knob on chromosome 2C at a distance of 2.1 cM.

While the lines developed by Jackson [7] are suitable for production under standard cultivation practices, they also possess much higher protein levels than common oats, exceeding 25% in the relatively new cultivar 'Avery'. *Avena magna* ssp. *domestica* also showed promise in improving dietary iron and zinc in comparison to other cereals, thus potentially reducing anemia [16,17]. These characteristics make *A. magna* a good grain resource for the development of high-quality protein products to address developing-world malnutrition, developed-world obesity, and high-quality livestock feed [11]. Since *A. magna* is already adapted to the semi-arid conditions of Morocco, it is a promising source of sustainable grain for a world increasingly affected by climate change. Nevertheless, there is still a need to continue breeding under Moroccan conditions for traits such as resistance to seed dehiscence, lodging, dormancy, productivity, and stability, as well as tolerance of diseases.

The main objective of this study was to assess the diversity and performance of *A. magna* ssp. *domestica* lines using 'Avery' as the control in seven diverse environments in Morocco. The evaluation included morphological and yield parameters, disease tolerance (crown rust, BYDV), and yield stability.

2. Materials and Methods

2.1. Plant Materials

Eleven *A. magna* ssp. *domestica* lines were used in this study along with 'Avery', which was registered in the Official Moroccan Catalog in 2019, as control (Table 1). These lines were selected from a set of 41 lines introduced in Morocco during the 2017–2018 and 2018–2019 cropping seasons for adaptation trials. *A. magna* was domesticated via hybridization with common hexaploid oat *A. sativa* followed by a single backcross cycle to produce line Ba13-13 [14]. Subsequently, Jackson [7] produced six foundational *A. magna* ssp. *domestica* lines from a domesticated Ba13-13 × wild *A. magna* # 169 population [15,18], segregating for the wild-type growth habit and resistance to field races of crown rust (*Puccinia coronata*) in Baton Rouge, LA, USA. According to Jellen et al. [19], a virtual pedigree using a genotype/phenotype model with the JMP Genomics software package version 10 (SAS Institute Cary, NC, USA) was used as instruction to produce the 41 lines and the internal control Avery by intercrossing the foundational lines.

Table 1. List of *A. magna* ssp. *domestica* lines used in this study.

IAV_ID	Correspond	LINE_ID	PEDIGREE
ATC (Avery)	A40	BAM_96-5-6	BAM_96-5-6
AT1	A18a	2013Y1193	BAM_34/55_1
AT2	A14	2013Y1397	BAM_6/235_44
AT3	A27	2013Y1291	BAM_55/231_22
AT4	A35	2013Y1302	BAM_55/231_33
AT5	A44	2013Y1307	BAM_55/231_38
AT6	A45	2013Y1200	BAM_34/55_36
AT7	A02	2013Y1297	BAM_55/231_28
AT9	A20	2013Y1275	BAM_55/231_6
AT13	A41	2013Y1508	BAM_34/235_21
AT14	A43	2013Y1310	BAM_55/231_41
AT15	A10	2013Y1373	BAM_6/235_20

Explanation: IAV_ID: Institut Agronomique et Vétérinaire Hassan II Identifier. ATC: *Avena magna* spp. domestica variety 'Avery'.

2.2. Experimental Locations

Field experiments were conducted in three consecutive growing seasons (2018–2019, 2019–2020, and 2020–2021), and at 4, 3, and 5 experimental sites in each of these respective winter growing seasons. The selected experimental sites belong to contrasting Emberger bioclimatic stages across the central part of Morocco including per-arid (Alnif in the Anti-Atlas/Sahara); arid (Bouchane in the Phosphate Plateau); semi-arid cold winter (El Kbab in the Middle Atlas); sub-humid (Ain Itto in the Saïs Plain); and sub-humid cold winter (Oukaimeden in the High Atlas; [20]).

Among the twelve trials conducted in this investigation, one was not successful; data from the other eleven trials were subjected to ANOVA analysis. As four tests did not reveal any productivity differences among the advanced lines, the productivity and stability evaluation comprised the seven remaining trials.

Site descriptions for the seven retained trials are reported in Table 2. During the 2018–2019 season, experimental trials were installed at El Kbab (mountain plateau) on 29 November and Bouchane (Phosphate Plateau) on 30 November. Experiments for the following season, 2019–2020, were conducted at only one location, Bouchane, with a sowing date of 23 November. The third season (2020–2021) consisted of four experimental stations: Ain Itto, Bouchane, Oukaimeden, and Alnif. Seeds were sown on 16 October in Oukaimeden, 18 October in Bouchane, 20 October in Ain Itto, and on 21 November in Alnif.

Table 2 summarizes the experimental locations' specifications, the type of environmental climates (warm to cool), and the altitudes at the trial sites. Photos of some experimental sites are shown in Figure 1.

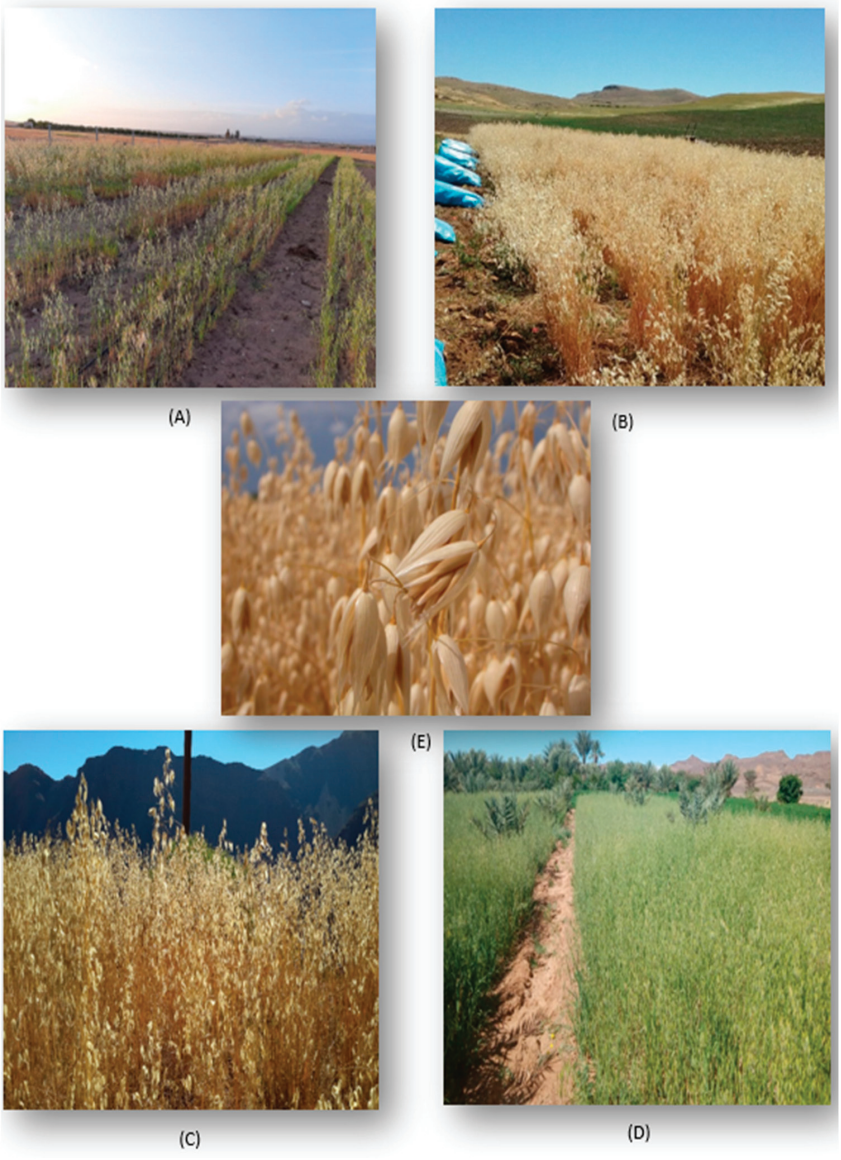

Figure 1. Experimental site photographs: (**A**) Bouchane, April 2020; (**B**) El Kbab, June 2019; (**C**) Oukaimeden, June 2021; (**D**) Alnif, April 2021; (**E**) *A. magna* panicle from Ain Itto site.

Table 2. Location and description of the experiment agro-climatic sites. Climate data were provided by worldweatheronline.com. Only data covering the periods of the experiments (between October and July) are reported.

Location	Zone	Geographic Position		Alt	Soil Type	Temp		Rain	Hum	S.H	Harvest Date
		Latitude	Longitude			Min	Max				
Ain Itto_21	Saïss Plain	34°05′33″ N	5°48′54″ W	855	Vertisols	8	36	609.8	61.8	3099	2 June 2021
Alnif_21	Oasis	31°06′37″ N	5°03′50″ W	1320	Fluvisols	9	43	43.2 *	26.2	3529	17 May 2021
Bouchane_21	Phosphate Plateau	32°14′35″ N	8°19′45″ W	830	Cambisols	9	38	250.2	54.1	3304	25 May 2021
Oukaimeden_21	Atlas Mounain	31°14′07″ N	7°48′42″ W	2530	Fluvisols	11	40	319.3	47.0	3369	25 June 2021
Bouchane_20	Phosphate Plateau	32°14′35″ N	8°19′45″ W	830	Cambisols	9	40	105.5	53.7	3376	22 June 2020
El kbab_19	Middle Atlas	32°42′25″ N	5°31′57″ W	1540	Fluvisols	2	35	573.0	50.9	3477	3 July 2019
Bouchane_19	Phosphate Plateau	32°14′35″ N	8°19′45″ W	830	Cambisols	9	33	313.1	53.4	3463	20 June 2019

With additional 200 m^3 of irrigation during the cycle development of plants. * By simplifying the number added on each location, the cropping season is specified, and each number is used for the rest of the article: 21 (season 2020–2021), 20 (season 2019–2020), and 19 (season 2018–2019). Alt: altitude (m); Temp: temperature (°C); Rain: rainfall (mm); Hum: humidity (%); S.H: sun hour (h).

In Alnif, Ain Itto, and Bouchane, mechanized moldboard plowing was used to prepare the soil for sowing, while for El Kbab and Oukaimeden, tillage was performed with a horse-drawn plow. Depending on the germination rate, the sowing dose was calculated to establish a density of 25 plants per linear meter. Trials were fertilized at the early tillering stage in the form of ammonium nitrate at the rate of 45 Kg/ha. Accessions were evaluated under rainfed conditions except for the Alnif site, where irrigation (1 m^3 of water per m^2) was supplied due to aridity. Weed control was performed manually at the tillering and flowering stages; if necessary, the number of weeding times exceeded two, depending on the degree of weed infestation, to avoid competition between plants.

2.3. Experimental Design

The field experiment design was a randomized complete block with three replications. The sowing plan varied from one site to another according to land availability for the trial. For the 2018–2019 season, the elementary plot included three six-meter rows at Bouchane and four three-meter rows at El Kbab with an inter-row spacing of 0.5 and 0.35 m, respectively. The space between elementary plots was 1.2 m for Bouchane and 1 m for El Kbab. Plots at Bouchane during the 2019–2020 season had four rows of 3.6 m length and were spaced 0.30 m apart. The 2020–2021 experimental plan was carried out in six rows of 12.5 m length and 0.3 m spacing. However, there was an exception at the Alnif and Oukaimeden sites, where eight rows of 8 m and four rows of 3 m were used, respectively, because of the land space limitations. The seeding rate per row was adjusted accordingly in those two sites.

2.4. Notations and Measurements

Crown rust (RC) and barley yellow dwarf virus (BYDV) assessments were made under natural infection at the flowering stage. The percentage of leaf area showing pathogen symptoms was scored for each accession and site where diseases were noticeable. At maturity, 12 agro-morphological traits were scored on harvested individual plants. Plant height (PH, cm) was measured at maturity from the soil surface to the tip of the panicle. After hand-harvesting of the four plants per elementary plot, the panicles were threshed and dried at 35 °C for seeds and 70 °C for other parts of the plant (stem weight SW (g) and root weight RW (g)). Grain yield per plant YP (g) and dry matter per plant DMP (g) were measured using a weighing scale. Harvest index (HI, %) was derived as the ratio of grain yield to total biomass by the formula: HI = (YP/(YP + DMP)) × 100. At harvest, plant density was estimated by counting the number of plants on a one-meter row length. Subsequently, the yield in quintals per hectare (Yield q/ha) and dry matter in quintals per hectare (DM q/ha) were estimated according to plant density, yield per plant, and the plot

area which varied between experimental sites. The root length RL (cm), number of fertile tillers NFT, and number of spikelets per panicle (NSP) were also assessed. Furthermore, the weight of a thousand unshelled kernels (TKW g) was estimated using three samples of 250 seeds.

2.5. Statistical Analysis

Collected data were subjected to a variety of statistical analyses. Descriptive statistics, two- and three-way analyses of variance (ANOVA), and multivariate analyses such as principal component analysis (PCA) and additive main effects and multiplicative interaction (AMMI) were performed to assess the genetic diversity in terms of productivity, yield stability, and disease tolerance among lines and experimental sites. The R software version 3.5.1 was used for these tests. The ANOVA tests were conducted to assess the variability among lines within and between sites. For significant ANOVAs, determination of homogeneous groups of lines was performed using the Newman–Keuls post hoc test. Associations among pertinent traits, which were useful for line classifications, as well as significant correlations between those traits, were performed through multivariate principal component analysis (PCA) with Factominer package version 2.4 [21]. The AMMI analysis via R [22] combines both ANOVA and PCA to determine the main effects and genotype-by-environment interactions (GEI) in multi-location trials. The interaction principal component axes, IPCA1 and IPCA2, are calculated and displayed as biplots to project GEI patterns graphically. Initially, adaptability and phenotype stability across the locations were performed by the AMMI method described by Zobel et al. [23]. Subsequently, Purchase [24] developed the AMMI stability value (ASV) based on the AMMI model's principal components axis 1 and 2 scores for each genotype, respectively. Genotypes with small values of IPCA1, IPCA2, and ASV are more stable across environments. Of course, yield stability is a critical factor to protect small-holding subsistence farmers from starvation in adverse growing seasons.

3. Results

3.1. Disease Assessments

Crown rust (RC; *Puccinia coronata* f. sp. *avenae*), barley yellow dwarf virus (BYDV), and powdery mildew (*Blumeria graminis* f. sp. *avenae*) are the three most common diseases found on oats in Morocco [19]. Powdery mildew was not noticeable in the experimental trials; consequently, only RC and BYDV infections were assessed at the flowering stage in Bouchane_19, El Kbab_19, Bouchane_21, Ain Itto_21, and Oukaimeden_21. Table 3 shows that BYDV symptoms were more frequent than the two other diseases in five out of seven trials. The ANOVA test for BYDV revealed significant differences among oat lines at three sites: Bouchane_21, Ain Itto_21, and Oukaimeden_21. The average leaf area covered by the virus was equal to 14.62 and 14.25% in Ain Itto_21 and Bouchane_21, respectively. El Kbab_19 BYDV infection was the lowest at only 4.09% and with no significant differences among lines. Regarding RC, the ANOVA test was significant in Bouchane_19 with an average infection value of 20.28%.

Table 3. Summary one-way ANOVA for BYDV and RC infestations.

Site	Season	Trait	F	Mean (%)	*p*_Value
Bouchane_19	2018–2019	BYDV	2.109 NS	6.11	0.061
		RC	6.811 ***	20.28	0.000
El Kbab_19	2018–2019	BYDV	0.731 NS	4.09	0.699
Bouchane_21	2020–2021	BYDV	7.928 ***	14.25	0.000
Ain Itto_21	2020–2021	BYDV	5.437 ***	14.62	0.000
Oukaimeden_21	2020–2021	BYDV	5.377 ***	9.38	0.000

NS = not significant; *** significant at $p = 0.001$. BYDV: barley yellow dwarf virus; RC: Crown rust.

The Student–Newman–Keuls test allowed ranking of the oat lines in locations where disease infections were significant (Table 4). There was an irregular ranking of the BYDV infection across sites apart from line AT6. This accession tended to show more tolerance than the others with a value of 9% at Bouchane_21 (Rank 1), 10% at Ain Itto_21 (Rank 2), and 5% at Oukaimeden_21 (Rank 1). It was also ranked second for RC at Bouchane_19 (13.33%).

Table 4. Disease rankings of the 12 lines using the Student–Newman–Keuls test.

BYDV (%)									RC (%)		
Bouchane_21			**Ain Itto_21**			**Oukaimeden_21**			**Bouchane_19**		
AT6	9.00	a	AT3	8.33	a	AT6	5.00	a	ATC	10.00	a
AT4	10.00	ab	AT6	10.00	ab	AT13	7.50	b	AT6	13.33	ab
AT13	11.00	ab	AT14	11.67	abc	AT1	8.75	b	AT2	13.33	ab
AT5	12.00	ab	AT1	13.33	abcd	AT5	8.75	b	AT5	13.33	ab
ATC	12.00	ab	ATC	13.33	abcd	AT14	10.00	bc	AT1	16.67	ab
AT3	12.50	ab	AT2	14.17	abcd	AT15	10.00	bc	AT3	16.67	ab
AT15	13.50	ab	AT9	15.83	bcd	AT2	10.00	bc	AT4	16.67	ab
AT14	16.00	bc	AT15	16.25	cd	AT3	10.00	bc	AT14	23.33	ab
AT2	16.00	bc	AT7	17.08	cd	AT7	10.00	bc	AT15	23.33	ab
AT1	19.00	c	AT13	17.50	cd	AT9	10.00	bc	AT13	26.67	bc
AT9	19.00	c	AT4	18.33	d	ATC	10.00	bc	AT7	30.00	c
AT7	21.00	c	AT5	19.58	d	AT4	12.5	c	AT9	40.00	d

Values within a column followed by a common (a–d) are not significantly different ($p < 0.05$). BYDV: barley yellow dwarf virus; RC: crown rust.

3.2. Analyses of Agro-Morphological Traits

The average values (means) and coefficients of variation (CVs) of the different morphological (PH, RL) and agronomic (NFT, Yield, DM, HI, etc.) traits across sites are presented in Table 5. Plant height (PH) was less variable than the other traits, with CVs of 9.97% at Oukaimeden_21 and 21.18% at Bouchane_19. The variable TKW also possessed small CVs among samples but was quite variable from site to site (6.82% and 55.58%, respectively). As expected, traits related to grain yield or biomass showed large variation. For example, the CV for yield was over 55% across sites. The Alnif_21 trial yield was the highest at 85.5 q/ha, while the Bouchane_21 trial was the least productive at just 6.89 q/ha. Bouchane_19 plants, in comparison to the other sites, were the shortest (48.93 cm) and had the deepest roots (16.16 cm).

Table 5. Descriptive statistics of the agro-morphological traits of domesticated *A. magna* for the three cropping seasons.

	Season 2018–2019				**Season 2019–2020**		**Season 2020–2021**							
	El Kbab_19		**Bouchane_19**		**Bouchane_20**		**Ain_Itto_21**		**Alnif_21**		**Bouchane_21**		**Oukaimeden_21**	
Traits	Mean	CV	Mean	CV	Mean	CV	Mean	CV	Mean	CV	Mean	CV	Mean	CV
PH	72.86	13.92	48.93	21.18	87.91	14.70	118.47	15.65	116.89	11.44	64.61	14.08	120.47	9.97
RL	15.41	19.84	16.16	22.28	15.66	21.83	14.19	20.05	12.58	19.69	14.42	22.6	11.87	14.10
NFT	4.35	69.81	3.10	34.25	4.80	44.98	4.42	43.24	11.09	32.09	3.59	51.99	5.60	36.07
DMP	15.36	56.65	9.87	74.84	9.35	88.19	12.54	41.16	35.51	40.92	4.08	58.74	13.59	48.41
YP	9.69	59.6	5.63	86.16	3.18	65.59	4.74	52.71	16.1	51.14	1.83	69.37	5.92	51.28
HI	25.74	79.56	20.43	86.38	27.23	27.33	27.12	22.53	30.68	23.67	31.33	24.14	30.37	17.32

Table 5. *Cont.*

	Season 2018–2019				Season 2019–2020		Season 2020–2021							
	El Kbab_19		Bouchane_19		Bouchane_20		Ain_Itto_21		Alnif_21		Bouchane_21		Oukaimeden_21	
Yield	51.96	77.79	23.19	85.76	11.85	62.79	20.17	55.77	85.5	55.78	6.89	87.64	18.99	60.83
DM	78.33	67.19	42.76	82.94	34.41	80.98	53.5	46.01	188.15	45.77	15.34	81.72	43.85	59.30
NSP	53.89	58.81	29.74	76.45	16.17	38.40	25.3	52.15	43.43	34.23	14.24	53.21	24.83	32.50
TKW	45.73	11.84	37.66	55.58	40.61	7.58	43.94	6.82	42.76	6.98	34.29	45.11	40.04	7.95
SW	13.74	56.7	8.55	77.51	NA	NA	10.86	41.64	26.63	41.7	2.83	60.01	11.61	46.57
RW	1.62	72.66	1.33	74.59	NA	NA	1.68	48.65	8.88	51.83	1.25	63.9	1.98	66.73

Explanations: CV: coefficient of variation; PH = plant height (cm); RL = root length (cm); NFT = number of fertile tillers; DMP = dry matter per plant (g); YP = grain yield per plant (g); HI = harvest index (%); Yield = grain yield per hectare (q); DM = dry matter per hectare (q); NSP = number of spikelets per panicle; TKW = thousand-seed weight (g); SW = stem weight (g); RW = root weight (g); NA: not available.

The two-way ANOVA detected significant differences among lines for all the investigated traits except for DMP, TKW, and SW at Bouchane_19.

Table 6 summarizes the line rankings for seed yield at the experimental sites based on the Student–Newman–Keuls test. Table 6 shows that there was no dominant line across all locations. For example, the ATC control performed well in El Kbab_19 (73.8 q/ha) and Alnif_21 (114.9 q/ha), while it ranked last at Bouchane_20 (6.67 q/ha) and Oukaimeden_21 (11.64 q/ha). Line AT5 had the highest yield at Bouchane_19 (39.45 q/ha) and El Kbab_19 (103.17 q/ha); it yielded relatively well at Bouchane_21 (9.13 q/ha) and Oukaimeden_21 (27.11 q/ha) but was less productive at the other locations.

Merely considering line performance through all sites combined does not allow for their correct ranking because they showed contrasting productivity potential. The three-way ANOVA was conducted to take into account line × environment interaction. The ANOVA_3 test revealed significant differences among genotypes for most of the traits except TKW. Furthermore, it showed a high location effect on genotype morphology and productivity.

The ranking of the experimental sites for productivity parameters showed that average Yield varied from 6.89 to 85.5 q/h; DM from 15.34 to 188.15 q/ha; and HI ranged from 20.43 to 31.33%. Alnif_21 and El Kbab_19 produced both high grain and biomass yields in comparison to the other sites. During the 2019_2020 and 2020_2021 seasons, the arid Bouchane site produced less than the other locations.

The Student–Newman–Keuls test results of the three-way ANOVA are reported in Table 7. Combining all the sites' data showed clearly that AT5 was the most productive line. It was ranked first for grain yield (43.41 q/ha), HI (34.76%), and TKW (49.73 g). For the DM, it was ranked second after AT1 with a value of 69.24 q/ha. On the other hand, the least productive lines were AT15 (23.90 q/ha) and AT9 (23.11). Regarding the morphological traits, the accession PH ranged between 84.07 cm (AT2) and 94.92 cm (AT15). Lines ATC (85.06 cm), AT6 (84.64 cm), and AT2 (84.07 cm) were the shortest. Root length (RL), NFT, and NSP varied between 13.52 (AT5) and 15.61 cm (AT15); between 4.03 (AT15) and 5.93 (AT1); and between 24.85 (AT2) and 36.06 (AT13), respectively.

Table 6. Ranking of the 12 lines for grain yield per hectare at each site where it was significant across the three cropping seasons.

Season 2018–2019						Season 2019–2020			Season 2020–2021										
Bouchane_19			El Kbab_19			Bouchane_20			Ain_Itto_21			Alnif_21			Bouchane_21			Oukaimeden_21		
AT5	39.45	a	AT5	103.17	a	AT14	22.13	a	AT3	31.64	a	ATC	114.9	a	AT4	12.26	a	AT9	34.83	a
AT9	28.86	ab	ATC	73.8	b	AT3	15.41	b	AT15	27	b	AT1	103.7	ab	AT7	11.84	a	AT5	27.11	ab
AT2	27.21	ab	AT1	68.52	bc	AT15	15	bc	AT13	22.29	bc	AT7	97.1	abc	AT1	9.28	ab	AT7	24.67	bc
AT3	25.09	ab	AT3	62.7	bc	AT13	14.14	bc	AT6	22.1	bc	AT14	93.5	abc	AT5	9.13	ab	AT14	19	bc
AT13	24.85	ab	AT6	59.01	bc	AT1	13.4	bc	AT1	21.69	bc	AT4	90.7	abc	AT2	8.88	ab	AT4	18.96	bc
AT7	24.17	ab	AT2	58.09	bc	AT4	11.23	bc	AT14	21.14	bc	AT15	90.3	abc	AT3	6.9	abc	AT13	18.48	bc
AT1	23.99	ab	AT7	44.8	bcd	AT9	10.82	bc	AT9	20.49	bc	AT6	88.2	abc	AT6	5.19	bc	AT15	17.24	bc
ATC	23.19	ab	AT13	38.34	bcd	AT5	9.99	bc	ATC	16.82	cd	AT13	87.7	abc	AT9	4.75	bc	AT2	15.47	bc
AT4	19.3	ab	AT4	36.12	bcd	AT7	9.99	bc	AT7	16.54	cd	AT5	86	abc	AT14	4.59	bc	AT6	14.24	c
AT14	15.24	b	AT14	30.76	cd	AT6	9.19	bc	AT5	16.46	cd	AT3	61.6	bc	AT13	4.2	bc	AT3	13.59	c
AT6	15.15	b	AT15	13.47	d	AT2	7.4	bc	AT4	15.93	cd	AT2	58.7	bc	ATC	2.83	c	AT1	12.6	c
AT15	9.08	b	AT9	10.35	d	ATC	6.67	c	AT2	9.99	d	AT9	53.7	c	AT15	2.81	c	ATC	11.64	c

Values within a column followed by a common (a–d) are not significantly different ($p < 0.05$).

Table 7. Ranking of 12 lines for principal agro-morphological traits with ATC (Avery) as control.

Agronomic Traits								Morphological Traits					
Yield		DM		HI		TKW		PH		RL		NTF		NSP	
AT5	43.41 ^{a}	AT1	80.05 ^{a}	AT5	34.76 ^{a}	AT5	49.73 ^{a}	AT15	94.92 ^{a}	AT15	15.61 ^{a}	AT1	5.93 ^{a}	AT7	36.06 ^{a}
AT1	35.93 ^{ab}	AT5	69.24 ^{ab}	AT4	31.78 ^{b}	AT4	42.94 ^{ab}	AT13	94.57 ^{a}	AT13	15.27 ^{ab}	AT14	5.69 ^{ab}	AT13	34.34 ^{ab}
ATC	35.66 ^{ab}	ATC	67.33 ^{abc}	AT3	31.33 ^{b}	AT9	41.93 ^{abc}	AT7	92.71 ^{ab}	AT14	15.23 ^{ab}	AT9	5.64 ^{ab}	AT14	33.13 ^{ab}
AT3	31.74 ^{bc}	AT13	66.75 ^{abc}	ATC	31.20 ^{b}	AT1	41.62 ^{abc}	AT5	89.93 ^{bc}	AT7	14.96 ^{abc}	AT4	5.6 ^{ab}	AT5	31.56 ^{abc}
AT7	31.64 ^{bc}	AT6	65.85 ^{abc}	AT6	30.35 ^{b}	AT7	41.27 ^{abc}	AT4	89.76 ^{bc}	AT4	14.83 ^{abcd}	AT6	5.51 ^{ab}	AT15	30.48 ^{abc}
AT6	30.15 ^{bc}	AT3	63.36 ^{abc}	AT2	29.67 ^{b}	AT6	40.99 ^{abc}	AT9	88.94 ^{bcd}	AT1	14.31 ^{bcd}	AT5	5.17 ^{abc}	ATC	30.47 ^{abc}
AT13	29.78 ^{bc}	AT4	62.83 ^{abc}	AT1	29.47 ^{b}	AT2	40.29 ^{bc}	AT1	88.58 ^{bcd}	AT6	14.13 ^{bcd}	ATC	4.98 ^{bc}	AT3	30.39 ^{abc}
AT14	28.75 ^{bc}	AT14	61.77 ^{bc}	AT7	22.57 ^{c}	AT14	40.19 ^{bc}	AT3	88.56 ^{bcd}	AT3	14.11 ^{bcd}	AT2	4.94 ^{bc}	AT1	28.77 ^{abc}
AT4	28.07 ^{bc}	AT2	61.28 ^{bc}	AT9	22.17 ^{c}	AT15	39.60 ^{bc}	AT14	88.07 ^{cd}	AT9	13.85 ^{cd}	AT13	4.86 ^{bc}	AT4	28.50 ^{abc}
AT2	27.32 ^{bc}	AT7	58.33 ^{bc}	AT14	20.33 ^{c}	AT13	38.72 ^{bc}	ATC	85.06 ^{de}	AT2	13.81 ^{cd}	AT3	4.58 ^{cd}	AT6	28.04 ^{bc}
AT15	23.90 ^{c}	AT15	52.64 ^{bc}	AT15	20.28 ^{c}	ATC	37.97 ^{bc}	AT6	84.64 ^{de}	ATC	13.65 ^{d}	AT7	4.45 ^{cd}	AT9	25.23 ^{c}
AT9	23.11 ^{c}	AT9	49.99 ^{c}	AT13	19.88 ^{c}	AT3	32.83 ^{c}	AT2	84.07 ^{e}	AT5	13.52 ^{d}	AT15	4.03 ^{d}	AT2	24.85 ^{c}

Values within a column followed by a common (a–e) are not significantly different ($p < 0.05$). Yield = grain yield per hectare (q); DM = dry matter per hectare (q); HI = harvest index (%); TKW = thousand-seed weight (g); PH = plant height (cm); RL = root length (cm); NFT = number of fertile tillers; NSP = number of spikelets per panicle.

3.3. Principal Components Analysis

The principal component analysis (PCA) was conducted to identify the main traits that contribute to differentiation among lines. PCA considers all the variables at the same time to cluster the oat lines through their similarities. The PCA outputs showed that 84.57% of the variability was explained by the first four principal components' axes. This high percentage reflects strong discrimination among the assessed lines. The main contributors to the first principal component (PC1) were PH, RL, HI, and RC (35.73%). Thus, PC1 can be considered an indicator of the plant morphology behind the RC disease. Both PC2 and PC3 accounted for 37.71% of the total variation; they were mainly linked to the grain and biomass yield components: NTF, NSP, SW, DMP, YP, DM, and Yield. The fourth axis was essentially explained by the TKW and BYDV degree of susceptibility.

According to the Pearson correlations matrix (Table 8), DMP exhibited both highly significant and positive correlations with YP and SW ($R^2 = 0.81$; $R^2 = 0.82$). Yield per plant (YP) was also positively correlated with NSP and RW ($R^2 = 0.63$ and $R^2 = 0.65$). Grain yield per hectare (Yield) and DM were positively correlated at 75%. A negative correlation was found between the HI and PH ($R^2 = -0.59$), RL ($R^2 = -0.74$), and RC ($R^2 = -0.78$). On the other hand, the HI showed a positive relationship with grain yield ($R^2 = 0.63$). The susceptibility to BYDV and RC diseases appeared together in oat plants up to 62%.

The biplot PC1 × PC2 revealed four accessions' clusters (Figure 2). Two accessions, AT5 and AT1, formed cluster I, which included high biomass and grain production potential. Cluster II gathered AT13 and AT14, which had good individual plant performance (grain yield and dry matter per plant). Cluster III included ATC and AT6, short size, and high harvest-index lines with better tolerance to BYDV and RC infection than AT7 and AT9. Cluster IV included AT4 with its high TKW.

Table 8. Pearson correlation with traits from principal component analysis results.

	PH	**RL**	**NFT**	**NSP**	**RW**	**SW**	**DMP**	**YP**	**Yield**	**DM**	**HI**	**TKW**	**RC**	**BYDV**
PH	1													
RL	**0.72**	1												
NFT	−0.48	−0.31	1											
NSP	**0.60**	0.54	−0.38	1										
RW	0.22	0.41	0.03	**0.63**	1									
SW	0.27	0.32	**0.62**	0.10	0.15	1								
DMP	0.36	0.55	0.51	0.39	0.49	**0.82**	1							
YP	0.43	0.34	0.36	**0.63**	**0.65**	**0.67**	**0.81**	1						
Yield	−0.15	−0.47	0.13	0.32	−0.07	0.00	−0.06	0.30	1					
DM	−0.26	−0.26	0.42	0.12	−0.27	0.29	0.25	0.19	**0.75**	1				
HI	**−0.59**	**−0.74**	0.25	−0.36	−0.50	−0.11	−0.41	−0.24	**0.63**	0.53	1			
TKW	0.06	−0.21	0.36	−0.04	0.10	0.28	0.10	0.35	0.40	0.14	0.23	1		
RC	0.54	0.38	−0.05	0.14	0.36	0.24	0.31	0.31	−0.56	**−0.63**	**−0.78**	−0.01	1	
BYDV	0.52	0.24	−0.10	0.23	0.13	0.17	0.10	0.30	−0.09	−0.29	−0.45	0.44	**0.62**	1

Bolded values are significant Pearson correlation. PH = plant height (cm); RL = root length (cm); NFT = number of fertile tillers; NSP = number of spikelets per panicle; RW = root weight (g); SW = stem weight (g); DMP = dry matter per plant (g); YP = grain yield per plant (g); Yield = grain yield per hectare (q); DM = dry matter per hectare (q); HI = harvest index (%); TKW = thousand-seed weight (g); RC: crown rust (%); BYDV: barley yellow dwarf virus (%).

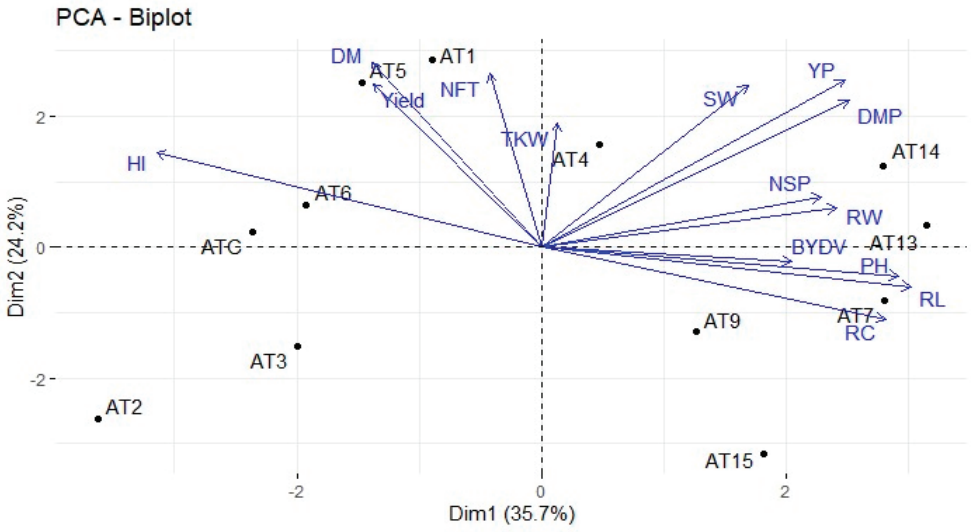

Figure 2. Biplot principal component 1 (PC1), principal component 2 (PC2) of the 12 lines, and traits derived from the average linkage cluster analysis. Explanation: traits: PH = plant height (cm); RL = root length (cm); NFT = number of fertile tillers; DMP = dry matter per plant (g); YP = grain yield per plant (g); HI = harvest index (%); Yield = grain yield per hectare (q); DM = dry matter per hectare (q); NSP = number of spikelets per panicle; TKW = thousand-seed weight (g); SW = stem weight (g); RW = root weight (g).

3.4. AMMI Analysis

An AMMI analysis was performed to scrutinize yield stability of the experimental lines across environments. The analysis of variance (ANOVA) associated with the AMMI model revealed highly significant site, line, and their interaction (S × L) effects (p-value ≤ 0.001). The environment explained the largest grain yield variability (78%), followed by the interaction (18%; Table 9). Only 4% of the total sum of squares was assigned to the genetic factor of the *A. magna* ssp. *domestica* lines—the large contrast between the sites was intended to assess the specific adaptation of the experimental lines through the GxE interactions. Differences among lines were more expressed within the experimental sites. The two first axes, IPCA1 and IPCA2, explained 59.7% and 31.7%, respectively, of the genotype×environment interaction (GEI) sum of squares.

Table 9. Additive main effects and multiplicative interaction analysis (AMMI) analysis of variance for grain yield of 12 lines for three cropping seasons.

Source	Df	Sum Sq	Mean Sq	F Value	Pr (>F)	% Variation
Site	6	596,996	99,499	12.32 ***	6.92×10^{-5}	78
Line	11	27,740	2522	6.04 ***	1.40×10^{-9}	4
S × L	66	136,793	2073	4.96 ***	2.20×10^{-16}	18
IPCA1	16	19,821.10	1238.82	2.97 ***	0.0001	59.7
IPCA2	14	10,539.33	752.81	1.80 *	0.0344	31.7
Residuals	897	374,620	418			

* significant at $p = 0.05$; *** significant at $p = 0.001$.

Figure 3 displays a scatter plot formed by genotypes and experimental locations according to their coordinates on the two first axes of GEI. The values of these coordinates

indicate the accessions' contribution to GEI. In this case, the lower the coordinate is, the lower its contribution to GEI and therefore the more stable the genotype is. Thus, lines AT7, AT6, AT13, and AT4 being closer to the biplot's center have more stable grain production across the experimental sites. In contrast, grain yields of the AT5, AT9, AT15, and ATC lines are unstable from site to site, as their position is far away from the biplot center. The other accessions are ranked intermediate with respect to their grain yield stability (AT1, AT2, AT3, and AT14). Furthermore, the length of vectors assigned to the experimental locations shows their ability to discriminate among the oat lines. El Kbab_19 and Alnif_21 sites showed more yield variation among lines. When a genotype projection is close to a site position on the biplot, that means the line has a specific adaptation to it; for example, AT5 was better suited to El Kbab_19 (103.17 q/ha), and ATC interacted positively with the Alnif_21 environment (114.9 q/ha), as did AT9 (34.83 q/ha) with Oukaimeden_21.

AMMI analysis provided comparisons between productivity and stability (Figure 4). We observed two main categories of the studied lines. The first group consisted of high-yielding lines that exceeded the experimental site average yield (30.76 q/ha). Among these lines, two were the most productive, AT5 and ATC, though they were quite unstable (ASV = 9.62 and 6.37, respectively). Line AT1 had intermediate stability and a yield equal to 36.17 q/ha, while AT7, which was the most stable (ASV = 1.69), yielded 32.73 q/ha. The other lines produced below the mean yield, with AT6 and AT13 showing good yield stability and a slightly lower yield than average (30.44 q/ha and 29.24 q/ha, respectively).

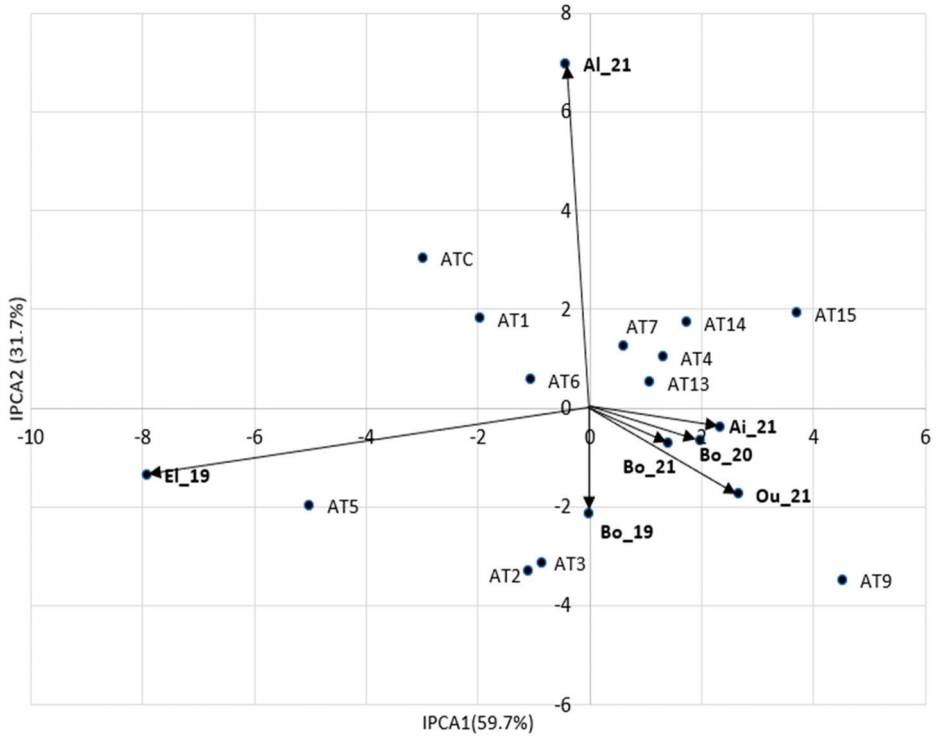

Figure 3. Biplot between the two first components (IPCA1 and IPCA2) of the genotype × environment interaction (GEI) for the grain yield of the 12 *Avena magna* domestica ssp. lines. Explanations: Bolds represent the locations Al_21: Alnif_21; Ai_21: Ain Itto_21; Bo_19: Bouchane_19; Bo_20: Bouchane_20; Bo_21: Bouchane_21; El_19: El Kbab_19; Ou_21: Oukaimeden_21.

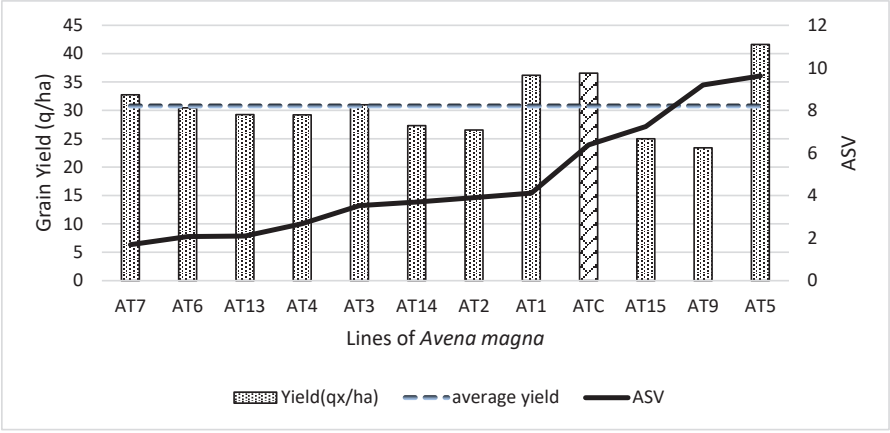

Figure 4. Average grain yield (Yield) and evolution of the AMMI stability values (ASV) of the 12 oat lines. The box ATC represents the control variety used in this investigation.

4. Discussion

The goal of this present work was to determine the agro-morphological variability of 11 *A. magna* ssp. *domestica* advanced lines and a control cultivar named Avery (ATC). *Avena sativa* (2n = 6x = 42) is the principal species of oat cultivated in Morocco, usually for fodder [25]. At the beginning of the local oat research program of the National Institute of Agricultural Research, varieties derived from the native hexaploid *A. byzantina* (red oat), which has a low water requirement and the ability to adjust its growth cycle to Moroccan environmental variability, were also released [26]. The array of wild *Avena* species native to Morocco—the center of origin of the genus—unfortunately lacks the required traits for broad cultivation such as resistance to shattering, semi-dwarfism, lodging resistance, erect growth habit, resistance to seed dormancy, etc. The neo-domesticated *A. magna* material first described by Ladizinsky [14] and later modified by Jackson [7] should have the potential to diversify the cultivated germplasm of oats. This new oat diversity contributes to the conservation of genetic resources of the genus and plays a positive role in maintaining crop diversity [6,17]. In addition, the significantly higher protein content of 'Avery' previously reported by Jackson [7] could encourage farmers and manufacturers to harness this asset to improve the crop's profitability for both human and animal feed. Over the course of the past 40 years, interest in oats for human consumption has gradually increased, concomitant with mounting clinical evidence regarding its nutritional benefits for cardiovascular health [27].

The disease assessment study had focused only on RC and BYDV, since there were no noticeable symptoms of powdery mildew at the heading stage when scoring was carried out. Several authors agree that RC (*Puccinia coronata*) is the major disease threatening global oat production [28]. This pathogen can drastically affect oat production by causing 10–40% yield loss [29]. Crown rust (RC) was only recorded at Bouchane in the 2018–2019 cropping season because at the other locations there were no noticeable symptoms in the experimental plots. The cause may be due to relatively dry and cool conditions at the experimental sites during 2020–2021. Nazareno et al. [28] reported that crown rust epidemics usually occur in warm areas as temperatures fluctuate between 20 and 25 °C and humidity surpasses 50–60%. At the El Kbab high-altitude site and in Alnif's dry environment, weather conditions would be expected to suppress crown rust development. The incidence of BYDV was more common than RC across the experimental locations. BYDV is probably the most economically important small-grain virus transmitted by insects, with 25 aphid species being involved as potential BYDV vectors [30]. High light intensity and low temperatures (15–18 °C) also promote increased intensity of BYDV symptoms [31]. All of these considerations and *A. magna*'s well-known susceptibility to

BYDV [14] may explain the high incidence of the virus observed in our experiments. The trials' results did not show consistent tolerance to diseases of tested lines at all sites, except for line AT6, which appeared to be more tolerant to BYDV and RC infections. Combining data from all sites, PCA revealed that the control variety Avery and AT6 were relatively less susceptible to the diseases, which was not the case for AT7 and AT9. Jellen et al. [19] had already noted A02 (line AT7 in this study) among the lines showing RC symptoms in the Lahri experiment in 2018.

Data analyses revealed significant agro-morphological diversity between the domesticated *A. magna* lines. Plant height (PH) varied between 48.93 and 120.47 cm across the sites. Through the different sites, PH fluctuated between 84.07 cm for AT2 and 94.92 cm for AT15. Previous studies reported similar plant height values. Dumlupinar et al. [32], who studied *A. sativa* pure-line varieties, reported variation for plant height between 46 and 112 cm. Among our investigated traits, PH gave the lowest CV, between 9.97 and 21.18% across the five sites. This finding is in line with Solange et al. [33] and Dumlupinar et al. [32], who reported CVs of 11.16 and 8.7%, respectively, for this trait. A possible explanation for these observations is that plant height is affected by a relatively small number of major genes, which in this case might be largely fixed through selection. PCA analysis showed that PH was positively correlated with RL (0.72) and NSP (0.60); on the other hand, PH was significantly negatively correlated with HI. Other authors reported a significant negative correlation between PH and grain yield and explained the relationship as being due to lodging [34,35]. Plant size has to be examined closely in varietal selection to avoid lodging, in our case with lines AT13 and AT15.

Root length across locations ranged from 11.87 to 16.16 cm at Oukaimeden_21 and Bouchane_19, respectively. The longest roots were observed in Bouchane in three successive seasons. This behavior is likely due to the sandy soil at Bouchane, which facilitates and encourages deep root penetration as capillary water drains downward through the soil profile. Finer roots were also more easily retained as the plants were uprooted in the light-textured soil to take RL measurements. The higher clay content at the other experimental sites allowed for better soil water retention. This supports the previous observation that A. *magna* ssp. *domestica* has the ability to deeply penetrate the soil under water-stress conditions [19].

The three-way ANOVA detected significant differences among lines according to their tillering ability: 4.03 NFT/plant for AT15 and 5.93 for AT1 on average (Table 7). The genetic control of tillering capacity has been discussed previously in oat genotypes [36,37]. The mean NFT was mostly equivalent among our test locations except for Alnif_21, where it reached an average of 11.09. Good crop management practices such as irrigation and fertilization have a positive influence on the tillering ability of plants; this may explain the significantly higher NFT value at this irrigated site.

The NSP varied among lines, ranging from 24.85 to 36.06 for AT2 and AT7, respectively. Solange et al. [33] observed an NSP mean of 26.63 for *A. sativa*, which is close to our findings. However, Jan et al. [6] counted 66 spikelets per panicle on average in their experiment. The number of spikelets is influenced by soil fertility, humidity, and photoperiod.

Thousand-kernel weight (TKW) is an important productivity and grain-quality trait for oats. According to our three-way ANOVA, TKW was more significantly influenced by growing location than genotype. Considering separately the experimental sites, two-way ANOVA showed a significant effect of the accessions at all testing sites except Bouchane_19. Our line TKW values, similar to previous results in *A. sativa*, varied between 32.83 and 49.73 g for AT3 and AT5, respectively. Our results correspond well with *A. sativa* TKW values [6,32,33].

Seed partitioning on the total biomass is evaluated through the HI. Statistical analyses showed that HI was influenced by both the line and the environment; it varied between 20.43 and 31.33% across the five testing locations. Regarding the effect of the lines, the HI varied between 19.88% for AT13 and 34.76% for AT5. Jan et al. [6] and Li et al. [38] reported

on variation for HI among *A. sativa* genotypes and between environments and years; their HI values were comparable to ours.

It has historically been a major challenge for plant breeders to consistently identify superior-yielding genotypes across environments when GEI is highly significant. Several researchers testing crops in multi-location conditions have reported larger environmental than genotypic effects on grain yield [39–42]. In our case, the environmental effect represented 78% of the total grain yield variation, while the genotype explained only 4%. Grain yield varied extensively among our sites: from 6.89 q/ha at Bouchane_19 to 85.50 q/ha at Alnif_21. Previously, within a larger set of *A. magna* lines, Jellen et al. [19] identified the environment as the most important factor influencing yield, with genotype being the second most significant factor. Our AMMI analysis allowed classification of the *A. magna* lines based on their ASVs. Combining ASV and yield into a single index should represent a better way to evaluate a genotype's potential across locations. The yield stability index has been used by several authors to rank their germplasm [40,43,44]. Stable lines are usually less productive than low-stability ones. Stable genotypes have large adaptation and intermediate yield potential, while low-stability lines yield the maximum in the environment in which they are best adapted while ranking among the lowest in other locations. In this study, we presented a hybrid graph to display the *A. magna* line performance and separated them into two groups according to their ASV and grain yield. The first group included *A. magna* lines whose grain yield across locations exceeded the average yield of 30.76 q/ha. Two of the genotypes produced relatively higher grain yields, but they were unstable: AT5 (mean yield of 43.31 q/ha) Avery (35.66 q/ha). Line AT5 performed the best at El Kbab_19 while Avery produced the most at Alnif_21, with respective yields of 103.17 q/ha and 114.9 q/ha. Gadisa et al. [40], while investigating germplasm consisting of 15 bread wheat lines, noticed that the two highest-yielding genotypes were among the most unstable. Each of these two wheat lines had interacted positively at a given site. These results are in agreement with our findings. Among the tested *A. magna* lines, AT1 was moderately stable, while AT7 had the highest stability in the collection. Using the yield stability index, AT7 ranked first as being the superior genotype among the tested germplasm in terms of stability and grain yield. This accession, however, appeared to be less tolerant to diseases. Among the *A. magna* lines that produced below the mean grain yield, AT6 exhibited good yield stability and will be further scrutinized for its apparent tolerance to the main common diseases and its yield, which approached 30.44 q/ha.

The average grain yield of this present study across five sites and three years of experimentation was 30,76 q/ha. It may be recalled when Tam [45] tested 101 oat varieties of *A. sativa* from Germany, Sweden, Russia, Canada, the USA, and other countries, where the average yields ranged between 32.88 and 58.24 q/ha. In our trials, Bouchane's relatively low average yield of 6.89 q/ha is explained by the semi-arid climate conditions; moreover, Morocco is an arid to semi-arid country, unlike Estonia where Tam carried out his experiment. At the most favorable Moroccan site, Ain Itto_21, rainfall barely reached 609.8 mm during the cropping season. However, it should be noted that with certain lines at certain locations, grain yield greatly exceeded the above-mentioned yield range: for example, AT5 at El Kbab_19 and Avery at Alnif_21. Tests of various *A. sativa* varieties selected for northern Morocco reached 45 q/ha under experimental conditions and 24 q/ha in farmers' production fields [46]; these previous results confirm that grain yield tends to decrease under working farm conditions, and some *A. magna* lines might express their best yield potential under good cultivation and environmental conditions.

5. Conclusions

This present study focused on the agronomic performance of advanced *A. magna* ssp. *domestica* lines under working farm conditions at five contrasting locations in Morocco. The results measured diversity among the investigated lines for agro-morphological traits. Grain yield was most highly influenced by the contrasted environments, followed by GEI, with genotype explaining very little of the variation for yield. The mountainous site of El

Kbab seems to be more suitable for growing *A. magna* under obligate rainfed conditions. The average grain yield obtained is in the range usually found for common oat production around the world, which justifies the adaptability of these *A. magna* ssp. *domestica* lines to their native zone. Line AT5 had the highest grain yield and is therefore expected to attain higher grain yields in different locations in Morocco experiencing ample rainfall. Line AT7 was interesting for its relatively high yield stability value, as measured by AMMI. We hope to be able to select one of these advanced lines for registration in Morocco along with the existing control variety, Avery. Further investigation of these lines' nutritional differences and molecular genotyping of these lines are the next steps for facilitating further improvement of domesticated *A. magna*.

Author Contributions: Conceptualization, O.B., E.N.J. and E.W.J.; methodology, O.B., E.W.J., E.h.T. and A.E.M.; formal analysis, E.h.T., O.B. and A.E.M.; execution of research, O.B., E.h.T., E.N.J., E.W.J., A.E.M., M.N. and W.R.; writing—original draft preparation, E.h.T., O.B. and E.N.J.; writing—review and editing, O.B., E.N.J., E.h.T. and M.N.; visualization, O.B., E.N.J. and E.h.T.; supervision, O.B., E.N.J., E.W.J., M.N. and W.R.; project administration, O.B., M.N., W.R., E.N.J. and E.W.J.; funding acquisition, O.B., E.W.J., E.N.J., M.N. and W.R. All authors have read and agreed to the published version of the manuscript.

Funding: This research was funded by Context Global Development (USA) under the Rich Oats for Africa project agreement with the Institut Agronomique et Vétérinaire Hassan II (Morocco).

Data Availability Statement: Data is contained within the article.

Acknowledgments: The authors would like to acknowledge Context Global Development (USA), SALL Family Foundation (USA), 25:2 Solutions (USA), Brigham Young University (USA), and Institut Agronomique et Vétérinaire Hassan II (Morocco) for their financial support and for conducting the field trials under the "Rich Oats for Africa" Project.

Conflicts of Interest: The authors declare no conflict of interest.

References

1. Loskutov, I.G.; Khlestkina, E.K. Wheat, Barley, and Oat Breeding for Health Benefit Components in Grain. *Plants* **2021**, *10*, 86. [CrossRef]
2. Galasso, E.; Wagstaff, A.; Naudeau, S.; Shekar, M. *Economic Costs of Stunting and How to Reduce Them*; World Bank Research Group Policy Research Note; October 2016. Available online: http://pubdocs.worldbank.org/en/536661487971403516/PRN05-March2017-Economic-Costs-of-Stunting.pdf (accessed on 9 July 2018).
3. Medek, D.E.; Schwartz, J.; Myers, S.S. Estimated Effects of Future Atmospheric CO_2 Concentrations on Protein Intake and the Risk of Protein Deficiency by Country and Region. *Environ. Health Perspect.* **2017**, *125*, 087002. [CrossRef] [PubMed]
4. Edge, M.S.; Tiffany, A. *The Importance of Protein in the Developing World—A Solution to Food and Nutrition Insecurity*; 2018. Available online: https://contextglobaldevelopment.medium.com/the-importance-of-protein-in-the-developing-world-79189e3ad67f (accessed on 23 May 2023).
5. Food and Agriculture Organization, United Nations. *Tackling Climate Change Through Livestock*; 2013. Available online: http://www.fao.org/3/a-i3437e.pdf (accessed on 6 July 2018).
6. Jan, S.F.; Khan, M.R.; Iqbal, A.; Khan, F.U.; Ali, S. Genetic diversity in exotic oat germplasm & resistance against barley yellow dwarf virus. *Saudi J. Biol. Sci.* **2020**, *27*, 2622–2631. [CrossRef] [PubMed]
7. Jackson, E.W. High Protein Oat Species. W.I.P.O. Patent Application WO 2017/070104 A1, 27 April 2017.
8. Leggett, J.M. Classification and speciation in Avena. In *Oat Science and Technology, Agronomy Monograph No. 33*; Marshall, H.G., Sorrells, M.E., Eds.; American Society of Agronomy, Crop Science Society of America Madison: Madison, WI, USA, 1992.
9. Ahola, H.G.; Sontag-Strohm, T.S.; Schulman, A.H.; Tanhuanpää, P.; Viitala, S.; Huang, X. Immunochemical analysis of oat avenins in an oat cultivar and landrace collection. *J. Cereal Sci.* **2020**, *95*, 103053. [CrossRef]
10. Song, M.; Wu, K.; Meyerhardt, J.A.; Ogino, S.; Wang, M.; Fuchs, C.S.; Giovannucci, E.L.; Chan, A.T. Fiber Intake and Survival After Colorectal Cancer Diagnosis. *JAMA Oncol.* **2018**, *4*, 71–79. [CrossRef]
11. Rasane, P.; Jha, A.; Sabikhi, L.; Kumar, A.; Unnikrishnan, V.S. Nutritional advantages of oats and opportunities for its processing as value added foods—A review. *J. Food Sci. Technol.* **2015**, *52*, 662–675. [CrossRef]
12. Kouřimská, L.; Sabolová, M.; Horčička, P.; Rys, S.; Božik, M. Lipid content, fatty acid profile, and nutritional value of new oat cultivars. *J Cereal Sci.* **2018**, *84*, 44–48. [CrossRef]
13. Gu, Y.; Qian, X.; Sun, B.; Ma, S.; Tian, X.; Wang, X. Nutritional composition and physicochemical properties of oat flour sieving fractions with different particle size. *LWT* **2021**, *154*, 112757. [CrossRef]

14. Ladizinsky, G. Domestication via hybridization of the wild tetraploid oats Avena magna and A. murphyi. *Theor. Appl. Genet.* **1995**, *91*, 639–646. [CrossRef]
15. Oliver, R.E.; Jellen, E.N.; Ladizinsky, G.; Korol, A.B.; Kilian, A.; Beard, J.L.; Dumlupinar, Z.; Wisniewski-Morehead, N.H.; Svedin, E.; Coon, M.; et al. New Diversity Arrays Technology (DArT) markers for tetraploid oat (Avena magna Murphy et Terrell) provide the first complete oat linkage map and markers linked to domestication genes from hexaploid *A. sativa* L. *Theor. Appl. Genet.* **2011**, *123*, 1159–1171. [CrossRef]
16. Kassebaum, N.J.; Jasrasaria, R.; Naghavi, M.; Wulf, S.K.; Johns, N.; Lozano, R.; Regan, M.; Weatherall, D.; Chou, D.P.; Eisele, T.P.; et al. A systematic analysis of global anemia burden from 1990 to 2010. *Blood* **2014**, *123*, 615–624. [CrossRef]
17. Manzali, R.; Douaik, A.; Bouksaim, M.; Ladizinsky, G.; Saidi, N. Assessment of important technological parameters of new Moroccan domesticated tetraploid oat lines of *Avena magna*. *Труды по прикладной ботанике, генетике и селекции* **2018**, *179*, 32–42. [CrossRef]
18. Jellen, E.; Beard, J. Geographical Distribution of a Chromosome 7C and 17 Intergenomic Translocation in Cultivated Oat. *Crop. Sci.* **2000**, *40*, 256–263. [CrossRef]
19. Jellen, E.N.; Jackson, E.W.; Elhadji, T.; Young, L.K.; El Mouttaqi, A.; Al Halfa, I.; El Fartassi, I.; Katile, L.S.; Linchangco, R.; Klassen, K.; et al. Adaptation and Agronomic Performance of Domesticated Moroccan Oat (*Avena magna* ssp. *domestica*) Lines under Subsistence Farming Conditions at Multiple Locations in Morocco. *Agronomy* **2021**, *11*, 1037. [CrossRef]
20. Mokhtari, N.; Mrabet, R.; Lebailly, P.; Bock, L. Spatialisation des bioclimats, de l'aridité et des étages de végétation du Maroc. *Rev. Mar. Sci. Agron. Vét.* **2014**, *2*, 50–66.
21. Husson, F.; Le, S.; Pages, J. *Exploratory Multivariate Analysis by Example Using R*; Chapman and Hall: London, UK, 2010.
22. R Core Team. *R: A Language and Environment for Statistical Computing*; R Foundation for Statistical Computing: Wien, Austria, 2016; ISBN 3-900051-07-0. Available online: https://www.R-project.org (accessed on 9 September 2022).
23. Zobel, R.W.; Wright, M.J.; Gauch, H.G., Jr. Statistical Analysis of a Yield Trial. *Agron. J.* **1988**, *80*, 388–393. [CrossRef]
24. Purchase, J.L. *Parametric Analysis to Describe Genotype x Environment Interaction and Yield Stability in Winter Wheat*; University of Free State: Bloemfontein, South Africa, 1997.
25. Al Faïz, C.; Saïdi, S.; Jaritz, G. Avoine fourragère (*Avena sativa* L.). In *Production et Utilisation des Cultures Fourragères au Maroc*; Jaritz, G., Bounejmate, M., Eds.; INRA: Rabat, Morocco, 1997; pp. 209–224.
26. Bari Abdellah. Oats in Morocco. 2016. Available online: https://www.researchgate.net/publication/31057526 (accessed on 22 February 2022).
27. Broeck, H.C.V.D.; Londono, D.M.; Timmer, R.; Smulders, M.J.M.; Gilissen, L.J.W.J.; Van der Meer, I.M. Profiling of Nutritional and Health-Related Compounds in Oat Varieties. *Foods* **2016**, *5*, 2. [CrossRef]
28. Nazareno, E.S.; Li, F.; Smith, M.; Park, R.F.; Kianian, S.F.; Figueroa, M. *Puccinia coronata* f. sp. *avenae*: A threat to global oat production. *Mol. Plant Pathol.* **2018**, *19*, 1047–1060. [CrossRef]
29. Behnken, L.M.; Breitenbach, F.R.; Miller, R.P. Impact of Foliar Fungicide to Control Crown Rust in Oats. 2009. Available online: https://www.extension.umn.edu/agriculture/forages/pest/docs/umn-ext-impact-offoliar-fungicide-to-control-crown-rusts-in-oats.pdf (accessed on 21 April 2017).
30. Halbert, S.; Voegtlin, D. Biology and taxonomy of vectors of barley yellow dwarf viruses. *Barley Yellow Dwarf* **1995**, *40*, 217–258.
31. D'Arcy, C.J.; Burnett, P.A. *Barley Yellow Dwarf: 40 Years of Progress*; The American Phytopathological Society Press: St. Paul, MN, USA, 1995.
32. Dumlupinar, Z.; Güngör, H.; Dokuyucu, T.; Herek, S.; Tekin, A.; Akkaya, A. Agronomical Screening of OGLE1040/TAM O-301 Oat Genetic Mapping Population. *Sains Malays.* **2019**, *48*, 975–981. [CrossRef]
33. Solange, F.d.S.S.; Danyela, d.C.S.O.; Latoia, E.M.; Tiago, C.; Victoria, F.d.O.; Cristiano, S.; Henrique, P.C.; Vianei, R.; Maraisa, C.H.; Luis, C.G.; et al. Associations between Agronomic Performance and Grain Chemical Traits in Oat. 2020; Volume 10. Available online: http://cpsjournal.org (accessed on 8 November 2021).
34. Dumlupinar, Z.; Kara, R.; Dokuyucu, T.; Akkaya, A. Correlation and path analysis of grain yield and yield components of some Turkish oat genotypes. *Pak. J. Bot.* **2012**, *44*, 321–325.
35. Buerstmayr, H.; Krenn, N.; Stephan, U.; Grausgruber, H.; Zechner, E. Agronomic performance and quality of oat (*Avena sativa* L.) genotypes of worldwide origin produced under Central European growing conditions. *Field Crop. Res.* **2007**, *101*, 343–351. [CrossRef]
36. Ahmad, G.; Ansar, M.; Kalem, S.; Nabi, G.; Hussain, M. Performance of early maturing oats (*Avena sativa* L.) cultivars for yield and quality. *J. Agric. Res.* **2008**, *46*, 341–346.
37. Ma, Y.; Liu, Z.; Bai, Y.; Wang, W.; Wang, H. Study on diversity of oats varieties in Xinjiang. *Xinjiang Agric. Sci.* **2006**, *43*, 510–513.
38. Li, P.-F.; Mo, F.; Li, D.; Ma, B.-L.; Yan, W.; Xiong, Y. Exploring agronomic strategies to improve oat productivity and control weeds: Leaf type, row spacing, and planting density. *Can. J. Plant Sci.* **2018**, *98*, 1084–1093. [CrossRef]
39. Thiam, E.; Allaoui, A.; Benlhabib, O. Quinoa Productivity and Stability Evaluation through Varietal and Environmental Interaction. *Plants* **2021**, *10*, 714. [CrossRef]
40. Gadisa, A.W.; Hussein, M.; Dawit, A.; Tesfahun, A. Genotype X Environment Interaction and Yield Stability of Bread Wheat Genotypes in Central Ethiopia. *J. Plant Breed. Genet.* **2019**, *7*, 87–94.
41. Machado, N.G.; Lotufo-Neto, N.; Hongyu, K. Statistical analysis for genotype stability and adaptability in maize yield based on environment and genotype interaction models. *Ciênciae Nat.* **2019**, *41*, 25. [CrossRef]

42. Doehlert, D.C.; McMullen, M.S.; Hammond, J.J. Genotypic and Environmental Effects on Grain Yield and Quality of Oat Grown in North Dakota. *Crop. Sci.* **2001**, *41*, 1066–1072. [CrossRef]
43. Farshadfar, E. Incorporation of AMMI Stability Value and Grain Yield in a Single Non-Parametric Index (GSI) in Bread Wheat. *Pak. J. Biol. Sci.* **2008**, *11*, 1791–1796. [CrossRef]
44. Atta, B.M.; Shah, T.M.; Abbas, G.; Haq, M.A. Genotype x environment interaction for seed yield in kabuli chickpea (*Cicer arietinum* L.) genotypes developed through mutation breeding. *Pak. J. Bot.* **2009**, *41*, 1883–1890.
45. Tamn, I. Genetic and environmental variation of grain yield of oat varieties. *Agron. Res.* **2003**, *1*, 93–97.
46. Noutfia, A.; El Mourabit, N.; Alfaiz, C. Selection of oat varieties to the North of Morocco. Need of diffusion and renewal of the varieties. In *New Approaches for Grassland Research in a Context of Climate and Socio-Economic Changes*; (Option s Méditerranéennes: Série A. Séminaires Méditerranéens; n. 102); Acar, Z., López-Francos, A., Porqueddu, C., Eds.; CIHEAM: Zaragoza, Spain, 2012; pp. 233–236.

agriculture

MDPI

Article

Searching for Novel Oat Crown Rust Resistance in Diploid Oat *Avena strigosa* Schreb. Reveals the Complexity and Heterogeneity of the Analyzed Genebank Accessions

Sylwia Sowa [1], Volker Mohler [2] and Edyta Paczos-Grzęda [1,*]

[1] Institute of Plant Genetics, Breeding and Biotechnology, University of Life Sciences in Lublin, 20-950 Lublin, Poland
[2] Institute for Crop Science and Plant Breeding, Bavarian State Research Center for Agriculture (LfL), 85354 Freising, Germany
* Correspondence: edyta.paczos@up.lublin.pl

Abstract: Crown rust, one of the most destructive diseases of oat, regularly occurs worldwide and leads to significant yield losses. The constant evolution of the *Puccinia coronata* f. sp. *avenae* pathogen causes a rapid decline in the effectiveness of currently used crown rust resistance genes, so new ones are urgently needed. In this study, 39 accessions of *Avena strigosa* Schreb. from ten countries gathered from the Polish National Genebank were evaluated at the seedling stage for crown rust reaction using a detached leaf assay and five isolates of *P. coronata* with diverse virulence profiles. Ten plants of each accession were tested, and 28 diverse infection profiles (IPs) were defined. One hundred and sixty-eight out of 390 plants revealed an IP of unidentified resistance. Thirty-eight (97%) of the accessions studied showed a heterogeneous infection pattern, none of the accessions displayed homogeneous susceptibility, and one (51887) was homogeneously resistant to all races used. The obtained results confirmed the complexity and heterogeneity of the accessions gathered in the genebanks. *A. strigosa* preserved as complex populations could be a valuable source of resistance to crown rust and potentially other pathogens. The variability of the analyzed populations was ascertained by a detailed diversity analysis of the transformed resistance/susceptibility data. The averaged resistance rating for the genebank specimens available in the databases may be an obstacle in revealing the beneficial alleles of genes hidden among the plants representing accessions preserved as complex populations. Potential donors of effective resistance may be discovered even in accessions with general susceptibility, which is a promising alternative at a time when making new collections of wild and weedy accessions is under threat from agricultural practice and climate change.

Keywords: *Avena strigosa*; *Puccinia coronata* f. sp. *avenae*; crown rust; accessions heterogeneity; resistance diversity

Citation: Sowa, S.; Mohler, V.; Paczos-Grzęda, E. Searching for Novel Oat Crown Rust Resistance in Diploid Oat *Avena strigosa* Schreb. Reveals the Complexity and Heterogeneity of the Analyzed Genebank Accessions. *Agriculture* **2023**, *13*, 296. https://doi.org/10.3390/agriculture13020296

Academic Editor: Peter Dracatos

Received: 17 November 2022
Revised: 18 January 2023
Accepted: 23 January 2023
Published: 26 January 2023

1. Introduction

Oat is a cereal cultivated worldwide with a high range of applications from animal feed to pharmaceuticals and the food industry [1]. The global production of oat is severely affected by rust diseases [2]. Crown rust caused by *Puccinia coronata* f. sp. *avenae* regularly occurs worldwide and poses a great threat to oat yield and quality. The use of fungicides is common to prevent crown rust development; however, it is becoming more and more unaffordable for consumers. Moreover, the number of registered fungicide active ingredients for the control of *P. coronata* is often limited. Therefore, genetic resistance is one of the most important modern oat breeding goals. The complex life cycle of *P. coronata* leads to the emergence of new rust races and causes high virulence dynamics and phenotypic diversity [3,4]. The efficient adaptability of the fungus is resulting in a rapid breakdown of crown rust resistance genes in existing oat varieties, hence the need for new sources

of *P. coronata* resistance genes for the introgression and genetic enhancement of existing oat varieties.

While most *Pc* genes have been identified in the wild hexaploid oat *A. sterilis* [5], some have come from lower ploidy species, although their introduction into hexaploid *A. sativa* is much more difficult and demanding due to the lack of chromosome homology and the special technical requirements [6,7]. *Pc91* is the only crown rust resistance gene successfully introduced into cultivated oat from a wild tetraploid. This gene was transferred from the accession *A. magna* CI 8330 [8] and remains effective in Europe, although virulence to *Pc91* has already been recorded in Canada [9–11], Australia [12], and the USA [13]. Slightly better results were obtained in the case of the diploid black oat *A. strigosa* Schreb. often called black, sand, or bristle oat. *Pc23* and *Pc94* have been incorporated into a stable *A. sativa* background and used in oat resistance breeding [6,14]. *Pc94* originating from *A. strigosa* accession RL1697 is still in use in the modern varieties 'Leggett' and 'Stride' [15,16]. Recently in the studies of Rines et al. [17], a new and highly effective source of adult plant resistance to oat crown rust was identified in the diploid oat *A. strigosa* accession PI 258731 and introgressed into the hexaploid cultivated oat.

According to Vavilov [18], the origin of *A. strigosa* is northwestern and western Europe with the diversity center in northern Portugal and northwestern Spain, where a whole complex of endemic forms of this species was found [19]. *A. strigosa* was widely cultivated for grain fodder in many European countries and is currently grown to a limited extent on the marginal soils of Scotland and Lithuania [20–22]. The grain of this species is distinguished from common oat by its high nutritional value, manifested in a higher content of polysaccharides (38–72% more), fat (14–27% more), and protein (27–52% more) as well as health-promoting ingredients such as phenolic alkaloids, phenolic acids, tocopherols, tocotrienols, and β-glucan [23]. *A. strigosa* has also been reported as a carrier of genes for resistance to *Ustilago avenae* (Pers.) Rostr. (smut), *Puccinia graminis Pers*. f. sp. *avenae* Eriks. & E. Henn. (stem rust), and *Heterodera avenae* Woll. (cereal cyst nematode) [24–26].

Many researchers have proven that *A. strigosa* is a rich source of useful genes and has a high potential for oat variety improvement. Despite the crossing barriers, the ever-evolving genome editing technology offers an opportunity for the easier insertion of the desired genes utilizing targeted genome engineering techniques [27]; so, it is worth characterizing possible donors of valuable breeding traits. Previous research focused on the screening of *A. strigosa* accessions gave the first insight into the resistance potential of this species [28–30]. The current work complements the existing data and reveals the spectrum of putative new resistance genes or alleles present in the diploid sand oat gathered by the Polish Genebank (National Centre For Plant Genetic Resources, The Plant Breeding and Acclimatization Institute, NRI, Radzików, Poland). Considering the presumable heterogeneity of the analyzed populations, testing many plants of one accession was conducted with the use of various *P. coronata* races. Such an approach enabled us to reveal the complexity of the studied wild species populations gathered in the genebanks and to identify the most resistant individuals.

2. Materials and Methods

2.1. Plant Material and Virulence Assessment

The study was carried out on 39 accessions of *A. strigosa* (Table 1) obtained from the National Centre for Plant Genetic Resources in Radzików, Poland. The accessions were landraces from Poland (22 accessions), the United Kingdom (5 accessions), Spain (2 accessions), Chile (2 accessions), Russia (2 accessions), France (1 accession), Uruguay (1 accession), the Netherlands (1 accession), Bulgaria (1 accession), and Brazil (1 accession). The origin of one accession was unknown.

The reactions of the seedlings to crown rust were recorded using five *P. coronata* race isolates with the virulence profile characterized based on the susceptibility/resistance reaction of 34 differential oat lines with single *Pc* genes [31,32], described by Paczos-Grzęda et al. [31,33]. CR230, CR241, and CR257 were obtained from the Morden Research and

Development Centre, AAFC, Canada, whereas 94(63) and 51(22) were selected from a collection of races' isolates originating from populations collected in Poland [34].

Ten seedlings from each *A. strigosa* accession were tested with all five *P. coronata* races using a detached leaf assay [35], according to the host–pathogen test methodology of Hsam et al. [36] with modifications [34]. The leaves were placed into Petri dishes or 12-well culture plates filled with agar medium (0.6%) with benzimidazole (3.4 mM) using susceptible cv. Kasztan as the infection control in each well [37]. The inoculations were performed in a settling tower, and the plates were incubated for 10 days and assessed using an infection type (IT) qualitative scale [38,39]. The infection results were transformed to HS, S, MS, MR, and R as described by Sowa and Paczos-Grzęda [34,37,40].

2.2. Data Mining and Analysis

The reactions to the isolate infections were grouped into two classes: the phenotypes described as HS, S, and MS were considered susceptible, and the remainder were considered resistant. The infection profiles (IP) of differential lines were compared with the infection profiles assigned to the analyzed *A. strigosa* seedlings to select the genotypes with crown rust resistance conditioned by genes not described so far. The infection scores were transformed into a binary matrix. Each plant's resistance response level to a particular *P. coronata* race was treated as a single variable. The resistance or susceptibility was considered as 1 or 0, respectively. The phenotypic diversity of the accessions was described by the Normalized Shannon diversity index (Sh) [41] and Nei's diversity (Hs) [42,43], calculated by the Virulence Analysis Tool (VAT) software [44,45]. For hierarchical clustering, dissimilarity matrices were used to construct a dendrogram using Ward's method. Principal component analysis (PCA) was performed to visualize the relationships between the accessions. The groups and subgroups were determined with 1000 bootstrap analyses performed in PAST 4.11 software [46]. The analysis of molecular variance (AMOVA), performed by GenAlex 6.502 [47], was used to partition the diversity [48]. The variance components were tested statistically using 9999 permutations. The binary data were also evaluated for population structure using a model-based Bayesian clustering in STRUCTURE v2.3.4 [49]. The models were computed for K = 1 ÷ 10 (K—number of subpopulations). Each model was tested ten times with 10,000 burn-in cycles and 100,000 iterations. The results were tested to find the best model with the highest ΔK value using the web-based software StructureSelector [50] integrating the Clumpak program [51].

Table 1. Crown rust resistance phenotypes of *Avena strigosa* L. genotypes. Accessions, within which fully resistant plants were present, are highlighted in grey.

No.	Plant ID	Origin	*Puccinia coronata* Race [1]					Infection Profile (Number of Resistant Seedlings) [2]	Diversity [3]	
			51(22)	94(63)	CR230	CR241	CR257		Sh	Hs
1	51022	Brazil	HS, S	MS, R	S, MS, R	S, R	HS, R	0 (2), 1.2 (6), 2.5 (1), 4.1 (1)	0.473	0.200
2	51199	Bulgaria	HS, S	HS, S, MS	S, MS, R	S, HS	HS, S, MS	0 (9), 1.3 (1)	0.141	0.036
3	51326	unknown	S	S, MS	MS, MR, R	HS	HS	0 (7), 1.3 (3)	0.265	0.084
4	51518	Poland	HS, S, MS, R	HS, MS	HS	HS, S, MS	HS	0 (7), 1.1 (3)	0.265	0.084
5	51520	Poland	HS, S, R	HS, MS, R	HS	HS, S, MS, MR	HS	0 (4), 1.1 (2), 1.2 (2), 1.4 (1), 2.1 (1)	0.639	0.204
6	51523	Poland	HS, S, MS, R	HS, MS, R	HS	HS, MS, R	HS, S, MR, R	1 (3), 1.2 (1), 1.5 (2), 2.4 (2), 2.8 (1), 3.7 (1)	0.736	0.280
7	51524	Poland	HS, S, MS, R	HS, MS, R	HS	HS, MS, MR, R	HS, S, MS	0 (3), 1.1 (3), 1.2 (1), 1.4 (1), 2.3 (1), 2.4 (1)	0.714	0.236
8	51575	Holland	S	MR, R	MR	HS, MS, R	HS, R	2.5 (2), 3.2 (5), 4.1 (3)	0.447	0.148
9	51578	Uruguay	HR	HR	R	R	HS, S, MS, MR	4.4 (9), 5 (1)	0.141	0.036
10	51579	Russia	HS, S, R	HS, S, MS	HS	HS, S, MS, R	HS	0 (4), 1.1 (5), 1.4 (1)	0.410	0.136
11	51581	Russia	HS, S, MS, R	HS, S, MS, R	HS	HS, S, MS	HS	0 (9), 2.1 (1)	0.141	0.072
12	51582	Spain	HS	R	MS, MR	S	MS	2 (1), 2.5 (9)	0.141	0.036
13	51583	Spain	R	MR, R	HS, R	R	HS, R	3.8 (1), 4.2 (1), 5 (8)	0.278	0.100
14	51584	France	HS, R	HS	HS	S, MS, R	HS, S	0 (8), 1.1 (1), 2.3 (1)	0.278	0.100
15	51585	Poland	HS, S, MS, R	HS, S	MR, R	S, MS, R	MS, R	3 (1), 2.7 (6), 3.1 (2), 3.6 (1)	0.473	0.136
16	51586	Poland	HS, S, MS, MR, R	HS, S, MR, R	HS, S, MR, R	HS, S, MS, R	HS, R	0 (3), 1.1 (2), 1.2 (2), 2.1 (1), 2.3 (1), 5 (1)	0.736	0.332
17	51596	Chile	HR	R	R	R	HS, HR	4.4 (9), 5 (1)	0.141	0.036
18	51597	Chile	HS, S, MS, MR, R	R	R	R	S	3.5 (3), 4.4 (7)	0.265	0.084
19	51598	Poland	S, MS	MS, MR, R	HS, S	S	HS, S, MS, R	0 (1), 1.2 (8), 1.5 (1)	0.278	0.100
20	51613	Poland	HS, R	S, MS, R	HS	HS, S	HS, S	0 (9), 2.1 (1)	0.141	0.072
21	51630	Poland	S, MR	MS, MR	HS	HS	HS	0 (8), 1.2 (1), 2.1 (1)	0.278	0.100
22	51732	Poland	S, MS, MR	MR, R	MR, R	MS, MR, R	S, MS, MR, R	2.5 (5), 3.2 (1), 3.5 (2), 4.1 (1), 4.4 (1)	0.590	0.196
23	51750	Poland	S, MS, MR, R	MR, R	MS, MR, R	S, MS, R	HS, MS, MR, R	2.9 (1), 2.8 (2), 3.2 (1), 4.1 (2), 4.4 (3), 5 (1)	0.736	0.360

Table 1. *Cont.*

No.	Plant ID	Origin	*Puccinia coronata* Race [1]					Infection Profile (Number of Resistant Seedlings) [2]	Diversity [3]	
			51(22)	94(63)	CR230	CR241	CR257		Sh	Hs
24	51751	Poland	HS, S, MS, R	HS	HS	HS, MS	HS, R	0 (5), 1.1 (4), 1.5 (1)	0.410	0.132
25	51753	Poland	S, MS, MR	MR, R	MS, R	MS	MS, MR, R	2 (1), 2.5 (1), 2.9 (5), 3.2 (1), 4.3 (2)	0.590	0.224
26	51754	Poland	S, MS, MR	S, MS, MR	MR, R	S	HS	3 (7), 2.5 (2), 3.4 (1)	0.348	0.120
27	51755	Poland	MS, R	MS, MR, R	MS, R	S, MS	HS	0 (1), 1.2 (7), 2.1 (1), 3.4 (1)	0.408	0.136
28	51887	Poland	MR, R	MR, R	R	MR, R	MR, R	5 (10)	0.000	0.000
29	51987	Poland	S, R	MS, MR, R	S, MS, R	S, MS, R	HS, S, MS, R	0 (1), 1.2 (1), 2.9 (2), 4.4 (2), 5 (4)	0.639	0.420
30	52339	Poland	S, MS	S, MS, MR, R	S, MS	S, MS, MR, R	HS	0 (3), 1.2 (2), 1.4 (3), 2.6 (2)	0.593	0.196
31	52340	Poland	S	MR, R	S, MS	S, R	HS, S, MS, R	2 (6), 2.6 (2), 2.9 (1), 3.3 (1)	0.473	0.148
32	52341	Poland	MR, R	S, MS	MS, MR, R	MS	S, MS, MR, R	7 (2), 2.4 (3), 3.1 (5)	0.447	0.148
33	52342	Poland	MS, MR, HR	MS, MR, HR	MR, HR	MS, MR, R	MS, R	3.1 (1), 3.5 (1), 4.3 (2), 5 (6)	0.473	0.192
34	501048	Poland	HS, S, MR, R	HS	HS, MS	HS	HS	0 (8), 1.1 (2)	0.217	0.064
35	502855	United Kingdom	MS, MR, HR	S	S, MS, MR, R	S	HS	1 (4), 1.3 (1), 2.2 (5)	0.410	0.132
36	502856	United Kingdom	MR, R	MS, R	MS, MR, R	MS, MR	HS, MS, MR, R	1 (5), 2.3 (1), 2.4 (1), 2.8 (1), 3.1 (1), 5 (1)	0.651	0.288
37	502857	United Kingdom	MS, MR	HS, R	MS	S, MS	HS, R	0 (8), 1.5 (1), 2.8 (1)	0.278	0.136
38	502858	United Kingdom	S, MS, MR	HS	S	MS	HS	0 (9), 1.1 (1)	0.141	0.036
39	502859	United Kingdom	S, MS	HS	S, MS, MR	S	HS	0 (9), 1.3 (1)	0.141	0.036

[1] Resistance phenotype: HS = 4 = highly susceptible—large pustules with little or no chlorosis; S = 3 = susceptible—moderately large pustules with little or no chlorosis; MS = 2 = moderately susceptible—moderately large pustules surrounded by extensive chlorosis; MR = 2N, 2C, ;1C = moderately resistant—small pustule surrounded by chlorosis or necrosis; R = ;-N, ;C, ;+C, ;1N = resistant—chlorotic or necrotic flecking; and 0 = HR = highly resistant—no visible reaction. [2] IP—infection profile—infection pattern determined for the five tested isolates characterized in Table 2; the number of resistant seedlings in brackets. [3] Sh—Normalized Shannon diversity index; Hs—Nei's diversity.

Table 2. The infection profiles (IP) of the tested *A. strigosa* accessions based on the reaction to *P. coronata* race infection.

IP	*Puccinia coronata* Race					Oat Differential Line with a Corresponding Phenotype
	51(22)	94(63)	CR230	CR241	CR257	
0	H [1]	H	H	H	H	-
1.1	L	H	H	H	H	Pc36, Pc39, Pc55, Pc61, Pc70, Pc71
1.2	H	L	H	H	H	-
1.3	H	H	L	H	H	-
1.4	H	H	H	L	H	-
1.5	H	H	H	H	L	-
2.1	L	L	H	H	H	Pc38, Pc63
2.2	L	H	L	H	H	-
2.3	L	H	H	L	H	-
2.4	L	H	H	H	L	-
2.5	H	L	L	H	H	-
2.6	H	L	H	L	H	-
2.7	H	H	L	H	L	-
2.8	L	L	H	H	L	-
2.9	H	L	H	H	L	Pc14
3.1	L	H	L	H	L	Pc48, Pc103-1
3.2	H	L	L	H	L	-
3.3	H	L	H	L	L	Pc35
3.4	L	L	L	H	H	-
3.5	H	L	L	L	H	-
3.6	H	H	L	L	L	Pc54, Pc62, Pc64, Pc96, Pc97, Pc98
3.7	L	H	H	L	L	-
3.8	L	L	H	L	H	-
4.1	H	L	L	L	L	Pc45, Pc51, Pc101, Pc104
4.2	L	L	H	L	L	Pc59, Pc60, Pc91
4.3	L	L	L	H	L	Pc52
4.4	L	L	L	L	H	Pc56, Pc68
5	L	L	L	L	L	-

[1] H = high infection (virulent reaction); L = low infection (avirulent reaction).

3. Results

Five *P. coronata* isolates were used to perform the host–pathogen tests on ten plants of each of the 39 *A. strigosa* accessions. The host reactions ranged from highly susceptible (HS) to highly resistant (HR) (Table 1). All of the tested *A. strigosa* accessions displayed heterogeneous phenotypes. None of the accessions was completely susceptible to all *P. coronata* races; however, 118 of all 390 tested plants were susceptible to all *P. coronata* pathotypes. The largest number of resistant plants (177) was found for the most aggressive race 94(63), which was virulent to 18 of 34 evaluated *Pc* genes. Resistance to the 51(22) race was shown by 146 plants, and 148 plants were resistant to CR230. The lowest number of resistant plants, 96 and 97 were obtained for race CR241 (virulent to 13 *Pc* genes) and CR257 (virulent to 11 *Pc* genes), respectively. For nine accessions (51199, 502858, 502859, 501048, 51326, 51518, 51751, 51579, and 51598), only single seedlings were rated as resistant or moderately resistant to one crown rust race. Thirty-three plants within nine accessions (Table 1) were fully resistant to all the crown rust races used. Within accessions 51578 from Uruguay and 51596 from Chile, one plant each was resistant to all races, and nine plants were immune only to CR257. The exceptional accession was 51887 originating from Poland, which was resistant or moderately resistant to all *P. coronata* races.

Based on the seedling reactions to the five *P. coronata* races, 28 infection profiles (IPs) were determined for the 390 *A. strigosa* plants (Table 2). IP 0 corresponded to virulent reactions to all of the rust races. Resistance to one of five races was assigned as IP 1.1–IP 1.5, while resistance to two races was described as IP 2.1–IP 2.8. IP 3.1–3.8 indicated a

combination of resistance to three crown rust races. Resistance to four races was assigned as IP 4.1–4.3, and resistance to all five races was assigned as IP 5.

The IPs of the *A. strigosa* accessions were compared with the IPs of the differential Pc lines. The infection profile of the reference lines containing genes *Pc36*, *Pc39*, *Pc55*, *Pc61*, *Pc70*, and *Pc71* corresponded to IP 1.1 (Table 2) and was present within nine accessions (Table 1). The Pc38 and Pc63 lines were identical with IP 2.1, as observed within six accessions. The resistance to 94(63) and CR257 was characteristic of the differential line for *Pc14*. This pattern was assigned as IP 2.9 and was observed for four accessions. IP 3.1 corresponded to Pc48 and Pc103-1 and was found in two accessions. IP 3.3 (Pc35), IP 3.6 (Pc54, Pc62, Pc64, Pc96, Pc97, and Pc98) and IP 4.2 (Pc59, Pc60, and Pc91) were observed in one accession each. IP 4.1 with a virulent reaction to 51(22) was identical with Pc45, Pc51, Pc101, and Pc104 and was present within four accessions. IP 4.3 corresponding to Pc52 was present within two accessions. IP 4.4 (Pc56, Pc68) was observed within six accessions.

The variation within the accessions was assessed based on the level of the resistance reaction of each plant inoculated with five isolates of *P. coronata*. The average values of both calculated coefficients were 0.383 for the Normalized Shannon index (Sh) and 0.143 for Nei's diversity index (Hs). In the group with the lowest variation, we found accessions wherein all individuals were characterized by a low level of resistance to the tested isolates (51199, 51581, 51582, 51613, 502858, and 502859), as well as accessions wherein all individuals were highly resistant to all (51887) or almost all (51578 and 51596) isolates (Table 1). The greatest diversity was observed in accessions 51586, 51750, 51523, and 51987. These were mixtures of individuals with different levels of resistance to all *P. coronata* isolates, displaying the highest level of heterogeneity.

The analysis of molecular variance (AMOVA) determined that the majority of the observed variability was due to variation among accessions (64%, $p = 0.001$). The variation within the accessions accounted for 36% of the total variation.

The first two axes of the principal component analysis (PCA) of the accessions explained 51.3% of the total variance (41% and 11.3%, respectively) (Figure 1). The plot presented a large variation; however, a clear identification of groups composed of resistant or moderately resistant accessions was possible. The most resistant accession 51887 was localized on the opposite side of the plot along with 51583 and 52342. The middle part of the plot was occupied by genotypes with large variations in the immune response, e.g., 52341 (Sh = 0.447; Hs = 0.148), 502856 (Sh = 0.651; Hs = 0.288), and 52340 (Sh = 0.473; Hs = 0.148).

A dendrogram based on the accessions' dissimilarity identified two main clusters, composed of 25 and 14 accessions, respectively (Figure 2). The second group consisted of eight accessions from Poland, two from Chile, two from Russia, one from the Netherlands, and one from Uruguay. These were generally the most resistant accessions largely corresponding to the PCA group of resistant genotypes. Some genotypes from the same countries with identical or very similar profiles could be seen, e.g., 502855 and 502856 as well as 502858 and 502859 from the United Kingdom or 51518 and 51630 from Poland.

For population structure analysis, the Bayesian model approach implemented in STRUCTURE software was used (Figure 3). The ΔK peak was the highest for $K = 2$, supporting the presence of two distinct populations. On the basis of the membership fraction, the accessions were categorized as homogeneous (probability ≥ 0.8) or admixed. P1 contained seven homogeneous accessions. In P2, fifteen homogeneous accessions were included. The remaining 17 accessions were classified as admixed. In general, P1 corresponded to resistance to most of the tested *P. coronata* race isolates, whereas P2 corresponded to susceptibility to these isolates. The analysis of the population structure in a graphical way refers to the results of the variation level within the accession obtained with the use of Shannon's index and the coefficient of Nei's diversity.

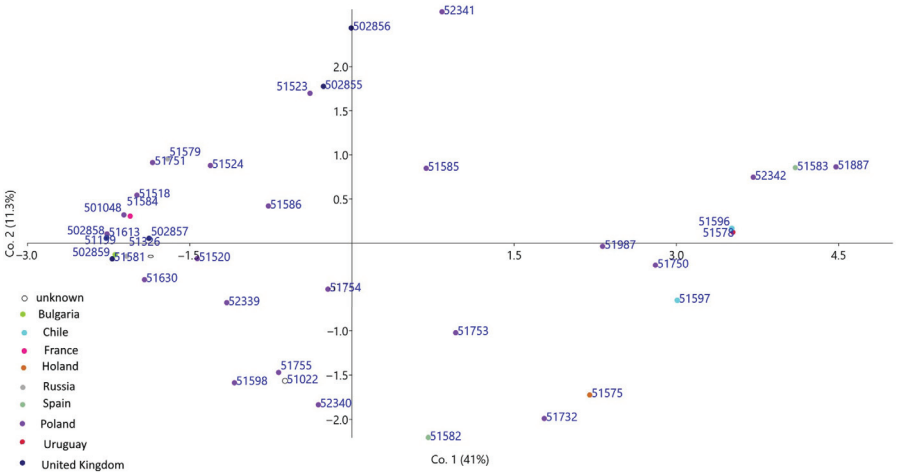

Figure 1. Principal component analysis of the *Avena strigosa* L. accessions. A scatter plot of PC1 (explaining 41% of the variance) versus PC2 (explaining 11.3% of the variance). Label colors indicate the origin countries of the samples.

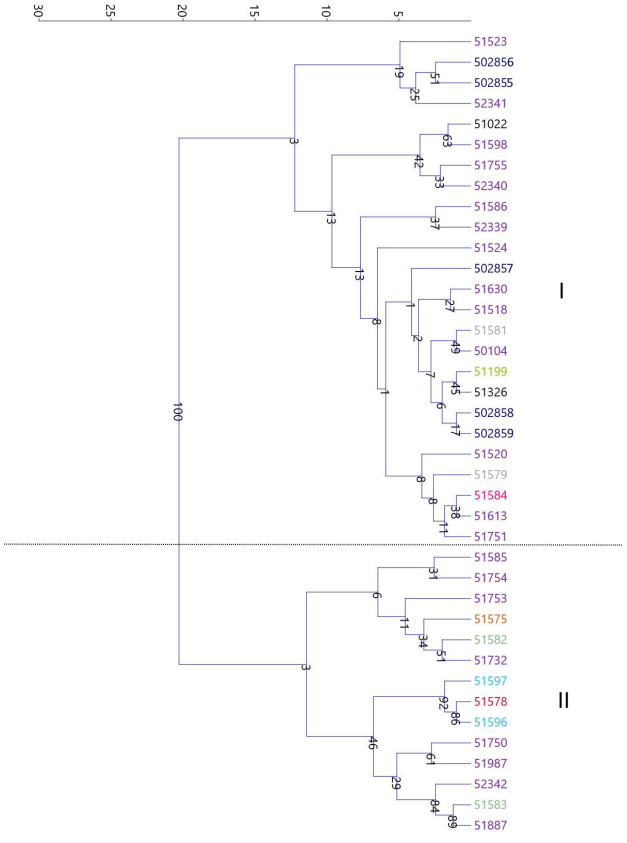

Figure 2. Ward's dendrogram of 39 accessions of *Avena strigosa* L. The accessions were assigned with the numbers used in Table 1 and the colors indicating the origin countries of the samples used in Figure 1.

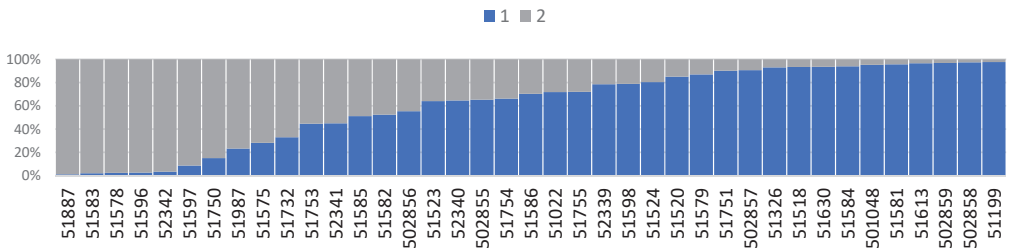

Figure 3. Bar graphs showing the population structure of 39 accessions of *Avena strigosa* L. based on the resistance to five isolates of *Puccinia coronata* f. sp. *avenae* as assessed using STRUCTURE. Each population is represented by a different color.

4. Discussion

The constant evolution of the *P. coronata* pathogen has caused the rapid loss of the effectiveness of the currently used crown rust resistance genes; therefore, the search for new ones is necessary. Wild oat progenitors have been proven to be a rich source of useful genes [32,33,35,52]; however, *A. strigosa* still remains unexploited. This study was carried out on 39 mostly European accessions from the Polish National Centre for Plant Genetic Resources with the majority originating from Poland (22 genotypes). A set of five *P. coronata* isolates was used to postulate the presence of potentially novel resistance genes.

Thirty-eight (97%) of the accessions studied showed a heterogeneous infection pattern; none of the accessions displayed homogeneous susceptibility, and only one, 51887, was homogeneously resistant to all *P. coronata* races. The heterogeneity of response to the rust inoculation within a single accession was already reported in the studies of wild oat species [32,33,53,54]; however, the level of phenotype variability within the analyzed *A. strigosa* was significantly higher, similar to the results obtained for *A. fatua*, where 85% of tested genotypes showed a heterogeneous infection pattern [31].

More than half of the *A. strigosa* genotypes screened in this research were characterized in terms of genetic (ISSR and SRAP), isoenzymatic, and morphological diversity by Podyma et al. [55,56]. According to Rodionova et al. [57], 17 botanical *A. strigosa* varieties can be distinguished based on clearly recognizable morphological traits. The results of the abovementioned authors revealed both genetic, botanical, and isoenzymatic variations in the analyzed objects. In terms of the morphology, within each accession, one to four varieties were recorded. Interestingly, within the most phenotypically variable *A. strigosa* accessions identified in our study (51586, 51520, 51523, and 51524), according to previous research, only one or two botanical varieties could be distinguished.

In this study, a detached leaf assay was used for resistance evaluation, allowing for the simultaneous testing of multiple rust isolates on a single plant. This is an important consideration when genotypes may be mixed as for many genebank accessions of landrace or previously uncharacterized material [35,58]. Additionally, the use of *P. coronata* races for the establishment of infection profiles (IP) allows postulating known and new *Pc* genes/alleles by matching the IPs of the tested plants with the profiles identified in differential lines. Twenty-eight infection profiles were defined within the 39 *A. strigosa* accessions, of which ten corresponded to the profile of known *Pc* genes. One hundred and sixty-eight out of 390 plants revealed an IP indicative of uncharacterized genes. Among the most resistant genotypes, 43 plants were immune to four of the five *P. coronata* races; each of these profiles corresponded to that of a highly efficient known *Pc* gene. However, this does not rule out that the identified profiles may correspond to new genes. To assess the genetic background of this resistance, it would be necessary to perform crosses with susceptible parents to determine the heredity model and conduct allelism tests to determine gene novelty.

Thirty-three plants within nine accessions were resistant to all crown rust races. A highly resistant response was shown by accessions 51578 from Uruguay and 51596 from Chile, with one plant in each resistant to all races and nine plants immune only to CR257.

The most homogeneous accession was 51887 from Poland, resistant or moderately resistant to all isolates. According to the Polish Genebank, 51578 was acquired by the USDA (United States Department of Agriculture, Agricultural Research Service Small Grains Collection in Aberdeen, ID) in 1951 from the Instituto Fitotecnico y Semillero Nacional, Montevideo, and the equivalent of this number is PI 194201. This accession obtained from the USDA was tested by Admassu-Yimer et al. [59] for seedling resistance against eight *P. coronata* races. PI 194201 along with PI 193040, PI 237090, and PI 247930 were resistant to all the races used; however, according to USDA, all of the genotypes are classified as *A. sativa.* In the study of Podyma et al. [56], 51578 obtained from Polish genebank was assessed in terms of a range of morphological traits, and two *A. strigosa* varieties within the analyzed plants were recorded, which confirms the correct species classification. Both PI 194201 and 51578 exhibited high crown rust resistance; moreover, PI 194201, according to the GRIN database, possesses resistance to other important diseases of oats, including stem rust, barley yellow dwarf virus, and smut. The classification of both accessions should be reexamined; regardless, both could prove valuable for oat breeding programs. The equivalent number of 51596 from Chile is PI 436103. Apart from the crown rust resistance exhibited by this accession in this study, it displayed a high level of seedling resistance to five of six *P. graminis* races used in the study of Gold Steinberg et al. [26], which further increases the agronomic value of the genotype. The highest level of resistance was observed in 51887 acquired by the IHAR genebank in 1994 and classified as a Polish landrace. No further data regarding the resistance of this accession to other oat diseases are available, so it is worth conducting additional analysis, as previous studies indicate that the *A. strigosa* species can exhibit a wide range of resistance to various pathogens.

5. Conclusions

The results obtained in this research confirmed the complexity and heterogeneity of the accessions gathered in genebanks. Here, we compared the resistance within as well as between the accessions based on PCA and agglomerative hierarchical clustering. The generalized average of resistance across individuals from a given accession, standardly available in the genebank databases, may obscure the presence of individuals with significant resistance to pathogens and reduce interest in looking for new resistance sources within it. Even accessions with poor overall resistance, such as 51586, may contain very resistant and often overlooked plants. At a time when many available sources of oat resistance have been overcome, it might be worth looking for desirable traits within susceptible accessions, which could be hidden donors of effective pathogen resistance.

Author Contributions: Conceptualization and methodology, E.P.-G., S.S., and V.M.; investigation, E.P.-G.; resources E.P.-G.; writing—original draft preparation, S.S.; writing—review and editing, E.P.-G. and V.M.; visualization, S.S. All authors have read and agreed to the published version of the manuscript.

Funding: This research received no external funding.

Conflicts of Interest: The authors declare no conflict of interest. The funders had no role in the design of the study; in the collection, analyses, or interpretation of data; in the writing of the manuscript, or in the decision to publish the results.

References

1. Boczkowska, M.; Podyma, W.; Łapiński, B. Oat. In *Genetic and Genomic Resources for Grain Cereals Improvement*; Singh, M., Upadhyaya, H.D., Eds.; Elsevier: Amsterdam, The Netherlands, 2016; pp. 159–225. ISBN 9780128020005.
2. Chaves, M.S.; Martinelli, J.A.; de Wesp, C.L.; Graichen, F.A.S. The cereal rusts: An overview. *Pest Technol.* **2008**, *2*, 38–55.
3. Paczos-Grzęda, E.; Sowa, S. Virulence structure and diversity of *Puccinia coronata* f. sp. *avenae* P. syd. & syd. in Poland during 2013 to 2015. *Plant Dis.* **2019**, *103*, 1559–1564. [CrossRef] [PubMed]
4. Sowa, S.; Paczos-Grzeda, E.; Paczos-Grzęda, E. Virulence structure of *Puccinia coronata* f. sp. *avenae* and effectiveness of *Pc* resistance genes in Poland during 2017–2019. *Phytopathology* **2021**, *111*, 1158–1165. [CrossRef] [PubMed]
5. CDL Cereal Disease Laboratory. Resistance Genes. Oat. *Pc* (Crown Rust). Available online: https://www.ars.usda.gov/midwest-area/stpaul/cereal-disease-lab/docs/resistance-genes/resistance-genes/ (accessed on 16 July 2021).

6. Aung, T.; Chong, J.; Leggett, M. The transfer of crown rust resistance Pc94 from a wild diploid to cultivated hexaploid oat. In *Proceedings of the 9th International European and Mediterranean Cereal Rust and Powdery Mildews Conference, Lunteren, The Netherlands, 2–6 September 1996*; Kema, G.H.J., Niks, R.E., Daamen, R.A., Eds.; Wageningen, European and Mediterranean Cereal Rust Foundation: Lunteren, The Netherlands, 1996; pp. 167–171.
7. Jellen, E.; Leggett, J.M. Cytogenetic Manipulation in Oat Improvement. In *Genetic Resources, Chromosome Engineering, and Crop Improvement*; Singh, R.J., Jauhar, P.P., Eds.; Genetic Resources Chromosome Engineering & Crop Improvement; CRC Press: Boca Raton, FL, USA, 2006; pp. 199–231. ISBN 978-0-8493-1432-2.
8. Rothman, P.G. Registration of four stem rust and crown rust resistant oat germplasm lines. *Crop Sci.* **1984**, *24*, 1217. [CrossRef]
9. Chong, J.; Gruenke, J.; Dueck, R.; Mayert, W.; Woods, S. Virulence of oat crown rust *Puccinia coronata* f. sp. *avenae* in Canada during 2002–2006. *Can. J. Plant Pathol.* **2008**, *30*, 115–123. [CrossRef]
10. McCartney, C.A.; Stonehouse, R.G.; Rossnagel, B.G.; Eckstein, P.E.; Scoles, G.J.; Zatorski, T.; Beattie, A.D.; Chong, J. Mapping of the oat crown rust resistance gene *Pc91*. *Theor. Appl. Genet.* **2011**, *122*, 317–325. [CrossRef]
11. Menzies, J.G.; Xue, A.; Dueck, R.; Greunke, J. Virulence of *Puccinia coronata* f. sp. *avenae* in Canada; 2010 to 2014. In Proceedings of the 14th International Cereal Rust and Powdery Mildew Conference, Denmark, Copenhagen, 5–8 July 2015; p. 95.
12. Park, R. New oat crown rust pathotype with virulence for *Pc91*. *Cereal Rust Rep.* **2013**, *11*, 8–10.
13. Carson, M.L. Crown rust development and selection for virulence in *Puccinia coronata* f. sp. *avenae* in an oat multiline cultivar. *Plant Dis.* **2009**, *93*, 347–353. [CrossRef]
14. Dyck, P.L.; Zillinsky, F.J. Inheritance of crown rust resistance transfrred from diploid to hexaploid oats. *Can. J. Genet. Cytol.* **1963**, *5*, 398–407. [CrossRef]
15. Mitchell Fetch, J.W.; Duguid, S.D.; Brown, P.D.; Chong, J.; Fetch, T.G.; Haber, S.M.; Menzies, J.G.; Ames, N.; Noll, J.; Aung, T.; et al. Leggett oat. *Can. J. Plant Sci.* **2007**, *87*, 509–512. [CrossRef]
16. Mitchell Fetch, J.W.; Tekauz, A.; Brown, P.D.; Ames, N.; Chong, J.; Fetch, T.G.; Haber, S.M.; Menzies, J.G.; Townley-Smith, T.F.; Stadnyk, K.D.; et al. Stride oat. *Can. J. Plant Sci.* **2013**, *93*, 749–753. [CrossRef]
17. Rines, H.W.; Miller, M.E.; Carson, M.; Chao, S.; Tiede, T.; Wiersma, J.; Kianian, S.F. Identification, introgression, and molecular marker genetic analysis and selection of a highly effective novel oat crown rust resistance from diploid oat, *Avena strigosa*. *Theor. Appl. Genet.* **2018**, *131*, 721–733. [CrossRef] [PubMed]
18. Vavilov, N.I. *Studies on the Origin of Cultivated Plants*; FAO: Leningrad, Russia, 1926. [CrossRef]
19. Vavilov, N.I. *World Resources of Varieties of Small Grains, Grain Legumes and Flax, and Their Use in Breeding*; Leningrad Izdvo AN SSSR: Moscow, Russia, 1957. (In Russian)
20. Kubiak, K. Genetic diversity of Avena strigosa Schreb. ecotypes on the basis of isoenzyme markers. *Biodivers. Res. Conserv.* **2009**, *15*, 23–28. [CrossRef]
21. Scholten, M.; Spoor, B.; Green, N. Machair corn: Management and conservation of a historical machair component. *Glas. Nat.* **2009**, *25*, 63–71.
22. Weibull, J.; Bojesen, L.; Rasomavieius, V. *Avena strigosa* in Denmark and Lithuania: Prospects for in situ conservation. *Plant Genet. Resour. Newsl.* **2002**, *131*, 1–6.
23. Smitterberg, M. *Differences among Variety Samples of Avena strigosa Regarding β-Glucan, Tocopherols, Tocotrienols and Avenanthramides*; Swedish University of Agricultural Sciences: Uppsala, Sweden, 2018.
24. Harder, D.; Chong, J.; Brown, P.; Sebesta, J.; Fox, S. Wild oat as a source of disease resistance: History, utilization, and prospects. In Proceedings of the Fourth International Oat Conference, Wild Oats in World Agriculture, Adelaide, Australia, 19–23 October 1992.
25. Leggett, J. The conservation and exploration of wild oat species. In Proceedings of the Fourth International Oat Conference, Wild Oats in World Agriculture, Adelaide, Australia, 19–23 October 1992; pp. 57–60.
26. Gold Steinberg, J.; Mitchell Fetch, J.; Fetch, T.G. Evaluation of *Avena* spp. accessions for resistance to oat stem rust. *Plant Dis.* **2005**, *89*, 521–525. [CrossRef]
27. Andolfo, G.; Iovieno, P.; Frusciante, L.; Ercolano, M.R. Genome-Editing Technologies for Enhancing Plant Disease Resistance. *Front. Plant Sci.* **2016**, *7*, 1813. [CrossRef]
28. Cabral, A.L.; Park, R.F. Genetic analysis of seedling resistance to crown rust in five diploid oat (*Avena strigosa*) accessions. *J. Appl. Genet.* **2016**, *57*, 27–36. [CrossRef]
29. Cabral, A.L.; Park, R.F. Seedling resistance to *Puccinia coronata* f. sp. *avenae* in *Avena strigosa*, *A. barbata* and *A. sativa*. *Euphytica* **2014**, *196*, 385–395. [CrossRef]
30. Sánchez-Martín, J.; Rubiales, D.; Sillero, J.C.; Prats, E. Identification and characterization of sources of resistance in *Avena sativa*, *A. byzantina* and *A. strigosa* germplasm against a pathotype of *Puccinia coronata* f.sp. *avenae* with virulence against the *Pc94* resistance g. *Plant Pathol.* **2012**, *61*, 315–322. [CrossRef]
31. Paczos-Grzęda, E.; Sowa, S.; Koroluk, A.; Langdon, T. Characteristics of resistance to *Puccinia coronata* f. sp. *avenae* in *Avena fatua*. *Plant Dis.* **2018**, *102*, 2616–2624. [CrossRef]
32. Chong, J.; Leonard, K.J.; Salmeron, J.J. A North American System of Nomenclature for *Puccinia coronata* f. sp. *avenae*. *Plant Dis.* **2007**, *84*, 580–585. [CrossRef] [PubMed]
33. Paczos-Grzęda, E.; Boczkowska, M.; Sowa, S.; Koroluk, A.; Toporowska, J. Hidden diversity of crown rust resistance within genebank resources of *Avena sterilis* L. *Agronomy* **2021**, *11*, 315. [CrossRef]

34. Sowa, S.; Paczos-Grzęda, E.; Koroluk, A.; Okoń, S.; Ostrowska, A.; Ociepa, T.; Chrząstek, M.; Kowalczyk, K. Resistance to *Puccinia coronata* f. sp. *avenae* in *Avena magna*, *A. murphyi*, and *A. insularis*. *Plant Dis.* **2016**, *100*, 1184–1191. [CrossRef] [PubMed]
35. Paczos-Grzęda, E.; Sowa, S.; Boczkowska, M.; Langdon, T. Detached leaf assays for resistance to crown rust reveal diversity within populations of *Avena sterilis* L. *Plant Dis.* **2019**, *103*, 832–840. [CrossRef]
36. Hsam, S.L.K.; Peters, N.; Paderina, E.V.; Felsenstein, F.; Oppitz, K.; Zeller, F.J. Genetic studies of powdery mildew resistance in common oat (*Avena sativa* L.) I. Cultivars and breeding lines grown in Western Europe and North America. *Euphytica* **1997**, *96*, 421–427. [CrossRef]
37. Sowa, S.; Paczos-Grzęda, E. A study of crown rust resistance in historical and modern oat cultivars representing 120 years of Polish oat breeding. *Euphytica* **2020**, *216*, 12. [CrossRef]
38. Nazareno, E.S.; Li, F.; Smith, M.; Park, R.F.; Kianian, S.F.; Figueroa, M. *Puccinia coronata* f. sp. *avenae*: A threat to global oat production. *Mol. Plant Pathol.* **2018**, *19*, 1047–1060. [CrossRef]
39. Murphy, H.C. Physiologic specialisation in *Puccinia coronata* f. sp. *avenae*. *Bull. U.S. Dep. Agric.* **1935**, *433*, 1–48.
40. Sowa, S.; Paczos-Grzęda, E. Identification of molecular markers for the *Pc39* gene conferring resistance to crown rust in oat. *Theor. Appl. Genet.* **2020**, *133*, 1081–1094. [CrossRef]
41. Simpson, E.H. Measurement of diversity. *Nature* **1949**, *163*, 688. [CrossRef]
42. Nei, M. Analysis of gene diversity in subdivided populations. *Proc. Natl. Acad. Sci. USA* **1973**, *70*, 3321–3323. [CrossRef] [PubMed]
43. Kosman, E. Nei's gene diversity and the index of average differences are identical measures of diversity within populations. *Plant Pathol.* **2003**, *52*, 533–535. [CrossRef]
44. Kosman, E.; Dinoor, A.; Herrmann, A.; Schachtel, G.A. Virulence Analysis Tool (VAT) User Manual. Available online: Ttp://www.tau.ac.il/lifesci/departments/plant_s/members/kosman/VAT.html (accessed on 15 September 2022).
45. Schachtel, G.A.; Dinoor, A.; Herrmann, A.; Kosman, E. Comprehensive Evaluation of Virulence and Resistance Data: A New Analysis Tool. *Plant Dis.* **2012**, *96*, 1060–1063. [CrossRef]
46. Hammer, Ø.; Harper, D.A.T.; Ryan, P.D. PAST: Paleontological Statistocs Software Package for education and data analysis. *Palaeontol. Electron.* **2001**, *4*, 1–9.
47. Peakall, R.; Smouse, P.E. GenAlEx 6.5: Genetic analysis in Excel. Population genetic software for teaching and research—An update. *Bioinformatics* **2012**, *28*, 2537–2539. [CrossRef]
48. Excoffier, L.; Smouse, P.E.; Quattro, J.M. Analysis of molecular variance inferred from metric distances among DNA haplotypes: Application to human mitochondrial DNA restriction data. *Genetics* **1992**, *131*, 479–491. [CrossRef]
49. Porras-Hurtado, L.; Ruiz, Y.; Santos, C.; Phillips, C.; Carracedo, A.; Lareu, M.V. An overview of STRUCTURE: Applications, parameter settings, and supporting software. *Front. Genet.* **2013**, *4*, 98. [CrossRef]
50. Li, Y.L.; Liu, J.X. StructureSelector: A web-based software to select and visualize the optimal number of clusters using multiple methods. *Mol. Ecol. Resour.* **2018**, *18*, 176–177. [CrossRef]
51. Kopelman, N.M.; Mayzel, J.; Jakobsson, M.; Rosenberg, N.A.; Mayrose, I. Clumpak: A program for identifying clustering modes and packaging population structure inferences across K. *Mol. Ecol. Resour.* **2015**, *15*, 1179–1191. [CrossRef]
52. Okoń, S.M.; Ociepa, T.; Paczos-Grzęda, E.; Ladizinsky, G. Evaluation of resistance to *Blumeria graminis* (DC.) f. sp. *avenae*, in *Avena murphyi* and *A. magna* genotypes. *Crop Prot.* **2018**, *106*, 177–181. [CrossRef]
53. Tan, M.Y.A.; Carson, M.L. Screening wild oat accessions from Morocco for resistance to *Puccinia coronata*. *Plant Dis.* **2013**, *97*, 1544–1548. [CrossRef] [PubMed]
54. Carson, M.L. Broad-spectrum resistance to crown rust, *Puccinia coronata* f. sp. *avenae*, in accessions of the tetraploid slender oat, *Avena barbata*. *Plant Dis.* **2009**, *93*, 363–366. [CrossRef] [PubMed]
55. Podyma, W.; Boczkowska, M.; Wolko, B.; Dostatny, D.F. Morphological, isoenzymatic and ISSRs-based description of diversity of eight sand oat (*Avena strigosa* Schreb.) landraces. *Genet. Resour. Crop Evol.* **2017**, *64*, 1661–1674. [CrossRef]
56. Podyma, W.; Bolc, P.; Nocen, J.; Puchta, M.; Wlodarczyk, S.; Lapinski, B.; Boczkowska, M. A multilevel exploration of *Avena strigosa* diversity as a prelude to promote alternative crop. *BMC Plant Biol.* **2019**, *19*, 291. [CrossRef]
57. Rodionova, N.; Soldatov, V.; Merezhko, V.; Jarosh, N.; Kobyljanskij, V. *Flora of Cultivated Plants*; Kolos: Moscow, Russia, 1994; Volume 2.
58. Jackson, E.W.; Obert, D.E.; States, U.; Agricultural, A.; Chong, J.; Avant, J.B.; Bonman, J.M. Detached-leaf method for propagating *Puccinia coronata* and assessing crown rust resistance in oat. *Plant Dis.* **2008**, *92*, 1400–1406. [CrossRef]
59. Admassu-Yimer, B.; Gordon, T.; Harrison, S.; Kianian, S.; Bockelman, H.; Bonman, J.M.; Esvelt Klos, K. New Sources of Adult Plant and Seedling Resistance to *Puccinia coronata* f. sp. *avenae* Identified among *Avena sativa* Accessions from the National Small Grains Collection. *Plant Dis.* **2018**, *102*, 2180–2186. [CrossRef]

agriculture

MDPI

Article

Application Marker-Assisted Selection (MAS) and Multiplex PCR Reactions in Resistance Breeding of Maize (*Zea mays* L.)

Aleksandra Sobiech [1,*], Agnieszka Tomkowiak [1], Jan Bocianowski [2], Bartosz Nowak [3], Dorota Weigt [1], Danuta Kurasiak-Popowska [1], Michał Kwiatek [1], Sylwia Mikołajczyk [1], Janetta Niemann [1] and Katarzyna Szewczyk [1]

[1] Department of Genetics and Plant Breeding, Poznan University of Life Sciences, Dojazd 11, 60-632 Poznan, Poland
[2] Department of Mathematical and Statistical Methods, Poznan University of Life Sciences, Wojska Polskiego 28, 60-637 Poznan, Poland
[3] Smolice Plant Breeding Sp. Z O. O. IHAR Group, Smolice 146, 63-740 Kobylin, Poland
* Correspondence: aleksandra.sobiech@up.poznan.pl

Abstract: Cultivated maize (*Zea mays* L.) is the oldest and one of the most important crop species in the world. Changing climatic conditions in recent years, warm weather, expansion of acreage and intensification of maize cultivation have resulted in an increase in the threat posed by diseases caused by, among others, *Fusarium* fungi. Breeding success in all plant species is determined by access to starting materials with possible high genetic diversity also in terms of disease resistance. Identification of parental combinations that produce offspring that are high-yielding and resistant to *Fusarium*, among other diseases, is one of the costliest steps in breeding programs. We used maize lines which, as a result of five-year field observations, were divided into resistant and susceptible to *F. verticillioides*. It is known that resistance to fusarium is a trait strongly dependent on environmental conditions. Due to the fact that the years of observation of the degree of infestation were hot and dry, the resistance of some lines could result from favorable environmental conditions. In view of the above, the aim of this study was to analyze the genetic basis of the resistance of these lines and to correlate molecular analyses with field observations. Comprehensive field and molecular analyses will allow the selection of reference lines that will be resistant to fusarium in the field and, at the same time, will have pyramidized resistance genes. Such lines can be used for crossbreeding to obtain fusarium-resistant varieties. In addition, an attempt was made to develop Multiplex PCR conditions for faster identification of the analyzed markers. As a result of the analyses, it was found that the resistance of the studied maize lines was correlated with the number of molecular markers identified in them. Both field and laboratory analyses have shown that the best line that can be used for crossbreeding as a source of fusarium resistance genes is the line number 25. It has a resistance level of 8–9 on the nine-point COBORU scale. In this line, as a result of molecular analyses, 10 out of 12 markers were identified (SSR 85, Bngl 1063, Bngl 1740, Umc 2082, Bngl 1621, Umc 2059, Umc 2013, SSR 93, SSR 105, STS 03) related to fusarium resistance genes, which may be the reason for such a high resistance to this pathogen. Similarly, 9 markers were identified for line number 35 (SSR 85, Bngl 1063, Bngl 1740, Umc 2082, Bngl 1621, Umc 2059, Umc 2013, SSR 93, STS 03). This line, however, was characterized by a slightly lower resistance at the level of 7–8. Line 254 turned out to be the least resistant, as the resistance was at the level of 4–5, and the number of identified molecular markers was 5. Lines numbered 25 and 35 can be successfully used as a source of fusarium resistance genes.

Keywords: maize; molecular markers; multiplex PCR; *Fusarium*

Citation: Sobiech, A.; Tomkowiak, A.; Bocianowski, J.; Nowak, B.; Weigt, D.; Kurasiak-Popowska, D.; Kwiatek, M.; Mikołajczyk, S.; Niemann, J.; Szewczyk, K. Application Marker-Assisted Selection (MAS) and Multiplex PCR Reactions in Resistance Breeding of Maize (*Zea mays* L.). *Agriculture* **2022**, *12*, 1412. https://doi.org/10.3390/agriculture12091412

Academic Editors: Edyta Paczos-Grzeda, Volker Mohler, Sylwia Sowa and Davinder Singh

Received: 7 July 2022
Accepted: 6 September 2022
Published: 7 September 2022

1. Introduction

The maize (*Zea mays* L.), along with rice, is the most commonly cultivated crop for human and animal consumption. It is also a species grown for grain and feed. In 2022, the

largest producers of maize for grain were the United States of America (367.3 million tons), Mexico (337.8 million tons) and China (266.2 million tons). Maize ranks first place in terms of production volume among grain crops in the world (about 1 billion tons). In comparison, in 2000, the leading positions in the production of this species were occupied by the same countries; however, the amount of grain they produced was 251 million tons, 106 million tons and 32 million tons, respectively. These data confirm that over the past 20 years, the global maize production for grain has increased significantly [1].

The prevailing warm weather in the last decade of the 20th century, the expansion of acreage and intensification of corn cultivation, as well as the introduced agrotechnical simplifications, resulted in an increase in the threat caused by diseases to the amount and quality of yields. In addition, epidemics are facilitated by the emergence of new agrophage species, and the invasive movement of those already present, into neighboring areas. Based on studies conducted over the past few years, it is estimated that corn diseases cause yield losses of up to 30% each year [2]. The quality of the grain yield is also significantly affected because early plant infection by fungi and bacteria causes the grain to become diminished, deteriorating the feed value and quality of the forage obtained [3].

Diseases caused by fungi of the genus *Fusarium*, which are the main culprits of seedling rot, root rot and stem base rot, but also the most dangerous cob fusariosis, are now considered the most dangerous. Maize cob fusariosis, except in cases of severe occurrence, causes little yield loss, but greatly impairs the quality of grain and feed as a product for further processing [2,4]. Fungal species responsible for the infestation, in addition to secreting substances necessary for life, have the ability to produce secondary metabolites, so-called mycotoxins, accumulated in grains and other parts of the plant (trichothecenes, among others: T-2 toxin and diacetoxyscirpenol-DAS, ochratoxin A, zearalenone, deoxynivalenone-DON, HT-2 toxin, alphatoxins and others). These substances can cause many diseases in humans, including various types of allergies, hormonal disorders, cancer (they activate oncogenic cells) [5]. Their presence in feed also poses a major threat to animal health and life, especially for pigs and poultry, as they cause increased susceptibility to infectious agents that under standard conditions, without the additional action of toxigenic fungal metabolites, would not be able to cause disease. In addition, they negatively affect production and reproductive performance and, most importantly, the health and quality of the final product going to the consumer [6].

Fusarium resistance is a polygenic and is strongly influenced by environmental factors. This type of resistance is very complex which makes breeding difficult and results in most commercial maize hybrids having a lower level of resistance than is desirable [7].

Integrated pest management involves the development of non-chemical methods as an alternative to the most commonly used fungicides. Breeding for plant resistance to pathogens is a sustainable way to produce more crops without using inputs that are harmful to the environment and humans [8]. Stagnati et al. [9] mapped quantitative trait loci (QTLs) for *F. verticillioides* resistance in two maize populations. As a result of the study, they found that they were not consistent between populations. Analyzing the transcriptome and identifying areas associated with *F. verticillioides* resistance may help to better understand the processes that occur when plants are infected by these fungi.

Salah et al. [10] using marker-assisted selection (MAS) identified molecular markers linked to *F. verticillioides* resistance (QTL) genes: RAPD (OPA02), ISSR (AD8), SSR (SSR93, SSR105, SSR225 and SSR337) and STS (STS03). It was shown that the SSR and STS markers were located on chromosome 10. The use of SNP markers coupled to yield structure traits in maize and barley, showed greater precision than methods based on the study of metabolic pathways [11]. Maschietto et al. [12] demonstrated, the utility of SSR, GBS, and transcriptomics markers and QLT mapping to improve the selection of *F. verticillioides* resistant lines. Abdel-Rahman et al. [13] showed that regression analysis for the relationship between SSR markers and phenotypes of maize F_2 populations evaluated for *F. verticillioides* head blight severity was highly significant. This indicates that SSR markers were associated with resistance to the disease. SRR markers have been the most widely used markers

for many years due to their ease of use and relatively low price. Nowadays, more and more research is being conducted using SNP markers, as they occur at a much higher frequency in the genome than SRRs. Authors Jones et al. [14], Hamblin et al. [15] and Van Inghelandt et al. [16] point to the advantage of SNP markers over SRRs in studying the genetic diversity of inbred lines in maize.

Today, in public databases, more than one million SNPs can be found for maize. With the development of association mapping using SNPs, it will be possible to accelerate the identification and use of new agronomically useful alleles [17].

Marker-assisted selection (MAS) reduces financial expenses and increases productivity. By increasing the efficiency of selecting varieties for crossbreeding, breeders can improve breeding programs in less time [18].

The process, referred to as multiplex polymerase chain reaction (PCR), saves considerable time and money by simultaneously amplifying multiple sequences in a single reaction. Optimization of the method consisted of selecting the appropriate primer volume for all markers in each variant and adjusting the appropriate primer annealing temperature in order to obtain uniformly intense bands on the gel. Developing an effective multiplex PCR usually requires strategic planning and multiple attempts to optimize reaction conditions. The testing of a number of molecular markers related to maize plant resistance to *F. verticillioides* and the development of multiplex PCR conditions will provide breeders with tools ready to guide selection.

In view of the above, the aim of this study was to analyze the genetic basis of resistance to the fusarium of the studied lines and to correlate molecular analyses with field observations. Comprehensive field and molecular analyses will allow the selection of reference lines that will be resistant to fusarium in the field, and at the same time, they will be characterized by pyramidized resistance genes. Such lines can be used for crossing to obtain fusarium-resistant varieties. Additionally, an attempt was made to develop Multiplex PCR conditions for faster identification of the analyzed markers

2. Materials and Methods

2.1. Plant Material

Plant material consisted of 30 genotypes (15 resistant and 15 susceptible) to *F. verticillioides* donated to the Department of Plant Genetics and Breeding by Plant Breeding Smolice Ltd. IHAR Group. Lines used for the research were derived from hybrid varieties available on the Polish market. They are mainly characterized by grain types of Dent. Hybrids from which the inbred lines were derived belong to the BSSS and non-BSSS origin groups, mainly Iodent and Lancaster. The plant material is shown in Table 1. These lines were monitored for 5 years for resistance to fusarium. Throughout the years of observation, the resistance of each line remained constant (on a COBORU scale of 1–9; 1, susceptible; 9, resistant). In order to establish the genetic basis of resistance to the fusarium of these lines, the above experiment was set up.

Table 1. Plant material used in the experiment.

Resistant Genotypes		Susceptible Genotypes	
No.	**Genotype Number**	**No.**	**Genotype Number**
1	9	16	16
2	25	17	23
3	28	18	24
4	35	19	41
5	45	20	57
6	47	21	58
7	52	22	67
8	66	23	68
9	71	24	78
10	74	25	103
11	80	26	253
12	114	27	254
13	255	28	256
14	257	29	258
15	260	30	259

2.2. Methodology

2.2.1. Field Experiment

The experiment with 30 *F. verticillioides*-resistant and -susceptible maize genotypes was established in 10 m^2 fields belonging to Plant Breeding Smolice, Smolice, Ltd., Co., Poland Plant Breeding and Acclimatization Institute—National Research Institute Group (51°41′23.16″ N, 17°4′18.241″ E)—in a randomized complete block design in three replicates, in 2021. During the conduct of the experiments, observations were made on the degree of maize cob infection by *F. verticillioides*. The observations were carried out on eight dates: term 1—development of the first blister stage kernels, which contain about 16% of dry matter (BBCH 71); date 2—the beginning of early milk (BBCH 73); term 3—milk stage, middle kernels are milky, containing about 40% of dry matter (BBCH 75); term 4—nearly all kernels have reaches final volume (BBCH 79); date 5—the beginning of the kernel's denting maturity, kernels are soft, containing 45% of dry matter (BBCH 83); date 6—full denting maturity of the kernels, kernels with a typical color, containing about 55% of dry matter (BBCH 85); term 7—physiological maturity, visible black layering at the base of the kernel, with kernels containing about 60% of dry matter (BBCH 87); date 8—full maturity, hard and shiny kernels containing about 65% dry weight (BBCH 89).

Meteorological conditions during the 2021 growing season were favorable for the growth and development of maize, although frosts in April delayed sowing. The month of May, which is very important for the growth and development of maize, should be counted as cool (12 °C) and wet as the amount of precipitation was 76 mm. In contrast to May, June and July 2021 turned out to be dry (June 52.7 mm; July 65 mm) and warm (June 19.3 °C; July 20.9 °C) months. The dry and warm weather did not favor the spread of fungal diseases during this period. Intensive infestation of European corn borer (*Ostrinia nubilalis*) was also not observed. European corn borer feeds on maize and increases its susceptibility to fusarium by laying eggs from mid-June to the end of August. In August, an increased infestation of maize by *Fusarium* spp. was observed, which was due to very high rainfall (140.1 mm) and fairly high temperature (17 °C). The very dry months of September (42.3 mm) and October (19.2 mm) affected the inhibition of the development of fungal diseases including cob fusariosis.

2.2.2. DNA Isolation

Isolation of genomic DNA from 30 susceptible and resistant genotypes to *F. verticillioides* was performed using the reagent kit (Genomic Mini AX Plant) from A&A Biotechnology (Gdańsk, Poland).

The concentration and purity of the isolated DNA samples were measured by a DS-11 spectrophotometer from DeNovix. The isolated DNA matrix was brought to a uniform concentration of 50 ng μL^{-1} by dilution with distilled water.

DNA concentration ranged from 155 ng/μL for line 28 to 950 ng/μL for line 24. Purity of individual samples was also very good and ranged from 1.7 to 2.1 for absorbance 260/280 and 260/230.

2.2.3. Molecular Marker Analysis and PCR Amplification

Identification of markers (Table 2) coupled to *F. verticillioides* resistance genes was carried out using polymerase chain reaction (PCR) and primers proposed by Abdel-Rahman et al. [13] and Salah et al. [10] (Table 2).

The polymerase chain reaction (PCR) was conducted in a BIO-RAD T1000 thermocycler. Reagents from Promega were used to prepare the mixture. The composition of the reaction mixture volume (μL) of reaction components per 20 μL sample: Buffer (5× Green Go Taq, Flexi Buffer), 4 μL; 25 mM $MgCl_2$, 1.6 μL; 10 mM Ultrapure dNTPs Mix, 0.32 μL; DNA polymerase (Go Taq G2 Flexi), 0.17 μL; Nuclease-free water, 11.91 μL (reaction mixture for a single primer pair), 10.91 μL (reaction mixture for multiplex PCR); Starter F, 0.5 μL; Starter F, marker 2–0.5 μL (reaction mixture for multiplex PCR); Starter R, 0.5 μL; Starter 1,

marker 2–0.5 µL (reaction mixture for multiplex PCR); DNA, 1 µL. Reaction profile for PCR is shown below:

Table 2. Molecular markers associated with *F. verticillioides* resistance genes for maize.

Polymorphism	Marker	Primer Sequences		Product Size (bp)	Melting Temperature (°C)	Reference
		Rewers	Forward			
	bnlg1621	GGATCTTCGTTGCAGTTCTT	CATCAGTGATCCTCCACCAT	135–160	54	[13]
	bnlg1063	GGAGACAACCCCGACGAC	GGTACCAGAGCCACAGATCC	105–120	55	[13]
	bnlg1740	TTTTCTCCTTGAGTTCGTTCG	ACAGGCAGAGCTCTCACACA	125–160	56	[13]
	umc2082	TAGCTGCCCCTCTTCCGTCT	GTCGTGGCGTAGAGACTAGGGT	100–130	54	[13]
	umc2059	CTCTTCGATCTTTAAGAGAGAGAGAG	ACACGAGGCACTGGTACTAACG	170–200	54	[13]
SSR	umc2013	GGAAAAGGAGGAACAGTGTAAGCA	AGCGTGATCAGACGTACAATGCTA	110–130	54	[13]
	SSR85	GGGACGAGAGTCTGTTGTTGTTG	GTTGATGCATGTGACTCTGGAAAC	110–125	55	[13]
	SSR93	CGCCGTACAGACTGCTATGA	CACATGCTACGACTGCGATG	210	57	[10]
	SSR105	GTTCATCCTGATTCCCATCC	CAGCCTTGCTTCTACACCAC	200	58	[10]
	SSR255	TCGACGAGATACGCGACTAC	CAGTACAAAGCCGATCCAAG	200	55	[10]
ISSR	AD8	$(AGC)_6GC$		410	55	[10]
STS	STS03	CTTGTATCATCAGCTAGGGCATGT	GTGATCTGAACGCCAACCTC	300	54	[10]

PCR conditions:

94 °C/2 min.
95 °C/1 min.
54 °C */0.50 min.
72 °C/1 min. } 39×
72 °C/5 min.
4 °C/∞.

* The primer binding temperature was different for each marker and depended on the melting temperature of the primer. The temperatures for each marker are given in Table 2. Melting point for multiplex PCR is 54 °C.

2.2.4. Electrophoretic Separation

Electrophoresis was conducted in a 2% agarose gel in 1× TBE buffer out at 120 V for 1.5 h.

Composition of the 2% agarose gel: 1× TBE buffer, 150 µL; Agarose, 3 g; Midori Green DNA Stain, 7.5 µL.

2.3. Statistical Analysis

The normality of the distribution of the degree of *F. verticillioides* infection of the maize lines was tested using Shapiro–Wilk's normality test. The homogeneity of variance was tested using Bartlett's test. A one-way analysis of variance (ANOVA) was carried out to determine the main line effect on the variability of the degree of *F. verticillioides* infection. The genetic similarity for each pair of the investigated lines was estimated based on the coefficient proposed by Nei and Li [19]. The lines were grouped hierarchically using the unweighted pair group method of arithmetic means (UPGMA) based on the calculated coefficients [20]. The relationships between the lines were presented in the form of a dendrogram. Results were also analyzed using multivariate methods. The principal component analysis (PCA) was applied to present a multi-markers assessment of similarity for the tested lines. The association between molecular markers and the degree of *F. verticillioides* infection was estimated using regression analysis [21]. All analyses were conducted in GenStat 18.2 (VSN International Ltd., Hemel Hempstead, England, UK).

3. Results

3.1. Field Experiment

As a result of field observations, it was confirmed that genotypes identified as resistant were characterized by higher resistance on a 9-level COBORU scale (1, susceptible; 9, resistant) than susceptible genotypes. The empirical distribution of the degree of *F. verticillioides* infection was normal. The results of the analysis of variance for *Fusarium* resistance

($F_{29;60}$ = 8.55) showed variability of the tested lines at the significant level α = 0.001. The lines with numbers 255, 260, 9, 25, 28, 52, 71 were the most resistant at levels 8 and 9 (Table 3). It is worth noting that during molecular analyses, the highest number of molecular markers linked to *F. verticillioides* resistance genes were identified in these lines (Table 3). The least resistant at level 4–6 were lines with numbers: 254, 257, 24, and 67.

Table 3. Degree of *Fusarium verticillioides* infection of individual genotypes and number of identified markers.

Line No.	Observation of the Degree of Resistance			Number of Molecular Markers Identified
	I Repetition	II Repetition	III Repetition	
253	7	7	8	6
254	4	5	4	5
255	9	9	9	9
256	5	7	6	7
257	5	5	6	6
258	7	8	7	7
259	7	7	7	8
260	9	9	8	9
9	9	9	8	9
16	7	6	7	7
23	6	6	7	8
24	6	5	4	6
25	9	8	9	10
28	9	8	8	8
35	8	8	7	9
41	8	7	6	7
45	7	7	8	8
47	8	7	8	8
52	9	8	8	8
57	5	6	5	7
58	6	6	5	7
66	8	7	7	8
67	4	5	6	6
68	5	7	4	7
71	8	8	9	8
74	8	6	5	8
78	6	8	6	7
80	6	6	7	8
103	8	6	6	7
114	9	8	9	8

3.2. Identification of Molecular Markers Linked to Fusarium verticillioides Resistance Genes

The analyzed markers were taken from literature reports. Table 4 shows the distribution of molecular markers associated with *F. verticillioides* resistance genes in the tested lines. ("+" -visible stripe, "-"-no stripe). As can be seen from the analyses, ten of the 12 markers tested were identified for one line number 25 (Table 4). This line has a fusarium resistance of 8–9 under field conditions Table 3). For lines numbered 255, 260, and 9, nine of twelve markers were identified. These lines also exhibited resistance at the 8–9 level under field conditions. Similarly, for the line with number 35, nine markers were identified; this line, however, exhibited slightly lower resistance at the 7–8 level. The least resistant was line 254, in which resistance was at the level of 4–5, and the number of identified markers was five. The same was true for lines 257, 24 and 67, which were characterized by resistance at the level of 4–6 and the number of identified markers was six (Tables 3 and 4).

Table 4. Molecular markers linked to plant resistance to fusarium present in the analyzed lines.

Line No.	Molecular Marker											
	SSR85	**bngl1063**	**bngl1740**	**umc2082**	**bngl1621**	**umc2059**	**umc2013**	**SSR93**	**SSR105**	**SSR255**	**AD8**	**STS03**
253	-	+	+	+	+	+	+	-	-	-	-	-
254	-	+	+	+	+	+	-	-	-	-	-	-
255	+	+	+	+	+	+	+	-	+	-	-	+
256	-	+	+	+	+	+	+	+	-	-	-	-
257	-	+	+	+	+	+	+	-	-	-	-	-
258	-	+	+	+	+	+	+	-	-	+	-	-
259	-	-	+	+	+	+	+	-	+	-	+	+
260	+	-	+	+	+	+	+	-	+	+	-	+
9	+	+	+	+	+	+	+	-	+	-	-	+
16	+	-	+	+	+	+	-	-	+	-	-	+
23	+	-	+	+	+	+	+	-	+	-	-	+
24	+	-	+	+	+	+	+	-	-	-	-	-
25	+	+	+	+	+	+	+	+	+	-	-	+
28	+	-	+	+	+	+	+	+	-	-	-	+
35	+	+	+	+	+	+	+	+	-	-	-	+
41	+	-	+	+	+	+	+	-	-	+	-	-
45	+	-	+	+	+	+	+	-	+	-	-	+
47	+	-	+	+	+	+	+	-	+	-	-	+
52	+	+	+	+	+	+	+	-	-	+	-	-
57	+	-	+	+	+	+	+	-	-	+	-	-
58	+	+	+	+	+	+	+	-	-	-	-	-
66	+	+	+	+	+	+	+	-	-	+	-	-
67	+	-	+	+	+	+	+	-	-	-	-	-
68	+	-	+	+	+	+	+	-	-	+	-	-
71	+	+	+	+	+	+	+	-	-	+	-	-
74	+	+	+	+	+	+	+	-	-	+	-	-
78	+	-	+	+	+	+	+	+	-	-	-	-
80	-	+	+	+	+	+	+	-	+	-	-	+
103	+	-	+	+	+	+	+	+	-	-	-	-
114	+	+	+	+	+	+	+	-	-	+	-	-

Below, photos 1 and 2, and 3 and 4 show sample electrophoretic images showing the identification of bngl1621 and umc2059 markers for the 30 maize genotypes tested (Figures 1–4). For the bngl1521 marker, the following products were obtained by polymerase chain reaction: for lines 253, 254, 257, 258, 260, 16, 23, 66, 67, 68, 71, 74, 80 and 114, a specific product of 170 bp was obtained. For lines: 255, 256, 259, 9, 24, 25, 28, 35 41, 45, 47, 52, 57, 58, 78 and 103 a specific product of 175 bp was obtained (Figures 1 and 2). For the umc 2059 marker, specific products of four different sizes were obtained: 110 bp (for lines: 260, 9, 16, 23, 24, 25, 28), 120 bp (for line: 254), 125 bp (for lines: 253 and 258) and 130 bp (for lines: 257 and 35) (Figure 3). In Figure 4, a product of 110 bp was observed in all analyzed lines.

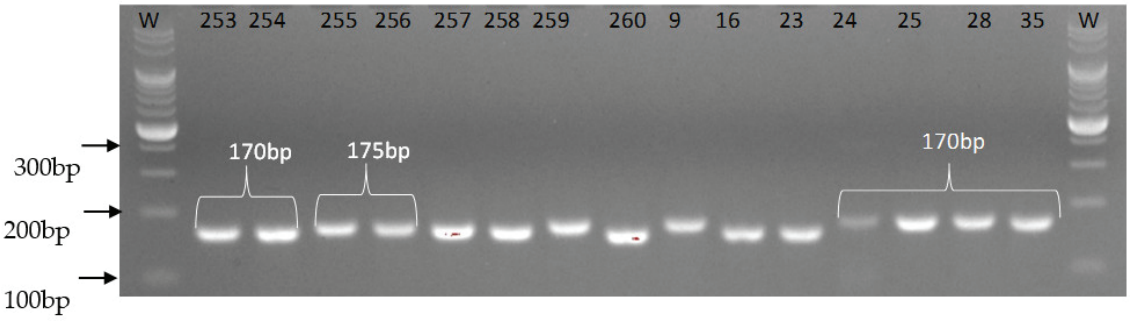

Figure 1. Electrophoretic image of PCR products in 2% agarose gel using bnlg1621 primer pair.

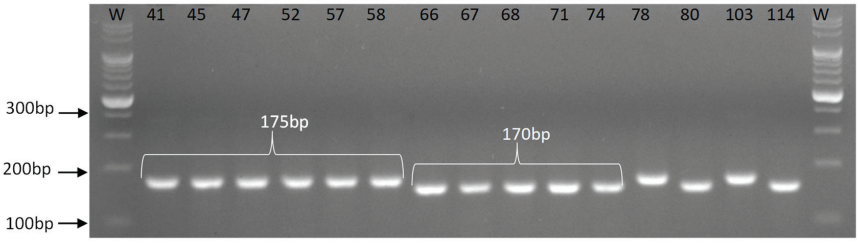

Figure 2. Electrophoretic image of PCR products in 2% agarose gel using bnlg1621 primer pair.

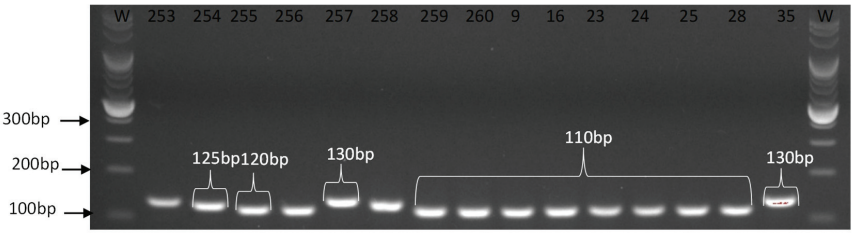

Figure 3. Electrophoretic image of PCR products in 2% agarose gel using umc2059 primer pair.

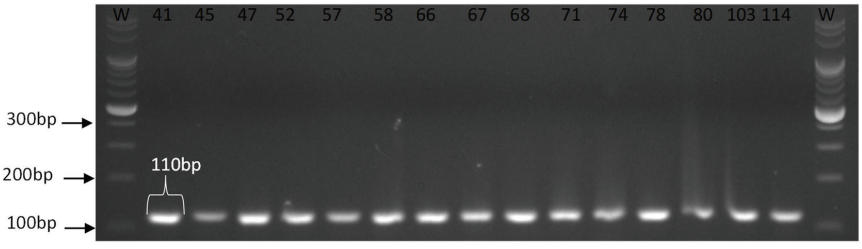

Figure 4. Electrophoretic image of PCR products in 2% agarose gel using umc2059 primer pair.

All markers, except AD8, were associated with *F. verticillioides* resistance of the maize lines (Table 5). Percentage variance accounted for particular markers ranged from 0.7% (for bngl1621 170 bp and bngl1621 175 bp) to 19.9% (for STS03 (Table 5).

The greatest genetic similarity (equal to 1) was found for lines 78 and 103, while the most diversity (equal to 0) for lines 28 and 258 (Figures 5 and 6).

Table 5. Characteristics of molecular markers associated with *Fusarium verticillioides* resistance.

Marker	Effect	Percentage Variance Accounted
SSR85	0.921 ***	9.9
bngl1063	0.565 ***	7.4
bngl1740 125 bp	−0.093 *	1.5
bngl1740 155 bp	−0.432 ***	6.7
bngl1740 160 bp	0.518 ***	2.8
umc2082 100 bp	0.503 ***	3.4
umc2082 115 bp	0.067 *	1.2
umc2082 120 bp	0.164 ***	4.7
bngl1621 170 bp	−0.521 ***	0.7
bngl1621 175 bp	0.521 ***	0.7
umc2059 110 bp	0.694 **	1.8
umc2059 120 bp	−2.7 **	11.2
umc2059 125 bp	0.417 *	7.5
umc2059 130 bp	−0.476 **	5.5
umc2013 120 bp	−0.224 *	2.8
umc2013 125 bp	−0.093 *	1.5
SSR93	0.486 **	3.6
SSR105	1.033 ***	11.3
SSR255	0.483 ***	5.7
AD8	0.06	
STS03	1.25 ***	19.9

* $p < 0.05$; ** $p < 0.01$; *** $p < 0.001$.

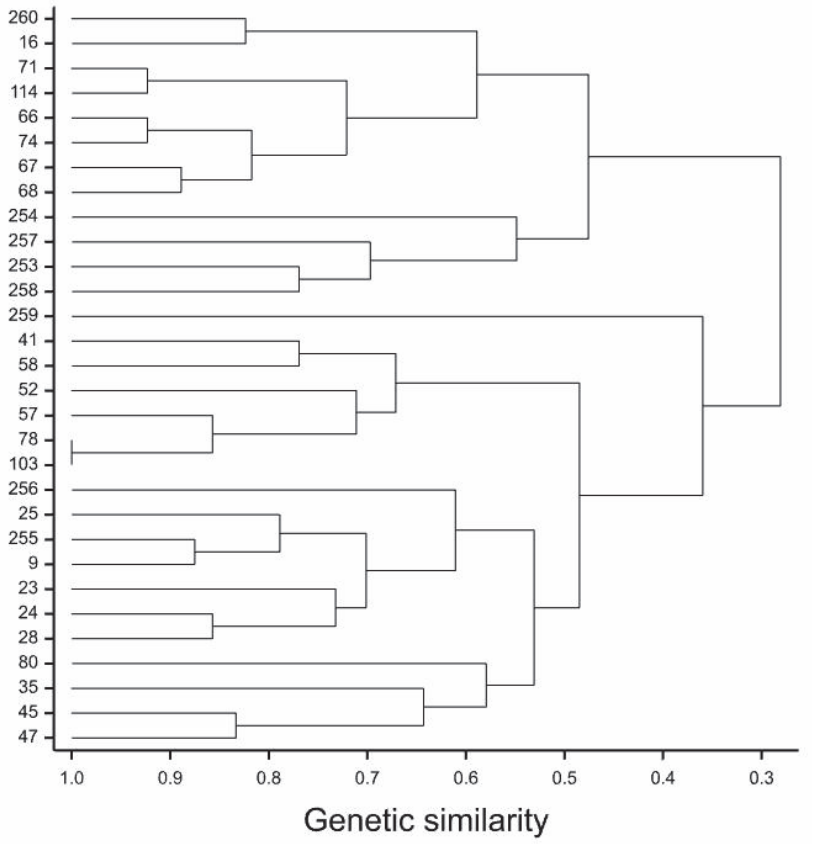

Figure 5. Dendrogram of cluster groupings of 30 maize lines based on all molecular markers.

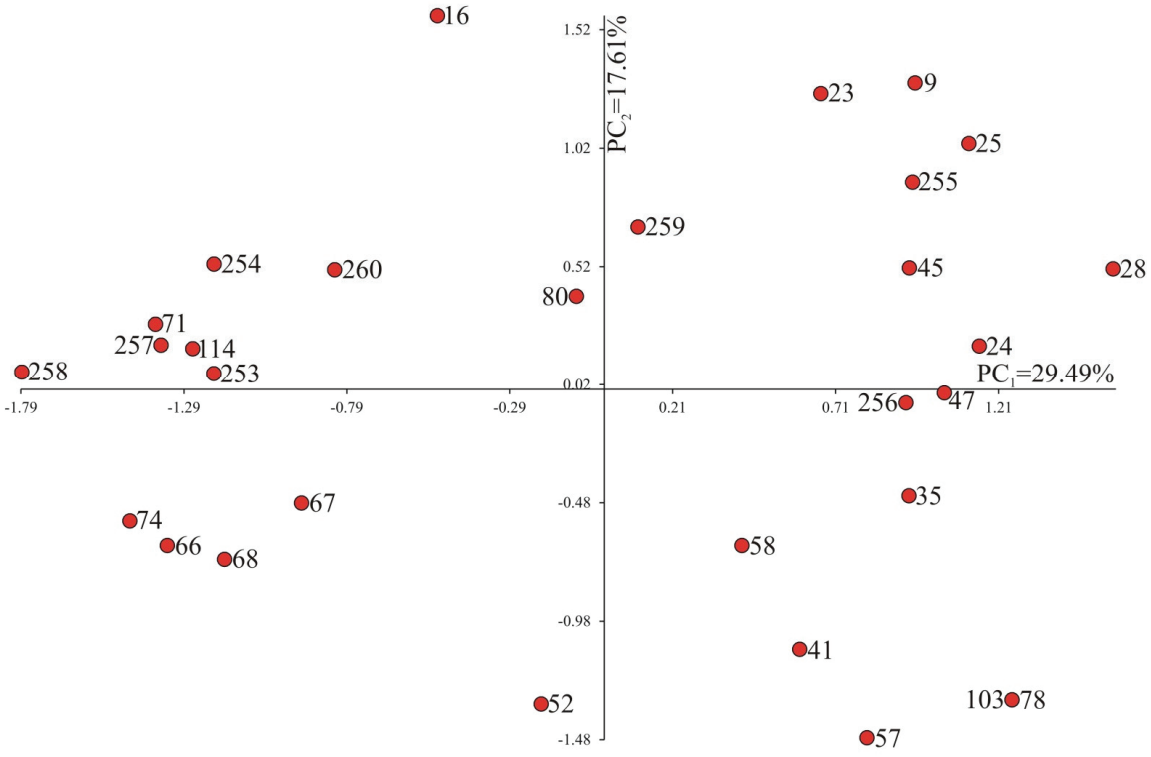

Figure 6. Distribution of 30 maize lines in the space of the first two principal components.

Analysis of the first two principal components for 30 maize lines regarding the all molecular markers is shown in Figure 6. In the graph, the coordinates of the point for a particular line were the values for the first and second principal component, respectively. The first two principal components accounted for 47.10% of the total variability between the individual lines.

3.3. Multiplex PCR Analyses

In order to simultaneously identify two markers associated with cob fusarium resistance genes, conditions were developed for multiplex PCR reactions. Figures 5 and 6 show the multiplex PCR results developed for the markers bnlg1621 and umc2059 (Figures 7 and 8). The multiplex PCR results corresponded to those from single marker analyses. Multiplex PCR was also developed for markers bnlg1621 and SSR85, bnlg1621 and bnlg1740, bnlg1740 and SRR85, STS03 and umc2013, and STS03 and SRR255 according to the methodology presented in Materials and Methods.

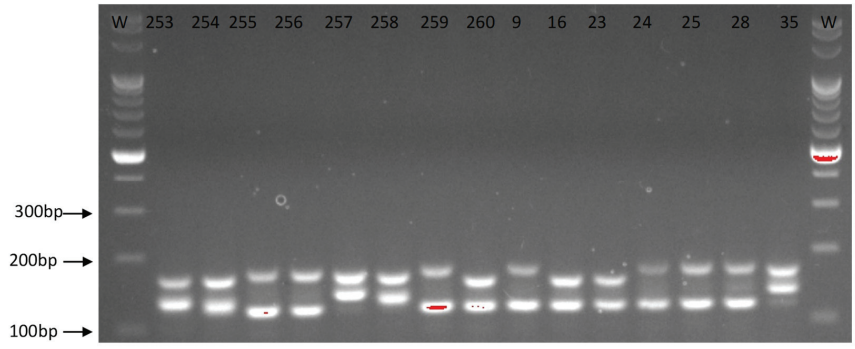

Figure 7. Electrophoretic image of PCR products after including bnlg1621 and umc2059 primer pairs in the reaction.

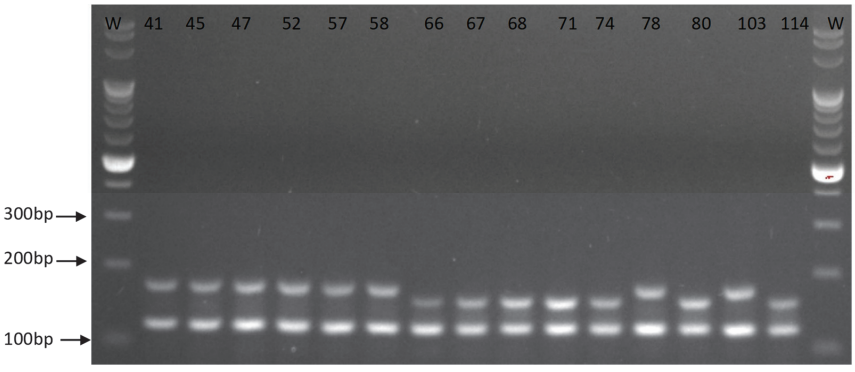

Figure 8. Electrophoretic image of PCR products after including bnlg1621 and umc2059 primer pairs in the reaction.

4. Discussion

Fungi of the genus *Fusarium* spp. are common pathogens among grain crops. They cause diseases associated with rot of ears, stems and roots, among others. Their negative effects cause large losses in yield. In addition, some races of these fungi have the ability to produce mycotoxins that are harmful to humans and animals [22]. Mycotoxins can be divided into three classes: fumonisins, compounds with a simple structure, cause complex and diverse harmful reactions; trichothecenes, a group of compounds with the most harmful effects on humans and animals, can cause fatal and chronic poisoning; zearalenones, the least harmful group of compounds, are toxic but cause death [23].

Mycotoxin toxicity is divided into four types: chronic, acute, teratogenic and mutagenic. The effect of acute poisoning is most often a decrease in kidney and liver function. In severe cases, it leads to the death of the individual [24].

As part of prevention, great emphasis is placed on the development of resistance breeding. Classical selection of resistant varieties based on phenotype analysis is time-consuming and costly. In view of the above, molecular biology tools are increasingly being used for selection. Sets of molecular markers are available that significantly augment traditional resistance breeding methods [25].

Maize resistance to *Fusarium* spp. is a quantitative trait determined by low-influence polygenes [12,26–28]. Over the past decade, many studies have been conducted on the genetic basis associated with resistance to the disease [29]. Genome-wide association and transcriptomic studies (transcriptomic and genome-wide association studies GWAS)

combined with QTL mapping have helped identify markers associated with increased resistance to *Fusarium* spp.

We know from literature reports that phytohormones, e.g., salicylic acid, jasmonic acid and abscisic acid, play a key role in maize's defense response to *Fusarium* spp. The induction of genes related to the benzoxazinoid biosynthetic pathway (i.e., an antimicrobial and insecticidal secondary compound in maize) has also been shown to be linked to plant defense mechanisms against pathogens. The involvement of genes encoding pathogenesis-related (PR) proteins, particularly β-1,3-glucanase, chitinase and pathogenesis-related protein 10 (PR10 protein), has also been observed in maize plant defense responses against *F. verticillioides* [30,31]. It is important to identify markers associated with genes affecting fusarium resistance to facilitate the selection of resistant genotypes. As a result of many studies to date, several SSR-type markers (SSR85, bnlg1063, bnlg1740, umc2082, bnlg1621, umc2059 or umc2013) have been selected for molecular-level selection of resistant varieties and lines.

As can be concluded from the analyses, the resistance of the maize plants tested was correlated with the number of molecular markers identified. An example is line number 25, in which ten (SSR 85, Bngl 1063, Bngl 1740, Umc 2082, Bngl 1621, Umc 2059, Umc 2013, SSR 93, SSR 105, STS 03) of the twelve markers tested were identified. This line is characterized by a *F. verticillioides* resistance of 8–9 under field conditions. For other lines with numbers 255, 260, and 9, nine (SSR 85, Bngl 1063, Bngl 1740, Umc 2082, Bngl 1621, Umc 2059, Umc 2013, SSR 105, STS 03 of twelve markers were identified. As in the case of the line with number 25, these lines also exhibited od resistance at the 8–9 level under field conditions. The same pattern was observed for the line with number 35, for which nine markers were identified. However, this line was characterized by a slightly lower resistance at the level of 7–8. The least resistant was line 254, in which resistance was at the level of 4–5 and the number of identified markers was five. The same was true for lines 257, 24 and 67, which were characterized by resistance at the level of 4–6, and the number of identified markers was six.

The molecular markers used for analysis in this work were taken from the literature of Abdel-Rahman et al. [13]. In their work, the authors studied *Fusarium* spp.—resistant and susceptible genotypes and two parental genotypes. This allowed them to select PCR reaction products responsible for increased resistance. In their study, the problematic markers were umc2082 and bngl1063. As many as four different products were obtained for the umc2082 marker. The resulting bands had similar lengths, making further analysis difficult. Park et al. [32] also studied this molecular marker to analyze the genetic diversity of maize in Korea. The course of the PCR reaction looked similar to the course in this work. However, Park et al. [32] in their work used a polyacrylamide gel for electrophoretic separation thus obtaining better separation of PCR reaction products. Hence, it can be inferred that by using this type of gel, a clearer electrophoretic image could be obtained. Abdel-Rahman et al. [13] obtained products of about 100 and 120 bp for this markers.

Sa et al. [33] evaluating the genetic diversity and structure of selected maize inbred lines studied the bnlg1621 marker, which is also analyzed in this work. According to the study, a total of as many as 15 different alleles were shown for this particular molecular marker, which occurred in the inbred lines studied. Their research work also analyzed other SSR-type markers, 50 in number, and a total of 381 alleles were distinguished in just 32 maize inbred lines.

As a result of the methods used, clear and readable electrophoretic images were obtained for all the molecular markers analyzed. The exceptions were the aforementioned markers umc2082 and bngl1063. Ignjatović-Micić et al. [34] studying the diversity as well as genetic structure of local maize populations also took into account the bngl1063 marker due to its high polymorphism. In their research work, they obtained a very clear electrophoretic image. However, they used different primer attachment temperatures (63.5 °C or 56 °C). The authors did not specify which exact temperature was used for this marker. However, the difference between those used in this paper is at least one degree. Therefore, it can

be concluded that using a slightly higher temperature for primer attachment would have yielded a better, clearer electrophoretic image.

Ashkani et al. [35] investigating multiplex PCR conditions using SSR markers concluded that such reactions often require extensive optimization to obtain relatively good results, and the reaction conditions themselves can differ significantly from single marker analyses. Very often, primers of both markers can hybridize with each other.

In order to improve the breeding cycle, multiplex PCR conditions were developed to identify two markers simultaneously. The multiplex PCR results corresponded to those from single marker analyses. Multiplex PCR was developed for markers bnlg1621 and umc2059 bnlg1621 and SSR85, bnlg1621 and bnlg1740, bnlg1740 and SRR85, STS03 and umc2013, STS03 and SRR255 according to the methodology presented in Materials and Methods.

Butrón et al. [2] investigated quantitative trait loci (QTLs) associated with resistance to corn cob fusariosis using a maize population called Multiparent Advanced Generation Intercross (MAGIC). The authors confirmed that maize cob fusariosis resistance is determined by quantitative trait genes, meaning that many loci manifest small additive effects [36–38].

In conclusion, it was found that the tested molecular markers may be useful for the selection of fusarium-resistant maize lines. In addition, multiplex PCR conditions were developed for the simultaneous identification of two markers. On the basis of the analysis of field experiments and molecular studies, maize lines with numbers 9, 25, 35, 255 and 260 were selected, which are characterized by very high resistance to fusarium and have accumulated markers linked with the genes of resistance to fusarium. These lines can be taken as reference lines and used in the breeding process as a source of fusarium resistance genes.

5. Conclusions

It is well known that advances in plant breeding depend on technologies to identify markers of quantitative traits. Statistical methods used in association mapping and genomic selection are playing an increasingly important role. Attempts are being made to identify and map new markers significantly associated with many traits, including *F. verticillioides* resistance. In recent years, there has been a change in the approach to selection. Instead of using single feature markers, multiple markers for these features are searched for, or the entire available pool of markers describing the population is used for selection. The research described in this paper shows that the presented markers can be successfully used for the selection of varieties resistant to *F. verticillioides*. In the course of molecular analyses and field observations, five lines were selected: 9, 25, 35, 255 and 260, which can be used to crossbreed in order to obtain varieties resistant to fusarium. In addition, conditions for multiplex PCR reactions were developed to shorten the breeding cycle. This tool can be used for the selection of resistant lines and varieties.

Author Contributions: Conceptualization, A.S. and A.T.; methodology, A.S. and J.B.; software, A.T., J.B. and A.S.; validation, A.T., J.B. and A.S.; formal analysis, A.S., J.B., A.T., B.N., K.S., D.W., D.K.-P., M.K., S.M. and J.N.; investigation, A.S., J.B., K.S. and A.T.; resources, A.S.; data curation, A.S., A.T. and J.B.; writing—original draft preparation, A.S., A.T. and J.B.; writing—review and editing, A.S., A.T. and J.B.; visualization, A.S., A.T. and J.B.; supervision, A.T. and J.B.; project administration, A.T. All authors have read and agreed to the published version of the manuscript.

Funding: The research presented in this publication was financed as part of the research project "Analysis of genetic determinants of heterosis effect and fusarium resistance in maize (*Zea mays* L.)". PL: "Analiza genetycznych uwarunkowań związanych z efektem heterozji oraz odpornością na fuzarium u kukurydzy (*Zea mays* L.)". The project is implemented under the grant from the Ministry of Agriculture and Rural Development "Biological progress in plant production (recruitment 2020)". Duration of the project 2021–2026.

Institutional Review Board Statement: Not applicable.

Data Availability Statement: Not applicable.

Conflicts of Interest: The authors declare no conflict of interest. The funders had no role in the design of the study, in the collection, analyses, or interpretation of data, in the writing of the manuscript, or in the decision to publish the results.

References

1. Yadav, M.K.; Lipsa, D.; Sandeep, R. Evaluation of Host Plant Resistance Traits in Certain Genotypes of Maize (*Zea Mays* L.) against Maize Spotted Stem Borer (Chilo Partellus Swinhoe, Crambidae). *Int. J. Entomol. Res.* **2021**, *6*, 64–69. Available online: www.entomologyjournals.com (accessed on 1 May 2022).
2. Butrón, A.; Santiago, R.; Cao, A.; Samayoa, L.F.; Malvar, R.A. QTLs for resistance to fusarium ear rot in a multiparent advanced generation intercross (MAGIC) maize population. *Plant Dis.* **2019**, *103*, 897–904. [CrossRef]
3. Scauflaire, J.; Mahieu, O.; Louvieaux, J.; Foucart, G.; Renard, F.; Munaut, F. Biodiversity of *Fusarium* species in ears and stalks of maize plants in Belgium. *Eur. J. Plant Pathol.* **2011**, *131*, 59–66. [CrossRef]
4. Logrieco, A.; Mule, G.; Moretti, A.; Bottalico, A. Toxigenic *Fusarium* species and mycotoxins associated with maize ear rot in Europe. In *Mycotoxins in Plant Disease*; Logrieco, A., Bailey, J.A., Corazza, L., Cooke, B.M., Eds.; Springer: Berlin/Heidelberg, Germany, 2002; pp. 597–609. ISBN 978-94-010-3939-0. [CrossRef]
5. Eckard, S.; Wettstein, F.E.; Forrer, H.-R.; Vogelgsang, S. Incidence of *Fusarium* Species and Mycotoxins in Silage Maize. *Toxins* **2011**, *3*, 949–967. [CrossRef]
6. Garcia-Ceron, D.; Lowe, R.G.T.; McKenna, J.A.; Brain, L.M.; Dawson, C.S.; Clark, B.; Berkowitz, O.; Faou, P.; Whelan, J.; Bleackley, M.R.; et al. Extracellular Vesicles from *Fusarium graminearum* Contain Protein Effectors Expressed during Infection of Corn. *J. Fungi* **2021**, *7*, 977. [CrossRef]
7. Bush, B.J.; Carson, M.L.; Cubeta, M.A.; Hagler, W.M.; Payne, G.A. Infection and Fumonisin Production by *Fusarium verticillioides* in Developing Maize Kernels. *Genet. Resist. Infect. Am. Phytopathol. Soc.* **2003**, *94*, 88–93. [CrossRef]
8. Uwe, L.; Miedaner, T.; Bürstmayr, H.; Vögele, R.T. *Breeding for Resistance to Fusarium Ear Diseases in Maize and Small-Grain Cereals Using Genomic Tools*; Faculty of Agricultural Sciences University of Hohenheim: Stuttgart, Germany, 2020; p. 144. Available online: http://opus.uni-hohenheim.de/volltexte/2021/1865/pdf/Gaikpa_Dissertation_phdKIM_print.pdf (accessed on 1 May 2022).
9. Stagnati, L.; Lanubile, A.; Samayoa, L.F.; Bragalanti, M.; Giorni, P.; Busconi, M.; Holland, J.; Mrocco, B.A. A Genome Wide Association Study Reveals Markers and Genes Associated with Resistance to *Fusarium Verticillioides* Infection of Seedlings in a Maize Diversity Panel. *G3 Genes Genomes Genet.* **2019**, *9*, 571–579. [CrossRef] [PubMed]
10. Salah, N.; Milad, S.I.; El-Rouby, M.M.; Barakat, M.N. Identification of New Molecular Markers Linked to Maize Stalk Rot Disease Resistance (*Fusarium Moniliforme*) in Maize. *Plant Omics J.* **2016**, *9*, 12–18. [CrossRef]
11. Michel, S.; Wagner, C.; Nosenko, T.; Steiner, B.; Samad-Zamini, M.; Buerstmayr, M.; Mayer, K.; Buerstmayr, H. Merging Genomics and Transcriptomics for Predicting Fusarium Head Blight Resistance in Wheat. *Genes* **2021**, *12*, 114. [CrossRef] [PubMed]
12. Maschietto, V.; Colombi, C.; Pirona, R.; Pea, G.; Strozzi, F.; Marocco, A.; Rossini, L.; Lanubile, A. QTL mapping and candidate genes for resistance to Fusarium ear rot and fumonisin contamination in maize. *BMC Plant Biol.* **2017**, *17*, 20. [CrossRef] [PubMed]
13. Abdel-Rahman, M.M.; Bayoumi, S.R.; Barakat, M.N. Identification of molecular markers linked to *Fusarium* ear rot genes in maize plants *Zea mays* L. *Biotechnol. Biotechnol. Equip.* **2016**, *30*, 692–699. [CrossRef]
14. Jones, E.S.; Sullivan, H.; Bhattramakki, D.; Smith, J.S.C. A comparison of simple sequence repeat and single nucleotide polymorphism marker technologies for the genotypic analysis of maize (*Zea mays* L.). *Theor. Appl. Genet.* **2007**, *115*, 361–371. [CrossRef] [PubMed]
15. Hamblin, M.T.; Fernandez, M.G.S.; Tuinstra, M.R.; Rooney, W.L.; Kresovich, S. Sequence Variation at Candidate Loci in the Starch Metabolism Pathway in Sorghum: Prospects for Linkage Disequilibrium Mapping. *Crop Sci.* **2007**, *47*, 125–134. [CrossRef]
16. Van Inghelandt, D.; Melchinger, A.E.; Lebreton, C.; Stich, B. Population structure and genetic diversity in a commercial maize breeding program assessed with SSR and SNP markers. *Theor. Appl. Genet.* **2010**, *120*, 1289–1299. [CrossRef] [PubMed]
17. Li, M.; Zhong, W.; Yang, F.; Zhang, Z. Genetic and Molecular Mechanisms of Quantitative Trait Loci Controlling Maize Inflorescence Architecture. *Plant Cell Physiol.* **2018**, *59*, 448–457. [CrossRef] [PubMed]
18. Arabzai, M.; Gul, H. Application Techniques of Molecular Marker and Achievement of Marker Assisted Selection (MAS) in Three Major Crops Rice, Wheat and Maize. *Int. J. Res. Appl. Sci. Biotechnol.* **2021**, *8*, 82–93. [CrossRef]
19. Nei, M.; Li, W.H. Mathematical model for studying genetic variation in terms of restriction endonucleases. *Proc. Natl. Acad. Sci. USA* **1979**, *76*, 5269–5273. [CrossRef]
20. Starzycka-Korbas, E.; Weber, Z.; Matuszczak, M.; Bocianowski, J.; Budzianowski, G.; Stefanowicz, M.; Starzycki, M. The diversity of *Sclerotinia sclerotiorum* (Lib.) de Bary isolates from western Poland. *J. Plant Pathol.* **2021**, *103*, 185–195. [CrossRef]
21. Bocianowski, J.; Kozak, M.; Liersch, A.; Bartkowiak-Broda, I. A heuristic method of searching for interesting markers in terms of quantitative traits. *Euphytica* **2011**, *181*, 89–100. [CrossRef]
22. Bottalico, A.; Perrone, G. Toxigenic *Fusarium* species and mycotoxins associated with head blight in small-grain cereals in Europe. *Eur. J. Plant Pathol.* **2002**, *108*, 611–624. [CrossRef]
23. Desjardins, A.E.; Proctor, R.H. Molecular biology of *Fusarium* mycotoxins. *Int. J. Food Microbiol.* **2007**, *119*, 47–50. [CrossRef]
24. Pitt, J.I. Toxigenic fungi: Which are important? *Med. Mycol.* **2000**, *38*, 17–22. [CrossRef] [PubMed]
25. Santiago, R.; Cao, A.; Malvar, R.A.; Butrón, A. Genomics of Maize Resistance to Fusarium Ear Rot and Fumonisin Contamination. *Toxins* **2020**, *12*, 431. [CrossRef] [PubMed]

26. Robertson, L.A.; Kleinschmidt, C.E.; White, D.G.; Payne, G.A.; Maragos, C.M.; Holland, J.B. Heritability and correlations of Fusarium ear rot resistance and fumonisin contamination resistance in two maize populations. *Crop Sci.* **2006**, *46*, 353–361. [CrossRef]
27. Ding, J.Q.; Wang, X.M.; Chander, S.; Yan, J.E.; Li, J.S. QTL mapping of resistance to Fusarium ear rot using a RIL population in maize. *Mol. Breed.* **2008**, *22*, 395–403. [CrossRef]
28. Chen, J.; Ding, J.; Li, H.; Li, Z.; Sun, X.; Li, J.; Wang, R.; Dai, X.; Dong, H.; Song, W.; et al. Detection and verification of quantitative trait loci for resistance to Fusarium ear rot in maize. *Mol. Breed.* **2012**, *30*, 1649–1656. [CrossRef]
29. Gaikpa, D.S.; Miedaner, T. Genomics-assisted breeding for ear rot resistances and reduced mycotoxin contamination in maize: Methods, advances and prospects. *Theor. Appl. Genet.* **2019**, *132*, 2721–2739. [CrossRef]
30. Baldwin, T.; Baldwin, S.; Klos, K.; Bregitzer, P.; Marshall, J. Deletion of the benzoxazinoid detoxification gene *NAT1* in *Fusarium graminearum* reduces deoxynivalenol in spring wheat. *PLoS ONE* **2019**, *14*, e0214230. [CrossRef]
31. Cotton, T.E.A.; Pétriacq, P.; Cameron, D.D.; Al Meselmani, M.; Schwarzenbacher, R.; Rolfe, S.A.; Ton, J. Metabolic regulation of the maize rhizobiome by benzoxazinoids. *ISME J.* **2019**, *13*, 1647–1658. [CrossRef]
32. Park, J.S.; Park, J.Y.; Park, K.J.; Lee, J.K. Genetic diversity among waxy corn accessions in Korea revealed by microsatellite markers. *Korean J. Breed. Sci.* **2008**, *40*, 250–257.
33. Sa, K.J.; Hong, T.K.; Lee, J.K. Genetic diversity and association analyses of canadian maize inbred lines with agronomic traits and simple sequence repeat markers. *Plant Breed. Biotechnol.* **2018**, *6*, 159–169. [CrossRef]
34. Ignjatović-Micić, D.; Drinić, S.M.; Nikolić, A.; Lazić-Jančić, V. SSR analysis for genetic structure and diversity determination of maize local populations from former Yugoslavia territories. *Russ. J. Genet.* **2008**, *44*, 1317–1324. [CrossRef]
35. Ashkani, S.; Rafii, M.Y.; Shabanimofrad, M.; Foroughi, M.; Azizia, P.; Akhtar, M.S.; Sahebi, M.; Harun, A.R.; Nasehi, A. Multiplex SSR–PCR approaches for semi-automated genotyping and characterization of loci linked to blast disease resistance genes in rice. *Comptes Rendus Biol.* **2015**, *388*, 709–722. [CrossRef]
36. Bocianowski, J.; Nowosad, K.; Wróbel, B.; Szulc, P. Identification of Associations between SSR Markers and Quantitative Traits of Maize (*Zea mays* L.). *Agronomy* **2021**, *11*, 182. [CrossRef]
37. Cyplik, A.; Sobiech, A.; Tomkowiak, A.; Bocianowski, J. Genetic Parameters for Selected Traits of Inbred Lines of Maize (*Zea mays* L.). *Appl. Sci.* **2022**, *12*, 6961. [CrossRef]
38. Sobiech, A.; Tomkowiak, A.; Nowak, B.; Bocianowski, J.; Wolko, Ł.; Spychała, J. Associative and Physical Mapping of Markers Related to *Fusarium* in Maize Resistance, Obtained by Next-Generation Sequencing (NGS). *Int. J. Mol. Sci.* **2022**, *23*, 6105. [CrossRef] [PubMed]

agriculture

MDPI

Article

Combining Ability and Testcross Performance for Carotenoid Content of S_2 Super Sweet Corn Lines Derived from Temperate Germplasm

Worawan Wasuwatthanakool [1], Bhornchai Harakotr [1,*], Yaowapha Jirakiattikul [1], Khomsorn Lomthaisong [2] and Khundej Suriharn [3,4]

[1] Department of Agricultural Technology, Faculty of Science and Technology, Thammasat University, Pathum Thani 12120, Thailand
[2] Department of Chemistry, Faculty of Science, Khon Kaen University, Khon Kaen 40002, Thailand
[3] Department of Agronomy, Faculty of Agriculture, Khon Kaen University, Khon Kaen 40002, Thailand
[4] Plant Breeding Research Center for Sustainable Agriculture, Faculty of Agriculture, Khon Kaen University, Khon Kaen 40002, Thailand
* Correspondence: harakotr@tu.ac.th; Tel.: +66-2564-4440-79 (ext. 2364)

Abstract: Understanding the impact of gene action and combining ability on targeted traits in a hybrid breeding program is imperative. The objective of this study was to estimate the genetic effect and combining ability of S_2 super sweet corn lines on carotenoid content. Twenty S_2 lines were crossed with two hybrid testers by using the line × tester mating design. Regarding parents, forty hybrids and two commercial checks were evaluated for carotenoid content across two different growing seasons between 2019 and 2020. The result indicated that the non-additive gene action governed the inheritance of carotenoid content. Several promising S_2 lines for individual carotenoids were identified; only L_{20} possessed different and positive GCA values for all observed carotenoids. Moreover, genotype T_2 was a promising tester to identify superior lines for creating biofortified sweet corn hybrids. Testcross hybrids with satisfactory performance, desirable SCA estimates, and involving at least one of the pairwise parents with positive and high GCA were successfully defined. Hybrid $T_2 \times L_{20}$ had high lutein, zeaxanthin, β-cryptoxanthin, and total carotenoids contents (ranging from 12.58 to 74.01 μg/g of dry weight), whereas hybrid $T_2 \times L_9$ showed the highest content of β-carotene (4.19 μg/g of dry weight). We propose that high GCA and line at least one of the pairwise parents be included in indirect selections for the hybrid breeding of high-carotenoid sweet corn.

Keywords: biofortification; general and specific combining ability; non-additive gene action; *Zea mays* L. var. *saccharata*

Citation: Wasuwatthanakool, W.; Harakotr, B.; Jirakiattikul, Y.; Lomthaisong, K.; Suriharn, K. Combining Ability and Testcross Performance for Carotenoid Content of S_2 Super Sweet Corn Lines Derived from Temperate Germplasm. *Agriculture* **2022**, *12*, 1561. https://doi.org/10.3390/agriculture12101561

Academic Editors: Edyta Paczos-Grzeda, Volker Mohler and Sylwia Sowa

Received: 24 August 2022
Accepted: 24 September 2022
Published: 27 September 2022

1. Introduction

Super sweet corn (*Zea mays* L. var. *saccharata*), one of the most preferred vegetable crops, is widely grown and consumed worldwide as a canned or frozen foodstuff. This corn type has an allelic mutant *shrunken*$_2$ (*sh*$_2$) gene that makes it suited for food processing because it accumulates starch at a constant rate and maintains high sugar levels [1]. Therefore, super sweet corn possesses significant shares in both national and global markets [2]. For instance, in Thailand, the domestic production of sweet corn increased from 100,000 tons in early 1992 to 357,118 tons at the end of 2019 [3]. Nowadays, Thailand is the world's leading exporter of canned sweet corn, and 73% of the total production is concentrated in four provinces: Chiang Mai, Chiang Rai, Lampang, and Kanchanaburi. Apart from economic advantages, sweet corn offers abundant nutritional values including protein, lipids, minerals [4], and phytochemicals such as phenolics, flavonoids, and carotenoids [5]. Carotenoids are recognized as potent antioxidants [6] that benefit human health through reducing the risk of cancer, cardiovascular disease, and age-related macular

degeneration (AMD) [7,8]. Carotenoids are the second largest group of naturally appearing lipid-soluble pigments, represented in yellow, orange, or red colors. Two of fifty carotenoid structures found in plants are predominant, namely xanthophylls (lutein, zeaxanthin, and β-cryptoxanthin) and carotenes (β-carotene and α-carotene) [9]. Within the xanthophylls group, lutein and zeaxanthin are major non-provitamin A in corn kernels. Several epidemiological studies have found that diets high in these two fractions can protect ocular tissues from phototoxic damage and improve visual acuity [7,9,10]. Likewise, provitamin A carotenoids, namely β-carotene and β-cryptoxanthin, are converted into retinol after ingestion, serving as the precursor of the light sensor molecules in the retina. An adequate intake of them can prevent degenerative eye damage, such as night blindness, xerophthalmia, Bitot's spots, corneal ulcerations, and lesions [9]. However, low dietary sources of provitamin A, lutein, and zeaxanthin in traditional sweet corn have been reported by Baseggio et al. [11]. In contrast, sweet corn genotypes with high β-carotene have been developed to combat hypovitaminosis A and released to targeted populations in several developing countries [2,12].

The success of sweet corn hybrid development can be achieved by selecting superior parents that could be used to develop biofortified commercial corn cultivars. A thorough understanding of combining ability, which comprises general combining ability (GCA) and specific combining ability (SCA), is essential to identify superior parental lines and hybrids [13,14]. While the GCA is determined by the additive genetic effect, the SCA is determined by the non-additive genetic effect, arising largely from the variance of dominance, overdominance, and epistasis with respect to certain traits [15,16]. Line × tester analysis is one of the mating designs commonly applied in biometrical studies and could provide useful information on combining ability and testcross performance [17]. Combining ability using line x tester analysis has been reported in various corn types on yield, yield components [18,19], kernel nutritional qualities [20,21], and disease resistance [22,23]. Moreover, the combining ability analysis is used to estimate the modes of gene actions on desired traits, which could be manipulated by heterosis breeding or by the accumulation of fixable genes through repeated selections [24]. Additive gene effect was predominant on carotenoid contents in maize [13,25], while other studies reported the equal importance of both additive and non-additive gene effects on this trait [21,26–29]. The Lycopene epsilon cyclase (*lcyE*) gene is the key gene influencing how much flux goes into the α- and β-carotene biosynthetic pathways (e.g., lutein and zeaxanthin, respectively), whose two parallel branches bifurcate after carotenogenesis [26]. Four genes, namely phythoene synthase (*PSY1*), cytochrome P450-type monooxygenase (*CYP97C*), ferredoxin-dependent di-iron monooxygenase (*HYD3*), and carotenoid dioxygenase (*ZmCCD1*), were found to be responsible for underlying the diversity of Brazilian maize landraces on the content and composition of carotenoids. While *PSY1*, *CYP97C*, and *HYD3* were more highly expressed at the late grain-filling stage and positively correlated with the total carotenoid content, *ZmCCD1* was expressed at the early grain-filling stage and negatively correlated with the total carotenoid content [27].

However, such kinds of studies focusing on sweet corn genotypes on improved carotenoid content are still lacking. In the present study, we examined the combining ability on both total carotenoids and their fractions, constructed from tropical super sweet corn lines derived from temperate corn germplasm. The introduced temperate corn germplasm differs in climatic regions and is expected to expand the genetic diversity in tropical breeding [28,29]. Therefore, the objective of this study was to determine the genetic effect and to estimate the combining ability of super sweet corn lines on carotenoid content. The information obtained from this study will be useful for sweet corn hybrid breeding with better nutritional values.

2. Materials and Methods

2.1. Plant Materials

Twenty S_2 super sweet corn lines and two F_1 hybrids as testers were used in this study (Table 1). These lines were developed from four tropical and temperate biparental crosses, which were obtained from the Plant Breeding Research Center for Sustainable Agriculture, Khon Kaen University, Thailand. Then, the progenies were backcrossed to tropical corn to enhance the adaptation and plant stand in the tropics. The top 10% of BC_1F_2 or BC_2F_2-derived lines were selected based on their phenotypic performance. The selected lines of each family were evaluated in the nursery of the Department of Agricultural Technology, Thammasat University, Thailand. The selection was made within and among families, and selected plants were self-pollinated to obtain $F_{2:3}$ lines. Further selections were performed, emphasizing germination rate, good plant architecture, low ear placement, and good kernel sets. Moreover, sweet corn kernels with a hue angle value of less than 85°, which is the maximum angle for rapid kernel identification with high carotenoid levels, were subsequently selected [12] (Figure 1). The two F_1 hybrids used as testers have a wide genetic distance, high yield, good adaptation, and light-yellow kernel pigmentation. A line × tester mating scheme was conducted by assigning 20 elite lines as lines and 2 hybrids as a tester, resulting in 40 progenies. This step was carried out in the dry season of 2018/2019 at the Research Farm in the Department of Agricultural Technology, Thammasat University, Pathum Thani, Thailand.

Table 1. List of S_2 super sweet corn lines, testers, and commercial check varieties used in this study.

No.	Code	Pedigree	Population	Description	Relative Carotenoid Content [1/]
1	L_1	Sugar-75/TSC-BC_2-4-5	1	Line	high
2	L_2	Sugar-75/TSC-BC_2-6-2	1	Line	low
3	L_3	Sugar-75/TSC-BC_2-8-1	1	Line	low
4	L_4	Sugar-75/TSC-BC_2-10-5	1	Line	high
5	L_5	Sugar-75/TSC-BC_2-11-2	1	Line	medium
6	L_6	Sugar-75/TSC-BC_2-16-5	1	Line	low
7	L_7	Sugar-75/TSC-BC2-22-1	1	Line	medium
8	L_8	Sugar-75/TSC-BC_2-25-1	1	Line	medium
9	L_9	Sugar-75/TSC-BC_2-28-3	1	Line	high
10	L_{10}	Sugar-75/TSC-BC_2-29-7	1	Line	medium
11	L_{11}	Sugar-75/TSC-BC_2-31-3	1	Line	medium
12	L_{12}	Sugar-75/TSC-BC_2-32-4	1	Line	medium
13	L_{13}	Hibrix-3//KV/Delectable-BC_1-11-9(2)	2	Line	medium
14	L_{14}	Hibrix-3//P4546/Montauk-BC_1-10-6(1)	2	Line	medium
15	L_{15}	Hibrix-3//P4546/Montauk-BC_1-11-7	2	Line	high
16	L_{16}	Hibrix-3//P4546/Montauk-BC_1-16-7	2	Line	medium
17	L_{17}	Hibrix-3//Jumbo Sweet/Delectable-BC_1-5-3	2	Line	high
18	L_{18}	Hibrix-3//Jumbo Sweet/Delectable-BC_1-5-5	2	Line	medium
19	L_{19}	Hibrix-3//Jumbo Sweet/Delectable-BC_1-13-5	2	Line	medium
20	L_{20}	Hibrix-3//Jumbo Sweet/Delectable-BC_1-17-4	2	Line	high
21	T_1	Dr.Pek's Wan 54		Tester 1	high
22	T_2	Hibrix-53		Tester 2	low
23	C_1	Dr.Pek's 1351		Check 1	high
24	C_2	Hibrix-59		Check 2	low

[1/] Total carotenoid contents were analyzed at maturity stage (35 days after anthesis).

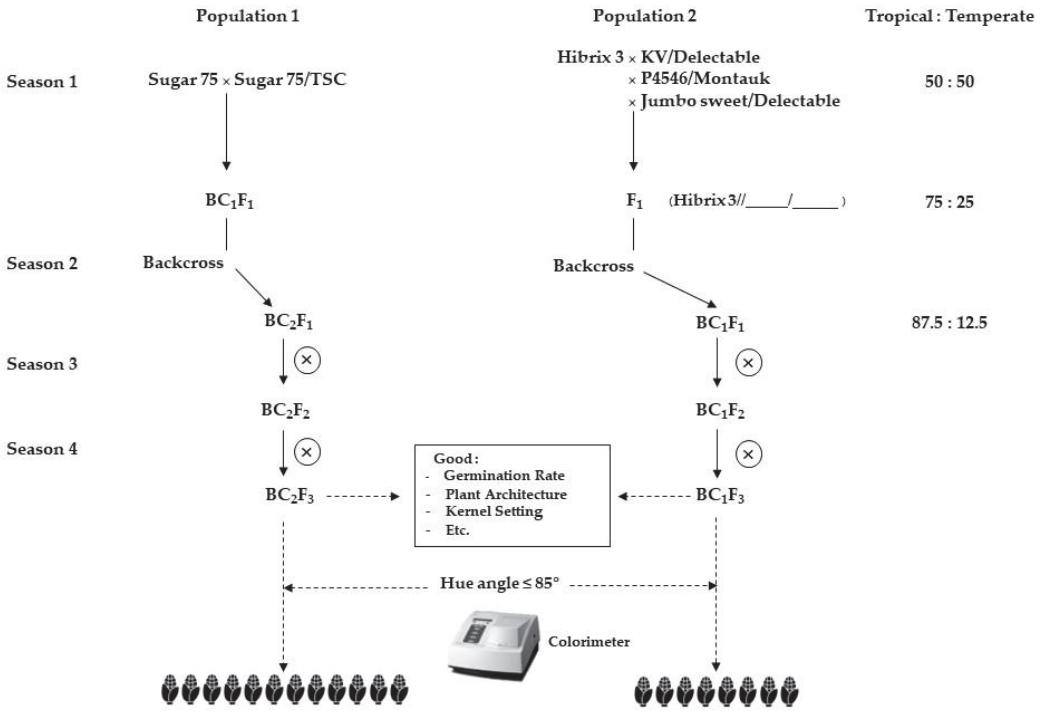

Figure 1. Scheme of the S_2 super sweet corn lines development from a cross between tropical and temperate germplasm.

2.2. Field Experiment

Twenty lines, two hybrid testers, forty hybrids, and two check varieties were evaluated at the Research Farm, Thammasat University, Thailand during May–August 2019 (wet season) and November 2019–February 2020 (dry season). The experiment was conducted in a randomized complete block design (RCBD) with three replications. Each plot consisted of 2 rows 5 m long with a spacing of 0.75 m between rows and 0.25 m between hills in a row; hence, the plant density was 5.33 plants/m^2. Thailand's agricultural recommendations were followed. Fertilizer formula 15-15-15 of NPK was applied at the rate of 312.5 kg/ha before planting, and 156.25 kg/ha of fertilizer formula 46-0-0 was applied twice 20 and 40 days after planting. Weed control was accomplished by hand weeding at critical periods of the crop, whereas pesticides were applied when reaching economic injury level.

Hand pollination was carried out to avoid unintended pollen contamination. Five ears from each plot were harvested at the milk stage, or 20 days after pollination, as a sample for carotenoid analysis. Kernels located in the middle of cobs were manually separated, frozen in liquid nitrogen to stop the enzymatic activity, and then dried using the freeze-drying technique. All the samples were finely ground in a sample mill, sieved through a 60-mesh screen, thoroughly mixed, and stored at −20 °C until analysis.

2.3. Soil and Weather Data

The experimental field is located at 14°04′28.2″ N, 00°36′33.9″ E, 7.3 m above sea level. This site had clay soil (pH = 4.91), very low total nitrogen (0.08%) and available phosphorus (3.85 ppm), and high extractable potassium (165.96 ppm). Weather data, including total rainfall, relative humidity, temperature, and solar radiation, were collected from the nearest meteorological stations. Weather data can be seen in Figure S1.

2.4. Carotenoid Extraction and Analysis

The extraction was performed according to the method of Schaub et al. [30] with slight modifications. The milled samples (1 g) were transferred to 6 mL ethanol (containing 0.1% BHT) and then mixed with a vortex mixer. The tubes were heated in hot water at 85 °C for 3 min and then shaken. This step was repeated twice. The extracts were saponified with 120 µL of 80% KOH and shaken gently by hand. The saponified solutions were placed in an ice bath for 5 min before adding 4 mL of DI water and thoroughly mixing with the vortex mixer. After that, the samples were added with 3 mL of diethyl ether (DE):petroleum ether (PE) (1:1, *v*/*v*) and carefully shaken until two layers separated. The aqueous solution was transferred into a new test tube. This step was repeated twice, and the resulting layers were pooled. Consequently, the solution was adjusted to a final volume of 10 mL with PE:DE. The extracted solution was separated equally into two factions. The first fraction was used to determine the total carotenoid content of each sample. A UV–Vis spectrophotometer (Shimadzu mod. UV-128, Japan) was used to measure the absorbance at 450 nm. The total carotenoid content was expressed as micrograms per gram of dry weight (µg/g of dry weight), and it was calculated according to the following formula:

$$\text{Total carotenoid content} = \frac{A \times \text{V(mL)} \times 10^4}{A1cm1\% \times \text{W}(g)}, \quad (1)$$

where A = absorbance; V = total extract volume; W = sample weight; $A1cm1\% = 2500$ (β-carotene extinction coefficient in PE).

The second fraction was used to quantify each carotenoid. The extracts were concentrated until dry under nitrogen flux. After, samples were stored at −20 °C until further analysis.

The frozen carotenoid extract was dissolved in 1 mL of methyl tert-butyl ether (MTBE):methanol (75:25, *v*/*v*) and filtered through a 0.22 µm nylon membrane filter. The composition of solvents and the gradient elution conditions used were those described by Gupta et al. [31] with slight modifications. Reversed-phase HPLC analysis of carotenoids was performed using a Shimadzu system (Shimadzu, Japan) equipped with a binary pump (LC-20AC pump) and a diode array detector (SPD-M20A). Chromatographic separations were performed on a reversed-phase C30 column (250 × 4.6 mm, 3 µm diameter) coupled to a 20 × 4.6 mm C30 guard column (YMC Co., Japan). The mobile phases were (A) methanol/water (98:2, *v*/*v*), (B) methanol/water (95:5, *v*/*v*), and (C) MTBE. Gradient elution was 80% A, 20% C at 0 min, followed by a linear gradient to 60% A, 40% C to 2 min at a flow rate of 1.4 mL/min. The 2.01 min flow rate was changed to 1.00 mL/min and the gradient was changed to 60% B, 40% C followed by a linear gradient to 0% B, 100% C by 12 min and was returned to the initial condition by 13 min. A re-equilibration (7 min) was carried out at the initial concentration of 80% A, 20% C. Operating conditions were as follows: column temperature of 25 °C, injection volume of 10 µL, and monitoring wavelength of 450 nm. Moreover, peaks were verified with retention time and spectral characteristics by a diode array detector (range 350–600 nm) in both standards and samples. The results for the carotenoids were expressed as micrograms per g of dry weight (µg/g of dry weight).

2.5. Statistical Analysis

Analysis of variance of each growing season was performed, and the error variances were then tested for homogeneity [32]. The line × tester analysis and combining ability estimates for all observed traits were computed by Analysis of Genetic Designs in R (AGD-R) version 5.0 software. Mean comparisons were performed with the least significant difference (LSD) test by Statistix 10.0 [33].

The mean squares for male and female parents are independent estimates of GCA line and GCA tester effects, respectively, while the mean square of line × tester interaction is an estimate of the SCA effect [34,35]. The statistical model followed for combining ability

analysis was that of Singh and Chaudhary [34] with proper modification regarding the line × tester multi-environment according to the AGD-R user manual [36]. The proportional contributions of lines (GCA_L), testers (GCA_T), and their interaction ($SCA_{L\times T}$) to the sum of squares of hybrids were assumed as the ratio between the sum of squares of each component and the sum of squares of hybrids [34]. Combining ability estimates (GCA and SCA), including their standard errors, were calculated following Singh and Chaudhary's formula [34].

3. Results and Discussion

3.1. Line and Tester Analysis

The season was significant for all observed carotenoids (Table 2), indicating that contrasting climate profiles between wet and dry seasons significantly altered the carotenoid contents. Changes in weather parameters such as temperature, solar radiation, relative humidity, and rainfall seemed to interfere with the accumulation of carotenoids among tested genotypes in this study. This assumption was supported by previous studies [37]. The hybrid was significant on all observed carotenoids, suggesting that our tested progenies derived from the line × tester mating fashion were diverse enough to evaluate. The existing variabilities of corn germplasm on carotenoids have been reported [21,25,28,38,39]. Hybrid × season interaction was also significant for all observed carotenoids, indicating that each tested hybrid had different responses to different growing seasons based on carotenoid content. This corroborated previous results [25]. Thus, evaluation of the effect of either germplasm or selected progenies on carotenoid content should be conducted across diverse environments. Moreover, this also revealed that there was a certain number of hybrids that were suitable for growing in specific environments.

Table 2. Combined analysis of variance for carotenoid contents of sweet corn evaluated across two seasons between 2019 and 2020.

SOV	df [1/]	Mean Squares				
		LUT [2/]	ZEA	β-CX	β-CT	TCC
Season (S)	1	537.00 **	1566.00 **	39.50 **	5.77 **	1090.00 **
Rep/S	2	1.37	0.80	0.09	0.02	1.77
Hybrid (H)	39	110.00 **	178.00 **	24.61 **	0.83 **	316.00 **
GCA_L	19	1042.00 **	213.00 **	30.24 **	0.91 **	264.00 **
GCA_T	1	84.78 **	109.00 **	181.63 **	0.77 **	3383.00 **
SCA	19	87.61 **	149.00 **	10.71 **	0.76 **	207.00 **
H × S	39	31.11 **	82.19 **	7.47 **	0.49 **	149.90 **
GCA_L × S	19	35.28 **	83.79 **	7.39 **	0.56 **	80.81 **
GCA_T × S	1	84.78 **	0.00	0.19	0.06	7.71
SCA × S	19	24.18 **	85.48 **	7.94 **	0.43 **	226.00 **
Pooled error	156	0.81	0.77	0.19	0.02	2.88
		Proportion of genetic variance (%)				
O^2_A		6.27	0	4.54	0	30.05
O^2_D		93.73	100	95.46	100	69.95
h^2_{ns} (%)		6	0	4	0	24

[1/] df, degree of freedom; GCA_L, general combining ability of line; GCA_T, general combining ability of tester; SCA, specific combining ability; O^2_A, additive genetic variance; O^2_D, non-additive genetic variance; h^2_{ns}, narrow-sense heritability. [2/] LUT, lutein, ZEA, zeaxanthin; β-CX, β-cryptoxanthin; β-CT, β-carotene; TCC, total carotenoid content. ** significant at $p \leq 0.01$ probability level.

The GCA effects of line and tester were significant on all observed carotenoids, indicating that our parental lines possessed diverse levels of favorable alleles during hybrid formation. Likewise, the SCA effect on these attributes was also significant. Moreover, this result exhibited that hybrids had better or worse performance than expected and had considerable complementation degrees in the frequency of alleles presenting dominance or

over-dominance [40]. The interaction between the GCA line and season was significant on all observed carotenoids. This result suggested that the GCA-based line selection should be applied to each environment; however, the interaction between SCA and season was also significant, and it supposed that the crossbreeding process was not stable across the assessed environments.

A better understanding of the magnitudes of additive and non-additive variance components is important for formulating a breeding strategy on desired traits. The proportion of dominance variance to the total variance was predominant for lutein (93.73%), zeaxanthin (100%), β-cryptoxanthin (95.46%), β-carotene (100%), and total carotenoid content (69.95%) (Table 2). The more dominant gene effect was important, and the less additive gene effect existed. The increased importance of the dominant gene effect on certain traits could be attributed to inbreeding and the accumulation of homozygotic loci [28]. The predominance of non-additive gene action was found in our study's selection criteria; therefore, selections could be performed at later generations. This means that low-intensity selection (*i*) is applied in early breeding cycles to avoid the fixation of deleterious alleles, and increasing selection intensities could be performed in further selection cycles (F_5–F_7) to fix the favorable alleles and harness heterosis.

On the other hand, previous investigations reported the large contribution of additive gene effect instead of non-additive effects on lutein, zeaxanthin, β-cryptoxanthin, and β-carotene of maize [13,25]. Halilu et al. [28] found the predominance of additive gene action on β-cryptoxanthin and non-additive gene actions on grain yield, β-carotene, α-carotene, and provitamin-A. Other studies reported the importance of additive and non-additive gene effects on dried kernel carotenoids of maize [21,38,41]. The contrasting reports on the carotenoid content of corn may be due to differences in the genetic background of materials used, experimental conditions, mating design, or even carotenoid analysis methods.

Low estimates of narrow-sense heritability were noticed on carotenoids, ranging from 0% to 24% (Table 1). Similar results have been reported by Halilu et al. [28], where zero broad- and narrow-sense heritability values for β-cryptoxanthin and α-carotene occurred in tropical-adapted maize. However, other research has found medium to high broad-sense heritability estimates for these traits [13,38,39,41,42]. These results confirmed that the contrasting of this key parameter correlated with genetic backgrounds and/or environmental factors. Moreover, low estimates of heritability indicated that phenotypic selection was not an effective method for improving carotenoid content in corn kernels. Harjes et al. [26] found that kernel color trends have a moderate positive correlation with total carotenoids but only a weak positive correlation with individual carotenoids. The molecular approaches may prove much more efficient than selection based on color alone. Marker-assisted selection (MAS) for favorable alleles of the carotenoid biosynthesis genes, for example, *lcyE* (*lycopene epsilon cyclase*) and *crtRB1* (*β-carotene hydroxylase 1*), has been used to increase the level of carotenoids [26,43]. On the other hand, recurrent selection could be used as a potential strategy for improving quantitative traits such as carotenoid content in corn kernels [24]. Dhliwayo et al. [44] reported that S_1 recurrent selection could increase lutein and zeaxanthin in three diverse maize populations. Additionally, during two cycles of selection, this method could enhance the contents of lutein, zeaxanthin, β-carotene, and total carotenoid of waxy corn populations, ranging from 18.5% to 196.6%, as compared with the base population [45]. Finally, because of the predominance of non-additive gene action and low heritability value, genetic gains from recurrent selection of carotenoids in the base population constructed from 20 S_2 lines presented a suitable breeding strategy for short- and long-term breeding goals.

3.2. Evaluation of Hybrid Performance

With this study, we aimed to establish new super sweet corn hybrids with high carotenoid contents. Thus, the performance of each tested hybrid on carotenoid compositions was investigated. Unfortunately, the superior hybrids having high contents of all carotenoid fractions were not able to be identified (Tables 3 and S1). Across two dif-

ferent growing seasons, the mean of total carotenoid content ranged from 29.78 µg/g of dry weight ($T_1 \times L_8$) (Table S1) to 74.01 µg/g of dry weight ($T_2 \times L_{20}$) (Tables 3 and S1). Among hybrids, the top 10 hybrids had higher total carotenoid content as much as 51.85% and 40.78% than that of average commercial checks and the best commercial check, respectively. On average, the top 10 hybrids produced 34.56 µg/g of dry weight of lutein content, surpassing both the mean of commercial checks by 12.27 µg/g of dry weight and the mean of the best commercial check (Check 1) by 11.26 µg/g of dry weight. For zeaxanthin content, the mean of the top 10 hybrids was 43.21 µg/g of dry weight that was 17.63 µg/g of dry weight (68.92%) higher than the mean of all checks and 11.02 µg/g of dry weight (34.23%) over the best check (Check 2). Fanning et al. [12] and O'Hare et al. [46] improved zeaxanthin concentration in sweet corn kernels, reaching about 80–100 µg/g DW, based on 75% moisture content, which is 2 times higher than the best hybrids of this study. However, this study is an early step in parental selection. Consequently, the selected promising lines could be further developed to be suitable parental lines. The top 10 hybrids on average showed 7.11 µg/g of dry weight of β-cryptoxanthin higher than that of the commercial checks means. Moreover, the β-carotene content of the top 10 hybrids was higher than the average checks and the best check, representing 25.84% and 18.31%, respectively. Among the top 10 hybrids, genotype $T_2 \times L_{20}$ possessed high contents of all observed carotenoids, excluding β-carotene, making this genotype a promising hybrid for biofortified sweet corn (Table 3). This hybrid was derived from T_2 and L_{20} parental lines with positive and high GCA for carotenoid contents (Table 4); this could explain the superiority of hybrid $T_2 \times L_{20}$. This result also illustrated that a proper selection of parental lines based on GCA would be effective to achieve superior hybrids.

Table 3. Performance of top ten hybrids sorted on total carotenoid contents and two commercial checks of super sweet corn evaluated across two seasons between 2019 and 2020.

Hybrids	Carotenoid Contents (µg/g of Dry Weight)				
	LUT [1/]	ZEA	β-CX	β-CT	TCC
$T_2 \times L_{20}$	35.83 ^{ab} [2/]	47.59 ^{a}	12.85 ^{a}	3.58 ^{c}	74.01 ^{a}
$T_2 \times L_{16}$	27.72 ^{def}	33.04 ^{gh}	7.81 ^{g}	3.25 ^{ef}	67.74 ^{b}
$T_2 \times L_{14}$	36.01 ^{ab}	29.79 ^{klm}	7.96 ^{g}	2.58 ^{opq}	65.03 ^{c}
$T_2 \times L_{11}$	24.64 ^{hi}	30.35 ^{kl}	9.37 ^{de}	3.34 ^{de}	64.08 ^{cd}
$T_1 \times L_{20}$	28.10 ^{de}	45.93 ^{b}	10.66 ^{c}	3.14 ^{efg}	62.46 ^{de}
$T_2 \times L_5$	34.90 ^{b}	34.62 ^{f}	9.02 ^{ef}	3.12 ^{fgh}	61.11 ^{e}
$T_2 \times L_{17}$	36.03 ^{ab}	27.77 ^{op}	5.79 ^{mno}	3.03 $^{g–k}$	61.08 ^{e}
$T_2 \times L_1$	29.95 ^{c}	32.54 ^{hi}	6.73 $^{h–l}$	2.83 ^{lmn}	60.61 ^{e}
$T_1 \times L_{13}$	22.39 $^{k–n}$	35.86 ^{e}	8.65 ^{f}	2.62 ^{opq}	60.20 ^{e}
$T_2 \times L_8$	29.58 ^{c}	29.08 ^{mn}	6.67 $^{h–l}$	2.74 ^{mno}	57.76 ^{f}
Mean of top ten hybrids	34.56	43.21	11.89	3.36	60.45
Check 1	23.30 ^{jk}	20.96 ^{u}	3.93 ^{tu}	2.50 ^{pqr}	42.94 ^{o}
Check 2	21.27 ^{opq}	32.19 ^{hij}	6.17 ^{lmn}	2.84 $^{j–n}$	36.67 ^{q}
Mean of checks	22.29	25.58	4.78	2.67	39.81
Grand mean	25.68	30.23	6.96	2.96	51.72
C.V. (%)	3.43	2.88	6.19	4.81	3.24

[1/] LUT, lutein; ZEA, zeaxanthin; β-CX, β-cryptoxanthin; β-CT, β-carotene; TCC, total carotenoid content. [2/] Means followed by the same letters in the same column are not significantly different at the 0.05 probability level as determined by LSD.

Table 4. Parental means and general combining ability (GCA) on carotenoid contents of super sweet corn evaluated across two seasons between 2019 and 2020.

Lines/ Testers	LUT [1/]		ZEA		β-CX		β-CT		TCC	
	Mean [2/]	GCA	Mean	GCA	Mean	GCA	Mean	GCA	Mean	GCA
Lines										
L_1	17.36 $^{c–g}$ [3/]	1.76 **	62.36 ^{a}	1.89 **	4.34 $^{d–h}$	−1.53 **	3.74 ^{bcd}	0.89 **	71.78 ^{bc}	8.71 **
L_2	12.97 $^{e–h}$	2.98 **	17.09 $^{f–i}$	3.89 **	5.69 $^{c–h}$	2.73 **	3.53 ^{cde}	−0.15 *	29.34 ^{m}	0.49
L_3	7.60 ^{h}	1.04 *	13.24 ^{hi}	−3.12 **	2.28 ^{h}	−1.26 **	2.54 ^{efg}	−0.49 **	22.03 ^{n}	−11.30 **
L_4	54.28 ^{a}	−1.25 **	55.54 ^{a}	−2.61 **	7.60 $^{b–e}$	−1.65 **	3.04 $^{d–g}$	−0.24 **	68.84 ^{c}	−9.69 **
L_5	14.36 $^{d–h}$	2.38 **	17.73 $^{f–i}$	2.29 **	9.74 ^{ab}	−0.00	4.30 ^{abc}	−0.21 **	40.71 ^{hi}	−0.98
L_6	13.44 $^{e–h}$	−4.86 **	22.59 $^{d–i}$	−3.69 **	2.34 ^{gh}	−0.77 **	3.10 $^{d–g}$	−0.29 **	25.17 ^{n}	5.40 **
L_7	18.51 $^{c–f}$	−0.30	34.70 ^{bc}	−1.98 **	4.03 $^{e–h}$	−1.46 **	2.67 ^{efg}	0.10	39.28 ^{ij}	5.57 **
L_8	9.34 ^{fgh}	3.17 **	26.92 $^{c–g}$	2.38 **	3.65 ^{fgh}	−0.90 **	2.45 ^{g}	−0.63 **	36.50 ^{jk}	−7.03 **
L_9	22.26 $^{b–e}$	−0.23	61.94 ^{a}	−3.21 **	9.99 ^{ab}	0.43 *	2.98 $^{d–g}$	1.38 **	82.24 ^{a}	3.68 **
L_{10}	20.27 $^{b–e}$	0.75 *	24.96 $^{c–h}$	2.39 **	13.25 ^{a}	2.06 **	4.91 ^{a}	0.79 **	43.15 ^{gh}	−2.81 **
L_{11}	20.78 $^{b–e}$	−4.43 **	25.08 $^{c–h}$	−3.36 **	5.74 $^{c–h}$	−1.32 **	4.52 ^{ab}	0.15 *	48.59 ^{f}	−0.36
L_{12}	20.42 $^{b–e}$	−2.82 **	34.10 ^{bcd}	−2.24 **	7.24 $^{b–f}$	0.75 **	4.73 ^{a}	−0.33 **	56.58 ^{e}	2.38 **
L_{13}	9.21 ^{fgh}	1.95 **	12.12 ^{i}	2.47 **	4.09 $^{e–h}$	1.85 **	3.27 $^{d–g}$	−0.40 **	33.89 ^{kl}	−1.56 *
L_{14}	13.40 $^{e–h}$	2.32 **	19.78 $^{f–i}$	−0.33	5.37 $^{c–h}$	−0.41 *	3.49 $^{c–f}$	−0.51 **	36.59 ^{jk}	−1.53 *
L_{15}	16.03 $^{c–h}$	−5.78 **	19.63 $^{f–i}$	−6.40 **	8.56 ^{bc}	−0.11 *	4.68 ^{ab}	−0.15 *	61.90 ^{d}	−2.83 **
L_{16}	16.82 $^{c–h}$	−4.14 **	33.75 ^{bcd}	3.20 **	2.36 ^{gh}	0.70 **	2.70 ^{efg}	−0.21 **	44.86 ^{fg}	10.34 **
L_{17}	44.59 ^{a}	1.35 **	41.30 ^{b}	−4.52 **	7.99 ^{bcd}	−2.35 **	3.11 $^{d–g}$	−0.51 **	72.54 ^{bc}	−1.68 *
L_{18}	29.24 ^{b}	2.24 **	28.80 $^{c–f}$	−2.76 **	5.40 $^{c–h}$	0.12	2.94 $^{d–g}$	−0.43 **	59.40 ^{de}	−0.43
L_{19}	8.51 ^{gh}	2.28 **	15.91 ^{ghi}	3.62 **	4.25 $^{d–h}$	−0.89 **	4.59 ^{ab}	0.52 **	32.62 ^{lm}	−12.55 **
L_{20}	24.27 ^{bc}	1.59 **	31.92 $^{b–e}$	12.09 **	9.84 ^{ab}	4.04 **	4.65 ^{ab}	0.44 **	72.99 ^{b}	16.16 **
Testers										
T_1	23.30 ^{bcd}	−1.83 **	20.96 $^{e–i}$	0.86 **	3.93 ^{eh}	−1.10 **	2.51 ^{fg}	−0.09 **	42.94 ^{ghi}	−4.82 **
T_2	21.22 $^{b–e}$	1.83 **	32.19 $^{b–e}$	−0.86 **	6.17 $^{b–e}$	1.10 **	2.84 $^{d–g}$	0.09 **	36.67 ^{jk}	4.82 **
SE_{Line}		0.58		0.61		0.28		0.10		1.20
SE_{Tester}		0.18		0.19		0.09		0.33		0.38

[1/] LUT, lutein; ZEA, zeaxanthin; β-CX, β-cryptoxanthin; β-CT, β-carotene; TCC, total carotenoid content. [2/] Means are expressed in μg/g of dry weight. [3/] Means followed by the same letters in the same column are not significantly different at the 0.05 probability level as determined by LSD. * and ** GCA estimates are significantly different from zero at ≥SE and ≥2SE, respectively.

3.3. General Combining Ability (GCA) and Specific Combining Ability (SCA)

General combining ability has been widely adopted in crop breeding to assist line selections instead of line per se alone. Promising lines with a good line per se and GCA on targeted traits are preferred. With a few exceptions, the contributions of sweet corn lines and testers to hybrids were not consistent across carotenoid profiles in this study (Table 4). Favorable genotypes with high carotenoid content were represented by high parental means and positive GCA values. The parental means of 20 lines on five carotenoid parameters differed significantly from the parental means with total carotenoid content. Parental line L_{20} was the only one with high contents of all observed carotenoids, while other lines showed adequate performances on certain fractions, e.g., L_4 and L_{17} on lutein; L_1, L_4, and L_9 on zeaxanthin; L_5, L_9, and L_{10} on β-cryptoxanthin; and L_{10}, L_{11}, L_{12}, L_{15}, and L_{19} on β-carotene.

Eight parental lines, L_1, L_2, L_9, L_{10}, L_{13}, L_{16}, L_{19}, and L_{20}, revealed adequate GCA on carotenoid content, of which genotype L_{20} was the best, presenting a large number of favorable alleles of carotenoid that existed in this genotype (Table 4). The GCA values of genotypes L_4 and L_{15} were negative, indicating that these lines had a lack of favorable alleles of lutein, zeaxanthin, β-cryptoxanthin, β-carotene, and total carotenoid content. Moreover, the S_2 lines had greater contributions than the testers on all observed carotenoids. Genetic materials and cross direction during hybrid formation using the line × tester scheme were plausible reasons.

The ideal tester for hybrid breeding should appeal following criteria including the one that performed well, was efficient at classifying the relative performances among lines, and was practical during hybrid formation. Several factors have been considered

to choose appropriate testers in hybrid breeding, including gene frequency of favorable alleles, average testcross performance, the magnitude of variance estimates, and GCA effects [23,47]. Elite inbred lines are the logical choice for testers in commercial hybrid breeding [48]. However, a single-cross hybrid with outstanding combining ability would be a reasonable tester for a breeding program that lacks reliable inbred testers [49]. A previous study on combining ability assigned maize F_1 hybrids as testers in their mating design, and this method could identify superior three-way cross hybrids and heterotic groups [50]. Moreover, in sweet corn, two parameters, seed germination rate and seedling vigor, are critical issues determining the efficiency of hybrid seed production. Assigning F_1 hybrids as female testers like in our study could enhance the germination rate and seedling vigor of female plants and hybrid seed production due to the good seed set of female ears; thus, this concept will benefit hybrid seed producers. Our preliminary study found that F_1 hybrids can be effectively assigned to identify our breeding lines better than the inbred lines. Therefore, in this study, two F_1 hybrids differing in carotenoid content and heterotic groups were used.

The results indicate that suitable testers for individual traits were identified, but not for multiple traits (Table 4). The T_2 tester had significant and positive GCA estimates for lutein, β-cryptoxanthin, β-carotene, and total carotenoid content across two seasons, while the T_1 tester had a positive GCA estimate for zeaxanthin, and they can thus be regarded as suitable testers. The T_2 tester consistently identified most of the tested lines that formed the best testcross identified carotenoid content in the present study, although the relative ranks were not identical (Tables 3 and S1). Moreover, the T_2 tester identified two lines forming testcrosses showing a significant and positive GCA estimate for most studies except zeaxanthin, whereas the T_1 tester did not identify any line (Table 4). All the criteria used to identify the best tester favored the selection of the T_2 testers as promising candidates to separate superior S_2 lines for the hybridization and development of biofortified sweet corn hybrids.

Both general and specific combining abilities should be considered when interpreting the results of inbred lines evaluation during hybrid formation. It was ideal to associate high GCA and SCA values since they were two fundamental criteria used in population selection, namely high mean and the greatest genetic variance [35,51]. Hybrids with high hybrid means and positive SCA values are favorable. The contribution of sweet corn hybrids to hybrids was not stable across carotenoids, with a few exceptions (Table S1). However, several hybrids showed impressive SCA for carotenoid content.

Two major fractions of carotenoids, namely lutein and zeaxanthin, were emphasized in this study. The two positive and highest SCA estimates were found in $T_2 \times L_{12}$ and $T_2 \times L_{18}$ for lutein, and in $T_1 \times L_{10}$ and $T_2 \times L_{12}$ for zeaxanthin (Table S1). These hybrids involved one to two parental pairs that had positive GCA estimates. Both the top five high-lutein hybrids ($T_2 \times L_2$, $T_2 \times L_{17}$, $T_2 \times L_{14}$, $T_2 \times L_{20}$, and $T_2 \times L_5$) and the top five high-zeaxanthin hybrids ($T_2 \times L_{20}$, $T_1 \times L_{20}$, $T_1 \times L_{10}$, $T_2 \times L_2$, and $T_1 \times L_{19}$) (Tables 2 and S1) were composed of at least a male line with adequate GCA. A similar pattern was also found in the other three carotenoid fractions. Regarding β-cryptoxanthin, β-carotene, and total carotenoid content, high and positive SCA estimates involved at least one parent presenting high GCA. However, we also noticed that a hybrid with high and positive SCA was derived from a parental pair with negative GCA. This result indicated that both S_2 lines and testers possessed genes that are complementary.

4. Conclusions

The non-additive variance was predominantly prevailing for all the carotenoid content that can be exploited in hybrid breeding. L_{20}, the superior line with positive and high GCA values, was the best general combiner for all the traits, whereas T_2 could be considered the best tester. Moreover, the testcross hybrids with efficient performance and desirable SCA estimates involve at least one of the parents with positive GCA. $T_2 \times L_{20}$ had high contents of all traits that were found in $T_2 \times L_9$, except β-carotene. Although sweet corn hybrids

with high carotenoids have a greater advantage for growers and consumers, high yield and satisfactory eating quality are the primary goals of breeding programs. Thus, the selected promising S_2 lines could be further developed to be elite inbred lines and selected through combining ability by intercrossing with lines originating from other gene pools with high yield and palatability for establishing single-cross hybrids in the future.

Supplementary Materials: The following supporting information can be downloaded at: https://www.mdpi.com/article/10.3390/agriculture12101561/s1, Figure S1: Total rainfall, relative humidity, temperature, and solar radiation during crop growth at the Experimental Field, Thammasat University, Thailand in the wet season 2019 (a) and dry season 2019/20 (b); Table S1: Mean and specific combining ability (SCA) of 40 super sweet corn hybrids and two commercial checks for carotenoid contents evaluated across two seasons between 2019 and 2020.

Author Contributions: Conceptualization, B.H., W.W., Y.J., K.L. and K.S.; Formal analysis, B.H., W.W., Y.J. and K.S.; Methodology, B.H., W.W. and K.L.; Writing—original draft, B.H. and W.W.; Writing—review and editing, B.H., Y.J. and K.S.; Project administration, B.H.; Funding acquisition, B.H. All authors have read and agreed to the published version of the manuscript.

Funding: This study was supported by the Thammasat University Research Fund, Contract No. TUFT 2/2564, and the Thailand Toray Science Foundation through Science and Technology Research Grants National Science and Technology for the year 2018.

Institutional Review Board Statement: Not applicable.

Data Availability Statement: The data that support the findings of this study are available from the corresponding author upon reasonable request.

Acknowledgments: We acknowledge the Department of Agricultural Technology, Faculty of Science and Technology, Thammasat University, Thailand for providing research facilities. The sweet corn germplasm used for improved base populations was supplied by the Plant Breeding Research Center for Sustainable Agriculture, Khon Kaen University, Thailand. The authors wish to thank Theerapun Chumroenphat for the guidance provided in the chemical analyses and Abil Dermail for proofreading of the manuscript.

Conflicts of Interest: The authors declare no conflict of interest.

References

1. Ruanjaichon, V.; Khammona, K.; Thunnom, B.; Suriharn, K.; Kerdsri, C.; Aesomnuk, W.; Yongsuwan, A.; Chaomueang, N.; Thammapichai, P.; Arikit, S.; et al. Identification of gene associated with sweetness in corn (*Zea mays* L.) by genome-wide association study (GWAS) and development of a functional SNP marker for predicting sweet corn. *Plants* **2021**, *10*, 1239. [CrossRef]
2. Mehta, B.K.; Muthusamy, V.; Baveja, A.; Chauhan, H.S.; Chhabra, R.; Bhatt, V.; Chand, G.; Zunjare, R.U.; Singh, A.K.; Hossain, F. Composition analysis of lysine, tryptophan and provitamin-A during different stages of kernel development in biofortified sweet corn. *J. Food Comp. Anal.* **2020**, *94*, 103625. [CrossRef]
3. Food and Agriculture Organization. FAOSTAT. Available online: http://www.fao.org/faostat/en/#home (accessed on 30 June 2020).
4. Swapna, G.; Jadesha, G.; Mahadevu, P. Sweet corn-A future healthy human nutrition food. *Int. J. Curr. Microbiol. App. Sci.* **2020**, *9*, 3859–3865. [CrossRef]
5. Sheng, S.; Li, T.; Liu, R.H. Corn phytochemicals and their health benefits. *J. Food Sci.* **2018**, *7*, 185–195.
6. Palozza, P.; Krinsky, N.I. Antioxidant effects of carotenoids in vivo and in vitro: An overview. *Meth. Enzymol.* **1992**, *213*, 403–452.
7. Moeller, S.M.; Jacques, P.F.; Blumberg, J.B. The potential role of dietary xanthophylls in cataract and age-related macular degeneration. *J. Am. Coll. Nutr.* **2000**, *19*, 522S–527S. [CrossRef]
8. Dwyer, J.H.; Navab, M.; Dwyer, K.M.; Hassan, K.; Sun, A.; Shircore, A.; Hama-Levy, S.; Hough, G.; Wang, X.; Drake, T.; et al. Oxygenated carotenoids lutein and progression of early atherosclerosis. *Circulation* **2001**, *103*, 2922–2927. [CrossRef]
9. Trono, D. Carotenoids in cereal food crops: Composition and retention throughout grain storage and food processing. *Plants* **2019**, *8*, 551. [CrossRef]
10. Abdel-Aal, E.-S.M.; Akhtar, H.; Zaheer, K.; Ali, R. Dietary source of lutein and zeaxanthin carotenoids and their role in eye health. *Nutrients* **2013**, *5*, 1169–1185. [CrossRef]
11. Baseggio, M.; Murray, M.; Magallanes-Lundback, M.; Nicholas Kaczmar, N.; Chamness, J.; Buckler, E.S.; Smith, M.E.; Penna, D.D.; Tracy, W.F.; Gore, M.A. Natural variation for carotenoids in fresh kernels is controlled by uncommon variants in sweet corn. *Plant Genome* **2020**, *13*, e20008. [CrossRef]

12. Fanning, K.; Martin, I.; Wong, L.; Keating, V.; Pun, S.; Hare, O.J. Screening sweetcorn for enhanced zeaxanthin concentration. *J. Sci. Food Agric.* **2010**, *90*, 91–96. [CrossRef]
13. Li, R.; Xiao, L.H.; Wang, J.; Lu, Y.L.; Rong, T.Z.; Pan, G.T.; Wu, Y.Q.; Tang, Q.; Lan, H.; Cao, M.J. Combining ability and parent-offspring correlation of maize (*Zea may* L.) grain β-carotene content with a complete diallel. *J. Integr. Agric.* **2013**, *12*, 19–26. [CrossRef]
14. Khokhar, E.S.; Shakeel, A.; Maqbool, M.A.; Abuzar, M.K.; Zareen, S.; Aamir, S.A.; Asadullah, M. Studying combining ability and heterosis in different cotton (*Gossypium hirsutum* L.) genotypes for yield and yield contributing traits. *Pak. J. Agric. Sci.* **2018**, *31*, 55–68. [CrossRef]
15. Rojas, B.A.; Sprague, G.F. A comparison of variance components in corn yield trials. III general and specific combining ability and their interactions with locations and years. *Agron. J.* **1952**, *44*, 462–466. [CrossRef]
16. Falconer, D.S. *Introduction to Quantitative Genetics*, 3rd ed.; Longman Scientific and Technical, Co.: New York, NY, USA, 1989.
17. Sharma, H.C.; Dhillan, M.K.; Reddy, B.V.S. Expression of resistance to *Atherigona soccata* in F_1 hybrids involving shoot fly-resistant and susceptible cytoplasmic male-sterile and restorer lines of sorghum. *Plant Breed.* **2006**, *125*, 473–477. [CrossRef]
18. Elmyhum, M. Estimation of combining ability and heterosis of quality protein maize inbred lines. *Afr. J. Agric. Res.* **2013**, *8*, 6309–6317.
19. Amin, M.N.; Amirurzaman, M.; Ahmed, A.; Ali, M.R. Evaluation of inbred lines of maize (*Zea mays* L.) through line x tester method. *Bangladesh J. Agric. Res.* **2014**, *39*, 675–683. [CrossRef]
20. Kahriman, F.; Egesel, C.Ö.; Orhun, G.E.; Alaca, B.; Avci, F. Comparison of graphical analyses for maize genetic experiments: Application of biplots and polar plot to line x tester design. *Chil. J. Agric. Res.* **2016**, *76*, 285–293. [CrossRef]
21. Maqbool, M.A.; Aslam, M.; Khan, M.S.; Beshir, A.; Ahan, M. Evaluation of single cross yellow maize hybrids for agronomic and carotenoid traits. *Int. J. Agric. Biol.* **2017**, *19*, 1087–1098. [CrossRef]
22. Fountain, J.C.; Abbas, H.K.; Scully, B.T.; Li, H.; Lee, R.D.; Kemerait, R.C.; Guo, B. Evaluation of maize inbred lines and topcross progeny for resistance to pre-harvest aflatoxin contamination. *Crop J.* **2019**, *7*, 118–125. [CrossRef]
23. Zebire, D.; Menkir, A.; Adetimirin, V.; Mengesha, W.; Meseka, S.; Gedil, M. Effectiveness of yellow maize testers with varying resistance reactions to *Striga hermonthica* for evaluating the combining ability of maize inbred lines. *Agronomy* **2020**, *10*, 1276. [CrossRef]
24. Maqbool, M.A.; Aslam, M.; Beshir, A.; Khan, M.S. Breeding for provitamin A biofortification of maize (*Zea mays* L.). *Plant Breed.* **2018**, *137*, 451–469. [CrossRef]
25. Egesel, C.O.; Wong, J.C.; Lambert, R.J.; Rocheford, T.R. Combining ability of maize inbred for carotenoid and tocopherols. *Crop Sci.* **2003**, *43*, 818–823. [CrossRef]
26. Harjes, C.E.; Rocheford, T.R.; Bai, L.; Brutnell, T.P.; Kandianis, C.B.; Sowinski, S.G.; Stapleton, A.E.; Vallabhaneni, R.; Williams, M.; Wurtzel, E.T.; et al. Natural genetic variation in lycopene epsilon cyclase tapped for maize biofortification. *Science* **2008**, *319*, 330–333. [CrossRef]
27. da Silva Messias, R.; Galli, V.; Silva, S.D.D.A.; Rombaldi, C.V. Carotenoid biosynthetic and catabolic pathways: Gene expression and carotenoid content in grains of maize landraces. *Nutrients* **2014**, *6*, 546–563. [CrossRef]
28. Halilu, A.D.; Ado, S.G.; Aba, D.A.; Usman, I.S. Genetics of carotenoids for provitamin A biofortification in tropical-adapted maize. *Crop J.* **2016**, *4*, 313–322. [CrossRef]
29. Menkir, A.; Olowolafe, M.O.; Ingelbrecht, I.; Fawole, I.; BaduApraku, B.; Vroh, B.I. Assessment of testcross performance and genetic diversity of yellow endosperm maize lines derived from adapted × exotic backcrosses. *Theor. Appl. Genet.* **2006**, *113*, 90–99. [CrossRef]
30. Maize Quick Carotenoid Extraction Protocol. Available online: http://www.cropsci.uiuc.edu/faculty/rocheford/quick_carotenoid_analysis_protocol.pdf (accessed on 20 June 2019).
31. Gupta, P.; Sreelakshmi, Y.; Sharma, R. A rapid and sensitive method for determination of carotenoids in plant tissues by high performance liquid chromatography. *Plant Methods* **2015**, *11*, 5–16. [CrossRef]
32. Gomez, K.A.; Gomez, A.A. *Statistical Procedures for Agricultural Research*, 2nd ed.; An International Rice Research Institute Book, Co., Inc.: New York, NY, USA, 1984.
33. Statistix 10 Data analysis Software for Researchers. Available online: https://www.statistix.com (accessed on 11 November 2014).
34. Singh, R.K.; Chaudhary, B.D. *Biometrical Methods in Quantitative Genetic Analysis*; Kalyani Publishers: New Delhi, India, 1985.
35. Hallauer, A.R.; Carena, M.J.; Miranda, J.B. *Quantitative Genetics in Maize Breeding*; Springer: New York, NY, USA, 2010.
36. Rodríguez, F.; Alvarado, G.; Pacheco, A.; Crossa, J.; Burgueno, J. *AGD-R (Analysis of Genetic Designs with R for Windows) Version 5.0*; International Maize and Wheat Improvement Center: Mexico City, Mexico, 2018.
37. Mengesha, T.; Cao, F.B.; Wasim, I.; Wu, F.B. Differences in physiological and biochemical characteristics in response to single and combined drought and salinity stresses between wheat genotypes differing salt tolerance. *Physiol. Plant* **2019**, *165*, 134–143.
38. Chander, S.; Guo, Y.; Zhang, Y.; Li, J. Comparison of nutritional traits variability in selected eighty-seven inbreds from Chinese maize (*Zea mays* L.) germplasm. *J. Agric. Food Chem.* **2008**, *56*, 6506–6511. [CrossRef]
39. Muthusamy, V.; Hossain, F.; Thirunavukkarasu, N.; Saha, S.; Agrawal, P.K.; Gupta, H.S. Genetic analyses of kernel carotenoids in novel maize genotypes possessing rare allele of ß-carotene hydroxylase gene. *Cereal Res. Commun.* **2016**, *44*, 669–680. [CrossRef]
40. Durães, N.N.L.; Crevelari, J.A.; Vettorazzi, J.C.F.; Ferreira, J.A.; de Abreu Santana, F.; Pereira, M.G. Combining ability for traits associated with yield and quality in super sweet corn (*Zea mays* L. saccharata). *Crop Sci.* **2017**, *11*, 1188–1194. [CrossRef]

41. Suwarno, W.B.; Pixley, K.V.; Palacios-Rojas, N.; Kaeppler, S.M.; Babu, R. Formation of heterotic groups and understanding genetic effects in a provitamin A biofortified maize breeding program. *Crop Sci.* **2014**, *54*, 14–24. [CrossRef]
42. Wong, J.C.; Lambert, R.J.; Wurtzel, E.T.; Rocheford, T.R. QTL and candidate genes phytoene synthase and zeta-carotene desaturase associated with the accumulation of carotenoids in maize. *Theor. Appl. Genet.* **2004**, *108*, 349–359. [CrossRef]
43. Yan, J.; Kandianis, C.B.; Harjes, C.E.; Bai, L.; Kim, E.H.; Yang, X.; Skinner, D.; Fu, Z.; Mitchell, S.; Li, Q.; et al. Rare genetic variation at *Zea mays crtRB1* increases β-carotene in maize grain. *Nat. Genet.* **2010**, *42*, 322–327. [CrossRef]
44. Dhliwayo, T.; Palacios-Rojas, N.; Crossa, J.; Pixley, K.V. Effects of S_1 recurrent selection for provitamin A carotenoid content for three open-pollinated maize cultivars. *Crop Sci.* **2014**, *54*, 2449–2460. [CrossRef]
45. Khamkhoh, W.; Ketthaisong, D.; Lomthaisong, K.; Lertrat, K.; Suriharn, K. Recurrent selection method for improvement of lutein and zeaxanthin in orange waxy corn populations. *Aust. J. Crop Sci.* **2019**, *13*, 566–573. [CrossRef]
46. O'Hare, T.J.; Fanning, K.; Martin, I. Zeaxanthin biofortification of sweet-corn and factors affecting zeaxanthin accumulation and colour change. *Arch. Biochem. Biophys.* **2015**, *572*, 184–187. [CrossRef]
47. Castellanos, J.S.; Hallauer, A.R.; Córdova, H.S. Relative performance of testers to identify elite lines of corn (*Zea mays* L.). *Maydica* **1998**, *43*, 217–226.
48. Bernardo, R. *Breeding for Quantitative Traits in Plants*, 3rd ed.; Stemma Press: Woodbury, MN, USA, 2020.
49. Fasahat, P.; Rajabi, A.; Rad, J.M.; Derera, J. Principles and utilization of combining ability in plant breeding. *Biom. Biostat. Int. J.* **2016**, *4*, 1–22. [CrossRef]
50. Pswarayi, A.; Vivek, B.S. Combining ability amongst CIMMYT's early maturing maize (*Zea mays* L.) germplasm under stress and non-stress conditions and identification of testers. *Euphytica* **2008**, *162*, 353–362. [CrossRef]
51. Sprague, G.F.; Tatum, L.A. General vs. specific combining ability in single crosses of corn. *J. Am. Soc. Agron.* **1942**, *34*, 923–932. [CrossRef]

agriculture

MDPI

Article

Statistical Multivariate Methods for the Selection of High-Yielding Rapeseed Lines with Varied Seed Coat Color

Agnieszka Łopatyńska [1], Joanna Wolko [1,*], Jan Bocianowski [2], Adrian Cyplik [2] and Katarzyna Gacek [1,†]

[1] Plant Breeding and Acclimatization Institute—National Research Institute, Poznań Division, Department of Oilseed Crops, Strzeszyńska 36, 60-479 Poznań, Poland
[2] Department of Mathematical and Statistical Methods, Poznań University of Life Sciences, Wojska Polskiego 28, 60-637 Poznań, Poland
* Correspondence: j.wolko@ihar.edu.pl; Tel.: +48-61-846-42-02
† Current address: IHAR Group, Plant Breeding Smolice Ltd., Smolice 146, 63-740 Kobylin, Poland.

Abstract: A crucial aim for rapeseed breeders is increasing the seed yield through improving yield- and silique-related traits. In this research, traits including the number of seeds per silique, silique length, silique width, and thousand-seed weight combined with seed coat color were investigated. Yellow-seeded lines of oilseed rape have a thinner seed coat, lower fiber content, and higher protein and oil content than traditional varieties. Hybrids of yellow- and black-seeded *Brassica napus*, which combine the advantages of both types of seeds, are tested for their suitability in breeding. Therefore, the aim of this study was to assess a population of 78 doubled haploid lines with different seed coat colors to select genotypes connecting a light color of seeds with good yielding characteristics. Multivariate methods such as analysis of variance, correlation analysis, regression analysis, canonical variate analysis, Mahalanobis distances, and estimation of gene effects were used. The results showed that all tested genotypes were significantly different regarding all five studied traits. The multidimensional analyses gave an accurate overview of the relationship between the examined features. The color and weight of seeds were considered the most important for breeding rapeseed with better seed properties. Although a negative correlation between these two characteristics occurs quite commonly, it was not present in our plant material, which allowed us to select lines with a-light seed color and high thousand-seed weight, which is a significant achievement. As a result, two doubled haploid lines were chosen as valuable breeding material for creating oilseed rape varieties with improved biochemical characteristics of seeds.

Keywords: *Brassica napus*; multivariate methods; thousand-seed weight; yellow-seeded rapeseed

Citation: Łopatyńska, A.; Wolko, J.; Bocianowski, J.; Cyplik, A.; Gacek, K. Statistical Multivariate Methods for the Selection of High-Yielding Rapeseed Lines with Varied Seed Coat Color. *Agriculture* **2023**, *13*, 992. https://doi.org/10.3390/agriculture13050992

Academic Editor: Rosario Paolo Mauro

Received: 24 March 2023
Revised: 18 April 2023
Accepted: 28 April 2023
Published: 29 April 2023

1. Introduction

Improving the seed yield in oilseed rape (*Brassica napus* L.) is a key task for breeders. The yield is one of the most important and complex traits in crop species determined by direct and indirect yield-related traits. The main features that define the seed yield in *Brassica napus* include the number of siliques per plant (NSPP), number of seeds per silique (NSPS), and thousand-seed weight (TSW) [1]. The number of siliques per plant and seeds per silique have the greatest impact on the amount of seeds produced by the plant; therefore, improving the NSPS without decreasing the seed weight is an important breeding goal in many crop species [2]. It may be complicated due to the negative correlation that has been observed between NSPS and TSW [3].

Various studies show that the seed yield is also determined indirectly by silique-related traits such as the silique length (SL) and silique width (SW). The silique length is an important yield trait and positively correlates with the number of seeds per silique and seed weight [4]. Previous studies have proved that the enhancement of silique length could effectively improve the seed yield [5–7]. Since the number of siliques per plant is very susceptible to the genotype and environment [8], improving the seed yield through

coordination between NSPS, SL, SW, and TSW is a crucial aim in rapeseed breeding. For this reason, these are the features that we focused on in this study.

Yellow- and light-color-seeded lines of oilseed rape are characterized by a thinner seed coat, lower fiber content, and higher protein and oil content than traditional rapeseed [9]. Due to the properties of yellow seeds, they could be better exploited, as the by-product of obtaining oil from them is a protein-rich rapeseed meal with good digestibility. This makes it different from the extracted meal obtained from black-seeded lines, which due to the high fiber content cannot be used, for example, in poultry farming [10]. Despite many positive features, yellow-seeded lines are not commonly cultivated, because they have many disadvantages, such as seeds sprouting in the siliques and self-pressing of oil from the seeds during storage [11]. In addition, the yield of yellow-seeded lines is usually lower than that of black-seeded [12]. Furthermore, Piotrowska et al. [13] observed in their research a reduced seed yield of yellow lines, but the oil content in their seeds was higher. However, the overall yield of oil from the yellow lines studied by them was lower than that of the reference cultivar—precisely because of the lower seed yield.

Summarizing all aspects, valuable hybrids of yellow- and black-seeded *Brassica napus*, which combine the advantages of both types of seeds, such as high yield and high oil and protein content, are searched and tested for their suitability in breeding. However, this requires a non-standard approach, such as using more complicated mathematical methods. Therefore, the aim of this study was to assess the population of DH lines with different seed coat color in order to select lines combining these components. For this purpose, multidimensional analyses were used, which allowed for the assessment of the tested lines in terms of many features simultaneously. Multivariate statistical methods, such as canonical variate analysis or Mahalanobis D^2 statistics, simplify the dimensionality of multi-feature object comparisons [14,15]. Using these methods allowed us to choose from the studied lines those combining the most desirable traits, which is a valuable achievement with promising results.

2. Materials and Methods

2.1. Plant Material

The plant material used in this study consisted of 78 doubled haploid (DH) lines of winter oilseed rape and their parental forms. The DH population (M305 × Z114) was developed from F_1 plants of a cross between M305 (black-seeded) and Z114 (yellow-seeded) *Brassica napus* DH lines selected for contrasting seed coat color and seed fiber content.

The DH lines were produced in the Laboratory of Plant Tissue Culture, Plant Breeding and Acclimatization Institute—National Research Institute in Poznań, Poland using the isolated microspore culture method according to the procedure described by Cegielska-Taras et al. [16]. Microspores were isolated from unopened flower buds of donor plants (M305 × Z114 hybrids), sterilized, and macerated in NLN medium. The microspore pellet was plated on Petri dishes for 10 days in the dark at 30 °C. The dishes with microspore-derived embryos (MDEs) visible to the naked eye were then placed on an illuminated rotary shaker at 25 °C. Twenty-one-day-old MDEs were plated on Petri dishes with B5 medium, and then conversion of the embryos to plantlets took place. The dishes were then placed for 14 days at 1 °C under 8 h light. After this time, the dishes were transferred to the conditions of the culture room: 24 °C temperature and 16 h lighting. Over the next three weeks, the development of normal shoots from the apical meristem of the embryo was observed, as well as the development of roots. The young plants were transferred to the soil.

2.2. Field Trial

The M305 × Z114 mapping population and parental lines were cultivated in the Plant Breeding and Acclimatization Institute—National Research Institute experimental field in Poznań, Poland (52°45′ N, 16°90′ E) during the growing season of 2017/2018. The field trial was carried out in a randomized block design with three replicates of double 2 m

long rows with 30 cm spacing. In each row 100 seeds were sown. The field was managed with standard methods. Accordingly, fertilizer was applied in the fall: K 90 kg/ha, P 60 kg/ha, N 18 kg/ha, and S 18 kg/ha. In the spring, N 26 kg/ha and S 13 kg/ha were used. Appropriate plant protection products were also applied in the fall and spring.

The silique length, silique width, and number of seeds per silique were estimated on 20 siliques from each replicate. The siliques were collected at the stage of mature seeds from the main branch of five random plants and then dried. The thousand-seed weight was estimated as the average of three measurements from the mixed seeds in each replication. The seed coat color was determined on the same seed samples with the Hunter Labs spectrocolorimeter (Colorflex) and classified using a 0 (black) to 5 (yellow) scale [17]. The results of detailed analyses of the content of oil, protein, fiber (ADF and NDF), and glucosinolates in the seeds of the studied population in two growing seasons (2015/2016 and 2017/2018), investigated with a near-infrared reflectance spectroscopy (NIRS), have been previously published in Wolko et al.'s [18] study. The studied DH population was also sequenced and the obtained SNPs markers were used for QTL genetic mapping to search for loci associated with the biochemical components of seeds and seed coat color. Several candidate genes connected to seed fiber and color were identified as a result, which was described in a publication by Gacek et al. [19].

2.3. Statistical Analysis

The normality of the distributions for the studied traits (silique length, silique width, number of seeds per silique, seed coat color, and thousand-seed weight) was tested using Shapiro–Wilk's normality test [20]. Multivariate analysis of variance (MANOVA) was performed based on the following model using a MANOVA procedure: Y = XT + E, where Y is an $(n \times p)$-dimensional matrix of observations, where n is the total number of observations and p is the number of traits; X is an $(n \times k)$-dimensional matrix of design, where k is the number of genotypes; T is a $(k \times p)$-dimensional matrix of unknown effects; and E is an $(n \times p)$-dimensional matrix of residuals. Next, one-way analyses of variance (ANOVA) were carried out to determine the effects of the DH lines on the variability of the examined traits, for each trait independently. The arithmetical means and standard deviations of the traits were calculated. Moreover, Fisher's least significant differences (LSDs) and coefficients of variation (CVs) were also estimated at the significance level $\alpha = 0.05$. Homogeneous groups for the analyzed traits were determined based on the least significant differences. The relationships among the observed traits were assessed based on Pearson's correlation. The results were also analyzed using multivariate methods. The effect of the silique length, silique width, number of seeds per silique, and seed coat color on thousand-seed weight was checked using multivariate regression analysis. The canonical variate analysis was applied to present a multitrait assessment of similarity for the tested DH lines and their parental forms in a lower number of dimensions with the least possible loss of information [21]. It allows illustrating the variation in genotypes in terms of all the observed traits in a graphic form. The Mahalanobis distance was suggested as a measure of "polytrait" genotype similarity [22], whose significance was verified by means of the critical value D_α, called "the least significant distance" [23]. The differences between the analyzed genotypes were verified with a cluster analysis using the nearest-neighbor method and Euclidean distances [24].

Estimation and testing of the additive gene effects and additive-by-additive interaction of homozygous loci (epistasis) effects as well as additive gene effects were performed based on the methods presented by Bocianowski and Krajewski [25], Bocianowski [26], and Bocianowski et al. [27].

All the analyses were conducted using the GenStat (18th edition) statistical software package.

3. Results

The results of the MANOVA indicated that all studied genotypes were significantly different regarding all five quantitative traits (Wilk's $\lambda = 0.01067$; $F_{79;160} = 2.95$; $p < 0.0001$). The results of analysis of variance for these traits [silique length ($F_{79;160} = 2.03$), silique width ($F_{79;160} = 1.44$), number of seeds per silique ($F_{79;160} = 1.96$), seed coat color ($F_{79;160} = 12.86$), and thousand-seed weight ($F_{79;160} = 1.68$)] showed variability of the tested genotypes at significance level $\alpha = 0.05$.

The mean values and standard deviations for the observed traits indicated high variability among the 80 tested genotypes, for which significant differences were found in terms of all the analyzed quantitative traits (Table 1), and on this basis homogeneous groups were distinguished (Table S1). The silique length varied from 41.98 mm (for DH 07) to 69.63 mm (for DH 69) with an average of 53.66 mm and allowed for the distinction of 17 homogeneous groups. The values of silique width ranged from 3.12 mm (for DH 05) to 4.26 mm (for DH 30), with an average of 3.65 mm, and divided the studied genotypes into 11 groups. The number of seeds per silique varied from 8.5 (for DH 07) to 18.88 (for DH 01), with an average of 15.44, and allowed the distinction of 20 homogeneous groups. The values of seed coat color ranged from 0.1 (for DH 26) to 4.75 (for parental form Z114), with an average of 1.52. This trait distinguished the greatest number of groups, which was 32. The thousand-seed weight varied from 3.72 g (for DH 77) to 6.57 g (for DH 08), with an average of 5.01 g, and divided the studied DH lines and parental forms into 18 homogeneous groups.

Table 1. Basic values and parameters for five quantitative traits in all tested genotypes of *Brassica napus*.

	Silique Length [mm]	Silique Width [mm]	Number of Seeds per Silique	Seed Coat Color [0–5]	Thousand-Seed Weight [g]
Mean	53.66	3.65	15.44	1.52	5.01
Min.	41.98	3.12	8.50	0.10	3.72
Max.	69.63	4.26	18.88	4.75	6.57
s.d.	3.88	0.29	2.15	0.42	0.64
$LSD_{0.05}$	7.72	0.53	3.92	0.84	1.19
CV [%]	7.24	7.88	13.90	27.52	12.82

Table 1 also contains the coefficients of variation (CVs). The lowest and similar variability was observed for silique length and silique width (7.24% and 7.88%, respectively). Moreover, a similar but slightly higher variability occurred in the number of seeds per silique and thousand-seed weight (13.90% and 12.82%, respectively). The highest coefficient of variation occurred for the seed coat color (27.52%), in which the largest number of homogeneous groups was distinguished.

The correlation coefficients between all pairs of observed traits are presented in the form of a heatmap in Figure 1. This analysis indicated a statistically significant positive correlation between the silique length and number of seeds per silique ($r = 0.582$), silique length and thousand-seed weight ($r = 0.296$), as well as silique width and thousand-seed weight ($r = 0.412$). At the same time, a statistically significant negative correlation was observed between the silique length and seed coat color ($r = -0.289$).

The effect of the silique length, silique width, number of seeds per silique and seed coat color on the thousand-seed weight was evaluated using a multivariate regression analysis (Table 2). The thousand-seed weight was significantly positively determined by the silique length and silique width, but negatively by the number of seeds per silique. These three quantitative traits accounted for 28.90% of the thousand-seed weight variability. The effect of the seed coat color on the thousand-seed weight was not significant.

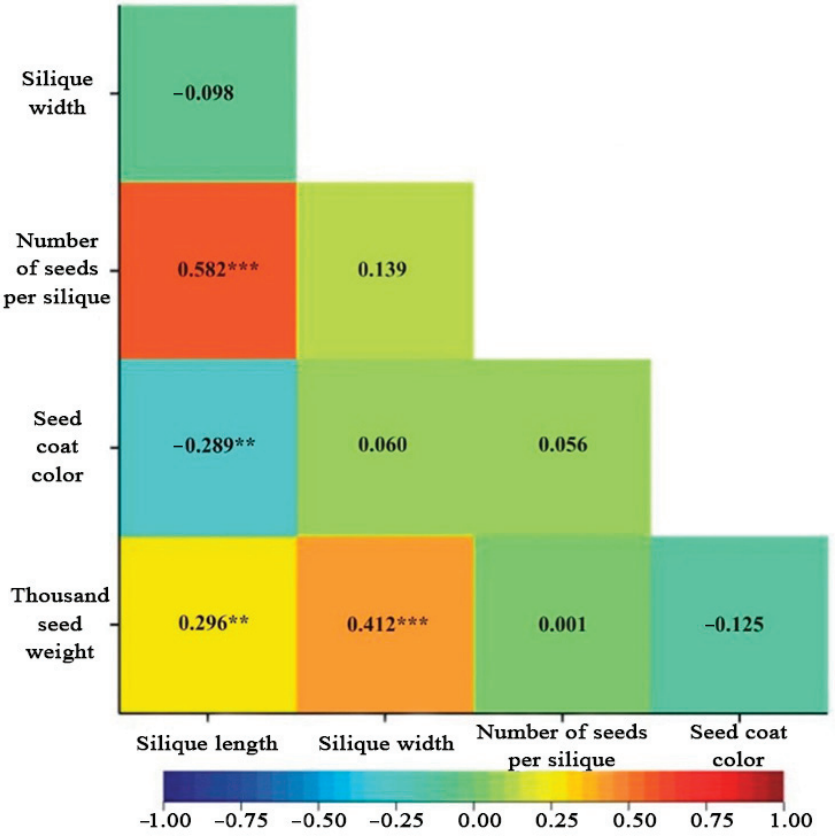

Figure 1. Heatmap for linear Pearson's correlation coefficients between observed traits of *Brassica napus*. ** $p < 0.01$; *** $p < 0.001$.

Table 2. Traits significantly affecting the thousand-seed weight.

Parameter	Estimate	Standard Error	*t*-Statistic
Constant	−0.229	1.043	−0.22 ns
Silique length [mm]	0.058	0.017	3.381 **
Silique width [mm]	0.875	0.208	4.205 ***
Number of seeds per silique	−0.066	0.026	−2.572 *
Seed coat color [0–5]	−0.010	0.050	−0.202 ns
Percentage variance accounted		28.90%	

* $p < 0.05$; ** $p < 0.01$; *** $p < 0.001$; ns—not significant.

Individual traits were of varying importance and had different shares in the joint multivariate variation of the studied genotypes. The analysis of the first two canonical variates for the DH population and parental lines regarding the five quantitative traits is shown in Figure 2. In the graph, the coordinates of the point for a particular genotype were the values for the first and second canonical variate, respectively. The studied population of the DH lines (apart from a few) was quite evenly distributed around the center of the coordinate system. The parental lines were located at opposite ends of the V_1 axis. The first two canonical variates accounted for 78.16% of the total variability among the individual genotypes. The most significant positive, linear relationship with the first canonical variate was found for the silique length, while the negative, for the seed coat color (Table 3). The

second canonical variate was significantly positively correlated with the silique length and thousand-seed weight, but negatively with the silique width. The silique length was the only trait positively correlated with both variates. The very strong (close to 1) correlation between the seed coat color and the first canonical variate means that the studied genotypes are distributed along this axis regarding this trait.

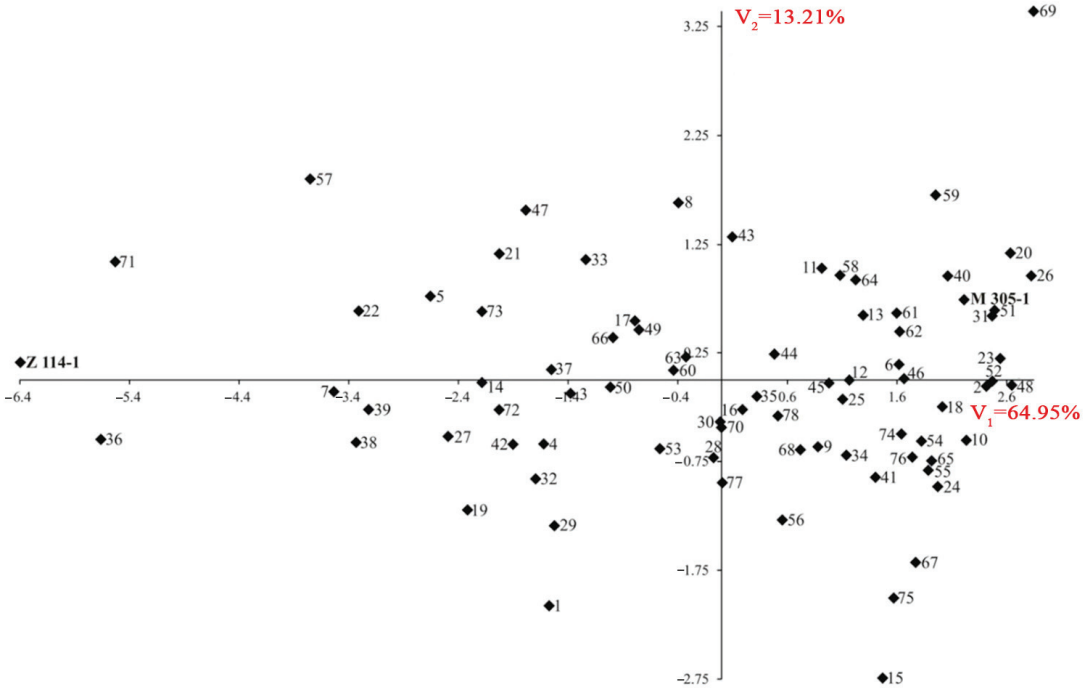

Figure 2. Distribution of the studied *Brassica napus* DH lines and their parental forms in the space of the first two canonical variates.

Table 3. Correlation coefficients between the first two canonical variates and studied traits.

Trait	First Canonical Variate	Second Canonical Variate
Silique length [mm]	0.289 **	0.64 ***
Silique width [mm]	−0.074	−0.374 ***
Number of seeds per silique	−0.129	−0.101
Seed coat color [0–5]	−0.995 ***	0.058
Thousand-seed weight [g]	0.12	0.378 ***
Percentage of explained multivariate variability	64.95%	13.21%

** $p < 0.01$; *** $p < 0.001$.

The greatest variation in terms of all five traits jointly measured with Mahalanobis distances was found for DH 69 and Z114 (the distance between them amounted to 9.926). The greatest similarity was found between DH 11 and DH 64 (0.502) (data not shown).

In the dendrogram presented in Figure 3, all the examined *B. napus* genotypes were divided into four groups as a result of agglomeration grouping using the Euclidean distance method. The first group (I) comprised two lines, DH 07 and DH 42, while the second one (II) consisted of five genotypes (DH 05, DH 36, DH 47, DH 71, and the yellow-seeded

parental line Z114). The third group (III) contained three lines, DH 08, DH 30, and DH 72, while the fourth group (IV) contained the rest of the genotypes and was divided into four subgroups: IVA consisted of 11 DH lines (DH 12, DH 24, DH 26, DH 31, DH 43, DH 46, DH 51, DH 61, DH 74, DH 75, DH 78) and the black–seeded parental line M305; IVB, four DH lines (DH 13, DH 20, DH 59, DH 69); IVC, 32 DH lines; and IVD comprised 22 DH lines.

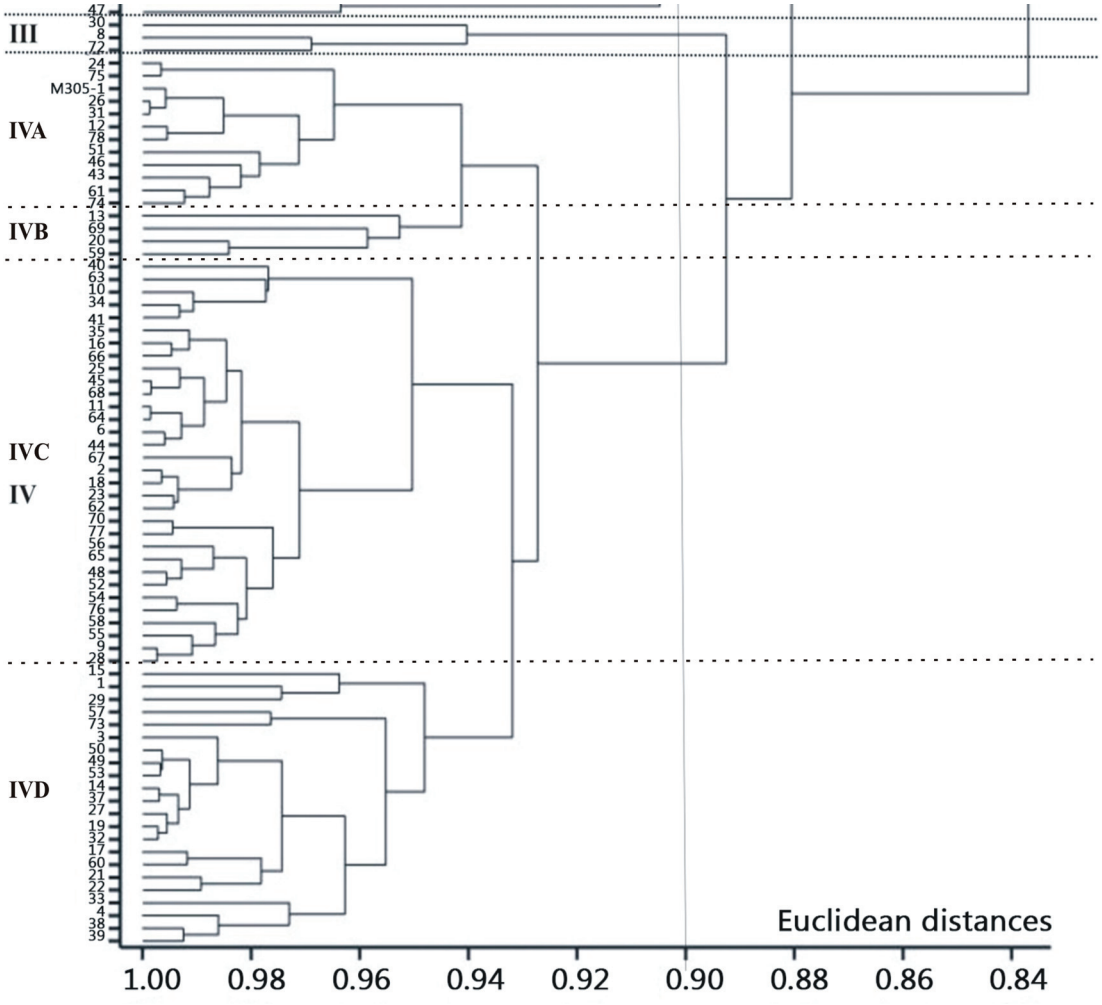

Figure 3. Dendrogram of cluster groupings of *Brassica napus* DH lines and their parental forms based on all five quantitative traits.

The additive gene action effect estimated based on the parental forms was significant only for seed coat color and based on DH lines it was significant for all five traits (Table 4). This effect for four observed features based on DH lines was larger than the parameter estimated based on the parental lines, and it was only on a similar level for seed coat color. The estimates of epistasis effects for all traits were statistically significant, but only positive for seed coat color.

Table 4. Estimates of additive and epistasis effects for observed traits of *Brassica napus*.

Effect	Silique Length [mm]	Silique Width [mm]	Number of Seeds per Silique	Seed Coat Color [0–5]	Thousand-Seed Weight [g]
			parental forms		
$a_{Parents}$ [1]	4.24	0.005	0.235	2.174 ***	0.337
			doubled haploid lines		
a_{DH} [2]	13.83 ***	0.570 *	5.190 ***	2.13 ***	1.423 **
aa_{DH} [3]	−39.83 ***	−3.087 ***	−10.233 ***	0.634 **	−3.586 ***

* $p < 0.05$; ** $p < 0.01$; *** $p < 0.001$. [1] the total additive effect estimated based on parental observations. [2] the total additive effect estimated based on doubled haploid lines observations. [3] the total additive-by-additive interaction effect estimated based on doubled haploid line observations.

4. Discussion

Breeding programs for winter oilseed rape cultivars are focused on improving the seed and oil yield; therefore, information about the genetic variability of traits is required [28]. The aim of this study was to estimate the variability of the silique- and seed-related traits in relation to the seed coat color using multivariate statistical methods. To achieve this goal, a population of DH lines with different seed color (from yellow to black) was used as a plant material. We decided to evaluate these lines because yellow seeds have a better biochemical composition than black seeds (mainly a lower fiber content). The mean content of neutral detergent fiber (NDF) in the yellow-seeded Z114 line was 17%, while in black-seeded M305 line it was 23%. The mean content of acid detergent fiber (ADF) was about 10% in the Z114 line and 17% in line M305 [18]. At the same time, yellow-seeded lines may be characterized by a lower yield [13] and a lower thousand-seed weight, which can be observed in the yellow-seeded parent of our DH population (3.97–4.81 g according to the year of research), while the thousand-seed weight of the M305 line ranged from 4.97 to 5.52 g [18]. Therefore, multivariate analysis was used to find lines with a light seed color, high thousand-seed weight, and good values of silique-related traits at the same time. In order to check whether the studied genotypes have sufficient variability for such statistical methods, an analysis of variance was initially performed. The results of the ANOVA showed variability of all the tested genotypes at a significance level $\alpha = 0.05$, and MANOVA indicated that all studied genotypes were significantly different regarding all five quantitative traits jointly. Thus, it confirmed that the tested population is suitable for carrying out the assumed multidimensional analyses.

The studied population of DH lines had very diverse seed coat colors, having a range from 0.1 to 4.75 on a scale from 0 to 5 (from black to light-yellow). Bartkowiak-Broda et al. [29], examining hybrids between yellow- and black-seeded lines, observed a seed coat color range from 1.7 to 5.0, which means they were slightly lighter than our material. The thousand-seed weight of the yellow lines they evaluated (between 3.5 and 5.2 g) was lower than in this study (3.72–6.57 g). The mean color value for our 78 DH lines was 1.52, while other authors noted it on the level of 3.5 for 58 yellow-seeded and seven black-seeded lines jointly [30]. The average thousand-seed weight observed by these authors (4.1 g) was much lower than in our genotypes (5.01 g). Therefore, compared to other studies, the population we observed had a wider range of seed coat color, but also heavier seeds.

The seed yield is a very complex feature that consists of direct and indirect yield-related traits. The number of siliques per plant, number of seeds per silique, and thousand-seed weight have the greatest impact on the size of the yield [7,31]. The last two features are related to indirect yield traits such as the length and width of the siliques. The silique length is positively correlated with the number of seeds per silique (the longer the siliques, the more seeds) and the silique width, with the thousand-seed weight (the wider the siliques, the bigger the seeds) [6,32,33]. We focused on these four features in our research. The values of silique length in our DH population (41.98–69.63 mm) had a narrower range than that observed by Wang et al. [7] in their DH population in four environments (19–118 mm). The

same situation occurred in reference to the silique width (3.12–4.26 mm in our study and 1.3–6.7 mm in Wang's study) and for the number of seeds per silique (8.50–18.88 and 0.6–39, respectively). These results show that our plant material, despite its origin from parents with different seed color, was more homogeneous in terms of these characteristics. A wider range of trait values tested in Wang's research is probably due to the fact that he conducted field trials in four environments, and we only in one. The features related to the structure of the crop are sensitive to environmental conditions. A relationship similar to that in our results for the three examined traits was also observed by Cai et al. [34] (38.4–93.9 mm for silique length, 10.35–27.66 for number of seeds per silique, and 2.20–5.49 g for thousand-seed weight). By analyzing these traits, it can be seen that our DH lines have shorter siliques with fewer seeds but a greater thousand-seed weight (average values: SL 53.66 mm, NSPS 15.44, TSW 5.01 g) than that observed by Cai et al. [34] (average values: SL 38.4 mm, NSPS 10.35, TSW 2.20 g) and Fu et al. [35] (average values: SL 56.7 mm, TSW 3.47 g).

The above-mentioned relationships are reflected in the calculated values of the standard deviation—they are lower in our study than in Cai et al.'s [34] for features such as silique length (3.88 and 7.8, respectively) or the number of seeds per silique (2.15 and 3.26, respectively) and higher for TSW (0.64 and 0.59, respectively). Analyzing the coefficients of variation, we can distinguish two features with significantly lower variability (silique length and silique width), two with a medium level (number of seeds per silique and thousand-seed weight), and one feature with a significantly higher variability than the others (seed coat color). Bartkowiak-Broda et al. [29], examining the variability of yellow- and black-seeded hybrids, noted a slightly lower coefficient of variation for the seed coat color (20.9%) and thousand-seed weight (8.2%) than in our study. All studied genotypes formed various numbers of homogeneous groups in terms of the tested traits. The largest number of groups was distinguished for the seed coat color, which indicates that for this trait, the objects were the most diverse. This is proved by the value of the coefficient of variation, which is the highest for this feature (27.52%). The high variability of the seed color, confirmed in this population, enables the selection of lines with the desired biochemical characteristics of the seeds and good yield-related traits.

In our research there was a statistically significant positive correlation between the silique length and number of seeds per silique, which is a commonly observed relationship [6,32,36]. We also noted a significant and positive correlation between the silique length and thousand-seed weight, similar to Fu et al. [35]. It indicates that longer siliques have heavier seeds. The opposite results, with a negative correlation for SL and TSW, were obtained by Zhang et al. [6]. Additionally, a statistically significant negative correlation was present in our study between the silique length and seed coat color, which suggests that the genotypes with darker seeds had longer siliques. The same result was achieved by Myszka et al. [30]. Another positive correlation was observed between the silique width and thousand-seed weight, indicating that wider siliques contain larger seeds. There was no statistically significant correlation between the seed coat color and thousand-seed weight. This means that genotypes in our population have varied seed sizes regardless of color, which allows the selection of genotypes connecting the desirable features of yellow seed color and high thousand-seed weight.

A regression analysis explains how the value of the dependent variable changes when any independent variable is modified. In most oilseed rape studies, regression analysis is evaluated for the seed yield per plot or plant. For example, Elliott et al. [37] and Sharafi et al. [38] observed a significant positive effect of the thousand-seed weight on the seed yield, which means that an increase in the TSW causes an increase in the yield. In our research, a linear regression was performed for the thousand-seed weight, because we wanted to check whether the color of the seeds affects their weight. As in our earlier studies [39], carried out on other rapeseed populations, the regression analysis showed that the thousand-seed weight was significantly positively affected by the silique length and negatively by the number of seeds per silique. An additional feature positively influencing the TSW in the current research was the silique width. There was no significant effect of

the seed coat color on the thousand-seed weight. Due to this, it is possible to select lines with large seeds and a light seed coat color at the same time.

Using canonical variate analysis, the tested DH lines and their parental lines were characterized in terms of five quantitative traits. The first two canonical variates together explained 78.16% of the total variability between the individual genotypes, which means that there was a small loss of information. A similar value (72.55%) was observed by Bocianowski et al. [40], who analyzed rapeseed hybrids and their parental lines in terms of 19 traits. Both canonical variates were significantly positively correlated with the silique length and only the second with thousand-seed weight. The seed color had a significant negative impact on the first variate, and the silique width on the second one. The conducted canonical variate analysis allowed for the assessment of the distribution of objects in terms of their features in the space of the first two canonical variates. As the first variate explained a significant percentage of the observed variability (64.95%), as well as the correlation value between it and the seed color being very high (close to -1), the studied genotypes are arranged along the V_1 axis in terms of this trait with high accuracy. Most of the studied DH lines were quite evenly distributed around the center of the coordinate system, while the parental lines were placed at the opposite ends of the V_1 axis, which reflects the difference in the color of their seeds. Genotypes characterized by a light seed color and low thousand-seed weight are placed in the bottom left quarter of the coordinate system, and genotypes with light seeds but a higher TSW in the upper left part. In the upper right part of the graph there are genotypes characterized by darker and heavier seeds, and in the last quarter (bottom right), lines with dark seeds and a low thousand-seed weight are located. This arrangement of lines in the coordinate system facilitates the selection of genotypes with the desired characteristics. Two lines in the upper left quarter attract attention—DH 71 (color 4.4, TSW 5.5 g) and DH 57 (color 3.5, TSW 5.6 g). They have a similar color level, but a higher thousand-seed weight than the yellow-seeded parental line Z114 (color 4.75, TSW 4.85 g). The position of these two lines in the upper left quarter also indicates their potential for long siliques, as this feature is highly significantly correlated with the V_2 variate (0.64).

The Mahalanobis distances between the examined objects allow us to assess the phenotypic similarity in the context of all examined traits. The Mahalanobis distances calculated in our study for all five quantitative traits ranged from 0.502 to 9.926. Very similar values were noticed by Parvin et al. [41] and Mili et al. [42] in *Brassica napus* genotypes—from 0.304 to 8.145 and from 0.378 to 12.433, respectively. An additional method in diversity studies is analysis of the specific clusters created on the dendrogram of similarity. The non-hierarchical Euclidean method of clustering is precise and critically identifies subclusters of the main groups at different levels, thus supporting the selection of diverse breeding materials [43]. The genotypes we studied were divided into four main clusters. From the fourth group, four subgroups were distinguished. As expected, the parental lines were placed in two separate groups. Most of the studied lines (69) were in group IV together with the black-seeded parent. In the second group of five genotypes, along with the yellow-seeded parent, there was line DH 71, which stands out from our plant material with a light color of seeds and a high thousand-seed weight.

The estimation of genetic parameters has a significant role in oilseed rape breeding. Our results indicate the importance of both additive and epistasis gene effects for all studied traits on the basis of doubled haploid lines observations. Additionally, the additive effect estimated based on parental observations was statistically significant for seed coat color. The importance of both additive and epistasis gene effects for the silique length and number of seeds per silique was also noted by Bocianowski et al. [44]. Luo et al. [45] observed that non-additive effects had a great influence on heritability and epistasis and noted the importance of environmental interactions. The significant additive and epistasis gene effects found in this study for all traits mean that they are regulated in a complex manner involving many genes with small effects and also by gene-by-gene interactions.

5. Conclusions

This study proves that multivariate statistical methods are useful for selecting breeding material in oilseed rape populations. In our opinion, out of the five traits we studied, the seed color and weight of seeds are the most important from the point of view of rapeseed breeding with better seed properties, combining the advantages of black- and yellow-seeded genotypes. Contrary to some published studies, in our population there was no negative correlation between the color of seeds and their weight, which allows us to select lines with desirable traits. The multidimensional analysis revealed an exact overview of the relationship between the examined features. As a result, two doubled haploid lines (DH 57 and DH 71) were selected as a valuable breeding material that could be used to create oilseed rape varieties with improved biochemical properties of seeds. Taking into account the parental genotypes used in this study, obtaining lines with such bright, large, and well-formed seeds is a significant achievement. The low fiber content in these yellow-seeded lines would provide an extracted meal with a better quality and better digestibility for farm animals. Rapeseed meal is already used as a supplement to protein feed, but the high fiber content limits its use in poultry farming. The use of yellow-seeded lines with a reduced fiber content would ensure a more comprehensive use of rapeseed not only as an oil plant, but also as a valuable source of feed protein.

Supplementary Materials: The following supporting information can be downloaded at: https://www.mdpi.com/article/10.3390/agriculture13050992/s1. Table S1: Mean values, homogenous groups, and standard deviations (s.d.) for five quantitative traits in all studied genotypes of *Brassica napus*.

Author Contributions: Conceptualization, A.Ł., J.B. and K.G.; formal analysis, J.B. and A.C.; investigation, A.Ł., J.W. and K.G.; data curation, A.Ł. and J.W.; writing—original draft preparation, A.Ł. and J.W.; writing—review and editing, J.B. and K.G.; visualization, J.B. and A.C.; supervision, K.G.; funding acquisition, K.G. All authors have read and agreed to the published version of the manuscript.

Funding: This research received no founding.

Institutional Review Board Statement: Not applicable.

Data Availability Statement: The data presented in this study are available on request from the corresponding author.

Acknowledgments: The authors would like to thank Laurencja Szała and Teresa Cegielska-Taras, Department of Oilseed Crop PBAI-NRI in Poznan for providing the plant material for this research.

Conflicts of Interest: The authors declare no conflict of interest.

References

1. Chen, W.; Zhang, Y.; Liu, X.; Chen, B.; Tu, J.; Fu, T. Detection of QTL for six yield-related traits in oilseed rape (*Brassica napus*) using DH and immortalized F_2 populations. *Theor. Appl. Genet.* **2007**, *115*, 849–858. [CrossRef]
2. Jiang, H.L.; Hong, J.; Jiang, Y.T.; Yu, S.X.; Zhang, Y.J.; Shi, J.X.; Lin, W.H. Genome-Wide Association Analysis Identifies Candidate Genes Regulating Seed Number Per Silique in *Arabidopsis thaliana*. *Plants* **2020**, *9*, 585. [CrossRef]
3. Wolko, J.; Dobrzycka, A.; Bocianowski, J.; Bartkowiak-Broda, I. Estimation of heterosis for yield-related traits for single cross and three-way cross hybrids of oilseed rape (*Brassica napus* L.). *Euphytica* **2019**, *215*, 156. [CrossRef]
4. Wang, H.; Zaman, Q.U.; Huang, W.; Mei, D.; Liu, J.; Wang, W.; Ding, B.; Hao, M.; Fu, L.; Cheng, H.; et al. QTL and Candidate Gene Identification for Silique Length Based on High-Dense Genetic Map in *Brassica napus* L. *Front. Plant Sci.* **2019**, *10*, 1579. [CrossRef] [PubMed]
5. Udall, J.A.; Quijada, P.A.; Lambert, B.; Osborn, T.C. Quantitative trait analysis of seed yield and other complex traits in hybrid spring rapeseed (*Brassica napus* L.): 2. Identification of alleles from unadapted germplasm. *Theor. Appl. Genet.* **2006**, *113*, 597–609. [CrossRef] [PubMed]
6. Zhang, L.W.; Yang, G.S.; Liu, P.W.; Hong, D.F.; Li, S.P.; He, Q.B. Genetic and correlation analysis of silique-traits in *Brassica napus* L. by quantitative trait locus mapping. *Theor. Appl. Genet.* **2011**, *122*, 21–31. [CrossRef]
7. Wang, X.; Chen, L.; Wang, A.; Wang, H.; Tian, J.; Zhao, X.; Chao, H.; Zhao, Y.; Zhao, W.; Xiang, J.; et al. Quantitative trait loci analysis and genome-wide comparison for silique related traits in *Brassica napus*. *BMC Plant Biol.* **2016**, *16*, 71. [CrossRef]
8. Zając, T.; Klimek-Kopyra, A.; Oleksy, A.; Lorenc-Kozik, A.; Ratajczak, K. Analysis of yield and plant traits of oilseed rape (*Brassica napus* L.) cultivated in temperate region in light of the possibilities of sowing in arid areas. *Acta Agrobot.* **2016**, *69*, 1696. [CrossRef]

9. Rahman, M.; McVetty, P.B.E. A review of *Brassica* seed color. *Can. J. Plant Sci.* **2011**, *91*, 437–446. [CrossRef]
10. Nesi, N.; Delourme, R.; Bregeon, M.; Falentin, C.; Renard, M. Genetic and molecular approaches to improve nutritional value of *Brassica napus* L. seed. *Comptes Rendus Biol.* **2008**, *331*, 763–771. [CrossRef]
11. Gawrysiak-Witulska, M.; Rudzińska, M.; Siger, A.; Bartkowiak-Broda, I. A high drying temperature causes degradation of sterols and tocopherols in yellow-seeded *Brassica napus* oils. *Eur. J. Lipid Sci. Technol.* **2015**, *117*, 483–490. [CrossRef]
12. Rakow, G.; Relf-Eckstein, J.A.; Raney, J.P. Rapeseed genetic research to improve its agronomic performance and seed quality. *Helia* **2007**, *30*, 199–206. [CrossRef]
13. Piotrowska, A.; Krótka, K.; Krzymański, J. Wartość gospodarcza żółtonasiennych linii rzepaku ozimego (*Brassica napus* L.). Economical value of yellow-seeded lines of winter oilseed rape (*Brassica napus* L.). *Rośliny Oleiste Oilseed Crops* **2000**, *21*, 359–368.
14. Daoyu, Z.; Lawes, G.S. Manova and discriminant analysis of phenotypic data as a guide for parent selection in kiwifruit (*Actinidia deliciosa*) breeding. *Euphytica* **2000**, *114*, 151–157. [CrossRef]
15. Vaylay, R.; van Santen, E. Application of canonical discriminant analysis for the assessment of genetic variation in tall fescue. *Crop Sci.* **2002**, *42*, 534–539. [CrossRef]
16. Cegielska-Taras, T.; Tykarska, T.; Szala, L.; Kuras, M.; Krzymański, J. Direct plant development from microspore-derived embryos of winter oilseed rape *Brassica napus* L. ssp *oleifera* (DC.) Metzger. *Euphytica* **2002**, *124*, 341–347. [CrossRef]
17. Michalski, K. Seed color assessment in rapeseed seeds using Color and Near Infrared Reflectance Spectrometers. *Rośliny Oleiste Oilseed Crops* **2009**, *30*, 119–132.
18. Wolko, J.; Dobrzycka, A.; Bocianowski, J.; Szala, L.; Cegielska-Taras, T.; Bartkowiak-Broda, I.; Gacek, K. Genetic variation of traits affecting meal quality in black × yellow seeded doubled haploid population of winter oilseed rape. *Agron. Res.* **2020**, *18*, 2259–2270. [CrossRef]
19. Gacek, K.; Bayer, P.E.; Anderson, R.; Severn-Ellis, A.A.; Wolko, J.; Łopatyńska, A.; Matuszczak, M.; Bocianowski, J.; Edwards, D.; Batley, J. QTL Genetic Mapping Study for Traits Affecting Meal Quality in Winter Oilseed Rape (*Brassica napus* L.). *Genes* **2021**, *12*, 1235. [CrossRef] [PubMed]
20. Shapiro, S.S.; Wilk, M.B. An analysis of variance test for normality (complete samples). *Biometrika* **1965**, *52*, 591–611. [CrossRef]
21. Rencher, A.C. Interpretation of canonical discriminant functions, canonical variates, and principal components. *Am. Stat.* **1992**, *46*, 217–225. [CrossRef]
22. Seidler-Łożykowska, K.; Bocianowski, J. Evaluation of variability of morphological traits of selected caraway (*Carum carvi* L.) genotypes. *Ind. Crops Prod.* **2012**, *35*, 140–145. [CrossRef]
23. Mahalanobis, P.C. On the generalized distance in statistics. *Proc. Natl. Acad. Sci. India A* **1936**, *12*, 49–55. [CrossRef]
24. Skomra, U.; Bocianowski, J.; Agacka, M. Agro-morphological differentiation between European hop (*Humulus lupulus* L.) cultivars in relation to their origin. *J. Food Agric. Environ.* **2013**, *11*, 1123–1128.
25. Bocianowski, J.; Krajewski, P. Comparison of the genetic additive effect estimators based on phenotypic observations and on molecular marker data. *Euphytica* **2009**, *165*, 113–122. [CrossRef]
26. Bocianowski, J. Analytical and numerical comparisons of two methods of estimation of additive × additive interaction of QTL effects. *Sci. Agric.* **2012**, *69*, 240–246. [CrossRef]
27. Bocianowski, J.; Warzecha, T.; Nowosad, K.; Bathelt, R. Genotype by environment interaction using AMMI model and estimation of additive and epistasis gene effects for 1000-kernel weight in spring barley (*Hordeum vulgare* L.). *J. Appl. Genet.* **2019**, *60*, 127–135. [CrossRef]
28. Liersch, A.; Bocianowski, J.; Nowosad, K.; Mikołajczyk, K.; Spasibionek, S.; Wielebski, F.; Matuszczak, M.; Szała, L.; Cegielska-Taras, T.; Sosnowska, K.; et al. Effect of Genotype × Environment Interaction for Seed Traits in Winter Oilseed Rape (*Brassica napus* L.). *Agriculture* **2020**, *10*, 607. [CrossRef]
29. Bartkowiak-Broda, I.; Piotrowska, A.; Hernacki, B.; Cegielska-Taras, T.; Michalski, K. Development of germplasm of yellow seeded winter oilseed rape (*Brassica napus* L. var. *oleifera*). In Proceedings of the GCIRC Technical Meeting, Manesar, India, 28–29 September 2009.
30. Myszka, K.; Boros, D.; Piotrowska, A.; Bartkowiak-Broda, I. Porównanie składu chemicznego śrut rzepakowych uzyskanych z rzepaku ozimego (*Brassica napus* L.) o zróżnicowanej barwie nasion. Comparison of chemical composition of rapeseed meals derived from winter rapeseed (*Brassica napus* L.) differing in colour of seeds. *Rośliny Oleiste Oilseed Crops* **2011**, *32*, 257–268.
31. Zhu, Y.; Ye, J.; Zhan, J.; Zheng, X.; Zhang, J.; Shi, J.; Wang, X.; Liu, G.; Wang, H. Validation and Characterization of a Seed Number Per Silique Quantitative Trait Locus qSN.A7 in Rapeseed (*Brassica napus* L.). *Front. Plant Sci.* **2020**, *11*, 68. [CrossRef]
32. Zhao, W.; Zhang, L.; Chao, H.; Wang, H.; Ta, N.; Li, H.; Wang, X.; Li, S.; Xiang, J.; Zhang, L.; et al. Genome-wide identification of silique-related traits based on high-density genetic linkage map in *Brassica napus*. *Mol. Breeding* **2019**, *39*, 86. [CrossRef]
33. Shi, J.Q.; Li, R.Y.; Qiu, D.; Jiang, C.C.; Long, Y.; Morgan, C.; Bancroft, I.; Zhao, J.Y.; Meng, J.L. Unraveling the complex trait of crop yield with quantitative trait loci mapping in *Brassica napus*. *Genetics* **2009**, *182*, 851–861. [CrossRef] [PubMed]
34. Cai, D.; Xiao, Y.; Yang, W.; Ye, W.; Wang, B.; Younas, M.; Wu, J.; Liu, K. Association mapping of six yield-related traits in rapeseed (*Brassica napus* L.). *Theor. Appl. Genet.* **2014**, *127*, 85–96. [CrossRef]
35. Fu, Y.; Wei, D.; Dong, H.; He, Y.; Cui, Y.; Mei, J.; Wan, H.; Li, J.; Snowdon, R.; Friedt, W.; et al. Comparative quantitative trait loci for silique length and seed weight in *Brassica napus*. *Sci. Rep.* **2015**, *5*, 14407. [CrossRef] [PubMed]
36. Diepenbrock, W. Yield analysis of winter oilseed rape (*Brassica napus* L.): A review. *Field Crop Res.* **2000**, *67*, 35–49. [CrossRef]

37. Elliott, R.H.; Mann, L.W.; Olfert, O.O. Effects of seed size and seed weight on seedling establishment, seedling vigour and tolerance of summer turnip rape (*Brassica rapa*) to flea beetles, *Phyllotreta* spp. *Can. J. Plant Sci.* **2007**, *87*, 385–393. [CrossRef]
38. Sharafi, Y.; Majidi, M.M.; Jafarzadeh, M.; Mirlohi, A. Multivariate Analysis of Genetic Variation in Winter Rapeseed (*Brassica napus* L.) Cultivars. *J. Agric. Sci. Technol.* **2015**, *17*, 1319–1331.
39. Łopatyńska, A.; Bocianowski, J.; Cyplik, A.; Wolko, J. Multidimensional Analysis of Diversity in DH Lines and Hybrids of Winter Oilseed Rape (*Brassica napus* L.). *Agronomy* **2021**, *11*, 645. [CrossRef]
40. Bocianowski, J.; Liersch, A.; Bartkowiak-Broda, I. Badanie zmienności fenotypowej mieszańców F1 CMS *ogura* rzepaku ozimego i ich form rodzicielskich za pomocą statystycznych metod wielowymiarowych. Investigation of phenotypic distance of F1 CMS *ogura* winter oilseed rape hybrids and parental lines using multivariate statistical methods. *Rośliny Oleiste Oilseed Crops* **2009**, *30*, 161–184.
41. Parvin, E.; Mahmud, F.; Bhuiyan, S.R.; Haque, M. Multivariate Analysis of Genetic Variation in Rapeseed (*Brassica napus* L.). *Agric. Food Sci. Res.* **2019**, *6*, 1–8. [CrossRef]
42. Mili, S.M.S.K.; Monalesa, N.; Rahman, M.J.; Afsana, N.; Zeba, N.; Mahmud, F. Genetic diversity analysis in F5 population of *Brassica napus* L. *Int. J. Biosci.* **2016**, *9*, 177–184. [CrossRef]
43. Singh, S.; Dwivedi, A.K.; Ashutosh, K.O.; Kumar, K. Genetic Divergence Analysis in Indian mustard (*Brassica juncea* L.). *Int. J. Curr. Microbiol. App. Sci.* **2018**, *7*, 2496–2503. [CrossRef]
44. Bocianowski, J.; Nowosad, K.; Dobrzycka, A.; Wolko, J. Estimation of additive and epistatic gene effects of doubled haploid lines of winter oilseed rape (*Brassica napus* L.). *Euphytica* **2017**, *213*, 122. [CrossRef]
45. Luo, X.; Ding, Y.; Zhang, L.; Yue, Y.; Snyder, J.H.; Ma, C.; Zhu, J. Genomic Prediction of Genotypic Effects with Epistasis and Environment Interactions for Yield-Related Traits of Rapeseed (*Brassica napus* L.). *Front. Genet.* **2017**, *8*, 15. [CrossRef] [PubMed]

agriculture

MDPI

Review

Loving the Alien: The Contribution of the Wild in Securing the Breeding of Cultivated Hexaploid Wheat and Oats

Volker Mohler [1,*,†], Edyta Paczos-Grzęda [2,*,†] and Sylwia Sowa [2]

[1] Bavarian State Research Center of Agriculture, Institute for Crop Science and Plant Breeding, Am Gereuth 2, 85354 Freising, Germany
[2] Institute of Plant Genetics, Breeding and Biotechnology, University of Life Sciences in Lublin, Akademicka 15, 20-950 Lublin, Poland; sylwia.sowa@up.lublin.pl
* Correspondence: volker.mohler@lfl.bayern.de (V.M.); edyta.paczos@up.lublin.pl (E.P.-G.)
† These authors contributed equally to this work.

Abstract: Cereal production is of strategic importance to the world economy. Although the primary aim of breeding programs is to develop cultivars with improved agronomic performance, including high grain yield and grain quality, as well as disease and lodging resistance, nowadays the adaptability to changing environmental conditions seems to be an extremely important feature. The achievement of these breeding objectives in diploid cereal species such as rice, barley, or maize is straightforward. The genetic improvement of polyploid crops such as hexaploid wheat and oats for increased crop production is highly demanding. Progenitor species and wild relatives, including taxa at lower ploidy levels, have preserved a high degree of useful genetic variation. The world's genebank collections of wheat and oat germplasm provide extremely rich resources for future breeding and utilization. This review highlights the immense potential of cultivated wild relatives as donors of genes for a wide range of biotic and abiotic traits and their impact on wheat and oat breeding. This review covers methods allowing access to these genetic resources, and it highlights the most (and most recently)-exploited related species for gene introgression in wheat and oats. Further, it will also deal with the impact of genomics and cloned genes on the advanced discovery, characterization, and utilization of genetic resources in these two cereals.

Keywords: crop wild relatives; wheat; oat; introgression breeding; pre-breeding; discovery breeding; wide crosses

Citation: Mohler, V.; Paczos-Grzęda, E.; Sowa, S. Loving the Alien: The Contribution of the Wild in Securing the Breeding of Cultivated Hexaploid Wheat and Oats. *Agriculture* **2023**, *13*, 2060. https://doi.org/10.3390/agriculture13112060

Academic Editor: Jaime Prohens

Received: 25 September 2023
Revised: 19 October 2023
Accepted: 25 October 2023
Published: 27 October 2023

1. Introduction

As major cereal crops cover a significant proportion of arable land [1], their continuous genetic improvement, particularly in terms of disease resistance and nitrogen-use efficiency, substantially supports, by the renunciation of pesticides and the saving on fertilizers, the movement to sustainable agriculture. Elite germplasm becomes short of useful genetic variation over time. This decrease periodically encourages breeders to remember the great allele diversity of crop wild relatives (CWR) and landraces that are stored globally in seed banks and intensify pre-breeding activities for elite germplasm enhancement. Although more challenging to explore, crop ancestors and widely related species meet great expectations as they reveal new alleles not only for traits such as resistance to diseases and tolerance to abiotic growth constraints, e.g., water deficits and heat, but also for yield and quality improvement.

The early work with alien germplasm was driven by common wheat (*Triticum aestivum*, 2n = 6x = 42, AABBDD genomes) and rapeseed (*Brassica napus*, 2n = 4x = 38, AACC) through attempts to unravel the wild relatives involved in polyploid formation [2,3]. A major success of introgression breeding was already reported in 1930, when the recessive and durable, race-non-specific adult plant stem rust-resistance gene *Sr2* was transferred from cultivated emmer (*T. dicoccum* syn. *T. dicoccon*, 2n = 4x = 28, AABB) into common

wheat [4]. The *Sr2* locus was later recognized also to confer partial resistance to leaf rust, stripe rust and powdery mildew [5], and a role for it was suggested in controlling cell death in response to stress [6]. The expansion of the gene pool concept by Harlan and de Wet [7], who proposed groupings of a crop and related species based on successful introgressions among them, paved the way for breeders to choose appropriate plant materials from CWR for successful introgression breeding. Along with the establishment of advanced molecular marker technologies, methods and resources, particularly noteworthy advanced backcross QTL analysis [8] and introgression libraries [9], were developed in the 1990s for coping with alien genes that determine quantitative traits. Finally, pan-genomics (reviewed, e.g., in [10]) guided in genotyping arrays the assembly of signatures for the variable gene fraction recognized through the comparison of the genome sequences from multiple, both closely and distantly related, individuals. These molecular tools use thousands of single nucleotide variants (SNV syn. SNP, single nucleotide polymorphism) markers and provide useful data for convoying introgression breeding. Genotyping-by-sequencing [11], another high-volume marker approach combining SNV discovery and scoring, was added to the molecular marker toolbox and shown to be highly useful for plant species for which whole genome sequence information is scarce. It appears that the potential of molecular marker technologies, 15 years ago identified as a shortcoming for assisting introgression breeding and gene deployment in breeding programs [12], can now be fully realized to produce new cultivars carrying genes from CWR. The shortening of the generation time through speed breeding [13], a technique employing easy protocols, can be seen as another milestone on the way to the exploration of CWR in a reasonable time. Complementing conventional breeding approaches, de novo domestication through genome editing was recently developed for several crops [14–17]. The conversion of wild into cultivated variants of cloned domestication and improvement genes makes CWR directly amenable for breeding, while retaining all other trait variation.

In this review, we present the contributions of wild relatives to the genetic enhancement of the two most important hexaploid temperate cereals, wheat and oats.

2. Wheat

2.1. Wheat, An Outstanding Grass Species

Wheat is one of the most consumed cereal species. This crop shows high adaptability to diverse environments as a result of genome plasticity, and thus has become the most widely cultivated species: it is grown on 221 million hectares with a production quantity of 771 million tons [18]. Sixty-six percent of global wheat production is used for food [19], and nutritional end-uses include different types of bread, noodles, cakes, pastries, cookies, crackers, bulgur, and even patties (from green spelt). Wheat trading, with 25% of the production in 2021 being exported [20], plays a major role in food security. As only several countries are central for the international wheat trade [21], supply shortages, such as experienced in the COVID-19 pandemic and now in the Ukraine war, have a severe impact on food availability. Wheat belongs to the Triticeae tribe within the *Poaceae* family. This genus group consists of nearly 500 species, most of which are perennials [22]. The embedding of common wheat, the most important representative of the *Triticum* species, into such a vast community of relatives has provided the basis for its successful continuous genetic improvement over the last century. Several of the many successful studies on the use of Triticeae members for the enhancement of cultivated wheat are reported in the following subsections.

2.2. Synthetic Hexaploid Wheat and Examples of Re-Synthesized Polyploids from Other Crops

Allopolyploids such as common wheat that have not recurrently formed suffer from a narrow genetic base [23]. However, this evolutionary constraint can be easily countered by using artificial polyploids for gene transfer. These important genetic resources are produced as chromosomally doubled hybrids (induced by treatment with colchicine or other antimitotic agents) from their progenitors, with interploid crosses requiring additional

embryo rescue and in vitro culture due to endosperm-development failure and embryo abortion [24,25]. Natural and artificial polyploids can be readily hybridized as they fully share the same genomes. Indeed, recurrent backcrossing (usually two rounds) to cultivated genetic backgrounds is needed to counter the low vigor of these primary polyploids, but, concurrently, homologous recombination-based introgressions are obtained.

Species re-synthesis was applied early in common wheat [26] and rapeseed [27], in the latter of which hybridization can be performed both sexually and somatically [28]. Since then, many primary synthetics and derivatives thereof, which provide new allele diversity from accessions of the lower ploidy level species *T. durum* (pasta wheat; 2n = 4x = 28, AABB), *T. dicoccum*, *T. dicoccoides* (wild emmer; 2n = 4x = 28, AABB) and *Aegilops tauschii* (2n = 2x = 14, DD), were developed and characterized in wheat [29]. A data survey on pre-breeding activities by the International Maize and Wheat Improvement Center revealed that at least 86 varieties have been selected from synthetic hexaploid wheat derivatives and released in 21 countries [30]. Of the released varieties, cultivar Largo and its derivatives were found to carry new major genes conferring resistance to insects [31–34] and stem rust [35]. Recently, Molero et al. [36] identified a locus of possibly dominant inheritance on chromosome 6D within an *Ae. tauschii* introgression that contributes to heat tolerance with no yield penalty in high-yield potential environments. An overview of documented genes captured in synthetic wheat from *Ae. tauschii* is presented in [37].

Recent work in the cultivated allotetraploid peanut (*Arachis hypogaea*, 2n = 4x = 40, AABB) reported neotetraploids that were obtained from crosses with accessions of *A. ipaënsis* (2n = 2x = 20, BB) and *A. duranensis* (2n = 2x = 20, AA), the two genome donors of the cultivated peanut, and other related wild diploid species, including *A. batizocoi* (BB), *A. magna* (BB), *A. valida* (BB), *A. correntina* (AA), and *A. stenosperma* (AA) [38,39]. The authors state that these synthetics are being used in breeding programs and carry alleles for traits including resistance to major diseases and adaptation to environmental stresses that frequently do not show genetic variation in cultivated peanut. These recent studies from the peanut clearly show that the creation of artificial polyploids through interspecific crosses is still a valid approach for accessing the genetic diversity of wild species.

2.3. Direct and Bridge Crosses

Gene introgression from wheat relatives can be achieved by direct hybridization with common wheat, which is used as female parent in the initial cross (Figure 1). Other methods that have been established for the exploitation of wheat species of lower ploidy level use bridge crosses with durum wheat.

2.3.1. Waiting for Rare Gametes: The Challenge Associated with the Exploitation of Lower Ploidy Level Species That Share Genomes with Common Wheat

The F1 hybrids between common wheat and diploid and tetraploid species that carry the haploid genomes of the species involved in the crosses are tetraploids and pentaploids, respectively. As fertile hybrids possessing gametes that are equipped with a full triploid chromosome complement are rare, many initial crosses must be made to obtain sufficient working material. Alternatively, embryo rescue of the hybrids can be employed [40]. Forty-two-chromosome wheat lines are recognized through chromosome counts in self-pollinated or backcross-derived progenies, while specific introgression lines are identified by phenotypic and/or genotypic assessments. Many designated genes conferring resistance to major diseases, such as powdery mildew and rusts, were directly transferred from compatible lower ploidy level species into common wheat (Table 1), and there was also a gene for increased protein and micronutrient (iron and zinc) content from wild emmer [41,42].

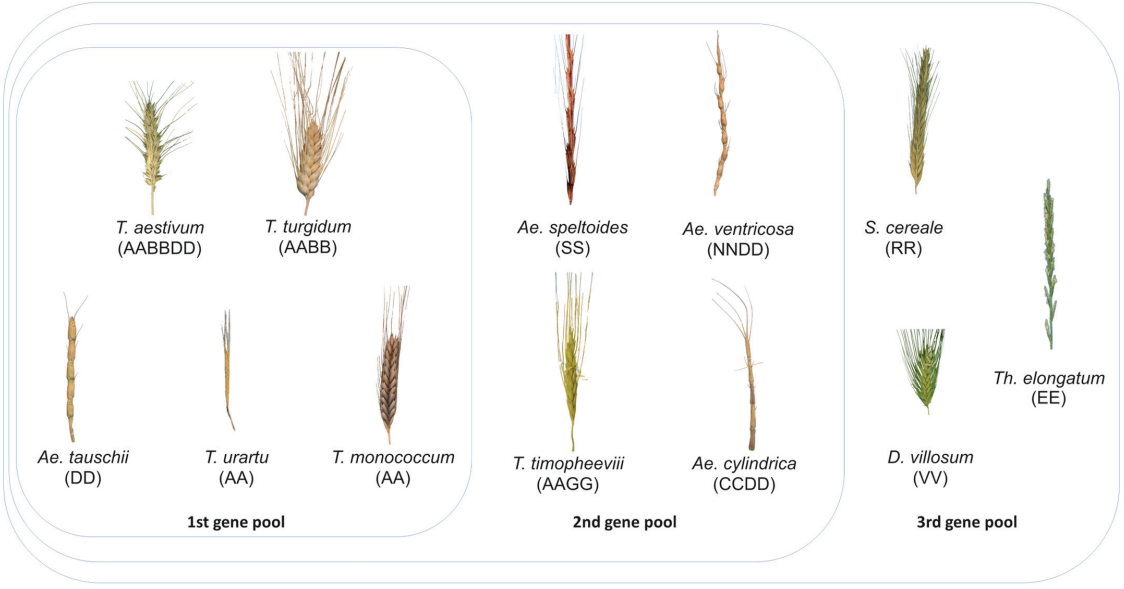

Figure 1. The gene pools of common wheat (*Triticum aestivum* L.) grouped based on the feasibility of gene transfer among species. Not all species are shown.

For gene transfer from wild emmer, three-way crosses using durum wheat as a bridge and hexaploid wheat as a pollinator (*T. dicoccoides*/*T. durum*//*T. aestivum*) were established, as the fertility of the F_1 pentaploid hybrids of these three-way crosses was increased compared to that of the direct crosses [43]. Recently, *PmG16* and the map-based cloned gene *Pm69* were transferred by this method (Table 1). Furthermore, tetraploid durum wheat can also be used to bridge the transfer of useful alleles from diploid species to common wheat. The triploid F_1 hybrids, similar as mentioned above, can then be either directly used for backcrossing with common wheat or, after establishment of an artificial hexaploid, through chemically induced genome doubling. This approach was followed for resistance genes *Sr22b* and *Sr60* from *T. monococcum*, and *Pm60* and *Pm60b* from *T. urartu* (2n = 2x = 14, A^uA^u) (Table 1). Notably, these genes were cloned in the diploid species before being transferred into common wheat. Besides using direct crosses with common wheat, *Sr21* and *Sr22* were also made available using the triploid hybrid bridge, whereas *Yr15* was additionally introgressed by durum wheat-assisted three-way crosses (Table 1).

Table 1. Gene transfers from fully compatible diploid and tetraploid wheat species (progenitors) into common wheat.

Gene	Origin	Introgression Method	Reference
Pm1b	*T. monococcum*	Direct cross	[44,45]
Pm4a	*T. dicoccum*	Direct cross	[46,47]
Pm4d	*T. monococcum*	Direct cross	[48]
Pm16 = Pm30	*T. dicoccoides*	Direct cross	[49,50]
Pm26	*T. dicoccoides*	Direct cross	[51]
Pm31	*T. dicoccoides*	Direct cross	[52]
Pm34	*Ae. tauschii*	Direct cross	[53,54]

Table 1. *Cont.*

Gene	Origin	Introgression Method	Reference
Pm35	*Ae. tauschii*	Direct cross	[55,56]
Pm50	*T. dicoccum*	Direct cross	[57]
Pm60	*T. urartu*	Triploid hybrid bridge	[58]
Pm60b	*T. urartu*	Triploid hybrid bridge	[58]
Pm64	*T. dicoccoides*	Direct cross	[59]
Pm69	*T. dicoccoides*	Three-way cross	[60]
MlZec1	*T. dicoccoides*	Direct cross	[61]
PmG16	*T. dicoccoides*	Three-way cross	[62]
Yr15	*T. dicoccoides*	Direct cross Three-way cross	[43,63,64]
Yr35	*T. dicoccoides*	Direct cross	[65]
YrAS2388R	*Ae. tauschii*	Direct cross	[66,67]
Lr14a	*T. dicoccum*	Direct cross	[4,68,69]
Lr21 [1]	*Ae. tauschii*	Direct cross	[70]
Lr39	*Ae. tauschii*	Direct cross	[71]
Lr42	*Ae. tauschii*	Direct cross	[72,73]
Lr53	*T. dicoccoides*	Direct cross	[65]
Sr21	*T. monococcum*	Direct cross Triploid hybrid bridge	[74,75]
Sr22	*T. boeoticum*	Direct cross Triploid hybrid bridge	[74,75]
Sr22b	*T. monococcum*	Triploid hybrid bridge	[76]
Sr35	*T. monococcum*	Direct cross	[77,78]
Sr60	*T. monococcum*	Triploid hybrid bridge	[79]
SrTA1662	*Ae. tauschii*	Direct cross	[80]
GPC-B1 [2]	*T. dicoccoides*	Direct cross	[81]

[1] *Lr21* introgressions were also made through synthetic hexaploid wheat line RL5406 [82]. [2] Also called *NAM-B1* as the gene encodes a NAC domain transcription factor [83].

2.3.2. The Induction of Homoeologous Pairing

Before methods for the targeted induction of homoeologous pairing were known, introgressions from the secondary and the tertiary gene pool of wheat were achieved via both compensating (substituting corresponding chromosome segments) and non-homoeologous (causing genetic imbalance through the loss and addition of chromosome segments) translocations that occurred spontaneously or were induced by facilitating the meiotic appearance of two homoeologous univalents (double monosomics), radiation treatment, or high-pairing lines (reviewed in [84]). The discovery of the genetic control of the strict pairing and recombination of homologous chromosomes in wheat [85,86] was essential for the conscious induction of homoeologous recombination. The disruption of meiotic pairing regulation in alien species-wheat F_1 hybrids was achieved with either deletion mutants [87] or suppressors (available from different wheat wild relatives) [88–90] for the *Ph1* locus on chromosome 5B and promoters for homoeologous recombination such as found in *Ae. geniculata* [91]. A recent study in common wheat combined *ph1b* and homoeologous recombination promoter factor(s) to further increase recombination, even in the proximal regions of the chromosomes where recombination is known to be rare [92].

Introgressions can finally also be achieved through the generation of addition and substitution lines. Single monosomic addition lines are obtained by crossing an amphidiploid such as historical triticale (2n = 8x = 56, AABBDDRR) with common wheat. To generate single monosomic substitution lines, single disomic addition lines, recovered after selfing, are then used to pollinate wheat lines that are monosomic for the homoeologous chromosome pair carried by the additions. For example, to produce hybrids of the genome constitution 20″ + 1B′ + 1R′, the gametes to combine must either have the constitution 20′ − 1B′ + 1R′ of the disomic addition line and 20′ + 1B′ of the monosomic line or 20′ + 1B′ + 1R′ of the disomic addition line and 20′ − 1B′ of the monosomic line. In subsequent segregating selfing progeny, lines without the single common wheat chromosome can be identified. Single disomic substitution lines are then used in *ph1*-based introgression programs.

In the secondary gene pool of wheat, consisting of Triticeae members with at least one genome common to bread wheat, useful variation is mostly obtained through translocations. Although several species belong to the secondary and tertiary gene pools, *Aegilops* is the largest genus in the secondary gene pool and most closely related to common wheat: *Ae. tauschii* is the direct progenitor of the wheat D genome (thus, per definition, a member of the primary gene pool) and *Ae. speltoides* (2n = 2x = 14, SS) of the section Sitopsis shares ancestry with an unknown, most likely extinct, diploid species that donated the wheat B genome [93]. The study also found that the four remaining Sitopsis species are phylogenetically clustered with the D genome lineage and may have contributed to the genome constitution of the unknown B genome progenitor. Members of the genus *Aegilops* have provided nearly 50 designated resistance genes against fungal diseases and pests [37,94–96]. Among them, *Ae. speltoides* is the most exploited species.

Dasypyrum villosum (2n = 2x = 14, VV) is an open-pollinating annual Mediterranean grass in the tertiary gene pool of wheat. Although known for its apparently high allele diversity, *D. villosum* was just recently explored in more detail, especially in China. Five documented *D. villosum* accessions, with genomes designated V#1 to V#5, have been used to develop wheat-*D. villosum* disomic addition, substitution, and translocation lines [97]. Of these accessions, at least three were donors of resistance genes to diverse pathogens (Table 2).

Table 2. Gene transfers from diploid *Dasypyrum villosum* into common wheat.

Disease	Gene	Line(s)	Chromosome Constitution	Reference
Powdery mildew	*Pm21*	Several	T6AL.6V#2S	[98]
		NAU427	Cryptic 6V#2S introgression	[99]
		DvRes-1	not published	[100]
	Pm55	NAU421	T5AL.5V#4S	[101]
	Pm62	NAU1823	T2BS.2V#5L	[102]
	Pm67	NAU1817	T1DL.1V#5S	[103]
	PmV	Pm97033	T6DL.6V#4S	[104]
		RIL 12401	T6AL.6V#4S-6V#2S	[105]
		Dv6T25	short distal 6VS segment	[106]
		Dv6T31	short proximal 6VS segment	[106]
	Pm5V	NAU1908	T5DL.5V#5S	[107]
Stripe rust	*YrCD-3*	22-12	T3DL.3V#3S	[108]
	Yr5V	NAU1908	T5DL.5V#5S	[107]
Stem rust	*Sr52*	Several	T6AS.6V#3L	[109]
Sharp eyespot	-	NAU2V–8	T2DS.2V#4L	[110]
Cereal cyst nematode	*CreV*	NAU423	T6AS.6V#4L	[111]
Wheat spindle streak mosaic virus	*Wss1*	NAU413	T4VS.4DL	[112]

As a major disease in the wheat-growing regions of China, resistance to powdery mildew was widely investigated and six genes have been characterized so far. Since its description in 1995, the all-stage resistance gene *Pm21* has been widely used in Chinese wheat-breeding and many cultivars were released [113]. To allow future use of this important resistance gene, new powdery mildew resistance genes from *D. villosum* including *PmV*, a *Pm21*-homolog carried by a wheat-*D. villosum* T6DL.6V#4S translocation for which small segmental translocation lines were identified in a large *ph1b*-based population, adult plant resistance genes *Pm55* and *Pm62*, and more recently, all-stage resistance gene *Pm67* are available for gene stacking with *Pm21*. In addition, the mining of 38 *Pm21* gene variants can also contribute to a longer use of the *Pm21* locus once their reaction to powdery mildew were characterized and the useful genes were transferred into common wheat [114].

Further overviews of wheat-alien translocations are presented in [84,115,116].

2.4. Impact of Genomics and Cloned Genes on the Advanced Utilization of Genetic Resources in Wheat

Developments in marker technologies over the last ten years have contributed, and still do contribute, to the systematic and large-scale exploration of species from the third gene pool of wheat. Molecular markers basically have the potential to identify chromatin of any wild relative in the common wheat background and are rapid when compared to cytological methods. Kompetitive allele-specific PCR (KASP) assays for single-copy SNPs that differentiate common wheat from wild relatives, and thus relatively easy heterozygous from homozygous hybrid lines in backcross populations, were recently developed for 10 wheat wild relatives ranging between 114 for *T. urartu* and 322 for *Thinopyrum intermedium* (2n = 6x = 42; $StStJ^rJ^rJ^{vs}J^{vs}$) [117]. This flexible molecular marker format was used at the Nottingham BBSRC Wheat Research Centre to study hundreds of homoeologous introgressions from *Ae. caudata* (2n = 2x = 14, CC) [118] and *Amblyopyrum muticum* (2n = 2x = 14, TT) [119] into wheat. Whole-genome sequencing of *Am. muticum* introgression lines has shown that KASP markers, despite an even genome coverage, have limited power for determining the precise size of incorporated segments and will likely overlook small segments [120]. Still, these and other resources [121,122] will make the species from the third gene pool of wheat among the most extensively exploited in future wheat breeding.

Linkage drag of detrimental alleles has regularly thwarted alien gene use in agriculture. For example, the introgression in common wheat of *Sr22* from *T. boeoticum* (2n = 2x = 14, A^bA^b) was burdened by a yield penalty [123]. After it was recognized that the gene was effective against Ug99 stem rust, efforts were undertaken to develop lines with reduced introgression fragments. Here, the availability of dense genetic maps was enough for the controlled targeting of the closely related chromosome fragment and the identification of recombinant lines in segregating populations [124]. The cloning of *Sr22* from a hexaploid introgression line [75] has allowed further allele-mining from diploid species, and the validation of predicted functional and nonfunctional alleles using transgenic assays in hexaploid wheat [125] enables the future transfer of effective alleles only. The *Th. ponticum* (2n = 10x = 70, $JJJJJJJ^sJ^sJ^s$)-derived genes *Lr19* and *Fhb7*, conferring a broad resistance without yield penalty to leaf rust [126,127] and Fusarium species [128,129], respectively, are closely linked to the yellow flour gene *Psy-E1* [130], which limits their use in wheat breeding. Three studies developed new small segment translocation lines based on *ph1b*-induced homoeologous recombination along with molecular marker enrichment for these segments to resolve this linkage drag effect: Li et al. 2023 [131] shortened the alien segment on wheat chromosome 7DL using wheat line SDAU 2028, whereas Zhang et al. 2022 [132] transferred a new *Fhb7* allele derived from diploid *Th. elongatum* (2n = 2x = 14, EE) and available in a Chinese Spring-*Th. elongatum* disomic substitution line 7E(7B) into chromosome 7B. Similarly, Xu et al. 2023 [133] obtained a smaller *Th. ponticum* chromosome segment on chromosome 7DL that retained *Lr19* but not *Psy-E1*, using translocation line K11695 [134].

Regarding the transfer of disease-resistance genes, the loss or reduced effectiveness of resistance (especially to the three wheat rust pathogens) from the progenitors was regularly observed in synthetic wheat. Thus, suppression was mediated by genes located either on the A and/or B genome chromosomes of some tetraploid genetic backgrounds such as Langdon durum [135] or on the D genome chromosomes of *Ae. tauschii* [136]. The stem rust suppressor *SuSr-D1* identified in Canthatch common wheat was cloned [137], allowing now for the targeted removal of the suppression allele by molecular markers or its inactivation by genome editing.

When cloned genes are available, the relationship of genes located in the target regions can be clearly answered as shown for the powdery mildew resistance loci *Pm3* [138], *Pm4* [47], *Pm5* [139], and *Pm24* [140]. Therefore, true allelism must also be questioned for *T. monococcum*-derived *Pm1b* [141], despite the fact that a genetic allelism test was carried out and a specific host response to powdery mildew isolates compared to other *Pm1* alleles was found [45]. The knowledge of whether genes are allelic or tightly linked is mandatory for creating virtually permanent gene stacks.

Among the genes that have been successfully cloned, the broad-spectrum all-stage resistance gene *Yr15* [64] and its allelic variants *YrG303* and *YrH52* [142] possibly have a high potential for longer use in agriculture, as they encode a tandem kinase-pseudokinase protein, like the barley stem rust-resistance gene *Rpg1* [143], a gene that has remained effective against most isolates in North America since its deployment in cultivar Kindred in 1942 [144]. *Yr15* has been now distributed in European commercial cultivars such as in the German spring wheat cultivar Kapitol and advanced breeding lines [145].

3. Oat

3.1. Oat—Common and Unique

Oat is a versatile crop with a wide range of applications, including human food, animal feed, and industrial materials. The primary aim of breeding programs is to develop cultivars with improved agronomic performance, including high grain yield and grain quality, disease and lodging resistance, as well as adaptability to changing environmental conditions.

It is significantly easier to achieve breeding objectives in diploid cereal species such as rice, barley or maize. It is much more difficult to conduct targeted breeding in polyploid crops such as wheat and oats. Despite the similarities in genome size between these hexaploids, wheat has immense significance in human nutrition, and substantial resources are allocated to research for this species. As a result, CWR utilization is more common in wheat than oats. *Hordeum*, *Secale*, and *Triticum* belong to the tribe Triticeae, *Avena* to the tribe Aveneae, and because of this the polyploid structure oat and wheat are not fully comparable [146]. Moreover, *Avena* has proven to be more recalcitrant to interspecies gene transfer compared to species from the tribe *Triticeae* due to postzygotic sterility barriers [147].

The main source of diversity for improving the cultivated oat has been the wild relatives of oats. Many genes providing desirable traits, especially disease-resistance genes, have been found in wild and weedy oat species as well as in landraces, breeding lines, or cultivars. However, it is mainly hexaploid taxa that have been utilized in oat breeding [148]. The main obstacle that is hindering oat improvement using wild or cultivated diploid and tetraploid species is the lack of chromosome pairing in hybrids [149]. Nonetheless, many oat cultivars now possess genes derived from wild relatives, and their contribution to global oat production is significant. This review highlights the immense potential of cultivated wild relatives as donors of genes for a wide range of biotic and abiotic traits and their impact on oat breeding.

3.2. Introduction to the Genus Avena

Understanding the relationships between species within the genus *Avena* is essential for genetics and breeding efforts, as well as for the efficient transfer of genes to the cultivated

oat. The genus *Avena* L. belongs to the tribe *Aveneae*, family *Gramineae*. It is divided into three karyological groups with 14, 28, and 42 chromosomes, and includes both wild and cultivated species [150]. Attempts to classify species within the genus *Avena* have been made many times [148,150–154]. Currently, most authors use the taxonomy based on Baum's numerical system [151] updated by Leggett [152], Zeller [154], and Loscutov and Rines [155]. According to this taxonomy, the genus *Avena* comprises 30 species, including 16 diploids (2n = 2x = 14), 8 tetraploids (2n = 4x = 28), and 6 hexaploids (2n = 6x = 42) (Table 3). Individual species were assigned to seven sections: *Ventricosa*, *Agraria*, *Ethiopica*, *Pachycarpa*, *Avenotrichon*, *Tenuicarpa*, and *Avena*. All species of the genus *Avena* are annual and self-pollinating, with the exception of *A. macrostachya*, which is a perennial and cross-pollinating species [156].

Table 3. Current classification of the genus *Avena* L.

Section/Species	Chromosome Number	Genomic Constitution
Section: *Avenotrichon*		
A. macrostachya Bal. ex Coss. et Dur.	2n = 4x = 28	CmCmCmCm
Section: *Ventricosa*		
A. clauda Dur.	2n = 2x = 14	CpCp
A. eriantha Dur.	2n = 2x = 14	CpCp
A. ventricosa Bal. ex Coss.	2n = 2x = 14	CvCv
Section: *Agraria*		
A. brevis Roth.	2n = 2x = 14	AsAs
A. hispanica Lag.	2n = 2x = 14	AsAs
A. nuda L.	2n = 2x = 14	AsAs
A. strigosa Schreb.	2n = 2x = 14	AsAs
Section: *Tenuicarpa*		
A. atlantica Baum et Fedak	2n = 2x = 14	AsAs
A. canariensis Baum Rajhathy et Sampson	2n = 2x = 14	AcAc
A. damascena Rajhathy et Baum	2n = 2x = 14	AdAd
A. hirtula Lag.	2n = 2x = 14	AsAs
A. longiglumis Dur.	2n = 2x = 14	AlAl
A. lusitanica (Table Mar.) Baum Comb et Stat.	2n = 2x = 14	AsAs
A. matritensis Baum Sp. Nov	2n = 2x = 14	AA?
A. prostrata Ladiz.	2n = 2x = 14	ApAp
A. wiestii Steud	2n = 2x = 14	AsAs
A. agadiriana Baum et Fedak	2n = 4x = 28	AABB (DDDD)
A. barbata Pott. ex Link.	2n = 4x = 28	AABB
Section: *Ethiopica*		
A. abyssinica Hochst	2n = 4x = 28	AABB
A. vaviloviana (Malz.) Mordv.	2n = 4x = 28	AABB
Section: *Pachycarpa*		
A. magna Murphy et Terrell	2n = 4x = 28	CCDD
A. murphyi Ladiz.	2n = 4x = 28	CCDD
A. insularis Ladiz.	2n = 4x = 28	CCDD
Section: *Avena*		
A. byzantina Koch.	2n = 6x = 42	AACCDD
A. fatua L.	2n = 6x = 42	AACCDD
A. ludoviciana Dur.	2n = 6x = 42	AACCDD
A. occidentalis Dur.	2n = 6x = 42	AACCDD
A. sativa L.	2n = 6x = 42	AACCDD
A. sterilis L.	2n = 6x = 42	AACCDD

Most species in the genus *Avena* are wild forms. Among cultivated forms, the following hexaploid species are of the greatest economic importance: *A. sativa* L. (common oat) and *A. byzantina* C. Koch. (red oat), and to a lesser extent diploid species *A. strigosa* Schreb. (grey oat). Diploid species *A. nuda* L., *A. brevis* Rotch., and *A. hispanica* Lag. [151] are of marginal economic importance among cultivated forms, similarly to tetraploid *A. barbata* Pott. ex Link and *A. abyssinica* Hochst (Ethiopian oat) [152].

Four primary genomes (A, B, C, and D) have been identified in the genus *Avena* based on the combined data from karyotype analysis, FISH, GISH, C-banding, and interspecific hybrid chromosome pairing experiments [154,157]. In diploid species, only the A or C genomes are present; in tetraploid species, the A, B, C, or D genomes can be found; and in hexaploid species, the A, C, and D genomes have been described. The A and C genomes are present in all karyological groups; the D genome is found in tetraploids and hexaploids, while the B genome is only present in certain tetraploids [158–160]. The B or D genomes have not been identified in any of the currently known diploid species [161]. Taking into account the structural differences in chromosomes, five subgenomes have been distinguished within the A genome of diploids: Ac, Ad, Al, Ap, and As. Similarly, two subgenomes have been identified within the C genome, i.e., Cp and Cv [149,150]. Diploid species belong to three sections, including *Ventricosa*, which comprises three species with the C genome, and sections *Agraria* and *Tenuicarpa*, which include four and nine diploids with the A genome, respectively.

Baum [151] has divided tetraploid species into three groups. The first group includes *A. macrostachya*, an autotetraploid, whose genome is a specific form of the C genome designated as Cm [162,163]. The second group, known as the "barbata group", includes species with an AABB genomic composition: *A. barbata, A. vaviloviana,* and *A. abyssinica.* The third group is composed of species with a CCDD genomic composition. The species belonging to the third group are *A. magna, A. murphyi* [160], and the relatively recently discovered (by Ladizinsky [164]) *A. insularis*. The genome composition of the tetraploid species *A. agadiriana* has not been definitively determined. However, research conducted by Tomaszewska et al. [165] has suggested that the genomic composition of this species may be DDDD, and not AABB as previously reported [166].

Based on the structural similarity of chromosomes and chromosomal pairing in hybrids, the genome composition of all hexaploids has been described by Rajhathy and Thomas [150] as AACCDD, which has been confirmed by whole-genome sequencing analyses [167]. There is much controversy regarding the distinctiveness of species among hexaploids, especially as intertaxa hybrids are fertile. Ladizinsky and Zohary [168], based on the identical genomic composition and fertility of hybrids, have suggested that all hexaploids belong to one species, *A. sativa*. Rajhathy [169] distinguishes four hexaploid species: *A. sativa*, *A. byzantina*, *A. fatua* and *A. sterilis*. Baum [151] and Zeller [154] in turn distinguish seven hexaploid species: *A. atheranta*, *A. fatua*, *A. hybrida*, *A. occidentalis*, *A. sativa*, *A. sterilis*, and *A. trichophylla*, while Jellen et al. [147] argue that there are eight hexaploid taxa and add *A. byzantina* to the seven mentioned above. On the other hand, Loscutov and Rines [155] identify six hexaploid taxa: *A. sativa*, *A. byzantina*, *A. fatua*, *A. sterilis*, *A. occidentalis*, and *A. ludoviciana.* Therefore, the taxonomic status of *Avena* hexaploids is ambiguous; however, Loscutow and Rines' [155] taxonomy seems to fit best in the context of contemporary research [159].

3.3. Use of Wild Relatives in Oat Improvement

Numerous studies have highlighted the common oat as a classic example of a cultivated species with a relatively narrow gene pool [170–172]. Historically, improvements since the end of the 19th century have focused on small but consistent increases in grain yield. A significant breakthrough occurred in the mid-twentieth century when researchers uncovered the potential of related wild oat species as valuable sources of genetic variability for cultivars [173–175]. As a result, breeders and researchers began exploring genebank resources to identify accessions carrying desirable genes.

Various genes have been identified in the oat species collected in global genebanks, including disease- and pest-resistance genes, genes enabling adaptation to specific or changing environmental conditions, genes conditioning high content and quality of protein, fat, or β-glucans in grains, tolerance to low and high temperatures, drought resistance, lodging resistance, early maturation, rapid vegetative growth, high yielding potential or insensitivity to day length [156,173,176–189]. A detailed characterization of gene resources and traits identified in various common oat relatives is discussed in reviews by Loscutow and Rines [155] and Boczkowska et al. [190].

3.4. Limitations in the Use of Wild Relatives of the Oat

Wild species variability is not always equally accessible to breeders and depends on the degree of genetic barriers separating some of these species [149]. The larger the phylogenetic distance between the crossed taxa, the greater the difficulty in obtaining fertile hybrid offspring. Interspecific crossing barriers result from the different levels of ploidy or lack of genome homology. They cause sterility in the obtained hybrids and constitute a significant limitation in the direct utilization of genes determining beneficial traits [150]. Understanding the genetic relationship between individual species at different ploidy levels is a prerequisite for effective selection of parental components for crossbreeding in order to obtain interspecific hybrids that carry desirable traits and could be the initial material for new cultivars [173,191–193].

An obstacle in expanding the oat gene pool is the presence of numerous translocations in the genome. The most common are translocations from the C to D genome; less common are those from A to C or from D to C [159,194]. However, rare translocations from A to D and from D to A genomes have also been identified [165]. Reconstruction of the ancestral state of oat chromosomes revealed the loss of at least 226 Mb of gene-rich regions from the C genome in favor of the A and D genomes [167]. The presence of large and fairly common intergenomic translocations 7C-17A (1C/1A) [163,195] and 3C-14D (6C/5D) [196] was detected within the cultivated hexaploid gene pool itself [197,198]. Kianian et al. [199] proposed describing the genomic organization of hexaploids as segmental homoeology, rather than whole-chromosome homoeology, due to the significant involvement of chromosomal rearrangements, such as translocations, inversions or duplications, in their evolution. Very frequent rearrangements of oat chromosomes result in pseudo-linkage and suppression of recombination and limit the improvement of cultivated oat forms [200]. The segmental chromosomes' homoeology affects segregation, localization, and deployment of QTLs in breeding programs [199].

Harlan and de Wet [7] presented a classification of wild species based on their crossing potential with cultivated forms. They distinguished three gene pools (Figure 2). A similar classification of wild species in the genus *Avena* was presented by Leggett and Thomas [148]. The first gene pool includes all wild hexaploid species. The free transfer of genes to cultivated forms occurs through conventional crossing, backcrossing, and recurrent selection [156]. The second gene pool includes tetraploids with a CCDD genomic composition, i.e., *A. magna*, *A. murphyi*, and *A. insularis*. The transfer of genes from this gene pool to hexaploid cultivated forms is partially limited. F_1 hybrids can be relatively easily obtained; they are self-sterile but partially female-fertile and their fertility can be restored through backcrossing [154,156]. The third gene pool comprises tetraploids with an AABB genomic composition, i.e., *A. barbata*, *A. abyssinica*, *A. vavilovonia*, and *A. agadiriana* as well as all diploids. The transfer of genes from these species to cultivated forms is limited and requires overcoming the crossing barriers through the use of in vitro cultures and polyploidization.

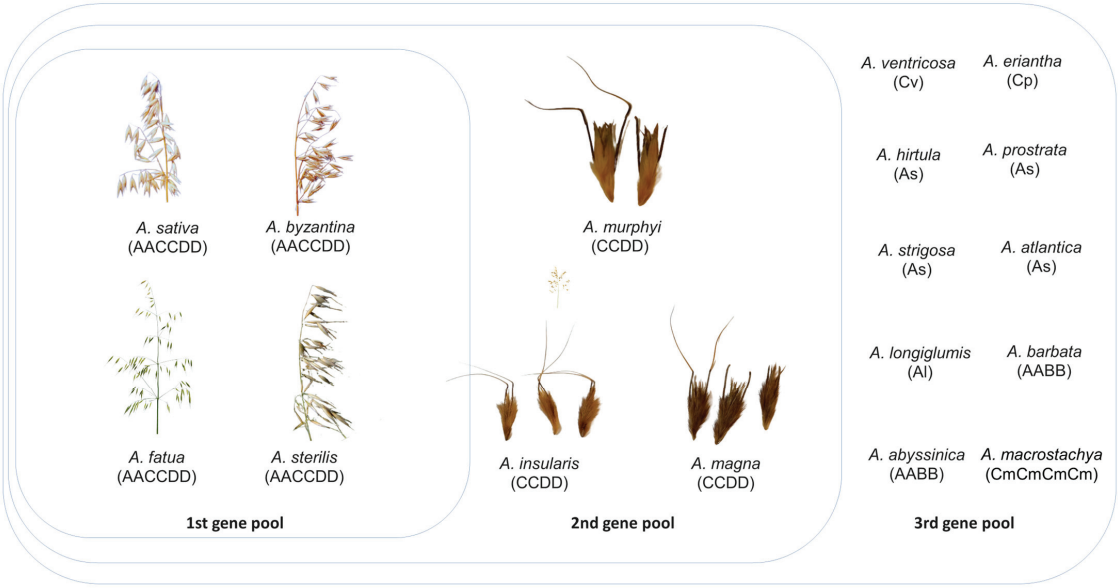

Figure 2. The gene pools of the common oat (*Avena sativa* L.) grouped based on the feasibility of gene transfer among species. Not all species are shown.

3.5. Cultivar Enhancement through Direct Crosses with Hexaploid Species

In the common oat breeding programs involving interspecific crosses, hexaploid species, which belong to the first gene pool, are most often used as the source of desirable genes [155,194]. Oat breeders have a broad spectrum of hexaploid species represented not only by wild or weedy species but also *A. sativa* and *A. byzantina* landraces. As a result, there are many examples of introgressions from these easily available resources. Nevertheless, Frey [173] considered the wild species *A. sterilis* as the most promising source of new genes available to breeders. Among the genotypes of this species, genes for BYDV tolerance and resistance to powdery mildew, crown rust, or nematodes have been identified. Additionally, this species is a source of genes that determine high protein and oil content in grains, as well as traits related to early maturity, rapid vegetative growth, and high yield [154,177,183,184,188,201–204]. Therefore, *A. sterilis* can be found in the pedigrees of many American cultivars, e.g., Starter, where this wild species contributed to increased grain protein content, Ozark (with improved winter hardiness [205]), or Sheldon (with high yielding potential [206]). However, most commonly, *A. sterilis* accessions have been used as a source of qualitatively inherited major disease-resistance genes, particularly against crown rust. The latter disease, caused by the fungus *Puccinia coronata* f. sp. *avenae* Eriks. (*Pc*), is one of the most widespread diseases of oats [207–209]. Crown rust infection causes a reduction in yield, decreases grain quality, and reduces plant resistance to lodging [208]. Genes determining resistance to specific races of this pathogen were initially identified in the cultivars of *A. sativa* and *A. byzantina*, and the first research in this field was conducted by Parker [210]. In subsequent years of breeding for resistance, alternative sources of *Pc* genes were sought, which turned out to be genotypes of *A. sterilis, A. strigosa*, and *A. abyssinica* [211]. Among over 100 identified genes conferring resistance to crown rust, approximately 50 originated from *A. sterilis*, 22 from *A. strigosa*, 1 from *A. abyssinica*, 1 from *A. magna*, and the remaining genes from cultivated forms [211–214]. The development of cultivars resistant to crown rust mainly utilized *A. sterilis* genes (*Pc38*, *Pc39*, *Pc48*, *Pc58*, *Pc59*, *Pc60*, *Pc61* and *Pc68*) [215,216]. An exception is the *A. magna*-derived *Pc91* gene, currently providing the most effective resistance to crown rust found in HiFi, Stainless or CDC Morrison cultivars. Genes conferring resistance to powdery mildew (*Pm1*, *Pm3*,

Pm11, *Pm12*, and *QPm.18*) [217–220], as well as stem rust (*Pg13*, *Pg15*, and *Pg17*) [221], also originated from *A. sterilis*. Among the aforementioned genes, *Pm1*, *Pm3*, *QPm.18*, and *Pg13* have been introduced into cultivars.

Grain protein content is one of the agronomically important traits improved with the use of *A. sterilis* genetic variation. Cox and Frey [178] identified transgressive segregants with high protein content in the progeny of *A. sativa* × *A. sterilis* hybrids. Lyrene and Shands [203] found that a higher protein proportion can be accompanied by an increase in husk content. Additionally, these authors pointed out that selecting progeny of *A. sativa* × *A. sterilis* hybrids based solely on grain protein content would also be associated with an increase in husk content in the grain, as well as a reduction in grain filling, decreased yield, and, in some cases, spikelets-shattering and awn formation. Hence, the authors suggested that breeding programs should prioritize maintaining a high level of agronomic traits, even if this approach may slow down progress in increasing grain protein content. Takeda and Frey [222], analyzing interspecific hybrids of *A. sativa* × *A. sterilis*, found that it is necessary to conduct three to five backcrosses to obtain lines with high grain protein content, while maintaining satisfactory levels of agronomic traits. The same authors [223] obtained lines with a very high level of grain protein content already in early backcross generations, but these traits were accompanied by unfavorable agronomic properties. Rossnagel and Bahtty [224] utilized American breeding lines containing *A. sterilis* in their pedigree as a source of genes for high grain protein content and obtained hybrids characterized by increased protein quantity, with retained high-yielding potential and grain quality. The recurrent selection method was also applied to increase oil content in groat up to 16% [206,225,226]. One of the important directions in oat breeding was to reduce straw height and improve lodging resistance by using dwarfing genes. The *Dw8* gene, which reduces plant height, was obtained from *A. fatua* [227,228]. However, the resulting dwarfism was too extreme to be used in *A. sativa* cultivars [229]. *A. fatua* germplasm was also used to improve adaptation to arid regions of the cultivars Sierra, Mesa, or Montezuma and introduce extreme earlines into the cultivar Rapida [230,231].

3.6. Non-Hexaploid Species as a Source of Desirable Genes

Attempts to transfer genes from di- and tetraploids to *A. sativa* have been carried out using, among others, addition and substitution lines [149]. Monosomic and disomic *A. sativa* addition lines were obtained by adding *A. strigosa* [232,233], *A. hirtula* [234], *A. barbata* [235], and *A. abyssinica* [233]. chromosomes. Similarly to wheat, the addition lines were utilized in oats for gene mapping on chromosomes and obtaining substitution lines, which are more stable and fertile than addition lines [149]. Substitution lines of *A. sativa* were obtained by replacing its chromosomes with their counterparts derived from *A. barbata*, *A. prostrata* [235], *A. strigosa* [236], and *A. abyssinica* [233].

The transfer of extraneous genetic variation can also occur through translocation induced by ionizing radiation. For the first time, translocation lines with resistance genes for stem rust [237] and powdery mildew [238] from *A. barbata* and crown rust from *A. strigosa* [239] were obtained by this means in *A. sativa*. The addition and substitution lines were the starting material for inducing translocations [233,238].

Another possibility for the transfer of extraneous genetic variation is the weakening or removal of the control mechanism for homologous pairing. The common oat (*A. sativa*) is a hexaploid, but cytologically it behaves like a diploid, forming 21 bivalents during meiosis [240]. Bivalent pairing and disomic inheritance indicate that homoeologous chromosomes do not normally conjugate [150]. In wheat, the gene controlling bivalent pairing (*Ph*) is located on the long arm of chromosome 5B [241]. The absence of chromosome 5B results in the formation of multivalents through homoeolog pairing. Jauhar [242] has argued that the process of homologous pairing control is more complex in *A. sativa* than in wheat, and it is likely that more genes are involved in regulating this mechanism. Gauthier and McGinnis [243] observed a lower degree of homologous chromosome pairing in nulli haploids of hexaploid oat compared to wheat, suggesting stronger control of bivalent

pairing in *A. sativa*. To date, no chromosomes of cultivated oats have been identified that could potentially harbor a specific gene or genes regulating bivalent pairing that would correspond to the wheat *Ph* gene [148,194].

The effect of weakening the control mechanism was observed in interspecific hybrids, when one of the crossing components was the CW57 genotype of the diploid species *A. longiglumis* [240]. This genotype is a suppressor of genes controlling bivalent pairing in interspecific hybrids, causing the induction of homoeologous conjugation and the formation of a large number of trivalents and quadrivalents. Utilization of the *A. longiglumis* CW57 homoeologous pairing system is constrained by the presence of a suppressor gene in this accession and is due to the sterility of *A. longiglumis* × *A. sativa* hybrids. Nevertheless, genes for powdery mildew resistance from *A. prostrata* and *A. barbata* [238] were transferred to *A. sativa* using this mechanism. In addition, a synthetic hexaploid, Amagalon, carrying a major crown rust resistance gene, *Pc91*, was developed from *A. magna* × *A. longiglumis* CW57 hybrids [244]. Understanding the pairing control system of *Avena* would make gene transfer from the secondary and tertiary gene pools less complicated.

In summary, only *Pc23* (*A. strigosa*), *Pc91* (*A. magna*), and *Pc94* (*A. strigosa*) genes were incorporated from non-hexaploid *Avena* species into *A. sativa* [245–247] (Table 4). Resistance to *Blumeria graminis* was introduced into hexaploid oat from *A. hirtula* (*Pm2*), *A. barbata* (*Pm4*), *A. macrostachya* Bal. (*Pm5*), and *A. eriantha* (*Pm7*) [248]. The *Pg16* gene, which confers resistance to *Puccinia graminis*, is also derived from *A. barbata*, while the *Pg6* and *Pg7* genes originate from *A. strigosa* [221]. Of the genes listed, only *Pc91* (HiFi, Stainless, CDC Morrison), *Pc94* (Leggett), and *Pm7* (Canyon, Yukon, Klaus, Harmony, Benny) were introduced into *A. sativa* cultivars.

Table 4. Gene transfers from diploid and tetraploid oat species into the common oat.

Disease	Gene	Origin	Introgression Method	Reference
Crown rust	*Pc15*	*A. strigosa*	Triploid hybrid bridge, monosomic substitution line irradiation	[239]
	Pc23	*A. strigosa*	Synthetic octoploid backcrosses	[246]
	Pc91	*A. magna*	Triploid hybrid bridge	[244]
	Pc92	*A. strigosa*	Autoteraploid, Triploid hybrid bridge	[247]
	Pc94	*A. strigosa*	Autoteraploid, Triploid hybrid bridge	[245]
Stem rust	*Pg6*	*A. strigosa*	Direct crosses Synthetic octoploid backcrosses	[244]
	Pg16	*A. barbata*	Direct crosses irradiation	[237,249]
Powdery mildew	*Pm2*	*A. hirtula*	-	[248]
	Pm4	*A. barbata*	Direct crosses, Disomic addition line irradiation	[238]
	Pm5	*A. macrostachya*	Direct crosses with *A. magna*, backcrosses with *A. sativa*	[250,251]
	Pm7	*A. eriantha*	Direct crosses with *A. sativa*, embryo rescue, backcrosses with *A. sativa*	[252]

The emergence of new pathogen races necessitates continuous efforts to search for new sources of resistance, leading to the discovery of new resistance genes [253–261]. Even though many highly effective resistance mechanisms can still be identified in hexaploid stocks stored especially in small national genebanks, diploid and tetraploid species have proven to be a better source, especially of adult plant resistance [190,213]. It is worth noting

that no effort to introduce resistance from diploid or tetraploid *Avena* species into hexaploid oats has been made in the last 15 years, with the most recent described by Rines et al. [262]. Furthermore, unlike in wheat, none of the *Avena* genes have been cloned [213].

3.7. Synthetic Polyploids

An alternative approach to breeding, based on introducing genes that determine desirable traits from non-cultivated species, is the domestication of selected wild species, or the synthesis of new artificial tetraploid, hexaploid, or octoploid forms [263,264]. Ladizinsky [265] presented an attempt to domesticate two wild tetraploid oat species, *A. magna* and *A. murphyi*, and selected domesticated *A. magna* lines are undergoing productivity evaluations in their native region of Morocco [266,267]. Domesticated tetraploids might be more successful than the common oat in the warm climate of North Africa or the Iberian Peninsula. In addition, domesticated tetraploids have been used to produce synthetic hexaploids. Although they may not be directly utilized as new cultivars, they can serve as bridging forms enabling gene transfer between di- and tetraploids and the cultivated hexaploid oat [264]. Amagalon, mentioned earlier, serves as an example of a synthetic hexaploid [244], and it was used as the parental form to develop a number of cultivars, with HiFi [268] being one of the most important among them. Another synthetic hexaploid is Strimagdo, obtained from a cross between *A. strigosa* Saia and domesticated *A. magna* [264]. The process of developing synthetic octoploids and hexaploids involved crossing *A. macrostachya* with *A. sativa*. As a result, F_1 hybrids were obtained through embryo rescue, vegetative cloning, and colchicine treatment. Afterwards, these hybrids were backcrossed with *A. sativa* cultivars to achieve the desired ploidy level. They gave rise to three groups of broad hybrid material, decaploids (2n = 10x = 70), octoploids (2n = 8x = 56), and plants with chromosome numbers between 40 and 49, which allowed selection of stable hexaploids (2n = 6x = 42). *A. macrostachya* derivatives were used as components to obtain breeding lines with improved winter hardiness and resistance to various diseases and pests, as well as larger seeds and higher protein content [269].

3.8. The Oat in the Genomic Era

For many years, research in oat genetics and breeding was severely hindered by the lack of highly saturated genetic maps, consistent chromosome nomenclature, and complete genome sequences. The breakthrough came initially with the publication of Chaffin et al. [270], where a consensus map of the cultivated hexaploid oat was developed based on 12 recombinant inbred line (RIL) populations. This facilitated the full utilization of molecular markers to confirm the transfer of external chromatin and select appropriate segregants in oat breeding. The next breakthrough occurred between 2020 and 2022, when the complete genome sequence of the oat *Avena sativa* line OT3098 was published [271], followed by the cultivars Sang [167] and Sanfesan [272]. The fully annotated cv. Sang reference genome plays a special role here, as it can assist breeders and researchers in better comprehending the segregation anomalies observed in various mapping studies and overcoming breeding barriers.

4. Conclusions

With the advent of molecular markers in the 1980s, to their high-throughput use over the last decade, introgression breeding in wheat has been constantly refined. Translocation lines can now be easily converted to true introgressions by employing the long-known *ph1b*-system for precisely following homoeologous recombination in segregating populations. Concurrently, approaches for obtaining small segmental introgressions at a large scale for individual species can be realized now to systematically assess their effects on the phenotype prior to implementation in costly breeding programs.

The progenitor species and wild relatives, including taxa at a lower ploidy level, are a valuable source of genes for the improvement of the cultivated oat; however, their use is limited by crossbreeding barriers and the lack of a wheat *ph1* system counterpart.

Recent advances in oat genetics and genomics have made molecular breeding possible and will enable the application of modern breeding strategies in future These advancements are instrumental in developing oat cultivars that are better adapted to changes in global climate conditions.

In recent years, the genomic selection of complex traits was successfully added to the molecular breeding toolbox of both wheat and oats, whereas genome editing has yet to come. It is expected that genomic selection can be more efficient than genome editing for improving complex traits, as more genetic components are considered simultaneously. However, genome-editing methods that involve targeted mutagenesis will become important for breeding both simple and complex traits because of the ease, speed, and cost-effectiveness with which beneficial gene signatures from species of the secondary and tertiary gene pools may be "utilized" for the fine-tuning of advanced breeding materials. Despite the unquestionable advantages of genome editing, in comparison with other major crops (e.g., rice or maize), the adoption of the CRISPR-Cas system for the improvement of wheat and oats has lagged behind. Among the factors that have contributed to this delay in the application of genome editing in these crops are the slow advances in wheat and oat transformation methods or, until recently, the lack of high-quality reference genomes. Nevertheless, continued progress in improving modern technologies and the allied application of available modern breeding techniques can contribute to the transition to true precision breeding.

Author Contributions: Writing—original draft preparation, review and editing, V.M. and E.P.-G.; writing—review and editing, S.S. All authors have read and agreed to the published version of the manuscript.

Funding: This research received no external funding.

Institutional Review Board Statement: Not applicable.

Data Availability Statement: No new data were created in this study.

Conflicts of Interest: The authors declare no conflict of interest.

References

1. Langridge, P.; Alaux, M.; Almeida, N.F.; Ammar, K.; Baum, M.; Bekkaoui, F.; Bentley, A.R.; Beres, B.L.; Berger, B.; Braun, H.-J.; et al. Meeting the challenges facing wheat production: The strategic research agenda of the Global Wheat Initiative. *Agronomy* **2022**, *12*, 2767. [CrossRef]
2. Kihara, H. Genomanalyse bei *Triticum* und *Aegilops*. *Cytologia* **1930**, *1*, 263–284. [CrossRef]
3. Nagaharu, U. Genome analysis in Brassica with special reference to the experimental formation of *B. napus* and peculiar mode of fertilization. *Japan. J. Bot.* **1935**, *7*, 389–452.
4. McFadden, E.S. A successful transfer of emmer characteristics to vulgare wheat. *J. Am. Soc. Agron.* **1930**, *22*, 1020–1034. [CrossRef]
5. Mago, R.; Tabe, L.; McIntosh, R.A.; Pretorius, Z.; Kota, R.; Paux, E.; Wicker, T.; Breen, J.; Lagudah, E.S.; Ellis, J.G.; et al. A multiple resistance locus on chromosome arm 3BS in wheat confers resistance to stem rust (*Sr2*), leaf rust (*Lr27*) and powdery mildew. *Theor. Appl. Genet.* **2011**, *123*, 615–623. [CrossRef]
6. Tabe, L.; Samuel, S.; Dunn, M.; White, R.; Mago, R.; Estavillo, G.; Spielmeyer, W. Phenotypes conferred by wheat multiple pathogen resistance locus, *Sr2*, include cell death in response to biotic and abiotic stresses. *Phytopathology* **2019**, *109*, 1751–1759. [CrossRef] [PubMed]
7. Harlan, J.R.; de Wet, J.M.J. Toward a rational classification of cultivated plants. *Taxon* **1971**, *20*, 509–517. [CrossRef]
8. Tanksley, S.D.; Nelson, J.C. Advanced backcross QTL analysis: A method for the simultaneous discovery and transfer of valuable QTLs from unadapted germplasm into elite breeding lines. *Theor. Appl. Genet.* **1996**, *92*, 191–203. [CrossRef]
9. Eshed, Y.; Zamir, D. An introgression line population of *Lycopersicon pennellii* in the cultivated tomato enables the identification and fine mapping of yield-associated QTL. *Genetics* **1995**, *141*, 1147–1162. [CrossRef]
10. Bayer, P.E.; Golicz, A.A.; Scheben, A.; Batley, J.; Edwards, D. Plant pan-genomes are the new reference. *Nat. Plants* **2020**, *6*, 914–920. [CrossRef]
11. Elshire, R.J.; Glaubitz, J.C.; Sun, Q.; Poland, J.A.; Kawamoto, K.; Buckler, E.S.; Mitchell, S.E. A robust, simple genotyping-by-sequencing (GBS) approach for high diversity cpecies. *PLoS ONE* **2011**, *6*, e19379. [CrossRef]
12. Hajjar, R.; Hodgkin, T. The use of wild relatives in crop improvement: A survey of developments over the last 20 years. *Euphytica* **2007**, *156*, 1–13. [CrossRef]

13. Watson, A.; Ghosh, S.; Williams, M.J.; Cuddy, W.S.; Simmonds, J.; Rey, M.D.; Asyraf Md Hatta, M.; Hinchliffe, A.; Steed, A.; Reynolds, D.; et al. Speed breeding is a powerful tool to accelerate crop research and breeding. *Nat. Plants* **2018**, *4*, 23–29. [CrossRef]
14. Lemmon, Z.H.; Reem, N.T.; Dalrymple, J.; Soyk, S.; Swartwood, K.E.; Rodriguez-Leal, D.; Van Eck, J.; Lippman, Z.B. Rapid improvement of domestication traits in an orphan crop by genome editing. *Nat. Plants* **2018**, *4*, 766–770. [CrossRef]
15. Li, T.; Yang, X.; Yu, Y.; Si, X.; Zhai, X.; Zhang, H.; Dong, W.; Gao, C.; Xu, C. Domestication of wild tomato is accelerated by genome editing. *Nat. Biotechnol.* **2018**, *36*, 1160–1163. [CrossRef]
16. Zsögön, A.; Čermák, T.; Naves, E.; Notini, M.M.; Edel, K.H.; Weinl, S.; Freschi, L.; Voytas, D.F.; Kudla, J.; Peres, L.E.P. *De novo* domestication of wild tomato using genome editing. *Nat. Biotechnol.* **2018**, *36*, 1211–1216. [CrossRef]
17. Yu, H.; Lin, T.; Meng, X.; Du, H.; Zhang, J.; Liu, G.; Chen, M.; Jing, Y.; Kou, L.; Li, X.; et al. A route to de novo domestication of wild allotetraploid rice. *Cell* **2021**, *184*, 1156–1170. [CrossRef]
18. FAOSTAT. 2021. Available online: https://www.fao.org/faostat/en/#data (accessed on 24 September 2023).
19. Erenstein, O.; Jaleta, M.; Mottaleb, K.A.; Sonder, K.; Donovan, J.; Braun, H.-J. Global Trends in Wheat Production, Consumption and Trade. In *Wheat Improvement*; Reynolds, M.P., Braun, H.-J., Eds.; Springer International Publishing: Cham, Switzerland, 2022; pp. 47–66.
20. International Grains Council. 2021. Available online: https://www.igc.int/en/default.aspx (accessed on 24 September 2023).
21. Raj, S.; Brinkley, C.; Ulimwengu, J. Connected and extracted: Understanding how centrality in the global wheat supply chain affects global hunger using a network approach. *PLoS ONE* **2022**, *17*, e0269891. [CrossRef]
22. Wang, R.; Lu, B. Biosystematics and evolutionary relationships of perennial Triticeae species revealed by genomic analyses. *J. Syst. Evol.* **2014**, *52*, 697–705. [CrossRef]
23. Soltis, P.S.; Soltis, D.E. The role of genetic and genomic attributes in the success of polyploids. *Proc. Natl. Acad. Sci. USA* **2000**, *97*, 7051–7057. [CrossRef]
24. Pennington, P.D.; Costa, L.M.; Gutierrez-Marcos, J.F.; Greenland, A.J.; Dickinson, H.G. When genomes collide: Aberrant seed development following maize interploidy crosses. *Ann. Bot.* **2008**, *101*, 833–843. [CrossRef]
25. Monnier, M. Culture of zygotic embryos of higher plants. In *Plant Cell and Tissue Culture. Methods in Molecular Biology*; Pollard, J.W., Walker, J.M., Eds.; Humana Press: Totowa, NJ, USA, 1990; Volume 6, pp. 129–139. [CrossRef]
26. McFadden, E.S.; Sears, E.R. The artificial synthesis of *Triticum spelta*. *Records Genet. Soc. Am.* **1944**, *13*, 26–27.
27. Olsson, G. Species crosses within the genus *Brassica*. II. Artificial *Brassica napus* L. *Hereditas* **1960**, *45*, 351–386. [CrossRef]
28. Sundberg, E.; Glimelius, K. Resynthesis of *Brassica napus* via somatic hybridization: A model for production of interspecific hybrids within *Brassiceae*. In *Genetic Manipulation in Plant Breeding: Proceedings International Symposium Organized by EUCARPIA, Berlin (West), Germany, 8–13 September 1985*; Horn, W., Jensen, C.J., Odenbach, W., Schieder, O., Eds.; De Gruyter: Berlin, Germany, 1986; pp. 709–712. [CrossRef]
29. Trethowan, R.; van Ginkel, M. Synthetic wheat—An emerging genetic resource. In *Wheat Science and Trade*; Carver, B.F., Ed.; Wiley-Blackwell: Hoboken, NJ, USA, 2009; pp. 369–385. [CrossRef]
30. Aberkane, H.; Payne, T.; Kishi, M.; Smale, M.; Amri, A.; Jamora, N. Transferring diversity of goat grass to farmer's fields through the development of synthetic hexaploid wheat. *Food Sec.* **2020**, *12*, 1017–1033. [CrossRef]
31. Joppa, L.R.; Williams, N.D. Registration of Largo, a greenbug resistant hexaploid wheat. *Crop Sci.* **1982**, *22*, 901–902. [CrossRef]
32. Hollenhorst, M.W.; Joppa, L.R. Chromosomal location of genes for resistance to greenbug in 'Largo' and 'Amigo' wheats. *Crop Sci.* **1983**, *23*, 91–93. [CrossRef]
33. Rudd, J.D.; Devkota, R.N.; Baker, J.A.; Peterson, G.L.; Lazar, M.D.; Bean, B.; Worrall, D.; Baughman, D.; Marshall, D.; Sutton, R.; et al. 'TAM 112' wheat, resistant to greenbug and wheat curl mite and adapted to the dryland production system in the southern high plains. *J. Plant Reg.* **2014**, *8*, 291–297. [CrossRef]
34. Dhakal, S.; Tan, C.-T.; Anderson, V.; Yu, H.; Fuentealba, M.P.; Rudd, J.C.; Haley, S.D.; Xue, Q.; Ibrahim, A.M.; Garza, L.; et al. Mapping and KASP marker development for wheat curl mite resistance in "TAM 112" wheat using linkage and association analysis. *Mol. Breed.* **2018**, *38*, 119. [CrossRef]
35. Sharma, J.S.; Overlander, M.; Faris, J.D.; Klindworth, D.L.; Rouse, M.N.; Kang, H.; Long, Y.; Jin, Y.; Lagudah, E.S.; Xu, S.S. Characterization of synthetic wheat line Largo for resistance to stem rust. *G3 Genes Genomes Genet.* **2021**, *11*, jkab193. [CrossRef]
36. Molero, G.; Coombes, B.; Joynson, R.; Pinto, F.; Piñera-Chávez, F.J.; Rivera-Amado, C.; Hall, A.; Reynolds, M.P. Exotic alleles contribute to heat tolerance in wheat under field conditions. *Commun. Biol.* **2023**, *6*, 21. [CrossRef]
37. Kishii, M. An update of recent use of *Aegilops* species in wheat breeding. *Front. Plant Sci.* **2019**, *10*, 585. [CrossRef]
38. Bertioli, D.J.; Gao, D.; Ballen-Taborda, C.; Chu, Y.; Ozias-Akins, P.; Jackson, S.A.; Holbrook, C.C.; Leal-Bertioli, S.C.M. Registration of GA-BatSten1 and GA-MagSten1, two induced allotetraploids derived from peanut wild relatives with superior resistance to leaf spots, rust, and root-knot nematode. *J. Plant Regist.* **2021**, *15*, 372–378. [CrossRef]
39. Chu, Y.; Stalker, H.T.; Marasigan, K.; Levinson, C.M.; Gao, D.; Bertioli, D.J.; Leal-Bertioli, S.C.M.; Corley Holbrook, C.; Jackson, S.A.; Ozias-Akins, P. Registration of three peanut allotetraploid interspecific hybrids resistant to late leaf spot disease and tomato spotted wilt. *J. Plant Regist.* **2021**, *15*, 562–572. [CrossRef]
40. Gill, B.S.; Raupp, W.J. Direct genetic transfers from *Aegilops squarrosa* L. to hexaploid wheat. *Crop Sci.* **1987**, *27*, 445–450. [CrossRef]
41. Joppa, L.R.; Cantrell, R.G. Chromosomal location of genes for grain protein content of wild tetraploid wheat. *Crop Sci.* **1990**, *30*, 1059–1064. [CrossRef]

42. Joppa, L.R.; Du, C.; Hart, G.E.; Hareland, G.A. Mapping gene(s) for grain protein in tetraploid wheat (*Triticum turgidum* L.) using a population of recombinant inbred chromosome lines. *Crop Sci.* **1997**, *37*, 1586–1589. [CrossRef]
43. Grama, A.; Gerechter-Amitai, Z.K. Inheritance of resistance to stripe rust (*Puccinia striiformis*) in crosses between wild emmer (*Triticum dicoccoides*) and cultivated tetraploid and hexaploid wheats. II. *Triticum aestivum. Euphytica* **1974**, *23*, 393–398. [CrossRef]
44. Valkoun, J.; Kučerova, D.; Bartoš, P. Transfer of a new gene for stem rust resistance from *Triticum monococcum* L. to hexaploid wheat, *T. aestivum* L. *Genet. Šlecht* **1989**, *25*, 209–214.
45. Hsam, S.L.K.; Huang, X.Q.; Ernst, F.; Hartl, L.; Zeller, F.J. Chromosomal location of genes for resistance to powdery mildew in common wheat (*Triticum aestivum* L. em Thell.). Alleles at the *Pm1* Locus. *Theor. Appl. Genet.* **1998**, *96*, 1129–1134. [CrossRef]
46. Briggle, L.W. Transfer of resistance to *Erysiphe graminis* f. sp. *tritici* from Khapli emmer and Yuma durum to hexaploid wheat. *Crop Sci.* **1966**, *6*, 459–461. [CrossRef]
47. Sánchez-Martín, J.; Widrig, V.; Herren, G.; Wicker, T.; Zbinden, H.; Gronnier, J.; Spörri, L.; Praz, C.R.; Heuberger, M.; Kolodziej, M.C.; et al. Wheat *Pm4* resistance to powdery mildew is controlled by alternative splice variants encoding chimeric proteins. *Nat. Plants* **2021**, *7*, 327–341. [CrossRef]
48. Schmolke, M.; Mohler, V.; Hartl, L.; Zeller, F.J.; Hsam, S.L.K. A new powdery mildew resistance allele at the *Pm4* wheat locus transferred from einkorn (*Triticum monococcum*). *Mol. Breed.* **2012**, *29*, 449–456. [CrossRef]
49. Reader, S.M.; Miller, T.E. The introduction into bread wheat of a major gene for resistance to powdery mildew from wild emmer wheat. *Euphytica* **1991**, *53*, 57–60. [CrossRef]
50. Liu, Z.Y.; Sun, Q.X.; Ni, Z.F.; Nevo, E.; Yang, T.M. Molecular characterization of a novel powdery mildew resistance gene *Pm30* in wheat originating from wild emmer. *Euphytica* **2002**, *123*, 21–29. [CrossRef]
51. Rong, J.K.; Millet, E.; Manisterski, J.; Feldman, M. A new powdery mildew resistance gene: Introgression from wild emmer into common wheat and RFLP-based mapping. *Euphytica* **2000**, *115*, 121–126. [CrossRef]
52. Xie, C.J.; Sun, Q.X.; Ni, Z.F.; Yang, T.M.; Nevo, E.; Fahima, T. Chromosomal location of a *Triticum dicoccoides*-derived powdery mildew resistance gene in common wheat by using microsatellite markers. *Theor. Appl. Genet.* **2003**, *106*, 341–345. [CrossRef]
53. Murphy, J.P.; Leath, S.; Huynh, D.; Navarro, R.A.; Shi, A. Registration of NC97BGTD7 and NC97BGTD8 wheat germplasms resistant to powdery mildew. *Crop Sci.* **1999**, *39*, 884–885. [CrossRef]
54. Miranda, L.M.; Murphy, J.P.; Marshall, D.; Leath, S. *Pm34*: A new powdery mildew resistance gene transferred from *Aegilops tauschii* Coss. to common wheat (*Triticum aestivum* L.). *Theor. Appl. Genet.* **2006**, *113*, 1497–1504. [CrossRef]
55. Murphy, J.P.; Leath, S.; Huynh, D.; Navarro, R.A.; Shi, A. Registration of NC96BGTD1, NC96BGTD2 and NC96BGTD3 wheat germplasm resistant to powdery mildew. *Crop Sci.* **1998**, *38*, 570–571. [CrossRef]
56. Miranda, L.M.; Murphy, J.P.; Marshall, D.; Cowger, C.; Leath, S. Chromosomal location of *Pm35*, a novel *Aegilops tauschii* derived powdery mildew resistance gene introgressed into common wheat (*Triticum aestivum* L.). *Theor. Appl. Genet.* **2007**, *114*, 1451–1456. [CrossRef]
57. Mohler, V.; Bauer, C.; Schweizer, G.; Kempf, H.; Hartl, L. *Pm50*: A new powdery mildew resistance gene in common wheat derived from cultivated Emmer. *J. Appl. Genet.* **2013**, *54*, 259–263. [CrossRef] [PubMed]
58. Zhang, Q.; Li, Y.; Li, Y.; Fahima, T.; Shen, Q.; Xie, C. Introgression of the powdery mildew resistance genes *Pm60* and *Pm60b* from *Triticum urartu* to common wheat using durum as a 'bridge'. *Pathogens* **2022**, *11*, 25. [CrossRef] [PubMed]
59. Zhang, D.; Zhu, K.; Dong, L.; Liang, Y.; Li, G.; Fang, T.; Guo, G.; Wu, Q.; Xie, J.; Chen, Y.; et al. Wheat powdery mildew resistance gene *Pm64* derived from wild emmer (*Triticum turgidum* var. *dicoccoides*) is tightly linked in repulsion with stripe rust resistance gene Yr5. *Crop J.* **2019**, *7*, 761–770. [CrossRef]
60. Li, Y.; Wei, Z.; Sela, H.; Govta, L.; Klymiuk, V.; Roychowdhury, R.; Chawla, H.S.; Ens, J.; Wiebe, K.; Bocharova, V.; et al. Long-read genome sequencing accelerated the dissection of a rapidly evolving resistance gene cluster and the cloning of *Pm69*. In Proceedings of the 2nd International Wheat Congress, Beijing, China, 11–15 September 2022.
61. Mohler, V.; Zeller, F.J.; Wenzel, G.; Hsam, S.L.K. Chromosomal location of genes for resistance to powdery mildew in common wheat (*Triticum aestivum* L. em Thell.). 9. Gene *MlZec1* from the *Triticum dicoccoides*-derived wheat line Zecoi-1. *Euphytica* **2005**, *142*, 161–167. [CrossRef]
62. Li, Y.; Wei, Z.; Fatiukha, A.; Jaiwar, S.; Wang, H.; Hasan, S.; Liu, Z.; Sela, H.; Krugman, T.; Fahima, T. *TdPm60* identified in wild emmer wheat is an ortholog of *Pm60* and constitutes a strong candidate for *PmG16* powdery mildew resistance. *Theor. Appl. Genet.* **2021**, *134*, 2777–2793. [CrossRef]
63. Gerechter-Amitai, Z.K.; van Silfhout, C.H.; Grama, A.; Kleitman, F. *Yr15*—A new gene for resistance to *Puccinia striiformis* in *Triticum dicoccoides* sel. G-25. *Euphytica* **1989**, *43*, 187–190. [CrossRef]
64. Klymiuk, V.; Yaniv, E.; Huang, L.; Raats, D.; Fatiukha, A.; Chen, S.; Feng, L.; Frenkel, Z.; Krugman, T.; Lidzbarsky, G.; et al. Cloning of the wheat *Yr15* resistance gene sheds light on the plant tandem kinase-pseudokinase family. *Nat. Commun.* **2018**, *9*, 3735. [CrossRef]
65. Marais, G.F.; Pretorius, Z.A.; Wellings, C.R.; McCallum, B.M.; Marais, A.S. Leaf rust and stripe rust resistance genes transferred to common wheat from *Triticum dicoccoides*. *Euphytica* **2005**, *143*, 115–123. [CrossRef]
66. Huang, L.; Zhang, L.Q.; Liu, B.L.; Yan, Z.H.; Zhang, B.; Zhang, H.G.; Zheng, Y.L.; Liu, D.C. Molecular tagging of a stripe rust resistance gene in *Aegilops tauschii*. *Euphytica* **2011**, *179*, 313–318. [CrossRef]

67. Lopez, S.R.; Wiersma, A.T.; Strauss, N.M.; Watkins, T.; Baik, B.-K.; Zhang, G.; Sehgal, S.K.; Kolb, F.L.; Poland, J.A.; Esten Mason, R.; et al. Description of U6719-004 wheat germplasm with *YrAS2388R* stripe rust resistance introgression from *Aegilops tauschii*. *J. Plant Regist.* **2022**, *17*, 26–33. [CrossRef]
68. Dyck, P.L.; Samborski, D.J. The genetics of two alleles for leaf rust resistance at the *Lr14* locus in wheat. *Can. J. Genet. Cytol.* **1970**, *12*, 689–694. [CrossRef]
69. Kolodziej, M.C.; Singla, J.; Sanchez-Martin, J.; Zbinden, H.; Simkova, H.; Karafiatova, M.; Dolezel, J.; Gronnier, J.; Poretti, M.; Glauser, G.; et al. A membrane-bound ankyrin repeat protein confers race-specific leaf rust disease resistance in wheat. *Nat. Commun.* **2021**, *12*, 956. [CrossRef] [PubMed]
70. Huang, L.; Brooks, S.A.; Li, W.; Fellers, J.P.; Trick, H.N.; Gill, B.S. Map-based cloning of leaf rust resistance gene *Lr21* from the large and polyploid genome of bread wheat. *Genetics* **2003**, *164*, 655–664. [CrossRef] [PubMed]
71. Raupp, W.J.; Singh, S.; Brown-Guedira, G.L.; Gill, B.S. Cytogenetic and molecular mapping of the leaf rust resistance gene *Lr39* in wheat. *Theor. Appl. Genet.* **2001**, *102*, 347–352. [CrossRef]
72. Cox, T.S.; Raupp, W.J.; Gill, B.S. Leaf rust-resistance genes *Lr41*, *Lr42* and *Lr43* transferred from *Triticum tauschii* to common wheat. *Crop Sci.* **1993**, *34*, 339–343. [CrossRef]
73. Lin, G.; Chen, H.; Tian, B.; Sehgal, S.K.; Singh, L.; Xie, J.; Rawat, N.; Juliana, P.; Singh, N.; Shresta, S.; et al. Cloning of the broadly effective wheat leaf rust resistance gene *Lr42* transferred from *Aegilops tauschii*. *Nat. Commun.* **2022**, *13*, 3044. [CrossRef]
74. The, T.T. Chromosome location of genes conditioning stem rust resistance transferred from diploid to hexaploid wheat. *Nat. New Biol.* **1973**, *241*, 256. [CrossRef]
75. Steuernagel, B.; Periyannan, S.; Hernández-Pinzón, I.; Witek, K.; Rouse, M.N.; Yu, G.; Hatta, A.; Ayliffe, M.; Bariana, H.; Jones, J.D.; et al. Rapid cloning of disease resistance genes in plants using mutagenesis and sequence capture. *Nat. Biotechnol.* **2016**, *34*, 652–655. [CrossRef]
76. Luo, J.; Rouse, M.N.; Hua, L.; Li, H.; Li, B.; Li, T.; Zhang, W.; Gao, C.; Wang, Y.; Dubcovsky, J.; et al. Identification and characterization of *Sr22b*, a new allele of the wheat stem rust resistance gene *Sr22* effective against the Ug99 race group. *Plant Biotechnol. J.* **2022**, *20*, 554–563. [CrossRef]
77. McIntosh, R.; Dyck, P.; Cusick, J.; Milne, D. Cytogenetical studies in wheat XIII. *Sr35*, a third gene from *Triticum monococcum* for resistance to *Puccinia graminis tritici*. *Z. Pflanzenzuecht.* **1984**, *92*, 1–14.
78. Saintenac, C.; Zhang, W.; Salcedo, A.; Rousse, M.; Trick, H.; Akhunov, E.; Dubcovsky, J. Identification of wheat gene *Sr35* that confers resistance to Ug99 stem rust race group. *Science* **2013**, *341*, 783–786. [CrossRef] [PubMed]
79. Chen, S.; Rouse, M.N.; Zhang, W.; Zhang, X.; Guo, Y.; Briggs, J.; Dubcovsky, J. Wheat gene *Sr60* encodes a protein with two putative kinase domains that confers resistance to stem rust. *New Phytol.* **2020**, *225*, 948–959. [CrossRef] [PubMed]
80. Olson, E.L.; Rouse, M.N.; Pumphrey, M.O.; Bowden, R.L.; Gill, B.S.; Poland, J.A. Simultaneous transfer, introgression, and genomic localization of genes for resistance to stem rust race TTKSK (Ug99) from *Aegilops tauschii* to wheat. *Theor. Appl. Genet.* **2013**, *126*, 1179–1188. [CrossRef] [PubMed]
81. Mesfin, A.; Frohberg, R.; Anderson, J.A. RFLP markers associated with high grain protein from *Triticum turgidum* L. var. *dicoccoides* introgressed into hard red spring wheat. *Crop Sci.* **1999**, *39*, 508–513. [CrossRef]
82. Rowland, G.G.; Kerber, E.R. Telocentric mapping in hexaploid wheat of genes for leaf rust resistance and other characters derived from *Aegilops squarrosa*. *Can. J. Genet. Cytol.* **1974**, *16*, 137–144. [CrossRef]
83. Uauy, C.; Distelfeld, A.; Fahima, T.; Blechl, A.; Dubcovsky, J. A NAC gene regulating senescence improves grain protein, zinc, and iron content in wheat. *Science* **2006**, *314*, 1298–1301. [CrossRef] [PubMed]
84. Friebe, B.; Jiang, J.; Raupp, W.J.; McIntosh, R.A.; Gill, B.S. Characterization of wheat-alien translocations conferring resistance to diseases and pests: Current status. *Euphytica* **1996**, *91*, 59–87. [CrossRef]
85. Okamoto, M. Asynaptic effect of chromosome V. *Wheat Inf. Serv.* **1957**, *5*, 19–58.
86. Riley, R.; Chapman, V. Genetic control of the cytologically diploid behavior of hexaploid wheat. *Nature* **1958**, *182*, 713–715. [CrossRef]
87. Sears, E.R. An induced mutant with homoeologous pairing in common wheat. *Can. J. Genet. Cytol.* **1977**, *19*, 585–593. [CrossRef]
88. Dover, G.A.; Riley, R. Prevention of pairing of homoeologous meiotic chromosomes of wheat by an activity of supernumerary chromosomes of *Aegilops*. *Nature* **1972**, *240*, 159–161. [CrossRef]
89. Riley, R.; Chapman, V.; Miller, T. The determination of meiotic chromosome pairing. In Proceedings of the 4th International Wheat Genetics Symposium, Columbia, MO, USA, 6–11 August 1973.
90. Dvořák, J. Chromosomal distribution of genes in diploid *Elytrigia elongata* that promote or suppress pairing of wheat homoeologous chromosomes. *Genome* **1987**, *29*, 34–40. [CrossRef]
91. Koo, D.-H.; Liu, W.; Friebe, B.; Gill, B.S. Homoeologous recombination in the presence of *Ph1* gene in wheat. *Chromosoma* **2017**, *126*, 531–540. [CrossRef] [PubMed]
92. Koo, D.-H.; Friebe, B.; Gill, B.S. Homoeologous recombination: A novel and efficient system for broadening the genetic variability in wheat. *Agronomy* **2020**, *10*, 1059. [CrossRef]
93. Li, L.-F.; Zhang, Z.-B.; Wang, Z.-H.; Li, N.; Sha, Y.; Wang, X.-F.; Ding, N.; Li, Y.; Zhao, J.; Wu, Y.; et al. Genome sequences of the five Sitopsis species of *Aegilops* and the origin of polyploid wheat B-subgenome. *Mol. Plant* **2022**, *15*, 488–503. [CrossRef]

94. Zhang, P.; Dundas, I.S.; McIntosh, R.A.; Xu, S.S.; Park, R.F.; Gill, B.S.; Friebe, B. Wheat– Aegilops introgressions. In *Alien Introgression in Wheat. Cytogenetics, Molecular Biology, and Genomics*; Molnár-Láng, M., Ceoloni, C., Doležel, J., Eds.; Springer: Cham, Switzerland, 2015; pp. 221–243.
95. Li, H.; Dong, Z.; Ma, C.; Xia, Q.; Tian, X.; Sehgal, S.; Koo, D.H.; Friebe, B.; Ma, P.; Liu, W. A spontaneous wheat-*Aegilops longissima* translocation carrying *Pm66* confers resistance to powdery mildew. *Theor. Appl. Genet.* **2020**, *133*, 1149–1159. [CrossRef]
96. Yu, G.T.; Matny, O.; Champouret, N.; Steuernagel, B.; Moscou, M.J.; Hernández-Pinzón, I.; Green, P.; Hayta, S.; Smedley, M.; Harwood, W.; et al. *Aegilops sharonensis* genome-assisted identification of stem rust resistance gene *Sr62*. *Nat. Commun.* **2022**, *13*, 1607. [CrossRef]
97. Li, S.; Wang, J.; Wang, K.; Chen, J.; Wang, K.; Du, L.; Ye, X. Development of PCR markers specific to *Dasypyrum villosum* genome based on transcriptome data and their application in breeding *Triticum aestivum-D. villosum#4* alien chromosome lines. *BMC Genom.* **2019**, *20*, 289. [CrossRef]
98. Li, H.; Xin, Z.Y.; Ma, Y.Z.; Xu, H.J.; Jia, X. Development and identification of wheat–*Haynaldia villosa* T6DL.6VS chromosome translocation lines conferring resistance to powdery mildew. *Plant Breed.* **2005**, *124*, 203–205. [CrossRef]
99. Xing, L.; Hu, P.; Liu, J.; Witek, K.; Zhou, S.; Xu, J.; Zhou, W.; Gao, L.; Huang, Z.; Zhang, R.; et al. *Pm21* from *Haynaldia villosa* encodes a CC-NBS-LRR protein conferring powdery mildew resistance in wheat. *Mol. Plant* **2018**, *11*, 874–878. [CrossRef]
100. He, H.; Zhu, S.; Zhao, R.; Jiang, Z.; Ji, Y.; Ji, J.; Qiu, D.; Li, H.-J.; Bie, T. *Pm21*, encoding a typical CC-NBS-LRR protein, confers broad-spectrum resistance to wheat powdery mildew disease. *Mol. Plant* **2018**, *11*, 879–882. [CrossRef]
101. Zhang, R.Q.; Sun, B.X.; Cheng, J.; Cao, A.Z.; Xing, L.P.; Feng, Y.G.; Lan, C.X.; Chen, P.D. *Pm55*, a developmental-stage and tissue-specific powdery mildew resistance gene introgressed from *Dasypyrum villosum* into common wheat. *Theor. Appl. Genet.* **2016**, *129*, 1975–1984. [CrossRef]
102. Zhang, R.Q.; Fan, Y.L.; Kong, L.N.; Wang, Z.J.; Wu, J.Z.; Xing, L.P.; Cao, A.Z.; Feng, Y.G. *Pm62*, an adult-plant powdery mildew resistance gene introgressed from *Dasypyrum villosum* chromosome arm 2VL into wheat. *Theor. Appl. Genet.* **2018**, *131*, 2613–2620. [CrossRef] [PubMed]
103. Zhang, R.; Xiong, C.; Mu, H.; Yao, R.; Meng, X.; Kong, L.; Xing, L.; Wu, J.; Feng, Y.; Cao, A. *Pm67*, a new powdery mildew resistance gene transferred from *Dasypyrum villosum* chromosome 1V to common wheat (*Triticum aestivum* L.). *Crop J.* **2021**, *9*, 882–888. [CrossRef]
104. Li, S.; Jia, Z.; Wang, K.; Du, L.; Li, H.; Lin, Z.; Ye, X. Screening and functional characterization of candidate resistance genes to powdery mildew from *Dasypyrum villosum*#4 in a wheat line Pm97033. *Theor. Appl. Genet.* **2020**, *133*, 3067–3083.
105. Zhao, R.; Liu, B.; Jiang, Z.; Chen, T.; Wang, L.; Ji, Y.; Hu, Z.; He, H.; Bie, T. Comparative analysis of genetic efects of wheat-*Dasypyrum villosum* translocations T6V#2S·6AL and T6V#4S·6DL. *Plant Breed.* **2019**, *138*, 503–512. [CrossRef]
106. Wan, W.; Zhao, R.; Chen, T.; Wang, L.; Zhang, X.; Li, H.; Wang, X.; Bie, T. Rapid development of wheat-*Dasypyrum villosum* compensating translocations resistant to powdery mildew using a triple marker strategy conducted on a large *ph1b*-induced population. *Theor. Appl. Genet.* **2023**, *136*, 148. [CrossRef]
107. Zhang, R.; Lu, C.; Meng, X.; Fan, Y.; Du, J.; Liu, R.; Feng, Y.; Xing, L.; Cápal, P.; Holušová, K.; et al. Fine mapping of powdery mildew and stripe rust resistance genes *Pm5V/Yr5V* transferred from *Dasypyrum villosum* into wheat without yield penalty. *Theor. Appl. Genet.* **2022**, *135*, 3629–3642. [CrossRef]
108. Zhang, J.; Tang, S.; Lang, T.; Wang, Y.; Long, H.; Deng, G.; Chen, Q.; Guo, Y.; Xuan, P.; Xiao, J.; et al. Molecular cytogenetic identification of the wheat–*Dasypyrum villosum* T3DL·3V#3S translocation line with resistance against stripe rust. *Plants* **2022**, *11*, 1329. [CrossRef]
109. Qi, L.L.; Pumphrey, M.O.; Friebe, B.; Zhang, P.; Qian, C.; Bowden, R.L.; Rouse, M.N.; Jin, Y.; Gill, B.S. A novel Robertsonian translocation event leads to transfer of a stem rust resistance gene (*Sr52*) effective against race Ug99 from *Dasypyrum villosum* into bread wheat. *Theor. Appl. Genet.* **2011**, *123*, 159–167. [CrossRef]
110. Liu, C.; Guo, W.; Wang, Y.; Fu, B.; Doležel, J.; Liu, Y.; Zhai, W.; Said, M.; Molnár, I.; Holušová, K.; et al. Introgression of sharp eyespot resistance from *Dasypyrum villosum* chromosome 2VL into bread wheat. *Crop J.* **2023**, *11*, 1512–1520. [CrossRef]
111. Zhang, R.Q.; Feng, Y.X.; Li, H.F.; Yuan, H.X.; Dai, J.L.; Cao, A.Z.; Xing, X.P.; Li, H.L. Cereal cyst nematode resistance gene *CreV* effective against *Heterodera filipjevi* transferred from chromosome 6VL of *Dasypyrum villosum* to bread wheat. *Mol. Breed.* **2016**, *36*, 122. [CrossRef]
112. Zhang, Q.P.; Li, Q.; Wang, X.E.; Wang, H.Y.; Lang, S.P.; Wang, Y.L.; Wang, S.L.; Chen, P.D.; Liu, D.J. Development and characterization of a *Triticum aestivum-Haynaldia villosa* translocation line T4VS.4DL conferring resistance to wheat spindle streak mosaic virus. *Euphytica* **2005**, *145*, 317–320. [CrossRef]
113. Wu, N.; Lei, Y.; Pei, D.; Wu, H.; Liu, X.; Fang, J.; Guo, J.; Wang, C.; Guo, J.; Zhang, J.; et al. Predominant wheat-alien chromosome translocations in newly developed wheat of China. *Mol. Breed.* **2021**, *41*, 30. [CrossRef] [PubMed]
114. He, H.; Ji, J.; Li, H.; Tong, J.; Feng, Y.; Wang, X.; Han, R.; Bie, T.; Liu, C.; Zhu, S. Genetic diversity and evolutionary analyses reveal the powdery mildew resistance gene *Pm21* undergoing diversifying selection. *Front. Genet.* **2020**, *11*, 489. [CrossRef]
115. Friebe, B.; Raupp, W.J.; Gill, B.S. Alien genes in wheat improvement. In *Wheat in a Global Environment*; Bedö, Z., Láng, L., Eds.; Kluwer Academic Publisher: Dordrecht, The Netherlands, 2001; Developments in Plant Breeding; Volume 9, pp. 709–720. [CrossRef]

116. Ceoloni, C.; Kuzmanović, L.; Forte, P.; Virili, M.E.; Bitti, A. Wheat-perennial Triticeae introgressions: Major achievements and prospects. In *Alien Introgression in Wheat. Cytogenetics, Molecular Biology, and Genomics*; Molnár-Láng, M., Ceoloni, C., Doležel, J., Eds.; Springer: Cham, Switzerland, 2015; pp. 273–313.
117. Grewal, S.; Hubbart-Edwards, S.; Yang, C.; Devi, U.; Baker, L.; Heath, J.; Ashling, S.; Scholefield, D.; Howells, C.; Yarde, J.; et al. Rapid identification of homozygosity and site of wild relative introgressions in wheat through chromosome-specific KASP genotyping assays. *Plant Biotechnol. J.* **2020**, *18*, 743–755. [CrossRef]
118. Grewal, S.; Othmeni, M.; Walker, J.; Hubbart-Edwards, S.; Yang, C.; Scholefield, D.; Ashling, S.; Isaac, P.; King, I.P.; King, J. Development of wheat-*Aegilops caudata* introgression lines and their characterisation using genome-specific KASP markers. *Front. Plant Sci.* **2020**, *11*, 606. [CrossRef]
119. Grewal, S.; Coombes, B.; Joynson, R.; Hall, A.; Fellers, J.; Yang, C.; Scholefield, D.; Ashling, S.; Isaac, P.; King, I.P.; et al. Chromosome-specific KASP markers for detecting *Amblyopyrum muticum* segments in wheat introgression lines. *Plant Genome* **2022**, *15*, e20193. [CrossRef]
120. Coombes, B.; Fellers, J.P.; Grewal, S.; Rusholme-Pilcher, R.; Hubbart-Edwards, S.; Yang, C.; Joynson, R.; King, I.P.; King, J.; Hall, A. Whole genome sequencing uncovers the structural and transcriptomic landscape of hexaploid wheat/*Ambylopyrum muticum* introgression lines. *Plant Biotechnol. J.* **2022**, *21*, 482–496. [CrossRef]
121. Grewal, S.; Yang, C.; Hubbart-Edwards, S.; Scholefield, D.; Ashling, S.; Burridge, A.; King, I.P.; King, J. Characterisation of *Thinopyrum bessarabicum* chromosomes through genome-wide introgressions into wheat. *Theor. Appl. Genet.* **2017**, *131*, 389–406. [CrossRef]
122. Baker, L.; Grewal, S.; Yang, C.-Y.; Hubbart-Edwards, S.; Scholefield, D.; Ashling, S.; Burridge, A.J.; Przewieslik-Allen, A.M.; Wilkinson, P.A.; King, I.P.; et al. Exploiting the genome of *Thinopyrum elongatum* to expand the gene pool of hexaploid wheat. *Theor. Appl. Genet.* **2020**, *133*, 2213–2226. [CrossRef] [PubMed]
123. The, T.T.; Latter, B.D.H.; McIntosh, R.A.; Ellison, F.W.; Brennan, P.S.; Fisher, J.; Hollamby, G.J.; Rathjen, A.J.; Wilson, R.E. Grain Yields of near-isogenic lines with added genes for stem rust resistance. In Proceedings of the 7th International Wheat Genetic Symposium, Cambridge, UK, 13–19 July 1988.
124. Olson, E.L.; Brown-Guedira, G.; Marshall, D.; Stack, E.; Bowden, R.L.; Jin, Y.; Rouse, M.; Pumphrey, M.O. Development of wheat lines having a small introgressed segment carrying stem rust resistance gene *Sr22*. *Crop. Sci.* **2010**, *540*, 1823–1830. [CrossRef]
125. Hatta, M.A.M.; Ghosh, S.; Athiyannan, N.; Richardson, T.; Steuernagel, B.; Yu, G.; Rouse, M.N.; Ayliffe, M.; Lagudah, E.S.; Radhakrishnan, G.V.; et al. Extensive genetic variation at the *Sr22* wheat stem rust resistance gene locus in the grasses revealed through evolutionary genomics and functional analyses. *Mol. Plant Microbe Interact.* **2020**, *33*, 1286–1298. [CrossRef] [PubMed]
126. Sharma, D.; Knott, D.R. The transfer of leaf-rust resistance from *Agropyron* to *Triticum* by irradiation. *Can. J. Genet. Cytol.* **1966**, *8*, 137–143. [CrossRef]
127. Reynolds, M.P.; Calderini, D.F.; Condon, A.G.; Rajaram, S. Physiological basis of yield gains in wheat associated with the *Lr19* translocation from *Agropyron elongatum*. *Euphytica* **2001**, *119*, 139–144. [CrossRef]
128. Shen, X.; Kong, L.; Ohm, H. Fusarium head blight resistance in hexaploid wheat (*Triticum aestivum*)-*Lophopyrum* genetic lines and tagging of the alien chromatin by PCR markers. *Theor. Appl. Genet.* **2004**, *108*, 808–813. [CrossRef]
129. Wang, H.; Sun, S.; Ge, W.; Zhao, L.; Hou, B.; Wang, K.; Lyu, Z.; Chen, L.; Xu, S.; Guo, J.; et al. Horizontal gene transfer of *Fhb7* from fungus underlies Fusarium head blight resistance in wheat. *Science* **2020**, *368*, eaba5435. [CrossRef]
130. Zhang, W.; Dubcovsky, J. Association between allelic variation at the *Phytoene synthase 1* gene and yellow pigment content in the wheat grain. *Theor. Appl. Genet.* **2008**, *116*, 635–645. [CrossRef]
131. Li, X.; Li, D.; Xuan, Y.; He, Z.; Zhao, L.; Hao, Y.; Ge, W.; Xu, S.; Hou, B.; Wang, B.; et al. Elimination of the yellow pigment gene *PSY-E2* tightly linked to the Fusarium head blight resistance gene *Fhb7* from *Thinopyrum ponticum*. *Crop J.* **2023**, *11*, 957–962. [CrossRef]
132. Zhang, W.; Danilova, T.; Zhang, M.; Ren, S.; Zhu, X.; Zhang, Q.; Zhong, S.; Dykes, L.; Fiedler, J.; Xu, S.; et al. Cytogenetic and genomic characterization of a novel tall wheatgrass-derived *Fhb7* allele integrated into wheat B genome. *Theor. Appl. Genet.* **2022**, *135*, 4409–4419. [CrossRef]
133. Xu, S.; Lyu, Z.; Zhang, N.; Li, M.; Wei, X.; Gao, Y.; Cheng, X.; Ge, W.; Li, X.; Bao, Y.; et al. Genetic mapping of the wheat leaf rust resistance gene *Lr19* and development of translocation lines to break the linkage with yellow pigment. *Theor. Appl. Genet.* **2023**, *136*, 200. [CrossRef]
134. Kim, N.S.; Armstrong, K.; Knott, D.R. Molecular detection of *Lophopyrum* chromatin in wheat-*Lophopyrum* recombinants and their use in the physical mapping of chromosome 7D. *Theor. Appl. Genet.* **1993**, *85*, 561–567. [CrossRef] [PubMed]
135. Athiyannan, N.; Zhang, P.; McIntosh, R.; Chakraborty, S.; Hewitt, T.; Bhatt, D.; Forrest, K.; Upadhyaya, N.; Steuernagel, B.; Arora, S.; et al. Haplotype variants of the stripe rust resistance gene *Yr28* in *Aegilops tauschii*. *Theor. Appl. Genet.* **2022**, *135*, 4327–4336. [CrossRef]
136. Kerber, E.R.; Green, G.J. Suppression of stem rust resistance in the hexaploid wheat cv. Canthatch by chromosome 7DL. *Can. J. Bot.* **1980**, *58*, 1347–1350. [CrossRef]
137. Hiebert, C.W.; Moscou, M.J.; Hewitt, T.; Steuernagel, B.; Hernández-Pinzón, I.; Green, P.; Pujol, V.; Zhang, P.; Rouse, M.N.; Jin, Y.; et al. Stem rust resistance in wheat is suppressed by a subunit of the mediator complex. *Nat. Commun.* **2020**, *11*, 1123. [CrossRef]

138. Yahiaoui, N.; Brunner, S.; Keller, B. Rapid generation of new powdery mildew resistance genes after wheat domestication. *Plant J.* **2006**, *47*, 85–98. [CrossRef]
139. Xie, J.; Guo, G.; Wang, Y.; Hu, T.; Wang, L.; Li, J.; Qiu, D.; Li, Y.; Wu, Q.; Lu, P.; et al. A rare single nucleotide variant in *Pm5e* confers powdery mildew resistance in common wheat. *New Phytol.* **2020**, *228*, 1011–1026. [CrossRef] [PubMed]
140. Lu, P.; Guo, L.; Wang, Z.; Li, B.; Li, J.; Li, Y.; Qiu, D.; Shi, W.; Yang, L.; Wang, N.; et al. A rare gain of function mutation in a wheat tandem kinase confers resistance to powdery mildew. *Nat. Commun.* **2020**, *11*, 680. [CrossRef]
141. Hewitt, T.; Mueller, M.C.; Molnár, I.; Mascher, M.; Holušová, K.; Šimková, H.; Kunz, L.; Zhang, J.; Li, J.; Bhatt, D.; et al. Highly differentiated region of wheat chromosome 7AL encodes a *Pm1a* immune receptor that recognizes its corresponding *AvrPm1a* effector from *Blumeria graminis*. *New Phytol.* **2021**, *229*, 2812–2826. [CrossRef]
142. Klymiuk, V.; Fatiukha, A.; Raats, D.; Bocharova, V.; Huang, L.; Feng, L.; Jaiwar, S.; Pozniak, C.; Coaker, G.; Dubcovsky, J.; et al. Three previously characterized resistances to yellow rust are encoded by a single locus *Wtk1*. *J. Exp. Bot.* **2020**, *71*, 2561–2572. [CrossRef]
143. Brueggeman, R.; Rostoks, N.; Kudrna, D.; Kilian, A.; Han, F.; Chen, J.; Druka, A.; Steffenson, B.; Kleinhofs, A. The barley stem rust-resistance gene *Rpg1* is a novel disease-resistance gene with homology to receptor kinases. *Proc. Natl. Acad. Sci. USA* **2002**, *99*, 9328–9333. [CrossRef] [PubMed]
144. Sharma Poudel, R.; Al-Hashel, A.F.; Gross, T.; Gross, P.; Brueggeman, R. Pyramiding *rpg4*- and *Rpg1*-mediated stem rust resistance in barley requires the *Rrr1* gene for both to function. *Front. Plant Sci.* **2018**, *871*, 1789. [CrossRef] [PubMed]
145. Kempf, H. (Secobra Saatzucht GmbH, Moosburg a. d., Isar, Germany). Personal communication, 2022.
146. Clayton, W.D.; Renvoize, S.A. *Genera Gramineum, Grasses of the World, Kew Bulletin Additional Series XIII*; Her Majesty's Stationary Office: London, UK, 1986.
147. Jellen, E.N.; Leggett, M. Cytogenetic Manipulation in Oat Improvement Genetic Resources, Chromosome Engineering, and Crop Improvement. In *Cereals*; Singh, R.J., Jauhar, P.P., Eds.; Taylor & Francis: London, UK, 2006; pp. 199–231, ISBN 978-1859723760.
148. Leggett, J.M.; Thomas, H. Oat evolution and cytogenetics. In *Oat Crop Production and Utilization*; Welch, R., Ed.; Chapman & Hall: London, UK, 1995.
149. Thomas, H. Cytogenetics of *Avena*. In *Oat Science and Technology*; Agronomy Monograf No.33; Marshall, H.G., Sorrells, M.E., Eds.; Merican Society of Agronomy: Madison, WI, USA, 1992; pp. 473–507.
150. Rajharthy, T.; Thomas, H. *Cytogenetics of oats (Avena L.)*; no. 2; Miscellaneous publications of the Genetics Society of Canada: Ottawa, ON, USA, 1974.
151. Baum, B.R. *Oats: Wild and Cultivated. A monograph of the genus Avena L. (Poaceae)*; Monogr. No. 14.; Department of Agriculture Supply and Services Canada: Ottawa, ON, Canada, 1977.
152. Legget, J.M. Classification and Speciation in *Avena*. In *Oat Science and Technology*; Agronomy Monograf, No.33; Marshall, H.G., Sorrells, M.E., Eds.; American Society of Agronomy: Madison, WI, USA, 1992; pp. 29–52.
153. Malzev, A.I. *Wild and Cutivated Oats. Section Euavena Griseb*; Works Appl. Bot. Plant. Breed. Suppl No: 38: Leningrad, Russia, 1930.
154. Zeller, F.J. Nutzung des genetischen Potentials der Avena-Wildarten zur Verbesserung des Saathafers (*Avena sativa* L.). *J. Appl. Bot.* **1998**, *72*, 180–185.
155. Loskutov, I.G.; Rines, H.W. Avena. In *Wild Crop Relatives: Genomic and Breeding Resources: Cereals*; Kole, C., Ed.; Springer: Berlin/Heidelberg, Germany, 2011; pp. 109–183.
156. Leggett, J.M. Using and conserving *Avena* genetic resources. In Proceedings of the 5th International Oats Conference, Saskatoon, SK, Canada, 29 July–6 August 1996; pp. 128–132.
157. Jellen, E.N.; Phillips, R.L.; Rines, H.W. C-banded karyotypes and polymorphisms in hexaploid oat accessions (*Avena* spp.) using Wright's stain. *Genome* **1993**, *36*, 1129–1137. [CrossRef] [PubMed]
158. Tomaszewska, P.; Kosina, R. Cytogenetic events in the endosperm of amphiploid *Avena magna* × *A. longiglumis*. *J. Plant Res.* **2021**, *134*, 1047–1060. [CrossRef]
159. Yan, H.; Bekele, W.A.; Wight, C.P.; Peng, Y.; Langdon, T.; Latta, R.G.; Fu, Y.-B.; Diederichsen, A.; Howarth, C.J.; Jellen, E.N.; et al. High-density marker profiling confirms ancestral genomes of *Avena* species and identifies D-genome chromosomes of hexaploid oat. *Theor. Appl. Genet.* **2016**, *129*, 2133–2149. [CrossRef]
160. Yan, H.; Ren, Z.; Deng, D.; Yang, K.; Yang, C.; Zhou, P.; Wight, C.P.; Ren, C.; Peng, Y. New evidence confirming the CD genomic constitutions of the tetraploid *Avena* species in the section *Pachycarpa* Baum. *PLoS ONE* **2021**, *16*, e0240703. [CrossRef]
161. Katsiotis, A.; Hagidimitriou, M.; Heslop-Harrison, J.S. The close relationship between the A and B genomes in *Avena* L. (*Poaceae*) determined by molecular cytogenetic analysis of total genomic, tandemly and dispersed repetitive DNA sequences. *Ann. Bot.* **1997**, *79*, 103–109. [CrossRef]
162. Hutchinson, J.; Postoyko, J. C-banding of Avena species. In *Genetic Manipulation in Plant Breeding*; De Gruyter: Berlin, Germany; New York, NY, USA, 1986; pp. 157–159.
163. Jellen, E.N.; Gill, B.S.; Cox, T.S. Genomic in situ hybridization differentiates between A/D and C-genome chromatin and detects intergenomic translocations in polyploid species (genus *Avena*). *Genome* **1994**, *37*, 613–618. [CrossRef]
164. Ladizinsky, G. A new species of *Avena* from Sicily, possibly progenitor of hexaploid oats. *Genet. Resour. Crop Evol.* **1998**, *45*, 263–269. [CrossRef]
165. Tomaszewska, P.; Schwarzacher, T.; Heslop-Harrison, J.S.P. Oat chromosome and genome evolution defined by widespread terminal intergenomic translocations in polyploids. *Front Plant Sci.* **2022**, *13*, 1026364. [CrossRef] [PubMed]

166. Markhand, G.S.; Leggett, J.M. The genomes of *A. lusitanica*, *A. hispanica* and *A. matritensis* confirmed using GISH. In Proceedings of the 5th International Oats Conference, Saskatoon, SK, Canada, 29 July–6 August 1996; pp. 347–349.
167. Kamal, N.; Tsardakas Renhuldt, N.; Bentzer, J.; Gundlach, H.; Haberer, G.; Juhász, A.; Lux, T.; Bose, U.; Tye-Din, J.A.; Lang, D.; et al. The mosaic oat genome gives insights into a uniquely healthy cereal crop. *Nature* **2022**, *606*, 113–119. [CrossRef] [PubMed]
168. Ladizinsky, G.; Zohary, D. Notes of species delimination, species relationships and polyploidy in *Avena*. *Euphytica* **1971**, *20*, 380–395. [CrossRef]
169. Rajhathy, T. The chromosomes of *Avena*. In *Chromosome Engineering in Plants: Genetics, Breeding and Evolution*; Gupta, P.K., Tsuchiya, T., Eds.; Elsevier Science Publishers: Amsterdam, The Netherlands, 1991; pp. 449–467.
170. Boczkowska, M.; Tarczyk, E. Genetic diversity among Polish landraces of common oat (*Avena sativa* L.). *Genet. Resour. Crop Evol.* **2013**, *60*, 2157–2169. [CrossRef]
171. Diederichsen, A. Assessments of genetic diversity within a world collection of cultivated hexaploid oat (*Avena sativa* L.) based on qualitative morphological characters. *Genet. Resour. Crop Evol.* **2007**, *55*, 419–440. [CrossRef]
172. Fu, Y.B.; Peterson, G.W.; Williams, D.; Richards, K.W.; Fetch, J.M. Patterns of AFLP variation in a core subset of cultivated hexaploid oat germplasm. *Theor. Appl. Genet.* **2005**, *111*, 530–539. [CrossRef]
173. Frey, K.J. Genetic resources and their use in oat breeding. In Proceedings of the Second International Oats Conference; Lawes, D.A., Thomas, H., Eds.; Springer: Aberystwyth, UK, 1985; pp. 9–15.
174. Langer, I.; Frey, K.J.; Bailey, T.B. Production response and stability characteristics of oat cultivars developed in different eras. *Crop Sci.* **1978**, *18*, 938–942. [CrossRef]
175. Rodgers, D.M.; Murphy, J.P.; Frey, K.J. Impact of plant breeding on the grain yield and genetic diversity of spring oats. *Crop Sci.* **1983**, *23*, 737–740. [CrossRef]
176. Burrows, V.D. Breeding oats for food and feed: Conventional and new techniques and materials. In *Oats: Chemistry and Technology*; Webster, F.H., Ed.; American Association of Cereal Chemists: St. Paul, MN, USA, 1986; pp. 13–46.
177. Comeau, A. Barley yellow dwarf virus resistance in the genus *Avena*. *Euphytica* **1984**, *33*, 49–55. [CrossRef]
178. Cox, T.S.; Frey, K.J. Complementarity of genes for high groat-protein percentage from *Avena sativa* L. and *A. sterilis* L. *Crop Sci.* **1985**, *25*, 106–109. [CrossRef]
179. Cox, D.J.; Frey, K.J. Improving cultivated oats (*Avena sativa* L.) with allels for vegetative growth index from *A. sterilis* L. *Theor. Appl. Genet.* **1984**, *68*, 239–245. [CrossRef]
180. Frey, K.J. Heritability of groat-protein percentage of hexaploid oats. *Crop Sci.* **1975**, *15*, 227–228. [CrossRef]
181. Hsam, S.L.K.; Paderina, E.V.; Gordei, S.; Zeller, F.J. Genetic studies of powdery mildew resistance in cultivated oat (*Avena sativa* L.) II. Cultivars and breeding lines grown in Northen and Eastern Europe. *Hereditas* **1998**, *129*, 227–230. [CrossRef]
182. Lawrence, P.K.; Frey, K.J. Backcross variability for grain yield in oat species crosses (*Avena sativa* L. × *A. sterilis* L.). *Euphytica* **1975**, *24*, 77–85. [CrossRef]
183. Leggett, J.M. The conservation and exploitation of wild oat species. In Proceedings of the 4th International Oats Conference, Adelaide, Australia, 19–23 October 1992; pp. 85–87.
184. Loskutov, I.G. The collection of wild oat species of C.I.S. as a source of diversity in agricultural traits. *Genet. Resour. Crop Evol.* **1998**, *45*, 291–295. [CrossRef]
185. Ohm, H.W.; Patterson, F.L. A six-parent diallel cross analysis for protein in *Avena sterilis* L. *Crop Sci.* **1973**, *13*, 27–30. [CrossRef]
186. Rines, H.W.; Stuthman, D.D.; Briggle, L.W.; Youngs, V.L.; Jedlinski, H.; Smith, D.H.; Webster, J.A.; Rothman, P.G. Collection and evaluation of *Avena fatua* for use in oat improvement. *Crop Sci.* **1980**, *20*, 65–68. [CrossRef]
187. Thro, A.M.; Frey, K.J. Inheritance of groat-oil content and high-oil selection in oats (*Avena sativa* L.). *Euphytica* **1985**, *34*, 251–263. [CrossRef]
188. Welch, R.W.; Brown, J.C.W.; Leggett, J.M. Interspecific and intraspecific variation in grain and groat characteristics of wild oat (*Avena*) species: Very high groat (1,3),(1,4)-β-D-glucan in an *Avena atlantica* genotype. *J. Cereal Sci.* **2000**, *31*, 273–279. [CrossRef]
189. Welch, R.W.; Leggett, J.M. Nitrogen content, oil content, oil composition of oat cultivars (*A. sativa*) and wild *Avena* species in relation to nitrogen fertility, yield and partioning of assimilates. *J. Cereal Sci.* **1997**, *26*, 105–120. [CrossRef]
190. Boczkowska, M.; Podyma, W.; Łapiński, B. Oat. In *Genetic and Genomic Resources for Grain Cereals Improvement*; Elsevier: London, UK, 2016; pp. 159–225.
191. Ladizinsky, G. Genetic resources and their use in the breeding of oats. In Proceedings of the Second International Oats Conference; Lawes, D.A., Thomas, H., Eds.; Springer: Aberystwyth, UK, 1986; pp. 52–53.
192. Ohm, H.W.; Shaner, G. Breeding oat for resistance to diseases. In *Oat Science and Technology*; Agronomy Monograf No.33; Marshall, H.G., Sorrells, M.E., Eds.; American Society of Agronomy: Madison, WI, USA, 1992; pp. 657–683.
193. Stalker, H.T. *Utilization of Wild Species for Crop Improvement*; Advances in Agronomy No. 33; Elsevier: Amsterdam, The Netherlands, 1980; pp. 111–147.
194. Jellen, E.N.; Jackson, E.W.; Maughan, P.J. Oat Improvement and Innovation Using Wild Genetic Resources (Poaceae, Avena spp.): Elevating "Oats" to a New Level and Stature. In *Polyploidy and Hybridization for Crop Improvement*; Mason, A.S., Ed.; CRC Press: Boca Raton, FL, USA, 2016; pp. 364–376.
195. Jellen, E.N.; Beard, J. Geographical distribution of a chromosome 7C and 17 intergenomic translocation in cultivated oat. *Crop Sci.* **2000**, *40*, 256–263. [CrossRef]

196. Jellen, E.N.; Rines, H.W.; Fox, S.L.; Davis, D.W.; Phillips, R.L.; Gill, B.S. Characterization of SUN II oat monosomics through C-banding and identification of eight new Sun II monosomics. *Theor. Appl. Genet.* **1997**, *95*, 1190–1195. [CrossRef]
197. Oliver, R.E.; Tinker, N.A.; Lazo, G.R.; Chao, S.; Jellen, E.N.; Carson, M.L.; Rines, H.W.; Obert, D.E.; Lutz, J.D.; Shackelford, I.; et al. SNP discovery and chromosome anchoring provide the first physically-anchored hexaploid oat map and reveal synteny with model species. *PLoS ONE* **2013**, *8*, e58068. [CrossRef]
198. Sanz, M.J.; Jellen, E.N.; Loarce, Y.; Irigoyen, M.L.; Ferrer, E.; Fominaya, A. A new chromosome nomenclature system for oat (*Avena sativa* L. and *A. byzantina* C. Koch) based on FISH analysis of monosomic lines. *Theor. Appl. Genet.* **2010**, *121*, 1541–1552. [CrossRef] [PubMed]
199. Kianian, S.F.; Wu, B.-C.; Fox, S.L.; Rines, H.W.; Phillips, R.L. Aneuploid marker assignment in hexaploid oat with the C genome as a reference for determining remnant homoeology. *Genome* **1997**, *40*, 386–396. [CrossRef] [PubMed]
200. Tinker, N.A.; Wight, C.P.; Bekele, W.A.; Yan, W.; Jellen, E.N.; Renhuldt, N.T.; Sirijovski, N.; Lux, T.; Spannagl, M.; Mascher, M. Genome analysis in *Avena sativa* reveals hidden breeding barriers and opportunities for oat improvement. *Commun. Biol.* **2022**, *5*, 474. [CrossRef]
201. Clamot, G.; Rivoal, R. Genetic resistance to cereal cyst nematode *Heterodera avenae* in wild oat *A. sterilis*. *Euphytica* **1984**, *33*, 27–32. [CrossRef]
202. Hsam, S.L.K.; Peters, N.; Paderina, E.V.; Felsenstein, F.; Oppitz, K.; Zeller, F.J. Genetic studies of powdery mildew resistance in common oat (*Avena sativa* L.) I. Cultivars and breeding lines grown in Western Europe and North America. *Euphytica* **1997**, *96*, 421–427. [CrossRef]
203. Lyrene, P.M.; Shands, H.L. Heading dates in six *A. sativa* × *A. sterilis* crosses. *Crop Sci.* **1975**, *15*, 359–360. [CrossRef]
204. Lyrene, P.M.; Shands, H.L. Associations among traits in progenies from *A. sativa* × *A. sterilis* crosses. *Crop Sci.* **1975**, *15*, 361–363. [CrossRef]
205. Bacon, R.K. Registration of 'Ozark' oat. *Crop Sci.* **1991**, *31*, 1383–1384. [CrossRef]
206. Frey, K.J. Oat improvement with genes from Avena species. In Proceedings of the 4th International Oat Conference, Vol 2: Wild Oats in Agriculture, Adelaide, SA, Australia, 19–23 October 1992; pp. 61–64.
207. Fox, S.L.; Brown, P.D.; Chong, J. Inheritance of crown rust resistance in four accessions of *Avena sterilis* L. *Crop Sci.* **1997**, *37*, 342–345. [CrossRef]
208. Gregory, J.W.; Wise, R.P. Linkage of genes conferring specific resistance to crown rust in diploid *Avena*. *Genome* **1994**, *37*, 92–96. [CrossRef] [PubMed]
209. O'Donoughue, L.S. The identification, localization and utilization of molecular markers for rust resistance genes in oat. In Proceedings of the 5th International Oats Conference, Saskatoon, SK, Canada, 29 July–6 August 1996; pp. 150–155.
210. Parker, J.H. A preliminary study of the inheritance of rust resistance in oats. *Agron. J.* **1920**, *12*, 23–38. [CrossRef]
211. Marshall, H.G.; Shaner, G.E. Genetics and inheritance in oat. In *Oat Science and Technology*; Agronomy Monograph, No.33; Marshall, H.G., Sorrells, M.E., Eds.; American Society of Agronomy: Madison, WI, USA, 1992; pp. 509–570.
212. Gnanesh, B.N.; Mitchell Fetch, J.; Zegeye, T.; McCartney, C.A.; Fetch, T. Oat. In *Alien Gene Transfer in Crop Plants*; Pratap, A., Kumar, J., Eds.; Springer: New York, NY, USA, 2014; Volume 2, pp. 51–73. [CrossRef]
213. Park, R.F.; Boshoff, W.H.P.; Cabral, A.L.; Chong, J.; Martinelli, J.A.; McMullen, M.S.; Mitchell Fetch, J.W.; Paczos-Grzęda, E.; Prats, E.; Roake, J.; et al. Breeding oat for resistance to the crown rust pathogen *Puccinia coronata* f. sp. *avenae*: Achievements and prospects. *Theor. Appl. Genet.* **2022**, *135*, 3709–3734. [CrossRef]
214. Simons, M.D. Transfer of field resistance to *Puccinia coronata* from *Avena sterilis* to cultivated oats by backcrossing. *Phytopathology* **1985**, *75*, 314–317. [CrossRef]
215. Chong, J.; Gruenke, J.; Dueck, R.; Mayert, W.; Woods, S. Virulence of oat crown rust [*Puccinia coronata* f. sp. *avenae*] in Canada during 2002–2006. *Can. J. Plant Pathol.* **2008**, *30*, 115–123. [CrossRef]
216. Leonard, K.; Martinelli, J.A. Virulence of oat crown rust in Brazil and Uruguay. *Plant Dis.* **2005**, *89*, 802–808. [CrossRef]
217. Admassu-Yimer, B.; Esvelt-Klos, K.; Griffiths, I.; Cowan, A.; Howarth, C. Mapping of crown rust (*Puccinia coronata* f. sp. *avenae*) resistance gene *Pc54* and a novel quantitative trait locus effective against powdery mildew (*Blumeria graminis* f. sp. *avenae*) in the oat (*Avena sativa*) line Pc54. *Phytopathology* **2022**, *112*, 1316–1322. [CrossRef] [PubMed]
218. Ociepa, T.; Okoń, S. Chromosomal location of *Pm12*—A novel powdery mildew resistance gene from *Avena sterilis*. *Genes* **2022**, *13*, 2409. [CrossRef]
219. Ociepa, T.; Okoń, S.M.; Nucia, A.; Leśniowska-Nowak, J.; Paczos-Grzęda, E.; Bisaga, M. Molecular identification and chromosomal localization of new powdery mildew resistance gene *Pm11* in oat. *Theor. Appl. Genet.* **2020**, *133*, 179–185. [CrossRef]
220. Roderick, H.W.; Jones, E.R.L.; Šebesta, J. Resistance to oat powdery mildew in Britain and Europe: A review. *Ann. Appl. Biol.* **2000**, *136*, 85–91. [CrossRef]
221. Fetch, T.G.; Jin, Y. Letter code system of nomenclature for *Puccinia graminis* f. sp. *avenae*. *Plant Dis.* **2007**, *91*, 763–766. [CrossRef]
222. Takeda, K.; Frey, K.J. Simultaneous selection for grain yield and protein percentage in backcross populations from *A. sterilis* × *A. sativa* matings by using independent culling levels procedure. *Theor. Appl. Genet.* **1985**, *69*, 375–382. [CrossRef] [PubMed]
223. Takeda, K.; Frey, K.J. Protein yield and its relationship to other traits in backcross population in from an *A. sativa* × *A. sterilis* cross. *Crop Sci.* **1979**, *19*, 623–628. [CrossRef]

224. Rossnagel, B.G.; Bhatty, R.S. Use of *A. sterilis* and *A. maroccana* derived *A. sativa* germplasm to increase groat protein concetration in oat for Western Canada. In Proceedings of the 4th International Oats Conference, Adelaide, Australia, 19–23 October 1992; pp. 134–137.
225. Frey, K.J.; Holland, J.B. Nine cycles of recurrent selection for increased groat-oil content in oat. *Crop Sci.* **1999**, *39*, 1636–1641. [CrossRef]
226. Schipper, H.; Frey, K.J. Observed gains from three recurrent selection regimes for increased groat-oil content of oat. *Crop Sci.* **1991**, *31*, 1505–1510. [CrossRef]
227. Morikawa, T. Genetic analysis on dwarfness of wild oats, *Avena fatua*. *Jpn. J. Genet.* **1989**, *64*, 363–371. [CrossRef]
228. Morikawa, T.; Sumiya, M.; Kuriyama, S. Transfer of new dwarfing genes from the weed species *Avena fatua* into cultivated oat mboxemphA. byzantina. *Plant Breed.* **2007**, *126*, 30–35. [CrossRef]
229. Milach, S.C.; Rines, H.W.; Phillips, R.L.; Stuthman, D.D.; Morikawa, T. Inheritance of a new dwarfing gene in oat. *Crop Sci.* **1997**, *38*, 356–360. [CrossRef]
230. Suneson, C.A. Registration of Montezuma oats. *Crop Sci.* **1969**, *9*, 527. [CrossRef]
231. Thompson, R.K. Registration of Mesa oats. *Crop Sci.* **1967**, *7*, 167. [CrossRef]
232. Dyck, P.L.; Rajharthy, T. Cytogenetics of a hexaploid oat with an extra pair of chromosomes. *Can. J. Genet. Cytol.* **1963**, *5*, 408–413. [CrossRef]
233. Sharma, D.C. Disomic alien chromosome substitution and addition in hexaploid oat. *Euphytica* **1978**, *27*, 581–586. [CrossRef]
234. Thomas, H. Evaluation of the use of species hybrids and synthetic amphiploids in the improvement of the oat crop. *Euphytica* **1968**, *17*, 404–413. [CrossRef]
235. Thomas, H.; Bahatti, I.M. Notes on the cytogenetic structure of the cultivated oat *Avena sativa* (2n = 6x = 42). *Euphytica* **1975**, *24*, 149–157. [CrossRef]
236. Sharma, D.C. Chromosome pairing problems in interploidy transfer of leaf rust resistance in oats. *Euphytica* **1975**, *24*, 503–510. [CrossRef]
237. Brown, P.D.; Forsberg, R.A.; McKenzie, R.I.H.; Martens, J.W. The use of disomic addition lines in the transfer of oat stem resistance to hexaploid oats. In *Proceedings of the Second International Oats Conference*; Lawes, D.A., Thomas, H., Eds.; Springer: Aberystwyth, UK, 1985; pp. 16–20.
238. Aung, T.; Thomas, H.; Jones, I.T. The transfer of the gene for mildew resistance from *Avena barbata* (4x) into the cultivated oat *A. sativa* by an induced translocation. *Euphytica* **1977**, *26*, 623–632. [CrossRef]
239. Sharma, D.C.; Forsberg, R.A. Spontaneous and induced interspecific gene transfer for crown rust resistance in *Avena*. *Crop Sci.* **1977**, *17*, 855–860. [CrossRef]
240. Rajhathy, T.; Thomas, H. Genetic control of chromosome pairing in hexaploid oats. *Nat. New Biol.* **1972**, *239*, 217–219. [CrossRef]
241. Riley, R.; Chapman, V. The effects of the deficiency of chromosom V (5B) of *Triticum aestivum* on the meiosis of synthetic amphiploids. *Heredity* **1963**, *18*, 473–484. [CrossRef]
242. Jauhar, P.P. Genetic regulation of diploid-like chromosome pairing in *Avena*. *Theor. Appl. Genet.* **1977**, *49*, 287–295. [CrossRef] [PubMed]
243. Gauthier, F.M.; McGinnis, R.C. The meiotic behavior of a nulliploid plant in *Avena sativa* L. *Can. J. Genet. Cytol.* **1968**, *10*, 186–189. [CrossRef]
244. Rothman, P.G. Registration of four stem rust and crown rust resistant oat germplasm lines. *Crop Sci.* **1984**, *24*, 1217–1218. [CrossRef]
245. Aung, T.; Chong, J.; Leggett, J.M. The transfer of crown rust resistance gene *Pc94* from a wild diploid to cultivated hexaploid oat. In Proceedings of the 9th European and Mediterranean Cereal Rusts and Powdery Mildews Conference, Lunteren, The Netherlands, 2–6 September 1996; p. 3.
246. Dyck, P.L.; Zillinsky, F.L. Inheritance of crown rust resistance transferred from diploid to hexaploid oats. *Can. J. Genet. Cytol.* **1963**, *5*, 398–407. [CrossRef]
247. Rooney, W.L.; Rines, H.R.; Phillips, R.L. Identification of RFLP markers linked to crown rust resistance genes *Pc91* and *Pc92* in oat. *Crop Sci.* **1994**, *34*, 940–944. [CrossRef]
248. Hsam, S.L.K.; Mohler, V.; Zeller, F.J. The genetics of resistance to powdery mildew in cultivated oats (*Avena sativa* L.): Current status of major genes. *J. Appl. Genet.* **2014**, *55*, 155–162. [CrossRef]
249. Brown, P.D. The transfer of oat stem rust resistance gene *Pg16* from tetraploid *Avena barbata* Pott. to hexaploidy *Avena sativa* L. *Dissert. Abstr. Int. B Sci. Eng.* **1985**, *45*, 2036B.
250. Pohler, W.; Hoppe, H.D. *Avena macrostachya*—A potential gene source for oat breeding. *Vortr Pflanzenzüchtg* **1991**, *20*, 66–71.
251. Yu, J.; Herrmann, M. Inheritance and mapping of a powdery mildew resistance gene introgressed from *Avena macrostachya* in cultivated oat. *Theor. Appl. Genet.* **2006**, *113*, 429–443. [CrossRef]
252. Hoppe, H.D.; Kummer, M. New productive hexaploid derivatives after introgression from *A. pilosa* features. *Vortr Pflanzenzüchtg* **1991**, *20*, 56–61.
253. Cabral, A.L.; Park, R.F. Seedling resistances to *Puccinia coronata* f. sp. *avenae* in *Avena strigosa*, *A. barbata* and *A. sativa*. *Euphytica* **2014**, *196*, 385–395. [CrossRef]
254. Cabral, A.L.; Singh, D.; Park, R.F. Identification and genetic characterisation of adult plant resistance to crown rust in diploid and tetraploid accessions of *Avena*. *Ann. Appl. Biol.* **2011**, *159*, 220–228. [CrossRef]

255. Okoń, S.; Paczos-Grzęda, E.; Ociepa, T.; Koroluk, A.; Sowa, S.; Kowalczyk, K.; Chrząstek, M. *Avena sterilis* L. Genotypes as a Potential Source of Resistance to Oat Powdery Mildew. *Plant Dis.* **2016**, *100*, 2145–2151. [CrossRef]
256. Okoń, S.; Ociepa, T.; Paczos-Grzęda, E.; Ladizinsky, G. Evaluation of resistance to *Blumeria graminis* (DC.) f. sp. *avenae*, in *Avena murphyi* and *A. magna* genotypes. *Crop Prot.* **2018**, *106*, 177–181. [CrossRef]
257. Paczos-Grzęda, E.; Sowa, S.; Koroluk, A.; Langdon, T. Characteristics of resistance to *Puccinia coronata* f. sp. *avenae* in *Avena fatua* L. *Plant Dis.* **2018**, *102*, 2616–2624. [CrossRef] [PubMed]
258. Paczos-Grzęda, E.; Sowa, S.; Boczkowska, M.; Langdon, T. Detached leaf assays for resistance to crown rust reveal diversity within populations of *Avena sterilis* L. *Plant Dis.* **2019**, *105*, 832–840. [CrossRef] [PubMed]
259. Paczos-Grzęda, E.; Boczkowska, M.; Sowa, S.; Koroluk, A.; Toporowska, J. Hidden Diversity of Crown Rust Resistance within Genebank Resources of *Avena sterilis* L. *Agronomy* **2021**, *11*, 315. [CrossRef]
260. Sowa, S.; Paczos-Grzęda, E.; Koroluk, A.; Okoń, S.; Ostrowska, A.; Ociepa, T.; Chrząstek, M.; Kowalczyk, K. Resistance to *Puccinia coronata* f. sp. *avenae* in *Avena magna*, *A. murphyi*, and *A. insularis*. *Plant Dis.* **2016**, *100*, 1184–1191. [CrossRef]
261. Sowa, S.; Mohler, V.; Paczos-Grzęda, E. Searching for novel oat crown rust resistance in diploid oat *Avena strigosa* Schreb. reveals the complexity and heterogeneity of the analyzed genebank accessions. *Agriculture* **2023**, *13*, 296. [CrossRef]
262. Rines, H.W.; Porter, H.L.; Carson, M.L.; Ochocki, G.E. Introgression of crown rust resistance from diploid oat *Avena strigosa* into hexaploid cultivated oat *A. sativa* by two methods: Direct crosses and through an initial 2x 4x synthetic hybrid. *Euphytica* **2007**, *158*, 67–79. [CrossRef]
263. Ladizinsky, G.; Fainstein, R. Introgression between the cultivated hexaploid oat *A. sativa* and the tetraploid wild *A. magna* and *A. murphyi*. *Can. J. Genet. Cytol.* **1977**, *19*, 59–60. [CrossRef]
264. Ladizinsky, G. A synthetic hexaploid (2n=42) oat from the cross of *Avena strigosa* (2n = 14) and domesticated *A. magna* (2x = 28). *Euphytica* **2000**, *116*, 231–235. [CrossRef]
265. Ladizinsky, G. Domestication via hybridization of the wild tetraploid oats *Avena magna* and *A. murphyi*. *Theor. Appl. Genet.* **1995**, *91*, 639–646. [CrossRef]
266. Jellen, E.N.; Jackson, E.W.; Elhadji, T.; Young, L.K.; El Mouttaqi, A.; Al Halfa, I.; El Fartassi, I.; Sanata Katile, L.; Linchangco, R.; Klassen, K.; et al. Adaptation and agronomic performance of domesticated moroccan oat (*Avena magna* ssp. *domestica*). Lines under subsistence farming conditions at multiple locations in Morocco. *Agronomy* **2021**, *11*, 1037. [CrossRef]
267. Thiam, E.; Jellen, E.N.; Jackson, E.W.; Nelson, M.; Rogers, W.; El Mouttaqi, A.; Benlhabib, O. Productivity and stability evaluation of 12 selected *Avena magna* ssp. *domestica* lines based on multi-location experiments during three cropping seasons in Morocco. *Agriculture* **2023**, *13*, 1486. [CrossRef]
268. McCartney, C.A.; Stonehouse, R.G.; Rossnagel, B.G.; Eckstein, P.E.; Scoles, G.J.; Zatorski, T.; Beattie, A.D.; Chong, J. Mapping of the oat crown rust resistance gene *Pc91*. *Theor. Appl. Genet.* **2011**, *122*, 317–325. [CrossRef]
269. Łapiński, B.; Nita, Z.; Szołkowska, A.; Wieczorek, P. A hybrid of cultivated oat with the wild species *Avena macrostachya* as a source of new variation for yield quality improvement in naked oats. *Biuletyn IHAR* **2013**, *270*, 43–54. [CrossRef]
270. Chaffin, A.S.; Huang, Y.-F.; Smith, S.; Bekele, W.A.; Babiker, E.; Gnanesh, B.N.; Foresman, B.J.; Blanchard, S.G.; Jay, J.J.; Reid, R.W.; et al. A consensus map in cultivated hexaploid oat reveals conserved grass synteny with substantial subgenome rearrangement. *Plant Genome* **2016**, *9*, 1–21. [CrossRef]
271. GrainGenes: A Database for Triticeae and Avena, Avena sativa, OT3098 v2, PepsiCo. Available online: https://wheat.pw.usda.gov/jb?data=/ggds/oat-ot3098v2-pepsico (accessed on 25 January 2023).
272. Peng, Y.; Yan, H.; Guo, L.; Deng, C.; Wang, C.; Wang, Y.; Kang, L.; Zhou, P.; Yu, K.; Dong, X.; et al. Reference genome assemblies reveal the origin and evolution of allohexaploid oat. *Nat. Genet.* **2022**, *54*, 1248–1258. [CrossRef]

agriculture

MDPI

Review

Portuguese *Castanea sativa* Genetic Resources: Characterization, Productive Challenges and Breeding Efforts

Megan Braga [1,*], Susana de Sousa Araújo [1], Hélia Sales [2], Rita Pontes [2] and João Nunes [2]

[1] Association BLC3—Technology and Innovation Campus, Centre Bio R&D Unit | North Delegation, Rua Comendador Emílio Augusto Pires, Edifício SIDE UP, 5340-257 Macedo de Cavaleiros, Portugal; susana.araujo@blc3.pt

[2] Association BLC3—Technology and Innovation Campus, Centre Bio R&D Unit, Rua Nossa Senhora da Conceição 2, Lagares da Beira, 3405-155 Oliveira do Hospital, Portugal; helia.sales@blc3.pt (H.S.); rita.pontes@blc3.pt (R.P.); joao.nunes@blc3.pt (J.N.)

* Correspondence: megan.braga@blc3.pt

Abstract: Chestnuts are multipurpose trees that grow mainly in the Northern Hemisphere due to their aptitude for fruit and wood production. These trees are vastly significant for the economy and wildlife. The widespread distribution of these trees demonstrates their genetic adaptability to many environmental conditions. The main varieties of European chestnut (*Castanea sativa* Miller) cultivated in Portugal, their productive challenges and breeding and biotechnological efforts developed over the last decades are described. This paper highlights the efforts focused on the improvement of varieties and rootstocks through selection and hybridization of European chestnut with the Asian species *Castanea crenata* Siebold and Zuccarini and *Castanea mollissima* Blume, which are resistant to ink disease, which have been the foundation of the Portuguese chestnut breeding programs. Breeding and biotechnological efforts developed over the last decades, focused on ink disease and chestnut blight resistance, are described. The potentialities of this research to stimulate the competitiveness of bioeconomy-based knowledge and innovation in the productive chestnut sector is also discussed.

Keywords: bioeconomy; chestnut; *Cryphonectria parasitica*; genetic resources; genetic variability; genomics; *Phytophthora cinnamomi*

Citation: Braga, M.; Araújo, S.d.S.; Sales, H.; Pontes, R.; Nunes, J. Portuguese *Castanea sativa* Genetic Resources: Characterization, Productive Challenges and Breeding Efforts. *Agriculture* **2023**, *13*, 1629. https://doi.org/10.3390/agriculture13081629

Academic Editors: Edyta Paczos-Grzeda, Volker Mohler and Sylwia Sowa

Received: 30 June 2023
Revised: 9 August 2023
Accepted: 10 August 2023
Published: 18 August 2023

1. Introduction

Chestnuts, genus *Castanea*, are multipurpose trees that grow mainly in the Northern Hemisphere due to their aptitude for fruit and wood production [1,2]. These are vastly significant for the economy and wildlife [1,2]. The name of the genus, *Castanea*, derived from "Kastah", which means "dried fruit, seed" in eastern Asia. It is suspected that chestnuts were introduced in Europe by Greeks, where the Latin word *Castanea* is derived from the Greek "Kastanon" [3,4]. The chestnut is incorporated in the *Fagaceae* family, in the *Castaneoidiae* subfamily and in the genus *Castanea*, which includes *sativa* and 12 other species, all diploid ($2n = 24$) [3]. The species were distributed mainly in three regions of the world: Europe and the Mediterranean basin (*C. sativa* Miller), Asia (China (*C. mollissima* Blume)), North Korea (*C. crenata* Siebold and Zuccarini), Republic of Korea (*C. seguinii* Dode), Japan (*C. davidii* Dode), Vietnam (*C. henryi* Rehder and Wilson), and in North America (*C. dentata* (Marsh.) Borkh, *C. pumila* Miller, *C. floridiana* Ashe, *C. ashei* Sudworth, *C. alnifolia* Nuttal, *C. paucispina* Ashe and *C. azarkensis*) [5,6]. Each species clearly differs from one another in terms of vegetative habits, fruit and wood characteristics, sizes, resistance to biotic and abiotic factors and adaptability. Altogether, these factors have influenced their distribution throughout time.

As result of its dispersal and use in Europe, the species name acquired the epithet *sativa* (derived from the Latin "*sativus*"), which means "cultivated" [4]. The introduction and dispersion of the chestnut tree in Portugal, as in other European countries, was made

by the Romans during their colonization [7]. *C. sativa*, which has hundreds of varieties with significant economic potential for fruit production, is one of the most-planted *Castanea* species in Europe [1]. According to official data made available by FAO [8], over the past few years, harvesting and production of chestnuts have expanded substantially around the world.

Although *Castanea* species have adapted to different environmental conditions, their production in Europe has been continuously threatened by biotic and abiotic stresses, presently exacerbated by climate change. To tackle this problem, the scientific community has been focusing on identifying the cellular, molecular and genetic interactions underlying all biotic and abiotic stresses in the chestnut tree [2]. Most efforts on this topic have been toward breeding and biotechnology to address the main chestnut's biotic stresses. Numerous biotic stressors affect *Castanea* species, but the two most damaging pathogens are *Cryphonectria parasitica* (Murr.) Barr. (*CP*) and *Phytophthora cinnamomi* Rands (*PC*) [9,10]. *C. parasitica* causes chestnut blight or chestnut canker, while *P. cinnamomi* causes the ink disease, also known as root rot. Despite the availability of chemical treatments, they have proven to be ineffective and harmful for the environment [9,10]. Biological treatments based on hypovirulence have successfully controlled chestnut blight in some locations in Europe [10]. Other diseases affect chestnuts, such as the leaf spot (*Marssonina ochroleuca*), twig canker (*Cryptodiaporthe castanea*) and chestnut mosaic virus (*ChMV*), although the damage they inflict is not as severe as that from the above-mentioned diseases [9]. The Asian chestnut gall wasp *Dryocosmus kuriphilus* is another pest that caused serious impacts on chestnut production and orchard health, but the introduction of the biological control agent *Torymus sinensis* seems to have had positive results on the issue [10]. Other approaches include, as an example, the use of *Castanea crenata* (Sieb and Zucc), a rootstock for *C. sativa* that created hybrid rootstock plants that are advantageously used today due to their growth and disease resistance [11,12], which will be discussed in more detail in the following sections.

The purpose of this review is to provide a description of the main varieties of chestnut cultivated in Portugal, their productive challenges and a description of the most recent accomplishments, as well as challenges underlying their improvement regarding biotic stresses.

2. Chestnut Varieties in Portugal

Portugal occupies the seventh position worldwide in chestnut production, with a production of 37,876 tons, as result of the expansion of chestnut grove planting areas [8]. Portuguese chestnuts have an enhanced quality recognized nationally and internationally. To protect the specificity of this product, and due to its economic and social importance, protected designations of origin (PDO) (EU Regulation no. 1151/2012, article 5) for Portuguese chestnuts were created. This agrarian policy of the European Union outlines territorial quality products as components of local development, whose primary objective is the improvement and preservation of the genetic heritage of the product, setting guidelines, parameters and rules to distinguish the production and market in the various regions [13,14]. Four PDO for chestnut were established: two of them in Trás-os-Montes ("Castanha da Padrela" and "Castanha da Terra Fria"), one in the region of Portalegre ("Castanha de Marvão-Portalegre") and another in Beira Alta ("Castanha dos Soutos da Lapa") [10]. A schematic representation of the 4 PDOs in Portugal is depicted in Figure 1, highlighting the municipalities included. Each PDO for chestnut production has its own history, predominant varieties and production area. The most popular and representative varieties in Portugal are "Boa ventura", "Judia", "Longal" and "Martaínha", but many more were identified and cultivated, namely "Amarelal", "Aveleira", "Bebim", "Benfeita", "Côta", "Lada", "Lamela", "Negral" and "Trigueira", among others [7,15].

In geographical terms, the main production areas are located in the most mountainous part of the North Centre "Soutos da Lapa" and Northeast region in Trás-os-Montes, which have optimal climatic characteristics to produce chestnuts [4]. Trás-os-Montes is the region

with the highest national production, and two PDOs can be found there [15]. The presence of the chestnut tree in Trás-os-Montes is millenary, having been one of the main sources of food in the region where the Padrela PDO is found [16]. The Judia is the principal variety of the "Castanha da Padrela PDO", but contributions from the "Lada", "Negral", "Côta", "Longal" and "Preta" varieties are also included [15]. The geographical production area (production, processing and packaging) is circumscribed to the municipality of Chaves, Murça, Valpaços and Vila Pouca de Aguiar [16]. The typical "Castanha da Padrela PDO" is very versatile and may be in peeled, frozen, candied or syrup form and have some special features, such as striped rind and a good peeling aptitude [16]. Similarly, to the previous PDO, the local rural community of the "Terra Fria PDO" has long depended on the chestnut trees that contribute significantly to the local economy and serve as a source of food [16]. The "Castanha da Terra Fria PDO" includes contribuitions of several varieties, such as the "Amarelal", "Aveleira", "Boa ventura", "Côta", "Judia", "Lamela", "Longal", "Martaínha", "Negral" and "Trigueira", among others. Its production is concentrated in the municipalities of Alfândega da Fé, Bragança, Chaves, Macedo de Cavaleiros, Mirandela, Valpaços and Vimioso e Vinhais [15,16].

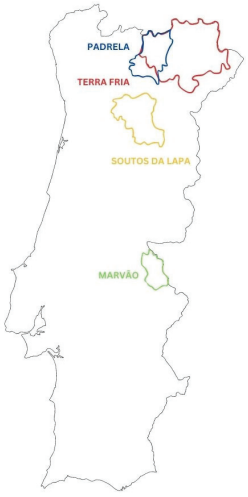

Figure 1. Chestnut protected designations of origin (PDO) in Portugal. In each PDO, the municipalities included in the PDO production area are depicted. Legend: PADRELA PDO (blue) (Murça, Vila Pouca de Aguiar, Chaves and Valpaços municipalities), TERRA FRIA PDO (red) (Alfândega da Fé, Bragança, Chaves, Macedo de Cavaleiros, Mirandela, Valpaços, Vimioso and Vinhais municipalities), SOUTOS DA LAPA PDO (yellow) (Lamego, Trancoso, Tarouca, Tabuaço, Armamar, Aguiar da Beira, S.João da Pesqueira, Moimenta da Beira, Sernancelhe and Penedono municipalities) and MARVÃO PDO (green) (Castelo de Vide, Marvão and Portalegre municipalities).

In the Beira Alta region, where the "Castanha de Soutos da Lapa PDO" is located, the chestnut tree stands out for its numerous applications in construction and handicraft, with the use of its wood and in the food sector, as well as for fruit consumption [16]. The geographical production area of this PDO is limited to the municipalities of Armamar, Aguiar da Beira, Lamego, Moimenta da Beira, Penedono, S. João da Pesqueira, Tabuaço, Tarouca, Trancoso and Sernancelhe [16]. The main varieties are the "Longal" and "Martaínha" [16].

The "Castanha de Marvão-Portalegre PDO", in the inner south of Portugal, includes the municipalities of Marvão, Castelo de Vide and Portalegre [16]. Similarly, the Alentejo chestnut orchards represent a considerable source of subsistence for the populations of this area, which have limited economic resources [16]. The color of the "Castanha de Marvão-Portalegre PDO" ranges from dark dull brown in the "Bárea" variety to lighter

brown in the "Clarinha" and "Enxerta" varieties and brilliant reddish-brown in the "Bravo" variety [16]. Additionally, the ability to peel varies from good to very good in the main varieties—"Clarinha", "Enxerta" and "Bravo"—and regular in the "Bárea" variety [16].

3. Ecophysiology and Fruit Characterization

3.1. Plant Growth Requirements

The chestnut (*C. sativa*) tree is a species of great interest due to its ability to be associated with different agricultural and forestry crops systems [5,17]. This species has great variability in morphological and ecological traits, wide biodiversity and the capacity to adapt to different ecosystems due to its high frugality, reproductive and vegetative growth habits, production (fruit size and wood characteristics), adaptability and resistance to biotic and abiotic stresses [5,17]. However, it is vital to understand the most advantageous environmental conditions to grow them to extract the full productive potential of this crop [5,17].

All chestnut varieties are heliophytic, needing sun exposure [18], with hypogeous germination—deciduous, megaphanerophyte and mesothermic—a characteristic that makes them quite suitable for establishment in mountainous areas and valleys [1]. It is considered a species also adapted to semi-arid to extremely humid climates, tolerating some aridity levels if they last no more than two months [19].

The chestnut tree prefers sub-Atlantic climates with temperatures below minus 15 °C, between 400 to 1000 m altitude, on slightly acidic soils [20]. However, it adapts to many regions with different climates [20]. The optimal conditions for the growth and production of the chestnut tree are found in the fresh, light and well-drained soils based on granitic gravel and siliceous sand or from the decomposition of gneisses, schists, volcanic soils, sandstone and alluvium with moderately high molybdenum rates with the pH below 6–6.5 [20]. It also requires at least 180 days of cold exposure and a growth temperature of −6 °C [1]. The root system adjusts, encouraging extensive horizontal root development rather than deep and strong roots, if penetration challenges occur [19].

3.2. Morphological Characterization

Numerous studies have shown that leaves can adapt, in terms of their morphological and photochemical characteristics, in changing environments. A relationship between temperature variations and changes in the anatomy, chemistry and morphology of chestnut varieties' leaves has been described [21]. The European chestnut tree has a long lifespan and displays a tremendous stature (it may grow to a height of 30–35 m) [22,23]. The deciduous leaves of the chestnut tree are characterized by their petiolate morphology, with a crenate-serrated or serrated marginal cut and an oblong-lanceolate limb [22,23]. On the extension of the secondary veins, they also have spatulate-aristate teeth that range in size from 5 to 8 cm in width and 10 to 25 cm in length and are subcordate to subtruncate at the base of the lamina [22,23]. This plant is monoicous, meaning that it has separate male and female flowers on the same plant [24]. The staminate flowers are arranged in glomerules of 5–6 flowers with yellow anthesis, from which emerge 10–20 stamens with yellow-greenish ovoid anthers [1]. The male flowers, usually gathered in catkins, either erect or subpendent, may be about 1 cm in diameter and 15–30 cm long and are inserted near the base of their leaves or in the terminal part of the year's branches [1]. In contrast, the androgynous female flowers are protected by a protective coriaceous envelope of green spinescent bracts with 2–3 flowers, which will give rise to the cupule [25]. A single viable seed-containing ovule (monospermic) or many fertile ovules (polyspermic) from each female flower are used to create fruit [25]. The pollen is viscous, and pollination can be anemophilous or entomophilous [25]. The *C. sativa* species has a single reddish-brown dry pseudo-fruit usually consisting of three ovoid to subglobose achenes with a small and irregular insertion scar at the base [1,12,25]. Aside from the embryo, each seed contains two cotyledons, the part of the fruit that is edible [25]. The following table represents the morphological characterization of the principal chestnut varieties (Table 1).

Table 1. Morphological characterization of the principal Portuguese chestnut varieties. Information in this table has been retrieved from [14].

Name	Port	Cup	Leaves	Catkins	Blooming	Fruit	Maturation
"Aveleira"	Open	Spherical-oval	Petiolate, mucronate, obtuse base, oblong-lanceolate, acute on some leaves, slightly asymmetric and slightly concave, light green on the abaxial surface and glabrous on the adaxial surface	Unisex male astaminates inserted very close to each other, in the axilla of the leaves, and androgynics at the base of the catkin	Early, 2nd week of June	Medium fruit, ovoid to broad ovoid, shiny strong brown, red tint with well-spaced dark streaks. Apex with sericeous star-shaped pubescence. Ventral surface predominantly planoconcave and convex dorsal surface, almost semispherical	Early, fall between the 2nd and 3rd decade of September
"Martaínha"	Semi-erect to open, branch insertion angles of branches 45° to 60°	Round-oval	Petiolate, base predominantly obtuse, oblong-lanceolate, toothed, straight to slightly concave and slightly asymmetric, glabrous only on the adaxial surface, light green on the abaxial surface, shiny medium green on the adaxial surface	Unisex male brachyaminates, inserted in the leaf axil of the shoots and androgynics	Early, 2nd week of June	Medium to large fruit, ovoid, brown, satiny luster, with dark bordeaux dissipated longitudinal stripes. Triangular pubescence sericeous at the apex on the dorsal side. Flat concave on the ventral surface and predominantly convex on the dorsal surface	Early, fall in the 3rd decade of September
"Longal"	Erect to semi-erect, branch insertion angles of branches $\leq$ 45°	Pyramidal	Petiolate, obtuse base oblong-lanceolate, dentate, slightly asymmetric and straight to slightly concave, glabrous only on the adaxial surface, light green on the abaxial surface and shiny light green on the adaxial surface	Unisex male mesostaminates, inserted in the leaf axil and androgynics	Average, 4th week of June	Medium to large fruit, ovoid, shiny light brown, reddish tint, with well-defined longitudinal stripes, forming slightly prominent, slightly protruding edges on the integument. Small, silky white pubescence at the apex, involving the stipes up to the stigmas. Planoconvex on the ventral surface and convex on the dorsal surface	Late, fall in the 2nd decade of October.
"Judia"	Erect to semi-erect, big insertion angles, small branches < 45° to more open angles (about 70°)	Spherical-pyramidal	Petiolate, obtuse base, oblong-lanceolate, toothed, slightly asymmetric and slightly concave, glabrous on the adaxial surface, shiny and more faded green on the abaxial surface and medium green on the adaxial surface	Unisex male astaminated with fillets and anthers not visible on the outside of the flower and androgynics	Average, 3rd week of June	Medium fruit, large ovoid, intense brightness brick-brown, lighter and dark brown tint. Apex with reduced sericeous pubescence. Ventral surface concave-plane to slightly convex in some fruits and convex on the dorsal surface	Average, fall in the 2nd decade of October

Table 1. *Cont.*

Name	Port	Cup	Leaves	Catkins	Blooming	Fruit	Maturation
"Côta"	Semi-erect	Pyramidal	Mucronate, lamina obtuse base, very concave, slightly asymmetrical cross-section leaf, whitish on the abaxial surface and medium green on the adaxial surface	Unisex male brachyaminates	Male flowering (1st week of July) and female flowering (2nd week of July)	Small fruit, large ovoid, dark brown	Average, fall between the 1st and 2nd decades of October
"Negral"	Erect	Rounded conic	Petiolate, cordiform limb base, oblong-lanceolate, asymmetrical leave, toothed, slightly asymmetrical cross-section, whitish abaxial surface and dark green adaxial surface	Unisex male brachyaminates	Male flowering (1st week of July) and female flowering (3rd week of July)	Large fruit, globular, dark brown	Average, fall in the 2nd decade of October
"Amarelal"	Semi-erect to open, branch insertion angles of branches 45° to 60°	Pyramidal	Petiolate, obtuse base, oblong-lanceolate, mucronate, slightly asymmetric, slightly concave in cross section. Glabrous light green on the abaxial surface and bright green on the adaxial surface	Unisex male mesostaminates, inserted in the axillae of the leaves and androgynics	Average, occurring in the 2nd/3rd weeks of June	Large to medium fruit, globular, light brown with clearly visible dark and shiny longitudinal well, occasionally with a slight concavity. Silky white pubescence on the apex. Almost flat ventral surface and convex on the dorsal surface	Early, occurring in the last week of September/1st week of October
"Lamela"	Open, the insertion angles of most of the lower branches > 45°	Rounded	Petiolate, limb with acute base, oblong-lanceolate, toothed, symmetrical, lighter green color on the abaxial surface and glabrous medium green on the adaxial surface	Unisex male brachyaminates to mesostaminates inserted in the leaf axils and androgynics	Average	Large, globular, light brown color, dull, near the hilum shows a dark brown color. Apex with reduced sericeous pubescence. Large hilum. Flat concave on ventral side	Average, fall in the 2nd decade of October

3.3. Fruit Nutritional Characterization

Many works characterize the nutritional qualities and technological aptitude of each chestnut variety. Chestnut is a gluten free fruit, mostly composed of complex carbs, but it also contains a considerable number of proteins (with high biological value) and fibers, which help to control insulin response and cholesterol levels [26]. Compared to other nuts and dried fruits, it is a fruit with a low-fat content [26,27] and an excellent source of vitamins, namely B6, vitamin C and folic acid [28]. It also has a relevant quantity of minerals such as calcium, copper, iron, manganese, magnesium, potassium, phosphorus, selenium and zinc [29]. Indeed, the phenolic compounds it contains further contribute to its nutritional importance [30]. Given its nutritional value and beneficial effects on health, it is a fruit that can be chosen as part of a balanced diet throughout the year. In addition, it can be used in both meat meals and sweets [13,31].

3.4. Commercialization and Uses

In Portugal, chestnut trees have a dual purpose, being planted and cultivated for their fruit as well as for their high-quality wood, which makes them a relevant income source for rural communities' economies [13]. The selection of the best varieties and the best trees was made through successive generations, choosing those that produced the best nuts and those that gave the best wood. The wood has a good density and is quite appreciated for furniture, cooperage and basketry [13]. Currently, the chestnut's main markets in Portugal are its commercialization in fresh form for traditional (street roasters) and domestic consumption (boiled, raw or roasted), as well as exportation to the international market in either fresh or frozen form, which has been increasing, particularly to Canada, France, Italy, Spain, Switzerland and the United States [13,32,33]. According to Portuguese data available in [32,33], for July 2022, the trade balance was positive (14,299€ (2010) vs. 20,461€ (2021)), with average export prices higher (24,461€) than import prices (3934€).

4. The *Castanea* Genetic Resources, Genetic Diversity and Biotechnology Based Approaches for Improvement

The foundation of agricultural progress is represented by plant genetic resources, which also serve as a genetic adaption reserve that serves as a biodiversity repository for defense against environmental changes [34,35]. Due to environmental disruptions, intense parasite infestations and cultivation in recent decades, the genetic variability of the chestnut tree has been significantly diminished in both natural populations and cultivated stands [34,35]. When handled properly, the plant genetic resources supply the raw material that results in new and improved varieties and are an unreplaceable source of features including greater yields, environmental adaptation and pest and disease resistance [34,35]. A huge number of genetic resources [36] has been developed for the American chestnut (*Castanea dentata* L.) and the Chinese chestnut (*Castanea mollissima*) throughout several research projects in the scope of the American Chestnut Foundation [37]. Importantly, the genome sequence for these two species is already available at Phytozome [38]. These resources were a relevant basis for comparative genetic and genomic studies in *C. sativa*, supporting the development of marker-assisted breeding programs for this species [38].

In situ and ex situ gene bank repositories play a major role in the conservation of genetic resources. Some studies about the *Castanea* species highlight the value of cryopreservation as an approach to conserve genetic resources [39,40]. Throughout cryopreservation, several plant materials/explants, such as recalcitrant seeds, somatic embryos, cell lines, genetically transformed material and vegetatively propagated species, could be safely and long-term conserved [39]. These repositories include the collection and cataloguing of germplasm information, identification, application, description of accessions, molecular research and preservation as part of the backing-up strategy for germplasm [40]. According to Costa [41], Columbano Taveira Fernandes, a member of Vieira Natividade's team, pioneered the controlled hybridization of chestnut trees in Portugal in the 1950s at Alcobaça. Consequently, a collection of clones that Columbano Fernandes identified has been hand-

picked and was made available at the Polytechnic Institute of Bragança's Escola Superior Agrária (ESA-IPB). Both Centro Nacional de Sementes Florestais (CENASEF, Amarante) and the University of Trás-os-Montes and Alto Douro (UTAD, Vila Real) received the same collection as a gift from IPB [41]. A collection of clones of the "Aveleira", "Bária", "Colarinha", "Côta", "Judia", "Lada", "Longal", "Martaínha", "Negral" and "Verdeal" varieties are maintained at the Agricultural Colony by Martim Rei. Clones of the "Martaínha", "Longal", "Judia" and "Verdeal" varieties and the hybrid "Marigoule" are maintained at the Agricultural Station of Viseu, while "Amarelal", "Martaínha" and "Longal" varieties are maintained at the "Quinta de Sergude" [14].

4.1. Intra- and Inter-Varietal Variability

The genetic variability of the regional chestnut varieties differs greatly, with certain varieties being more stable than others [14]. The results of a preliminary study using single sequence repeats (SSR) has been successfully used for typing Portuguese traditional chestnut varieties [42]. These results evidenced a low genetic variability among the varieties, explained to some extent by reduced variability for fruit orchard populations compared to the populations explored for wood or mixed purposes [42]. Despite being mainly propagated by grafting, Portuguese chestnut varieties are polyclonal, which means that a single variety might have many genotypes, indicating the existence of multiple clones of the same variety, possibly due to mutations and cross-pollination between varieties [14]. According to the literature, there are varieties with highly repeated genotypes that may thus be regarded as the primary clone from which additional clones within the same variety have been descended or even having given rise to other varieties through seed [14]. The genetic variability and stability of the varieties are directly related to the common practice of exchanging plant material for grafting [14]. This practice is regularly used in the Northern regions for production purposes [14].

Intra- and inter-varietal diversity studies have been conducted in Portuguese chestnut populations. Dinis et al. [43] used SSR markers to assess the heterogeneity of the genotype of the cultivar "Judia" in Trás-os-Montes, and they describe some intra-varietal differences within the studied accessions. In another approach, seven different types of isoenzyme markers were utilized by Pereira and colleagues [44], allowing for the differentiation of 32 genotype classes in Portuguese varieties. Each class has a matching cultivar or varieties, which have various names (synonymy) and may be genetically extremely similar or genetically different and have the same name but belong to separate classes (homonymy) [44].

According to [42] and [44]'s molecular characterization investigations of Portuguese chestnut varieties, a heteronymy between the varieties "Martaínha" and "Verdeal" can exists, which is supported by the 82% similarity value observed between the two varieties. The varieties "Longal" and "Martaínha" are also mentioned in these articles as being genotypically unstable, meaning that they exhibit high intra-varietal variability. The sets of varieties that emphasize this quality can only be alternative names for the same genotype:

"Cancela" (Lamego) and "Negral" (Valpaços); "Cota" (Murça) and "Negral" (Moimenta da Beira); "Cota" (Valpaços) and "Demanda" (Tarouca); "Lamela" (Vinhais) and "Pelada" (Moimenta da Beira); "Pelada" (Boticas) and "Redonda" (Montalegre); "Riscal" and "Verdeal" (from Armamar).

4.2. Portuguese Breeding Programs and Candidate Gene Identification

Chestnut breeding in Portugal has been focused on the improvement of varieties and rootstocks through selection and hybridization with Asian species resistant to ink disease. Interspecific crosses between the European chestnut and the Asian species of *C. crenata* and *C. mollissima* have been the foundation of the Portuguese chestnut breeding programs [45]. The first interspecific crosses in Portugal were made in 1948 by Bernardino Gomes using *C. crenata* (Tamba variety) as the pollen donor [46–48]. At the University Trás-os-Montes e Alto Douro, in the 1990s, Professor Lopes Gomes launched a breeding program that resulted in the development of 53 genotypes resistant to ink disease [49,50].

One of the most well-documented outcomes of this breeding program was the selection of the COLUTAD (COLumbano + UTAD), a hybrid between *Castanea sativa* × *Castanea crenata* found resistant to *PC* and broadly used as rootstock [49].

Another breeding program was started more recently by Costa et al. [50], focused on development of *C. sativa* × *C. crenata* and *C. sativa* × *C. mollissima* hybrids. Four F1 hybrids were chosen for extensive propagation according to their potential to proliferate and root in vitro, ink disease resistance levels and field development [51–53]. The selection process began with the identification of genotypes, in vitro establishment, large-scale propagation and characterization of molecular basis behind susceptible and resistant genotypes [45,54]. The elucidation of the genetic basis and molecular mechanism of *P. cinnamomi* resistance is a need for the implementation of marker-assisted selection in the breeding programs for resistance, since they will allow the selection of molecular markers and candidate genes to support breeding purposes. Costa et al. [50] performed a DNA marker:trait association analysis to identify quantitative trait loci (QTLs) related to ink disease and also to identify putative resistance genes to *P. cinnamomi* using a transcriptomic approach. Since the genome of *C. sativa* is still not available, the authors took advantage of the genetic resources developed and genome sequence available for *C. molissima.* The genetic linkage map and QTLs developed in an interspecific cross between *C. sativa* and *C. crenata* by Santos et al. [51] constituted the first effort to map genomic regions (QTLs) associated with *P. cinnamomi* resistance. Serrazina et al. [55] compared the root transcriptome of the susceptible species *C. sativa* and the resistant species *C. crenata* after *P. cinnamomi* inoculation in an approach to elucidate chestnut defense mechanisms. These results evidenced that the *C. crenata* response triggered more relevant changes in expressed genes related with biotic stress upon pathogen inoculation than the same situation in *C. sativa*, suggesting that despite both species recognizing the pathogen attack, the resistant species (*C. crenata*) may involve more genes in the defense response than the susceptible species (*C. sativa*) [55].

Two distinct strategies, genetic mapping and transcriptomics, were combined to better understand the molecular and genetic pathways and to find molecular markers that enable the early selection of resistant genotypes from the ongoing breeding program. Indeed, the genetic linkage maps created allowed the identification of regions of the genome associated with resistance (Table 2) [45].

Table 2. Summary of efforts to control *Cryphonectria parasitica* (*CP*) and *Phytophthora cinnamomi* (*PC*) using mapping and identification of Quantitative Trait Loci (QTL) in *Castanea*.

Plant Material	Approach for Improvement	Resources	Description	References
C. molissima × *C. dentata* F2 hybrids	Disease resistance (chestnut blight)	Study genetic architecture of *CP* resistance; future MAS	3 QTLs: *Cbr1* (LG B), *Cbr2* (LG F), *Cbr3* (LG G)	[56]
BC1, BC4 *C. dentata* × *C. dentata molíssima* " Nanking" and "Mahogany"	Disease resistance (chestnut blight and ink disease)	Study genetic architecture of *CP* and *PC* resistance; future MAS	1 QTL: LG E	[57]
BC1F1 *BC3F1* *C. dentata* × *C. dentata molíssima* " Nanking" and "Mahogany"	Disease resistance (chestnut blight and ink disease)	Study genetic architecture of *CP* and *PC* resistance; future MAS	22 QTLs: hb52208, hb39959 (LG A), nk12394 (LG C), h25723, h54539, hb54410, jb79599, jb32342, jb13258, nk29352, nk35044, nk19473 (LG E), h31744, hb7824, hb27106 (LG K)	[58]

Table 2. *Cont.*

Plant Material	Approach for Improvement	Resources	Description	References
C. sativa × *C. crenata* F1 hybrids	Disease resistance (ink disease)	Study genetic architecture of *PC* resistance; future MAS	17 QTLs: CC_3129_774, CmSNP00773E, CC_48142_849_ CmSNP00522E, AC_32934_470, AC_36335_960 (LG E), CC_46475_1222, CC_6279_2669, AC_14650_453 (LG K)	[59]

Legend: *CP* (*Cryphonectria parasitica*); MAS (marker-assisted selection); *PC* (*Phytophthora cinnamomi)*; QTL (quantitative trait loci); LG (linkage groups)

4.3. The Potential of Genetic Transformation and Genome Editing as a Tool for Pathogen Control

Genetic transformation and breeding have been combined by researchers due to their ability to speed up restoration when compared to standard backcross breeding. Chestnut genetic transformation systems have made tremendous advances, and, today, it is possible to evaluate genes for their capacity to confer pathogen resistance. In the 1990s, Carraway et al. [60] carried out the first attempt on *Castanea* spp. genetic transformation through embryogenic regeneration systems using microprojectile bombardment; however, they only obtained transgenic *calli*. Later, Seabra and Pais [61] successfully transformed and regenerated *C. sativa* shoots expressing the *uidA* gene encoding for the β-*GLUCURONIDASE* by *Agrobacterium*-mediated transformation and regeneration. Nevertheless, and despite many woody crops, the regeneration of transformed plants and their ex vitro acclimation remains a challenge to be addressed.

Since then, chestnut researchers have been dedicated to improving genetic *Agrobacterium*-mediated transformation of this recalcitrant species. The method involves co-culturing somatic embryos with liquid *Agrobacterium* suspension, while still in semi-solid multiplication media, and micropropagation of the plants. Several works were published on the *Agrobacterium*-mediated transformation in *C. sativa* with pathogen resistance genes as genes of interest, either as an attempt to validate gene function or modulate their resistance levels. Nowadays, cisgenes are the focus of increased investigation [2]. Corredoira et al. [62,63] obtained cisgene overexpressing lines with a thaumatin-like protein (*CsTL1*) gene and an *endochitinase* gene (*CsCH3*) (Table 3).

Table 3. Genetic transformation studies performed in European and American chestnuts with the goal of developing pathogen control strategies.

Explant	Gene of Interest	Gene Function	Target Pathogen	References
C. sativa somatic embryos	*CsTL1*	Thaumatin-like protein; promotes osmotic rupture in the pathogen	*Phytophthora cinnamomi*	[62]
C. sativa somatic embryos	*CsCH3*	Chitinase-like protein; hydrolyses chitin from pathogen's cell wall	*Cryphonectria parasitica*	[63]
C. dentata somatic embryos	*OxO*	Detoxifying enzyme; degrades oxalic acid	*Cryphonectria parasitica*	[64–67]
C. dentata somatic embryos	*Cast_Gnk2-like*	Antifungal	*Phytophthora cinnamomi*	[67]

Legend: *CsTL1* (CYSTATIN-LIKE 1 gene); *CsCH3* (ENDOCHITINASE gene); *OxO* (OXALATE OXIDASE gene); *Cast_Gnk2-like* (GINKBILOBIN-2 HOMOLOGOUS DOMAIN gene).

The functional characterization of genes involved in plant–pathogen interaction now has new directions thanks to genome editing [68]. Two S-genes, *POWDERY MILDEW*

RESISTANCE 4 (*pmr4*) and *DOWNY MILDEW RESISTANCE* 6 (*dmr6*), which are likely candidates for functional validation via *CRISPR/Cas9* knockdown, were identified and chosen by the same research team in *C. sativa* after *PC* and *CP* infection [69]. The potentialities of the genome editing tools and the research on S-genes may enable us to determine if *PC* has been adapted to the vulnerable chestnuts, possibly inducing effector-triggered susceptibility, and how it is interfering with their immunity [69].

5. Conclusions

Chestnuts are under threat from several biotic pressures, yet numerous initiatives are being developed to overcome the obstacles and conserve this valuable species. In the context of climate change, the prevalence of *Phytophthora cinnamomi* and *Cryphonectria parasitica* infections might increase due to the potential emergence of new strains. Several breeding programs have been implemented to improve chestnut resistance, particularly to ink disease. The next phase of chestnut breeding may involve strengthening resistance to both pathogens and searching for long-lasting resistance. Exploring the pathogen's virulence/avirulence variables specific to chestnut interactions may be beneficial for the future *Castanea*–pathogen study plan. The resistant genotypes, as a result of the successful approach to develop *C. sativa* × *C. crenata* and *C. sativa* × *C. mollissima*, are being mass-propagated using micropropagation and tested in the field conditions under various edaphoclimatic conditions, as well as for graft compatibility with Portuguese varieties for fruit production. Still, to overcome the lack of improved germplasm for plantation in Portugal and Europe, several biotechnology-based or conventional breeding approaches are being tested. Understanding the genetic basis of disease resistance, as well as the identification of candidate genes, will support the development of new tools and genotypes capable of coping with the threating scenarios. The use of modern techniques such as *CRISPR/Cas* systems in trees is opening up new avenues for the functional investigation and characterization of genes. Applying these technical advancements, along with biotic stressors, will enhance our capacity to respond to chestnut challenges and are expected to bring innovation and competitiveness to the productive chestnut sector.

Author Contributions: Conceptualization, J.N.; writing—original draft preparation, M.B.; writing—review and editing, M.B., S.d.S.A., H.S., R.P. and J.N.; supervision, S.d.S.A., H.S., R.P. and J.N.; funding acquisition, J.N. All authors have read and agreed to the published version of the manuscript.

Funding: This research was funded by the I-CERES project, NORTE-01-0145- FEDER-000082—Norte Portugal Regional Operational Program (NORTE2020), under the PORTUGAL 2020 Partnership Agreement, through the European Regional Development Fund (ERDF); RHAQ NORTE, NORTE-06-3559-FSE-000103—Norte Portugal Regional Operational Program (NORTE2020), under the PORTUGAL 2020 Partnership Agreement, through the European Social Fund (ESF) and RHAQ CENTRO, CENTRO-04-3559-FSE-000146—Centro Portugal Regional Operational Program (CENTRO2020), under the PORTUGAL 2020 Partnership Agreement, through the European Social Fund (ESF); the Centre Bio R&D Unit (UIDB/05083/2020) funded by Fundação para a Ciência e Tecnologia and the Interface Mission RE-C05-i02, under the Portuguese Recovery and Resilience Plan, through the European Union NextGenerationEU Fund.

Institutional Review Board Statement: Not applicable.

Data Availability Statement: Data sharing is not applicable to this article.

Acknowledgments: The authors would like to thank Marta Bobiano (BLC3) for her support during the constructive discussion made on the topic.

Conflicts of Interest: The authors declare no conflict of interest.

References

1. Gomes-Laranjo, J.; Cardoso-Ferreira, J.; Portela, E.; Abreu, G.C. Castanheiros. 2007. Available online: https://www.cm-sabugal.pt/wp-content/uploads/Castanheiros-livro.pdf (accessed on 29 May 2023).

2. Fernandes, P.; Colavolpe, M.B.; Serrazina, S.; Costa, R.L. European and American Chestnuts: An Overview of the Main Threats and Control Efforts. *Front. Plant Sci.* **2022**, *13*, 1–26. [CrossRef] [PubMed]
3. Lage, J. *Castanea: Uma Dádiva Dos Deuses*, 2nd ed.; Oficina São José: Braga, Portugal, 2006; pp. 1–325.
4. Moura, A.R.; Gomes-Laranjo, J.C.; Cardoso, J.V. Seleção Clonal Na Variedade de Castanha "Longal" Visando a Sua Aptidão Agronómica e Agroalimentar. Master's Thesis, University of Trás-os-Montes and Alto Douro, Vila Real, Portugal, 2018.
5. Mellano, M.G.; Beccaro, G.L.; Donno, D.; Marinoni, D.T.; Boccacci, P.; Canterino, S.; Cerutti, A.K.; Bounous, G. Castanea Spp. Biodiversity Conservation: Collection and Characterization of the Genetic Diversity of an Endangered Species. *Genet. Resour. Crop. Evol.* **2012**, *59*, 1727–1741. [CrossRef]
6. Bounous, G. The Chestnut: A Multipurpose Resource for New Millenium. *Acta Hortic.* **2005**, *693*, 33–40. [CrossRef]
7. Gomes-Laranjo, J.; Peixoto, F.; Costa, R.; Ferreira-Cardoso, J. Portugal, Following Chestnut Footprints, Cultivation and Culture, Folklore and History, Traditions and Uses. *Scr. Hortic.* **2009**, *9*, 106–111.
8. Food and Agriculture Organization of the United Nations. Available online: https://www.fao.org/faostat/en/#home (accessed on 29 May 2023).
9. Serdar, U.; Saito, T.; Cuenca, B.; Akyüz, B.; Laranjo, J.G.; Beccaro, G.; Bounous, G.; Costa, R.L.; Fernandes, P.; Mellano, M.G. Advances in cultivation of Chestnuts. In *Achieving Sustainable Cultivation of Tree Nuts*, 1st ed.; Serdar, U., Fulbright, D., Eds.; Burleigh Dodds Science Publishing: Cambridge, UK, 2019; Volume 1, pp. 349–388. [CrossRef]
10. Instituto Nacional de Investigação Agrária e Veterinária (INIAV). Novos Porta-Enxertos de Castanheiro Com Resistência à Doença Da Tinta. 2018, pp. 1–36. Available online: https://projects.iniav.pt/NewCastRootstocks/images/Manual_INIAV_web.pdf (accessed on 29 May 2023).
11. Freitas G.M.; Igrejas, G.; Santos, H. Caracterização de Cultivares Portuguesas de *Castanea Sativa* Mill: Uma Análise Proteómica. Master's Thesis, University of Trás-os-Montes and Alto Douro, Vila Real, Portugal, 2017.
12. Brito, D.; Gomes-Laranjo, J.; Álvaro, R.C. Produção de Novos Porta-Enxertos Híbridos Para Castanheiro. Caracterização Ecofisiológica Da Geração F1. Master's Thesis, University of Trás-os-Montes and Alto Douro, Vila Real, Portugal, 2014.
13. Silva, A.P. Castanha. Um Fruto Saudável. In *Projeto Agro 939, Dinamização do Consumo da Castanha Com Denominação de Origem*, 1st ed.; Mingo Gráfica: Braga, Portugal, 2007; Volume 1, pp. 1–178.
14. Costa, R.; Ribeiro, C.; Valdiviesso, T.; Afonso, S.; Borges, O.; Soeiro de Carvalho, J.; Costa, H.A.; Assunção, A.; Fonseca, L.; Augusta, C.; et al. *Variedades Portuguesas de Castanha das Regiões Centro e Norte de Portugal*, 1st ed.; Instituto Nacional dos Recursos Biológicos, I.P. (INRB, I.P.): Oeiras, Portugal, 2008; pp. 1–78.
15. Europeia, C. *Jornal Oficial Das Comunidades Europeias*; European Union: Maastricht, The Netherlands, 1996.
16. Direção-Geral de Agricultura e Desenvolvimento Rural. Produtos Tradicionais Portugueses. 2018. Available online: https://tradicional.dgadr.gov.pt/pt/ (accessed on 29 May 2023).
17. Queijeiro, J.M.; Diaz-Raviña, M.; de la Montaña, J. Edaphic Characterization of Chestnut Tree Orchards in Monterrei (Southeast Galicia, Spain). *Ecol. Mediterr.* **2000**, *26*, 163–167. [CrossRef]
18. Rojo, D.; Santín, J.; Sánchez, J.A. *Guía de Buenas Prácticas Para La Conservación y Custodia Del Território Del Castãno*; Imprenta Manolete: Asturias, Spain, 2016; pp. 1–37.
19. Suarez, P.C. Fitopatologia Del Castaño (*Castanea Sativa* Miller). In *Boletin de Sanidad Vegetal*; Secretaría General Técnica Ministerio de Agricultura, Pesca y Alimentación: Madrid, Spain, 1989; Volume 3, pp. 1–130.
20. Gonçalves, J.C. Influência de Alguns Factores Na Micropropagação Do Castanheiro (*Castanea* Miller). Ph.D. Thesis, Higher Institute of Agronomy, Lisbon, Portugal, 1991.
21. Dinis, L.; Peixoto, F.; Pinto, T.; Costa, R.; Bennett, R.N.; Gomes-Laranjo, J. Study of Morphological and Phenological Diversity in Chestnut Trees ("Judia" Variety) as a Function of Temperature Sum. *Environ. Exp. Bot.* **2011**, *70*, 110–120. [CrossRef]
22. Bradford, M.; Bradford, M.M. A Rapid and Sensitive Method for the Quantitation of Microgram Quantities of Protein Utilizing the Principle of Protein-Dye Binding. *Anal. Biochem.* **1976**, *72*, 248–254. [CrossRef]
23. Irigoyen, J.J.; Einerich, D.W.; Sánchez-Díaz, M. Water stress induced changes in concentrations of proline and total soluble sugars in nodulated alfalfa (*Medicago sativa*) plants. *Physiol. Plant.* **1992**, *84*, 55–60. [CrossRef]
24. Valdiviesso, T.; Mederia, C.; Pinto de Abreu, C. Contribution for The Study of the Chestnut Floral Biology. In Proceedings of the International Congress on Chestnut, Spoleto, Italy, 20–23 October 1993; pp. 95–97.
25. Giordano, E. *Biology, Physiology and Ecology of Chestnut, Comunità Montana Monti Martani e Serano of Spoleto and Istituto di Coltivazioni Arboree*; University of Perugia: Perugia, Italy, 1993.
26. De Vasconcelos, M.C.; Bennett, R.N.; Rosa, E.A.; Ferreira-Cardoso, J.V. Composition of European Chestnut (*Castanea Sativa* Mill.) and Association with Health Effects: Fresh and Processed Products. *J. Sci. Food Agric.* **2010**, *90*, 1578–1589. [CrossRef]
27. Sales, R.L.; Costa, N.M.B.; Monteiro, J.B.R.; Peluzio, M.D.C.G.; Coelho, S.B.; de Oliveira, C.G.; Mattes, R. Efeitos Dos Óleos de Amendoim, Açafrão e Oliva Na Composição Corporal, Metabolismo Energético, Perfil Lipídico e Ingestão Alimentar de Indivíduos Eutróficos Normolipidêmicos. *Rev. Nutr.* **2005**, *18*, 499–511. [CrossRef]
28. Manela-Azulay, M.; Mandarim-De-Lacerda, C.A.; da Perez, M.A.; Filgueira, A.L.; Cuzzi, T. Vitamina C. *An. Bras. Dermatol.* **2003**, *78*, 265–272. [CrossRef]
29. Borges, O.; Gonçalves, B.; de Carvalho, J.L.S.; Correia, P.; Silva, A.P. Nutritional Quality of Chestnut (*Castanea Sativa* Mill.) Cultivars from Portugal. *Food Chem.* **2008**, *106*, 976–984. [CrossRef]

30. Dinis, L.R.; Gomes-Laranjo, J.; Peixoto, F.; Costa, R. Castanheiros: Seleção Clonal Na Variedade Judia. Ph.D Thesis, University of Trás-os-Montes and Alto Douro, Vila Real, Portugal, 2011.
31. Montanhas de Investigação. A Castanha Da Terra Fria DOP Inclui 10 Variedades Do Castanheiro (Castanea Sativa Mill)? Available online: https://morecolab.pt/2020/06/15/castanha-da-terra-fria-10-variedades-do-castanheiro/ (accessed on 29 May 2023).
32. Gabinete de Planeamento, Políticas e Administração Geral. Available online: https://www.gpp.pt/ (accessed on 29 May 2023).
33. Instituto Nacional de Estatística. Available online: https://www.ine.pt/xportal/xmain?xpgid=ine_main&xpid=INE (accessed on 29 May 2023).
34. Esquinas-Alcázar, J.T. Plant Breeding. In *Plant Breeding: Principles and Prospects*; Hayward, M.D., Bosemark, N.O., Romagosa, I., Cerezo, M., Eds.; Springer: Dordrecht, The Netherlands, 1993; pp. 33–51. [CrossRef]
35. Carvalho, C. Detecção de Cromatina de Centeio e Análise Da Biodiversidade N landrace de Trigo "Barbela", Através de Marcadores Genéticos. Ph.D Thesis, University of Trás-os-Montes and Alto Douro, Vila Real, Portugal, 2003.
36. Kremer, A.; Abbott, A.G.; Carlson, J.E.; Manos, P.S.; Plomion, C.; Sisco, P.; Staton, M.E.; Ueno, S.; Vendramin, G.G. Genomics of Fagaceae. *Tree Genet. Genomes* **2012**, *8*, 583–610. [CrossRef]
37. American Chestnut Foundation. Available online: https://acf.org/ (accessed on 29 May 2023).
38. Goodstein, D.M.; Shu, S.; Howson, R.; Neupane, R.; Hayes, R.D.; Fazo, J.; Mitros, T.; Dirks, W.; Hellsten, U.; Putnam, N.; et al. Phytozome: A comparative platform for green plant genomics. *Nucleic Acids Res.* **2012**, *40*, D1178–D1186. [CrossRef]
39. Vidal, N.; Vieitez, A.M.; Fernández, M.R.; Cuenca, B.; Ballester, A. Establishment of Cryopreserved Gene Banks of European Chestnut and Cork Oak. *Eur. J. For. Res.* **2010**, *129*, 635–643. [CrossRef]
40. Guo-Tian, L.; Cheng-Xiang, A.; Li-Si, Z.; Hai-Rong, W.; Qing-Zhong, L. Chestnut Genebank In China National Clonal Plant Germplasm Repository. *Acta Hortic.* **2009**, 199–206. [CrossRef]
41. Costa, R. Variedades e porta-enxertos. *Man. Boas Práticas Frutic.* **2020**, *6*, 4. Available online: https://www.iniav.pt/images/publicacoes/livros-manuais/manual_de_fruticultura_castanheiro.pdf (accessed on 29 May 2023).
42. Costa, R.; Valdiviesso, T.; Marum, L.; Fonseca, L.; Borges, O.; Soeiro, J.; Soares, F.M.; Sequeira, J.; Assunção, A.; Correia, P. Characterisation of Traditional Portuguese Chestnut Cultivars by Nuclear SSRS. *Acta Hortic.* **2005**, 437–440. [CrossRef]
43. Dinis, L.-T.; Peixoto, F.; Costa, R.; Gomes-Laranjo, J. Molecular Characterization Of "Judia" (*Castanea Sativa* Mill.) From Several Trás-Os-Montes Regions By Nuclear Microsatellite Markers. *Acta Hortic.* **2010**, 225–232. [CrossRef]
44. Pereira, M.; Castro, L.; Torres-Pereira, J.; Lorenzo, S. Isozyme Polymorphisms in Portuguese Chestnut Cultivars. *Acta Hortic.* **1999**, 283–286. [CrossRef]
45. Santos, C.; Machado, H.; Serrazina, S.; Gomes, F.; Gomes-Laranjo, J.; Correia, I.; Zhebentyayeva, T.; Duarte, S.; Bragança, H.; Fevereiro, P. Comprehension of Resistance to Diseases in Chestnut. *Rev. Ciências Agrárias* **2016**, *39*, 189–193. [CrossRef]
46. Natividade, J.V. *Quatro Anos Na Defesa Da Campanha e Reconstituição Dos Soutos*; Boletim Junta Nacional das Frutas: Lisbon, Portugal, 1947; pp. 1–21.
47. Gomes Guerreiro, M. Alguns Estudos Do Género *Castanea*. Relatório. Tomos I e II. In *Alcobaça: Publicação da Direcção Geral dos Serviços Florestais e Aquícolas*; Topografia Alcobacence lda: Alcobaça, Portugal, 1948; Volume XV.
48. Gomes Guerreiro, M. Castanheiros Alguns Estudos Sobre a Sua Ecologia e o Seu Melhoramento Genético. Master's Thesis, Higher Institute of Agronomy, Lisbon, Portugal, 1957.
49. Martins, L.; Anjos, R.; Costa, R.; Gomes-Laranjo, J. Colutad. Um Clone de Castanheiro Resistente à Doença Da Tinta. In *Castanheiros. Técnicas e Práticas*; Gomes-Laranjo, J., Peixoto, F., Ferreira-Cardoso, J., Eds.; Indústria Criativa and University of Trás-os-Montes and Alto Douro: Vila Real, Portugal, 2009; pp. 135–142.
50. Costa, R.; Santos, C.; Tavares, F.; Machado, H.; Gomes-Laranjo, J.; Kubisiak, T.; Nelson, C.D. Mapping and Transcriptomic Approches Implemented for Understanding Disease Resistance to Phytophthora Cinammomi in *Castanea* Sp. *BMC Proc.* **2011**, *5*, O18. [CrossRef]
51. Santos, C.; Machado, H.; Correia, I.; Gomes, F.; Gomes-Laranjo, J.; Costa, R. Phenotyping Castanea Hybrids for Phytophthora Cinnamomi Resistance. *Plant Pathol.* **2015**, *64*, 901–910. [CrossRef]
52. Fernandes, P.; Amaral, A.; Colavolpe, B.; Pereira, A.; Costa, R. Avaliação Agronómica de Genótipos de Castanheiro Selecionados Do Programa de Melhoramento Genético Para a Resistência à Tinta. *Vida Rural* **2021**, *1*, 76–82. Available online: https://www.researchgate.net/publication/352878064 (accessed on 29 May 2023).
53. Fernandes, P.; Amaral, A.; Colavolpe, B.; Balonas, D.; Serra, M.; Pereira, A.; Costa, R.L. Propagation of New Chestnut Rootstocks with Improved Resistance to *Phytophthora cinnamomi*—New Cast Rootstocks. *Silva Lusit.* **2020**, *28*, 15–29. [CrossRef]
54. Kubisiak, T.L.; Nelson, C.D.; Staton, M.E.; Zhebentyayeva, T.; Smith, C.; Olukolu, B.A.; Fang, G.-C.; Hebard, F.V.; Anagnostakis, S.; Wheeler, N.; et al. A Transcriptome-Based Genetic Map of Chinese Chestnut (*Castanea Mollissima*) and Identification of Regions of Segmental Homology with Peach (Prunus Persica). *Tree Genet. Genomes* **2013**, *9*, 557–571. [CrossRef]
55. Serrazina, S.; Santos, C.; Machado, H.; Pesquita, C.; Vicentini, R.; Pais, M.S.; Sebastiana, M.; Costa, R. Castanea Root Transcriptome in Response to Phytophthora Cinnamomi Challenge. *Tree Genet. Genomes* **2015**, *11*, 6. [CrossRef]
56. Zhang, J.; Bernatzky, R.; Anagnostakis, S.L.; Doudrick, R.L.; Kubisiak, F.V.H.T.L.; Ji, F.; Wei, W.; Liu, Y.; Wang, G.; Zhang, Q.; et al. Molecular Mapping of Resistance to Blight in an Interspecific Cross in the Genus Castanea. *Phytopathology* **1997**, *87*, 751–759. [CrossRef]

57. Zhebentyayeva, T.; Chandra, A.; Abbott, A.; Staton, M.; Olukolu, B.; Hebard, F.; Georgi, L.; Jeffers, S.; Sisco, P.; James, J.; et al. Genetic and Genomic Resources For Mapping Resistance To Phytophthora Cinnamomi In Chestnut. *Acta Hortic.* **2014**, 263–270. [CrossRef]
58. Zhebentyayeva, T.N.; Sisco, P.H.; Georgi, L.L.; Jeffers, S.N.; Perkins, M.T.; James, J.B.; Hebard, F.V.; Saski, C.; Nelson, C.D.; Abbott, A.G. Dissecting Resistance to Phytophthora Cinnamomi in Interspecific Hybrid Chestnut Crosses Using Sequence-Based Genotyping and Qtl Mapping. *Phytopathology* **2019**, *109*, 1594–1604. [CrossRef]
59. Santos, C.; Nelson, C.D.; Zhebentyayeva, T.; Machado, H.; Gomes-Laranjo, J.; Costa, R.L. First Interspecific Genetic Linkage Map for Castanea Sativa x Castanea Crenata Revealed QTLs for Resistance to Phytophthora Cinnamomi. *PLoS ONE* **2017**, *12*, e0184381. [CrossRef] [PubMed]
60. Carraway, D.; Wilde, H.; Merkle, S. Somatic Embryogenesis and Gene Transfer in American Chestnut. *J. Am. Chestnut* **1994**, *6*, 29–33.
61. Seabra, R.C.; Pais, M.S. Genetic transformation of European chestnut. *Plant Cell Rep.* **1998**, *17*, 177–182. [CrossRef] [PubMed]
62. Corredoira, E.; Valladares, S.; Allona, I.; Aragoncillo, C.; Vieitez, A.M. Ballester, Genetic Transformation of European Chestnut Somatic Embryos with a Native Thaumatin-like Protein (CsTL1) Gene Isolated from Castanea Sativa Seeds. *Tree Physiol.* **2012**, *32*, 1389–1402. [CrossRef] [PubMed]
63. Corredoira, E.; José, M.C.S.; Vieitez, A.M.; Allona, I.; Aragoncillo, C.; Ballester, A. Agrobacterium-Mediated Transformation of European Chestnut Somatic Embryos with a Castanea Sativa (Mill.) Endochitinase Gene. *New For.* **2016**, *47*, 669–684. [CrossRef]
64. Carlson, E.; Stewart, K.; Baier, K.; McGuigan, L.; Ii, T.C.; Powell, W. Pathogen-induced Expression of a Blight Tolerance Transgene in American Chestnut. *Mol. Plant Pathol.* **2022**, *23*, 370–382. [CrossRef]
65. Polin, L.D.; Liang, H.; Rothrock, R.E.; Nishii, M.; Diehl, D.L.; Newhouse, A.E.; Nairn, C.J.; Powell, W.A.; Maynard, C.A. Agrobacterium-Mediated Transformation of American Chestnut (Castanea Dentata (Marsh.) Borkh.) Somatic Embryos. *Plant Cell Tissue Organ Cult. (PCTOC)* **2006**, *84*, 69–79. [CrossRef]
66. Rothrock, R.E.; Polin-McGuigan, L.D.; Newhouse, A.E.; Powell, W.A.; Maynard, C.A. Plate Flooding as an Alternative Agrobacterium-Mediated Transformation Method for American Chestnut Somatic Embryos. *Plant Cell Tissue Organ Cult. (PCTOC)* **2007**, *88*, 93–99. [CrossRef]
67. McGuigan, L.; Fernandes, P.; Oakes, A.; Stewart, K.; Powell, W. Transformation of American Chestnut (*Castanea Dentata* (Marsh.) Borkh) Using RITA®Temporary Immersion Bioreactors and We Vitro Containers. *Forests* **2020**, *11*, 1196. [CrossRef]
68. Pavese, V.; Moglia, A.; Corredoira, E.; Martínez, M.T.; Marinoni, D.T.; Botta, R. First Report of CRISPR/Cas9 Gene Editing in Castanea Sativa Mill. *Front. Plant Sci.* **2021**, *12*, 1–11. [CrossRef]
69. Pavese, V.; Moglia, A.; Gonthier, P.; Marinoni, D.T.; Cavalet-Giorsa, E.; Botta, R. Identification of Susceptibility Genes in *Castanea sativa* and Their Transcription Dynamics following Pathogen Infection. *Plants* **2021**, *10*, 913. [CrossRef] [PubMed]

agriculture

MDPI

Review

The Use of the Polish Germplasm Collection of *Nicotiana tabacum* in Research and Tobacco Breeding for Disease Resistance

Anna Czubacka

Institute of Soil Science and Plant Cultivation–State Research Institute, 8 Czartoryskich Street, 24-100 Puławy, Poland; annacz@iung.pulawy.pl

Abstract: The Polish germplasm collection of *Nicotiana tabacum* was started in the 1920s. Up to now, more than eight hundred accessions originating from different regions of the world have been gathered in the collection. It includes valuable breeding lines and obsolete cultivars, among them cytoplasmic male-sterile lines. Numerous cultivars are rich sources of features desired in tobacco breeding. Therefore, the accessions are continually characterised in terms of their various features, one of the most important of which is disease resistance. Much research is being done to explain the nature of resistance and its genetic basis. Moreover, cultivars with good agronomic characteristics are used in wide hybridisation, being recipients of resistance genes from wild species or are genetically modified with transgenes conditioning resistance. The biological diversity of cultivars also allows a proper selection of plant material for pathogen studies, while the large number of the accessions facilitates research into the conditions for long seed storage. Numerous examples of the use of Polish tobacco germplasm in research and breeding, specifically in disease resistance, have been presented in this paper.

Keywords: tobacco breeding; resistance; potato virus Y; tomato spotted wilt virus; tobacco mosaic virus; black root rot; blue mould; seed storing; cytoplasmic male sterility

Citation: Czubacka, A. The Use of the Polish Germplasm Collection of *Nicotiana tabacum* in Research and Tobacco Breeding for Disease Resistance. *Agriculture* **2022**, *12*, 1994. https://doi.org/10.3390/agriculture12121994

Academic Editors: Edyta Paczos-Grzeda, Volker Mohler and Sylwia Sowa

Received: 20 October 2022
Accepted: 19 November 2022
Published: 24 November 2022

1. Introduction

The Polish collection of *Nicotiana tabacum* cultivars initiated in the 1920s was started by Prof. Lucjan Kaznowski. He started to collect cultivars imported from abroad for use in domestic breeding. The first accessions included in the collection were Bulgarian cultivars Enidże Stary and Kaba-Kułak. By 1930, the collection consisted of 25 tobacco cultivars coming from different European countries. In the next decade, the collection was expanded to include 150 more cultivars. In subsequent years, it was gradually enriched with cultivars and valuable breeding lines, and currently there are 803 accessions in the collection. The latest ones were added in 2019.

One third of accessions are cultivars or breeding lines obtained in Polish plant breeding centres. Many have been derived as a result of breeding programs conducted for several decades at the Institute of Soil Science and Plant Cultivation (IUNG), Puławy, Poland. Over seventy accessions originate from the USA and a similar number were obtained from the former USSR, mostly from its European part, the Krasnodar Region. Numerous accessions come from France, Germany, Romania, Italy, Hungary, Canada and Australia. There are also cultivars obtained from other European countries, as well as from South America, Asia and Africa, totalling 30 countries in all. The gathered tobacco germplasm is diverse and represents all known tobacco types. There we can find light, dark, flue-cured, air-cured, oriental, broadleaf and cigar tobacco. Moreover, besides standard cultivars, there are alloplasmic lineages and mutants. Many cultivars have resistance to common tobacco threatening diseases and are therefore a valuable material that can be used in breeding.

Collection accessions are stored as seed samples in the storage room at a temperature of 4 °C at IUNG. They are regenerated every few years. For this purpose, seeds are sown and seedlings are planted in the field of the agricultural experimental station near Puławy. Duplicate seed samples are preserved in the storage of the National Centre for Plant Genetic Resources: Polish Genebank, located in The Plant Breeding and Acclimatization Institute (IHAR), Radzików, Poland. The accessions are distributed to researchers, breeders, farmers and hobbyists all over the world.

2. Characterisation of Tobacco Accessions in Terms of Resistance to Diseases

One of the aims of a plant collection is to maintain biodiversity. Tobacco cultivars and breeding lines are sources of various traits that can be used for further breeding. An essential goal is to obtain cultivars resistant to diseases. Therefore, it is important to characterise accessions in respect of resistance sources. For the purpose of resistance breeding in tobacco, genotypes are being screened for resistance to diseases (Table 1).

Table 1. Sources of resistance to the most important diseases of tobacco within accessions maintained in the Polish Genebank of *N. tabacum*.

Cultivar	Origin of Resistance	Inheritance	References
	blue mould (*Peronospora tabacina*)		
Sirogo, Sirone	*N. goodspeedii*	unknown	[1]
Criollo Correntino, Chileno Correntino	unknown	-	[2]
Hicks Resistant, Bel 61-9, Bel 61-10	*N. debneyi*	oligogenic, partially dominant	[2–4]
Chemical Mutant	induced mutation of cv. Virginia Gold	monogenic, partially dominant	[2]
GA 955	*N. excelsior*	unknown	[2]
Wiślica	*N. tabacum* cv. Ovens 62	unknown	[5]
	powdery mildew (*Erysiphe cichoracearum*)		
Kokubu	mutation within genes *NtMLO1* and *NtMLO2*	digenic, recessive	[6]
	black root rot (*Berkeleyomyces sp.*)		
AC Gayed	*N. debneyi*	monogenic, dominant	[7]
TN 86, TN 90	*N. debneyi*	monogenic, dominant	[2,8]
	tobacco mosaic virus (TMV)		
Samsun H, Buley 21, Kutsaga Mammoth, Vamorr 50	*N. glutinosa*	monogenic, dominant	[4,7,9,10]
Ambalema	unknown	digenic, ressessive	[4,10]
	potato virus Y (PVY)		
VAM (Virginia A Mutant)	gene *va* (mutation within susceptibility gene)	monogenic, recessive	[11]
TN 86, TN 90	gene *va* from VAM	monogenic, recessive	[2,12]
Havana IIC, V.SCR (Virginia SCR), Bursan, Wiecha, Bachus, Wiktoria, Weneda	gene *va*	monogenic, recessive	[5,13]
Virginia Kaznowskiego, Wilia, Wisła, Złotolistny IHAR	probably from oriental cultivars	-	[2]
Wiślica, Elka 245, Wika	gene *va*	monogenic, recessive	[14]
Węgierski Ogrodowy	unknown	-	[13]
Lechia A, Zamojska 4	gene *NtTPN1*	monogenic, recessive	[15]
	tomato spotted wilt virus (TSWV)		
Polalta, Wiktoria	*N. alata*	monogenic, dominant	[16]

The table contains an updated description presented by Laskowska [2].

One of the most economically important viral diseases is tobacco veinal necrosis, caused by some strains of potato virus Y (PVY). Isolates belonging to strain groups PVY^O and PVY^C induce only mosaic symptoms on tobacco while these from groups PVY^N and PVY^{NTN} cause veinal necrosis [17]. There are numerous tobacco cultivars with recessive resistance of *va* type, which is the result of a deletion within the gene of translation initiation factor 4E (eIF4E) [14]. The effectiveness of *va* type of resistance present at different cultivars gathered in the Polish Genebank was tested in many studies. Depta et al. [18] observed the development of PVY infection on four tobacco cultivars: susceptible Samsun H and Burley 21, as well as resistant VAM and Wiślica. They showed that highly virulent isolates (PVY^N and PVY^{NTN}) can break the resistance of VAM and Wiślica but symptoms developed more slowly compared to susceptible cultivars.

Korbecka-Glinka et al. [19] widened these studies using nine cultivars and one breeding line in inoculation tests with ten diverse PVY isolates belonging to PVY^{NTN} and PVY^N groups. They selected resistant cultivars: V.SCR, PBD6, TN 86, VAM and Wiślica and susceptible ones: BP-210, K 326, NC 95 and Samsun H. Both VAM and Wiślica proved to be the most effective sources of resistance as they developed no symptoms and had no virus detected in a serological test of four PVY^NW isolates. In the case of cultivars TN 86 and V.SCR the virus was not found in the tissues of plants inoculated with three isolates and one isolate, respectively. In contrast, the tested breeding line BPA, which was derived from a cross *N. tabacum* cv. BP-210 × *N. africana* [20], showed tolerance to all ten PVY isolates, which was manifested by only mild symptoms of vein clearing, chlorotic spots and absence of veinal necrosis despite the presence of the virus in plant tissues.

Depta et al. [13] determined the presence of the *va* type of resistance in the case of 25 cultivars from the genebank resources and tested its effectiveness by inoculating plants with four PVY isolates. Their studies confirmed the resistance of VAM, Wiślica and V.SCR and showed PVY resistance of light flue-cured cultivars Wiecha, Wiktoria, Weneda and light air-cured cv. Bachus. An ineffectiveness of the *va* gene was revealed for a few other accessions which developed necrotic symptoms. Some tested materials showed PVY tolerance manifested by only mild symptoms without necrosis in spite of the lack of a resistance gene as was the case for the above-mentioned BPA line. Interestingly, the authors found that Hungarian dark air-cured cv. Węgierski Ogrodowy, which amplified markers associated with PVY susceptibility, remained symptomless after inoculation with a mild PVY isolate. Such results indicate a different genetic basis of resistance of this cultivar.

As the cultivars vary in their degree of resistance, researchers are looking for reasons for these differences. VAM is supposed to carry two recessive alleles va^1 (limiting virus cell-to-cell movement) and va^2 (limiting virus accumulation) [14,21] which contribute to the high effectiveness of its resistance. Michel et al. [14] studied durability of PVY resistance depending on the type of deletion and, among other things, they included Polish cultivars Wiślica, Wika and Elka 245. They indicated that Wiślica has large deletion of over 1 Mb at *eIF4E-1* gene-like cultivars regarded as the most resistant, such as VAM, TN 86 and PBD6. However, the durability of its resistance is a little weaker compared to TN 86 and VAM because of a lower expression level of the *eIF4E-2* gene (being an ortholog of the *eIF4E-1* gene) which was proved through RNAseq and qRT-PCR analyses. In turn, the resistance of cvs Wika and Elka 245 is even weaker as they have a smaller deletion.

Julio et al. [5] tested 92 *N. tabacum* accessions coming from different research facilities including cultivars Wiślica and Bursan from the Polish Genebank. The authors identified polymorphic fragments associated with sources of resistance to three pathogens. It was demonstrated that Wiślica did not show resistance to *Thielaviopsis basicola* (currently *Berkeleyomyces basicola*, syn. *Chalara elegans*) but it had resistance to two pathogens: potato virus Y (*va* type of resistance) and *Peronospora tabacina* (inherited from Australian cv. Ovens 62) while Bursan had the same type of resistance to PVY. In fact, the neighbour joining method indicated close relationship between both cultivars.

Some cultivars show a tolerance to the virus that is only mild symptoms without necrosis, in spite of the lack of a resistance gene. French researchers studied the genetic basis

of PVY tolerance of several accessions from the Imperial Tobacco germplasm collection [15]. Among them there were cultivars originally from the Polish gene resources such as Lechia A, Lechia LB, Zamoyska and Zamojska 4. The locus responsible for tolerance was mapped in F_2 populations coming from crossing two tolerant cultivars Lechia A and Zamojska 4 with susceptible Virginia 115 and Yellow Special, respectively. Using the previously developed SSR (Simple Sequence Repeat) markers [22,23], the researchers found the gene conferring tolerance on chromosome 13 and named it as *NtTPN1* [15]. Lechia (syn. LB-838) is a flue–cured cultivar bred at IUNG, derived from crossing Polish cv. LB-Koro with Australian cv. Hicks Resistant, carrying resistance to blue mould. PVY tolerance of LB-Koro, Zamojska 4 and a few other cultivars was also shown by Depta et al. [13].

The interesting accessions maintained in the Polish Genebank are cultivars resistant to tomato spotted wilt virus (TSWV). One of them is Polalta: a Polish cultivar with resistance originating from *N. alata* [24]. Polalta belongs to the group of dark-cured tobacco similar to the Puławski type [25]. The introgression from the wild species has been located in linkage group 7 in the region between 0 and 40 cM, which was indicated by comparing the genome sequence of Polalta with those of *N. tabacum* and *N. alata* [26]. Resistance of Polalta is conditioned by a single dominant gene: *RTSV-al* [27]. Unfortunately, it is associated with other genes responsible for morphological deformations such as thickened, abnormal ribbon-shaped leaves as well as the tendency to form tumours [16,24]. Moreover, deformations are more severe in hybrid forms obtained, which hinder the use of Polalta in breeding. Therefore, AFLP (Amplified Fragment Length Polymorphism) markers and then, on their basis, SCAR (Sequence Characterised Amplified Region) markers have been developed for TSWV resistance which could be helpful in reducing the size of *N. alata* introgression in backcrossed hybrids. The markers were tested also in cv. Wiktoria originating from the same interspecific hybrid as cv. Polalta [24]. Wiktoria comes from crossing this hybrid with cvs Virginia Skroniowska 78, V.SCR and Wiślica [28]. As a result of the morphological deformations, neither Polalta nor Wiktoria are commercially cultivated, but they have been included into the genebank as a source of valuable resistance to an important tobacco disease. Their resistance is the hypersensitive type which was proved by Laskowska et al. [16] in tests including artificial inoculation with TSWV, whereby all tested plants belonging to Polalta and only 4 of 15 plants within Wiktoria showed resistance. The rest of Wiktoria plants did not amplify SCAR markers and remained susceptible.

Tobacco collection accessions have been also tested for resistance to black root rot caused by fungal pathogen *Thielaviopsis basicola*. Berbeć and Trojak-Goluch [29] tested six flue-cured tobacco cultivars originating from Germany cv. V.SCR (syn. VD), Polish cultivars Wilia and Wiślica (accessions in the Polish Genebank) and Hungarian ones: Hevesi 9, VJ 1 and VJ 17. Moreover, they tested two breeding lines TB-570N and PTU-1098. On the basis of the results, they described VJ 17 as very resistant, VJ 1 and line PTU-1098 as moderately resistant, Wilia, Wiślica and Hevesi 9 as moderately susceptible and line TB-570N as susceptible.

There are some cultivars demonstrating resistance to tobacco mosaic virus (TMV) among tobacco accessions in the Polish Genebank. Sixty-two cultivars were tested by Depta et al. [10] in respect of reaction to TMV inoculation. One of them was Samsun H, a cultivar bred in 1938 by Holmes, who transferred resistance to *N. tabacum* cv. Samsun from *N. glutinosa* which possessed a single dominant *N* gene responsible for hypersensitive reaction to TMV infection [30,31]. Samsun H and other oriental cultivars such as Diubek 556, Newrokop 261 and Samsun 155 showed hypersensitivity [10]. Similar reactions were noticed in the case of a few other cultivars belonging to dark-cured, Burley and Virginia types. The presence of an *N* gene was detected in all these cultivars. In turn, dark-cured cv. Ambalema, in spite of the lack of an *N* gene, showed tolerance in that its mosaic symptoms were not observed in the infected plants but the presence of the virus was detected with serological tests. However, both resistance and tolerance of tested accessions were broken after increasing the temperature above 28 °C, causing systemic necrotic response.

3. Tobacco Breeding

Changing climatic conditions, increasing pathogen pressure and the growing demands of the tobacco industry are contributing to continual progress in breeding new cultivars. The Polish Genebank is rich resource of *N. tabacum* cultivars which have been used in tobacco breeding (Table 2).

Table 2. The use of tobacco cultivars from the Polish germplasm collection in breeding.

Cultivar	Tobacco Type	Origin	Source of Resistance	Resistance for	Transfer Method	Effect	References
AC Gayed	flue-cured	Canada	transgene with PVY replicase gene	PVY	*Agrobacterium* transformation	resistant breeding lines	[32–35]
BP-210	flue-cured	Poland	*N. africana*	PVY	interspecific hybridisation	tolerant breeding line	[20,32]
			N. benavidesii	PVY	interspecific hybridisation	resistant hybrids BC_1F_3	[36,37]
BY 103	air-cured	Japan	*N. glauca*	black root rot	interspecific hybridisation	amphidiploids, post-sesquidiploids with diverse resistance	[38,39]
			transgene with PVY replicase gene; transgene with LMV coat protein gene	PVY	*Agrobacterium* transformation	resistant breeding lines, DH lines	[32–34,40]
Izyda	flue-cured	Poland	*N. knightiana*	PVY	interspecific hybridisation	amphihaploids	[36]
K236	flue-cured	USA	*N. debneyi*	black root rot	crossing with cv. Wentura	resistant doubled haploids	[41]
			N. glauca	black root rot	interspecific hybridisation	post-sesquidiploids with diverse resistance	[38,39]
			transgene with PVY replicase gene; transgene with LMV coat protein gene	PVY	*Agrobacterium* transformation	resistant breeding lines	[32–34]
Mc Nair 944 (MN 944)	flue-cured	USA	transgene with PVY replicase gene; transgene with LMV coat protein gene	PVY	*Agrobacterium* transformation	resistant breeding lines	[32–34]
Nadwiślański Mały	dark air-cured	Poland	*N. africana*	PVY	interspecific hybridisation	amphihaploids	[42,43]
Nadwiślański Mały tetraploid	dark air-cured	Poland	*N. alata*	TSWV	interspesific hybridisation	sesquidiploids	[44]
Puławski 66	dark-cured	Poland	*N. wuttkei*	blue mould	interspesific hybridisation	amphihaploids	[45]
TB 566 tetraploid	flue-cured	Poland	*N. alata*	TSWV	interspecific hybridisation	sesquidiploids	[46]
TN 90	air-cured	USA	*N. wuttkei*	blue mould	interspecific hybridisation	non-viable hybrids	[45]
VAM	flue-cured	Germany	*N. africana*	PVY	interspecific hybridisation	amphidiploids	[47]
Virginia 278	flue-cured	Germany	*N. africana*	PVY	interspecific hybridisation	sesquidiploids	[42,43]
Virginia Gold Dollar	flue-cured	USA	*N. africana*	PVY	interspecific hybridisation	amphidiploids	[42,43]
Virginia SCR	flue-cured	Germany	*N. africana*	PVY	interspecific hybridisation	sesquidiploids	[42,43]
Virginia Skroniowska 78, V.SCR, Wiślica	flue-cured	Poland	*N. alata*	TSWV	interspecific hybridisation	resistant cv. Wiktoria	[28]

Table 2. *Cont.*

Cultivar	Tobacco Type	Origin	Source of Resistance	Resistance for	Transfer Method	Effect	References
Wiślica	flue-cured	Poland	*N. alata*	TSWV	intercultivar hybridisation with cv. Polalta	resistant DH lines	[48]
			N. africana	PVY	interspecific hybridisation	amphidiploids	[47]
			N. wuttkei	blue mould	interspecific hybridisation	sesquidiploids	[45,49]
			N. glauca	black root rot	interspecific hybridisation	resistant breeding lines WGL	[50,51]
Zamojska 4	flue-cured	Poland	*N. raimondii*	PVY	interspecific hybridisation	amphihaploids	[36]

3.1. Breeding for PVY Resistance

When tobacco veinal necrosis became a serious problem in Poland in the late 1950s and then the early 1960s [37], the breeders were faced with the need to breed resistant cultivars that were also adapted to the country's climatic conditions. Since then, there has been an ongoing search for sources of PVY resistance within *Nicotiana* species that could be used in the breeding of new tobacco cultivars [52].

At that time, cultivar BP-210 became popular with breeders. It is a good quality flue-cured cultivar bred at IUNG by selection from an Australian breeding line. It is resistant to blue mould but because of a high susceptibility to PVY it has been withdrawn from cultivation [53]. As a result of crossing with *N. benavidesii*, carrying resistance to PVY, the interspecific hybrids have been obtained [36]. Moreover, the tetraploid form of BP-210 was fertilised with pollen of *N. benavidesii* to obtain sesquidiploids which then were backcrossed with diploid BP-210, resulting in obtaining resistant plants [37].

A promising source of resistance has been transferred to *N. tabacum* from a wild species by Doroszewska and Berbeć [42,43], who crossed *N. africana* with five tobacco cultivars selected from among Polish Genebank accessions. They used flue-cured cultivars: V.SCR, Virginia 278 and BP-210 (Polish cultivars) and American cv. Gold Dollar and dark-cured Polish cv. Nadwiślański Mały. Next, hybrids resulting from crossing BP-210 and *N. africana* served to obtain breeding line BPA which showed tolerance to all tested PVY isolates [20,32,54]. A further attempt to transfer resistance from *N. africana* was crossing this species with VAM and Wiślica in order to enhance the resistance of these cultivars [47].

In turn, Polish flue-cured cultivar Izyda was applied in an attempt to transfer resistance from a wild species *N. knightiana* [36]. Another Polish cv. Zamojska 4 was crossed first with cv. LB-838 (syn. Lechia) and the hybrids showed tolerance to PVY; that is, they developed only mild vein clearing after inoculation but no systemic symptoms. Then the hybrids were used as the male parent in crossing with *N. raimondii* and, in the case of the amphidiploid of the hybrid and segregating backcross populations, an interesting phenomenon was observed. Both factors, i.e., tolerance from the tabacum parent (both Lechia and Zamojska 4 have tolerance to PVY) and resistance from *N. raimondii*, stopped each other resulting in strong susceptibility [36,55].

Resistance to PVY has been also obtained by genetic transformation of four flue-cured cultivars; two American ones MN 944 and K 326 and Japanese BY 103 as well as one coming from Canada, AC Gayed [32]. All of them are accessions of the Polish Genebank. They were transformed with three constructs containing modified PVY replicase gene with in sense (ROKY1) and antisense (ROKY2) orientation as well as coat protein gene of lettuce mosaic virus (LMV CP). Analysis of the resistance in successive generations of transgenic plants and their agronomic traits has allowed for selection of the two most promising lines: cv. MN 944 with transgene LMV CP and cv. AC Gayed with transgene ROKY2 [33,34]. Next, they have been crossed to obtain advanced generations [56] as well as stable double transgenic hybrid lines with high resistance [57]. Moreover, transgenic lines MN 944 LMV CP and AC Gayed ROKY2 were crossed with cultivars with resistance of *va* type, VAM

and Wiślica, which resulted in obtaining hybrid lines carrying two different sources of resistance to PVY. Of these VAM × MN 944 LMV CP and Wiślica × MN 944 LMV CP proved to be resistant even to a strong PVY isolate [58]. Moreover, a hybrid line originating from crossing MN 944 LMV CP and cv. Wiślica served as a material for obtaining double haploids [35]. The tobacco transgenic lines with resistance to PVY, and enhancing it by combining with *va* resistance, widened variability within the species *N. tabacum*.

3.2. Breeding for TSWV Resistance

The attempt to transfer TSWV resistance to *N. tabacum* was made by Berbeć [44], who crossed one of the cultivars maintained in the Polish Genebank, Nadwiślański Mały, with *N. alata*, which is a source of resistance to the virus. However, he obtained hybrids with low survival rates and complete sterility, which made continuation of the breeding process impossible. It was only by using a tetraploid form of *N. tabacum*, cv. Nadwiślański Mały or cv. TB 566, that viable hybrids could be obtained [44,46]. However, backcrossing to *N. tabacum* failed [46]. The use of a bridging species proved to be key to breeding success. The first cultivar resistant to TSWV was obtained by Gajos who used *N. otophora* as bridging species and thereby managed to transfer the resistance from *N. alata* to *N. tabacum* [7,25]. Unfortunately, these breeding efforts were not sufficiently documented, as it is not clear to which tobacco cultivar. Nevertheless, this way cv. Polalta was obtained [24,25,59]. An interspecies hybrid, which was used to obtain Polata, was also crossed with cultivars in the Polish collection such as Virginia Skroniowska 78, V.SCR and Wiślica. The results of these efforts was cultivar Wiktoria [28]. Both Polalta and Wiktoria have been included into the Polish Genebank as a source of valuable germplasm because they represent very few sources of TSWV resistance available today within *N. tabacum*. So far, attempts to use Polalta in crossbreeding with other tobacco cultivars have been unsuccessful because the hybrids show a number of morphological malformations. Laskowska and Berbeć [48] tried to break this phenomenon by anther culture obtaining haploid plants, originating from crossing Polalta with Wiślica and then doubled haploids. As a result, they bred three double haploid lines PW-833, PW-834 and PW-900 resistant to TSWV and simultaneously showing morphological deformations milder than those characteristic for Polalta.

3.3. Breeding for Resistance to Fungal Diseases

Resistance to black root rot has been transferred to *N. tabacum* from a wild species *N. glauca*. From the Polish germplasm collection, two cultivars, BY103 and K326, have been selected for interspecific hybridisation [38]. The obtained amphihaploids showed high resistance while the level of resistance of the sesquidiploids and post-sesquidiploids varied [39]. The resistance from *N. glauca* was also transferred to cv. Wiślica [50] which resulted in the obtention of resistant breeding lines WGL [51], and finally a resistant commercial cultivar [60]. It is noteworthy that breeding line WGL was also crossed with doubled haploid line PW-834 carrying resistance from Polalta in order to obtain first haploids and then doubled haploid lines DH3 and DH6 with resistance to both black root rot and TSWV [26,61,62]. Next, the lines were crossed with a high-quality flue-cured cultivar WAC 121D7 renamed as Wentura (with resistance to both black root rot and PVY) and the obtained plants of F_4 generation carrying *N. alata* introgression showed resistance to TSWV and simultaneously had morphology without deformations characteristic for Polalta [63]. One of the WGL lines was also crossed with line BPA carrying resistance to PVY [64]. Moreover, cv. K 326 served also as a good quality component in crossing with cv. Wentura carrying resistance to black root rot transferred from *N. debneyi*. Next, 24 doubled haploid lines were produced from the hybrids and five of them were completely resistant [41].

Tobacco cultivars were also crossed with *N. wuttkei* carrying resistance to another fungal disease dangerous for tobacco plantations: blue mould caused by *Peronospora tabacina*. The initial studies on the possibility of crossing *N. tabacum* with the wild species were made with the use of three cultivars from the Polish Genebank: Wiślica, Puławski

and TN 90. All of them are somewhat resistant to blue mould. The seedlings F_1 were not able to survive but the authors managed to obtain amphihaploids originating from crossing *N. wuttkei* × *N. tabacum* cv. Wiślica and *N. wuttkei* × *N. tabacum* cv. Puławski from cotyledons under in vitro conditions [45]. Next, the amphidiploids from hybrids *N. wuttkei* × *N. tabacum* cv. Wiślica were produced by in vitro chromosome doubling and backcrossed with Wiślica giving a single sesquidiploid plant [49]. Unfortunately, the amphidiploid plants could not be backcrossed, as male parents to *N. tabacum* and sesquidiploids would not cross as male components with *N. tabacum*. Therefore, the cytoplasmic inheritance could not be reversed to that of *N. tabacum*. Hence, further breeding progress was not possible because of the massive onset of cytoplasmic male sterility in further backcrossed populations [45,49]. Nevertheless, the obtained hybrids can be regarded as a new synthetic species carrying resistance to blue mould.

The use of cultivars from the Polish Genebank in breeding to combine sources of resistance to different diseases in a single genome is presented in the diagram (Figure 1).

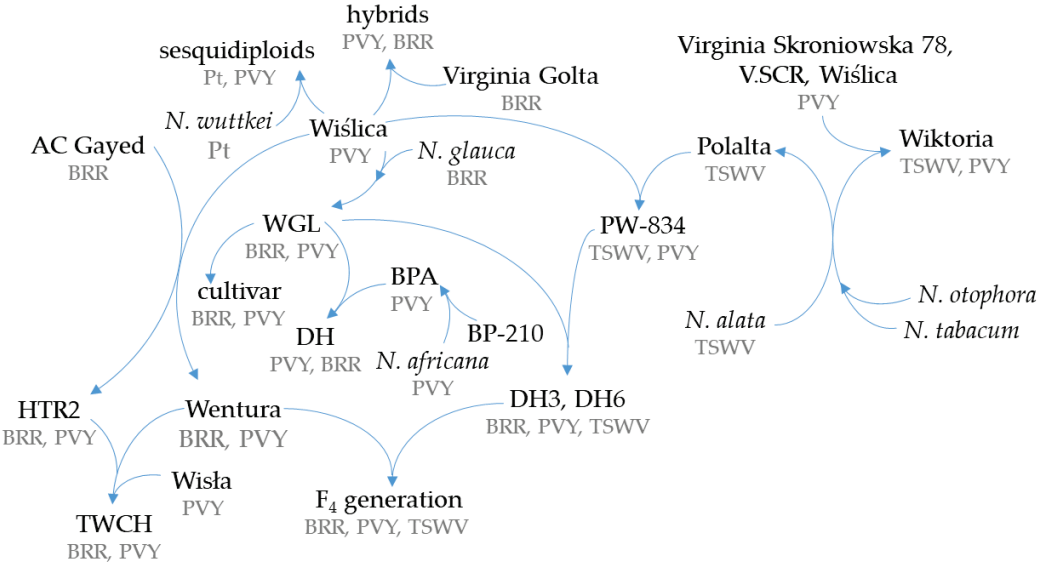

Figure 1. The use of cultivars from the Polish germplasm collection in tobacco breeding leading to combining resistance sources to different diseases. Breeding materials: *Nicotiana* species: *N. tabacum*, *N. alata*, *N. africana*, *N. othophora*, *N. wuttkei*; cultivars: AC Gayed, Wiślica, Virginia Golta, Virginia Skroniowska 78, V.SCR, Polalta, Wiktoria, BP-210, HTR2, Wentura, Wisła; breeding lines: WGL, BPA, PW-834, TWCH (three-way-cross hybrid), DH, DH3, DH6 (doubled haploid lines). BRR, PVY, TSWV, Pt–resistance to black root rot, PVY, TSWV and *Peronospora tabacina*, respectively, carrying in breeding materials.

4. Cultivars with Cytoplasmic Male Sterility (cms) and Their Application in Breeding for Disease Resistance

Cytoplasmic male sterility, which is the result of incompatibility between the genome of the cell nucleus and the cytoplasm, is used in plant breeding to obtain forms incapable of self-pollination which makes it easier for a breeder to carry out controlled production of hybrids for commercial use and prevents unauthorised reproduction of seeds [65]. Cytoplasmic male-sterility is mostly obtained as a result of the substitution of cytoplasm from a different species in place of the native cytoplasm and, in autogamic plants, less frequently may be the result of a spontaneous mutation [66,67].

The Polish collection of *N. tabacum* includes over fifty accessions which are cytoplasmic male sterile. Most of them are the result of the work of scientists from IUNG, obtained on

the base of Polish cultivars BP-210, BP-Koro, Lechia, Nadwiślański and Puławski. Moreover, there are several accessions of Zamojska 4 and Wiślica with cytoplasm originating from different wild *Nicotiana* species, and Wiślica with cytoplasm from an *N. tabacum* mutant. However, some alloplasmic forms such as Zamojska 4 cms *goodspeedii*, Zamojska 4 cms *bigelovii* and Zamojska 4 cms *suaveolens* were received from the Tobacco Research Board in Zimbabwe while other ones with cytoplasm replaced from *N. glutinosa*, *N. megalosiphon*, *N. occidentalis*, *N. plumbaginifolia* and *N. undulata* were obtained from the Russian research facility WITIM in Krasnodar [67]. A few more alloplasmic forms were obtained from other foreign breeding centres such as cv. Erzegowina cms from Italy or a breeding line from USA.

Alloplasmic forms develop modified, non-functional male generative organs or none at all. The morphological changes may also affect other parts of the flower and sometimes the entire plant, for example the habit of forms cms with cytoplasm from *N. goodspeedii* and *N. megalosiphon* differ significantly from the initial cv. Zamojska 4 [67]. Moreover, alloplasmic forms of that cultivar developed no stamens, malformed ones or petaloid, stigmatoid structures in their place [66,67]. In the case of Wiślica, most of the alloplasmic forms develop abnormal or no stamens. A few cms forms differed in leaf area and plant height relative to their fertile counterpart and, for example, Wiślica cms *bigelovii* provided higher yield [68]. Among the many alloplasmic forms gathered in the tobacco germplasm collection, Zamojska 4 *knightiana* stands out because it has retained partial fertility in contrast to the others which are completely sterile. Therefore, this particular cms form was used by Berbeć [69] to conduct studies to determine whether the presence of alien cytoplasm caused changes in the nuclear genome. For this purpose, he compared offspring of Zamojska 4 cms *knightiana* obtained by self-pollination and that backcrossed with Zamojska 4. The selfed progeny showed depressive agronomic performance; therefore, the author concluded that it may be a result of mutations within the nuclear genome which accumulated over generations while such a phenomenon did not occur in the case of the use of pollen of autoplasmic Zamojska 4.

The presence of alien cytoplasm can also affect other characteristics, including the plant resistance to pathogens [65,66]. That is why cms forms must be well characterised in order to determine their real suitability for breeding. Forms of Zamojska 4 with cytoplasm substituted from *N. eastii* and *N. plumbaginifolia* species were severely infected with powdery mildew under field conditions in a season characterised by a high incidence of the pathogen, while the other cms forms showed tolerance [67].

As far as the response to PVY infection was tested, under conditions of artificial inoculation it was found that the use of cytoplasm from the species *N. amplexicaulis*, *N. debneyi*, *N. exigua*, *N. glauca*, *N. glutinosa*, *N. knightiana* and *N. raimondii* did not contribute to changes in the level of tolerance responses of alloplasmic male-sterile forms of Zamojska 4. On the contrary, the use of cytoplasm from the species *N. goodspeedii*, *N. megalosiphon* and *N. undulata* resulted in an increased tolerance of the cms forms and delayed symptoms, whereas the presence of cytoplasm from the species *N. eastii*, *N. occidentalis* and *N. suaveolens* resulted in decreased tolerance. Changes in the resistance response also affected the cms form with cytoplasm of the *N. tabacum* mutant [66]. The type of cytoplasm also differentiated the occurrence of symptoms of PVY infection and cercosporiosis on male-sterile forms of Wiślica under natural pressure of the pathogens causing these diseases. Alloplasmic forms with cytoplasm substituted from *N. bigelovii*, *N. occidentalis*, *N. undulata*, *N. exigua* and *N. suaveolens* showed increased symptoms of *Cercospora* sp. infection, with the last two showing an additional decreased resistance to PVY compared to cv. Wiślica [68].

Hybrids originating from crossing Wiślica and Virginia Golta (maintained in the Polish Genebank German cultivar carrying resistance to black root rot) with four kinds of alien cytoplasm also varied in respect of susceptibility to PVY, black root rot, cercosporiosis, as well as in respect of agronomic performance, which demonstrates one more time that the choice of cytoplasm source is important in cultivar breeding [70].

Cytoplasmically male-sterile cvs HTR2 and Wentura were used by Berbeć [71] in comparing three-way cross hybrids of tobacco to single-cross ones. The cultivars originated from crossing of two cultivars maintained in the Polish Genebank: Wiślica and AC Gayed (Figure 1). The hybrid F_1 resulting from crossing of HTR2 cms × Wentura was crossed with another cultivar from the Polish collection, Wisła, or with the local cvs VP 06 and VB 08. The resulting three-way cross hybrids were compared in respect of agronomic performance to single-cross ones in which HTR2 cms and Wentura cms were used as maternal parents in crossing with Wisła, VP 06 or VB 08. Currently, at least two three-way cross hybrids are grown as commercial cultivars in Poland (VRG 5 TL and VRG 10 TL) [72].

5. Studies on Viral Pathogens

Some collection accessions are used in research, of which they are not the subject but play an important role in the preparation of the experiment proper. This is because the collection accessions are well characterised in terms of their numerous features, so the researcher can choose from among them the one that best meets his/her expectations. An example of a cultivar often used in numerous studies on viral pathogens or plant resistance, is the oriental cv. Samsun H. It is in the plants of Samsun H that the multiplication of viruses is carried out. Indeed, Samsun H shows hypersensitivity-type resistance to tobacco mosaic virus–the pathogen which is very common in tobacco crops and often accompanies infection with less common viruses. Therefore, the multiplication of the virus in Samsun H makes it possible to purify a viral isolate from TMV.

Moreover, cv. Samsun was used in the identification of a virus that had been noticed in tobacco crops for the first time in 2004 in Poland, Germany and Hungary [73]. Artificial inoculation of Samsun plants resulted in chlorotic lesions and severe necrosis of leaves as well as stunting of plants. The molecular and serological studies led to the identification of the virus as Colombian Datura virus.

In turn, other tobacco cultivars, whose resistance to the PVY virus was already well established, were used in the studies of this virus. Three cultivars Wiślica, VAM and Samsun H differing in resistance to PVY were the test set in studies identifying molecular point mutations in several viral isolates coming from Poland, Germany and Croatia [74]. The use of three cultivars allowed formation of a characteristic of isolates in terms of symptom severity depending on the kind of source of resistance. Samsun H reacted with susceptibility to all isolates while Wiślica and VAM showed disease symptoms as a result of inoculation with 8 of 15 PVY isolates. Sequencing viral genomes revealed that point mutations within their VPg region were responsible for the ability to break resistance in VAM and Wiślica. The authors deduced that there has been a change in the amino acid sequence by substitution of lysine with threonine in position 105 in resistance-breaking isolates. They also conferred another changes previously found by other researchers [75,76].

6. Seed Response for Long-Term Preservation

When plant gene resources are stored in the form of seeds, it is extremely important to optimise the conditions of the storage facility in such a way that the seed samples will remain viable for as long as possible. The longer the seeds remain viable, the longer the periods between their regeneration can be. The lower the frequency of regeneration, the lower the cost of maintaining the collection and labour intensity, but most importantly the lower the risk of genetic erosion of accessions.

Therefore, it is important to conduct research to determine the viability of seeds maintained in storage facilities. Such kinds of test should be made for each plant species. Accessions from the tobacco collection served as research material in studies of the viability of seeds stored under conditions of different humidity and ambient temperature [77]. The authors showed that the storage in reduced relative humidity (RH = 50.5 ± 6.3 %) was essential for maintenance of the seeds in a viable state. A proportion of 0.4 of seed lots stored under these conditions for 12 years still were able to spawn the normal seedlings from at least 75% of seeds, while none of those maintained in the conditions with higher

humidity (RH of about 77%) retained that ability. In turn, germination tests on *N. tabacum* seeds belonging to 227 collection accessions stored at 0 °C for 33 years indicated that only 10% of accessions retained the ability to germinate in no less than 75% of seeds [78]. In comparison, seeds stored in the Genebank of the Leibniz-Institut (IPK, Gatersleben, Germany) at a temperature of −15/−18 °C maintained a longer vitality at this level; that is, more than half of tested *Nicotiana* accessions had a high capacity of germination even after 40 years. The seeds stored in IPK had an approximate moisture content of 6% while the content of those in the Polish Genebank was 4%. Therefore, one should bear in mind that although temperature proved to be a key factor in seed viability, seed moisture may also be essential.

7. Conclusions

Maintaining the Polish germplasm collection of tobacco is primarily done to protect valuable breeding materials and obsolete cultivars which are no longer commercially grown. The need for long-term storage of seeds makes it possible to study the impact of external conditions on preserving their viability. However, caring for a collection is not limited to keeping accessions in a viable condition and genetically pure, but also presents a challenge in that one is obliged to constantly learn about them. This is especially true, as *N. tabacum* accessions come from many regions of the world and therefore represent a huge genetic diversity. Research aims are dictated, on the one hand, by the development of modern research methods, and on the other hand, by the needs of farmers and the tobacco product market. That is why many researchers focus on the study of resistance sources and the possibility of using them to breed new cultivars that will be used in current commercial cultivation. It seems that the direction of further research on *N. tabacum* should be to search for accessions resistant to biotic and abiotic stresses resulting from climate change.

Funding: This research received no external funding.

Institutional Review Board Statement: Not applicable.

Data Availability Statement: Not applicable.

Conflicts of Interest: The authors declare no conflict of interest.

References

1. Spring, O.; Gomez-Zeledon, J.; Hadziabdic, D.; Trigiano, R.N.; Thines, M.; Lebeda, A. Biological Characteristics and Assessment of Virulence Diversity in Pathosystems of Economically Important Biotrophic Oomycetes. *Crit. Rev. Plant Sci.* **2019**, *37*, 439–495. [CrossRef]
2. Laskowska, D. Różnorodność biologiczna w kolekcji *Nicotiana tabacum* L. zgromadzonej w Instytucie Uprawy Nawożenia i Gleboznawstwa—PIB w Puławach. *Zeszyty Problemowe Postępów Nauk Rolniczych* **2007**, *517*, 73–81.
3. Zhang, S.; Zaitlin, D. Genetic resistance to Peronospora tabacina in *Nicotiana langsdorffii*, a South American wild tobacco. *Phytopathology* **2008**, *98*, 519–528. [CrossRef]
4. Shava, J.G.; Richardson-Kageler, S.; Dari, S.; Magama, F.; Rukuni, D. Breeding for Flue-cured Tobacco (*Nicotiana tabacum* L.) Foliar Pest and Disease Resistance in Zimbabwe: A Review. *Agric. Rev.* **2019**, *40*, 104–112. [CrossRef]
5. Julio, E.; Verrier, J.L.; Dorlhac de Borne, F. Development of SCAR markers linked to three disease resistances based on AFLP within *Nicotiana tabacum* L. *Theor. Appl. Genet.* **2006**, *112*, 335–346. [CrossRef]
6. Fujimura, T.; Sato, S.; Tajima, T.; Arai, M. Powdery mildew resistance in the Japanese domestic tobacco cultivar Kokubu is associated with aberrant splicing of MLO orthologues. *Plant Pathol.* **2016**, *65*, 1358–1365. [CrossRef]
7. Berbeć, A.; Doroszewska, T. *The Use of Nicotiana Species in Tobacco Improvement In The Tobacco Plant Genome*; Ivanov, N.V., Sierro, N., Peitsch, M.C., Eds.; Springer: Cham, Switzerland, 2020; pp. 101–146.
8. Hood, M.E.; Shew, H.D. Pathogenesis of *Thielaviopsis basicola* on a susceptible and a resistant cultivar of burley tobacco. *Phytopathology* **1996**, *86*, 38–44. [CrossRef]
9. Chaplin, J.F.; Mann, T.J. Evaluation of tobacco mosaic resistance factor transferred from burley to flue-cured tobacco. *J Hered.* **1987**, *69*, 175–178. [CrossRef]
10. Depta, A.; Kursa, K.; Doroszewska, T.; Laskowska, D.; Trojak-Goluch, A. Reaction of *Nicotiana* species and cultivars of tobacco to *Tobacco mosaic virus* and detection of the *N* gene that confers hypersensitive resistance. *Czech J. Genet. Plant Breed.* **2018**, *54*, 143–146.

11. Koelle, G. Genetische Analyse einer Y-virus (Rippen-braune) resistenten Mutante der Tabaksorte Virgin A. *Der Zuchter* **1961**, *31*, 71–72.
12. Dluge, K.L.; Song, Z.; Wang, B.; Tyler Steede, W.; Xiao, B.; Liu, Y.; Dewey, R.E. Characterization of *Nicotiana tabacum* genotypes possessing deletion mutations that affect potyvirus resistance and the production of trichome exudates. *BMC Genom.* **2018**, *19*, 484. [CrossRef]
13. Depta, A.; Doroszewska, T.; Czubacka, A. Zróżnicowanie reakcji odpornościowej wybranych odmian tytoniu (*Nicotiana tabacum*) w zależności od użytego izolatu wirusa Y ziemniaka (PVY). *Pol. J. Agron.* **2020**, *42*, 3–13.
14. Michel, V.; Julio, E.; Candresse, T.; Cotucheau, J.; Decorps, C.; Volpatti, R.; Moury, B.; Glais, L.; Jacquot, E.; de Borne, F.D.; et al. A complex eIF4E locus impacts the durability of *va* resistance to *Potato virus Y* in tobacco. *Mol. Plant Pathol.* **2019**, *20*, 1051–1066. [CrossRef]
15. Michel, V.; Julio, E.; Candresse, T.; Cotucheau, J.; Decorps, C.; Volpatti, R.; Moury, B.; Glais, L.; Dorlhac de Borne, F.; Decroocq, V.; et al. *NtTPN1*: A *RPP8*-like *R* gene required for *Potato virus Y*-induced veinal necrosis in tobacco. *Plant J.* **2018**, *95*, 700–714. [CrossRef]
16. Laskowska, D.; Doroszewska, T.; Depta, A.; Kursa, K.; Olszak-Przybyś, H.; Czubacka, A. A survey of *Nicotiana* germplasm for resistance to *Tomato spotted wilt virus* (TSWV). *Euphytica* **2013**, *193*, 207–219. [CrossRef]
17. Glais, L.; Bellstedt, D.U.; Lacomme, C. The Diversity of PVY: A Constant Challenge for Its Classification and Characterisation. In *Potato Virus Y: Biodiversity, Pathogenicity, Epidemiology and Management*; Lancome, C., Glais, L., Bellstedt, D.U., Dupuis, B., Karasev, A.V., Jacquot, E., Eds.; Springer International Publishing AG: Cham, Switzerland, 2017.
18. Depta, A.; Olszak-Przybyś, H.; Korbecka, G. Development of *Potato virus Y* (PVY) infection in susceptible and resistant tobacco cultivars. *Pol. J. Agron.* **2014**, *18*, 3–6.
19. Korbecka-Glinka, G.; Czubacka, A.; Przybys, M.; Doroszewska, T. Resistance vs. tolerance to *Potato virus Y* in tobacco-comparing effectiveness using virus isolates from Central Europe. *Breed. Sci.* **2017**, *67*, 459–465. [CrossRef] [PubMed]
20. Doroszewska, T. Transfer of tolerance to different *Potato virus Y* (PVY) isolates from *Nicotiana africana* Merxm. to *Nicotiana tabacum* L. *Plant Breed.* **2010**, *129*, 76–81. [CrossRef]
21. Acosta-Leal, R.; Xiong, Z. Complementary functions of two recessive R-genes determine resistance durability of tobacco 'Virgin A Mutant' (VAM) to Potato virus Y. *Virology* **2008**, *379*, 275–283. [CrossRef] [PubMed]
22. Julio, E.; Cotucheau, J.; Decorps, C.; Volpatti, R.; Sentenac, C.; Candresse, T.; Dorlhac de Borne, F. A Eukaryotic Translation Initiation Factor 4E (eIF4E) is Responsible for the "*va*" Tobacco Recessive Resistance to Potyviruses. *Plant Mol. Biol. Rep.* **2015**, *33*, 609–623. [CrossRef]
23. Bindler, G.; Bakaher, N.; Gunduz, I.; Ivanov, N.; Van der Hoeven, R.; Donini, P. A high density genetic map of tobacco (*Nicotiana tabacum* L.) obtained from large scale microsatellite marker development. *Theor. Appl. Genet.* **2011**, *123*, 219–230. [CrossRef]
24. Moon, H.; Nicholson, J.S. AFLP and SCAR Markers Linked to *Tomato Spotted Wilt Virus* Resistance in Tobacco. *Crop Sci.* **2007**, *47*, 1887–1894. [CrossRef]
25. Gajos, Z. Polalta—Odmiana tytoniu odporna na wirus brązowej plamistości pomidora (TSWV) i czarną zgniliznę korzeni (*Thielaviopsis basicola* Ferr.) [Polalta—A tobacco cultivar resistant to *Tomato spotted wilt virus* and black root rot (*Thielaviopsis basicola* Ferr.)]. *Biuletyn CLPT* **1988**, *1–4*, 7–25.
26. Korbecka-Glinka, G.; Trojak-Goluch, A.; Doroszewska, T.; Goepfert, S. The influence of *Nicotiana alata*-derived introgression on plant malformations of tobacco breeding lines resistant to tomato spotted wilt virus. In Proceedings of the CORESTA Congress, Kunming, China, 22–26 October 2018. Agronomy/Phytopathology Groups, AP 49.
27. Huang, C.; Liu, Y.; Yu, H.; Yuan, C.; Zeng, J.; Zhao, L.; Tong, Z.; Tao, X. Non-Structural Protein NSm of *Tomato Spotted Wilt Virus* Is an Avirulence Factor Recognized by Resistance Genes of Tobacco and Tomato via Different Elicitor Active Sites. *Viruses* **2018**, *10*, 660. [CrossRef]
28. Gajos, Z. Virginia ZG-4 (Wiktoria)—Nowa odmiana tytoniu odporna na wirus brązowej plamistości pomoidora (TSWV) i czarną zgniliznę korzeni (*Thielaviopsis basicola*) (Virginia ZG-4 (Wiktoria)—A new variety resistant to *Tomato spotted wilt virus* (TSWV) and black root rot (*Thielaviopsis basicola*). *Biuletyn CLPT* **1993**, *1–4*, 5–19.
29. Berbeć, A.; Trojak-Goluch, A. Response to black root rot *Thielaviopsis tabacina* Ferr. of several flue-cured tobacco *Nicotiana tabacum* L. genotypes in different testing environments. *Plant Breed. Seed Sci.* **2001**, *45*, 11–20.
30. Marathe, R.; Anandalakshmi, R.; Liu, Y.; Dinesh-Kumar, S.P. The tobacco mosaic virus resistance gene, N. *Mol. Plant Pathol.* **2002**, *3*, 167–172. [CrossRef]
31. Lewis, R.S.; Milla, S.R.; Levin, J.S. Molecular and Genetic Characterization of *Nicotiana glutinosa* L. Chromosome Segments inTobacco mosaic virus-Resistant Tobacco Accessions. *Crop Sci.* **2005**, *45*, 2355–2362. [CrossRef]
32. Doroszewska, T. Wide Hybridization and Genetic Transformation in Breeding for Resistance to Potato virus Y (PVY) in Tobacco (*Nicotiana tabacum* L.). In *Habilitation Proceedings, Monographs and Dissertations*; IUNG: Puławy, Poland, 2004; Volume 9. (In Polish)
33. Czubacka, A.; Doroszewska, T. Estimating agronomic traits of transgenic tobacco lines. *Euphytica* **2009**, *172*, 35–47. [CrossRef]
34. Czubacka, A.; Doroszewska, T. Resistance of transgenic tobacco lines to *Potato Virus Y* (in Polish). *Biotechnologia* **2010**, *2*, 72–82.
35. Czubacka, A.; Doroszewska, T.; Trojak-Goluch, A. Agronomic characteristics of transgenic tobacco doubled haploids resistant to *Potato virus Y*. *J. Food Agric. Environ.* **2012**, *10*, 374–378.
36. Berbeć, A. Chromosome pairing and pollen fertility in the interspecific F_1 hybrids *Nicotiana tabacum* L. × *N. benavidesii* Goodspeed, *N. knightiana* Goodspeed × *N. tabacum*, and *N. raimondii* Macbride × *N. tabacum*. *Genet. Pol.* **1987**, *28*, 263–269.

37. Berbeć, A.; Głażewska, Z. Transfer of resistance to *Potato virus Y* from *Nicotiana benavidesii* Goodspeed to *N. tabacum* L. *Genet. Pol.* **1988**, *29*, 323–333.
38. Trojak-Goluch, A.; Berbeć, A. Cytological investigations of the interspecific hybrids of *Nicotiana tabacum* L. × *N. glauca* Grah. *J. Appl. Genet.* **2003**, *44*, 45–54.
39. Trojak-Goluch, A.; Berbeć, A. Potential of *Nicotiana glauca* Grah. as a source of resistance to black root rot *Thielaviopsis basicola* (Berk. and Broome) Ferr. in tobacco improvement. *Plant Breed.* **2005**, *124*, 507–510. [CrossRef]
40. Czubacka, A.; Doroszewska, T. Evaluation of agronomic characteristics of transgenic tobacco doubled haploids. In Proceedings of the CORESTA Meeting, Agronomy/Phytopathology, AP 30, Santiago, Chile, 6–10 November 2011.
41. Trojak-Goluch, A.; Berbeć, A. Resistance to black root rot (*Chalara elegans* Nag. Raj and Kendrick) and some growth characteristics in doubled haploid derivatives of the F1 hybrid of tobacco (*Nicotiana tabacum* L.). *Pol. J. Agron.* **2009**, *1*, 52–55.
42. Doroszewska, T.; Berbeć, A. Chromosome pairing and microsporogenesis in interspecific F_1 hybrids of *Nicotiana africana* with different cultivars of *N. tabacum*. *J. Genet. Breed.* **1996**, *50*, 75–82.
43. Doroszewska, T.; Berbeć, A. Cytogenetical investigations of poliploid interspecific hybrids of *Nicotiana africana* with different cultivars of *N. tabacum*. *J. Genet. Breed.* **2000**, *54*, 77–82.
44. Berbeć, A. Cytogenetical study on *Nicotiana tabacum* L. cv. Nadwiślański Mały (2x and 4x) x *Nicotiana alata* Link et Otto hybrids. *Genet. Pol.* **1987**, *28*, 253–261.
45. Laskowska, D.; Berbeć, A. Production and characterization of amphihaploid hybrids between *Nicotiana wuttkei* Clarkson et Symon and *N. tabacum* L. *Euphytica* **2011**, *183*, 75–82. [CrossRef]
46. Laskowska, D.; Berbeć, A. Cytology and fertility of viable hybrids of *Nicotiana tabacum* L. cv. TB-566 with *N. alata* Link et Otto. *J. Appl. Genet.* **2005**, *46*, 11–18. [PubMed]
47. Depta, A.; Doroszewska, T. Development and cytometric evaluation of interspecific F_1 hybrids *Nicotiana tabacum* × *N. africana*. *Pol. J. Agron.* **2019**, *38*, 3–14.
48. Laskowska, D.; Berbeć, A. TSWV resistance in DH lines of tobacco (*Nicotiana tabacum* L.) obtained from a hybrid between 'Polalta' and 'Wiślica'. *Plant Breed.* **2010**, *129*, 731–733. [CrossRef]
49. Laskowska, D.; Berbeć, A.; Van Laere, K.; Kirov, I.; Czubacka, A.; Trojak-Goluch, A. Cytology and fertility of amphidiploid hybrids between *Nicotiana wuttkei* Clarkson et Symon and *N. tabacum* L. *Euphytica* **2015**, *206*, 597–608. [CrossRef]
50. Trojak-Goluch, A.; Berbeć, A. Meiosis and fertility in interspecific hybrids of *Nicotiana tabacum* L. × *N. glauca* Grah. and their derivatives. *Plant Breed.* **2007**, *126*, 201–206. [CrossRef]
51. Trojak-Goluch, A.; Berbeć, A. Growth, development and chemical characteristics of tobacco lines carrying black root rot resistance derived from *Nicotiana glauca* (Grah.). *Plant Breed.* **2011**, *130*, 92–95. [CrossRef]
52. Doroszewska, T.; Depta, A. Resistance of wild *Nicotiana* species to different PVY isolates. *Phytopathologia* **2011**, *59*, 9–24.
53. Doroszewska, T.; Institute of Soil Science and Plant Cultivation—State Research Institute, Puławy, Poland; Berbeć, A.; Institute of Soil Science and Plant Cultivation—State Research Institute, Puławy, Poland. Characterics of cv. BP-210. Personal communication, 2022.
54. Korbecka-Glinka, G.; Czubacka, A.; Depta, A.; Doroszewska, T. Inheritance of *Potato virus Y* tolerance introgressed from *Nicotiana africana* to cultivated tobacco. *Pol. J. Agron.* **2017**, *31*, 39–44.
55. Berbeć, A. Morphology, cytogenetics, and resistance of amphidiploid *Nicotiana raimondii* Macbride × *N. tabacum* L. (F_1 cv. Zamojska 4 × cv. LB-838) to *Potato virus Y*. *Genet. Pol.* **1988**, *29*, 41–52.
56. Czubacka, A.; Sacco, E.; Olszak-Przybys, H.; Doroszewska, T. Inheritance and effectiveness of two transgenes determining PVY resistance in progeny from crossing independently transformed tobacco lines. *J. Appl. Genet.* **2017**, *58*, 179–184. [CrossRef]
57. Czubacka, A.; Doroszewska, T. Obtaining resistant to PVY tobacco double haploids containing different sources of resistance. In Proceedings of the 44th TWC—Tobacco Workers' Conference, Lexington, KY, USA, 19–21 January 2010. abstr. 115.
58. Czubacka, A.; Doroszewska, T. Effectiveness of combining *va*-mediated resistance with a lettuce mosaic virus coat protein gene and a potato virus Y polymerase RNA gene in protection of tobacco hybrids from *Potato virus Y*. *J. Food Agric. Environ.* **2015**, *13*, 36–42.
59. Gajos, Z. Przeniesienie odporności na wirus brązowej plamistości pomidora (*Tomato spotted wilt virus*) z *Nicotiana alata* Link et Otto do tytoniu szlachetnego poprzez skrzyżowanie obu gatunków [Transmission of resistance to *Tomato spotted wilt virus* from *Nicotiana alata* Link et Otto to *N. tabacum* by crossing both species]. *Biuletyn CLPT* **1981**, *1–2*, 3–24.
60. Trojak-Goluch, A.; Institute of Soil Science and Plant Cultivation—State Research Institute, Puławy, Poland. Tobacco breeding processes. Personal communication, 2022.
61. Trojak-Goluch, A.; Laskowska, D.; Agacka, M.; Czarnecka, D.; Kawka, M.; Czubacka, A. Effectiveness of combining resistance to *Thielaviopsis basicola* and *Tomato spotted wilt virus* in haploid tobacco genotypes. *Breed Sci.* **2011**, *61*, 389–393. [CrossRef]
62. Trojak-Goluch, A.; Laskowska, D.; Kursa, K. Morphological and chemical characteristics of doubled haploids of flue-cured tobacco combining resistance to *Thielaviopsis basicola* and TSWV. *Breed Sci.* **2016**, *66*, 293–299. [CrossRef]
63. Korbecka-Glinka, G.; Trojak-Goluch, A.; Bakaher, N.; Goepfert, S. Agronomic performance of Polalta derived breeding lines resistant to tomato spotted wilt virus. In Proceedings of the CORESTA Meeting, Agronomy/Phytopathology, AP 11, Online, 4–14 October 2021.
64. Trojak-Goluch, A. Regeneracja pędów i stopień ploidalności roślin uzyskanych w kulturach in vitro fragmentów walca osiowego haploidalnych łodyg tytoniu (*Nicotiana tabacum* L.). *Pol. J. Agron.* **2020**, *41*, 3–10.

65. Doroszewska, T.; Depta, A.; Czubacka, A. *Album Gatunków z Rodzaju Nicotiana/Album of Nicotiana Species*; IUNG-PIB: Puławy, Poland, 2009.
66. Czubacka, A.; Depta, A.; Doroszewska, T. Zróżnicowanie reakcji odpornościowej na wirus Y ziemniaka wśród alloplazmatycznych form tytoniu. *Pol. J. Agron.* **2019**, *39*, 27–34.
67. Berbeć, A. Floral Morphology and Some Other Characteristics of Iso-genomic Alloplasmics of *Nicotiana tabacum* L. *Beitrage zur Tabakforschung Int.* **2001**, *19*, 309–314.
68. Berbeć, A.; Laskowska, D. Investigations of Isogenomic Alloplasmics of Flue-Cured Tobacco *Nicotiana tabacum* cv. Wiślica. *Beitr. Table Int.* **2005**, *21*, 258–263.
69. Berbeć, A. Variation among offspring of alloplasmic tobacco *Nicotiana tabacum* L. cv 'Zamojska 4' with the cytoplasm of *N. knightiana* Goodspeed. *Theor. Appl. Genet.* **1994**, *89*, 127–132. [CrossRef]
70. Berbeć, A.; Laskowska, D. Agronomic Performance of Flue-Cured Tobacco F1 Hybrids Obtained with Different Sources of Male Sterile Cytoplasm. *Beitr. Table Int.* **2004**, *21*, 234–239. [CrossRef]
71. Berbeć, A. Three-Way Crosses vs. Single Crosses in Tobacco: First Agronomic Assessment. *Crop Sci.* **2017**, *57*, 1363–1372. [CrossRef]
72. Berbeć, A.; Institute of Soil Science and Plant Cultivation—State Research Institute, Puławy, Poland. Tobacco breeding processes. Personal communication, 2022.
73. Schubert, J.; Doroszewska, T.; Chrzanowska, M.; Sztangret-Wiśniewska, J. Natural Infection of Tobacco by *Colombian Datura virus* in Poland, Germany and Hungary. *J. Phytopathol.* **2006**, *154*, 343–348. [CrossRef]
74. Przybyś, M.; Doroszewska, T.; Berbeć, A. Point mutations in the viral genome-linked (VPg) of *Potato virus Y* probably correspond with ability to overcome resistance of tobacco. *J. Food Agric. Environ.* **2013**, *11*, 986–989.
75. Masuta, C.; Nishimura, M.; Morishita, H.; Hataya, T. A single amino acid change in viral genome-associated protein of potato virus Y correlates with resistance breaking in 'Virgin A Mutant' tobacco. *Phytopathology* **1999**, *89*, 118–123. [CrossRef] [PubMed]
76. Lacroix, C.; Glais, L.; Verrier, J.-L.; Jacquot, E. Effect of passage of a *Potato virus Y* isolate on a line of tobacco containing the recessive resistance gene va^2 on the development of isolates capable of overcoming alleles 0 and 2. *Eur. J. Plant Pathol.* **2011**, *130*, 259–269. [CrossRef]
77. Agacka, M.; Depta, A.; Börner, M.; Doroszewska, T.; Hay, F.R.; Börner, A. Viability of *Nicotiana* spp. seeds stored under ambient temperature. *Seed Sci. Technol.* **2013**, *41*, 474–478. [CrossRef]
78. Agacka, M.; Laskowska, D.; Doroszewska, T.; Hay, F.R.; Börner, A. Longevity of *Nicotiana* seeds conserved at low temperatures in ex situ genebanks. *Seed Sci. Technol.* **2014**, *42*, 355–362. [CrossRef]

MDPI
St. Alban-Anlage 66
4052 Basel
Switzerland
www.mdpi.com

Agriculture Editorial Office
E-mail: agriculture@mdpi.com
www.mdpi.com/journal/agriculture

Academic Open
Access Publishing

mdpi.com

ISBN 978-3-0365-9842-0